frontiers | Research Topics

MorphoEvoDevo: A multilevel approach to elucidate the evolution of metazoan organ systems

Edited by
Andreas Wanninger, Pedro Martinez and Neva P. Meyer

Published in
Frontiers in Cell and Developmental Biology
Frontiers in Ecology and Evolution

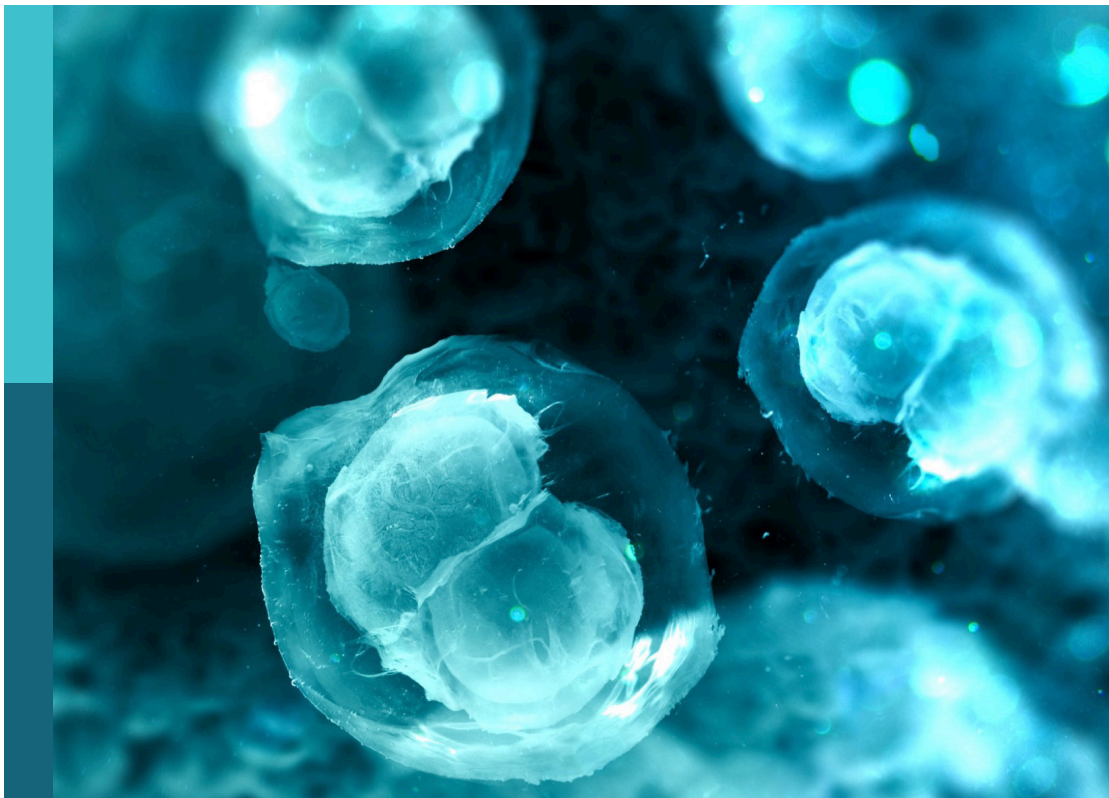

ISSN 1664-8714
ISBN 978-2-8325-3859-3
DOI 10.3389/978-2-8325-3859-3

About Frontiers

Frontiers is more than just an open access publisher of scholarly articles: it is a pioneering approach to the world of academia, radically improving the way scholarly research is managed. The grand vision of Frontiers is a world where all people have an equal opportunity to seek, share and generate knowledge. Frontiers provides immediate and permanent online open access to all its publications, but this alone is not enough to realize our grand goals.

Frontiers journal series

The Frontiers journal series is a multi-tier and interdisciplinary set of open-access, online journals, promising a paradigm shift from the current review, selection and dissemination processes in academic publishing. All Frontiers journals are driven by researchers for researchers; therefore, they constitute a service to the scholarly community. At the same time, the *Frontiers journal series* operates on a revolutionary invention, the tiered publishing system, initially addressing specific communities of scholars, and gradually climbing up to broader public understanding, thus serving the interests of the lay society, too.

Dedication to quality

Each Frontiers article is a landmark of the highest quality, thanks to genuinely collaborative interactions between authors and review editors, who include some of the world's best academicians. Research must be certified by peers before entering a stream of knowledge that may eventually reach the public - and shape society; therefore, Frontiers only applies the most rigorous and unbiased reviews. Frontiers revolutionizes research publishing by freely delivering the most outstanding research, evaluated with no bias from both the academic and social point of view. By applying the most advanced information technologies, Frontiers is catapulting scholarly publishing into a new generation.

What are Frontiers Research Topics?

Frontiers Research Topics are very popular trademarks of the *Frontiers journals series*: they are collections of at least ten articles, all centered on a particular subject. With their unique mix of varied contributions from Original Research to Review Articles, Frontiers Research Topics unify the most influential researchers, the latest key findings and historical advances in a hot research area.

Find out more on how to host your own Frontiers Research Topic or contribute to one as an author by contacting the Frontiers editorial office: frontiersin.org/about/contact

MorphoEvoDevo: A multilevel approach to elucidate the evolution of metazoan organ systems

Topic editors

Andreas Wanninger — University of Vienna, Austria

Pedro Martinez — University of Barcelona, Spain

Neva P. Meyer — Clark University, United States

Citation

Wanninger, A., Martinez, P., Meyer, N. P., eds. (2023). *MorphoEvoDevo: A multilevel approach to elucidate the evolution of metazoan organ systems*. Lausanne: Frontiers Media SA. doi: 10.3389/978-2-8325-3859-3

Table of contents

frontiers | Frontiers in Ecology and Evolution

TYPE Editorial
PUBLISHED 19 October 2023
DOI 10.3389/fevo.2023.1307280

OPEN ACCESS

EDITED AND REVIEWED BY
Maria Ina Arnone,
Stazione Zoologica Anton Dohrn, Italy

*CORRESPONDENCE
Andreas Wanninger
andreas.wanninger@univie.ac.at
Pedro Martinez
pedro.martinez@ub.edu
Néva P. Meyer
nmeyer@clarku.edu

†These authors have contributed equally to this work

RECEIVED 04 October 2023
ACCEPTED 12 October 2023
PUBLISHED 19 October 2023

CITATION
Wanninger A, Martinez P and Meyer NP (2023) Editorial: MorphoEvoDevo: a multilevel approach to elucidate the evolution of metazoan organ systems. *Front. Ecol. Evol.* 11:1307280. doi: 10.3389/fevo.2023.1307280

Editorial: MorphoEvoDevo: a multilevel approach to elucidate the evolution of metazoan organ systems

Andreas Wanninger[1*†], Pedro Martinez[2,3*†] and Néva P. Meyer[4*†]

[1]Unit for Integrative Zoology, Department of Evolutionary Biology, University of Vienna, Vienna, Austria, [2]Departament de Genètica, Microbiologia i Estadística, Universitat de Barcelona, Barcelona, Spain, [3]Institut Català de Recerca i Estudis Avançats (ICREA), Barcelona, Spain, [4]Biology Department, Clark University, Worcester, MA, United States

KEYWORDS

morphology, development, metazoa, organ system, fossil, phylogeny, embryo, ScRNA-seq

Editorial on the Research Topic
MorphoEvoDevo: a multilevel approach to elucidate the evolution of metazoan organ systems

1 Introduction

The evolution of animal morphologies has been a preoccupation of biologists at least since the XVIII century, when comparative methods were first used to model the transformations of animal form over evolutionary time. This relevance was encapsulated in Darwin's dictum: "Morphology [is] the most interesting department of natural history, [which] may be said to be its very soul" (page 434 of *On the Origin of Species*). Morphology, understood as a hierarchical construct (from molecules to cells, organs, and individuals), is still the central focus of the new field of EvoDevo.

Over the last 15 years, the International Society for Invertebrate Morphology (ISIM) has been meeting regularly to discuss the most current issues in the field. We have witnessed the incorporation of powerful technologies (i.e., single-cell RNA sequencing (scRNA-seq), serial transmission electron microscopy (TEM), and genomics), enabling the study of older problems in a new light. Moreover, the analysis of structures and processes now involves gathering data at different levels of complexity, from transcripts through cell types, tissues, and organs to whole bodies. With the help of phylogenetics and paleontology, the scales of our analyses have both spatial and temporal components. Integrating these data leads us to a more comprehensive study of morphology and easy movement across different scales, a prominent characteristic of presentations at past and present International Congress on Invertebrate Morphology (ICIM) meetings. The last of these, ICIM5, took place in Vienna between the 8th and 12th of August, 2022, and was organized by one of us (Andreas Wanninger). The presentations, ranging from the genomic control of development to cell lineage specification as well as the architecture and function of tissues and organs, showcased a variety of intellectual and methodological

approaches that attested to our community's vibrant activities. Accordingly, ICIM5 embraced a wide field of research areas as is reflected in the meeting's following core topics: MorphovoDevo; Functional Morphology; Molecular Basis of Morphological Diversity; Morphology in Deep Time; Morphology, Integrative Taxonomy and Phylogeny; Senses, Neurons and Behavior; Technological Advances in Microscopy and Imaging; Evolution of Multicellularity.

Some of these contributions, but also work that has not been presented at ICIM5 including studies on vertebrates, are included in this Research Topic entitled "MorphoEvoDevo: A Multilevel Approach to Elucidate the Evolution of Metazoan Organ Systems." We thank all colleagues who presented and shared their data and participated in the vital discussions on various topics of animal morphology, function, and evolution during ICIM5, 2022, and to those who contributed to this Research Topic. In the following, we summarize the essence of the papers published herein, grouping them by subject. Papers are bundled together based on the major level of analysis used, thereby being aware that they often tackle similar problems at different scales, an approach that we very much encourage (see also the final discussion for a critical assessment of the state of the field).

2 Genomes, transcriptomes, phylogeny: from single genes to gene collectives

As sequencing technologies and methods improve, the number and taxonomic coverage of sequenced genomes and transcriptomes continue to increase. Paps et al. discuss how these advances have informed our hypotheses of major evolutionary events within animals and plants such as the origin of multicellularity, and what challenges, such as poor taxon sampling, still remain. The authors compare evolutionary transitions in metazoans with those that occurred in plants, highlighting the multiple versus single origins of multicellularity, respectively, evolution of genomic novelty, and adaptations to terrestrial life. Genomic novelty in plants has been previously linked to the activity of transposable elements, and in this issue, Mukherjee and Moroz demonstrate the convergent generation of clusters of new transcription factors by transposable elements across different metazoan clades including *Hydra*, annelids, and mollusks (cephalopods, oysters, and sea slugs). Within Metazoa, there are abundant examples of morphological innovations, and comparative scRNA-seq is beginning to help us unravel the origins of these novelties. One morphological novelty that has long been studied is the molluscan shell. Salamanca-Díaz et al. compared the genetic toolkit for shell formation (embryonic shell or protoconch I and larval shell or protoconch II) in a conchiferan, the invasive quagga mussel *Dreissena rostriformis*, by generating single-cell transcriptomes for embryonic and larval cells. They found significant differences between gene complements across the two developmental stages as well as many novel genes with no clear ortholog, bringing into question the homology of the shell field across life history stages within a species and across molluscan taxa. Continued integration of phylogenomics, comparative genomics, and single-cell transcriptomics will enable us to continue answering questions surrounding the origins and diversification of major taxonomic clades and their morphological properties, providing insight into how multicellular life evolved.

3 Cellular and tissue diversity of animals

With the recent establishment of scRNA-seq, evolutionary biologists have now a tool at hand that allows for comparative analysis of gene expression signatures of individual cells or tissues of animals, thereby grouping them into so-called clusters and trajectories. Depending on how distinct the expression profile of a given cell cluster is from others, individual cell types that express key marker genes may be defined. If used in a comparative context across species, novel hypotheses on putative cell type homologies may be formulated. In order to facilitate such studies, Paganos et al. have established an easy-to-use method (whole animal freeze-fracture scanning electron microscopy; WAFFSEM), where small marine animals (embryos, larvae) are processed in such a way that cell types can be readily identified by scanning electron microscopy. They argue that a combination of their technique and other microscopic and molecular tools such as scRNA-seq will facilitate such comparative cell type analyses. Following their own rationale, a second paper of this group (Paganos et al.) combines serial block-face scanning electron microscopy and scRNA-seq to characterize pancreatic cells in developing sea urchins. They found that the sea urchin exocrine pancreas-like cells are molecularly and morphologically distinct from other cell types of the digestive tract and propose homology between these and the pancreatic cell of mammals, implying that such a cell type was already present in the last common deuterostome ancestor. Moroz and Romanova use a combination of morphological and scRNA-seq data in order to tackle the long-standing question about the identity and homology of neurons. They argue that neurons and synapses evolved multiple times independently in the animal tree of life and that nervous systems comprise different, non-homologous cell types. Using hemichordates as models for comparative research into genes that govern animal regeneration, Humphreys et al. found that these deuterostomes, during head regeneration, express genes that are closely related to those used by regenerating planarian flatworms and the cnidarian *Hydra*. These "stem cell reprogramming factors" appear to also be present in mammalian cells, although these animals do not show extensive regeneration abilities, raising the question as to what underlying mechanisms trigger the activation of these regeneration circuits in hemichordates.

In their quest to identify and characterize the expression profiles of cells that contribute to the tissues that form distinct morphological features in mollusks, such as the shell, foot, and neuromuscular systems, Salamanca-Díaz et al. provide a detailed atlas that identifies cell clusters in the trochophore larva of a bivalve

mollusk using scRNA-seq. The developmental trajectories of cells were traced, resulting in the reconstruction of the common origin of cells, e.g., from ectodermal precursors. Identified marker genes for each cell cluster were used to test for their *in situ* expression patterns in the respective stages of the developing bivalve. The data provided show that the identified cell populations indeed contribute to distinct morphological features, thus providing an important framework for future comparative cell genealogical studies into mollusks and other lophotrochozoans.

4 The architecture of animal tissues

Both gene expression as well as cellular and tissue dynamics during morphogenesis have long been used to infer the nature and evolutionary trajectories of key animal features such tissues or organs. In vertebrates, *Pax3/7* genes regulate the closure and patterning of the neural tube. Extending these studies to tunicates by using gene expression and CRISPR/Cas9-mediated mutagenesis, Kim et al. found that this is also the case in the model tunicate *Ciona*, suggesting that this key function of *Pax3/7* was already present in the last common vertebrate-tunicate ancestor. Neural crest and craniofacial development are two additional classical fields of research that have entered a new era by incorporating novel molecular tools into their research programs. In his topical review, Newton explores the possibilities of including "comparative evo-devo-omics" into assessing how different phenotypes are established during vertebrate development, in particular with respect to facial morphology. Thereby, he introduces the fat-tailed dunnart as a new marsupial model that, by comparing its developmental patterns with those known from mouse, should allow us to discern conserved from species-specific processes that generate craniofacial variation in mammals. Hampl et al. focus on another cranial component of vertebrates, the secondary palate, that in mammals forms a bony plate separating nose and mouth from each other. While in mammals two shelves are formed that subsequently fuse in the midline, development of these shelves varies considerably among reptile species ranging from open to fully closed phenotypes. The authors found that in chameleons the secondary palate closes after hatching. They identified various molecular factors that play a role in the growth of the palatal shelves and discuss variation in palate formation among amniotes.

Moving away from cranial hard part development, Macrì and Di-Poi studied cerebellar development in a lizard and a snake in order to assess differences of brain subdivision among vertebrates. They found that ontogenetic processes that were thought to be constrained to birds and mammals are also at play during cerebellogenesis in squamates, and that heterochronic shifts most likely influence mechanisms of molecular interactions between neural cell types in snakes. Painting an even bigger picture of neural evolution, Martinez and Sprecher ask the question about the factors that have allowed for the evolution of complex, centralized neural systems (brains, or "central processing units", CPUs, as they call them). They propose a scenario where, in a first step, receptors and then, in their proximity, neurons evolved, that were capable of transmitting signals. In areas with condensed neurons, the production of additional receptors was promoted, thus increasing signal processing in these areas (e.g., anteriorly in a prospective "head"). The increased presence of receptors would in turn have stimulated further neuron production, thereby generating a positive feedback loop that provided the prerequisite for shaping the vast amount of distinct neuronal phenotypes in the animal kingdom.

Not only skeleto- and neurogenetic processes but virtually all developmental pathways are highly dynamic. This becomes obvious if seemingly simple systems (e.g., at early ontogenetic stages that only comprise a few dozen or so cells) are studied. Zieger et al. looked into this phenomenon by analyzing intercellular lumen formation that is crucial for osmoregulation during early embryonic stages in the freshwater bivalve *Dreissena*. Their study showed that the water channel protein aquaporin is only associated with the midbody, a structure that is part of the intercellular cytokinetic bridge that is crucial for lumen formation. The direction of cavity expansion during cleavage depends on the location of the aquaporin-bearing midbodies, and if the microtubules that form the cytokinetic bridge are disrupted, no lumen is formed. Such embryos are incapable of expelling excess inflowing water and thus of osmoregulation. Since lumen formation during cleavage is a widely known phenomenon in freshwater invertebrates, the authors hypothesize that the mechanism they found in *Dreissena* may be widespread among such animals.

5 Animal organs and body parts: identity, variation, and evolution

The nature and function of animal organ systems and body regions has been a key topic in zoological research for centuries. In his review, Minelli outlines how the study of organs and body parts has changed over the past 200 years. While earlier morphologists either defined organs based on their very structure (morphology) or their function, today's evolutionary biologists incorporate the developmental mechanisms by which these structures are formed during ontogeny, thereby including morphogenetic, molecular, as well as cell type composition in their analyses. However, using the evolution of hermaphroditism as an example, Minelli argues that a sharp distinction between a morphological- and functional-based definition is vital when assessing the evolutionary pathways of respective body plan features in given animal lineages.

In order to reconstruct the evolutionary origin of the novel mammalian jaw joint, Anthwal and Tucker compared its development in the mouse and the tooth-less monotremes. They found that during platypus and echidna development a fibrocartilage disc primordium is formed, a structure that is associated with the mammalian jaw joint. However, this disc is not fully formed in the monotremes and resembles a state similar to that in mutagenic mice with reduced overall cranial musculature, leading the authors to conclude that the monotreme situation is due to a secondary loss of the jaw joint disc and dentition, and that the last common ancestor of Mammalia did carry teeth.

6 Fossils and development as windows into the evolutionary past: changing morphologies and ontogenetic strategies over time

The three papers of this topic ideally illustrate that both paleontology and developmental studies provide important insights as to how organisms or individual traits may have evolved over evolutionary time. In their study on the morphology, function, and replacement of teeth in the common Triassic sauropterygian *Keichosaurus*, Liao et al. used thin sectioning and X-ray computed microtomography. By comparing their findings to those on recent and Paleozoic piscivore vertebrates, they conclude that *Keichosaurus* likely fed on small fish and soft body invertebrates such as shrimps. At a branch of the animal tree of life far distant to the vertebrates are the placozoans, seemingly simple-built multicellular creatures without distinct neurons, muscles, or body axes. Employing long-term culturing of these "pre-bilaterians", Romanova et al. found that in addition to the well-known asexual reproductive strategies by fission and the production of ciliated swarmers, placozoans may also use the epithelial spheres to produce juvenile offspring. The diverse modes of asexual reproduction in placozoans prompts the authors to suggest these animals as potentially suitable experimental models for research into animal regeneration.

On a more theoretical side of evolutionary biology, Martynov et al. revisits the linkage of ontogeny and phylogeny by elaborating on traditional concepts such as Ernst Haeckel's biogenetic law ("ontogeny recapitulates phylogeny") or the hypothesis of a conserved phylotypic stage for given animal lineages. They argue that ontogeny is not only a result of phylogeny, but instead generates animal diversity through variations introduced during evolution, thereby affecting the (adult morphological) phenotype. As such, it should be possible to infer phylogenetic relationships using ontogenetic data, and the authors propose "ontogenetic systematics" as a crucial discipline in biology. According to them, this also requires a refined definition of the often interchangeably used terms "paedomorphosis", "neoteny", and "progenesis".

7 The future of MorphoEvoDevo

The contributions to this Research Topic demonstrate not just the vitality of the field but also the analytical complexity that contemporary investigators require to understand the evolution of morphologies. This is a field that lies at the intersection of different disciplines, from molecular genomics to morphological comparisons and paleontology. To a large extent, it still relies on the use of comparative methods and extrapolation from well-understood datasets. The fact that most evolutionary transitions occurred over long, hidden periods of time make some of these extrapolations rather difficult, if not far-flung. Ideas about the origin of key taxa and morphological innovations such as metazoans, bilaterians, brains, and mesoderm, are hinted at, at best. The scenarios proposed are undoubtedly based on inferences but, more and more, on well-informed ones. Data gathered by the new technologies—including genomics, scRNA-seq, knockdown technologies, and spatial transcriptomics—are helping us to dissect developmental processes with unprecedented detail, providing valuable data to revisit the diverse (old and new) evolutionary hypotheses. In addition, the recent incorporation and refinement of phylogenetic methods improve the understanding of highly debated clade affinities and, thus, permit more informed predictions of how morphological changes might have happened over evolutionary time.

But this is, perhaps, still a rosy picture. We noticed—particularly during the meeting but also reflected in these papers—that there remains room for improvement. Single-cell data (identification of cell types and subtypes) still lack proper resolution in most invertebrates. Moreover, the cross-species comparison and identification of cell type homologies is in its infancy; it is still challenging to infer the evolutionary history of cell types across animal groups. The cell atlases need to be transformed into cell maps of whole animals, specifying where all those identified cell types reside in the animal body. We also need to know how these cell types are organized into tissues. Clear progress has been made in mapping the positions of cell types, mainly in the context of high-throughput TEM reconstructions (e.g., connectomics). However, these approaches are still limited to very few animals. Highly automated systems in electron microscopy (i.e., serial block face scanning, etc.) are paving the way to more extensive analyses of tissue architectures. Needless to say, these maps should represent a broad taxonomic range; otherwise, transformations of tissues in evolutionary time are difficult to trace and will remain highly speculative. Genomics seems to be an area of fast progress, primarily due to the reduced costs of sequencing and increased computational power. A flurry of papers, plus huge sequencing projects (e.g., Earth Biogenome), are spearheading a bloom of comparative genome studies. Such advances have been complemented recently with the exploration, via epigenetic analysis, of the response of whole genomes to processes such as development and regeneration. Again, while this is encouraging, the transition from accumulating tons of data to distilling critical biological information is still wanting. The idea that huge datasets per se can inform us directly about specific biological processes is still a sign of over-optimism. More needs to be done to bridge these levels.

One relevant consequence of genome analysis and the use of technologies in the molecular realm is the development of functional assays. In the last decade, the introduction of CRISPR technologies (plus the extension of RNAi methods) has allowed us to analyze gene function in several animals and developmental contexts. We have moved from speculation about gene function (primarily based on homologies or just *in situ* patterns) to evaluating these functions *in vivo*. In addition, the generation of transgenic animals, a necessary complementary tool, is a pressing need. These methods are promising but need to be implemented in more animal systems and at a larger scale; otherwise, deciphering complex gene regulatory networks would need some time.

While the above-described use of new technologies has illuminated speculations on the origin of morphological and

molecular novelties, we should not forget that the path leading to a specific morphological transition can best be directly evaluated by searching for appropriate fossils, the only real transitional forms (maybe with the sole exception of ontogenetic sequences of morphogenesis that may provide a window into the evolutionary past and relatedness of organisms). Without a proper investigation of the fossil record, our scenarios lack a solid testing ground. More and more fossils corresponding to critical transitional periods (i.e., Precambrian-Cambrian) have been unearthed during the last few decades. This is particularly interesting, given that most of these deposits have revealed previously unimagined transitional forms, forcing us to reconsider evolutionary trajectories.

All in all, we believe that investment in emerging technologies and expansion of the phylogenetic range of our analyses open up the field of MorphoEvoDevo to a bright future. Integrating knowledge gathered across different scales should be a clear objective for the near future, since it is only by moving between them that we can suggest solid (informed) scenarios for the evolution of morphologies. Those at ICIM5 have witnessed a clear movement in this direction, and we anticipate that the following meetings will bring many new surprises to the field. On a particularly positive side of things, we believe that the diverse assemblage of contributions at ICIM5 and in the present Research Topic of Frontiers in Ecology and Evolution, that all identify themselves as revolving around animal morphology in the broadest sense, clearly demonstrates that we are about to overcome the long-standing methods-based rivalry between "morphologists" and "molecular biologists". More and more evolutionary zoologists are using methods just the way one should: as undogmatic tools to answer important questions. In doing so, we should get closer to describing biological reality more accurately as more suitable technologies are employed—often in form of larger collaborations where individual partners contribute their expertise to joint research programs.

Author contributions

AW: Conceptualization, Writing – original draft, Writing – review & editing. PM: Conceptualization, Writing – original draft, Writing – review & editing. NM: Conceptualization, Writing – original draft, Writing – review & editing.

Funding

The author(s) declare that no financial support was received for the research, authorship, and/or publication of this article.

Conflict of interest

The authors declare that the research was conducted in the absence of any commercial or financial relationships that could be construed as a potential conflict of interest.

The handling editor MA declared a past co-authorship with the author PM.

The author(s) declared that they were an editorial board member of Frontiers, at the time of submission. This had no impact on the peer review process and the final decision.

Publisher's note

frontiers | Frontiers in Ecology and Evolution

TYPE Review
PUBLISHED 02 June 2023
DOI 10.3389/fevo.2023.1185566

OPEN ACCESS

EDITED BY
Andreas Wanninger,
University of Vienna, Austria

REVIEWED BY
Jose Maria Martin-Duran,
Queen Mary University of London,
United Kingdom
Pedro Martinez,
University of Barcelona, Spain

*CORRESPONDENCE
Jordi Paps
✉ jordi.paps@bristol.ac.uk

†PRESENT ADDRESS
Marta Álvarez-Presas,
Institute of Evolutionary Biology (UPF-CSIC),
Barcelona, Spain

RECEIVED 13 March 2023
ACCEPTED 08 May 2023
PUBLISHED 02 June 2023

CITATION
Paps J, Rossi ME, Bowles AMC and Álvarez-Presas M (2023) Assembling animals: trees, genomes, cells, and contrast to plants. *Front. Ecol. Evol.* 11:1185566. doi: 10.3389/fevo.2023.1185566

Assembling animals: trees, genomes, cells, and contrast to plants

Jordi Paps[1]*, Maria Eleonora Rossi[2], Alexander M. C. Bowles[3] and Marta Álvarez-Presas[1†]

[1]School of Biological Sciences, University of Bristol, Bristol, United Kingdom, [2]School of Earth Sciences, University of Bristol, Bristol, United Kingdom, [3]School of Geographical Sciences, University of Bristol, Bristol, United Kingdom

The Animal Kingdom is an astonishingly diverse group. Together with plants and fungi is one of the three major lineages of multicellular eukaryotes. Due to anthropocentrism and/or genuine scientific interest, their origin and diversification are pivotal to modern evolutionary biology. In the last few decades, dramatic technological advances in molecular biology and computational power have generated new phylogenetic proposals, as well as new tools to compare genomes or study cell type evolution. These new approaches complement the insights from fields such as comparative morphology, evodevo, or palaeontology, which all together provide an integrative view of animal evolution, including major evolutionary transitions such as the origin of animals or the emergence of animals with bilateral symmetry. In this paper, we review recent developments in animal phylogenetics, comparative genomics, and cell type evolution related to these two transitions, and we compare animals to another major lineage of multicellular eukaryotes, plants.

KEYWORDS

metazoa, comparative genomics, phylogenetics, cell types, plants

Assembling trees

Animals (Metazoa) are multicellular eukaryotic organisms loosely characterized by their ability to move, sense, and react to their environment, as well as consuming other organisms. They play fundamental roles in the biosphere and in many ecological processes. Most animals display bilateral symmetry, like worms, molluscs, arthropods, or vertebrates, forming a monophyletic group called Bilateria. While other animals —sponges, ctenophores, placozoans, and cnidarians— display other body plans (Paps, 2018).

Paraphrasing Theodosius Dobzhansky, "*nothing makes sense in macroevolution except in the light of phylogeny*." A robust evolutionary tree is central to comparative biology, including the study of genomes or cell types. Early phylogenies were based on morphological traits, and the advent of PCR, expanded the range of characters to one or few genes. In the last 20 years (Delsuc et al., 2005; Philippe et al., 2005; Dunn et al., 2008), massive animal phylogenomic matrices containing hundreds or thousands of genes have dominated the narrative of animal evolution. Often, they have improved the resolution of major lineages like molluscs (Kocot et al., 2011; Smith et al., 2011), annelids (Struck et al., 2011), flatworms (Laumer and Giribet, 2014; Egger et al., 2015; Laumer et al., 2015), and insects (Rota-Stabelli et al., 2011; Misof et al., 2014). In contrast, the radiations of early animals and bilaterians have been more problematic, resulting in major controversies.

Previous articles have thoroughly reviewed the phylogeny of animals and its main problems (Edgecombe et al., 2011; Dunn et al., 2014; Jékely et al., 2015; Telford et al., 2015; Giribet, 2016; Ruiz-Trillo and Paps, 2016; Paps, 2018; Giribet and Edgecombe, 2019). Briefly, most pre-phylogenomic trees supported sponges as the sister group to other animals (Figure 1; hypothesis affectionately called #porosis or sponges-first; Hejnol, 2016). However, phylogenomic datasets have invariably been ambiguous with some supporing sponges-first (Philippe et al., 2009; Pick et al., 2010; Nosenko et al., 2013; Simion et al., 2017) and others recovering ctenophores in that same position (#ctenosis or ctenophores-first; Dunn et al., 2008; Hejnol et al., 2009; Ryan et al., 2013; Moroz et al., 2014). Later datasets, sometimes with expanded gene and taxa sampling, have controversially provided support for one hypothesis or the other based on the analytical methods used (see summary in Table 1 in Li et al., 2021). This debate has major consequences in our understanding of the nature of the last common ancestor (LCA) of all animals and the evolution of essential animal traits such as the nervous or muscle systems.

A similar controversy haunts the origin of bilateral animals (Hejnol and Pang, 2016; Ruiz-Trillo and Paps, 2016; Telford and Copley, 2016; Marlétaz, 2019; Pisani et al., 2022). The Xenoacoelomorpha (Xenoturbellida, Acoela, and Nemertodermatida; XAN from now on) is a lineage of simple animals central to this transition. Often linked to flatworms in morphological trees, early molecular phylogenies placed acoels and nemertodermatids as sister to the other bilaterians (Nephrozoa hypothesis; Ruiz-Trillo et al., 1999, 2002; Paps et al., 2009a), position backed by later phylogenomic analyses and expanded to all XAN (Hejnol et al., 2009; Cannon et al., 2016; Rouse et al., 2016). This would suggest that the first bilaterian was a simple benthic acoelomate animal with direct development and no brain (Baguñà et al., 2001; Baguñà and Riutort, 2004). However, other phylogenomic studies identified XAN as sister to the Ambulacraria (echinoderms and hemichordates; Xenambulacraria hypothesis), which sparked the War of the Worms (Telford and Copley, 2016). These studies recover (1) Xenambulacraria as sister to chordates, together forming the deuterostomes (Brinkmann et al., 2011) or, intriguingly, (2) Xenambulacraria as sister to all the other bilaterians, formed by chordates as sister to protostomes (Marlétaz, 2019; Marlétaz et al., 2019; Philippe et al., 2019). The later would effectively mean the demise of deuterostomes, although these topologies usually show low statistical support. In any case, the Xenambulacraria hypothesis implies that XAN body plans would be the result of body plan simplification rather than the ancestral condition of bilaterians.

These two controversies, origin of animals and bilaterians, share similar challenges. First, they both share branch length issues. Often short branches flank the nodes of interest, probably due to molecular saturation or rapid radiations. In addition, some of the key lineages (e.g., XAN, ctenophores) show fast evolutionary rates, making them susceptible to long branch attraction artifacts (LBA; Felsenstein, 1978). Amongst the different strategies that minimize the impact of LBA (Bergsten, 2005; Paps et al., 2009b), expanding the taxon sampling of fast evolving taxa to shorten the long branches has proven to be effective with different lineages such as nematodes or acoels (Aguinaldo et al., 1997; Ruiz-Trillo et al., 1999). Remarkably,

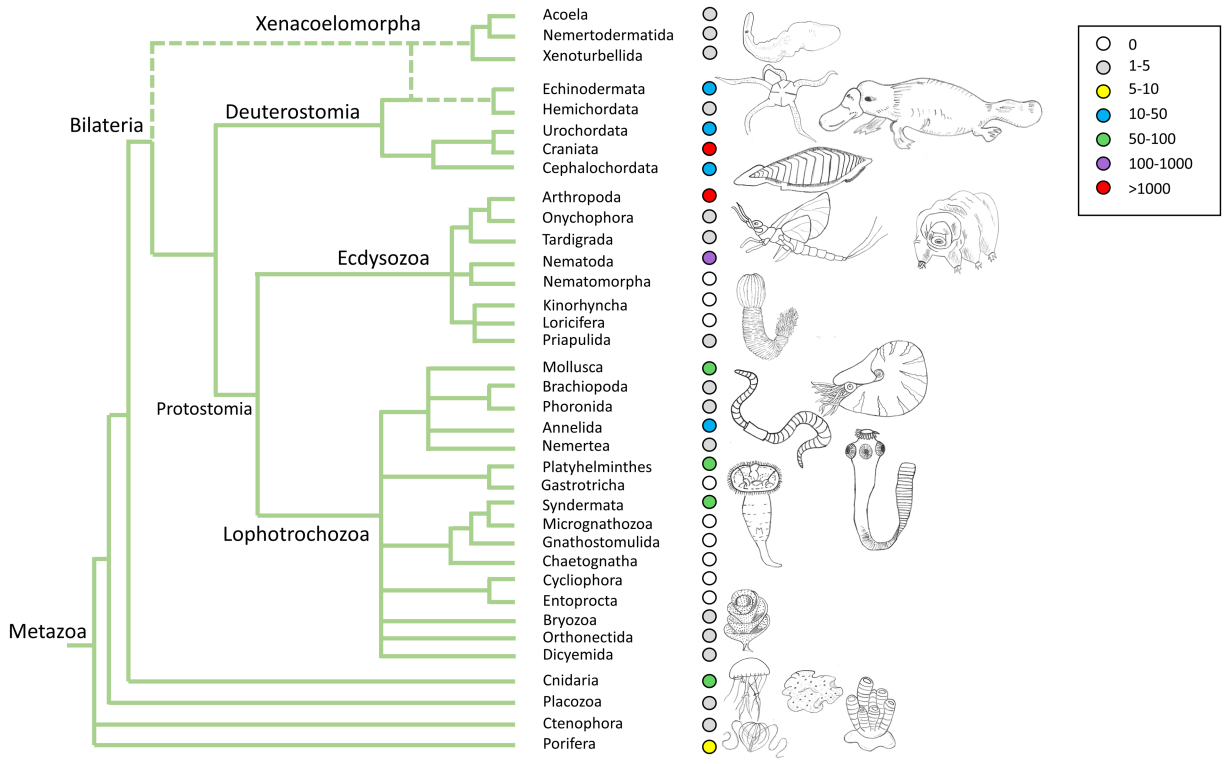

FIGURE 1
Genome data availability across the animal tree of life.

the molecular phylogenies of extant ctenophores resemble a "duster," with a long branch from their first ancestor to the most recent one, with all the extant taxa radiating in a recent short period of time. This entails a relatively young ctenophoran LCA (Podar et al., 2001), with earlier ctenophore lineages lost to time due to extinction; the recent discoveries of new stem fossil ctenophores seem to support this view (Ou et al., 2015; Zhao et al., 2019). Therefore, expanding the taxon sampling of extant ctenophores may not help to shorten their branch, although new environmental DNA studies indicate that we might be able to find new undescribed lineages (Arroyo et al., 2016; Christianson et al., 2022).

All these branch problems reflect the heterogeneity of molecular data, especially in key lineages like XAN or ctenophores, where the evolutionary models available may fail to adequately describe the data (Giacomelli et al., 2022), possibly resulting in model misspecification and inaccurate trees. Different approaches aim to reduce the impact of compositional rate, including the CAT model (Lartillot and Philippe, 2004; Lartillot Brinkmann et al., 2007; Philippe et al., 2009; Pick et al., 2010; Pisani et al., 2015), recoding (Feuda et al., 2017; Redmond and McLysaght, 2021; Giacomelli et al., 2022), expansion of gene and taxon sampling (Laumer et al., 2019), or —conversely— the significant removal markers that introduce phylogenetic noise (Mulhair et al., 2022; Pisani et al., 2022; McCarthy et al., 2023). In general, these approaches favor sponges-first and Xenambulacraria. However, some of these strategies have been criticized in studies that generally support ctenophores-first (Whelan et al., 2017; Whelan and Halanych, 2017; Hernandez and Ryan, 2021; Li et al., 2021). Moreover, sources of systematics errors have also been identified in the phylogeny of early bilaterians, which require further consideration when tackling these phylogenetic questions (Kapli and Telford, 2020; Natsidis et al., 2021; Kapli et al., 2021a,b).

A second common issue in these controversies stems from the datasets used. Most phylogenomic studies rely on data mostly derived from transcriptomes rather than whole genomes. Transcriptomes are a convenient and affordable way to expand taxon and gene sampling, at the expense of only capturing a subset of all the genes and isoforms present in an organism, the ones highly expressed in the tissue and/or developmental stages (usually adults) sampled to generate the data. Thus, transcriptomes do not reflect the full set of genes in an organism, and some genes will be missing, truncated, or split into two or more transcripts. These issues introduce missing data into matrices and confound the orthology assignment (Paps and Holland, 2018; Bowles et al., 2020; Guijarro-Clarke et al., 2020), an essential step in phylogenetic inference. The use of only complete genomes should overcome these concerns but, unfortunately, not many new genomes for sponges or ctenophores have been released in the recent years, with exceptions (Kenny et al., 2020). Genomes for XAN representatives have started to be available only very recently (Figure 1; Philippe et al., 2019; Martinez et al., 2022; Schiffer et al., 2022).

Generating new data is central to moving away from previous datasets. As a result of the lack of new data, many recent studies reanalyze earlier datasets, some over 10 years old, with new methods rather than compiling new dataset matrices. These analyses provide many interesting insights into methodological issues and datasets behaviors, but overall they do not provide a conclusive answer. For external observers, the succession of publications with opposing outcomes may resemble an endless tennis match with no resolution in sight. The lack of data has also introduced alternative interpretations of the analytical outcomes and the general outlook of ancestors. Sometimes a topology is favored because it is retrieved in most analyses even if suboptimal methods were used, following an implicit "democratic" criterion rather than integrating method optimality into the discrimination of topologies. In others, a topology is rejected because it is recovered by suboptimal approaches affected by systematic errors, or supported by simulations that integrate systematic error; however, in these cases no alternative hypothesis is strongly supported by optimal approaches or empirical data. Even a broken clock is right twice a day, and scientific hypotheses must be rejected using the best methods rather than flawed ones.

More genomes are being quickly produced by initiatives like the Darwin Tree of Life, Earth Biogenome, or the Global Invertebrate Genomics Alliance (Bracken-Grissom et al., 2014; Wellcome Sanger Institute, 2020). This will finally allow the generation of new datasets based on complete genomes, reducing the issues with orthology, hopefully moving the field forward from the current phylotranscriptomics era to a real phylogenomics stage. Complete genomes will also improve the curation of genome databases, reducing issues with contaminant sequences, misannotated genes, genes without functional annotation, etc. Moreover, this new high quality data will offer the chance to exploit genome-level information to reconstruct phylogenies and developing new methods, in addition to classical phylogenomic analyses, fulfilling the promise of rare genomic changes (Rokas and Holland, 2000). These include characters such indels, microRNAs, ancient linkage groups, etc. A recent example of this is the use of gene content to infer the phylogeny of animals, supporting porifera-first and Nephrozoa (Pett et al., 2019; Juravel et al., 2022; but see Schiffer et al., 2022). These recent developments and others to come will certainly move forward our understanding of animal evolution.

Assembling genomes

The characterization of the genetic toolkit in early animals is one of the main research goals of evolutionary biologists (Dunn and Ryan, 2015). Inferring the evolution of gene gains and losses, gene duplications, or horizontal gene transfer at different key points of the tree of life could help to better understand how extant species have evolved. In addition, it might answer some of the questions that have led to debate in recent years and that have been discussed in the previous section, such as whether the sponges or ctenophores came first or what is the phylogenetic position of XAN.

With the advent of next-generation sequencing (NGS) methods, a wealth of genomic data is available for a larger diversity of organisms. However, the taxon sampling is still highly biased in terms of the quality of genomes (referred to as reference genomes) and taxonomic diversity, which hinders the comprehensive comparative study at the kingdom level (Figure 1). As mentioned above, there are several initiatives trying to speed up the sequencing process of all existing animal species' genomes. However, there are still some underrepresented groups, mainly due to the difficulty in sampling and obtaining good quality data. The comparative genomics methods advance almost at the same speed as the number

of available genomes, ranging from whole genome comparisons to analysis of gene expression. The integration of machine and deep learning in the study of genomes is also advancing rapidly, beginning to replace traditional comparison methods, which are much slower and computationally imprecise (Zou et al., 2018). One of the critical points for conducting comparative genomics studies is the definition of orthologs and paralogs. In recent years, new sophisticated but also faster methods have emerged for the detection of orthologs that are facilitating robust genomic comparisons (Paps and Holland, 2018; Emms and Kelly, 2019; Miller et al., 2019; Buchfink et al., 2021; Grau-Bové and Sebé-Pedrós, 2021).

Evolutionary genomics can reconstruct ancestral animal genomes, inferring ancient gene complements or, more recently, even chromosome-level ancestral genomes (Nakatani and McLysaght, 2017; Simakov et al., 2020, 2022; Nakatani et al., 2021). Some preconceptions that have been rejected with the advancement of genomic study are the correlation between the number of genes and complexity (Dunn and Ryan, 2015), although the definition of organismal complexity has been always complex. Still, gene gains and losses play a significant role in evolution, with gene loss being associated with the loss of anatomical structures in evolution, in accordance with the view that evolution can lead to both increases and decreases in complexity (Lankester, 1880). The prevalence of gains and losses of genes and protein domains at the dawn of distinct groups of animals have been demonstrated (Albalat and Cañestro, 2016; Guijarro-Clarke et al., 2020).

A key element of comparative biology is the use of outgroups to polarise evolutionary changes. In recent years, the genomes of the close relatives of animals have become increasingly available. One of the main divisions of the eukaryotic Tree of Life is Opisthokonta, which includes fungi and choanoflagellates, some single-celled taxa such as Ichthyosporea or Filasterea, and of course, metazoans (or animals). Unicellular eukaryotes are key to revealing the origin of animal multicellularity (Paps et al., 2010; Sebé-Pedrós et al., 2017; Paps, 2018). The analysis of animal genomes and their close relatives in a phylogenetic context, facilitated the reconstruction of the minimum gene complement present in the genome of the last common ancestor of all animals, revealing an unprecedented increase in the degree of genomic novelty during the origin of metazoans (Paps and Holland, 2018). This genomic novelty involves biological functions characteristic of animal multicellularity (Brunet and King, 2017), especially gene regulation (e.g., transcription factors, signaling pathways) but also cell adhesion and the cell cycle. However, the functions and roles of these genes in opisthokonts are still pending to be deciphered.

Analyzing a large number of genomes, a reductive evolution pattern was observed on protein-coding genes complement, with a notable loss of genes during the emergence of two main groups of bilateral animals, Ecdysozoa and Deuterostomia (Guijarro-Clarke et al., 2020). At the phylum level, flatworms, nematodes, and tardigrades showed the greatest reduction in genetic complement, along with genetic novelty. A parallel study using different methods and datasets obtained remarkably similar results, describing that the origin of animals was characterized by the duplication of genes (Fernández and Gabaldón, 2020). Using transcriptome data, they incorporated the XAN to the dataset, which was characterized by rampant gene loss. Significant gene loss was also detected in Deuterostomia and Ecdysozoa. Novel genes in all nodes from Metazoa to specific phyla were enriched in functions related to the nervous system, suggesting that this system has been continuously and independently reformed throughout evolution inanimals. Thus, it appears that numerous duplication events occurred at the origin of the animals, followed later by the massive loss of some genes in certain lineages. These big gene losses are contrary to a "supposed" increase in complexity during evolution.

However, the taxon sampling for high quality genomes is still too scarce to be able to draw clear conclusions (Figure 1), and the picture may change with the addition of genomes in key phyla, such as Priapulida, Kinorhyncha, Gnathostomulida, and Chaetognatha, for example. The effect of taxon sampling bias is also a critical issue to address, as it can completely change the results of studies, as well as which external group is used for genomic comparison (Richter et al., 2018) and the detection of gene orthology also present serious challenges (Weisman et al., 2020; Natsidis et al., 2021).

Assembling cells

Understanding the evolution of cell types is key to reconstruct the evolutionary history of animals. We know that one of the major events that shaped animal evolution is the acquisition of multicellularity. In eukaryotes, it has evolved independently at least 25 times (Parfrey and Lahr, 2013), and the last common ancestor of animals was multicellular (Brunet and King, 2017). The diversification of the Animal Kingdom is concomitant to the enormous number of cell types they present. However, how multicellularity evolved and what shaped the diversity of cell types remains an open question.

Multicellularity is the result of a single cell dividing and differentiating into cell types, that differ in functions, morphology, and organization. It requires a process of spatial and temporal differentiation, and the resulting cell identity is regulated by a hierarchy of gene regulation (Arendt, 2008). With the recent development of NGS, cell identity was strictly associated by gene regulatory networks and the expression of specific transcription factors, and it became necessary to extend the definition of cell types, including the cell-type specific regulatory mechanisms (Arendt et al., 2016; Wang et al., 2021). Moreover, it has been suggested that cells undergo evolutionary changes, and they can be considered evolutionary units (Arendt et al., 2016). Historically, similar cell types of different animals have always been compared to one another to highlight similarities, question homology, and finally understand the evolutionary history of animals. This is the case of choanoflagellates compared to the choanocytes of the sponges, and the nervous system in ctenophores and other animals (Mah et al., 2014; Moroz et al., 2014; Jékely et al., 2015; Moroz and Kohn, 2016; Sogabe et al., 2019).

During the last decade, the advent of single cell RNA sequencing (scRNA-seq) made it possible to investigate gene expression at the cellular level. This enabled the mapping of all the different cell types present in an organism or a tissue (i.e., Atlas) using gene regulatory networks (Fiers et al., 2018) and gave the possibility to pose phylogenies of closely related cell types (Kin et al., 2015; Posada, 2020). In addition, it also showed the potential of comparative studies to question the origin of animals and their cell types, when applied to the earliest-branching taxa in the Animal Tree of Life,

being sponges, ctenophores, cnidarians, and placozoan (Tanay and Sebé-Pedrós, 2021). The first atlases generated for early metazoans showed a greater variety of cell lineages within species, identified by specific transcription factors. Across species comparison of similar cell types highlighted that most genes involved in co-regulation have evolved independently (e.g., convergent evolution), with only housekeeping function, ribosomal apparatus and flagellar apparatus being conserved. Moreover, genes expressed more broadly across tissues have older phylogenetic origin, while genes expressed in a subset of tissues should be considered more recent; this trend is reflected in the cell lineages as well (Sebé-Pedrós et al., 2018). A similar approach has been used in bilaterians, where muscle cells show conserved markers shared among epithelial cells, like cadherin involved in cell–cell adhesion, but across taxa comparison underline the presence of clade-specific transcripts, as in the case of XAN, which may be linked to specific cell types (Duruz et al., 2021).

Finally, an early hierarchical clustering analysis of cell types has been performed across animals, including the cnidarian *Nematostella* and bilaterian species model (Wang et al., 2021). Similarities have been found among stromal cells, smooth muscle cells, and endothelial cells which form a cluster with neurons closely related, this entire cluster is related to a second major cluster formed by stem cells, epithelial cells, and striated muscle cells, and highlights the amount of genes shared among different cell types across animals. These recent studies show that scRNA-seq can be a powerful tool to infer the evolutionary history of animals. However, this field is extremely young, and it faces many challenges. First being the restricted taxon sampling available, that does not reflect the diversity in the animal tree of life and in cell categories. The lack of knowledge regarding the gene regulatory networks that does not allow to characterize new cell types, followed by the plethora of sequencing techniques that have been developed in the last 10 years that provide a broad range of sequencing depth and sensibility, which makes it difficult to compare data. Finally, there is no shared consensus across the scientific community regarding the bioinformatic tools needed to correctly handle and analyze the scRNA-seq data under a phylogenomic framework. Nevertheless, scRNA-seq is a useful and powerful technique, that will allow us to understand better how cells function, and possibly disentangle the evolutionary history of animals if applied wisely.

Assembling plants

As highlighted above, insights from the analysis of genes, genomes and cell types have revealed that there are complex mechanisms regulating the development of animals. Plants represent another evolutionary distinct group with complex evolutionary development, with common elements emerging convergently in both plants and animals. Indeed, Szathmáry and Smith (1995) defined the evolution of multicellularity in animals, plant and fungi as a major evolutionary transition. However, the extent to which the mechanisms and innovations governing the origin of animals are unique or ubiquitous across multicellular organisms is only now being understood. As such, evolutionary developmental analyses are contrasted below, with parallels drawn between land plants (embryophytes) and animals.

Land plants are divided into the vascular plants (tracheophytes) and bryophytes, which originated from a single common ancestor that emerged onto land approximately 500 million years ago (Morris et al., 2018). The radiation of land plants changed the biosphere, enabling the establishment of terrestrial animal life (Julca et al., 2021). In comparison to animals, the phylogeny of land plant evolution is reasonably well resolved with bryophytes considered as a monophyletic group that is sister to vascular plants (Leebens-Mack et al., 2019; Harris et al., 2020). The closest relatives of land plants are the streptophyte algae, a paraphyletic group, with Zygnematophyceae identified as sister group to land plants (Wickett et al., 2014; Leebens-Mack et al., 2019).

Common features required for plant life on land and therefore present in the first land plants are rhizoids (root-like structures), stomata (pores) and the alternation of generations (Harrison, 2017). The latter of these involves two distinct phases in the plant life cycle, alternating between sporophyte (non-sexual phase) and gametophyte (sexual phase) forms. Additionally, three-dimensional growth was present in the ancestor of land plants. This is juxtaposed to streptophyte algal relatives which represent a plethora of forms with filamentous Zygnematophyceae, multicellular two-dimensional Coleochaetophyceae, three-dimensional Charophyceae and single-celled Mesostigmatophyceae (Umen, 2014). Therefore, the evolution of multicellularity and terrestrialisation occurred at distinct points in the evolution of plants (Hess et al., 2022), which contrasts with animals, whose obligated multicellular origins coincided with the origin of Metazoa (Bowles et al., 2020). There are additional examples of convergent evolution of multicellularity, with multicellular lineages found outside the streptophytes, in the chlorophytes and rhodophytes (Parfrey and Lahr, 2013; Bowles et al., 2022).

Comparative analysis of transcriptomes and genomes of streptophyte algae and land plants is beginning to reveal the evolutionary novelties associated with life on land. For example, gene content analysis suggests that the transition of plants from water onto land (terrestrialisation) was preceded by major innovations previously thought to be land plant specific (Hori et al., 2014; Nishiyama et al., 2018; Cheng et al., 2019). These include the symbiotic association of plants with beneficial fungi (Delaux et al., 2015), a partial genetic toolkit for directing stress responses (Bowman et al., 2017; de Vries et al., 2018; de Vries and Archibald, 2018), as well as cell wall modifications (Nishiyama et al., 2018; Cheng et al., 2019; Jiao et al., 2020).

Recent genomic studies have shown that the evolution of plants was coordinated by the development of increasingly complex signaling molecules (Bowman et al., 2017) and genetic networks (Catarino et al., 2016). Furthermore, the genomes of early land plants was associated with gene family expansions related to cutin and lignin biosynthesis and phytohormone production (Bowman et al., 2017). Further analysis of diverse plant genomes identified that the origin of land plants was accompanied by an unprecedented level of genomic novelty, with a second smaller burst in the ancestor of streptophytes (Bowles et al., 2020). This is in comparison to a single burst seen in the origin of animals (Paps and Holland, 2018). These patterns are reinforced based on the analysis from the one thousand plant transcriptome project, which identified gene family birth and expansion in some of the largest plant gene families in Streptophyta and land plants (Leebens-Mack et al., 2019).

These molecular innovations led to the evolution of embryogenesis in land plants, one of the defining features of embryophytes. In multicellular organisms, embryogenesis begins simply with a single cell, the zygote. This is true for both multicellular plants and animals, but the subsequent stages of development differ drastically (Radoeva et al., 2019). Comparative analysis of embryonic and post-embryonic transcriptomes in *Arabidopsis thaliana* revealed a unique transcriptomic profile coordinating embryo development which is distinct from all other tissue types (Hofmann et al., 2019). Importantly for most land plants, after embryogenesis, the mature embryo does not represent the architecture of the adult organism. The stem cells of meristems, undifferentiated plant tissue (e.g., shoots, roots), develop after embryonic development, defining different plant cell and tissue types (Radoeva et al., 2019). Since the origin of land plants, major plant groups have emerged, accompanied by the emergence of distinct plant cell types (e.g., xylem and phloem cells of vascular plants).

One of the main techniques, scRNA-seq, is used to understand animal cell types, as highlighted above, and only very recently in plants (Seyfferth et al., 2021; Otero et al., 2022; Tung et al., 2023). Recent analysis using scRNA-seq of 10,000 *A. thaliana* root cells identified all major cell and tissue types across multiple developmental stages, including the root cap, epidermis, and endodermis as well as xylem and phloem cells (Ryu et al., 2019). Application of scRNA-seq has also been used to investigate cell differentiation in the shoot apical meristem, the above-ground organ, in maize. Similar to root cells, the shoot apical meristem has distinct transcriptomic signatures, which enabled the identification of cell types including epidermal, tip, meristem, and vascular cells (Satterlee et al., 2021). Both studies aimed to track the developmental trajectory of individual cells identifying key genes involved in cellular development and differentiation (Ryu et al., 2019; Satterlee et al., 2021). Ultimately, these analyses provide insights into the processes governing cell fate specification and the identification of distinct cell types.

Much of the work aiming to understand plant cell types has been completed in model (e.g., *A. thaliana*) and crop species (e.g., *Zea mays*; Denyer and Timmermans, 2022). However, there is an important debate about how well cell and tissue development in model and crop species represents processes of more distant evolutionary groups (e.g., bryophytes, lycophytes). To address this question, gene expression atlases were developed for different tissues (e.g., shoot and root meristems, spores, seeds) of 10 species from across the land plant phylogeny. Comparative analysis across species and tissues found highly conserved developmental transcriptomes with many gene groups identified as organ specific across phylogenetic distance (Julca et al., 2021). This is in contrast to the development of some animal cell types where a large number of clade specific genes are responsible for distinct cell types (Duruz et al., 2021). The first land plants evolved new reproductive structures such as spores and embryo sacs through coordinated changes in gene expression and co-option of existing genes. It was identified that cell specific gene groups did not accompany the origin of the corresponding tissue, rather that cell specific gene expression is correlated with the age of the gene group. Based on Gene Ontology annotations, these gene groups also have biological functions relevant with their associated tissues (Julca et al., 2021). These broad patterns of changes in gene expression are familiar to animal cell type evolution (Sogabe et al., 2019; Duruz et al., 2021; Tarashansky et al., 2021).

Conclusion

The incoming wave of genome data and ever-increasing computational power, together with the development of new theoretical and analytical frameworks, will no doubt provide many surprises and new insights into the origins of animals and bilaterians. A comprehensive and representative taxon sampling will always remain central to any comparative study, including phylogenetics, comparative genomics, and cell type analyses. Integrating genome-level phylogenomic trees, comparative genomics, and the study of cell types with comparative morphology, evodevo, and palaeobiology will pose a difficult but interesting challenge. Comparing these findings with the evolution of other eukaryotic groups, plants, and fungi— will unveil the genomic forces driving major evolutionary transitions. Altogether, the near future looks like a great place to be an evolutionary biologist.

Author contributions

All authors listed have made a substantial, direct, and intellectual contribution to the work and approved it for publication.

Funding

MR is funded by NERC DTP GW4+, AB is funded by the Leverhulme Trust (RPG-2020-199 “iDAPT”), and MÁ-P and JP are supported by the Wellcome Trust (210101/Z/18/Z) and the School of Biological Sciences (University of Bristol).

Acknowledgments

The authors would like to thank Davide Pisani (University of Bristol) and the two reviewers (PM and JM-D) for their feedback on this manuscript.

Conflict of interest

The authors declare that the research was conducted in the absence of any commercial or financial relationships that could be construed as a potential conflict of interest.

Publisher’s note

References

Aguinaldo, A. M., Turbeville, J. M., Linford, L. S., Rivera, M. C., Garey, J. R., Raff, R. A., et al. (1997). Evidence for a clade of nematodes, arthropods and other moulting animals. *Nature* 387, 489–493. doi: 10.1038/387489a0

Albalat, R., and Cañestro, C. (2016). Evolution by gene loss. *Nat. Rev. Genet.* 17, 379–391. doi: 10.1038/nrg.2016.39

Arendt, D. (2008). The evolution of cell types in animals: emerging principles from molecular studies. *Nat. Rev. Genet.* 9, 868–882. doi: 10.1038/nrg2416

Arendt, D., Musser, J. M., Baker, C. V. H., Bergman, A., Cepko, C., Erwin, D. H., et al. (2016). The origin and evolution of cell types. *Nat. Rev. Genet.* 17, 744–757. doi: 10.1038/nrg.2016.127

Arroyo, A. S., López-Escardó, D., de Vargas, C., and Ruiz-Trillo, I. (2016). Hidden diversity of Acoelomorpha revealed through metabarcoding. *Biol. Lett.* 12:20160674. doi: 10.1098/rsbl.2016.0674

Baguñà, J., and Riutort, M. (2004). The dawn of bilaterian animals: the case of acoelomorph flatworms. *BioEssays* 26, 1046–1057. doi: 10.1002/bies.20113

Baguñà, J., Ruiz-Trillo, I., Paps, J., Loukota, M., Ribera, C., Baguna, J., et al. (2001). The first bilaterian organisms: simple or complex? New molecular evidence. *Int. J. Dev. Biol.* 45, 133–134. doi: 10.1387/ijdb.01450133

Bergsten, J. (2005). A review of long-branch attraction. *Cladistics* 21, 163–193. doi: 10.1111/j.1096-0031.2005.00059.x

Bowles, A. M. C., Bechtold, U., and Paps, J. (2020). The origin of land plants is rooted in two bursts of genomic novelty. *Curr. Biol.* 30, 530–536.e2. doi: 10.1016/j.cub.2019.11.090

Bowles, A. M. C., Williamson, C. J., Williams, T. A., Lenton, T. M., and Donoghue, P. C. J. (2022). The origin and early evolution of plants. *Trends Plant Sci.* 28, 312–329. doi: 10.1016/j.tplants.2022.09.009

Bowman, J. L., Kohchi, T., Yamato, K. T., Jenkins, J., Shu, S., Ishizaki, K., et al. (2017). Insights into land plant evolution garnered from the *Marchantia polymorpha* genome. *Cells* 171, 287–304. doi: 10.1016/j.cell.2017.09.030

Bracken-Grissom, H., Collins, A. G., Collins, T., Crandall, K., Distel, D., Dunn, C., et al. (2014). The global invertebrate genomics Alliance (GIGA): developing community resources to study diverse invertebrate genomes. *J. Hered.* 105, 1–18. doi: 10.1093/jhered/est084

Brinkmann, H., Copley, R. R., Moroz, L. L., Nakano, H., Poustka, A. J., Wallberg, A., et al. (2011). Acoelomorph flatworms are deuterostomes related to Xenoturbella. *Nature* 470, 255–258. doi: 10.1038/nature09676

Brunet, T., and King, N. (2017). The origin of animal multicellularity and cell differentiation. *Dev. Cell* 43, 124–140. doi: 10.1016/j.devcel.2017.09.016

Buchfink, B., Reuter, K., and Drost, H. G. (2021). Sensitive protein alignments at tree-of-life scale using DIAMOND. *Nat. Methods* 18, 366–368. doi: 10.1038/s41592-021-01101-x

Cannon, J. T., Vellutini, B. C., Smith, J., Ronquist, F., Jondelius, U., and Hejnol, A. (2016). XAN is the sister group to Nephrozoa. *Nature* 530, 89–93. doi: 10.1038/nature16520

Catarino, B., Hetherington, A. J., Emms, D. M., Kelly, S., and Dolan, L. (2016). The stepwise increase in the number of transcription factor families in the Precambrian predated the diversification of plants on land. *Mol. Biol. Evol.* 33, 2815–2819. doi: 10.1093/molbev/msw155

Cheng, S., Xian, W., Fu, Y., Marin, B., Keller, J., Wu, T., et al. (2019). Genomes of subaerial Zygnematophyceae provide insights into land plant evolution. *Cells* 179, 1057–1067. doi: 10.1016/j.cell.2019.10.019

Christianson, L. M., Johnson, S. B., Schultz, D. T., and Haddock, S. H. D. (2022). Hidden diversity of Ctenophora revealed by new mitochondrial COI primers and sequences. *Mol. Ecol. Resour.* 22:283. doi: 10.1111/1755-0998.13459

de Vries, J., and Archibald, J. M. (2018). Plant evolution: landmarks on the path to terrestrial life. *New Phytol.* 217, 1428–1434. doi: 10.1111/nph.14975

de Vries, J., Curtis, B. A., Gould, S. B., and Archibald, J. M. (2018). Embryophyte stress signaling evolved in the algal progenitors of land plants. *Proc. Natl. Acad. Sci. U. S. A.* 115, 3471–3480. doi: 10.1073/pnas.1719230115

Delaux, P. M., Radhakrishnan, G. V., Jayaraman, D., Cheema, J., Malbreil, M., Volkening, J. D., et al. (2015). Algal ancestor of land plants was preadapted for symbiosis. *Proc. Natl. Acad. Sci. U. S. A.* 112, 13390–13395. doi: 10.1073/pnas.1515426112

Delsuc, F., Brinkmann, H., and Philippe, H. (2005). Phylogenomics and the reconstruction of the tree of life. *Nat. Rev. Genet.* 6, 361–375. doi: 10.1038/nrg1603

Denyer, T., and Timmermans, M. C. P. (2022). Crafting a blueprint for single-cell RNA sequencing. *Trends Plant Sci.* 27, 92–103. doi: 10.1016/j.tplants.2021.08.016

Dunn, C. W., Giribet, G., Edgecombe, G. D., and Hejnol, A. (2014). Animal phylogeny and its evolutionary implications. *Annu. Rev. Ecol. Evol. Syst.* 45, 371–395. doi: 10.1146/annurev-ecolsys-120213-091627

Dunn, C. W., Hejnol, A., Matus, D. Q., Pang, K., Browne, W. E., Smith, S. A., et al. (2008). Broad phylogenomic sampling improves resolution of the animal tree of life. *Nature* 452, 745–749. doi: 10.1038/nature06614

Dunn, C. W., and Ryan, J. F. (2015). The evolution of animal genomes. *Curr. Opin. Genet. Dev.* 35, 25–32. doi: 10.1016/j.gde.2015.08.006

Duruz, J., Kaltenrieder, C., Ladurner, P., Bruggmann, R., Martìnez, P., and Sprecher, S. G. (2021). Acoel Single-Cell Transcriptomics: cell type analysis of a deep branching Bilaterian. *Mol. Biol. Evol.* 38, 1888–1904. doi: 10.1093/molbev/msaa333

Edgecombe, G. D., Giribet, G., Dunn, C. W., Hejnol, A., Kristensen, R. M., Neves, R. C., et al. (2011). Higher-level metazoan relationships: recent progress and remaining questions. *Org. Divers. Evol.* 11, 151–172. doi: 10.1007/s13127-011-0044-4

Egger, B., Lapraz, F., Tomiczek, B., Müller, S., Dessimoz, C., Girstmair, J., et al. (2015). A transcriptomic-phylogenomic analysis of the evolutionary relationships of flatworms. *Curr. Biol.* 25, 1347–1353. doi: 10.1016/j.cub.2015.03.034

Emms, D. M., and Kelly, S. (2019). OrthoFinder: phylogenetic orthology inference for comparative genomics. *Genome Biol.* 20:238. doi: 10.1186/s13059-019-1832-y

Felsenstein, J. (1978). Cases in which parsimony or compatibility methods will be positively misleading. *Syst. Biol.* 27, 401–410. doi: 10.1093/sysbio/27.4.401

Fernández, R., and Gabaldón, T. (2020). Gene gain and loss across the metazoan tree of life. *Nat. Ecol. Evol.* 4, 524–533. doi: 10.1038/s41559-019-1069-x

Feuda, R., Dohrmann, M., Pett, W., Philippe, H., Rota-Stabelli, O., Lartillot, N., et al. (2017). Improved modeling of compositional heterogeneity supports sponges as sister to all other animals. *Curr. Biol.* 27, 3864–3870.e4. doi: 10.1016/j.cub.2017.11.008

Fiers, M. W. E. J., Minnoye, L., Aibar, S., Bravo González-Blas, C., Kalender Atak, Z., and Aerts, S. (2018). Mapping gene regulatory networks from single-cell omics data. *Brief. Funct. Genomics* 17, 246–254. doi: 10.1093/bfgp/elx046

Giacomelli, M., Rossi, M. E., Lozano-Fernandez, J., Feuda, R., and Pisani, D. (2022). Resolving tricky nodes in the tree of life through amino acid recoding. *iScience* 25:105594. doi: 10.1016/j.isci.2022.105594

Giribet, G. (2016). New animal phylogeny: future challenges for animal phylogeny in the age of phylogenomics. *Org. Divers. Evol.* 16, 419–426. doi: 10.1007/s13127-015-0236-4

Giribet, G., and Edgecombe, G. D. (2019). "Perspectives in animal phylogeny and evolution: a decade late" in *Perspectives on evolutionary and developmental biology essays for Alessandro Minelli*. ed. G. Fusco (Padova (Italy): Padova University Press), 167–178.

Grau-Bové, X., and Sebé-Pedrós, A. (2021). Orthology clusters from gene trees with Possvm. *Mol. Biol. Evol.* 38, 5204–5208. doi: 10.1101/2021.05.03.442399

Guijarro-Clarke, C., Holland, P. W. H., and Paps, J. (2020). Widespread patterns of gene loss in the evolution of the animal kingdom. *Nat. Ecol. Evol.* 4, 519–523. doi: 10.1038/s41559-020-1129-2

Harris, B. J., Harrison, C. J., Hetherington, A. M., and Williams, T. A. (2020). Phylogenomic evidence for the Monophyly of bryophytes and the reductive evolution of stomata. *Curr. Biol.* 30, 2001–2012. doi: 10.1016/j.cub.2020.03.048

Harrison, C. J. (2017). Development and genetics in the evolution of land plant body plans. *Philos. Trans. R. Soc. B Biol. Sci.* 372:e2015.0490. doi: 10.1098/rstb.2015.0490

Hejnol, A. (@Hejnol_Lab) (2016). No "undetected systematic bias" in Chang et al detected so far (for ctenosis). Tweet. Available at: https://twitter.com/Hejnol_Lab/status/697740643209232384 (Accessed May 23, 2023).

Hejnol, A., Obst, M., Stamatakis, A., Ott, M., Rouse, G. W., Edgecombe, G. D., et al. (2009). Assessing the root of bilaterian animals with scalable phylogenomic methods. *Proc. R. Soc. B Biol. Sci.* 276, 4261–4270. doi: 10.1098/rspb.2009.0896

Hejnol, A., and Pang, K. (2016). XAN's significance for understanding bilaterian evolution. *Curr. Opin. Genet. Dev.* 39, 48–54. doi: 10.1016/j.gde.2016.05.019

Hernandez, A. M., and Ryan, J. F. (2021). Six-state amino acid recoding is not an effective strategy to offset compositional heterogeneity and saturation in phylogenetic analyses. *Syst. Biol.* 70, 1–34. doi: 10.1093/sysbio/syab027

Hess, S., Williams, S. K., Busch, A., Irisarri, I., Delwiche, C. F., Vries, S.De, et al. (2022). A phylogenomically informed five-order system for the closest relatives of land plants. *Curr. Biol.* 32, 4473–4482. doi: 10.1016/j.cub.2022.08.022

Hofmann, F., Schon, M. A., and Nodine, M. D. (2019). The embryonic transcriptome of *Arabidopsis thaliana*. *Plant Reprod.* 32, 77–91. doi: 10.1007/s00497-018-00357-2

Hori, K., Maruyama, F., Fujisawa, T., Togashi, T., Yamamoto, N., Seo, M., et al. (2014). *Klebsormidium flaccidum* genome reveals primary factors for plant terrestrial adaptation. *Nat. Commun.* 5:3978. doi: 10.1038/ncomms4978

Jékely, G., Paps, J., and Nielsen, C. (2015). The phylogenetic position of ctenophores and the origin(s) of nervous systems. *EvoDevo* 6:1. doi: 10.1186/2041-9139-6-1

Jiao, C., Sørensen, I., Sun, X., Sun, H., Behar, H., Alseekh, S., et al. (2020). The *Penium margaritaceum* genome: hallmarks of the origins of land plants. *Cells* 181, 1097–1111. doi: 10.1016/j.cell.2020.04.019

Julca, I., Flores, M., Proost, S., Lindner, A.-C., Hackenberg, D., Steinbachova, L., et al. (2021). Comparative transcriptomic analysis reveals conserved transcriptional programs underpinning organogenesis and reproduction in land plants. *Nat. Plants* 7, 1143–1159. doi: 10.1038/s41477-021-00958-2

Juravel, K., Porras, L., Höhna, S., Pisani, D., and Wörheide, G. (2022). Exploring genome gene content and morphological analysis to test recalcitrant nodes in the animal phylogeny. *bioRxiv*:2021.11.19.469253. doi: 10.1101/2021.11.19.469253

Kapli, P., Flouri, T., and Telford, M. J. (2021a). Systematic errors in phylogenetic trees. *Curr. Biol.* 31, R59–R64. doi: 10.1016/J.CUB.2020.11.043

Kapli, P., Natsidis, P., Leite, D. J., Fursman, M., Jeffrie, N., Rahman, I. A., et al. (2021b). Lack of support for Deuterostomia prompts reinterpretation of the first Bilateria. *Sci. Adv.* 7:eabe2741. doi: 10.1126/SCIADV.ABE2741/SUPPL_FILE/ABE2741_SM.PDF

Kapli, P., and Telford, M. J. (2020). Topology-dependent asymmetry in systematic errors affects phylogenetic placement of Ctenophora and XAN. *Sci. Adv.* 6, 5162–5173. doi: 10.1126/SCIADV.ABC5162/SUPPL_FILE/ABC5162_SM.PDF

Kenny, N. J., Francis, W. R., Rivera-Vicéns, R. E., Juravel, K., de Mendoza, A., Díez-Vives, C., et al. (2020). Tracing animal genomic evolution with the chromosomal-level assembly of the freshwater sponge *Ephydatia muelleri*. *Nat. Commun.* 11, 1–11. doi: 10.1038/s41467-020-17397-w

Kin, K., Nnamani, M. C., Lynch, V. J., Michaelides, E., and Wagner, G. P. (2015). Cell-type phylogenetics and the origin of endometrial stromal cells. *Cell Rep.* 10, 1398–1409. doi: 10.1016/j.celrep.2015.01.062

Kocot, K. M., Cannon, J. T., Todt, C., Citarella, M. R., Kohn, A. B., Meyer, A., et al. (2011). Phylogenomics reveals deep molluscan relationships. *Nature* 477, 452–456.

Lankester, E. R. (1880). "*Degeneration: A chapter in Darwinism*," in (London: Macmillan and Co

Lartillot Brinkmann, H., Philippe, H., Lartillot, N., Brinkmann, H., and Philippe, H. (2007). Suppression of long-branch attraction artefacts in the animal phylogeny using a site-heterogeneous model. *BMC Evol. Biol.* 7:S4. doi: 10.1186/1471-2148-7-S1-S4

Lartillot, N., and Philippe, H. H. (2004). A Bayesian mixture model for across-site heterogeneities in the amino-acid replacement process. *Mol. Biol. Evol.* 21, 1095–1109. doi: 10.1093/molbev/msh112

Laumer, C. E., Fernández, R., Lemer, S., Combosch, D., Kocot, K. M., Riesgo, A., et al. (2019). Revisiting metazoan phylogeny with genomic sampling of all phyla. *Proc. R. Soc. B Biol. Sci.* 286:20190831. doi: 10.1098/rspb.2019.0831

Laumer, C. E., and Giribet, G. (2014). Inclusive taxon sampling suggests a single, stepwise origin of ectolecithality in Platyhelminthes. *Biol. J. Linn. Soc.* 111, 570–588. doi: 10.1111/bij.12236

Laumer, C. E., Hejnol, A., Giribet, G., Appeltans, W., Ahyong, S. T., Anderson, G., et al. (2015). Nuclear genomic signals of the "microturbellarian" roots of platyhelminth evolutionary innovation. *elife* 4, 2189–2202. doi: 10.7554/eLife.05503

Leebens-Mack, J. H., Barker, M. S., Carpenter, E. J., Deyholos, M. K., Gitzendanner, M. A., Graham, S. W., et al. (2019). One thousand plant transcriptomes and the phylogenomics of green plants. *Nature* 574, 679–685. doi: 10.1038/s41586-019-1693-2

Li, Y., Shen, X. X., Evans, B., Dunn, C. W., and Rokas, A. (2021). Rooting the animal tree of life. *Mol. Biol. Evol.* 38, 4322–4333. doi: 10.1093/molbev/msab170

Mah, J. L., Christensen-Dalsgaard, K. K., and Leys, S. P. (2014). Choanoflagellate and choanocyte collar-flagellar systems and the assumption of homology. *Evol. Dev.* 16, 25–37. doi: 10.1111/ede.12060

Marlétaz, F. (2019). Zoology: worming into the origin of Bilaterians. *Curr. Biol.* 29, R577–R579. doi: 10.1016/j.cub.2019.05.006

Marlétaz, F., Peijnenburg, K. T. C. A., Goto, T., Satoh, N., and Rokhsar, D. S. (2019). A new Spiralian phylogeny places the enigmatic arrow Worms among Gnathiferans. *Curr. Biol.* 29, 312–318.e3. doi: 10.1016/j.cub.2018.11.042

Martinez, P., Ustyantsev, K., Biryukov, M., Mouton, S., Glasenburg, L., Sprecher, S. G., et al. (2022). Genome assembly of the acoel flatworm *Symsagittifera roscoffensis*, a model for research on body plan evolution and photosymbiosis. *G3: Genes Genomes Genet.* 13. doi: 10.1093/G3JOURNAL/JKAC336

McCarthy, C. G. P., Mulhair, P. O., Siu-Ting, K., Creevey, C. J., and O'Connell, M. J. (2023). Improving orthologous signal and model fit in datasets addressing the root of the animal phylogeny. *Mol. Biol. Evol.* 40, 1–16. doi: 10.1093/molbev/msac276

Miller, J. B., Pickett, B. D., and Ridge, P. G. (2019). JustOrthologs: a fast, accurate and user-friendly ortholog identification algorithm. *Bioinformatics* 35, 546–552. doi: 10.1093/bioinformatics/bty669

Misof, B., Liu, S., Meusemann, K., Peters, R. S., Donath, A., Mayer, C., et al. (2014). Phylogenomics resolves the timing and pattern of insect evolution. *Science* 1979, 763–767. doi: 10.1126/SCIENCE.1257570/SUPPL_FILE/1257570S9.XLS

Moroz, L. L., Kocot, K. M., Citarella, M. R., Dosung, S., Norekian, T. P., Povolotskaya, I. S., et al. (2014). The ctenophore genome and the evolutionary origins of neural systems. *Nature* 510, 109–114. doi: 10.1038/nature13400

Moroz, L. L., and Kohn, A. B. (2016). Independent origins of neurons and synapses: insights from ctenophores. *Philos. Trans. R. Soc. Lond. Ser. B Biol. Sci.* 371:20150041. doi: 10.1098/rstb.2015.0041

Morris, J. L., Puttick, M. N., Clark, J. W., Edwards, D., Kenrick, P., Pressel, S., et al. (2018). The timescale of early land plant evolution. *Proc. Natl. Acad. Sci.* 115, 2274–2283. doi: 10.1073/pnas.1719588115

Mulhair, P. O., McCarthy, C. G. P., Siu-Ting, K., Creevey, C. J., and O'Connell, M. J. (2022). Filtering artifactual signal increases support for XAN and Ambulacraria sister relationship in the animal tree of life. *Curr. Biol.* 32, 5180–5188.e3. doi: 10.1016/j.cub.2022.10.036

Nakatani, Y., and McLysaght, A. (2017). Genomes as documents of evolutionary history: a probabilistic macrosynteny model for the reconstruction of ancestral genomes. *Bioinformatics* 33, i369–i378. doi: 10.1093/BIOINFORMATICS/BTX259

Nakatani, Y., Shingate, P., Ravi, V., Pillai, N. E., Prasad, A., McLysaght, A., et al. (2021). Reconstruction of proto-vertebrate, proto-cyclostome and proto-gnathostome genomes provides new insights into early vertebrate evolution. *Nat. Commun.* 12, 1–14. doi: 10.1038/s41467-021-24573-z

Natsidis, P., Kapli, P., Schiffer, P. H., and Telford, M. J. (2021). Systematic errors in orthology inference and their effects on evolutionary analyses. *iScience* 24:102110. doi: 10.1016/j.isci.2021.102110

Nishiyama, T., Sakayama, H., de Vries, J., Buschmann, H., Saint-Marcoux, D., Ullrich, K. K., et al. (2018). The Chara genome: secondary complexity and implications for plant Terrestrialization. *Cells* 174, 448–464. doi: 10.1016/j.cell.2018.06.033

Nosenko, T., Schreiber, F., Adamska, M., Adamski, M., Eitel, M., Hammel, J., et al. (2013). Deep metazoan phylogeny: When different genes tell different stories. *Mol. Phylogenet. Evol.* 67, 223–233. doi: 10.1016/j.ympev.2013.01.010

Otero, S., Gildea, I., Roszak, P., Lu, Y., Vittori, V.Di, Bourdon, M., et al. (2022). A root phloem pole cell atlas reveals common transcriptional states in protophloem-adjacent cells. *Nat. Plants* 8, 954–970, doi: 10.1038/s41477-022-01178-y

Ou, Q., Xiao, S., Han, J., Sun, G., Zhang, F., Zhang, Z., et al. (2015). A vanished history of skeletonization in Cambrian comb jellies. *Sci. Adv.* 1, 1–9. doi: 10.1126/sciadv.1500092

Paps, J. (2018). What makes an animal? The molecular quest for the origin of the animal kingdom. *Integr. Comp. Biol.* 58, 654–665. doi: 10.1093/icb/icy036

Paps, J., Baguñà, J., and Riutort, M. (2009a). Bilaterian phylogeny: a broad sampling of 13 nuclear genes provides a new Lophotrochozoa phylogeny and supports a paraphyletic basal acoelomorpha. *Mol. Biol. Evol.* 26, 2397–2406. doi: 10.1093/molbev/msp150

Paps, J., Baguñà, J., Riutort, M., and Baguñà, J. (2009b). Lophotrochozoa internal phylogeny: new insights from an up-to-date analysis of nuclear ribosomal genes. *Proc. R. Soc. B Biol. Sci.* 276, 1245–1254. doi: 10.1098/rspb.2008.1574

Paps, J., and Holland, P. W. H. (2018). Reconstruction of the ancestral metazoan genome reveals an increase in genomic novelty. *Nat. Commun.* 9:1730. doi: 10.1038/s41467-018-04136-5

Paps, J., Ruiz-Trillo, I., and de Barcelona, U. (2010). "Animals and their unicellular ancestors" in *Encyclopedia of Life Sciences* (Chichester: John Wiley & Sons Ltd), 1–8.

Parfrey, L. W., and Lahr, D. J. G. (2013). Multicellularity arose several times in the evolution of eukaryotes. *BioEssays* 35, 339–347. doi: 10.1002/bies.201200143

Pett, W., Adamski, M., Adamska, M., Francis, W. R., Eitel, M., Pisani, D., et al. (2019). The role of homology and orthology in the phylogenomic analysis of metazoan gene content. *Mol. Biol. Evol.* 36, 643–649. doi: 10.1093/molbev/msz013

Philippe, H. H., Derelle, R., Lopez, P., Pick, K., Borchiellini, C., Boury-Esnault, N., et al. (2009). Phylogenomics revives traditional views on deep animal relationships. *Curr. Biol.* 19, 706–712. doi: 10.1016/j.cub.2009.02.052

Philippe, H. H., Lartillot, N., and Brinkmann, H. (2005). Multigene analyses of Bilaterian animals corroborate the Monophyly of Ecdysozoa, Lophotrochozoa, and Protostomia. *Mol. Biol. Evol.* 22, 1246–1253. doi: 10.1093/molbev/msi111

Philippe, H., Poustka, A. J., Chiodin, M., Hoff, K. J., Dessimoz, C., Tomiczek, B., et al. (2019). Mitigating anticipated effects of systematic errors supports sister-group relationship between XAN and Ambulacraria. *Curr. Biol.* 29, 1818–1826.e6. doi: 10.1016/j.cub.2019.04.009

Pick, K. S., Philippe, H., Schreiber, F., Erpenbeck, D., Jackson, D. J., Wrede, P., et al. (2010). Improved phylogenomic taxon sampling noticeably affects non-bilaterian relationships. *Mol. Biol. Evol.* 27, 1983–1987. doi: 10.1093/molbev/msq089

Pisani, D., Pett, W., Dohrmann, M., Feuda, R., Rota-Stabelli, O., Philippe, H., et al. (2015). Genomic data do not support comb jellies as the sister group to all other animals. *Proc. Natl. Acad. Sci. U. S. A.* 112, 15402–15407. doi: 10.1073/pnas.1518127112

Pisani, D., Rossi, M. E., Marlétaz, F., and Feuda, R. (2022). Phylogenomics: is less more when using large-scale datasets? *Curr. Biol.* 32, R1340–R1342. doi: 10.1016/J.CUB.2022.11.019

Podar, M., Haddock, S. H., Sogin, M. L., and Harbison, G. R. (2001). A molecular phylogenetic framework for the phylum Ctenophora using 18S rRNA genes. *Mol. Phylogenet. Evol.* 21, 218–230. doi: 10.1006/mpev.2001.1036

Posada, D. (2020). CellCoal: coalescent simulation of single-cell sequencing samples. *Mol. Biol. Evol.* 37, 1535–1542. doi: 10.1093/molbev/msaa025

Radoeva, T., Vaddepalli, P., Zhang, Z., and Weijers, D. (2019). Evolution, initiation, and diversity in early plant embryogenesis. *Dev. Cell* 50, 533–543. doi: 10.1016/j.devcel.2019.07.011

Redmond, A. K., and McLysaght, A. (2021). Evidence for sponges as sister to all other animals from partitioned phylogenomics with mixture models and recoding. *Nat. Commun.* 12, 1–14. doi: 10.1038/s41467-021-22074-7

Richter, D. J., Fozouni, P., Eisen, M. B., and King, N. (2018). Gene family innovation, conservation and loss on the animal stem lineage. *elife* 7:e34226. doi: 10.7554/eLife.34226

Rokas, A., and Holland, P. W. H. (2000). Rare genomic changes as a tool for phylogenetics. *Trends Ecol. Evol.* 15, 454–459. doi: 10.1016/S0169-5347(00)01967-4

Rota-Stabelli, O., Campbell, L., Brinkmann, H., Edgecombe, G. D., Longhorn, S. J., Peterson, K. J., et al. (2011). A congruent solution to arthropod phylogeny: phylogenomics, microRNAs and morphology support monophyletic Mandibulata. *Proc. R. Soc. B Biol. Sci.* 278, 298–306. doi: 10.1098/rspb.2010.0590

Rouse, G. W., Wilson, N. G., Carvajal, J. I., and Vrijenhoek, R. C. (2016). New deep-sea species of Xenoturbella and the position of XAN. *Nature* 530, 94–97. doi: 10.1038/nature16545

Ruiz-Trillo, I., and Paps, J. (2016). Acoelomorpha: earliest branching bilaterians or deuterostomes? *Org. Divers. Evol.* 16, 391–399. doi: 10.1007/s13127-015-0239-1

Ruiz-Trillo, I., Paps, J., Loukota, M., Ribera, C., Jondelius, U., Baguna, J., et al. (2002). A phylogenetic analysis of myosin heavy chain type II sequences corroborates that Acoela and Nemertodermatida are basal bilaterians. *Proc. Natl. Acad. Sci. U. S. A.* 99, 11246–11251. doi: 10.1073/pnas.172390199

Ruiz-Trillo, I., Riutort, M., Littlewood, D. T., Herniou, E. A., Baguña, J., and And Baguna, J. (1999). Acoel flatworms: earliest extant bilaterian metazoans, not members of Platyhelminthes. *Science* 1979, 1919–1923.

Ryan, J. F., Pang, K., Schnitzler, C. E., Nguyen, A.-D., Moreland, R. T., Simmons, D. K., et al. (2013). The genome of the ctenophore Mnemiopsis leidyi and its implications for cell type evolution. *Science* 342:1242592. doi: 10.1126/science.1242592

Ryu, K. H., Huang, L., Kang, H. M., and Schiefelbein, J. (2019). Single-cell RNA sequencing resolves molecular relationships among individual plant cells. *Plant Physiol.* 179, 1444–1456. doi: 10.1104/pp.18.01482

Satterlee, J. W., Strable, J., and Scanlon, M. J. (2021). Plant stem-cell organization and differentiation at single-cell resolution. *Proc. Natl. Acad. Sci. U. S. A.* 117, 33689–33699. doi: 10.1073/PNAS.2018788117

Schiffer, P. H., Natsidis, P., Leite, D. J., Robertson, H. E., Lapraz, F., Marlétaz, F., et al. (2022). The slow evolving genome of the xenacoelomorph worm *Xenoturbella bocki*. *bioRxiv*:2022.06.24.497508. doi: 10.1101/2022.06.24.497508

Sebé-Pedrós, A., Chomsky, E., Pang, K., Lara-Astiaso, D., Gaiti, F., Mukamel, Z., et al. (2018). Early metazoan cell type diversity and the evolution of multicellular gene regulation. *Nat. Ecol. Evol.* 2, 1176–1188. doi: 10.1038/s41559-018-0575-6

Sebé-Pedrós, A., Degnan, B. M., and Ruiz-Trillo, I. (2017). The origin of Metazoa: a unicellular perspective. *Nat. Rev. Genet.* 18, 498–512. doi: 10.1038/nrg.2017.21

Seyfferth, C., Renema, J., Wendrich, J. R., Eekhout, T., Seurinck, R., Vandamme, N., et al. (2021). Advances and opportunities in single-cell transcriptomics for plant research. *Annu. Rev. Plant Biol.* 72, 847–866. doi: 10.1146/annurev-arplant-081720-010120

Simakov, O., Bredeson, J., Berkoff, K., Marletaz, F., Mitros, T., Schultz, D. T., et al. (2022). Deeply conserved synteny and the evolution of metazoan chromosomes. *Sci. Adv.* 8:5884. doi: 10.1126/SCIADV.ABI5884/SUPPL_FILE/SCIADV.ABI5884_DATA_FILES_S1_TO_S5.ZIP

Simakov, O., Marlétaz, F., Yue, J. X., O'Connell, B., Jenkins, J., Brandt, A., et al. (2020). Deeply conserved synteny resolves early events in vertebrate evolution. *Nat. Ecol. Evol.* 4, 820–830. doi: 10.1038/s41559-020-1156-z

Simion, P., Philippe, H., Baurain, D., Jager, M., Richter, D. J., Di Franco, A., et al. (2017). A large and consistent phylogenomic dataset supports sponges as the sister group to all other animals. *Curr. Biol.* 27, 958–967. doi: 10.1016/j.cub.2017.02.031

Smith, S. A., Wilson, N. G., Goetz, F. E., Feehery, C., Andrade, S. C. S., Rouse, G. W., et al. (2011). Resolving the evolutionary relationships of molluscs with phylogenomic tools. *Nature* 480, 364–367. doi: 10.1038/nature10526

Sogabe, S., Hatleberg, W. L., Kocot, K. M., Say, T. E., Stoupin, D., Roper, K. E., et al. (2019). Pluripotency and the origin of animal multicellularity. *Nature* 570, 519–522. doi: 10.1038/s41586-019-1290-4

Struck, T. H., Paul, C., Hill, N., Hartmann, S., Hösel, C., Kube, M., et al. (2011). Phylogenomic analyses unravel annelid evolution. *Nature* 471, 95–98. doi: 10.1038/nature09864

Szathmáry, E., and Smith, J. M. (1995). The major evolutionary transitions. *Nature* 374, 227–232. doi: 10.1038/374227a0

Tanay, A., and Sebé-Pedrós, A. (2021). Evolutionary cell type mapping with single-cell genomics. *Trends Genet.* 37, 919–932. doi: 10.1016/j.tig.2021.04.008

Tarashansky, A. J., Musser, J. M., Khariton, M., Li, P., Arendt, D., Quake, S. R., et al. (2021). Mapping single-cell atlases throughout metazoa unravels cell type evolution. *elife* 10:e66747. doi: 10.7554/eLife.66747

Telford, M. J., Budd, G. E., and Philippe, H. (2015). Phylogenomic insights into animal evolution. *Curr. Biol.* 25, 876–887. doi: 10.1016/j.cub.2015.07.060

Telford, M. J., and Copley, R. R. (2016). Zoology: war of the worms. *Curr. Biol.* 26, R335–R337. doi: 10.1016/j.cub.2016.03.015

Tung, C.-C., Kuo, S.-C., Yang, C.-L., Yu, J.-H., Huang, C.-E., Liou, P.-C., et al. (2023). Single-cell transcriptomics unveils xylem cell development and evolution. *Genome Biol. Evol.* 24. doi: 10.1186/s13059-022-02845-1

Umen, J. G. (2014). Green algae and the origins of multicellularity in the plant kingdom. *Cold Spring Harb. Perspect. Biol.* 6:a016170. doi: 10.1101/cshperspect.a016170

Wang, J., Sun, H., Jiang, M., Li, J., Zhang, P., Chen, H., et al. (2021). Tracing cell-type evolution by cross-species comparison of cell atlases. *Cell Rep.* 34:108803. doi: 10.1016/j.celrep.2021.108803

Weisman, C. M., Murray, A. W., and Eddy, S. R. (2020). Many, but not all, lineage-specific genes can be explained by homology detection failure. *PLoS Biol.* 18:e3000862. doi: 10.1371/journal.pbio.3000862

Wellcome Sanger Institute (2020). Darwin tree of life. Available at: https://www.darwintreeoflife.org/

Whelan, N. V., and Halanych, K. M. (2017). Who let the CAT out of the bag? Accurately dealing with substitutional heterogeneity in Phylogenomic analyses. *Syst. Biol.* 66, 232–255. doi: 10.1093/sysbio/syw084

Whelan, N. V., Kocot, K. M., Moroz, T. P., Mukherjee, K., Williams, P., Paulay, G., et al. (2017). Ctenophore relationships and their placement as the sister group to all other animals. *Nat. Ecol. Evol.* 1, 1737–1746. doi: 10.1038/s41559-017-0331-3

Wickett, N. J., Mirarab, S., Nguyen, N., Warnow, T., Carpenter, E., Matasci, N., et al. (2014). Phylotranscriptomic analysis of the origin and early diversification of land plants. *Proc. Natl. Acad. Sci.* 111, 4859–4868. doi: 10.1073/pnas.1323926111

Zhao, Y., Vinther, J., Parry, L. A., Wei, F., Green, E., Pisani, D., et al. (2019). Cambrian sessile, suspension feeding stem-group ctenophores and evolution of the comb jelly body plan. *Curr. Biol.* 29, 1112–1125.e2. doi: 10.1016/j.cub.2019.02.036

Zou, J., Huss, M., Abid, A., Mohammadi, P., Torkamani, A., and Telenti, A. (2018). A primer on deep learning in genomics. *Nat. Genet.* 51, 12–18. doi: 10.1038/s41588-018-0295-5

frontiers | Frontiers in Cell and Developmental Biology

TYPE Original Research
PUBLISHED 07 March 2023
DOI 10.3389/fcell.2023.1113046

OPEN ACCESS

EDITED BY
Pedro Martinez,
University of Barcelona, Spain

REVIEWED BY
Stephane Boissinot,
New York University Abu Dhabi, United Arab Emirates
Kirill Ustyantsev,
University Medical Center Groningen, Netherlands
Manuel Fernández Moreno,
Center for Genomic Regulation (CRG), Spain

*CORRESPONDENCE
Leonid L. Moroz,
moroz@whitney.ufl.edu
Krishanu Mukherjee,
krishanu@ufl.edu

SPECIALTY SECTION
This article was submitted to Evolutionary Developmental Biology, a section of the journal Frontiers in Cell and Developmental Biology

RECEIVED 01 December 2022
ACCEPTED 09 February 2023
PUBLISHED 07 March 2023

CITATION
Mukherjee K and Moroz LL (2023), Transposon-derived transcription factors across metazoans.
Front. Cell Dev. Biol. 11:1113046.
doi: 10.3389/fcell.2023.1113046

Transposon-derived transcription factors across metazoans

Krishanu Mukherjee[1]* and Leonid L. Moroz[1,2]*

[1]Whitney Laboratory for Marine Biosciences, University of Florida, St. Augustine, FL, United States, [2]Departments of Neuroscience and McKnight Brain Institute, University of Florida, Gainesville, FL, United States

Transposable elements (TE) could serve as sources of new transcription factors (TFs) in plants and some other model species, but such evidence is lacking for most animal lineages. Here, we discovered multiple independent co-options of TEs to generate 788 TFs across Metazoa, including all early-branching animal lineages. Six of ten superfamilies of DNA transposon-derived conserved TF families (ZBED, CENPB, FHY3, HTH-Psq, THAP, and FLYWCH) were identified across nine phyla encompassing the entire metazoan phylogeny. The most extensive convergent domestication of potentially TE-derived TFs occurred in the hydroid polyps, polychaete worms, cephalopods, oysters, and sea slugs. Phylogenetic reconstructions showed species-specific clustering and lineage-specific expansion; none of the identified TE-derived TFs revealed homologs in their closest neighbors. Together, our study established a framework for categorizing TE-derived TFs and informing the origins of novel genes across phyla.

KEYWORDS

placozoa, ctenophora, porifera, cnidaria, mollusca, convergent domestication, transcription factors, class II DNA transposons

1 Introduction

Transposable elements (TEs) or transposons identified by Barbara McClintock during the 1940-the 50s are now recognized as pivotal regulatory elements (Biemont and Vieira, 2006) controlling roughly 25% of the human genes (Jordan et al., 2003). TEs are also major constituents of all eukaryotic genomes, frequently occupying from 20% to more than 70% of genomes. The inherent ability of TEs to self-replicate, move and mutate transformed the initial assessment of TEs as "selfish gene" parasites and "junk DNA" into powerful evolutionary forces (Miller et al., 1999). The process of genomic integration of TE and thus generating or expanding cis-regulatory elements, genes, and other elements such as micro (microRNAs) or non-coding RNAs (ncRNAs) followed by suppression of parasitic self-propagation properties is called molecular domestication or exaptation (Gould and Vrba, 1982; Miller et al., 1999; Volff, 2006).

A domesticated TE-derived gene regulator can benefit the host and be an adaptive advantage (Miller et al., 1999; Biemont and Vieira, 2006; Volff, 2006; Feschotte and Pritham, 2007). The TE-associated domestication events can be sources of novel genes (Miller et al., 1999), ncRNAs, microRNAs, etc., (Borchert et al., 2011; Li et al., 2011; Chuong et al., 2013; Henaff et al., 2014; Zhang et al., 2016). There are multiple examples of such beneficial domestication events, and the scope of this process is expanding with sequenced genomes (Miller et al., 1999; Jordan et al., 2003; Volff, 2006; Feschotte and Pritham, 2007; Koonin et al., 2020; Sundaram and Wysocka, 2020). There are also examples of convergent domestication, reflecting TE's nature (Casola et al., 2008; Mateo and Gonzalez, 2014). For example, the emergence of the placenta from the TE-derived *Syncytin* gene in

mammals and lizards occurred through two independent occurrences of TE domestication; it is portrayed as a classic example of convergent evolution (Miller et al., 1999; Lavialle et al., 2013; Cornelis et al., 2017).

Perhaps, the most critical domestication episodes associated with the rise of biological novelties are the recruitments of TEs in the evolution of transcription factors (TFs). TFs are known to be master regulators of gene expression across Metazoa (Lewis, 1978; Gehring, 1996), including body patterning (Pearson et al., 2005; Peter and Davidson, 2011) and cell fate commitment (Lin et al., 2010; Vervoort and Ledent, 2001). Mechanisms of the origins and lineage-specific TF gene expansion are primarily unknown. A classical hypothesis implies ancestral TF gene duplication, followed by the divergence of the duplicated gene (Ohno et al., 1968). However, this scenario does not apply to the TFs that are solely organism-specific and have no *bona fide* one-to-one orthologs in closest relatives.

The complementary scenario is the origin of TFs and the novel TF-binding sites with the contribution of TEs. DNA-binding properties of TEs, in particular the evidence that TEs contain TF-binding sites, perfectly match structural genome constraints as a potential "pre-adaptation" and sources to form novel cis-regulatory elements and TFs. Thus, incorporating non-coding and new TF genes into existing transcriptional networks (Sundaram and Wysocka, 2020) can also lead to the origins of new functions and transformative biological innovations, as well as the diversification of both genes and forms.

The most notable examples of TE-derived TFs came from plants (Lin et al., 2007; Henaff et al., 2014) and such model animal species as insects, e.g., *Drosophila* (Miller et al., 1999; Casola et al., 2007; Mateo and Gonzalez, 2014) or vertebrates (Hammer et al., 2005; Cayrol et al., 2007; Balakrishnan et al., 2009; Markljung et al., 2009; Hayward et al., 2013; Majumdar et al., 2013). However, the broad comparative scope of these events is less explored, with little knowledge about the majority of animal phyla.

Practically nothing is known about the most diverse bilaterian lineage–Lophotrochozoa. This clade consists of more than a dozen phyla (Kocot et al., 2017), including Mollusca—the second most species-rich phylum and one of the most diverse groups of animals (Ponder and Linderg, 2008). The evidence of TE domestication events outside Bilateria in four other basal metazoan lineages (Ctenophora, Porifera, Placozoa, and Cnidaria) is also lacking.

Here, we generated a catalog of potentially TE-derived TFs across Metazoa and proposed independent co-option of six out of ten superfamilies of TEs to create hundreds of TFs in all early-branching animal lineages.

2 Results and discussion

1. Mosaic distribution and parallel evolution of transposon-derived transcription factors across metazoans

Using tblastn searches against target genomes we first identified and curated a complete dataset of transcription factors (TFs) encoded in representatives of four animal phyla with the sequenced genomes, including two bilaterians (*Aplysia californica* and *Octopus bimaculoides*), one ctenophore (*Pleurobrachia bachei*), a sponge (*Amphimedon queenslandica*), and a placozoan (*Trichoplax adhaerens*). As a query, we used the most completed, annotated, and published dataset of 1,600 TFs encoded in the human genome to represent the deuterostomes clade (Lambert et al., 2018) and 755 predicted sequence-specific TFs in *Drosophila*, the model representative of the Ecdysozoa clade, as the initial queries for the tblastn searches (Shokri et al., 2019). Utilizing these complete and initial datasets, we identified that the sea slug *Aplysia* genome encodes 824 transcription factors. Similarly, using all *Aplysia*, *Drosophila,* and human TFs as queries in tblastn searches against their genomes, we identified the complete repertoire of TFs encoded in the *Octopus bimaculoides,* and the other three (*Trichoplax*, *Amphimedon*, *Pleurobrachia*) basal metazoan genomes.

Next, we identified TF families in these five animal phyla that have undergone lineage-specific TFs gene expansions, including the ones that have originated through tandem duplications. To our surprise, we found that the full-length TFs that derived from the class II DNA transposable elements (TEs) were primarily associated with species-specific TFs family gene expansion (Figure 1). Within this framework, Cosby et al. (Cosby et al., 2021) not only described the tendency of class II TE for being domesticated as TFs in mammals but also study mechanisms and proposed a model for this process, taking into count the binding sites of transposases. There are ten superfamilies of Class II TEs that are known to use the "*cut-and-paste*" mechanism for transposition from one position in the genome to another (Feschotte and Pritham, 2007; Zattera and Bruschi, 2022). Representatives of each of these subfamilies TE encoded full-length TF proteins were used as a query to screen for potentially TE-derived TFs across nine metazoan phyla (Figure 1; Supplementary Table S1). We determined that six of these TEs superfamilies could be independently recruited into the metazoan TFs: ZBED, CENPB, FHY3, HTH-Psq, THAP, and FLYWCH (Figure 1). Phylogenetic reconstruction suggested independent recruitment due to the absence of a "one-to-one" homolog in the closest species (Figure 2). The domain organization of newly identified potentially TE-derived metazoan TFs (summarized in Figure 3) also revealed the presence of transposon-like components within the protein-coding open reading frames (ORFs). The occurrence of TEs components within the TFs was further supported by sequence similarity searches against the *de novo* assembled transcriptome (RNA-Seq) dataset (https://neurobase.rc.ufl.edu).

All predicted TE-derived TF families identified in our analysis showed low (<1; Z-test $p < 0.05$) non-synonymous substitutions *versus* synonymous substitution (Ka/Ks) ratios (Supplementary Excel File S2, S3), indicating negative or purifying selection acting to maintain evolutionarily conserved sets of amino acid sequences. Similarly, the low Ka/Ks ratio of predicted TE-derived TFs suggests stationary domesticated genes (Gao et al., 2020). Furthermore, maintaining low Ka/Ks also suggest that their transposition ability can be maintained (Dazeniere et al., 2022). In addition to the Z test, Fast Unbiased Bayesian Approximation (FUBAR) (Murrell et al., 2013) estimation of the dN/dS ratio also confirmed negative or purifying selection pressure acting on these TFs (Figure 4). The total number of the proposed transposon-derived TFs is 788 (Supplementary Excel File S1). Supplementary Table S3 includes species such as the sea slug, *Elysia chlorotica*, the hemipteran insect *Myzus persicae*, and the rainbow trout *Oncorhynchus mykiss* (Supplementary Excel File S1).

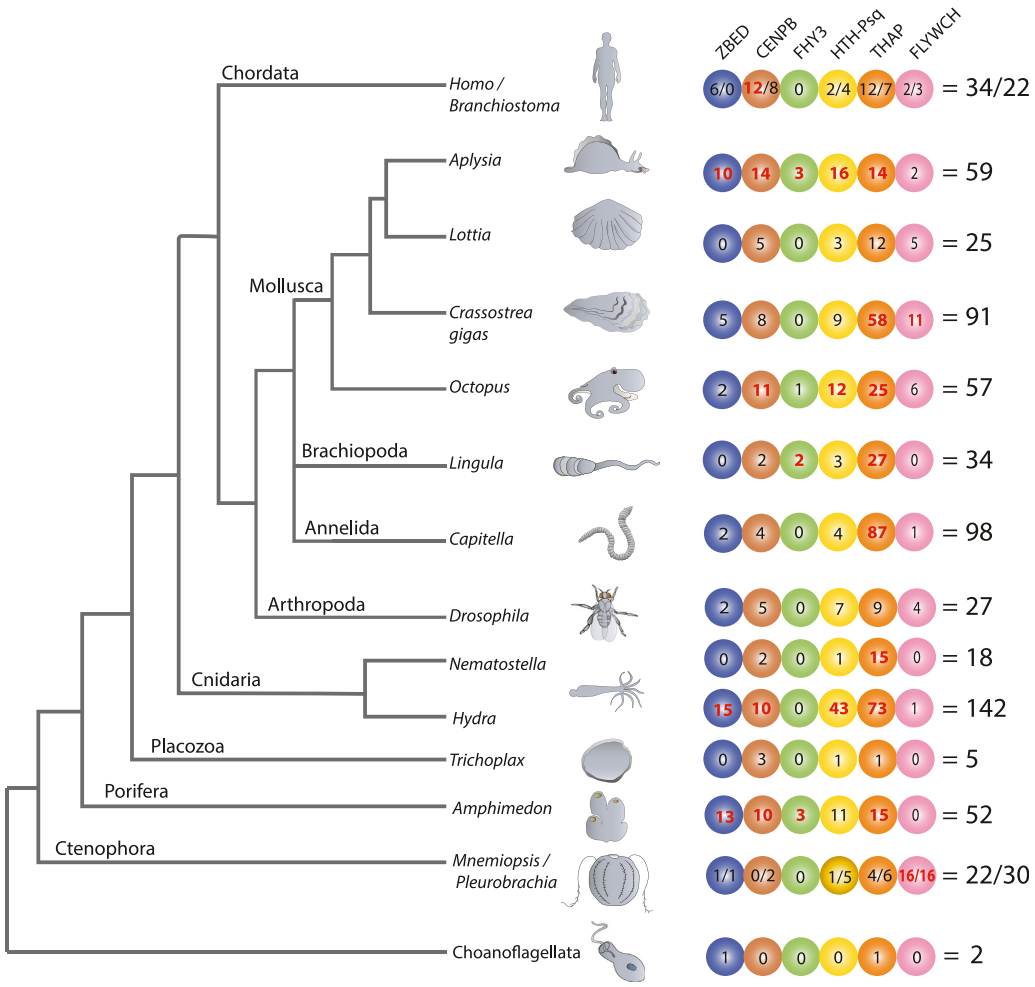

FIGURE 1
Transposon-derived transcription factors across metazoans. The diagram shows lineage-specific expansion and mosaic distributions of six families of transposon-derived transcription factors (TFs) across metazoans. All TFs depicted in the tree are lineage-specific genes that have no homolog in other classes or phyla. Each colored circle represents one of the six potentially TE-derived TF gene families: ZBED, CNPB, FHY3, HTH-Psq, THAP, and FLYWCH. Figures within circles indicate several independent species-specific events of the domestication of a particular TF family. The total numbers of transposon-derived TFs identified in each reference species are shown on the right. We observed the most extensive expansion of transposon-derived TFs in four bilaterian lineages led to the hydrozoan polyp—*Hydra* (142), the oligochaete—*Capitella* (98), the sea slug—*Aplysia* (59), and the bivalve—*Crassostrea* (91). Of note, a significant expansion of the THAP gene family occurred in *Capitella* (87), *Hydra* (73), and *Crassostrea* (58). Independent species-specific expansions of the FLYWCH gene family occurred in ctenophores *Mnemiopsis* (16) and *Pleurobrachia* (16). The "/" symbol is used to differentiate the numbers identified under both species, such as in *Homo*/*Branchostoma* and *Mnemiopsis*/*Pleurobrachia*, etc., The bold red letter indicates when the values are significantly higher in numbers compared to other species.

Figure 1 illuminates the mosaic-type distribution in the recruitments of transposon-derived TF subfamilies across major metazoan lineages studied here. In the sister group to all Metazoa—Choanoflagellata—we found only two genes likely encoding transposon-derived TFs from ZBED and THAP superfamilies, respectively.

Ctenophores are often viewed as the earliest branching lineage of animals, sister to the rest of Metazoa (Ryan et al., 2013; Moroz et al., 2014; Whelan et al., 2015; Whelan et al., 2017), although the reconstruction of the basal metazoan phylogeny is still a highly debated topic (Kapli and Telford, 2020; Li et al., 2021; Redmond and McLysaght, 2021), and might not be convincingly resolved. Unlike other studied metazoans, both the ctenophores *Mnemiopsis* and *Pleurobrachia* showed tremendous expansions of the FLYWCH transcription factor gene family (Figure 2A). FLYWCH (Dorn and Krauss, 2003; Ow et al., 2008), which is a distinct DNA-binding zinc finger domain-containing protein family known to have originated from the *Mutator* transposase (Marquez a Pritham, 2010). FLYWCH domains are evolutionary conserved but relatively rarely occur in animals. They were initially identified in *Drosophila* (Dai et al., 2004) and then in *C. elegans*, where it plays regulatory roles during embryogenesis by repressing microRNAs (Ow et al., 2008). The most recent evidence suggests that FLYWCH, in complex with β-catenin, repressed specific genes of the Wnt pathways and, therefore, can control cell polarity, migration, and metastasis (Muhammad et al., 2018). Surprisingly, none of the newly identified FLYWCH domain-containing genes have homologs in each other ctenophore species (Figure 2A; Supplementary Figure S1). Unfortunately, there are no

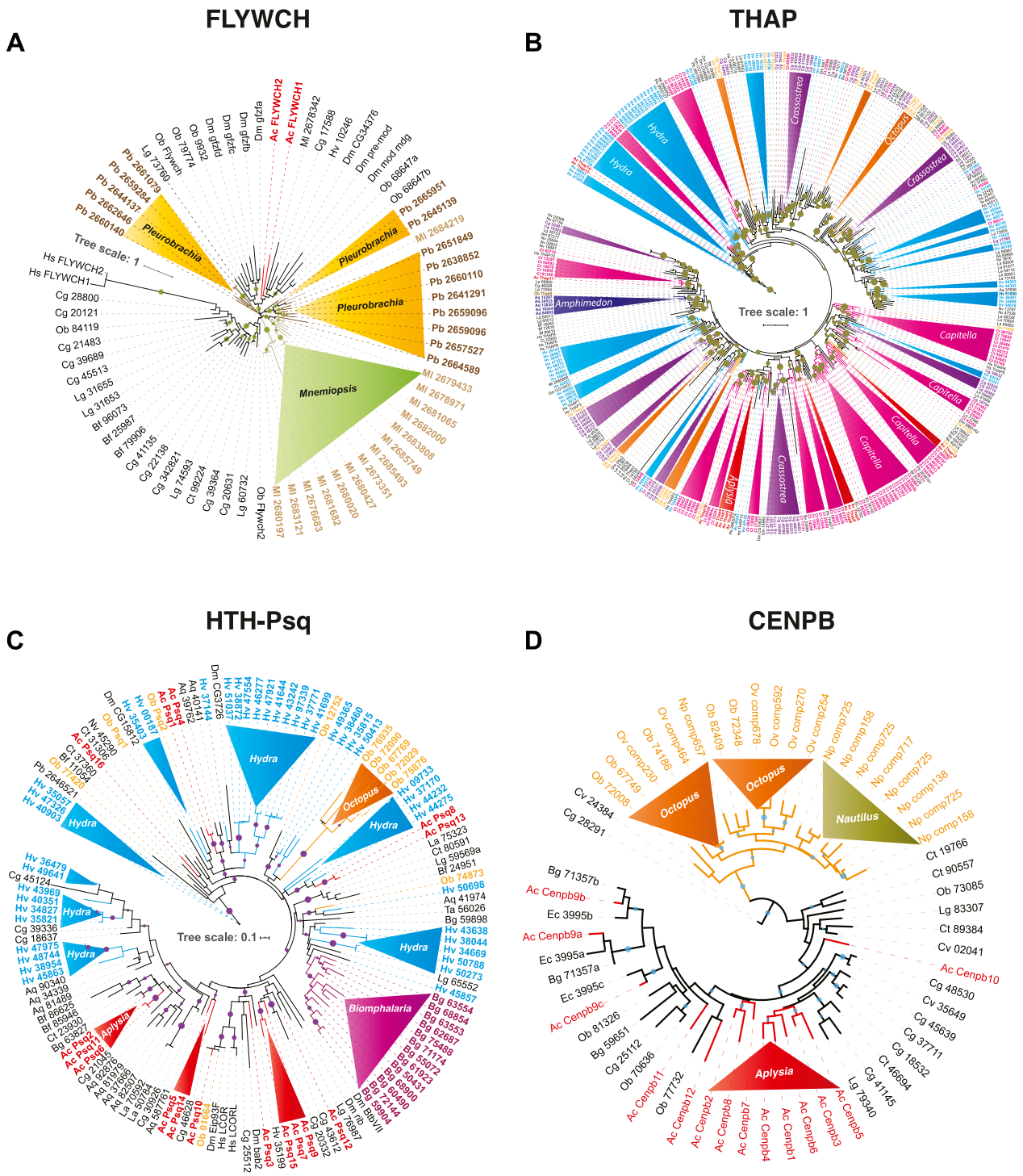

FIGURE 2
Independent expansion and convergent evolution of transposon-derived transcription factors in Metazoa. The phylogenetic tree represents the independent expansion and evolution of transposon-derived transcription factors protein families across metazoans. Each solid-color triangle represents species-specific expansion that has no homologs in related species. We used the following DNA binding domains–FLYWCH **(A)**, THAP **(B)**, HTH-Psq **(C)**, and CENPB **(D)**—as illustrative examples to build the maximum likelihood (ML) tree. The trees show independent FLYWCH gene expansion in the ctenophores *Mnemiopsis* and *Pleurobrachia* **(A)**. Similarly, independent THAP genes expansion in *Capitella*, *Octopus*, *Crassostrea*, *Hydra* **(B)**, HTH-Psq expansion in *Hydra*, *Biomphalaria*, *Aplysia,* and *Octopus* **(C)**, and Independent convergent domestication of CENPB genes in *Octopus*, *Nautilus,* and *Aplysia* **(A)**. High-resolution images of each of these trees are presented in Supplementary Figures.S1–S4.

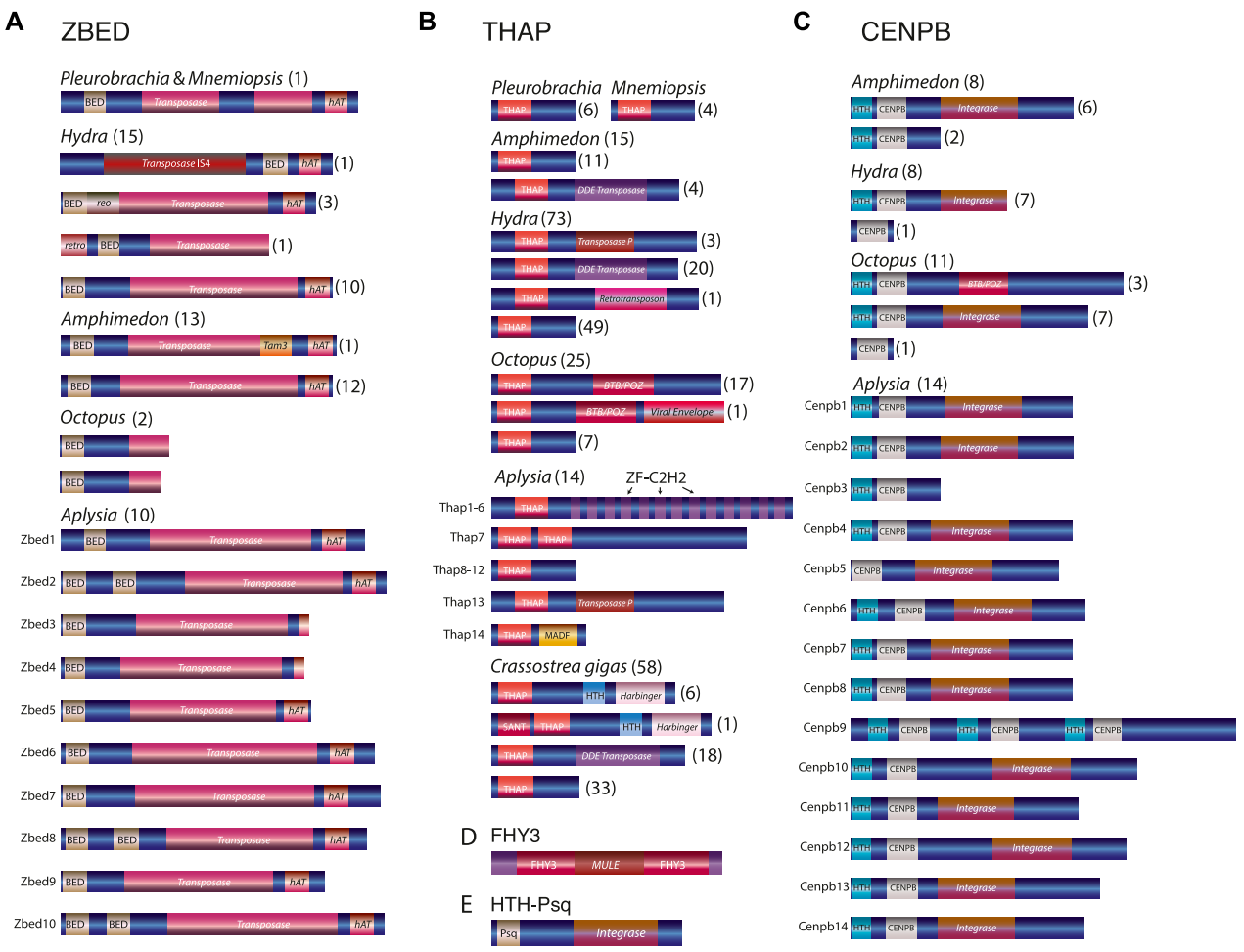

FIGURE 3
Domain organizations of the transposon-derived transcription factors across metazoans **(A–E)**. Transposon insertions domains are shown in shaded red color and labeled as *integrase*, *transposase*, *Harbinger*, *BTB/POZ*, etc., Note that the same transcription factor protein families have different transposon components. For example, *Octopus* CENPB and THAP proteins have derived mostly from BTB/Poxvirus BTB (Godt et al., 1993)/POZ (Bardwell and Treisman, 1994) transposable elements, whereas, in other species, the same TFs have originated from multiple different transposable elements. Similarly, *Hydra* ZBED genes could have derived from at least three transposon sources such as *retrotransposon*, *reoviruses*, and *transposon IS4*, whereas all *Aplysia* ZBED genes seem to have derived from *Ac* transposon (Supplementary Figures S5, S6). Numbers within parentheses indicate the number of genes identified with a similar domain organization.

functional studies of these genes, and the roles of these TFs in ctenophores will be subjects of future studies.

There are three species with the broadest overall domestication of TEs: the hydroid polyp—*Hydra* (142 TFs), the polychaete annelid—*Capitella* (98 TFs), and the gastropod mollusk, *Aplysia* (59 TFs). In these animals, the identified domestication events are both species-specific and TF-type-specific. In other words, for each animal studied, we noticed an independent expansion of one or more families of potentially TE-derived TFs (Figure 1). The most notable examples of predicted TE exaptation we found in *Hydra* and the ctenophore *Pleurobrachia* (5 out of 6 superfamilies), *Aplysia* (6 out of 6 superfamilies), and the sponge *Amphimedon* (5 out of 6 superfamilies). Surprisingly, the lineage that led to the sponges also revealed multiple examples of independent domestication and expansion of potentially TE-derived TFs compared to other non-bilaterian metazoans (except *Hydra*), which correlate to astonishing diversification within the phylum Porifera in general.

In contrast, the placozoan *Trichoplax*—the simplest known free-living animal (Grell and Ruthmann, 1991; Srivastava et al., 2008; Romanova et al., 2021; 2022), had the smallest number (5) of predicted TE-derived TFs, which might reflect the observed morphological simplicity of these disk-shaped benthic animals with only three layers of cells gliding on algal substrates (Srivastava et al., 2008; Smith et al., 2014; Eitel et al., 2018).

Likewise, the anthozoan *Nematostella* also had a modest representation of potentially TE-derived TFs, mostly related to just one superfamily; there are 15 Thanatos and associated protein (THAP) domain-containing genes. THAP genes were found in *Drosophila*, and they are known to have originated from P element transposes (Roussigne et al., 2003). Our analysis support events of the

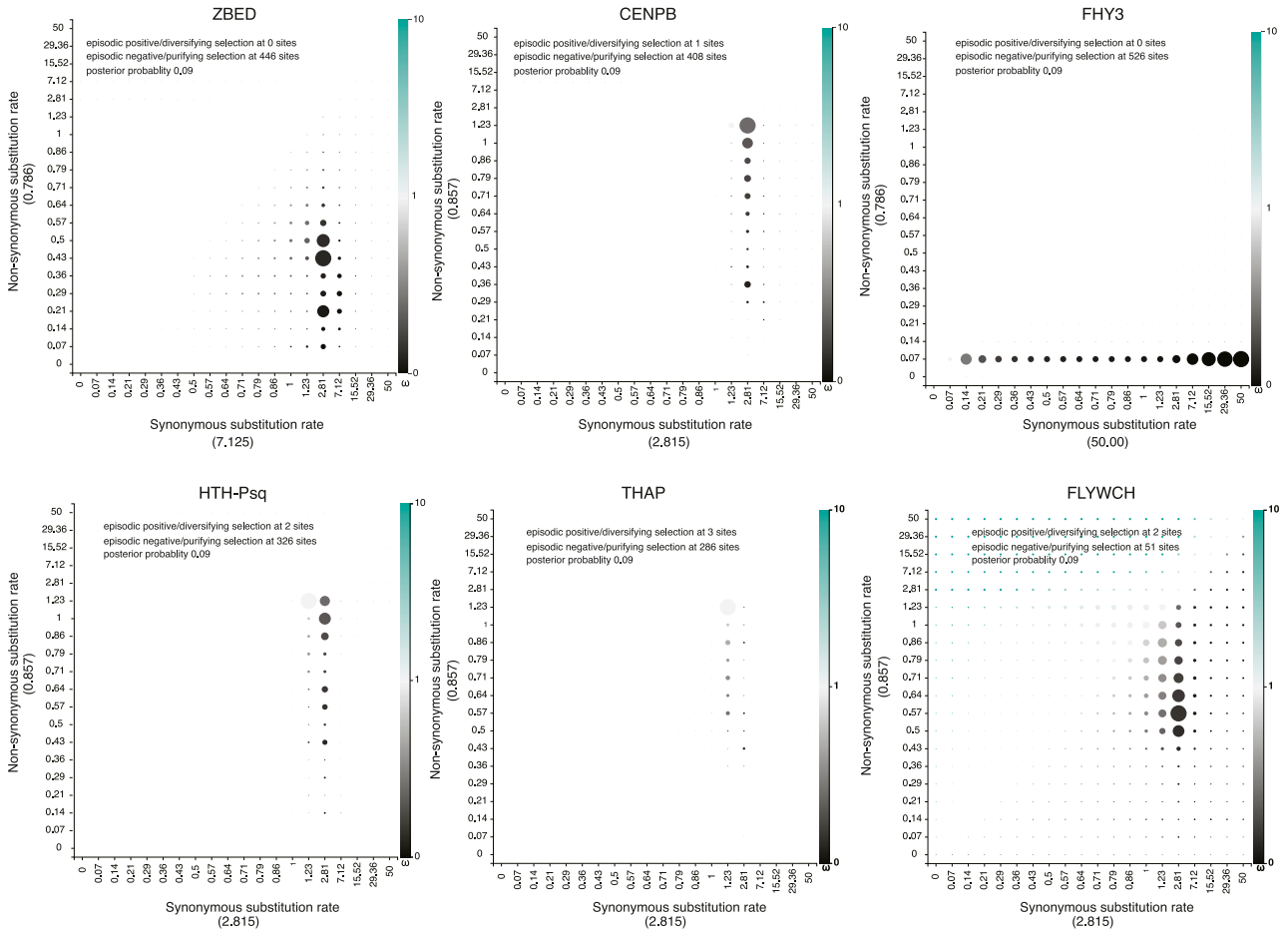

FIGURE 4
Non-synonymous (dN) versus synonymous substitution (dS) ratio show transposon-derived transcription factors evolving under purifying selection pressure. Non-synonymous *versus* synonymous substitutions were calculated across all potentially TE-derived TF families using the Fast Unbiased Bayesian Approximation (FUBAR) approach (Murrell et al., 2013). Synonymous substitutions (dS) rates calculated under each family are shown in *X*-axis inside the parentheses. Similarly, Non-synonymous substitutions (dN) rates calculated under each family showed in the Y axis inside the parentheses. Gray to intense black color-coding dots signifies negative or purifying (dN/dS < 1) selection, while light green to intense green represents sites under diversifying or positive (dN/dS > 1) selection.

independent diversification of THAP genes in *Hydra* (73), *Capitella* (87), *Crassostrea* (58) (see details in the next section and Figure 2B; Supplementary Figure S2); and at a lesser degree in a living fossil—the brachiopod, *Lingula* (27) and *Octopus* (25).

In summary, THAP genes represent the largest class of potentially TE-derived TFs identified in this study, including the basally branched chordate amphioxus (*Branchiostoma*) and humans. THAP- TF functions in invertebrates are primarily unknown (Nicholas et al., 2008). On the other hand, THAP TFs in humans were implicated in epigenetic regulation, maintenance of pluripotency, transposition, cancers, and other disorders like hemophilia. For example, THAP0 is a member of the apoptotic cascade induced by IFN-γ (Lin et al., 2002). THAP1, with RRM1, regulates cell proliferation (Cayrol et al., 2007). THAP5 acts as a cell cycle inhibitor (Balakrishnan et al., 2009). THAP9 is an active transposase in humans (Majumdar et al., 2013). The THAP11 homolog in mice is essential for embryogenesis (Dejosez et al., 2008).

Two other groups presently identified TE-derived TFs are also prominent in humans and *Branchiostoma*: ZBED and CENPB (Figure 1; Supplementary Figures S5–S7).

BED zinc fingers or ZBED genes reported having derived from the *hAT* (hobo, Ac, Tam3) superfamily of DNA transposon (Aravind, 2000), and members of this superfamily regulate an extensive array of functions in vertebrates. For example, ZBED6 affects development, cell proliferation, wound healing, and muscle growth (Markljung et al., 2009). ZBEDs are present in mammals, birds, reptiles, and fish; however, they are absent from jawless fishes. Based on these findings, it was proposed that ZBED genes in vertebrates originated due to at least two independent *hAT* DNA transposon domestication events in primitive jawed-vertebrate ancestors (Hayward et al., 2013). Our searches against the *Branchiostoma belcheri* genome uncovered a full-length ZBED gene, which was surprisingly absent from the *Branchiostoma floridae* genome, further suggesting species-specific and mosaic exaptation of TE-encoded genes.

Also, using both the DNA binding BED domain and known full-length ZBED genes, we find that ZBED genes form a monophyletic cluster in three mollusks (*Aplysia*, *Biomphalaria*, *Crassostrea*), the sponge *Amphimedon,* and *Hydra* (Supplementary Figures S5–S6).

Centromere-binding proteins-B (CENPB) transcription factor (Lein et al., 2007) involved in chromosome segregation maintenance and genome stability (Morozov et al., 2017) recurrently domesticated from *pogo*-like transposons (Casola et al., 2008; Mateo and Gonzalez, 2014) across Metazoa (Supplementary Figure S7). CENPB homologs were found in mammals (Sullivan and Glass, 1991) but not in other vertebrates. Nevertheless, we identified CENPB TFs from both *Branchiostoma belcheri* and *B. floridae* genomes, indicating their presence before the divergence of vertebrates. Thus, this finding suggests either loss of CENPBs in most of the extant lineages of vertebrates or their independent domestication in mammalian species, which is a more likely scenario (Casola et al., 2008). There is also a remarkable diversification and independent expansion of the CENPB superfamily in Mollusca (Supplementary Figure S7), which we will discuss in the following section.

The most stunning example of mosaic recruitment of TEs can be illustrated using *Mule* transposons. *Mule* transposon-derived transcription factor far-red elongated hypocotyls 3 (FHY3) group are critical for far-red (near-infrared) light signaling and survival of chloroplast in plants (Lin et al., 2007; Chang et al., 2015). Here for the first time, we identified FHY3 in animals (Figures 1, 3D). Our cross-species comparison across metazoans showed that FHY3 was present in three copies, both in the demosponge *Amphimedon* and the sea slug *Aplysia* genomes. There are two copies in the brachiopod *Lingula* and one in *Octopus* genomes (Figure 1). However, we did not find FHY3 in the sequenced ctenophores (*Pleurobrachia* and *Mnemiopsis*), placozoan (*Trichoplax*), and cnidarian (*Nematostella* and *Hydra*) and human genomes. Thus, FHY3 can be absent or present in a mosaic fashion without a recognized taxonomical specification. Our phylogenetic analysis (Supplementary Excel File S1) showed that FHY3 had been repeatedly domesticated over 550 + million years of animal evolution (see Supplementary Figure 8S), including examples from selected molluscs (e.g., the algae-eating sea slugs *Aplysia californica*, *Elysia chlorotica,* and the oyster—*Crassostrea*), some arthropods (*Myzus persicae* and *Limulus polyphemus*) and chordates (*Branchiostoma*).

In conclusion, we obtained evidence that the majority of TFs are the results of the species-specific convergent domestication events across animal phyla tested here. Figure 2; Supplementary Figures S1–S8 illustrate these cases. Of note, although some of the studied species show a predominant exaptation of just one or two categories of genes, many domesticated events occurred independently, even within the same superfamily of potentially TE-derived TFs (Figure 2; Supplementary Figures S1–S8). This situation is summarized below, focusing on the Lophotrochozoan lineage.

2. Transposon-derived TFs showed independent species-specific expansion and evolution in Molluscs.

Lophotrochozoa or Spiralia, including the phylum Mollusca, is the most morphologically and biochemically diverse animal clade (Kocot et al., 2017). None of the predicted TE-derived TFs were previously reported in Lophotrochozoa (Table 1). The phylum Mollusca in our analysis is represented by seven species (*Aplysia*, *Biomphalaria*, *Elysia*, *Lottia*, *Crassostrea, Octopus,* and *Nautilus*), with *Aplysia* showing the most remarkable expansion of potentially TE-derived TFs (Figure 1). First, we systematically scanned the complete set of the TFs encoded in the *Aplysia californica* genome a prominent neuroscience model (Kandel, 2001; Moroz et al., 2006; Moroz, 2011), resulting in the identification of 824 transcription factors.

Then, we identified 59 novel (~7%) transposon-derived TFs that have no homolog in closely related species such as in *Biomphalaria* the freshwater pulmonated snail (Adema et al., 2017) or the limpet *Lottia* (Simakov et al., 2013). This finding indicates that these TFs did not originate from canonical gene duplication events (Supplementary Excel File S1); they do not follow the canonical subfunctionalization (Stoltzfus, 1999) and neofunctionalization (Force et al., 1999) characteristics. Of these 59 *Aplysia* lineage-specific TFs, 42 were coupled with the transposase (TPase) domain (Figure 3), confirming the hypothesis that these genes, including their DNA-binding domain, may have originated by unique mechanisms involving "*cut-and-paste*" DNA transposons.

In molluscs, we also revealed that the lineage-specific TFs, even those belonging to identical TF families, originated both from similar and different transposon sources: the majority of potentially TE-derived TF domestication events were not detected from related species. Thus, the most likely parsimonious scenario is a broad scope of independent domestication events leading to the convergent evolution of TE-derived TFs within animal lineages studied here. Figure 2; Supplementary Figures S1–S8 illustrates bursts of parallel expansions of transposon-derived TFs subfamilies. Three examples are outlined below.

(1) There are convergent domestications of *pogo*-derived CENPB sequences in *Aplysia*, cephalopods, and other Lophotrochozoan species, such as in *Crassostrea* (Figure 2D). Within the cephalopod lineage, we identified two distinct events of *pogo* domestication—one, in the lineage leading to *Nautilus* and another event occurring in the lineage leading to *Octopus* (Figure 2D).

(2) Helix-turn-helix motif of pipsqueak (HTH-Psq) proteins form a family of transcription factors known to have derived from *Drosophila* pogo transposase (Siegmund and Lehmann, 2002). We find the *Aplysia* genome encodes 16 HTH-Psq subfamily transcription factors while the *Biomphalaria* genome encodes 15. Surprisingly none of these *Biomphalaria* TFs has direct homologs in the *Aplysia* genome and *vice versa* (Figure 2C; Supplementary Figure S3), indicating species-specific expansion event. Similarly, both *Hydra* and *Octopus* showed independent species-specific expansions of transposon-derived HTH-Psq genes. Thus, independent domestication of Psq genes might occur at least five times in *Aplysia*, *Biomphalaria*, *Octopus,* and the *Hydra* and *Amphimedon* genomes (Figure 2C).

(3) Myb-SANT, like in Adf (MADF) domain-containing genes initially identified in *Drosophila* known to have originated from the P instability factor or PIF superfamily of DNA transposon (Lin et al., 2007). We find that MADF genes were expanded in *Amphimedon*, *Drosophila,* and, most of all,

TABLE 1 The total number of potentially TE-derived TFs identified in this study. (See Figure 1; Supplementary Table S1 for details).

TE-derived TF families	Total numbers identified	Comments on 1st time identification	Top 3–4 species highlighted*
ZBED	71	1st for Lophotrochozoa	*Aplysia* (10), *Amphimedon* (13), ***Hydra*** **(15)**
CENPB	121	1st for Lophotrochozoa	***Aplysia*** **(14)**, *Homo* (12), *Octopus* (7)
FHY3	23	**1st for Metazoa**	***Aplysia*** **(3)**, *Amphimedon* (**3**), *Lingula* (2), *Octopus* (1)
HTH-Psq	136	1st for Lophotrochozoa	*Aplysia* (16), ***Hydra*** **(43)**, *Octopus* (12)
THAP	370	1st for Lophotrochozoa	***Capitella*** **(87)**, *Hydra* (73), *Crassostrea* (58)
FLYWCH	67	1st for Ctenophora and Lophotrochozoa	Expansion in Ctenophores
	Total = 788		

* Topmost 3–4 species that have the highest expansion of TE-derived TFs are shown. The number of TE-derived TFs identified is shown inside the parenthesis. The bold letter is used to highlight the significant increase over other species or the first time detected in the entire metazoan phylogeny.

Aplysia with at least six predicted independent domestication events. Although MADF genes are likely derived from the PIF superfamily of DNA transposon, we have excluded MADF genes from this analysis owing to the growing concern that these genes do not harbor a recognized transposon-derived transposase domain within the protein-coding gene.

Altogether our results suggest a substantial lineage-specific diversification and independent evolution of new genes originating from a modular diversity of *cut-and-paste* DNA transposons, as outlined in the next section.

3 Domain analysis revealed the presence of transposons derived components within the protein-coding TFs

All subfamilies of transposon-derived TFs predicted in this analysis have a modular domain architecture (Figure 3). Within each subfamily, most TFs encode recognizable transposon-derived components within exons of these protein-coding genes. For example, transposon-derived ZBED TFs, besides encoding the canonical DNA-binding BED zinc finger motif, also encoded a transposon-derived *transposase* domain and an *hAT* dimerization domain (Figure 3A). Strikingly, we find that ZBED genes across metazoans derived from diverse transposable element components (Supplementary Figures S5, S6). For instance, Homo ZBED5 is known to have derived from Buster DNA transposon (Hayward et al., 2013), which, in our analysis, forms a robust clade with one of the *Octopus* ZBED genes indicating its *Buster* transposon origin (Supplementary Figures S5, S6). In contrast, the second *Octopus* ZBED gene forms a robust cluster with the *Hydra retrotransposon-derived* ZBED gene (Supplementary Figures S5, S6). The two truncated ZBED genes from the *Octopus bimaculoides* genome lack an intact transposase and an *hAT* dimerization domain. In addition, we could not recover the full-length transposase domain and the *hAT* dimerization domain from the *Octopus bimaculoides* genome associated with them. This result indicates that the two *Octopus* ZBED genes may have evolved from two independent transposon components.

Similarly, the *Hydra retrotransposon-derived* ZBED gene encodes an intron that separates the N-terminal reverse transcriptase (RT) domain against the C-terminal BED finger and the transposase domain. This result suggests that the *Hydra* BED and the transposase domains are no longer part of the retrotransposon component. In addition, *Hydra* ZBED genes contained at least three transposon components, such as *retrotransposons*, *reoviruses,* and *transposon* IS4 (Figure 3A; Supplementary Figures S5, S6). Likewise, while *Octopus* THAP genes are mostly derived from BTB (Godt et al., 1993) (Broad-Complex, Tramtrack, Bric a Brac) or POZ (Bardwell and Treisman, 1994) (poxvirus and zinc finger) transposon sources—the *Hydra* THAP genes, however, found to be derived from versatile transposon sources such as *Transposase P* element, *DDE transposase* (*DDE_Tnp_4*) and *retrotransposon*. In contrast, some *Crassostrea gigas* THAP genes contained sequences associated with the *Harbinger*-derived transposon domain (Figure. 3B).

Also, while most of the *Octopus* CENPB TFs were associated with the transposon-derived BTB/POZ domain, none of the genes from another mollusc, *Aplysia*, contained this domain (Figure 3C).

Both CENPB and HTH-Psq genes had a signature of the viral *rve* superfamily of the retroviral integrase domain (Figure 3C, E). Integrase is the retroviral enzyme that catalyzes the integration of virally derived DNA into the host cell's nuclear DNA, forming a provirus that can be activated to produce viral proteins (Delelis et al., 2008). In the same way, FHY3 genes share remarkable sequence similarities with MURA (Hudson et al., 2003), the transposable element encoded by the *Mutator* element of maize, and the predicted transposase of the maize mobile element *Jittery* (Xu et al., 2004). Both transposons are a member of the Mutator-like elements (*MULE*) (Lisch, 2002) (Figure 3D).

These results, for the first time, indicate that even within the same subfamily of transposon-derived TFs—similar domains have derived from multiple transposon components across the animal kingdom. Together our phylogenetic analysis and the revealed domain organizations suggest that similar domain architecture originated in parallel from numerous transposon resources across phyla.

4 Conclusion

By systematic analysis of about seven thousand animal TFs, we have predicted a total of 788 (>10%) novel DNA transposons-derived TFs across metazoans (Figure 1; Supplementary Excel File S1). Our study was limited to 6 previously known TE-derived TF families used as a query to search for the new domestication events. Although predictably derived from the TE components, we had to exclude the MADF genes from the current analysis owing to the absence of a potential transposase domain.

The *Aplysia* genome encodes 41 MADF genes, and a many of them expressed in developmental stages as well as in specific neuronal populations, suggesting their involvement in the control of cell-specific phenotypes (data not shown) as well as contributing to the very origin of neuronal organizations and diversification events (Erwin, 2009; Mustafin and Khusnutdinova, 2020; Moroz and Romanova, 2021). Homologs of these *Aplysia* MADF genes are missing in the sequenced *Biomphalaria* genome a related gastropod species (Adema et al., 2017; Kocot et al., 2011), which encodes only three of these MADF genes. Thus, careful systematic analysis is needed to identify novel domestication events in the evolution of TE-derived TFs within molluscs.

Overall, predicted TE-derived TFs show mosaic patterns in their distribution with extreme heterogeneity and with a 'sudden' appearance in one lineage and, at the same time, found to be 'missing' in more closely related species.

Although most studied species predict a predominant exaptation of just one category of genes, many domesticated events might occur independently in evolution, even within the same superfamily of potentially TE-derived TFs (Figure 2).

Our results suggest a substantial lineage-specific diversification and independent origins of new TF genes originated from a broad array and a modular diversity of *cut-and-paste* DNA transposons and related viroid-like elements. Many described TFs preserved the original modular gene organization (Figure 3) and could act as highly dynamic modules shaping the genome-wide reorganization within Metazoa.

5 Materials and Methods

5.1 Identification of potentially TE-derived TFs

We used representatives of published and confirmed domesticated transposable element-derived TFs protein families from plants and animals as a query (Supplementary Table S2). Both PSI-BLAST, as well as Tblastn searches, were performed using both the command-line version at the NCBI standalone BLAST (version 2.2.18) (Camacho et al., 2009) as well as at the online BLAST web interface (Boratyn et al., 2013; Shi et al., 2018) using default e-value cut off for the online version and 10^{-5} to 10^{-10} cut off for the stand-alone blast to identify all potential homologs. Homologs were detected not solely based on e-value cut-off but other criteria such as coverage statistics, bit score, etc., were considered. Protein sequences recovered from one round of TBLASTN or PSI-BLAST searches were recursively used as queries until no further sequences were detected. Each protein blast hit was manually inspected following multiple sequence alignment (MSA) and validated utilizing several databases including the NCBI conserved domain database (CDD) (Marchler-Bauer et al., 2011), Hmmer (Finn et al., 2011), Pfam (Punta et al., 2011), and SMART (Letunic and Bork, 2018). In the case of the non-availability of the gene model (exome), genome sequences surrounding the coding region were excised, and homology-based gene prediction based on hidden Markov models (HMMs) was performed in FGENESH+ (www.softberry.com) to identify the complete open reading frame. Finally, TE insertions within the TFs were further validated by similarity searches against the *de novo* assembled RNA-Seq (transcriptome) datasets obtained in Moroz lab (https://neurobase.rc.ufl.edu).

5.2 Multiple sequence alignment and protein domain identification

Protein functional domains were identified by sequence search of the NCBI conserved domain databases (Marchler-Bauer et al., 2011; Marchler-Bauer et al., 2017). Results were verified *via* sequence searches of the SMART (Letunic and Bork, 2018) and Pfam database (Punta et al., 2011). Also, sequences were aligned in MUSCLE (Edgar, 2004a; Edgar, 2004b) and displayed in clustalX (Larkin et al., 2007) and manually confirmed the domain architecture by examining the sequences based on protein secondary structure analysis and profile alignments. Multiple sequence alignment (MSA) obtained through MUSCLE was used to build the HMMER v3.1b2 (Finn et al., 2011) position-specific scoring matrix (PSM) to search against the reference proteome datasets.

5.3 Phylogeny reconstruction

Maximum-likelihood (ML) trees were inferred using PhyML v3.0 (Guindon and Gascuel, 2003; Guindon et al., 2010), with the best-fit evolutionary model identified using the AIC criterion estimated by ProtTest (Abascal et al., 2005). ML phylogenies were performed using the JTT model of rate heterogeneity, estimated proportion of invariable sites, four rate categories, and estimated alpha distribution parameter. Tree topology searches were optimized using the best of both NNI (nearest-neighbor interchanges) and SPR (subtree pruning and regrafting) moves (Hordijk and Gascuel, 2005). Clade support was calculated using the SH-like approximate likelihood ratio test (Anisimova et al., 2011). Unless otherwise mentioned, all phylogenetic trees presented throughout the manuscript show SH-support of 80 or greater. The resulting phylogenetic trees were viewed and edited with iTol version 2.0 (Letunic and Bork, 2007).

5.4 Estimation of codon substitution pattern and inference of selective pressure

Protein sequences of potentially TE-derived transcription factors under each family were aligned using MUSCLE (Edgar, 2004a), and the conversion of protein alignments to corresponding nucleotide coding sequences was obtained using PAL2NAL webserver (Suyama et al., 2006). Codon-based tests of neutrality and negative or purifying selection were conducted using MEGA with a Z test by calculating the substitution ratio of the number of non-synonymous substitutions per non-synonymous site (Ka) *versus* synonymous substitution per

synonymous sites (Ks) using the Nei-Gojobori method (Nei and Gojobori, 1986). Orthologous sequences with a Ka/Ks value of <1 (Z-test, $p < 0.05$) were defined as having been under purifying selection shown with yellow color (Supplementary Excel files S3, S4).

Of note that the extended methods section is summarized in the Supplementary Method section online.

Data availability statement

The datasets presented in this study can be found in online repositories. The names of the repository/repositories and accession number(s) can be found in the article/Supplementary Material.

Author contributions

KM and LM: Conceptualization; Writing an original draft, Writing-review and editing, Data obtaining, and curation. KM: Formal computational analysis, Investigation, Methodology, Software, Validation, Data Visualization, LM: Funding Acquisition, Project Administration, Resources, and Supervision.

Funding

This work was supported by the Human Frontiers Science Program (RGP0060/2017), National Science Foundation (Grants 1146575, 1557923, 1548121, and 1645219), National Institute of Health (R01 NS114491) to LM.

Acknowledgments

The authors would like to thank Drs. Caleb Bostwick, Peter Williams, and Andrea Kohn for the generation of RNA-seq libraries and initial annotations. Thanks to Gayle Prevatt for the initial drawing of the animal sketches.

Conflict of interest

The authors declare that the research was conducted in the absence of any commercial or financial relationships that could be construed as a potential conflict of interest.

Publisher's note

All claims expressed in this article are solely those of the authors and do not necessarily represent those of their affiliated organizations, or those of the publisher, the editors and the reviewers. Any product that may be evaluated in this article, or claim that may be made by its manufacturer, is not guaranteed or endorsed by the publisher.

Supplementary material

The Supplementary Material for this article can be found online at: https://www.frontiersin.org/articles/10.3389/fcell.2023.1113046/full#supplementary-material

References

Abascal, F., Zardoya, R., and Posada, D. (2005). ProtTest: Selection of best-fit models of protein evolution. *Bioinformatics* 21, 2104–2105. doi:10.1093/bioinformatics/bti263

Adema, C. M., Hillier, L. W., Jones, C. S., Loker, E. S., Knight, M., Minx, P., et al. (2017). Whole genome analysis of a schistosomiasis-transmitting freshwater snail. *Nat. Commun.* 8, 15451. doi:10.1038/ncomms15451

Anisimova, M., Gil, M., Dufayard, J. F., Dessimoz, C., and Gascuel, O. (2011). Survey of branch support methods demonstrates accuracy, power, and robustness of fast likelihood-based approximation schemes. *Syst. Biol.* 60, 685–699. doi:10.1093/sysbio/syr041

Aravind, L. (2000). The BED finger, a novel DNA-binding domain in chromatin-boundary-element-binding proteins and transposases. *Trends Biochem. Sci.* 25, 421–423. doi:10.1016/s0968-0004(00)01620-0

Balakrishnan, M. P., Cilenti, L., Mashak, Z., Popat, P., Alnemri, E. S., and Zervos, A. S. (2009). THAP5 is a human cardiac-specific inhibitor of cell cycle that is cleaved by the proapoptotic Omi/HtrA2 protease during cell death. *Am. J. Physiol. Heart Circ. Physiol.* 297, H643–H653. doi:10.1152/ajpheart.00234.2009

Bardwell, V. J., and Treisman, R. (1994). The POZ domain: A conserved protein-protein interaction motif. *Genes. Dev.* 8, 1664–1677. doi:10.1101/gad.8.14.1664

Biemont, C., and Vieira, C. (2006). Genetics: Junk DNA as an evolutionary force. *Nature* 443, 521–524. doi:10.1038/443521a

Boratyn, G. M., Camacho, C., Cooper, P. S., Coulouris, G., Fong, A., Ma, N., et al. (2013). Blast: A more efficient report with usability improvements. *Nucleic Acids Res.* 41, W29–W33. doi:10.1093/nar/gkt282

Borchert, G. M., Holton, N. W., Williams, J. D., Hernan, W. L., Bishop, I. P., Dembosky, J. A., et al. (2011). Comprehensive analysis of microRNA genomic loci identifies pervasive repetitive-element origins. *Mob. Genet. Elem.* 1, 8–17. doi:10.4161/mge.1.1.15766

Camacho, C., Coulouris, G., Avagyan, V., Ma, N., Papadopoulos, J., Bealer, K., et al. (2009). BLAST+: Architecture and applications. *BMC Bioinforma.* 10, 421. doi:10.1186/1471-2105-10-421

Casola, C., Hucks, D., and Feschotte, C. (2008). Convergent domestication of pogo-like transposases into centromere-binding proteins in fission yeast and mammals. *Mol. Biol. Evol.* 25, 29–41. doi:10.1093/molbev/msm221

Casola, C., Lawing, A. M., Betran, E., and Feschotte, C. (2007). PIF-like transposons are common in drosophila and have been repeatedly domesticated to generate new host genes. *Mol. Biol. Evol.* 24, 1872–1888. doi:10.1093/molbev/msm116

Cayrol, C., Lacroix, C., Mathe, C., Ecochard, V., Ceribelli, M., Loreau, E., et al. (2007). The THAP-zinc finger protein THAP1 regulates endothelial cell proliferation through modulation of pRB/E2F cell-cycle target genes. *Blood* 109, 584–594. doi:10.1182/blood-2006-03-012013

Chang, N., Gao, Y., Zhao, L., Liu, X., and Gao, H. (2015). *Arabidopsis* FHY3/CPD45 regulates far-red light signaling and chloroplast division in parallel. *Sci. Rep.* 5, 9612. doi:10.1038/srep09612

Chuong, E. B., Rumi, M. A., Soares, M. J., and Baker, J. C. (2013). Endogenous retroviruses function as species-specific enhancer elements in the placenta. *Nat. Genet.* 45, 325–329. doi:10.1038/ng.2553

Cornelis, G., Funk, M., Vernochet, C., Leal, F., Tarazona, O. A., Meurice, G., et al. (2017). An endogenous retroviral envelope syncytin and its cognate receptor identified in the viviparous placental Mabuya lizard. *Proc. Natl. Acad. Sci. U. S. A.* 114, E10991–E11000. doi:10.1073/pnas.1714590114

Cosby, R. L., Judd, J., Zhang, R., Zhong, A., Garry, N., Pritham, E. J., et al. (2021). Recurrent evolution of vertebrate transcription factors by transposase capture. *Science* 371, eabc6405. doi:10.1126/science.abc6405

Dai, M. S., Sun, X. X., Qin, J., Smolik, S. M., and Lu, H. (2004). Identification and characterization of a novel *Drosophila melanogaster* glutathione S-transferase-containing FLYWCH zinc finger protein. *Gene* 342, 49–56. doi:10.1016/j.gene.2004.07.043

Dazeniere, J., Bousios, A., and Eyre-Walker, A. (2022). Patterns of selection in the evolution of a transposable element. *G3 (Bethesda)* 12, jkac056. doi:10.1093/g3journal/jkac056

Dejosez, M., Krumenacker, J. S., Zitur, L. J., Passeri, M., Chu, L. F., Songyang, Z., et al. (2008). Ronin is essential for embryogenesis and the pluripotency of mouse embryonic stem cells. *Cell.* 133, 1162–1174. doi:10.1016/j.cell.2008.05.047

Delelis, O., Carayon, K., Saib, A., Deprez, E., and Mouscadet, J. F. (2008). Integrase and integration: Biochemical activities of HIV-1 integrase. *Retrovirology* 5, 114. doi:10.1186/1742-4690-5-114

Dorn, R., and Krauss, V. (2003). The modifier of mdg4 locus in *Drosophila*: Functional complexity is resolved by trans splicing. *Genetica* 117, 165–177. doi:10.1023/a:1022983810016

Edgar, R. C. (2004a). Muscle: A multiple sequence alignment method with reduced time and space complexity. *BMC Bioinforma.* 5, 113. doi:10.1186/1471-2105-5-113

Edgar, R. C. (2004b). Muscle: Multiple sequence alignment with high accuracy and high throughput. *Nucleic Acids Res.* 32, 1792–1797. doi:10.1093/nar/gkh340

Eitel, M., Francis, W. R., Varoqueaux, F., Daraspe, J., Osigus, H. J., Krebs, S., et al. (2018). Comparative genomics and the nature of placozoan species. *PLoS Biol.* 16, e2005359. doi:10.1371/journal.pbio.2005359

Erwin, D. H. (2009). Early origin of the bilaterian developmental toolkit. *Philos. Trans. R. Soc. Lond B Biol. Sci.* 364, 2253–2261. doi:10.1098/rstb.2009.0038

Feschotte, C., and Pritham, E. J. (2007). DNA transposons and the evolution of eukaryotic genomes. *Annu. Rev. Genet.* 41, 331–368. doi:10.1146/annurev.genet.40.110405.090448

Finn, R. D., Clements, J., and Eddy, S. R. (2011). HMMER web server: Interactive sequence similarity searching. *Nucleic Acids Res.* 39, W29–W37. doi:10.1093/nar/gkr367

Force, A., Lynch, M., Pickett, F. B., Amores, A., Yan, Y. L., and Postlethwait, J. (1999). Preservation of duplicate genes by complementary, degenerative mutations. *Genetics* 151, 1531–1545. doi:10.1093/genetics/151.4.1531

Gao, B., Wang, Y., Diaby, M., Zong, W., Shen, D., Wang, S., et al. (2020). Evolution of pogo, a separate superfamily of IS630-Tc1-mariner transposons, revealing recurrent domestication events in vertebrates. *Mob. DNA* 11, 25. doi:10.1186/s13100-020-00220-0

Gehring, W. J. (1996). The master control gene for morphogenesis and evolution of the eye. *Genes. cells.* 1, 11–15.

Godt, D., Couderc, J. L., Cramton, S. E., and Laski, F. A. (1993). Pattern formation in the limbs of Drosophila: Bric a brac is expressed in both a gradient and a wave-like pattern and is required for specification and proper segmentation of the tarsus. *Development* 119, 799–812.

Gould, S. J., and Vrba, E. S. (1982). Exaptation—A missing term in the science of form. *Paleobiology* 8, 4–15. doi:10.1017/S0094837300004310

Grell, K. G., and Ruthmann, A. (1991). "Placozoa," in *Microscopic anatomy of invertebrates*. Editor F. W. Harrison (New York: Wiley-Liss), 13–27.

Guindon, S., Dufayard, J. F., Lefort, V., Anisimova, M., Hordijk, W., and Gascuel, O. (2010). New algorithms and methods to estimate maximum-likelihood phylogenies: Assessing the performance of PhyML 3.0. *Syst. Biol.* 59, 307–321. doi:10.1093/sysbio/syq010

Guindon, S., and Gascuel, O. (2003). A simple, fast, and accurate algorithm to estimate large phylogenies by maximum likelihood. *Syst. Biol.* 52, 696–704. doi:10.1080/10635150390235520

Hammer, S. E., Strehl, S., and Hagemann, S. (2005). Homologs of *Drosophila* P transposons were mobile in zebrafish but have been domesticated in a common ancestor of chicken and human. *Mol. Biol. Evol.* 22, 833–844. doi:10.1093/molbev/msi068

Hayward, A., Ghazal, A., Andersson, G., Andersson, L., and Jern, P. (2013). ZBED evolution: Repeated utilization of DNA transposons as regulators of diverse host functions. *PLoS One* 8, e59940. doi:10.1371/journal.pone.0059940

Henaff, E., Vives, C., Desvoyes, B., Chaurasia, A., Payet, J., Gutierrez, C., et al. (2014). Extensive amplification of the E2F transcription factor binding sites by transposons during evolution of Brassica species. *Plant J.* 77, 852–862. doi:10.1111/tpj.12434

Hordijk, W., and Gascuel, O. (2005). Improving the efficiency of SPR moves in phylogenetic tree search methods based on maximum likelihood. *Bioinformatics* 21, 4338–4347. doi:10.1093/bioinformatics/bti713

Hudson, M. E., Lisch, D. R., and Quail, P. H. (2003). The FHY3 and FAR1 genes encode transposase-related proteins involved in regulation of gene expression by the phytochrome A-signaling pathway. *Plant J.* 34, 453–471. doi:10.1046/j.1365-313x.2003.01741.x

Jordan, I. K., Rogozin, I. B., Glazko, G. V., and Koonin, E. V. (2003). Origin of a substantial fraction of human regulatory sequences from transposable elements. *Trends Genet.* 19, 68–72. doi:10.1016/s0168-9525(02)00006-9

Kandel, E. R. (2001). The molecular biology of memory storage: A dialogue between genes and synapses. *Science* 2 (294), 1030–1028. doi:10.1126/science.1067020

Kapli, P., and Telford, M. J. (2020). Topology-dependent asymmetry in systematic errors affects phylogenetic placement of Ctenophora and Xenacoelomorpha. *Sci. Adv.* 6, eabc5162. doi:10.1126/sciadv.abc5162

Kocot, K. M., Cannon, J. T., Todt, C., Citarella, M. R., Kohn, A. B., Meyer, A., et al. (2011). Phylogenomics reveals deep molluscan relationships. *Nature* 4 (477), 452–456. doi:10.1038/nature10382

Kocot, K. M., Struck, T. H., Merkel, J., Waits, D. S., Todt, C., Brannock, P. M., et al. (2017). Phylogenomics of Lophotrochozoa with consideration of systematic error. *Syst. Biol.* 66, 256–282. doi:10.1093/sysbio/syw079

Koonin, E. V., Makarova, K. S., Wolf, Y. I., and Krupovic, M. (2020). Evolutionary entanglement of mobile genetic elements and host defence systems: Guns for hire. *Nat. Rev. Genet.* 21, 119–131. doi:10.1038/s41576-019-0172-9

Lambert, S. A., Jolma, A., Campitelli, L. F., Das, P. K., Yin, Y., Albu, M., et al. (2018). The human transcription factors. *Cell.* 175, 598–599. doi:10.1016/j.cell.2018.09.045

Larkin, M. A., Blackshields, G., Brown, N. P., Chenna, R., McGettigan, P. A., McWilliam, H., et al. (2007). Clustal W and clustal X version 2.0. *Bioinformatics* 23, 2947–2948. doi:10.1093/bioinformatics/btm404

Lavialle, C., Cornelis, G., Dupressoir, A., Esnault, C., Heidmann, O., Vernochet, C., et al. (2013). Paleovirology of 'syncytins', retroviral env genes exapted for a role in placentation. *Philos. Trans. R. Soc. Lond B Biol. Sci.* 368, 20120507. doi:10.1098/rstb.2012.0507

Lein, E. S., Hawrylycz, M. J., Ao, N., Ayres, M., Bensinger, A., Bernard, A., et al. (2007). Genome-wide atlas of gene expression in the adult mouse brain. *Nature* 445, 168–176. doi:10.1038/nature05453

Letunic, I., and Bork, P. (2018). 20 years of the SMART protein domain annotation resource. *Nucleic Acids Res.* 46, D493–D496. doi:10.1093/nar/gkx922

Letunic, I., and Bork, P. (2007). Interactive tree of life (iTOL): An online tool for phylogenetic tree display and annotation. *Bioinformatics* 23, 127–128. doi:10.1093/bioinformatics/btl529

Lewis, E. B. (1978). A gene complex controlling segmentation in *Drosophila*. *Nature* 276, 565–570. doi:10.1038/276565a0

Li, Y., Li, C., Xia, J., and Jin, Y. (2011). Domestication of transposable elements into MicroRNA genes in plants. *PLoS One* 6, e19212. doi:10.1371/journal.pone.0019212

Li, Y., Shen, X. X., Evans, B., Dunn, C. W., and Rokas, A. (2021). Rooting the animal tree of life. *Mol. Biol. Evol.* 38, 4322–4333. doi:10.1093/molbev/msab170

Lin, R., Ding, L., Casola, C., Ripoll, D. R., Feschotte, C., and Wang, H. (2007). Transposase-derived transcription factors regulate light signaling in *Arabidopsis*. *Science* 318, 1302–1305. doi:10.1126/science.1146281

Lin, Y. C., Jhunjhunwala, S., Benner, C., Heinz, S., Welinder, E., Mansson, R., et al. (2010). A global network of transcription factors, involving E2A, EBF1 and Foxo1, that orchestrates B cell fate. *Nat. Immunol.* 11, 635–643. doi:10.1038/ni.1891

Lin, Y., Khokhlatchev, A., Figeys, D., and Avruch, J. (2002). Death-associated protein 4 binds MST1 and augments MST1-induced apoptosis. *J. Biol. Chem.* 277, 47991–48001. doi:10.1074/jbc.M202630200

Lisch, D. (2002). Mutator transposons. *Trends Plant Sci.* 7, 498–504. doi:10.1016/s1360-1385(02)02347-6

Majumdar, S., Singh, A., and Rio, D. C. (2013). The human THAP9 gene encodes an active P-element DNA transposase. *Science* 339, 446–448. doi:10.1126/science.1231789

Marchler-Bauer, A., Bo, Y., Han, L., He, J., Lanczycki, C. J., Lu, S., et al. (2017). CDD/SPARCLE: Functional classification of proteins via subfamily domain architectures. *Nucleic Acids Res.* 45, D200–D203. doi:10.1093/nar/gkw1129

Marchler-Bauer, A., Lu, S., Anderson, J. B., Chitsaz, F., Derbyshire, M. K., DeWeese-Scott, C., et al. (2011). Cdd: A conserved domain database for the functional annotation of proteins. *Nucleic Acids Res.* 39, D225gkq1189–229. doi:10.1093/nar/gkq1189

Markljung, E., Jiang, L., Jaffe, J. D., Mikkelsen, T. S., Wallerman, O., Larhammar, M., et al. (2009). ZBED6, a novel transcription factor derived from a domesticated DNA transposon regulates IGF2 expression and muscle growth. *PLoS Biol.* 7, e1000256. doi:10.1371/journal.pbio.1000256

Marquez, C. P., and Pritham, E. J. (2010). Phantom, a new subclass of Mutator DNA transposons found in insect viruses and widely distributed in animals. *Genetics* 185, 1507–1517. doi:10.1534/genetics.110.116673

Mateo, L., and Gonzalez, J. (2014). Pogo-like transposases have been repeatedly domesticated into CENP-B-related proteins. *Genome Biol. Evol.* 6, 2008–2016. doi:10.1093/gbe/evu153

Miller, W. J., McDonald, J. F., Nouaud, D., and Anxolabehere, D. (1999). Molecular domestication--more than a sporadic episode in evolution. *Genetica,* 107, 197–207.

Moroz, L. L. (2011). Aplysia. *Curr. Biol.* 21, R60–R61. doi:10.1016/j.cub.2010.11.028

Moroz, L. L., Edwards, J. R., Puthanveettil, S. V., Kohn, A. B., Ha, T., Heyland, A., et al. (2006). Neuronal transcriptome of Aplysia: Neuronal compartments and circuitry. *Cell* 29 (127), 1453–1467. doi:10.1016/j.cell.2006.09.052

Moroz, L. L., Kocot, K. M., Citarella, M. R., Dosung, S., Norekian, T. P., Povolotskaya, I. S., et al. (2014). The ctenophore genome and the evolutionary origins of neural systems. *Nature* 510, 109–114. doi:10.1038/nature13400

Moroz, L. L., and Romanova, D. Y. (2021). Selective advantages of synapses in evolution. *Front. Cell. Dev. Biol.* 9, 726563. doi:10.3389/fcell.2021.726563

Morozov, V. M., Giovinazzi, S., and Ishov, A. M. (2017). CENP-B protects centromere chromatin integrity by facilitating histone deposition via the H3.3-specific chaperone Daxx. *Epigenetics Chromatin* 10, 63. doi:10.1186/s13072-017-0164-y

Muhammad, B. A., Almozyan, S., Babaei-Jadidi, R., Onyido, E. K., Saadeddin, A., Kashfi, S. H., et al. (2018). FLYWCH1, a novel suppressor of nuclear beta-catenin, regulates migration and morphology in colorectal cancer. *Mol. Cancer Res.* 16, 1977–1990. doi:10.1158/1541-7786.MCR-18-0262

Murrell, B., Moola, S., Mabona, A., Weighill, T., Sheward, D., Kosakovsky Pond, S. L., et al. (2013). Fubar: A fast, unconstrained bayesian approximation for inferring selection. *Mol. Biol. Evol.* 30, 1196–1205. doi:10.1093/molbev/mst030

Mustafin, R. N., and Khusnutdinova, E. K. (2020). Involvement of transposable elements in neurogenesis. *Vavilovskii Zhurnal Genet. Sel.* 24, 209–218. doi:10.18699/VJ20.613

Nei, M., and Gojobori, T. (1986). Simple methods for estimating the numbers of synonymous and nonsynonymous nucleotide substitutions. *Mol. Biol. Evol.* 3, 418–426. doi:10.1093/oxfordjournals.molbev.a040410

Nicholas, H. R., Lowry, J. A., Wu, T., and Crossley, M. (2008). The *Caenorhabditis elegans* protein CTBP-1 defines a new group of THAP domain-containing CtBP corepressors. *J. Mol. Biol.* 375, 1–11. doi:10.1016/j.jmb.2007.10.041

Ohno, S., Wolf, U., and Atkin, N. B. (1968). Evolution from fish to mammals by gene duplication. *Hereditas* 59, 169–187. doi:10.1111/j.1601-5223.1968.tb02169.x

Ow, M. C., Martinez, N. J., Olsen, P. H., Silverman, H. S., Barrasa, M. I., Conradt, B., et al. (2008). The FLYWCH transcription factors FLH-1, FLH-2, and FLH-3 repress embryonic expression of microRNA genes in *C. elegans*. *Genes. Dev.* 22, 2520–2534. doi:10.1101/gad.1678808

Pearson, J. C., Lemons, D., and McGinnis, W. (2005). Modulating Hox gene functions during animal body patterning. *Nat. Rev. Genet.* 6, 893–904. doi:10.1038/nrg1726

Peter, I. S., and Davidson, E. H. (2011). Evolution of gene regulatory networks controlling body plan development. *Cell.* 144, 970–985. doi:10.1016/j.cell.2011.02.017

Ponder, W. F., and Linderg, D. R. (2008). *Molluscan Evolution and Phylogeny: An introduction*. Berkeley (CA): Univ of California Press.

Punta, M., Coggill, P. C., Eberhardt, R. Y., Mistry, J., Tate, J., Boursnell, C., et al. (2011). The Pfam protein families database. *Nucleic Acids Res.* 40, D290–D301. doi:10.1093/nar/gkr1065

Redmond, A. K., and McLysaght, A. (2021). Evidence for sponges as sister to all other animals from partitioned phylogenomics with mixture models and recoding. *Nat. Commun.* 12, 1783. doi:10.1038/s41467-021-22074-7

Romanova, D. Y., Nikitin, M. A., Shchenkov, S. V., and Moroz, L. L. (2022). Expanding of Life Strategies in Placozoa: Insights From Long-Term Culturing of *Trichoplax* and *Hoilungia*. *Front. Cell Dev. Biol.* 10, 823283. doi:10.3389/fcell.2022.823283

Romanova, D. Y., Varoqueaux, F., Daraspe, J., Nikitin, M. A., Eitel, M., Fasshauer, D., et al. (2021). Hidden cell diversity in Placozoa: Ultrastructural insights from *Hoilungia hongkongensis*. *Cell Tissue Res.* 385, 623–637. doi:10.1007/s00441-021-03459-y

Roussigne, M., Kossida, S., Lavigne, A. C., Clouaire, T., Ecochard, V., Glories, A., et al. (2003). The THAP domain: A novel protein motif with similarity to the DNA-binding domain of P element transposase. *Trends Biochem. Sci.* 28, 66–69. doi:10.1016/S0968-0004(02)00013-0

Ryan, J. F., Pang, K., Schnitzler, C. E., Nguyen, A. D., Moreland, R. T., Simmons, D. K., et al. (2013). The genome of the ctenophore *Mnemiopsis leidyi* and its implications for cell type evolution. *Science* 342, 1242592. doi:10.1126/science.1242592

Shi, M., Lin, X. D., Chen, X., Tian, J. H., Chen, L. J., Li, K., et al. (2018). The evolutionary history of vertebrate RNA viruses. *Nature* 556, 197–202. doi:10.1038/s41586-018-0012-7

Shokri, L., Inukai, S., Hafner, A., Weinand, K., Hens, K., Vedenko, A., et al. (2019). A comprehensive *Drosophila melanogaster* transcription factor interactome. *Cell. Rep.* 27, 955–970.e7. doi:10.1016/j.celrep.2019.03.071

Siegmund, T., and Lehmann, M. (2002). The *Drosophila* Pipsqueak protein defines a new family of helix-turn-helix DNA-binding proteins. *Dev. Genes. Evol.* 212, 152–157. doi:10.1007/s00427-002-0219-2

Simakov, O., Marletaz, F., Cho, S. J., Edsinger-Gonzales, E., Havlak, P., Hellsten, U., et al. (2013). Insights into bilaterian evolution from three spiralian genomes. *Nature* 493, 526–531. doi:10.1038/nature11696

Smith, C. L., Varoqueaux, F., Kittelmann, M., Azzam, R. N., Cooper, B., Winters, C. A., et al. (2014). Novel cell types, neurosecretory cells, and body plan of the early-diverging metazoan *Trichoplax adhaerens*. *Curr. Biol.* 24, 1565–1572. doi:10.1016/j.cub.2014.05.046

Srivastava, M., Begovic, E., Chapman, J., Putnam, N. H., Hellsten, U., Kawashima, T., et al. (2008). The Trichoplax genome and the nature of placozoans. *Nature* 454, 955–960. doi:10.1038/nature07191

Stoltzfus, A. (1999). On the possibility of constructive neutral evolution. *J. Mol. Evol.* 49, 169–181. doi:10.1007/pl00006540

Sullivan, K. F., and Glass, C. A. (1991). CENP-B is a highly conserved mammalian centromere protein with homology to the helix-loop-helix family of proteins. *Chromosoma* 100, 360–370. doi:10.1007/BF00337514

Sundaram, V., and Wysocka, J. (2020). Transposable elements as a potent source of diverse cis-regulatory sequences in mammalian genomes. *Philos. Trans. R. Soc. Lond B Biol. Sci.* 375, 20190347. doi:10.1098/rstb.2019.0347

Suyama, M., Torrents, D., and Bork, P. (2006). PAL2NAL: Robust conversion of protein sequence alignments into the corresponding codon alignments. *Nucleic Acids Res.* 34, W609–W612. doi:10.1093/nar/gkl315

Vervoort, M., and Ledent, V. (2001). The evolution of the neural basic Helix-Loop-Helix proteins. *ScientificWorldJournal* 1, 396–426. doi:10.1100/tsw.2001.68

Volff, J. N. (2006). Turning junk into gold: Domestication of transposable elements and the creation of new genes in eukaryotes. *Bioessays* 28, 913–922. doi:10.1002/bies.20452

Whelan, N. V., Kocot, K. M., Moroz, L. L., and Halanych, K. M. (2015). Error, signal, and the placement of Ctenophora sister to all other animals. *Proc. Natl. Acad. Sci. U. S. A.* 112, 5773–5778. doi:10.1073/pnas.1503453112

Whelan, N. V., Kocot, K. M., Moroz, T. P., Mukherjee, K., Williams, P., Paulay, G., et al. (2017). Ctenophore relationships and their placement as the sister group to all other animals. *Nat. Ecol. Evol.* 1, 1737–1746. doi:10.1038/s41559-017-0331-3

Xu, Z., Yan, X., Maurais, S., Fu, H., O'Brien, D. G., Mottinger, J., et al. (2004). Jittery, a mutator distant relative with a paradoxical mobile behavior: Excision without reinsertion. *Plant Cell.* 16, 1105–1114. doi:10.1105/tpc.019802

Zattera, M. L., and Bruschi, D. P. (2022). Transposable elements as a source of novel repetitive DNA in the eukaryote genome. *Cells* 11, 3373. doi:10.3390/cells11213373

Zhang, H., Tao, Z., Hong, H., Chen, Z., Wu, C., Li, X., et al. (2016). Transposon-derived small RNA is responsible for modified function of WRKY45 locus. *Nat. Plants* 2, 16016. doi:10.1038/nplants.2016.16

frontiers | Frontiers in Cell and Developmental Biology

ORIGINAL RESEARCH
published: 09 June 2022
doi: 10.3389/fcell.2022.883755

Comparative Single-Cell Transcriptomics Reveals Novel Genes Involved in Bivalve Embryonic Shell Formation and Questions Ontogenetic Homology of Molluscan Shell Types

David A. Salamanca-Díaz[1†], *Elena A. Ritschard*[2†], *Hannah Schmidbaur*[2†] *and Andreas Wanninger*[1*†]

[1]Unit for Integrative Zoology, Department of Evolutionary Biology, University of Vienna, Vienna, Austria, [2]Division of Molecular Evolution and Development, Department of Neuroscience and Developmental Biology, University of Vienna, Vienna, Austria

Mollusks are known for their highly diverse repertoire of body plans that often includes external armor in form of mineralized hardparts. Representatives of the Conchifera, one of the two major lineages that comprises taxa which originated from a uni-shelled ancestor (Monoplacophora, Gastropoda, Cephalopoda, Scaphopoda, Bivalvia), are particularly relevant regarding the evolution of mollusk shells. Previous studies have found that the shell matrix of the adult shell (teleoconch) is rapidly evolving and that the gene set involved in shell formation is highly taxon-specific. However, detailed annotation of genes expressed in tissues involved in the formation of the embryonic shell (protoconch I) or the larval shell (protoconch II) are currently lacking. Here, we analyzed the genetic toolbox involved in embryonic and larval shell formation in the quagga mussel *Dreissena rostriformis* using single cell RNA sequencing. We found significant differences in genes expressed during embryonic and larval shell secretion, calling into question ontogenetic homology of these transitory bivalve shell types. Further ortholog comparisons throughout Metazoa indicates that a common genetic biomineralization toolbox, that was secondarily co-opted into molluscan shell formation, was already present in the last common metazoan ancestor. Genes included are *engrailed*, *carbonic anhydrase*, and *tyrosinase* homologs. However, we found that 25% of the genes expressed in the embryonic shell field of *D. rostriformis* lack an ortholog match with any other metazoan. This indicates that not only adult but also embryonic mollusk shells may be fast-evolving structures. We raise the question as to what degree, and on which taxonomic level, the gene complement involved in conchiferan protoconch formation may be lineage-specific or conserved across taxa.

Keywords: Mollusca, Bivalvia, Dreissena, eco-evodevo, trochophore, larval shell, single-cell seq, proteomics

OPEN ACCESS

Edited by:
Stefano Tiozzo,
Université Paris-Sorbonne, France

Reviewed by:
Marco Gerdol,
University of Trieste, Italy
Eve Gazave,
UMR7592 Institut Jacques Monod (IJM), France

***Correspondence:**
Andreas Wanninger
andreas.wanninger@univie.ac.at

***ORCID:**
David A. Salamanca-Díaz
orcid.org/0000-0003-2082-3939
Elena A. Ritschard
orcid.org/0000-0002-4956-9703
Hannah Schmidbaur
orcid.org/0000-0002-0099-7491
Andreas Wanninger
orcid.org/0000-0002-3266-5838

Specialty section:
This article was submitted to Evolutionary Developmental Biology, a section of the journal Frontiers in Cell and Developmental Biology

Received: *25 February 2022*
Accepted: *19 May 2022*
Published: *09 June 2022*

Citation:
Salamanca-Díaz DA, Ritschard EA, Schmidbaur H and Wanninger A (2022) Comparative Single-Cell Transcriptomics Reveals Novel Genes Involved in Bivalve Embryonic Shell Formation and Questions Ontogenetic Homology of Molluscan Shell Types. Front. Cell Dev. Biol. 10:883755. doi: 10.3389/fcell.2022.883755

INTRODUCTION

Mollusca constitutes one of the most diverse metazoan phyla. It is composed of two major subclades, Aculifera and Conchifera, which diverged from one another in the Cambrian (Vinther, 2015; Wanninger and Wollesen, 2015; Parkhaev, 2017; Wanninger and Wollesen, 2019). The Aculifera includes the vermiform, spicule-bearing Solenogastres (Neomeniomorpha) and Caudofoveata (Chaetodermomorpha), as well as the dorso-ventrally flattened Polyplacophora with eight shell plates. The primarily single-shelled Conchifera contains the Monoplacophora, Scaphopoda, Gastropoda, Bivalvia, and Cephalopoda (Kocot et al., 2011; Smith et al., 2011; Vinther, 2015). One molluscan key characteristic is the presence of a mineralized exoskeleton that may come in form of spicules and scales, single or bipartite shells, or serially arranged shell plates. This external armor might have played a crucial role in the evolutionary success of the phylum (Marin et al., 2014).

Molluscan shells and spicules are highly versatile morphological innovations that provide protection and, together with an elaborated musculature, often aid in maintaining structural support (Lowenstam and Weiner, 1989; Simkiss and Wilbur, 2012). They are formed as mineralized secretions from epithelial cells of the mantle (Marin et al., 2007; Furuhashi et al., 2009; Kocot et al., 2016). Once mineralized, shells present a considerable amount of variation in form and shape up to the microstructural level across the different taxa (Chateigner et al., 2000; Furuhashi et al., 2009). In conchiferan mollusks, the shell matrix, i.e., the outer layer of the mantle, is primarily composed of polysaccharides, glycoproteins, chitin, and calcium carbonate (Addadi et al., 2006; Marin et al., 2007). Previous studies that analyzed gene expression in adult mantle tissues of various bivalves and gastropods found that, despite sharing a common set of genes, the expression profiles in the shell matrix differ considerably between taxa, irrespective of their phylogenetic position. This has been used to argue that conchiferan adult shells (teleoconchs) are rapidly evolving features, thus providing an explanation for their high degree of morphological variation across lineages (Jackson et al., 2006; Aguilera et al., 2017; Clark et al., 2020; Yarra et al., 2021).

While conchiferan teleoconchs are continuously secreted from the mantle margin and are highly variable in shape and color, the first-formed embryonic shell (protoconch I) emerges in the gastrula or in the early trochophore larva from the dorsally situated embryonic shell gland (or shell field) in a short time window. It is typically of smooth, non-sculptured appearance (see Wanninger and Wollesen, 2015 for review). Some gastropods with long-lived veliger stages as well as most bivalves form an additional, intermediate shell type, the larval shell (protoconch II) that—similar to its developmental successor, the teleoconch—is secreted from the mantle edge. Only very few studies have focused on the cell lineage, morphological, biochemical, and molecular aspects of the formation of these elusive and microscopic protoconch types (Henry et al., 2004; Kakoi et al., 2008; Lyons et al., 2017; Liu et al., 2018; Liu et al., 2020). While embryonic and larval shell-forming cells have shown to express a common toolbox of markers such as chitin-binding proteins, von Willebrand factor type A domain-containing proteins, and carbonic anhydrases, they display numerous shell matrix proteins (SMPs) that are likely lineage-specific and also differ from those involved in teleoconch formation (Zhao et al., 2018, 2020). However, detailed analyses to assess the number and type of genes that are expressed during protoconch I and protoconch II formation are currently lacking. To fill this gap in knowledge, we reconstructed the shell formation toolbox during protoconch I development in the trochophore larva of the quagga mussel, *Dreissena rostriformis*, using a previously generated single-cell RNA-Seq dataset (Salamanca-Díaz et al., 2022). We also analyzed previously annotated genes which were shown to be expressed in the developing embryonic shell field across conchiferan mollusks for insights into the putative involvement of conserved versus hitherto unknown genes in this key developmental process in the bivalve life cycle.

MATERIALS AND METHODS

Single Cell RNA Sequencing Data Resources

Single cell RNA sequencing data from *Dreissena rostriformis* that had previously been generated (Salamanca-Díaz et al., 2022) were used for the assessment of unknown genes expressed in the shell field as well as for further analyses. In the following, a summary of all major steps from animal acquisition through the in silico analyses performed herein is provided.

Animal Collection and Cultures

Sexually mature individuals of *Dreissena rostriformis* were collected from the Danube River in Vienna, Austria (N 48°14′45.812″, O 16°23′38.145″). Collection took place between April and September 2019. Adults were gathered from underneath stones and transferred to the laboratory where they were cleaned and maintained in aquaria with filtered river water (FRW) at 19°C.

Spawning of animals was induced by incubating sexually mature specimens in a 10^{-3} M solution of serotonin for 15 min (Sigma-Aldrich, Darmstadt, Germany) in FRW, followed by one wash and subsequent maintenance in FRW. Individuals were kept isolated in FRW in 50 ml glass beakers and after approximately 30 min, up to 50% of the treated specimens started to spawn. Fertilization occurred when three to four drops of sperm-containing water were added to 50 ml glass beakers with oocytes. After fertilization, water was changed every half an hour for the first 3 h and then every 6 h to remove excess sperm and avoid bacterial and fungal growth. The embryos were cultured at 23°C.

10X Single-Cell 3′RNAseq

Sample Preparation

Cell dissociations of *Dreissena* larvae were generated by first washing 13 h post fertilization (hpf) old trochophore larvae over a 20 μm mesh with sterile media (autoclaved fresh river water; AFRW). Larvae were concentrated and dissociated by first passing them through a syringe with a hypodermic needle

with 0.4 mm diameter. A single-cell suspension was loaded into a 10x Chromium Controller using Chromium Single Cell 3' Kit v2 reagents (Cat #120237, 10xGenomics, United States). cDNA synthesis and library construction were made according to specifications from the manufacturer. Library quantification was performed on a bioanalyzer (High Sensitivity DNA reagents, Agilent Technology #5067-4626; Agilent 2100 Bioanalyzer) and sequenced on the Illumina platform as previously described (Salamanca-Díaz et al., 2022).

Mapping Tool Preparation and Cell Clustering

The transcriptomes used for creating the mapping tool and the reference genome used to map the reads against were previously generated (Calcino et al., 2019). In our study, gene models were elongated by 2 kilobases in the 3′ direction to account for poorly annotated three-prime ends in the gene models (Levin et al., 2016). In order to obtain a reference gene nomenclature for the transcriptome of *Dreissena*, we performed a BLASTX search against both human and the Pacific giant oyster (*Crassostrea gigas*) genome for each individual gene sequence. For each transcript, the BLAST hit with the highest E-value was selected for annotation. We utilized InterProScan v5.46-81.0 (Jones et al., 2014) to search for gene ontology and to allocate domains on the reference genome by surveying publicly available databases such as GO terms, Pfam, and PANTHER (**Supplementary Table S3**). The reference database used in this study was generated by Salamanca-Díaz et al. (2022) using CellRanger Makeref v3.1.0 and demultiplexed using CellRanger Makefastq v3.1.0 with default settings and filtered according to cell barcode and Unique Molecular Markers (UMIs). The resulting cell count gene expression matrix was analyzed in R v3.6.1 (R Development Core Team, 2015) with the Seurat v4.0.1 package (Satija et al., 2015). The count matrix was processed through a standard Seurat pipeline using default parameters. We then generated a KNN graph and clustered the data. Marker genes were identified according to the enrichment and expression of these in at least 10% of the cells in each population (min.pct = 0.1) and with a log fold difference larger than 0.6 (logfc.threshold = 0.6). After this, we selected the differentially expressed genes from the cluster annotated as "shell field" from Salamanca-Díaz et al. (2022) for in-depth homology assessments with respective sequences from other metazoan taxa.

Assessment of Unknown Genes and Gene Architecture Annotations

To assess the orthology relationships of shell field-specific genes in the trochophore stage of *D. rostriformis* with genes of other metazoan species, we performed a comparative analysis using OrthoFinder2 (Emms & Kelly, 2019). The genomes, transcriptomes, and gene models for 30 species were analyzed in addition to the previously generated *D. rostriformis* transcriptome and genome assembly (Calcino et al., 2019). These 30 species represent major sub-phylum-level metazoan lineages and were obtained from publicly available data (**Supplementary Table S1**). At first, proteins were filtered for the longest transcript per gene and used as an input to OrthoFinder. After this, all-versus-all similarity search was obtained using DIAMOND v0.9.15 (Buchfink et al., 2015) and used as input to OrthoFinder2 to identify orthogroups, which are groups of proteins that are likely homologous. Subsequently, proteins belonging to each orthogroup were aligned using MAFFT v7.221 (Katoh & Standley, 2013) for multiple sequence alignments to generate gene trees using FastTree (Price et al., 2009) (-a 16 -b WorkingDirectory -M msa -A mafft -T fasttree). The resulting trees were parsed with the OrthoFinder2 pipeline to discriminate between orthologs and paralogs within each orthogroup. Afterwards, we overlapped these results with the gene sets previously characterized through differentially expressed genes in the single-cell RNA sequencing of the shell field. This resulted in identification of the orthogroups which contain differentially expressed genes in the shell field of the trochophore larva.

For insights into the architecture of genes that are differentially expressed in the shell field, we used the webserver of SignalP v5.0 with default parameters (Almagro Armenteros et al., 2019) to search for signal peptides in each corresponding sequence. Additionally, TMHMM v2.0 webserver (Krogh et al., 2001) was used to screen transmembrane domains and predict which amino acid sequences have domains on the outer side of the plasma membrane. For insights into the tertiary structure of the peptide sequence of each gene from this set, we used the Phyre2 webserver (Kelley et al., 2015). Further gene annotations, corresponding to Pfam, PANTHER, GO term, human, and *Crassostrea gigas* ortholog similarity, were implemented from a previous study (Salamanca et al., 2022). Gene expression levels of the 17 existing transcriptome libraries (Calcino et al., 2019) were quantified with Kallisto (transcripts per million, TPM) (Bray et al., 2016). Expression data from *Crassostrea gigas* were collected from public databases (**Supplementary Table S1**) and TPM values were calculated following the pipeline of a previous study (Zieger et al., 2021). Heatmaps showing normalized quantitative expression of genes were plotted with R (R Developement Core Team, 2015) with the heatmap function from the ComplexHeatmap R package (Gu et al., 2016) (**Figure 1**, **Supplementary Table S3**).

RESULTS

Overall Orthogroup Statistics of the *Dreissena rostriformis* Genome

To discard false positives while screening for novel genes in the shell field, the orthology assessment was made using the whole genome of *Dreissena rostriformis*. After that, we analyzed the genes that are exclusively part of the transcriptomic signature from the shell field of the trochophore larva. Around one third of all orthogroups (31.4%) predicted from 30 different metazoan species contain *Dreissena rostriformis* ("DRERO") genes (cf. **Supplementary Table S3**). In addition, we identified *D. rostriformis* lineage-specific orthogroups with non-annotated genes, meaning there is a noteworthy number of genes that have no known match with any other animal sampled. However, all other species used in our analysis show similar low percentages of genes that can be assigned to known orthogroups (**Supplementary Table S3**), corroborating the common notion of the vital role of lineage specific genes or families during animal genome evolution (Fernández and Gabaldón, 2020). In *D. rostriformis*, such

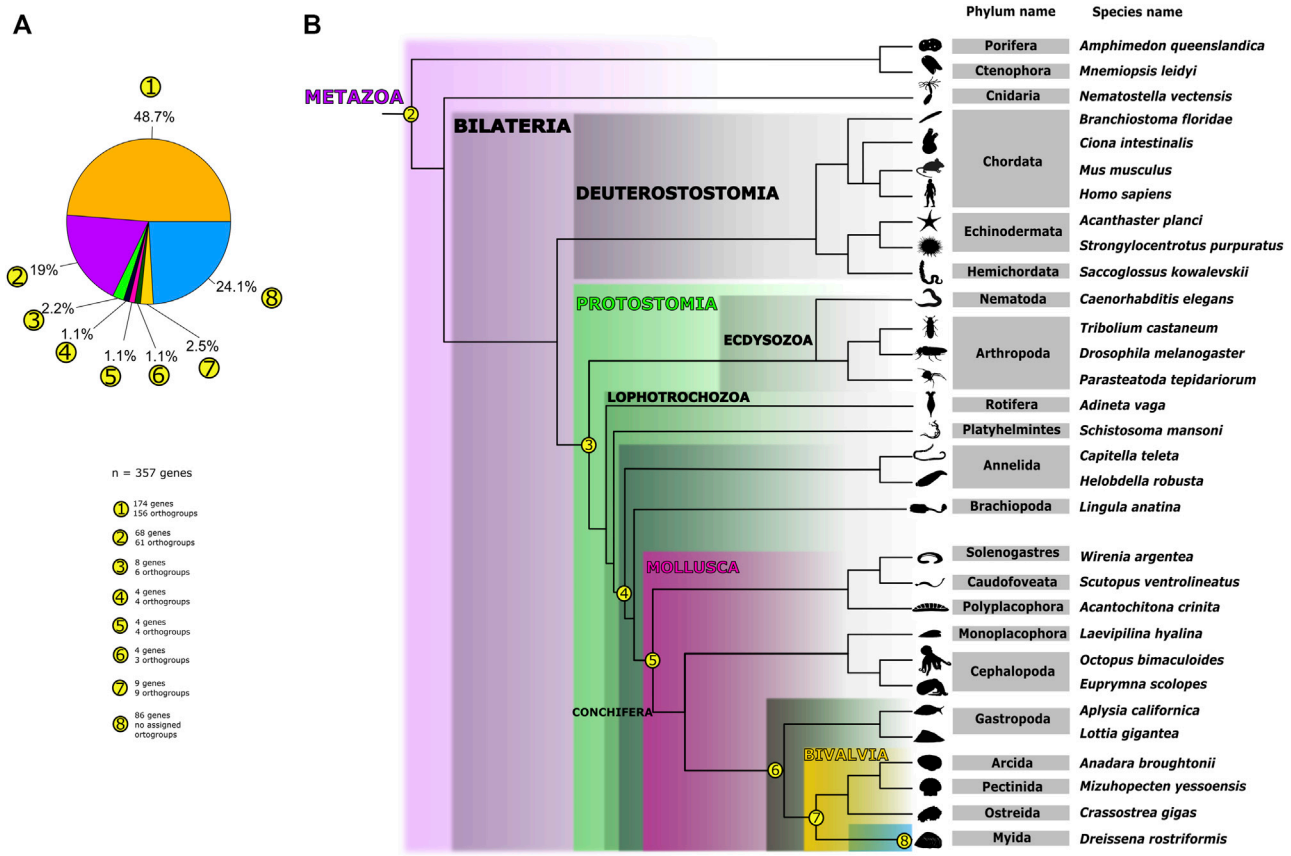

FIGURE 1 | Distribution of orthogroups containing shell field-specific genes from *Dreissena rostriformis* across Metazoa. **(A)** Pie chart representing the number of orthogroups and genes found in the respective taxa. Each subset of orthogroups is numbered (1-8), indicating how many shell field-specific genes are contained in each taxon, together with the total amount of shell field-specific genes analyzed. **(B)** Dendrogram representing phylogenetic relationships of the sampled species and the presence of orthogroups and genes on each node. Phylogenetic relationships of the sampled species are plotted on a class-level tree based on previous studies (Smith et al., 2011; Laumer et al., 2019; Lemer et al., 2019; Fernández and Gabaldón, 2020; Li et al., 2021). Numbers correspond to those in **(A)**. Number 1 refers to all shell field orthogroups that are randomly distributed (i.e., diverse and without distinct pattern) among the sampled metazoans (48.7%). Numbers 2–8 depict the shell field genes/orthogroups identified for the respective nodes in the phylogeny. Node (2) refers to the 19% of all shell field orthogroups present in all sampled metazoan genomes in this study. Node (3) is equivalent to 2.2% of all shell field orthogroups present in sampled protostome organisms. Node (4) corresponds to the 1.1% of orthogroups present in the sampled organisms classified as Lophotrochozoa. Node (5) refers to all shell field orthogroups present exclusively in the sampled mollusks (1.1%). Node (6) represents all shell field orthogroups (1.1%) present in the gastropod and bivalve genomes sampled. Node (7) depicts all shell field orthogroups (2.5%) present in bivalve genomes analyzed here. Node (8) represents all *D. rostriformis*-specific shell field genes that could not be assigned to any orthogroup. Species silhouettes were obtained from www.phylopic.org and are either licensed under Creative Commons Attribution 3.0 Unported or are available under public domain.

genes identified from the genome mount up to 19.8% (7469 genes; see **Supplementary Tables S2, S3**).

Orthogroups Containing Genes From the Trochophore Shell Field

Using the outputs from the OrthoFinder and Single-cell seq pipelines, we characterized the shell field-specific genes and their orthogroup correspondence (**Supplementary Table S2**). In total, we analyzed 357 genes differentially expressed in shell field cells from the trochophore stage of *Dreissena rostriformis*. Gene ontology terms of these genes showed enrichment in shell formation-associated processes such as vesicle-mediated transport, phospholipid metabolic processing, integrin-mediated signaling pathway, and positive regulation of cell cycle G2/M phase progress (Salamanca-Díaz et al., 2022; **Supplementary Table S2**). Tertiary structure analysis using the Phyre2 webserver coincide with and thus confirm the results from SignalP and Interproscan (**Supplementary Tables S2, S5, S6** and **Supplementary File S1**). In addition, expression dynamics of shell matrix genes during development of the trochophore of *D. rostriformis* were analyzed and compared with shell field-specific genes from pre-metamorphosis stages of the oyster *Crassostrea gigas* using previously published RNA-seq data (**Figure 2**, **Supplementary Tables S7, S8**) (Zhao et al., 2018; Calcino et al., 2019). Expression of most of these genes starts early in development, i.e., shortly after fertilization, likely by maternal transcripts. High normalized peaks of transcription are seen throughout the late gastrula and trochophore stages (during which the protoconch I is established) and continue in the veliger stages (continuous protoconch II formation) *i.e.*, between 13 and 48 hpf. *In situ* hybridization experiments of some of these

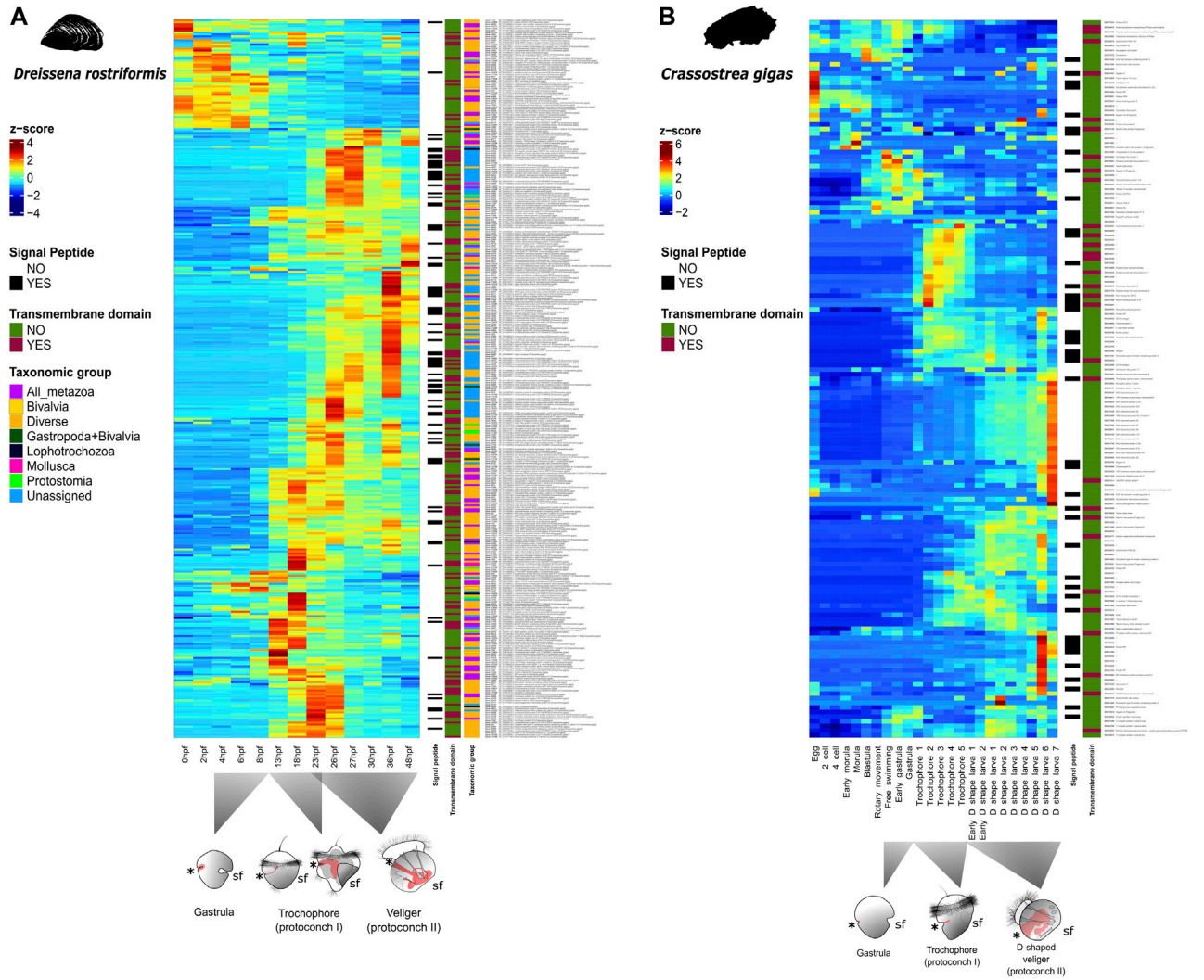

FIGURE 2 | Relative quantitative expression of shell field-specific genes during development of two bivalve species. **(A)** Heat map showing relative normalized expression levels for each isolated gene from the shell field of the trochophore of *Dreissena rostriformis*. Normalized gene expression (transcripts per million; TPM) is depicted in graded shades of red when values are above the median, those below this threshold and with a value close to zero are in shades of blue. Details on gene annotations, orthogroup assignments to the respective taxonomic level, presence of signaling peptides, and transmembrane domains are provided in **Supplementary Table S2**. Blast top hit to the Pacific oyster is next to each gene name. Time after fertilization (hpf) and corresponding developmental stages at 23°C are ordered chronologically at the bottom of the *x* axis. Germ layers and their major derivatives in animal schemes are depicted in grey (mesoderm), red (endoderm), and white (ectoderm), respectively. Asterisks mark the blastopore/mouth, sf indicates the shell field. **(B)** Heat map showing relative normalized expression levels of genes isolated from larval and adult shells of *Crassostrea gigas* as described in Zhao et al. (2018). Normalized gene expression is depicted in graded shades of red when values are above the median, those below this threshold and with a value close to zero are in shades of blue. Each developmental stage is organized chronologically from left to right on the *x* axis. Details on gene annotations, orthogroup assignments, presence of signaling peptides, and transmembrane domains are provided in **Supplementary Table S9** (cf. Zhao et al., 2018).

genes have previously shown a high level of expression in stages of embryonic shell (protoconch I) formation (e.g., *Hox 1*, *hic31*) (Salamanca-Díaz et al., 2021; Salamanca-Díaz et al., 2022). Furthermore, numerous orthogroups that contain genes that are specific to the embryonic shell field are shared across Metazoa (**Supplementary Tables S2, S4**. This demonstrates multiple cooption events of these genes into various functions in the respective metazoan lineages (**Supplementary Table S1**). However, we also found a group of genes (68 genes in 61 orthogroups; e.g., *engrailed*, *cyclin-A2, carbonic anhydrase*, *tyrosinase* homologs) active in *D. rostriformis* shell field formation that are also involved in shell formation of other mollusks (Nederbragt et al., 2002; Iijima et al., 2008; Kin et al., 2009; Samadi and Steiner, 2009; Huan et al., 2020; Zhao et al., 2020). These genes are also present in all other metazoans screened for herein and are commonly known to be related to body plan specification, cell cycle, and metalloenzyme activity (**Figure 1** and **Supplementary Table S2**).

A closer analysis of specific taxonomic orthogroups (e.g., Protostomia, Lophotrochozoa) revealed that the majority of the genes (48.7%) that are differentially expressed in the shell field in *D. rostriformis* have orthologs in other taxa. However, their distribution between the given taxa is highly variable (**Figure 1**, **Supplementary Tables S2, S4**). While 19% of the shell field-specific genes are shared with other metazoan taxa, only 2.24% of the total number of shell field-specific genes are shared with other protostome species (8 genes in 6 orthogroups), and 1.1% of the same total number of genes are restricted to lophotrochozoans (4 genes in 4 orthogroups). Within molluscs, 1.1% of the shell field-specific genes are shared with other conchiferans, another 1.1% were only found in the sampled bivalves and gastropods, and 2.5% are possibly bivalve-specific. A quarter of the shell field-specific genes were only found in *D. rostriformis* and are not shared with other taxa. These may either genus- or species-specific genes, however their evolutionary history needs to be assessed in more depth once more bivalve datasets become available. The majority of genes in all orthogroups do not have a match in the InterPro database but show low level similarities with human orthologs (e-values higher than 1). Among the few genes with annotations in these groups, there is a member of the Claudin protein family, a *keratin* ortholog, epidermal growth factor domains, *heat shock 70 kDa protein*, and an *endonuclease 2* ortholog. Genes expressed in the shell field which are restricted to Mollusca lack confident annotations (**Supplementary Table S2**). Human blast hits show only few domain commonalities to genes with a role in protein modification, DNA repair, nuclear envelope component and ion exchange, i.e., *DDB1 and CUL4 associated factor 4*, *DNA repair protein XRCC1, nuclear envelope integral membrane protein 2*, and *sodium-driven bicarbonate exchanger*.

The number of hitherto non-annotated genes shows a tendency to decrease when analyzing the different lineages inside Mollusca. This suddenly changes in the branch leading to *Dreissena rostriformis*, where the number of shell field-specific genes notably increases (**Figure 1**). Within Conchifera, a putative Bivalvia + Gastropoda clade shows 2 hitherto undescribed genes in 2 separate orthogroups and Bivalvia alone presents a unique set of 9 genes in 9 orthogroups (**Figure 1**, **Supplementary Table S2**). In this gene set, there are low e-values and little similarity to human as well as *Crassostrea gigas* orthologs, with blast hits to genes associated to antioxidant reactions, cell migration, cell attachment, and cellular proliferation, i.e., *superoxide dismutase*, *myomegalin*, *laminin subunit beta-4*, and *ETS domain-containing transcription factor ERF*. Additionally, from the genes expressed in the *D. rostriformis* embryonic shell field which were not assigned to any orthogroup or have a specific identity, and thus are considered here for *Dreissena* to be lineage-specific (86 genes in total, 24% of all shell field genes), 39 have transmembrane domains and 41 have signal peptides. This suggests that almost half of this gene subset is probably crucial for cell signaling since it has domains that interact directly with the outside of the cell membrane (**Supplementary Tables S2, S5, S6**). Altogether, our results show that, while there is a core gene set expressed in the embryonic shell field which is present throughout Metazoa, there is also strong indication of novel gene emergence that is specific to the embryonic shell field of the *Dreissena* trochophore.

DISCUSSION

High Number of Putative Novel Lineage-Specific Genes Involved in Embryonic Shell Formation

Previous studies have characterized the shell secretomes from larval and adult stages of two marine bivalves, *Pinctada fucata* and *Crassostrea gigas*. They found that, despite having some common gene expression signatures (e.g., *carbonic anhydrase*, *chitin binding protein*, and *von Willebrand factor type A*), they also show distinct expression patterns of larval shell matrix proteins depending on species and developmental stages. One significant subset of the genes (around 90 out of 156 genes) involved in shell secretion is expressed in trochophore stages, while the other genes are expressed during the later D-shape veliger stages, suggesting different molecular signatures underlying embryonic versus larval shell formation (Zhao et al., 2018). This calls into question the homology of embryonic and larval shells in Bivalvia. Since solid data on the genes involved in bivalve teleoconch formation are still lacking, evolutionary relationships between the adult and the two transitory protoconch shell types currently remain unknown. This underlines that more in-depth comparative studies are needed to assess the decades-old question of (ontogenetic) homology of conchiferan embryonic, larval, and adult shells within the respective sublineages (particularly bivalves, gastropods, and scaphopods).

Our study shows that 24% (86) of the genes differentially expressed in the shell field of the trochophore of *D. rostriformis* could not be assigned to any orthogroup and may thus be genus- or species-specific (**Figure 1A**). From these, 13 unassigned genes have only incomplete annotations in specific regions of each gene sequence, 41 have low e-value similarity with human or *Crassostrea* orthologs, and 32 of these genes have no known annotation or ortholog match (**Supplementary Table S2**). Similar trends are also known from other mollusks, where unassigned and undescribed genes expressed in shell- and plate-forming cells appear to be highly taxon-specific. For example, secretomes from adult gastropods, bivalves, polyplacophorans, and a nautiloid cephalopod show considerable levels of lineage-specific orphan genes (Jackson et al., 2006, 2009; Immel et al., 2016; Kocot et al., 2016; Marin, 2020; Setiamarga et al., 2021). It has been argued previously that the rapid evolutionary rate of these genes may be a possible reason for the lack of orthology detection of these shell matrix toolbox genes (Aguilera et al., 2017). This, in turn, could be the result of evolutionary responses to the widely varying ecological conditions shell-bearing mollusks are exposed to, since most of the gene products in the shell field are in direct contact with the environment. Interestingly, almost half of these lineage-specific orphan genes have transmembrane domains and/or signaling peptides (**Supplementary Tables S2, S5, S6**). This suggests that genes expressed in the shell field at the trochophore stage might be significantly influenced by the ecology of the larva. Previous studies

have found that molluscan shell proteomes drastically change when ecological factors such as the pH or the temperature are altered, but combined experimental and transcriptomic studies are currently too scarce for robust conclusions on an evolutionary level (Timmins-Schiffman et al., 2014; Wei et al., 2015). However, since the environmental conditions during protoconch I and protoconch II formation are identical in *D. rostriformis*, this might hint towards an independent evolutionary origin (and thus argue against ontogenetic homology) of these shell types. This is further supported by the fact that, after shell field formation, there is a fluctuation of gene expression throughout development, *i.e.*, *Chitin binding domain* ortholog (Gene.49769) and *voltage-dependent calcium channel subunit alpha-2/delta-4* human ortholog (Gene.25093) (**Figure 2A**), demonstrating putatively different expression dynamics during protoconch I and protoconch II formation, respectively. A similar tendency emerges when comparing temporal expression dynamics of shell-specific genes of *D. rostriformis* with *C. gigas* (**Figure 2B**). The Pacific oyster seems to have different sets of genes with alternate expression throughout developmental stages where shell field formation is active, just as in *Dreissena,* thus calling into question the homology of bivalve ontogenetic shell types (cf. Zhao et al., 2018). However, further comparative studies employing different developmental stages of the same as well as similar developmental stages of different species are needed to further assess this assumption.

Metazoan Biomineralization Gene Repertoires

Our single-cell RNAseq and OrthoFinder analyses grouped 271 (76%) out of 357 identified genes that are differentially expressed in shell field cells from the trochophore stage of *Dreissena rostriformis* into orthogroups shared with different taxa. From these resulting orthogroups, there is a fraction of *Dreissena* trochophore shell field-specific genes that are shared with the rest of the sampled metazoans (68 genes in 61 orthogroups, 19%) (**Figure 1**, **Supplementary Table S2**). It has been shown previously that mantle secretomes in other bivalves and gastropods also possess a wide range of gene families that originated prior to the emergence of the conchiferan clade (Kocot et al., 2016; Aguilera et al., 2017). Among this, a set of genes from the shell field of *Dreissena*, which are present in other metazoans, is known to be involved in extracellular matrix formation, such as orthologs of *laminin*, *C-type lectin* domains, and immunoglobulins (**Supplementary Table S2**). Additionally, among this set there are genes containing leucine-rich repeat domains and semaphorins, which are also found throughout metazoans (**Supplementary Table S2**). Moreover, genes from this subset of orthogroups were coopted into embryonic shell formation in conchiferan mollusks such as *Dreissena*, e.g., *Hox 1* (Gene.152834), *Hox 4* (Gene.66474), *Lox 4* (Gene.142102), and *engrailed* (Gene.126286) (**Figure 1**, **Supplementary Table S2**) as previously described for other species of mollusks (Samadi & Steiner, 2009; Fritsch et al., 2015; Wollesen et al., 2018; Huan et al., 2020; Liu et al., 2020; Salamanca-Díaz et al., 2021). Furthermore, in these orthogroups there are genes that have been found to be also involved in biomineralization processes in echinoderms and vertebrates, e.g., *Cyclophilin-type* (Gene.103270) and *Carbonic anhydrase* (Gene.82229) (Livingston et al., 2006; Mann et al., 2008; Mann et al., 2010; Mann and Edsinger, 2014). Such an organic matrix is formed prior to secretion of the mineralized part of the shell and is thus of crucial importance for conchiferan mollusks, but the respective factors involved are also present in other metazoans that lack a shell (**Supplementary Table S2**) (Marie et al., 2010; Marie et al., 2011a; Marie et al., 2011b; Marie et al., 2012; Marin et al., 2014). Altogether, our data point towards a shared "molecular biomineralization toolbox" across Metazoa, but a broader taxon sampling especially from key invertebrate phyla are required for deeper evolutionary insights. Given the fact that numerous animal phyla contain taxa with mineralized hard parts, including accessible representatives such as annelids, brachiopods, other lophotrochozoans, as well as numerous arthropods, this hypothesis can be tested by comparative studies using single-cell RNA transcriptomic approaches.

Taken together, the quagga mussel *Dreissena rostriformis* shows a mosaic of co-option of known metazoan genes and *de novo* recruitment of genes with hitherto unknown function or ortholog match into embryonic (protoconch I) shell formation. Our data suggest that not only adult but also embryonic bivalve shells are highly plastic in the gene repertoire that underlie their ontogeny, which may be indicative of non-homology of bivalve—and possibly conchiferan - ontogenetic shell types.

DATA AVAILABILITY STATEMENT

The data presented in this study are deposited in NCBI's Gene Expression Omnibus and are accessible through the GEO series accession number GSE192624 (https://www.ncbi.nlm.nih.gov/geo/query/acc.cgi?acc=GSE192624).

AUTHOR CONTRIBUTIONS

DS and AW designed the research. DS performed the experiments and generated data with contribution of ER and HS. DS performed the data analysis with assistance of ER. DS drafted the manuscript with input from AW, ER and HS. DS and AW interpreted and discussed the findings and finalized the manuscript. All authors contributed to interpretation of data and approved the final version of the manuscript.

FUNDING

This work was supported by the completion grant of the Vienna Doctoral School Ecology and Evolution (VDSEE) to DS and by the Austrian Science Fund (FWF) (grant P29455-B29 to AW).

ACKNOWLEDGMENTS

The authors thank Nicolas S. M. Robert (Vienna) for his support and valuable input when developing the OrthoFinder pipeline and for advice during data acquisition.

SUPPLEMENTARY MATERIAL

The Supplementary Material for this article can be found online at: https://www.frontiersin.org/articles/10.3389/fcell.2022.883755/full#supplementary-material

Supplementary Table S1 | Genome and proteomes of publicly available data. Columns show species scientific names, common names, their respective abbreviation used in this study, databases where the data were obtained from, as well as the molecular nature (either genome or transcriptome assembly) of each sample.

Supplementary Table S2 | Annotations of shell field genes from *Dreissena rostriformis*. Results show the orthofinder, InterProScan, TMHMM, SignalP, and BLAST searches against the human genome. Each column corresponds to the gene code from the quagga mussel, the analysis performed on the aminoacid sequence, the signature accession result of the analysis, signature description, accession code on the InterPro database, InterPro description, associated gene ontology terms, similarity index of the analysis (e-value), blast top hit against the human genome and the Pacific oyster with the respective e-value, presence of transmembrane domains and signal peptides, orthogroup containing the corresponding gene and the taxonomic clades containing that orthogroup, and the length of the protein sequence of each gene.

Supplementary Table S3 | Statistics result of the orthofinder analysis showing the number of genes assigned to each orthogroup for all species used in the analysis.

Supplementary Table S4 | Resulting orthogroups that contain at least one shell field gene obtained from the single cell RNA seq analysis from *D. rostriformis*.

Supplementary Table S5 | Transmembrane helices domains predicted for trochophore shell field genes from *D. rostriformis* with the TMHMM 2.0 webserver.

Supplementary Table S6 | Signal peptide-positive proteins prediction for the trochophore shell field genes from *D. rostriformis* with the SignalP 5.0 software.

Supplementary Table S7 | Raw data of relative expression levels (transcripts per million, TPM) of *Dreissena rostriformis* shell field genes throughout development.

Supplementary Table S8 | Raw data of relative expression levels (transcripts per million, TPM) of *Crassostrea gigas* shell field genes throughout development [based on Zhao et al. (2018)].

Supplementary Table S9 | Annotations of shell-related genes from *Crassostrea gigas*. Results from annotations of shell protein matrix genes taken from Zhao et al. (2018). Each column corresponds to annotations assigned in Zhao et al. (2018). Indicated is the gene code from the NCBI database, the result of the analysis performed on the aminoacid sequence showing the presence of transmembrane domains and signal peptides, and the assigned signature description.

Supplementary File S1 | Output generated from the Phyre2 webserver. Summary results and files are in pdb format for the predicted tertiary structure of each amino acid sequence of the dataset.

REFERENCES

Addadi, L., Joester, D., Nudelman, F., and Weiner, S. (2006). Mollusk Shell Formation: a Source of New Concepts for Understanding Biomineralization Processes. *Chem. Eur. J.* 12 (4), 980–987. doi:10.1002/chem.200500980

Aguilera, F., McDougall, C., Degnan, B. M., and Irwin, D. (2017). Co-option and De Novo Gene Evolution Underlie Molluscan Shell Diversity. *Mol. Biol. Evol.* 34 (4), msw294–792. doi:10.1093/molbev/msw294

Almagro Armenteros, J. J., Tsirigos, K. D., Sønderby, C. K., Petersen, T. N., Winther, O., Brunak, S., et al. (2019). SignalP 5.0 Improves Signal Peptide Predictions Using Deep Neural Networks. *Nat. Biotechnol.* 37 (4), 420–423. doi:10.1038/s41587-019-0036-z

Bray, N. L., Pimentel, H., Melsted, P., and Pachter, L. (2016). Near-optimal Probabilistic RNA-Seq Quantification. *Nat. Biotechnol.* 34, 525–527. doi:10.1038/nbt.3519

Buchfink, B., Xie, C., and Huson, D. H. (2015). Fast and Sensitive Protein Alignment Using DIAMOND. *Nat. Methods* 12 (1), 59–60. doi:10.1038/nmeth.3176

Calcino, A. D., de Oliveira, A. L., Simakov, O., Schwaha, T., Zieger, E., Wollesen, T., et al. (2019). The Quagga Mussel Genome and the Evolution of Freshwater Tolerance. *DNA Res.* 26 (5), 411–422. doi:10.1093/dnares/dsz019

Chateigner, D., Hedegaard, C., and Wenk, H.-R. (2000). Mollusc Shell Microstructures and Crystallographic Textures. *J. Struct. Geol.*, 22(11), 1723–1735. doi:10.1016/S0191-8141(00)00088-2

Clark, M. S., Peck, L. S., Arivalagan, J., Backeljau, T., Berland, S., Cardoso, J. C. R., et al. (2020). Deciphering Mollusc Shell Production: the Roles of Genetic Mechanisms through to Ecology, Aquaculture and Biomimetics. *Biol. Rev.*, n a. doi:10.1111/brv.12640

Emms, D. M., and Kelly, S. (2019). OrthoFinder: Phylogenetic Orthology Inference for Comparative Genomics. *Genome Biol.* 20 (1), 238. doi:10.1186/s13059-019-1832-y

Fernández, R., and Gabaldón, T. (2020). Gene Gain and Loss across the Metazoan Tree of Life. *Nat. Ecol. Evol.* 4 (4), 524–533. doi:10.1038/s41559-019-1069-x

Fritsch, M., Wollesen, T., de Oliveira, A. L., and Wanninger, A. (2015). Unexpected Co-linearity of Hox Gene Expression in an Aculiferan Mollusk. *BMC Evol. Biol.* 15 (1), 151. doi:10.1186/s12862-015-0414-1

Furuhashi, T., Schwarzinger, C., Miksik, I., Smrz, M., and Beran, A. (2009). Molluscan Shell Evolution with Review of Shell Calcification Hypothesis. *Comp. Biochem. Physiology Part B Biochem. Mol. Biol.*, 154(3), 351–371. doi:10.1016/j.cbpb.2009.07.011

Gu, Z., Eils, R., and Schlesner, M. (2016). Complex Heatmaps Reveal Patterns and Correlations in Multidimensional Genomic Data. *Bioinformatics* 32 (18), 2847–2849. doi:10.1093/bioinformatics/btw313

Henry, J. Q., Okusu, A., and Martindale, M. Q. (2004). The Cell Lineage of the Polyplacophoran, *Chaetopleura apiculata*: Variation in the Spiralian Program and Implications for Molluscan Evolution. *Dev. Biol.*, 272(1), 145–160. doi:10.1016/j.ydbio.2004.04.027

Huan, P., Wang, Q., Tan, S., and Liu, B. (2020). Dorsoventral Decoupling of Hox Gene Expression Underpins the Diversification of Molluscs. *Proc. Natl. Acad. Sci. U.S.A.* 117 (1), 503–512. doi:10.1073/PNAS.1907328117

Iijima, M., Takeuchi, T., Sarashina, I., and Endo, K. (2008). Expression Patterns of Engrailed and dpp in the Gastropod Lymnaea Stagnalis. *Dev. Genes Evol.* 218 (5), 237–251. doi:10.1007/s00427-008-0217-0

Immel, F., Broussard, C., Catherinet, B., Plasseraud, L., Alcaraz, G., Bundeleva, I., et al. (2016). The Shell of the Invasive Bivalve Species *Dreissena polymorpha*: Biochemical, Elemental and Textural Investigations. *PLOS ONE* 11 (5), e0154264. doi:10.1371/journal.pone.0154264

Jackson, D. J., McDougall, C., Green, K., Simpson, F., Wörheide, G., and Degnan, B. M. (2006). A Rapidly Evolving Secretome Builds and Patterns a Sea Shell. *BMC Biol.* 4 (1), 40. doi:10.1186/1741-7007-4-40

Jackson, D. J., McDougall, C., Woodcroft, B., Moase, P., Rose, R. A., Kube, M., et al. (2009). Parallel Evolution of Nacre Building Gene Sets in Molluscs. *Mol. Biol. Evol.* 27 (3), 591–608. doi:10.1093/molbev/msp278

Jones, P., Binns, D., Chang, H.-Y., Fraser, M., Li, W., McAnulla, C., et al. (2014). InterProScan 5: Genome-Scale Protein Function Classification. *Bioinformatics* 30 (9), 1236–1240. doi:10.1093/bioinformatics/btu031

Kakoi, S., Kin, K., Miyazaki, K., and Wada, H. (2008). Early Development of the Japanese Spiny Oyster (Saccostrea Kegaki): Characterization of Some Genetic Markers. *Zoological Sci.* 25 (5), 455–464. doi:10.2108/zsj.25.455

Katoh, K., and Standley, D. M. (2013). MAFFT Multiple Sequence Alignment Software Version 7: Improvements in Performance and Usability. *Mol. Biol. Evol.* 30 (4), 772–780. doi:10.1093/molbev/mst010

Kelley, L. A., Mezulis, S., Yates, C. M., Wass, M. N., and Sternberg, M. J. E. (2015). The Phyre2 Web Portal for Protein Modeling, Prediction and Analysis. *Nat. Protoc.* 10 (6), 845–858. doi:10.1038/nprot.2015.053

Kin, K., Kakoi, S., and Wada, H. (2009). A Novel Role for dpp in the Shaping of Bivalve Shells revealed in a Conserved Molluscan Developmental Program. *Dev. Biol.* 329 (1), 152–166. doi:10.1016/j.ydbio.2009.01.021

Kocot, K. M., Aguilera, F., McDougall, C., Jackson, D. J., and Degnan, B. M. (2016). Sea Shell Diversity and Rapidly Evolving Secretomes: Insights into the Evolution of Biomineralization. *Front. Zool.* 13 (1), 23. doi:10.1186/s12983-016-0155-z

Kocot, K. M., Cannon, J. T., Todt, C., Citarella, M. R., Kohn, A. B., Meyer, A., et al. (2011). Phylogenomics Reveals Deep Molluscan Relationships. *Nature* 477 (7365), 452–456. doi:10.1038/nature10382

Krogh, A., Larsson, B., Von Heijne, G., and Sonnhammer, E. L. L. (2001). Predicting Transmembrane Protein Topology with a Hidden Markov Model: Application to Complete genomes11Edited by F. Cohen. *J. Mol. Biol.* 305 (3), 567–580. doi:10.1006/jmbi.2000.4315

Laumer, C. E., Fernández, R., Lemer, S., Combosch, D., Kocot, K. M., Riesgo, A., et al. (2019). Revisiting Metazoan Phylogeny with Genomic Sampling of All Phyla. *Proc. R. Soc. B* 286, 20190831. doi:10.1098/rspb.2019.0831

Lemer, S., Bieler, R., and Giribet, G. (2019). Resolving the Relationships of Clams and Cockles: Dense Transcriptome Sampling Drastically Improves the Bivalve Tree of Life. *Proc. R. Soc. B* 286, 20182684. doi:10.1098/rspb.2018.2684

Levin, M., Anavy, L., Cole, A. G., Winter, E., Mostov, N., Khair, S., et al. (2016). The Mid-developmental Transition and the Evolution of Animal Body Plans. *Nature* 531 (7596), 637–641. doi:10.1038/nature16994

Li, Y., Shen, X.-X., Evans, B., Dunn, C. W., and Rokas, A. (2021). Rooting the Animal Tree of Life. *Mol. Biol. Evol.* 38 (10), 4322–4333. doi:10.1093/molbev/msab170

Liu, G., Huan, P., and Liu, B. (2020). Identification of Three Cell Populations from the Shell Gland of a Bivalve Mollusc. *Dev. Genes. Evol.* 230, 39–45. doi:10.1007/s00427-020-00646-9

Liu, X., Jin, C., Li, H., Bai, Z., and Li, J. (2018). Morphological Structure of Shell and Expression Patterns of Five Matrix Protein Genes during the Shell Regeneration Process in Hyriopsis Cumingii. *Aquac. Fish.*, 3(6), 225–231. doi:10.1016/j.aaf.2018.09.005

Livingston, B. T., Killian, C. E., Wilt, F., Cameron, A., Landrum, M. J., Ermolaeva, O., et al. (2006). A Genome-wide Analysis of Biomineralization-Related Proteins in the Sea Urchin *Strongylocentrotus purpuratus*. *Dev. Biol.* 300 (1), 335–348. doi:10.1016/j.ydbio.2006.07.047

Lowenstam, H. A., and Weiner, S. (1989). *On Biomineralization*. Oxford University Press on Demand.

Lyons, D. C., Perry, K. J., and Henry, J. Q. (2017). Morphogenesis along the Animal-Vegetal axis: Fates of Primary Quartet Micromere Daughters in the Gastropod Crepidula Fornicata. *BMC Evol. Biol.* 17 (1), 217. doi:10.1186/s12862-017-1057-1

Mann, K., and Edsinger, E. (2014). The *Lottia gigantea* Shell Matrix Proteome: Re-analysis Including MaxQuant iBAQ Quantitation and Phosphoproteome Analysis. *Proteome Sci.* 12 (1), 28–12. doi:10.1186/1477-5956-12-28

Mann, K., Poustka, A. J., and Mann, M. (2008). The Sea Urchin (*Strongylocentrotus purpuratus*) Test and Spine Proteomes. *Proteome Sci.* 6 (1), 22–10. doi:10.1186/1477-5956-6-22

Mann, K., Wilt, F. H., and Poustka, A. J. (2010). Proteomic Analysis of Sea Urchin (*Strongylocentrotus purpuratus*) Spicule Matrix. *Proteome Sci.* 8 (1), 33–12. doi:10.1186/1477-5956-8-33

Marie, B., Marie, A., Jackson, D. J., Dubost, L., Degnan, B. M., Milet, C., et al. (2010). Proteomic Analysis of the Organic Matrix of the Abalone Haliotis Asinina Calcified Shell. *Proteome Sci.* 8 (1), 54–11. doi:10.1186/1477-5956-8-54

Marie, B., Joubert, C., Tayalé, A., Zanella-Cléon, I., Belliard, C., Piquemal, D., et al. (2012). Different Secretory Repertoires Control the Biomineralization Processes of Prism and Nacre Deposition of the Pearl Oyster Shell. *Proc. Natl. Acad. Sci. U.S.A.* 109 (51), 20986–20991. doi:10.1073/pnas.1210552109

Marie, B., Trinkler, N., Zanella-Cleon, I., Guichard, N., Becchi, M., Paillard, C., et al. (2011a). Proteomic Identification of Novel Proteins from the Calcifying Shell Matrix of the Manila Clam Venerupis Philippinarum. *Mar. Biotechnol.* 13 (5), 955–962. doi:10.1007/s10126-010-9357-0

Marie, B., Zanella-Cléon, I., Guichard, N., Becchi, M., and Marin, F. (2011b). Novel Proteins from the Calcifying Shell Matrix of the Pacific Oyster *Crassostrea gigas*. *Mar. Biotechnol.* 13 (6), 1159–1168. doi:10.1007/s10126-011-9379-2

Marin, F., Le Roy, N., Marie, B., Ramos-Silva, P., Bundeleva, I., Guichard, N., et al. (2014). Metazoan Calcium Carbonate Biomineralizations: Macroevolutionary Trends - Challenges for the Coming Decade. *Bull. La Société Géologique Fr.* 185 (4), 217–232. doi:10.2113/gssgfbull.185.4.217

Marin, F., Luquet, G., Marie, B., and Medakovic, D. (2007). Molluscan Shell Proteins: Primary Structure, Origin, and Evolution. In *Curr. Top. Dev. Biol.* (Vol. 80, pp. 209–276). doi:10.1016/S0070-2153(07)80006-8

Marin, F. (2020). Mollusc Shellomes: Past, Present and Future. *J. Struct. Biol.*, 212(1), 107583. doi:10.1016/j.jsb.2020.107583

Nederbragt, A. J., van Loon, A. E., and Dictus, W. J. (2002). Expression of Patella Vulgata Orthologs of Engrailed and dpp-BMP2/4 in Adjacent Domains During Molluscan Shell Development Suggests a Conserved Compartment Boundary Mechanism. *Dev. Biol.* 246 (2), 341–55. doi:10.1006/dbio.2002.0653

Parkhaev, P. Y. (2017). Origin and the Early Evolution of the Phylum Mollusca. *Paleontol. J.* 51 (6), 663–686. doi:10.1134/s003103011706003x

Price, M. N., Dehal, P. S., and Arkin, A. P. (2009). FastTree: Computing Large Minimum Evolution Trees with Profiles Instead of a Distance Matrix. *Mol. Biol. Evol.* 26 (7), 1641–1650. doi:10.1093/molbev/msp077

R Developement Core Team (2015). *R: A Language and Environment for Statistical Computing*. Vienna, Austria: R Foundation for Statistical Computing. Available at: https://www.R-project.org

Salamanca-Díaz, D. A., Calcino, A. D., de Oliveira, A. L., and Wanninger, A. (2021). Non-collinear Hox Gene Expression in Bivalves and the Evolution of Morphological Novelties in Mollusks. *Sci. Rep.* 11 (1), 3575. doi:10.1038/s41598-021-82122-6

Salamanca-Díaz, D. A., Schulreich, S. M., Cole, A. G., and Wanninger, A. (2022). Single-Cell RNA Sequencing Atlas from a Bivalve Larva Enhances Classical Cell Lineage Studies. *Front. Ecol. Evol.* 9, 783984. doi:10.3389/fevo.2021.783984

Samadi, L., and Steiner, G. (2009). Involvement of Hox Genes in Shell Morphogenesis in the Encapsulated Development of a Top Shell Gastropod (Gibbula Varia L.). *Dev. Genes. Evol.* 219 (9–10), 523–530. doi:10.1007/s00427-009-0308-6

Satija, R., Farrell, J. A., Gennert, D., Schier, A. F., and Regev, A. (2015). Spatial Reconstruction of Single-Cell Gene Expression Data. *Nat. Biotechnol.* 33 (5), 495–502. doi:10.1038/nbt.3192

Setiamarga, D. H. E., Hirota, K., Yoshida, M.-a., Takeda, Y., Kito, K., Ishikawa, M., et al. (2021). Hydrophilic Shell Matrix Proteins of Nautilus Pompilius and the Identification of a Core Set of Conchiferan Domains. *Genes.* 12 (Issue 12), 1925. doi:10.3390/genes12121925

Simkiss, K., and Wilbur, K. M. (2012). *Biomineralization*. Elsevier.

Smith, S. a., Wilson, N. G., Goetz, F. E., Feehery, C., Andrade, S. C. S., Rouse, G. W., et al. (2011). Resolving the Evolutionary Relationships of Molluscs with Phylogenomic Tools. *Nature* 480 (7377), 364–367. doi:10.1038/nature10526

Timmins-Schiffman, E., Coffey, W. D., Hua, W., Nunn, B. L., Dickinson, G. H., and Roberts, S. B. (2014). Shotgun Proteomics Reveals Physiological Response to Ocean Acidification in *Crassostrea gigas*. *BMC Genomics* 15 (1), 951. doi:10.1186/1471-2164-15-951

Vinther, J. (2015). The Origins of Molluscs. *Palaeontology*, 58(1), 19–34. doi:10.1111/pala.12140

Wanninger, A., and Wollesen, T. (2015). "Mollusca," in *Evolutionary Developmental Biology of Invertebrates 2: Lophotrochozoa (Spiralia)*. Editor A. Wanninger (Springer-Verlag Wien), 103, 153–154. doi:10.1007/978-3-7091-1871-910.1007/978-3-7091-1871-9_7)

Wanninger, A., and Wollesen, T. (2019). The Evolution of Molluscs. *Biol. Rev.* 94 (1), 102–115. doi:10.1111/brv.12439

Wei, L., Wang, Q., Ning, X., Mu, C., Wang, C., Cao, R., et al. (2015). Combined Metabolome and Proteome Analysis of the Mantle Tissue from Pacific Oyster *Crassostrea gigas* Exposed to Elevated pCO2. *Comp. Biochem. Physiology Part D Genomics Proteomics* 13, 16–23. doi:10.1016/j.cbd.2014.12.001

Wollesen, T., Rodríguez Monje, S. V., Luiz de Oliveira, A., and Wanninger, A. (2018). Staggered Hox Expression Is More Widespread Among Molluscs Than Previously Appreciated. *Proc. R. Soc. B* 285, 20181513. doi:10.1098/rspb.2018.1513

Yarra, T., Blaxter, M., and Clark, M. S. (2021). A Bivalve Biomineralization Toolbox. *Mol. Biol. Evol.* 38, 4043–4055. doi:10.1093/molbev/msab153

Zhao, R., Takeuchi, T., Koyanagi, R., Villar-Briones, A., Yamada, L., Sawada, H., et al. (2020). Phylogenetic Comparisons Reveal Mosaic Histories of Larval and

Adult Shell Matrix Protein Deployment in Pteriomorph Bivalves. *Sci. Rep.* 10 (1), 22140. doi:10.1038/s41598-020-79330-x

Zhao, R., Takeuchi, T., Luo, Y.-J., Ishikawa, A., Kobayashi, T., Koyanagi, R., et al. (2018). Dual Gene Repertoires for Larval and Adult Shells Reveal Molecules Essential for Molluscan Shell Formation. *Mol. Biol. Evol.* 35 (11), 2751–2761. doi:10.1093/molbev/msy172

Zieger, E., Robert, N. S. M., Calcino, A., and Wanninger, A. (2021). Ancestral Role of Ecdysis-Related Neuropeptides in Animal Life Cycle Transitions. *Curr. Biol.*, 31(1), 207–213. doi:10.1016/j.cub.2020.10.004

Conflict of Interest: The authors declare that the research was conducted in the absence of any commercial or financial relationships that could be construed as a potential conflict of interest.

Publisher's Note: All claims expressed in this article are solely those of the authors and do not necessarily represent those of their affiliated organizations, or those of the publisher, the editors and the reviewers. Any product that may be evaluated in this article, or claim that may be made by its manufacturer, is not guaranteed or endorsed by the publisher.

frontiers | Frontiers in Ecology and Evolution

TYPE Methods
PUBLISHED 02 June 2023
DOI 10.3389/fevo.2023.1146749

OPEN ACCESS

EDITED BY
Pedro Martinez,
University of Barcelona, Spain

REVIEWED BY
Olga Zueva,
Marine Biological Laboratory, United States
Noriyuki Satoh,
Okinawa Institute of Science and Technology Graduate University, Japan

*CORRESPONDENCE
Giovanna Benvenuto
✉ giovanna.benvenuto@szn.it

RECEIVED 17 January 2023
ACCEPTED 19 May 2023
PUBLISHED 02 June 2023

CITATION
Paganos P, Caccavale F, Cocurullo M, D'Aniello E, Arnone MI and Benvenuto G (2023) Whole animal freeze-fracture scanning electron microscopy: an easy-to-use method to investigate cell type morphology of marine embryos and larvae.
Front. Ecol. Evol. 11:1146749.
doi: 10.3389/fevo.2023.1146749

Whole animal freeze-fracture scanning electron microscopy: an easy-to-use method to investigate cell type morphology of marine embryos and larvae

Periklis Paganos, Filomena Caccavale, Maria Cocurullo, Enrico D'Aniello, Maria Ina Arnone and Giovanna Benvenuto*

Stazione Zoologica Anton Dohrn, Naples, Italy

Morphological and molecular characterization of cell types, organs and individual organisms is essential for understanding the origins of morphogenesis. The increased implementation of high throughput methods as a means to address cell type evolution, during the last decade, created the need for an efficient way to assess cell type morphology. Here in order to create a new tool to study cell type morphology, we optimized a fast and easy-to-use whole animal freeze-fracture scanning electron microscopy (WAFFSEM) method. This method was applied on marine experimental systems (echinoderms, mollusks, tunicates, and cephalochordates), that have been widely used to assess environmental, developmental, and evolutionary questions. Our protocol does not require any specialized equipment and the processed specimens are compatible with scanning electron microscopy. This protocol was able to successfully expose the internal cell types of all specimens in which it was tested and to reveal their cellular and subcellular characteristics. We strongly believe that the combination of our protocol with other methods (e.g., light microscopy and single cell transcriptomics) will be beneficial to further improve the way to classify and describe cell types.

KEYWORDS

echinoderms, tunicates, mollusks, cephalochordates, morphology, cell types, SEM, freeze fracture

1. Introduction

Cells are the building blocks of life, and their development, specification, differentiation, and function are tightly orchestrated by the genetic program operating within them and by how this is properly executed. Multicellular organisms consist of various cell types that can either be found dispersed within the body fluids or organized in distinct units such as tissues and organs. Each specific cell type consists of cells with similar morphological features that are the result of specific gene regulatory programs and epigenetic mechanisms dictating their identity and function (Davidson and Erwin, 2006). Nowadays, high throughput technologies have been developed to assess cell type complexity in an unprecedented resolution. For instance, advances in transcriptomics have allowed the capture of the molecular signature of a given organism, tissue, or organ at a single cell resolution, resolving the identification of putative cell types in an

unbiased way. These technologies have been applied on plenty of animals across the evolutionary tree of life including representatives from both invertebrates and vertebrates. Specifically, single cell transcriptomics has been successfully applied on a variety of organisms spanning from sponges, planarians, mollusks, crustaceans, cnidarians and echinoderms to tunicates, cephalochordates, and mammals (Plass et al., 2018; Cao et al., 2019; Tabula Muris, 2020; Chari et al., 2021; Massri et al., 2021; Musser et al., 2021; Paganos et al., 2021; Satoh et al., 2021; Almazan et al., 2022; Murat et al., 2023). The implementation of such approaches has contributed to the reconstruction of distinct cell type atlases as well as the revaluation of embryonic development and cell type evolution. However, in order to fully define a given cell type apart from the identification of the expressed genes within it, it is imperative to understand how this genetic information is translated into phenotypic features. In other words, the assessment of the molecular signature of a given cell type should always go hand in hand with its morphological assessment.

Traditionally, light microscopy has been used to describe the morphology of animals' cell types and has been heavily exploited in cases where the specimens are optically transparent. On the other hand, for specimens that lack this feature, clearing methods have been developed to allow a better visualization of tissues that otherwise would remain hidden due to the presence of extensive lipid membranes, protective organs, or pigments.

In order to facilitate the study of cell type morphology we optimized a simple, efficient, and low-cost whole animal freeze-fracture scanning electron microscopy (WAFFSEM) protocol. Marine organisms as experimental systems are ideal to approach Evo-Devo research questions. They offer many advantages, such as a high number of transparent embryos/larvae, as well as a well resolved evolutionary history and distances that allow meaningful comparisons (Stracke and Hejnol, 2023). We, therefore, applied the WAFFSEM protocol on a variety of extensively used marine organisms including mollusks, echinoderms, tunicates, and cephalochordates. This freeze fracture protocol combined with subsequent scanning electron microscopy observation allowed us to spatially recognize well-known cell types and to further describe their phenotypic features. Moreover, focusing on echinoderms we also used correlative approaches as proof of concept of the complementarity of our method with other techniques, always in respect to cell type characterization.

2. Materials and methods

2.1. Animal collection, *in vitro* fertilization and rearing of embryos and larvae

2.1.1. Sea urchin

Adult *Paracentrotus lividus* individuals were collected from the Gulf of Naples (Italy), while the Pacific Ocean sea urchin *Strongylocentrotus purpuratus* individuals were collected from the Gulf of Santa Catalina (CA, United States) and distributed by Patrick Leahy (Kerckhoff Marine Laboratory, California Institute of Technology, Pasadena, CA, United States). Gametes were obtained by vigorous shaking of the adult individuals. Fertilization of eggs was performed by using approximately 1:1,000 dry sperm diluted in filtered sea water (FSW) and larvae were let to develop according to their species salinity and temperature biological needs. *P. lividus* larvae were cultured at 18°C in Mediterranean FSW and *S. purpuratus* at 15°C in Mediterranean FSW diluted 9:1 with deionized water.

2.1.2. Sea star

Adult *Patiria miniata* individuals were collected from the Gulf of Santa Catalina (CA, United States) and distributed by Patrick Leahy (Kerckhoff Marine Laboratory, California Institute of Technology, Pasadena, CA, United States). Gametes were collected by performing a 4 mm diameter incision on one side of each animal's arm. A piece of each gonad was extracted and placed in calcium and magnesium-free artificial sea water (CMF-ASW). In the case of female gametes, immature eggs were treated with 10 µM 1-Methyladenine in Mediterranean FSW for approximately 1 h until the germinal vesicle (GV) disappears, indicating their maturity. Mature eggs were then fertilized with approximately 1:1,000 dry sperm diluted in FSW, and zygotes were let to develop, until they reached the desired developmental stage at 15°C in Mediterranean FSW diluted 9:1 with deionized water.

2.1.3. Sea squirt

Adult *Ciona robusta* individuals were collected from the Gulf of Taranto (Italy). Gametes from adult individuals were collected for *in vitro* fertilization and chemical dechorionation was performed prior to fertilization as previously described (D'aniello, 2009). Embryos were allowed to grow until the stage of interest at 18°C in Mediterranean FSW.

2.1.4. Mussel

Adult individuals of *Mytilus galloprovincialis* were purchased from Irsvem Srl (Naples, Italy) and were used immediately for spawning. Spawning of male and female individuals was induced through mechanical stimulation. Approximately 20–30 mussels were placed in a tank with Mediterranean FSW at 18°C and spread to easily monitor the spawning. When spawning started, each individual was washed and then transferred into a Becker containing 200 mL of Mediterranean FSW to isolate males and females. Mature eggs were fertilized with an eggs/sperm ratio 1:15 in a volume of 50 mL. The resulting zygotes were let to develop at 18°C in Mediterranean FSW until the developmental stage of interest.

2.1.5. Amphioxus

Branchiostoma lanceolatum embryos and larvae were reared from animals collected in Argelès-sur-mer (France) and spawned at Observatoire Océanologique de Banyuls-sur-Mer (France). Gametes were obtained during late spring/early summer period and the spawning was induced through thermal shock (Fuentes et al., 2007). Mature eggs were then fertilized with approximately 1:1,000 dry sperm diluted in FSW. Embryos were let to develop until they reached the desired developmental stage at 18°C in Mediterranean FSW.

2.2. Fluorescent *in situ* hybridization, immunohistochemistry and F-actin detection

2.2.1. Fluorescent *in situ* hybridization

Strongylocentrotus purpuratus and *P. lividus* larvae, intended to be used for FISH, were fixed as previously described in Paganos et al.

(2022a). Synthesis of antisense mRNA probes against the genes of interest and FISH were performed as described by Perillo et al. (2021) and Paganos et al. (2022a). Briefly, genes of interest were isolated from a pool of cDNAs, and the amplified products were sequenced. Probes were generated through *in vitro* transcription using Digoxigenin RNA labeling mix solutions (Roche) and signal was developed through cyanine-based signal amplification (Akoya Biosciences). DAPI was added (1 µg/mL) and specimens were imaged using a Zeiss LSM 700 confocal microscope.

2.2.2. Immunohistochemistry and F-Actin detection

Mytillus galloprovinicialis, *P. miniata*, *P. lividus* and *S. purpuratus* embryos and larvae, intended to be used for IHC and F-Actin detection, were fixed as described in Perillo et al. (2021). In brief, specimens were fixed in 4% PFA in FSW for 15 min at RT. After fixation, samples were washed several times with MOPS Buffer and stored at 4°C. IHC was carried out as described in Perillo et al. (2021) with minor modifications. Specimens were washed several times with MOPS buffer, then they were placed in a blocking solution containing 1 mg/mL Bovine Serum Albumin (BSA) and 4% sheep serum in MOPS buffer for 1 h at room temperature (RT). Primary antibodies were added in the appropriate dilution and incubated for 1 h and 30 min at 37°C. Anti-Endo1 (gift from Dr. David McClay) was used undiluted to mark the sea urchin mid and hindgut domains; anti-Sp-Brn1/2/4 (gift from Dr. Robert Burke) was used instead to label sea urchin neurons and the esophageal regions and used diluted 1:200 in blocking solution; anti-Msp130 labeling the sea urchin skeletal spicules (gift from Dr. David McClay) was used with a dilution factor 1:10 in blocking solution; anti-Acetylated tubulin (Sigma) was chosen to label cilia and was used diluted 1:200 in blocking solution. Specimens were washed with MOPS Buffer (5 times) and incubated for 1 h with the appropriate secondary antibody (AlexaFluor) diluted 1:1,000 in MOPS buffer. F-actin staining was performed using phalloidin solution (Invitrogen) diluted 1:20 in MOPS buffer. Samples were let to incubate for 1 h at RT. Next, specimens were washed 5 times with MOPS buffer and DAPI was added (1 µg/mL). Specimens were imaged using a Zeiss LSM 700 confocal microscope.

2.3. Catecholamine staining (FaGlu)

Paracentrotus lividus early pluteus larvae were collected and placed in a solution containing 4% formaldehyde and 0.5% glutaraldehyde in FSW (FaGlu). Specimens were incubated for 1 h at RT in the dark. Next, a drop of specimens was transferred on a glass slide and FaGlu was used as mounting medium. A coverslip was added and samples were imaged using a Zeiss LSM 700 confocal microscope. Dopaminergic neurons were detected using the 475–480 nm emission peak.

2.4. Whole animal freeze-fracture scanning electron microscopy protocol

- Whole embryos at the developmental stage of interest were fixed in 2.5% glutaraldehyde in FSW and placed at 4°C overnight. The day after, the samples were washed five times with FSW and were let to settle. The duration of each wash was 15 min at RT.
- FSW was then removed and replaced with 25% DMSO in double distilled water (ddH_20) in which specimens were incubated for 30 min at RT. This step was repeated twice.
- The 25% DMSO solution was removed and replaced with 50% DMSO in ddH_20 and embryos or larvae were incubated for 30 min at RT. This step was repeated twice.
- During the last 30 min of incubation a metal key, a pair of forceps, an aluminum tray and a razor blade were placed in a polyurethane ice bucket and covered with liquid nitrogen to pre-cool.
- Pre-chilled forceps were used to remove the key from the liquid nitrogen bath and placed on the bench. This step is necessary to avoid the immediate freezing of the sample, while being transferred onto the pre-chilled key. Approximately 100 µL of specimens were quickly transferred with a P200 pipette inside the groove of the key and spread throughout the groove surface. The key was quickly returned inside the pre-chilled aluminum tray.
- Using the same pair of forceps, the pre-chilled razor blade was collected and placed in parallel and on top in respect to the key's groove. Using a hammer, the razor blade was stricken multiple times in a downward motion until complete fracturing of the pellet.
- The key was transferred on the bench and the fractured pellet was let to thaw at RT. Then, using a P200 pipette, the solution was placed in clean Eppendorf tubes.
- Once the fractured specimens settled down, DMSO solution was removed, and specimens were gradually dehydrated by passing them in 30, 50 and 70%, 80, 90% molecular grade ethanol diluted in ddH_20. The incubation time for each dehydration step was 15 min.
- To ensure the complete dehydration, samples were incubated 3 times (15 min each) in absolute ethanol.
- Samples were then subjected to the standard processing for SEM including critical point drying and sputtering and were analyzed using a Jeol field emission scanning electron microscope (JSM 6700-F).

3. Results

The accurate characterization of cell type morphology is essential to better understand which are the key features responsible for cell type diversification and to gain insight into their function and interconnectivity with other cells, tissues, or organs. In this study we developed an easy-to-use WAFFSEM protocol that we tested on a variety of marine embryos and larvae. A schematic and detailed representation of this protocol is depicted in Figure 1.

The idea for developing this protocol is based on a previous study led by MacDonald et al. (2017), in which the authors developed a method for freeze-fracturing and subsequent observation with scanning electron microscopy of isolated murine mitochondria. Our method is a simplified version of that protocol that has been adapted to be suitable for whole organisms. Here we present WAFFSEM examples for several marine organisms including representatives of both protostomes and deuterostomes. In detail, this protocol was successful to visualize phenotypic features for the tunicate *C. robusta*,

10.3389/fevo.2023.1146749

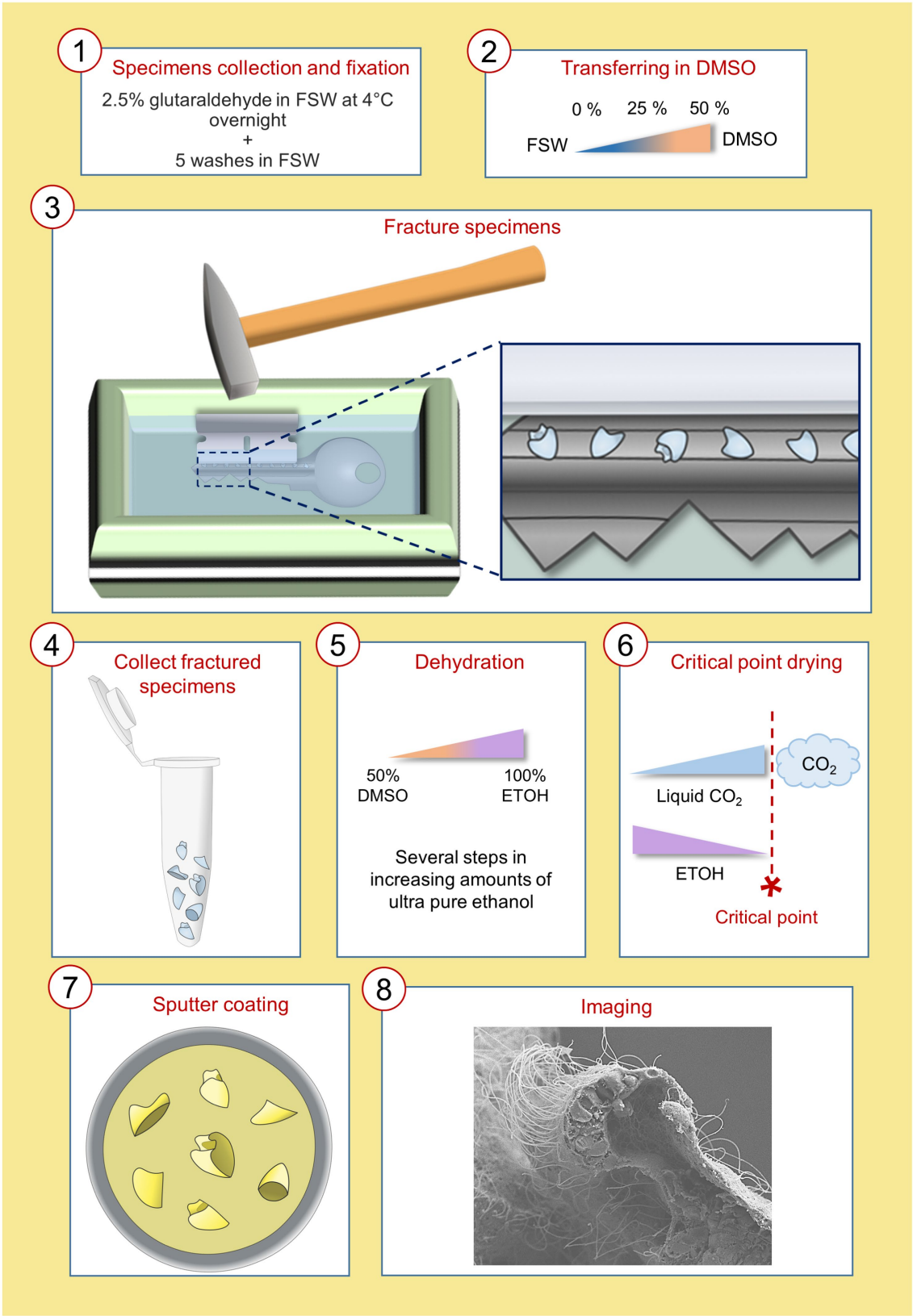

FIGURE 1
Schematic representation of the WAFFSEM protocol steps from specimen fixation to imaging. Details on the precise steps of the protocol can be found in materials and methods, section 2.4.

the cephalochordate *B. lanceolatum*, the mollusk *M. galloprovincialis*, the sea star *P. miniata* and for the two sea urchin species *P. lividus* and *S. purpuratus*.

3.1. Tunicates, cephalochordates, and mollusks

The WAFFSEM protocol applied on *C. robusta* and *B. lanceolatum* embryos and larvae was shown to have high efficiency. An advantage for using those species as test subjects were the availability of great numbers of starting material from each fertilization and their relatively big size (*C. robusta* mid-tailbud stage ~ 450 µm; T0 stage *B. lanceolatum* larva ~ 350 µm; L0 stage *B. lanceolatum* larva ~ 750 µm) that increases the likelihood of specimens being successfully fractured. Taking advantage of the available information about cell types in *C. robusta* and *B. lanceolatum*, we were able to recognize key features. In the case of the *C. robusta* embryo at the mid tailbud stage (Figure 2A) WAFFSEM was able to successfully reveal the morphology of cell type derivatives from all germ layers (Figures 2A–I). In detail, we were able to visualize putative epidermal, mesenchymal, and endodermal cells (Figures 2C,D,F). Furthermore, details on the spatial position of neuronal cell types, such as the ones constituting the nerve cord, are shown and especially in respect to supportive cell types such as muscles and the notochord (Figures 2F–I). Our WAFFSEM protocol was also effective on the cephalochordate *B. lanceolatum* (Figures 2J–O). We recovered a T0 stage larva approximately longitudinally fractured at the pharynx level, and we were able to recognize morphological characteristics of cell types related to the neural tube, the notochord, longitudinal muscles, and the gut (Figure 2K). Moreover, at the anterior portion of this specimen, we observed a structure potentially related to the primordium of the club-shaped gland (Figure 2K). Immediately posterior to the presumptive club-shaped gland domain, a thickening of the endoderm on the right side of the pharyngeal region is visible and this can be identified as the primordium of the first gill slit (Figure 2K). Concerning the L0 stage larva, depicted in Figures 2L–O and fractured transversally at the posterior part of the body, we can clearly see the lumen of the gut and the cell types around it. Moving from the dorsal to the ventral part of the specimen we observed the anatomy and cell morphology of the neural tube and especially of the cells comprising its wall and the central hollow tube (Figures 2M,N). Immediately below the neural tube we see the notochord and the gut (Figures 2N,O). Moreover, we can clearly see the longitudinal muscles positioned bilaterally to the notochord (Figure 2N).Taken together, we concluded that the WAFFSEM protocol is applicable on marine organisms and is able to reveal the morphological features of various tunicate and cephalochordate cell types.

In order to test whether our protocol gives similar results on smaller specimens we also applied it on the D-Larva of the bivalve mollusk *M. galloprovincialis* (Figures 3A–F). Furthermore, using a specimen that has a calcium-based shell offers the possibility to test whether such structures interfere with the efficiency of our method. Surprisingly, the efficiency of our WAFFSEM protocol did not seem to be altered either by the smaller size of the specimen or the presence of the shell and the results of this are shown in Figures 3C,F. In this case, we also implemented the use of light microscopy in order to recognize distinct cell types and to show the correlative potential of using WAFFASEM combined with other imaging techniques (Figures 3B,E). In Figure 3 panels C, F fractured *M. galloprovincialis* D-larvae are depicted in oral view and we can see various cell types such as muscles, branchial gills and ciliated cells as well as parts of the gut luminary epithelium. Noteworthy, the combination of our WAFFSEM protocol with light microscopy allowed us to map on the SEM images cell types such as muscles and ciliated cells (Figures 3B,C,E,F). In conclusion, our WAFFSEM protocol can be used as a tool to assess cell type morphology of the *M. galloprovincialis* larva at a cellular resolution, information that when combined with other imaging approaches can be used for further cell type characterizations.

3.2. Echinoderms

Echinoderms are non-chordate deuterostomes and represent an ideal model for comparative Evo-Devo approaches at a cell-type resolution level. Historically, echinoderms have been extensively used to describe cell type specific morphological features (Ernst, 2011). Moreover, several molecular biology tools such as ATAC-seq and single cell transcriptomics have been successfully implemented to address chromatin dynamics, cell type composition and evolution during echinoderm embryonic and larval development. Therefore, echinoderms were the perfect candidates to apply our WAFFSEM protocol in a correlative perspective.

To this end we performed the WAFFSEM protocol on early bipinnaria larvae of the sea star *P. miniata*, which enabled us to assess the cell type morphology of distinct larval cell types (Figure 4). In Figure 4 panel B, a larva in lateral view is depicted in which the foregut and midgut domains have been successfully fractured. In this specimen, we report the presence of distinct muscle fibers and ciliated cells in the esophageal region (Figure 4C), while the midgut domain is enriched in ciliated cells projecting their cilia within the lumen region (Figures 4C,F). In this case the direction of the fracture allowed us to also observe several subcellular components of the midgut cells including nuclei, round structures that are indicative of vesicles as well as small protrusions, corresponding to microvilli (Figure 4C). In the same figure, panels D and E, a larva in oral view is shown and we report fractured cells corresponding to the oral hood and apical organ domains of the larva known to be enriched in neuronal cell types (Zheng et al., 2022). Interestingly, on the same specimen, but focusing on another fractured region, spanning from the lower foregut to the midgut domains, we were able to observe the morphology of the cells forming the constriction between the foregut and midgut domains, known as the cardiac sphincter (Figure 4H). Moreover, the great resolution of these images allowed us also to clearly distinguish two hollow tubes corresponding to the left and right coeloms of the animal (Figures 4D,G,H). In addition to the previous structures observed from this view, we can also see the cell consistency of the posterior enterocoel, a structure that arises from the dorsal side of the digestive tract and later buds off the left endodermal epithelium (Figures 4I,J). This structure has been associated with the metamorphosis process in this species and has been also hypothesized to be a stem cell reservoir (Wessel et al., 2014). Furthermore, we were able to detect many vesicle-like structures and filaments expanding towards the epidermal cells of the larva and the connective tissue holding this structure in place. Ultimately, we report the presence of

10.3389/fevo.2023.1146749

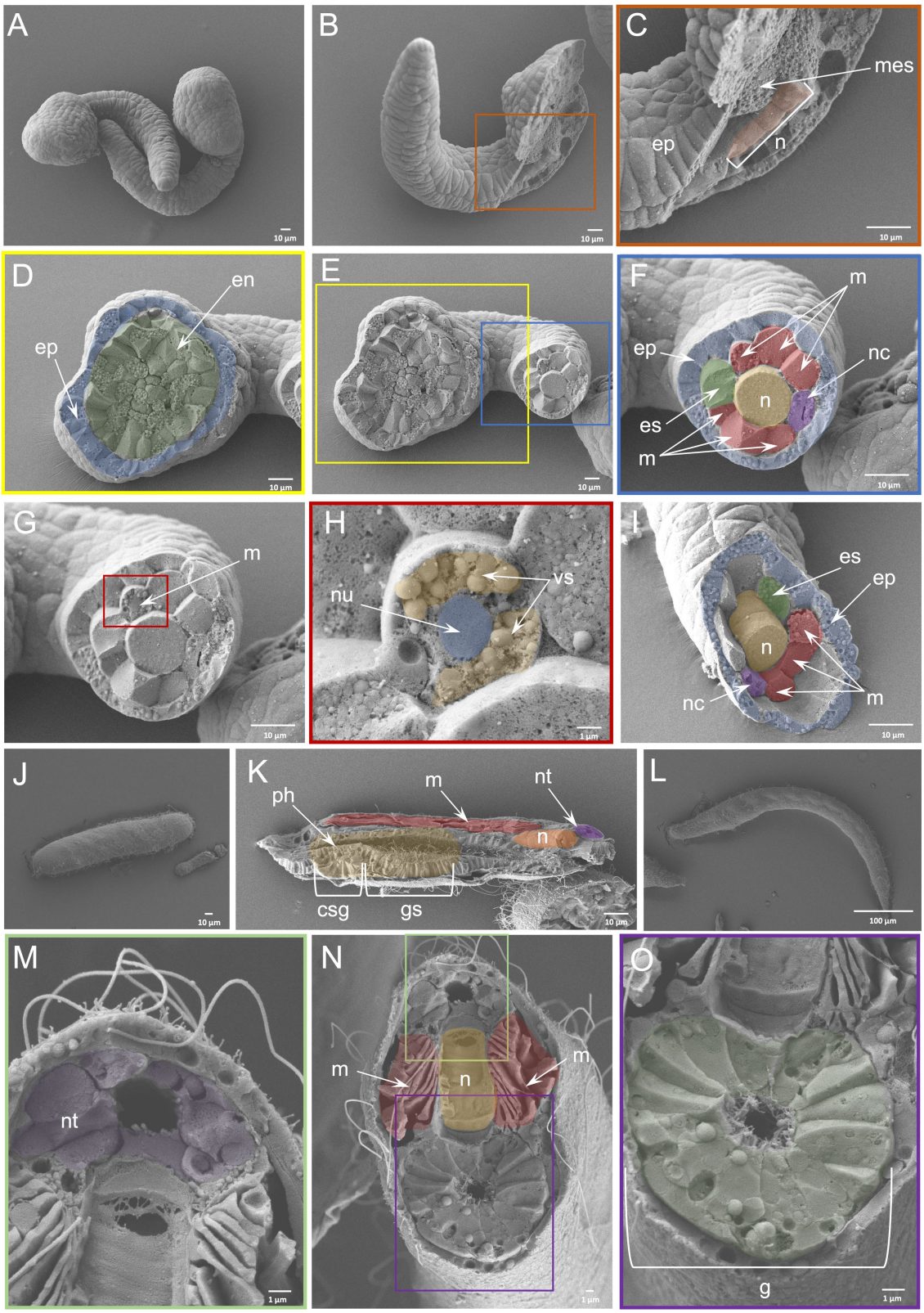

FIGURE 2
Efficiency of WAFFSEM protocol on tunicate and cephalochordate embryos and larvae. **(A)** Intact *C. robusta* mid-tailbud stage embryos. **(B)** Fractured *C. robusta* embryo in lateral view. **(C)** Inset of panel B focused on the fractured region depicting mesenchymal cells and the notochord. **(D)** Inset showing the head region of the fractured specimen shown in **(E)**, displaying endodermal and epidermal cells. **(E)** Fractured *C. robusta* embryo in ventral view. **(F)** Inset focused on the tail region of the fractured specimen shown in **E.** A variety of cell types including muscles, notochord, nerve cord, epidermis, and endodermal strand are visible. **(F, G)** SEM image depicting a *C. robusta* fractured tail. **(H)** Inset showing a fractured muscle cell and its ultrastructure. The nucleus and vesicle-like structures are visible. **(I)** SEM image of fractured *C. robusta* mid-tailbud stage embryo focused on the tail

(Continued)

FIGURE 2 CONTINUED
region and containing the same cell types as labeled in **F**. **(J)** SEM image of intact *B. lanceolatum* T0 stage larva. **(K)** SEM image of fractured *B. lanceolatum* T0 stage larva. Several cell types including the primordium of the club-shaped gland and gill slit as well as muscles, notochord, neural tube and pharynx are visible. **(L)** SEM image of intact *B. lanceolatum* L0 stage larva. **(M–O)** SEM images of fractured *B. lanceolatum* L0 stage larva. **(M)** Inset showing details of the dorsal region of the specimen depicted in **N**. **(O)** Inset depicting the digestive tract of the specimen shown in **N**. csg, club-shaped gland primordium; en, endoderm, ep, epidermis; es, endodermal strand; **(G)**, gut; gs, gill slit primordium; mes, mesenchyme; **(M)**, muscles; **(N)**, notochord; nc, nerve cord; nt, neural tube; nu, nucleus; ph, pharynx; vs., vesicle. Pseudo-coloring was applied to enhance the visualization of the cell types of interest.

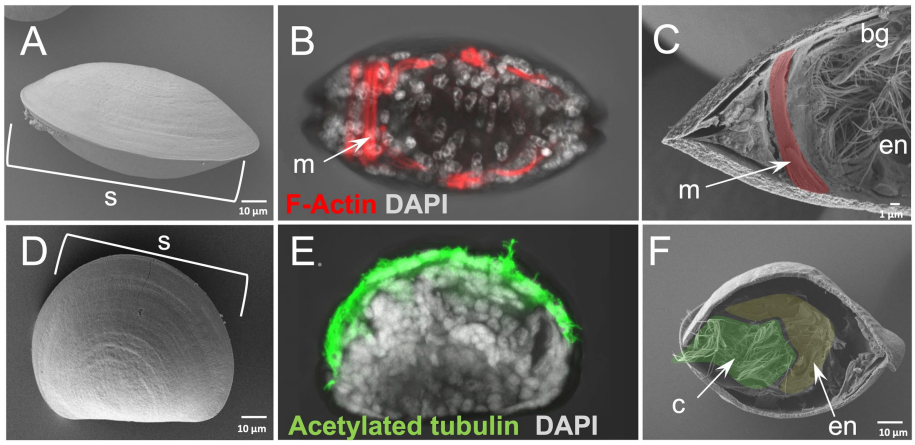

FIGURE 3
Whole animal freeze-fracture scanning electron microscopy (WAFFSEM) protocol applied on mollusk larvae. **(A)** SEM image of intact *Mytilus galloprovincialis* 3dpf D-larva stage in oral view. **(B)** Phalloidin staining showing the F-Actin localization in muscle cells seen in oral view. **(C)** SEM image of a fractured *M. galloprovincialis* 3 dpf D-larva stage oriented in oral view. Muscle fibers, endodermal structures and the brachial gills are visible. **(D)** SEM image of intact *M. galloprovincialis* 3 dpf D-larva stage in lateral view. **(E)** Immunohistochemical detection of acetylated tubulin enriched cilia in a *M. galloprovincialis* 3dpf D-larva stage positioned in lateral view. **(F)** SEM image of fractured *M. galloprovincialis* 3dpf D-larva stage seen in oral view. Cilia and endodermal regions are visible. Nuclei in panels B and E are labeled with DAPI (in gray). bg, branchial gills; c, cilia; en, endoderm; m, muscles; s, shell; Pseudo-coloring was applied to enhance the visualization of the cell types of interest.

an extensive extracellular matrix (ECM) network that can be seen in all panels presented in Figure 4.

In the case of the sea urchin *P. lividus* early pluteus larva, a stage for which plenty of molecular information is available (Figure 5A) WAFFSEM was able to reveal distinct features of various larval cell types. In Figure 5 panels B,C, a larva in abanal view is shown and we can easily observe the midgut domain of the digestive tract and the morphology of the cells constituting it, including small vesicle-like structures, the nuclei, microvilli, and cilia. Moreover, we can observe a cell that, based on its spatial location, we hypothesize it to be corresponding to an immune cell that is in contact with the midgut region, but not embedded with it. Interestingly, in Figures 5 panels B, D, we also observed cells that based on their relative position could correspond to the post oral dopaminergic neurons known to be present at sea urchin early pluteus stage as approximately 1–2 cell clusters positioned bilaterally to the midgut region. The distribution of dopaminergic neurons in *P. lividus* early larvae was visualized using catecholamine staining (FaGlu) and can be seen in Figure 5 panel E. Taking into account the shared morphological features of the dopaminergic neuron shown in Figure 5 panel E and the cell shown in Figure 5 panel D, such as the presence of two axonal-like projections and the spatial position in respect to the post oral arms of the larva, we hypothesize that the cells shown in B and D corresponds to post oral neurons. Furthermore, we can see epidermal cells of various shapes in the regions that correspond to the ciliary band and specifically to the post oral arms of the larva (Figures 5B,D).

On another specimen, seen from a dorsal view and fractured longitudinally, we report the presence of cells in various shapes in the apical plate region (Figures 5F,G). Cross-referencing the SEM images showing the exposed apical plate region (Figures 5F,G) with FISH against the paneuronal sea urchin marker *Synb* (Figure 5H) carried out at the same developmental stage, we speculate that most of the cells shown in panel G correspond to neurons. In support of this, several apical plate cells seem to contain vesicle-like structures and to have a flask-like cell body shape (Figures 5F,G), a known feature of sea urchin apical organ serotonergic neurons. Moreover, in the same specimen we can clearly see the ciliated epithelium of the same region as well as an extensive ECM network. Moving on to a different region of the same specimen, we can clearly see features of the digestive tract and the midgut domain, including cilia, microvilli, and vesicle-like structures (Figures 5G,H). One of the easily observed regions in the fractured specimen in panel I is the constriction corresponding to the cardiac sphincter that is separating the midgut from the foregut domain. Noteworthy, the architecture of the sphincter in the fractured specimen was confirmed when we performed *in situ* hybridization and compared to the confocal image of *Fgf9/16/20*, a marker labeling larval sphincters, further showing the power of the combination of these two approaches (Figures 5I,J).

Finally, we applied the WAFFSEM protocol on the 3 dpf *S. purpuratus* pluteus larva (Figure 6A), a species and developmental stage, for which we recently generated a detailed cell type atlas allowing us to determine its specific cell type composition (Paganos

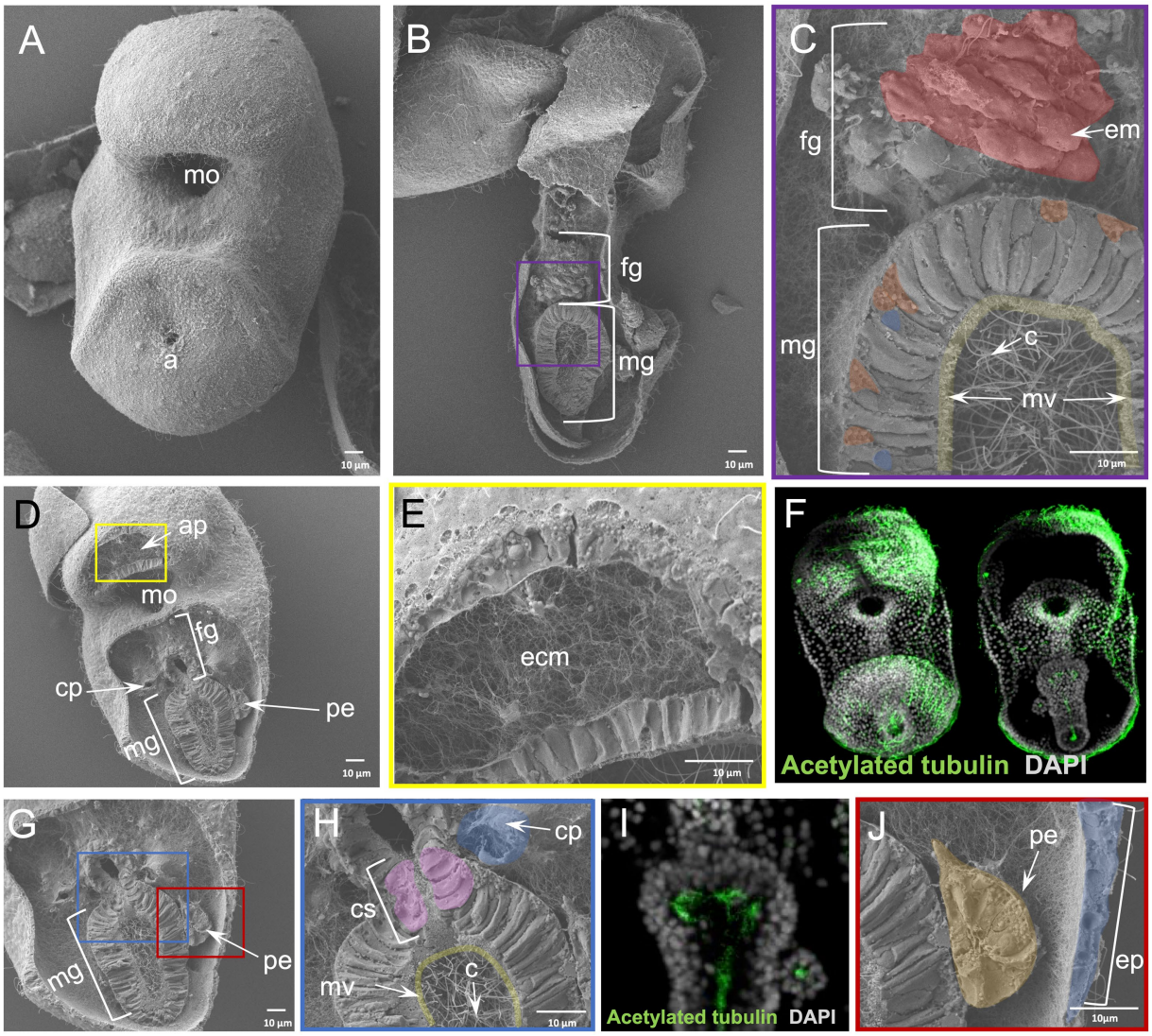

FIGURE 4
Results of WAFFSEM protocol applied on sea star larvae. **(A)** SEM image of an intact *Patiria miniata* ~3dpf bipinnaria larva. **(B)** SEM image of a fractured *P. miniata* ~3dpf bipinnaria larva placed in lateral view. **(C)** Inset of panel B showing in higher magnification the foregut and midgut regions. Muscles patterning the foregut region as well as cilia and microvilli inside the midgut area are highlighted. **(D)** SEM image of a fractured *P. miniata* ~3dpf bipinnaria larva placed in oral view. **(E)** Inset of panel D showing the extensive extracellular matrix (ECM) network in the apical organ/oral hood region of the specimen. **(F)** Immunohistochemical detection of cilia using anti-acetylated tubulin. **(G)** SEM image of a fractured *P. miniata* ~3dpf bipinnaria larva placed in lateral view focused on the digestive tract region. **(H)** Inset of panel G showing the lower foregut and upper midgut regions of the larva. The cardiac sphincter, left coelom as well as cilia and microvilli of the midgut are evident. **(I)** Immunohistochemical detection of cilia within the digestive tract, in dorsal view, using anti-acetylated tubulin. **(J)** Inset of panel G focusing on the posterior enterocoel and the epidermis of the ~3dpf larva. Nuclei in panels F and I are labeled with DAPI (in gray). ap, apical plate; c, cilia; cp, coelomic pouches; cs, cardiac sphincter; e, epidermis; em, esophageal muscle; ecm, extracellular matrix; fg, foregut; mg, midgut; mo, mouth; mv, microvilli; pe, posterior enterocoel. Pseudo-coloring was applied to enhance the visualization of the cell types of interest.

et al., 2021). Briefly, we previously demonstrated that this stage consists of 21 cell type families that we mapped into distinct domains of the larva (Figures 6B,C). Moreover, we recently showed that the implementation of single cell transcriptomics analyses and electron microscopy is sufficient to assess cell type homology (Paganos et al., 2022b).

The WAFFSEM protocol applied on 3 dpf pluteus larvae allowed us to correlate the molecular signatures identified with single cell transcriptomics to distinct cell type features. Focusing on the digestive tract of the larva, only WAFFSEM was able to depict morphological diversity of the cell types composing it, while FISH and IHC, as well as single-cell transcriptomics, are able to reveal distinct molecular signatures of the sphincter, esophageal, stomach and intestinal domains (Figures 6D–I). For example, this is the case of the larval pyloric sphincter, in which we can clearly see the constriction formed by the endodermally derived muscles that are morphologically diversified in comparison to the rest of the posterior gut cells (Figure 6H). Specific features of these cells are the elongated cell shape and the presence of vesicle-like structures. Similar cell characteristics can be appreciated in the cardiac sphincter domain, suggesting that the two sphincters share morphological features (Figure 6I). Once more we can clearly see that the blastocoel is full of ECM as well as a

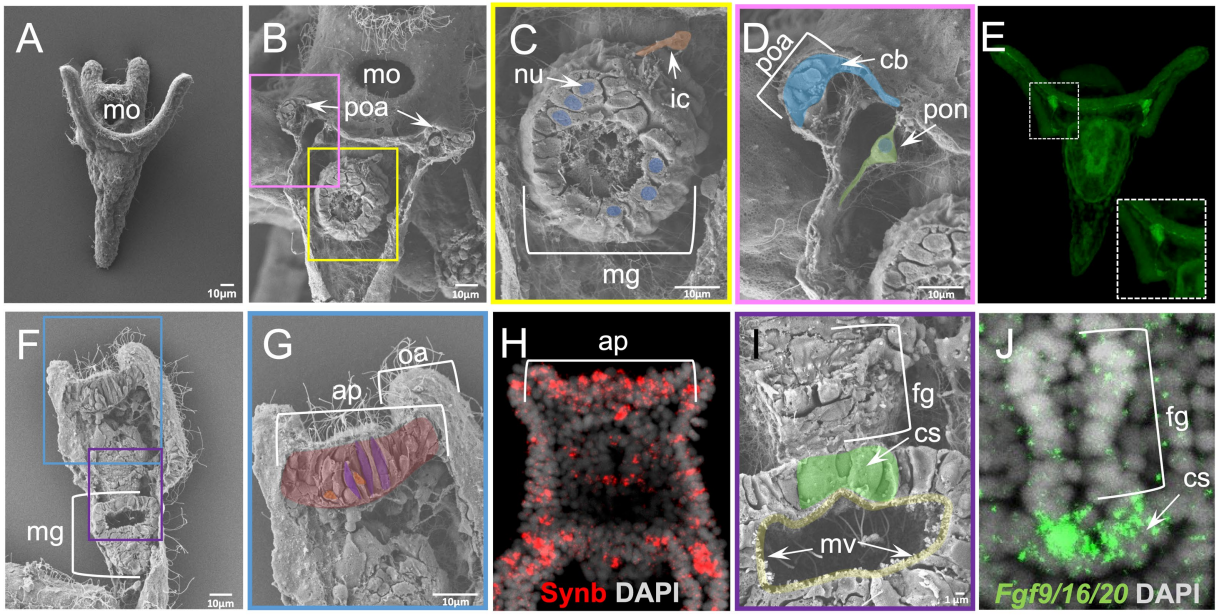

FIGURE 5
Results of WAFFSEM protocol applied on *Paracentrotus lividus* early larvae. **(A)** SEM image of an intact *P. lividus* 4 arm pluteus larva. **(B)** SEM image of a fractured *P. lividus* 4 arm larva seen in abanal view. The post oral arms and midgut regions are visible. **(C)** Inset of panel B showing in higher magnification the midgut region. An immune cell that is in contact with the midgut region as well as nuclei of midgut cells are visible. **(D)** Inset of panel B showing in higher magnification the post oral arm cell consistency and the post oral neuron. **(E)** Fluorescent detection of dopamine through FaGlu staining in a *P. lividus* larva. The dopaminergic post oral neurons are organized in bilaterally symmetric cell clusters in respect to the digestive tract. Axonal projections are found across the post oral arms and ciliary band. **(F)** SEM image of a fractured *P. lividus* 4 arm larva placed in dorsal view. **(G)** Inset of panel F showing the apical plate region of the specimen. **(H)** FISH using antisense probe against the sea urchin paneuronal marker *Synb*. **(I)** Inset of panel F showing the lower foregut and upper midgut regions of the larva in higher magnification. The cardiac sphincter and midgut microvilli are visible. **(J)** FISH using antisense probe for *Fgf9/16/20* marking the cardiac sphincter region. Nuclei in panels H and J are labeled with DAPI (in gray). ap, apical plate; cb, ciliary band; cs, cardiac sphincter; fg, foregut; ic, immune cell; mg, midgut; mo, mouth; mv, microvilli; nu, nucleus; oa, oral arm; ps, pyloric sphincter; poa, post oral arm; pon, post oral neuron. Pseudo-coloring was applied to enhance the visualization of the cell types of interest.

complex network of blastocoelar cells that are interconnecting most of the cell types of the larva (Figure 6H).

Moving on to a fractured larva seen from a dorsal view, we can see the two coelomic pouches of the larva at a cell resolution and their relative position and connectivity to the foregut region of the animal (Figure 6J). Furthermore, we also report the presence of distinct ciliated cells patterning those domains, a feature that was also evident by anti-acetylated tubulin immunohistochemistry, although lacking defined cell resolution (Figures 6J,K). Last but not least, a specimen that is placed in lateral view and fractured along the longitudinal axis allowed us to observe the cell morphology of the cells constituting the ciliary band, stomach and left coelomic pouch domains (Figures 6L,M). Especially for the coelomic pouch region, our approach allows us to speculate that the well-known *Vasa* positive cells, shown by FISH are potentially ciliated as revealed by WAFFSEM (Figures 6M,N). Moreover, on the same specimen, we observed the morphology of the skeletal spicules forming the larval skeleton that we highlighted as Msp130 immunopositive structures (Figure 6O). We identified, as well, the presence of a cell containing filopodia-like structures that appears to be in contact with the skeletal rod and potentially corresponds to a blastocoelar/immune cell (Figure 6M). This hypothesis is based on the previously shown evidence that sea urchin immune cells use the skeletal structures as a scaffold to migrate to different regions inside the larva (Allen et al., 2022). Taken together, our data set an example on how our WAFFSEM protocol combined with gene expression visualization methods, as well as transcriptomics, is able to provide complementary and useful information on assessment of cell type morphology and identity.

4. Discussion

Traditionally the classification of cell types was based on microscopy observation of the phenotypic characteristics of isolated cells, tissues, and organs. Nowadays, technologies have enabled the characterization and re-evaluation of cell types at an unprecedented resolution. However, most of these technologies focus on the identification of cell types at a molecular level and are not able to address their morphological features. On the other hand, electron microscopy-based methods such as Serial Block-face Electron Microscopy (SBEM) and Focused Ion Beam Scanning Electron Microscopy (FIBSEM) are able to successfully address cell type morphology, but currently due to their high price and sample size limitations are not applicable to a wide range of specimens. In this study, we optimized a low-cost method that is easy to use and is sufficient to reveal the cellular and subcellular characteristics of the specimens.

Our WAFFSEM method was tested on different developmental stages of six widely used marine experimental systems allowing the visualization of distinct cell type characteristics that were otherwise undetectable or detectable at a lower resolution with light microscopy. The efficiency of our method does not seem to bear any

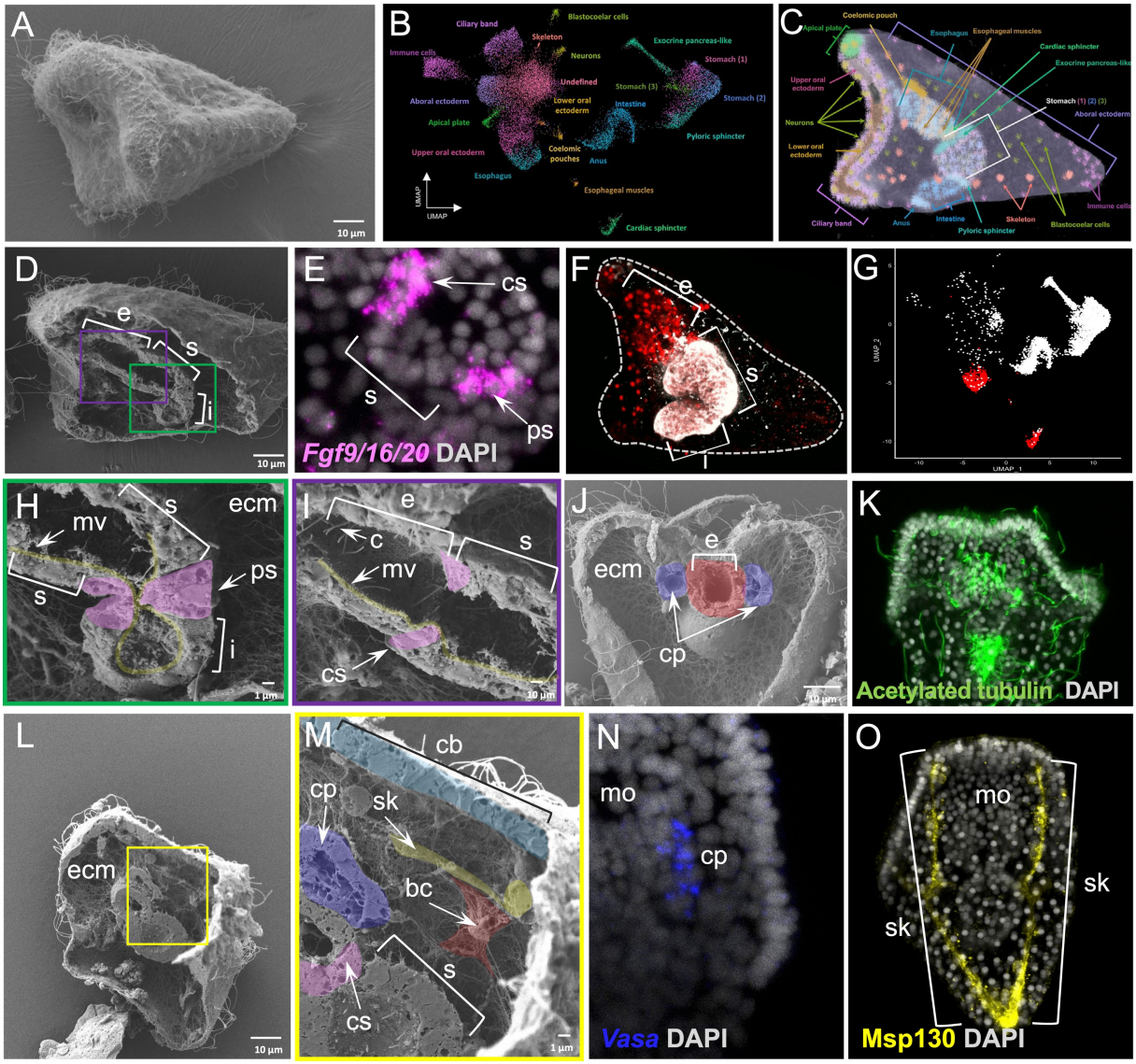

FIGURE 6
Whole animal freeze-fracture scanning electron microscopy protocol applied on *Strongylocentrotus purpuratus* 3dpf larvae combined with FISH, IHC and scRNA-seq. **(A)** SEM image of an intact *S. purpuratus* 3dpf pluteus larva. **(B)** UMAP representing the cell type atlas of the 3dpf pluteus larva [adapted from Paganos et al., 2022b]. **(C)** X-ray microtomography (MicroCT) of the 3dpf *S. purpuratus* pluteus larva, placed in lateral view, in which the different cell type families are labeled with pseudo-coloring [adapted from Paganos et al. (2022b)]. **(D)** SEM images of a fractured *S. purpuratus* 3dpf larva seen in lateral view. The three partitions of the digestive tract (esophagus, stomach, and intestine) are visible. **(E)** FISH using antisense probe for *Fgf9/16/20* marking the cardiac and pyloric sphincter regions. **(F)** Immunohistochemical staining using the Sp-Brn1/2/4 (red) and 5c7 (white) antibodies labeling the esophagus and the rest of the digestive tract regions, respectively, seen in lateral view. **(G)** Feature plot showing the esophageal (red) and the rest of the digestive tract regions (white) at a single cell resolution. **(H)** Inset of panel D showing the midgut and posterior gut regions of the larva's digestive tract in higher magnification. The morphology of the pyloric sphincter cells as well as microvilli are evident. **(I)** Inset of panel D focused on the esophageal and stomach domains of the digestive tract. The cardiac sphincter, cilia and microvilli are visible. **(J)** SEM image of a fractured *S. purpuratus* 3dpf larva seen in dorsal view. Extensive ECM networks and fractured pieces of the coelomic pouches and esophagus are evident. **(K)** Immunohistochemical detection of cilia using the antibody against acetylated tubulin. The larva is seen in dorsal view. **(L)** SEM image of a fractured *S. purpuratus* 3dpf larva seen in lateral view. **(M)** Inset of panel L showing a variety of cell types including the stomach, cardiac sphincter, ciliary band, left coelomic pouch, blastocoelar cells and skeleton. **(N)** FISH using antisense probe against *Vasa* mRNA marking the coelomic pouch of the larva. **(O)** Immunohistochemical detection of the larval skeleton using the antibody against Msp130. Larvae in N and O are seen in ventral view. Nuclei in panels E, K, N, and O are labeled with DAPI (in gray). bc, blastocoelar cell; c, cilia; cp, coelomic pouch; cs, cardiac sphincter; e, esophagus; ecm, extracellular matrix; i, intestine; mo, mouth; mv, microvilli; ps, pyloric sphincter; s, stomach; sk, skeleton. Pseudo-coloring was applied to enhance the visualization of the cell types of interest.

size or specimen shape restrictions; however, a high number of embryos or larvae is strongly recommended to ensure a high ratio of fractured versus not fractured specimens. In conclusion, we believe that the WAFFSEM protocol we optimized, is a useful and easy-to-use tool to characterize cell types. Nowadays, no matter how powerful, there is no sole technique that is able to solve every biological mystery. Therefore, correlative approaches are needed to thoroughly address complex scientific questions. Along this line we hope that our WAFFSEM protocol combined with other technologies and methods, will promote the advancement of the

Evo-Devo research field by improving our understanding of animal cell types from both a morphological and a molecular fingerprint point of view.

Data availability statement

The original contributions presented in the study are included in the article/supplementary material, further inquiries can be directed to the corresponding author.

Author contributions

PP, MIA, and GB: conceptualization. PP, FC, and GB: methodology. PP, FC, MC, ED'A, MIA, and GB: validation and writing—review and editing. PP: writing—original draft preparation. PP, FC, MC, and ED'A: visualization. GB: supervision. All authors contributed to the article and approved the submitted version.

Funding

PP was supported by Marie Curie ITN EvoCELL (H2020 grant number: 766053 to MIA) and Human Frontiers Science Program grant number (RGP0002/2019 to MIA). FC was supported by MUR CIR_0029 Human Capital and by Assemble Plus project (BA010618 and 360BA0619) to visit Observatoire Océanologique de Banyuls-sur-Mer (France).

Acknowledgments

The authors would like to thank Davide Caramiello for taking care of the adult sea urchins at Stazione Zoologica Anton Dohrn and Erica Riccio for her assistance in spawning the animals. We are also grateful to the microscopy facility at Stazione Zoologica Anton Dohrn for their assistance in sample preparation for SEM.

Conflict of interest

The authors declare that the research was conducted in the absence of any commercial or financial relationships that could be construed as a potential conflict of interest.

Publisher's note

References

Allen, R. L., George, A. N., Miranda, E., Phillips, T. M., Crawford, J. M., Kiehart, D. P., et al. (2022). Wound repair in sea urchin larvae involves pigment cells and blastocoelar cells. *Dev. Biol.* 491, 56–65. doi: 10.1016/j.ydbio.2022.08.005

Almazan, A., Cevrim, C., Musser, J. M., Averof, M., and Paris, M. (2022). Crustacean leg regeneration restores complex microanatomy and cell diversity. *Sci. Adv.* 8:eabn9823. doi: 10.1126/sciadv.abn9823

Cao, C., Lemaire, L. A., Wang, W., Yoon, P. H., Choi, Y. A., Parsons, L. R., et al. (2019). Comprehensive single-cell transcriptome lineages of a proto-vertebrate. *Nature* 571, 349–354. doi: 10.1038/s41586-019-1385-y

Chari, T., Weissbourd, B., Gehring, J., Ferraioli, A., Leclere, L., Herl, M., et al. (2021). Whole-animal multiplexed single-cell Rna-seq reveals transcriptional shifts across Clytia medusa cell types. *Sci. Adv.* 7:eabh1683. doi: 10.1126/sciadv.abh1683

D'aniello, E. (2009). *Studies on Rx Gene Function and Its Involvement in Ciona intestinalis ocellus Differentiation*. PhD thesis The Open University.

Davidson, E. H., and Erwin, D. H. (2006). Gene regulatory networks and the evolution of animal body plans. *Science* 311, 796–800. doi: 10.1126/science.1113832

Ernst, S. G. (2011). Offerings from an urchin. *Dev. Biol.* 358, 285–294. doi: 10.1016/j.ydbio.2011.06.021

Fuentes, M., Benito, E., Bertrand, S., Paris, M., Mignardot, A., Godoy, L., et al. (2007). Insights into spawning behavior and development of the European amphioxus (Branchiostoma lanceolatum).. *J. Exp. Zool. B. Mol. Dev. Evol.* 308, 484–493. doi: 10.1002/jez.b.21179

Macdonald, J. A., Fowle, W. H., and Woods, D. C. (2017). New insights on mitochondrial heterogeneity observed in prepared mitochondrial samples following a method for freeze-fracture and scanning electron microscopy. *Micron* 101, 25–31. doi: 10.1016/j.micron.2017.05.002

Massri, A. J., Greenstreet, L., Afanassiev, A., Berrio, A., Wray, G. A., Schiebinger, G., et al. (2021). Developmental single-cell transcriptomics in the *Lytechinus variegatus* sea urchin embryo. *Development* 148:dev198614. doi: 10.1242/dev.198614

Murat, F., Mbengue, N., Winge, S. B., Trefzer, T., Leushkin, E., Sepp, M., et al. (2023). The molecular evolution of spermatogenesis across mammals. *Nature* 613, 308–316. doi: 10.1038/s41586-022-05547-7

Musser, J. M., Schippers, K. J., Nickel, M., Mizzon, G., Kohn, A. B., Pape, C., et al. (2021). Profiling cellular diversity in sponges informs animal cell type and nervous system evolution. *Science* 374, 717–723. doi: 10.1126/science.abj2949

Paganos, P., Caccavale, F., La Vecchia, C., D'aniello, E., D'aniello, S., and Arnone, M. I. (2022a). Fish for all: a fast and efficient fluorescent in situ hybridization (Fish) protocol for marine embryos and larvae. *Front. Physiol.* 13:878062. doi: 10.3389/fphys.2022.878062

Paganos, P., Ronchi, P., Carl, J., Mizzon, G., Martinez, P., Benvenuto, G., et al. (2022b). Integrating single cell transcriptomics and volume electron microscopy confirms the presence of pancreatic acinar-like cells in sea urchins. *Front. Cell Dev. Biol.* 10:991664. doi: 10.3389/fcell.2022.991664

Paganos, P., Voronov, D., Musser, J. M., Arendt, D., and Arnone, M. I. (2021). Single-cell RNA sequencing of the *Strongylocentrotus purpuratus* larva reveals the blueprint of major cell types and nervous system of a non-chordate deuterostome. *elife* 10:e70416. doi: 10.7554/eLife.70416

Perillo, M., Paganos, P., Spurrell, M., Arnone, M. I., and Wessel, G. M. (2021). Methodology for whole mount and fluorescent Rna in situ hybridization in echinoderms: single, double, and beyond. *Methods Mol. Biol.* 2219, 195–216. doi: 10.1007/978-1-0716-0974-3_12

Plass, M., Solana, J., Wolf, F. A., Ayoub, S., Misios, A., Glazar, P., et al. (2018). Cell type atlas and lineage tree of a whole complex animal by single-cell transcriptomics. *Science* 360:eaaq1723. doi: 10.1126/science.aaq1723

Satoh, N., Tominaga, H., Kiyomoto, M., Hisata, K., Inoue, J., and Nishitsuji, K. (2021). A preliminary single-cell Rna-Seq analysis of embryonic cells that express Brachyury in the Amphioxus, *Branchiostoma japonicum*. *Front. Cell Dev. Biol.* 9:696875. doi: 10.3389/fcell.2021.696875

Stracke, K., and Hejnol, A. (2023). Marine animal evolutionary developmental biology–advances through technology development. *Evol. Appl.* 16, 580–588. doi: 10.1111/eva.13456

Tabula Muris, C. (2020). A single-cell transcriptomic atlas characterizes ageing tissues in the mouse. *Nature* 583, 590–595. doi: 10.1038/s41586-020-2496-1

Wessel, G. M., Fresques, T., Kiyomoto, M., Yajima, M., and Zazueta, V. (2014). Origin and development of the germ line in sea stars. *Genesis* 52, 367–377. doi: 10.1002/dvg.22772

Zheng, M., Zueva, O., and Hinman, V. F. (2022). Regeneration of the larval sea star nervous system by wounding induced respecification to the Sox2 lineage. *elife* 11:e72983. doi: 10.7554/eLife.72983

frontiers | Frontiers in Cell and Developmental Biology

TYPE Original Research
PUBLISHED 19 August 2022
DOI 10.3389/fcell.2022.991664

OPEN ACCESS

EDITED BY
Katherine Buckley,
Auburn University, United States

REVIEWED BY
Shunsuke Yaguchi,
University of Tsukuba, Japan
Smadar Ben-Tabou De-Leon,
University of Haifa, Israel

*CORRESPONDENCE
Maria Ina Arnone,
miarnone@szn.it

SPECIALTY SECTION
This article was submitted to Evolutionary Developmental Biology, a section of the journal Frontiers in Cell and Developmental Biology

RECEIVED 16 August 2022
ACCEPTED 21 July 2022
PUBLISHED 19 August 2022

CITATION
Paganos P, Ronchi P, Carl J, Mizzon G, Martinez P, Benvenuto G and Arnone MI (2022), Integrating single cell transcriptomics and volume electron microscopy confirms the presence of pancreatic acinar-like cells in sea urchins.
Front. Cell Dev. Biol. 10:991664.
doi: 10.3389/fcell.2022.991664

Integrating single cell transcriptomics and volume electron microscopy confirms the presence of pancreatic acinar-like cells in sea urchins

Periklis Paganos[1], Paolo Ronchi[2], Jil Carl[2], Giulia Mizzon[2], Pedro Martinez[3,4], Giovanna Benvenuto[1] and Maria Ina Arnone[1]*

[1]Stazione Zoologica Anton Dohrn (SZN), Naples, Italy, [2]European Molecular Biology Laboratory (EMBL), Heidelberg, Germany, [3]Institut Català de Recerca i Estudis Avancats (ICREA), Barcelona, Spain, [4]Genetics Department, University of Barcelona, Barcelona, Spain

The identity and function of a given cell type relies on the differential expression of gene batteries that promote diverse phenotypes and functional specificities. Therefore, the identification of the molecular and morphological fingerprints of cell types across taxa is essential for untangling their evolution. Here we use a multidisciplinary approach to identify the molecular and morphological features of an exocrine, pancreas-like cell type harbored within the sea urchin larval gut. Using single cell transcriptomics, we identify various cell populations with a pancreatic-like molecular fingerprint that are enriched within the *S. purpuratus* larva digestive tract. Among these, in the region where they reside, the midgut/stomach domain, we find that populations of exocrine pancreas-like cells have a unique regulatory wiring distinct from the rest the of the cell types of the same region. Furthermore, Serial Block-face scanning Electron Microscopy (SBEM) of the exocrine cells shows that this reported molecular diversity is associated to distinct morphological features that reflect the physiological and functional properties of this cell type. Therefore, we propose that these sea urchin exocrine cells are homologous to the well-known mammalian pancreatic acinar cells and thus we trace the origin of this particular cell type to the time of deuterostome diversification. Overall, our approach allows a thorough characterization of a complex cell type and shows how both the transcriptomic and morphological information contribute to disentangling the evolution of cell types and organs such as the pancreatic cells and pancreas.

KEYWORDS

sea urchin, pancreas, acinar cells, morphology, evolution of cell types, scRNAseq, SBEM

Introduction

Cell types consist of cells with common developmental origins and similar gene expression profiles that execute a specific gene regulatory program. The gene regulatory program associated to each cell type is tightly linked to its physiology and includes a periphery of terminal genes in charge of regulating its distinct morphological features and function. In this context, each distinct gene repertoire executing specific functions is uniquely deployed in that given cell type. One of the most intriguing scientific questions in the biology of organisms is how complex cell types arose during metazoan evolution and to how early the emergence of specific cell types can be traced.

Nowadays, technological advances in transcriptomics and imaging have increased the ease with which the combination of molecular fingerprint plus high-resolution morphology of cell types enable the tackling of such complex questions. For instance, single cell RNA sequencing (scRNA-seq) applied on organisms including both vertebrates and invertebrates, such as sponges, planarians, mollusks, cnidarians and echinoderms has led to the recognition of novel cell type families and the understanding of developmental and gene regulatory processes in these animals at an unprecedented level of detail (Fincher et al., 2018; Sebe-Pedros et al., 2018; Cao et al., 2019; Tabula Muris, 2020; Chari et al., 2021; Musser et al., 2021; Paganos et al., 2021; Salamanca-Díaz et al., 2022). Furthermore, single cell inventories have also allowed the reevaluation of developmental and evolutionary relationships of animals' cell types. Cross-species comparison of the developmental program at a cell type level has resulted in the identification of hidden homologies between cell types and organs across taxa, sometimes separated by enormous evolutionary time spans. Examples of this are the identification of homologous cell types across flatworm species, such is the case of neoblasts, or differentiated metazoan cell types such as muscles and neurons; but also identified closely linked relationships between contractile and neural cells in the sponge, jellyfish (Hydra) and mouse atlases (Tarashansky et al., 2021).

An interesting case of an organ lacking resolved evolutionary history is the vertebrate pancreas. Pancreas is a multifunctional organ that bears specialized cell types responsible for food digestion and organismal homeostatic regulation. In brief, digestion relies on the production and secretion of digestive enzymes that catabolize large biomolecules such as proteins to amino acids, plus the hormones involved in the metabolism of glucose derivatives. The complex cell type composition, and the precise architectural organization of the pancreas, allows it to act both as endocrine and exocrine gland.

The exocrine pancreas partition consists of cells that are spatially organized into acini (Slack, 1995; Karpińska and Czauderna, 2022) and are responsible for the synthesis, storage and secretion of digestive (zymogen) enzymes such as carboxypeptidases, amylases, lipases as well as proteases and their ontogeny has been thoroughly described in the past (Husain and Thrower, 2009). Once mature, acinar cells produce and secrete the zymogen enzymes, through a mechanism involving the vesicle transport into the pancreatic lumen, thus connecting the pancreas with the digestive tract (Husain and Thrower, 2009). On the other hand, the endocrine function of pancreas, which is mainly the production of hormones with homeostatic function such as insulin, glucagon and pancreatic polypeptide (PP), is executed by diverse populations of endocrine cells that in mammals are grouped into islets (islets of Langerhans). Noteworthy, both mammalian exocrine and endocrine glands are in direct contact with a ductal epithelium, whose role is to neutralize those enzymes (Karpińska and Czauderna, 2022).

Interestingly, although the cellular composition of pancreas is widely conserved among vertebrates, the spatial distribution of the different cell types varies across taxa. For instance, a specific feature of mammalian clade is that the pancreas contains different endocrine cell types with diverse functions (α-cells, β-cells, δ-cells, ε-cells and pancreatic polypeptide producing cells), which are clustered together in the islets of Langerhans, embedded within the same tissue as acini, a specific feature of mammals (Mastracci and Sussel, 2012). In other vertebrates, such as teleost fish, the organization of the pancreatic cell types appears to be rather simple, with all cells being grouped in pancreas-like organs consisting of endocrine cells organized also in islets, but here not embedded within the exocrine tissue (Falkmer et al., 1985; Yui and Fujita, 1986; Youson et al., 2006). The formation of a distinct pancreatic organ (with different cellular architectures) seems to be a vertebrate innovation as no such structure has been so far identified in invertebrates or even non-vertebrate chordates. However, gene expression studies identified the presence of distinct cell types employing a pancreatic genetic program. However, since these animals lack pancreas as a distinct organ, they are referred to as pancreatic-like cell types. For instance previous studies have shown that while no pancreas is present in cephalochordates and tunicates, several pancreatic-like cell types are there, dispersed throughout their digestive tract (Reinecke and Collet, 1998; Olinski et al., 2006; Arda et al., 2013; Lecroisey et al., 2015). Moreover, pancreatic-like cell types have been identified even in cnidarian species suggesting that a pancreatic-like molecular machinery might have been present in the last common ancestor of cnidarians and bilaterians (the Nephrozoa). In fact, scRNA-seq of *Nematostella vectensis* revealed the presence of several genes encoding for secreted digestive enzymes that were restricted to the pharynx cnidoglandular tract (Sebe-Pedros et al., 2018). Furthermore, a similar spatial distribution of exocrine and insulin-producing cells has been reported in ectodermally-derived cell types of the sea anemone (Steinmetz et al., 2017). All the previous evidence points toward the existence of a regulatory program in the common ancestor of the Nephrozoa, which is instantiated as a fully organized pancreas only in the vertebrates.

The molecular decisions, developmental pathways, and gene regulatory networks of all stages of pancreas development have been

reconstructed in great detail in various taxa, although most of the available data come from studies carried out exclusively in mammals. Such studies have highlighted the important role of several transcription factors in the specification of pancreatic progenitors, those that gives rise to both endocrine and exocrine lineages. In addition, distinct terminal differentiation gene batteries have been identified. Functional analysis has corroborated the specific role of some regulatory genes in the pancreas formation. For instance, the silencing of either the *pancreatic and duodenal homeobox 1 (Pdx1)* or the *pancreas-specific transcription factor 1a (Ptf1a)*, which are amongst the first transcription factors to be activated within the primitive murine gut tube (Burlison et al., 2008), leads to pancreatic agenesis (Ahlgren et al., 1996; Kawaguchi et al., 2002; Marty-Santos and Cleaver, 2016). Both transcription factors have been found to have a dual role, both in the initial steps of pancreatic progenitor specification and in the cell type's differentiation. In particular, *Ptf1a* is known as essential for the differentiation of acinar cells (Zecchin et al., 2004), while *Pdx1* is re-utilized later in development to promote specifically β-cells differentiation (Macfarlane et al., 1999; Afelik et al., 2006). The tightly modulated serial activation of different transcription factor regulatory modules will give rise to distinct pancreatic types. For instance, the differentiation of β-cells depends on a gene regulatory core consisting of the transcription factors *Pdx1, NeuroD, Islet1, Nkx2.2, Pax6, Mnx, Rfx6*, and *Rfx3* with the silencing of any of those genes resulting in the impairment of β-cell maturation and function (Ait-Lounis et al., 2010; Gu et al., 2010; Gosmain et al., 2012; Ediger et al., 2014; Piccand et al., 2014; Pan et al., 2015; Gutierrez et al., 2017). In contrast, the transcription factor *Brn4* is the dominant regulator of glucagon expression in another endocrine cell population, the α-cells (Hussain et al., 2002). Here, Notch signaling has been found to promote exocrine fate through the activation of *Ptf1a, Mist1 and Rbpj* and the repression of *Ngn3* (Pin et al., 2001; Fujikura et al., 2007).

Among deuterostomes, echinoderms, in particular sea urchin larva is a unique model to address pancreas evolution and the origination of the vertebrate structure. Their phylogenetic position as non-chordate deuterostomes, the thorough characterization of their cell lineages, the availability of genomic resources and the presence of resolved at a great detail gene regulatory networks make sea urchins suitable for addressing the question of organogenesis evolution. In the larvae of the sea urchin *S. purpuratus*, cells located in the upper part of the larval stomach co-express a subset of typical pancreatic digestive enzymes. Their gene regulatory program depends on the Notch signaling pathway and the activation of the transcription factor *Sp-Ptf1a* (Perillo et al., 2016) and due to their gene expression similarities to the mammalian exocrine pancreas cells were annotated as exocrine pancreas-like cells. Furthermore, it has been demonstrated that apart from the gene expression conservation, the sea urchin homolog of the vertebrate *Ptf1a* gene can substitute for its vertebrate homolog in activating downstream gene targets (Perillo et al., 2016). In addition to the exocrine pancreas-like cells, sea urchin larva also contains specialized gut cells that produce a structurally similar protein to that of the cephalochordate amphioxus insulin-like peptide (Perillo and Arnone, 2014). Interestingly, the insulin positive cells were found in the intestinal region of the larva, which is known to be patterned and controlled by the sea urchin homolog of the vertebrate *Pdx1* gene (Cole et al., 2009; Annunziata et al., 2014). It is important to stress out that previous studies from our group demonstrated that sea urchin could potentially represent an intermediate stage in pancreas evolution, since the larva contains, apart from the endodermally-derived endocrine and exocrine-like cell types (Perillo et al., 2016). Moreover we recently provided evidence that sea urchin larvae possess an additional neuronal population with a pancreatic-like gene toolkit, whose differentiation is *Pdx1*-dependent, and was probably co-opted by modern endocrine pancreatic cells (Paganos et al., 2021). This scenario is also supported by the molecular and functional similarities of mammalian neurons and β pancreatic cells (Arntfield and van der Kooy, 2011).

Despite our previous knowledge, little is known of these pancreatic-like cell types present in the sea urchin digestive tract. There are still some open questions regarding the number of pancreatic-like cell types that need to be resolved, in particular, whether they are endocrine or exocrine-like. Additionally, it is still not clear to which extent the molecular similarity also reflects a morphological resemblance with the vertebrate pancreatic cells. In order to address these questions, we undertook a thorough molecular and morphological characterization of those cell types. Here we demonstrate that the pancreatic signature is present in distinct populations of cells within the larval digestive tract, supporting the hypothesis that the cell types constituting the pancreas are already present in a deuterostome and prior to the late coalescence in a distinctly organized multifunctional unit, the pancreas. Furthermore, we characterize molecularly and morphologically an exocrine cell type that is present in the upper part of the larval stomach, and whose specification is remarkably guided by a specific gene regulatory network used in the differentiation of mammalian pancreatic progenitors of acinar cells. Moreover, we provide evidence that the sea urchin acinar-like cells are homologous to the building blocks making the pancreatic acini in mammals. This was estimated by their molecular signature as identified using single cell transcriptomics and their distinct morphological features as shown by volume electron microscopy paired with confocal microscopy.

Materials and methods

Animal husbandry and larval cultures

Adult *Strongylocentrotus purpuratus* individuals were collected from the San Diego coast by Peter Halmay and shipped by Patrick Leahy (Kerckhoff Marine Biological Laboratory, California Institute of Technology, Pasadena, CA, United States). Sea urchins were

housed in circulating seawater and temperature controlled aquaria at both the Stazione Zoologica Anton Dohrn, Naples, Italy and the European Molecular Biology Laboratory, Heidelberg, Germany. Gametes were collected after *in vitro* induced spawning of the adult individuals; oocytes were fertilized, and embryos/larvae were reared at 15°C in FSW diluted 9:1 with distilled H_2O (Filtered seawater) until the developmental time-points of interest. Larval cultures were maintained by exchanging half of the FSW with fresh FSW) two times per week. After the 3 days post fertilization (dpf) pluteus stage, the larvae were fed three times per week with the unicellular micro-algae *Dunaliella* sp at an approximate concentration of 1,000 cells/mL.

Fluorescent *in situ* hybridization and immunohistochemistry

Fluorescent *in situ* hybridization (FISH) was performed as described in Paganos et al. (2022). Embryos and larvae were fixed in 4% PFA in MOPS Buffer overnight at 4°C, washed with MOPS buffer and then stored in 70% ethanol at −20°C. Antisense mRNA probes against the genes of interest were generated as described in Perillo et al. (2021). Probes for *Pdx1, Cdx, Brn1/2/4, ManrC1a* were generated as described in Annunziata and Arnone (2014); for *Fgf9/16/20* and *SoxE* as described in Andrikou et al. (2015); for *Cpa2L* and *Ptf1a* as shown in Perillo et al., 2016; for *Islet* as described in Perillo et al., 2018 and for *Rfx6* and *Serp2/3* in Paganos et al., 2021. Primers used for the amplification of *Rfx3, Mnx, FoxA* and *Trypsin 2* can be found in Supplementary Table 1. Briefly, genes of interest were isolated from a pool of cDNAs, and the amplified products were sequenced. Probes were generated through *in vitro* transcription using Digoxigenin or Fluorescein RNA labeling mix solutions (Roche) and signal was developed through cyanine based signal amplification (Akoya Biosciences). Immunohistochemistry (IHC) was carried out as described in Perillo et al., 2021 with minor modifications. Once FISH procedure was completed specimens were placed in blocking solution containing 1 mg/ml Bovine Serum Albumin (BSA) and 4% sheep serum in MOPS buffer for 1 h at room temperature (RT). Primary antibodies were added in the appropriate dilution and incubated for 1 h and 30 min at 37°C. Endo1 (gift from Dr. David McClay) was used to mark the mid and hindgut domains (undiluted). Specimens were washed with MOPS Buffer (five times) and incubated for 1 h with the appropriate secondary antibody (AlexaFluor) diluted 1:1,000 in MOPS buffer. Samples were washed several times with MOPS buffer and imaged using a Zeiss LSM 700 confocal microscope.

X-ray micro computed tomography

EM prepared samples (3 dpf *S. purpuratus* larvae) fixed in 2% Glutaraldehyde in FSW and embedded in resin were manually trimmed with a razor blade to reduce the size and the amount of empty resin around the larvae. When necessary, further trimming with an ultramicrotome (Leica UC7) and a diamond trimming knife (Cryotrim 90, Diatome) was done to smoothen the surfaces of the blocks and reduce potential imaging artifacts. The obtained samples were then imaged using a Bruker Skyscan 1272, using the X-ray source at a voltage of 50 kV and 200 µA current. The samples ware rotated 180° on the stage and images were collected every 0.2° with an exposure time of 519 ms at 1 µm voxel size. The 3D volume was finally reconstructed using the software NRecon (Bruker).

Volume electron microscopy

S. purpuratus 3 dpf larvae were frozen at a high pressure with an HPM010 (Abra Fluid) high pressure freezer using 20% Ficoll 70 (Sigma) in FSW as a cryoprotectant. The samples were then freeze substituted with a solution of 1% OsO_4, 0.5% Uranyl Acetate and 5% H_2O in acetone, using a Leica AFS2. They were left afterwards for 64 h at −90°C before increasing the temperature to −30°C using a speed of 5°C/h. After 4 h incubation at −30°C the temperature was gradually increased to +20°C (5°C/h), and the samples were further incubated for 5 h. After this, samples were manually rinsed with dry acetone before putting them in a solution of 0.1% Thiocarbohydrazide and 10% H_2O in acetone for 20 min at room temperature. The contrast was then further increased by a second OsO_4 incubation (1% in acetone). Infiltration in Durcupan (Sigma) was performed with a Pelco Biowave (Ted Pella). The samples were flat-embedded, and the resulting blocks were scanned with an X-ray micro computed tomography apparatus [Skyscan 1272, Bruker, referred to as micro computed tomography (microCT)] in order to identify and target the best preserved larvae. The sample was then trimmed (UC7, Leica) using a 90° cryo-trimmer (Diatome) to generate a small block face (~400 µm × 400 µm) and to approach in depth the larva of interest. The resulting resin block was mounted on a pin stub using silver conductive epoxy resin (Ted Pella). The serial block face acquisition was performed with a Zeiss Gemini2 equipped with a Gatan 3view microtome and a focal charge compensation device (Zeiss). The SEM was operated at 1.5 kV 300 pA, using a pixel size of 15 nm, a dwell time of 0.8 µs and a slice thickness of 50 nm. The acquisition of the full larva images was performed using the software SBEMimage (Titze et al., 2018). After acquisition, alignment of the sections and the tiles containing the volume of interest (covering the larva stomach) were aligned and blended using the FiJi plugin TrackEM2 (Cardona et al., 2012). Segmentation and analysis were performed using the software package Amira (Thermo Fischer Scientific). The aligned SBEM dataset was imported in a x,y binned form to identify regions of interest, which were then imported at full resolution for further study. Nuclei, vesicles and plasma membranes were segmented in a semi manual fashion using the thresholding and Magic Wand tools in Amira. The

resulting segmented objects were further rendered for three-dimensional visualization using the surface rendering module and analyzed using the label analysis module to quantify organelle volumes and positions. Vesicles were classified as apical based on their position below the base of the nucleus in direction of the apical plasma membrane.

Single cell RNA sequencing analysis

The Single cell RNA data analyzed in this study originate from the study by Paganos et al. (2021) as they have been deposited in Dryad under the unique identifier https://doi.org/10.5061/dryad.n5tb2rbvz. Subclustering analysis has been performed as described in Paganos et al. (2021) using the Seurat scRNA-seq R package (Butler et al., 2018; Stuart et al., 2019). Subclustering analysis was performed by selecting and subsetting the cell type families of endodermal origin (esophagus, cardiac sphincter, exocrine pancreas-like, stomach 1, 2, and 3, pyloric sphincter, intestine and anus). Datasets were normalized and variable genes were found using the vst method with a maximum of 2,000 variable features. These datasets were scaled, and principal component (PCA) analysis was performed. Nearest Neighbor (SNN) graph was computed with 20 dimensions (resolution 1.0) and Uniform Manifold Approximate and Projection (UMAP) was used to perform clustering dimensionality reduction. Cluster markers were found using the genes that are detected in at least 0.01 fraction of min.pct cells. The average score of pancreatic gene markers was estimated using the AddModuleScore function incorporated in Seurat R package. The presence of transcripts per cluster was visualized using the DotPlot or DoHeatmap functions incorporated in the Seurat package.

Results

Pancreatic-like signature across larval cell type families

Single cell RNA sequencing has been shown to be a great resource in analyzing fine developmental events as well as identifying complex molecular signatures during sea urchin embryogenesis (Massri et al., 2021; Paganos et al., 2021). Previously, we have used single cell RNA sequencing originating from 3 dpf *S. purpuratus* larvae to reconstruct the cell type family composition of the *S. purpuratus* pluteus larva (Paganos et al., 2021). The results of that analysis resulted in the identification of 21 cell type families with diverse regulatory signatures (Figures 1A,B) as well as 12 distinct neuronal types, one of which was found to utilize, surprisingly, a gene regulatory toolkit that is present in mammalian endocrine cells. Based on those findings, confirming the presence of neuroendocrine sea urchin cells that employ an evolutionary conserved pancreatic gene regulatory program led by *Pdx1*, we decided to investigate whether a pancreatic-like molecular signature is deployed in other sea urchin larval cell type families. To do so, we selected, as guides, a core (module) of typical mammalian transcription factors that are known to be essential for pancreatic cells specification and/or differentiation (Figure 1C). Plotting for the average score of the sea urchin orthologs of these markers reveals an enrichment of this module in ectodermally-derived upper oral ectodermal and neuronal cell type families as well as in endodermally-derived cells corresponding to anal, intestinal, exocrine pancreas-like and esophageal clusters (Figure 1D), all suggesting a broad use of this module in a variety of larval cell types. Similar data were obtained by plotting for the average expression of each member of this module highlighting the expression of endocrine pancreas gene markers in both neurons (*FoxA2, Ngn3, Pdx1, NeuroD1, Mnx, Islet, Rfx3, Brn4* and *Mist*) and intestinal cells (*FoxA2, Pdx1, NeuroD1, Mnx, Nkx2.2* and *Rfx6*), thus suggesting a shared pancreatic regulatory wiring in these two cell type groups (Figure 1E). Interestingly, the same plot reveals the presence of an endocrine pancreas regulatory wiring also in the pyloric sphincter cell types expressing *Gata6, Pdx1, Nkx6.1, Rfx3* and *Rfx6* genes. Moreover, these data, taken together, suggest the presence of at least two distinct endocrine and exocrine cell fates, with the endocrine deployed in both ectodermally- and endodermally-derived cell type families, and the exocrine limited to a well-defined cluster (Figures 1D,E).

Assessing the pancreatic signature of the digestive tract at a single cell resolution

In order to further investigate the pancreatic-like signature of the digestive tract at a higher resolution, we performed subclustering analysis solely of clusters representing endodermally-derived cell type families. This analysis, originating from nine initial clusters resulted in the generation of 15 distinct subclusters (Figure 2A) for which the marker genes were extracted (Supplementary File 3). Next, we used the marker genes in combination with already known lineage and cell type specific gene markers (Supplementary Figures S1A,B to annotate them. For instance, such markers included the transcription factors *Sp-Bra* and *Sp-Hox11/13b* known to be expressed in cells located in the anal region of the digestive tract (Annunziata et al., 2014; Paganos et al., 2021), *Sp-Ffg9/16/20* expressed in the anal, pyloric and cardiac sphincters domains (Paganos et al., 2021), *Sp-ManrC1A* which is a midgut/stomach molecular marker (Annunziata et al., 2014; Paganos et al., 2021), and *Sp-Brn1/2/4* expressed specifically in the esophageal domain (Cole et al., 2009; Perillo et al., 2018; Paganos et al., 2021). Interestingly, we detected the presence of an unexpected cluster composed of cells that, based on their molecular signature, correspond to an anal subtype. These cells appear to also co-express genes related to the

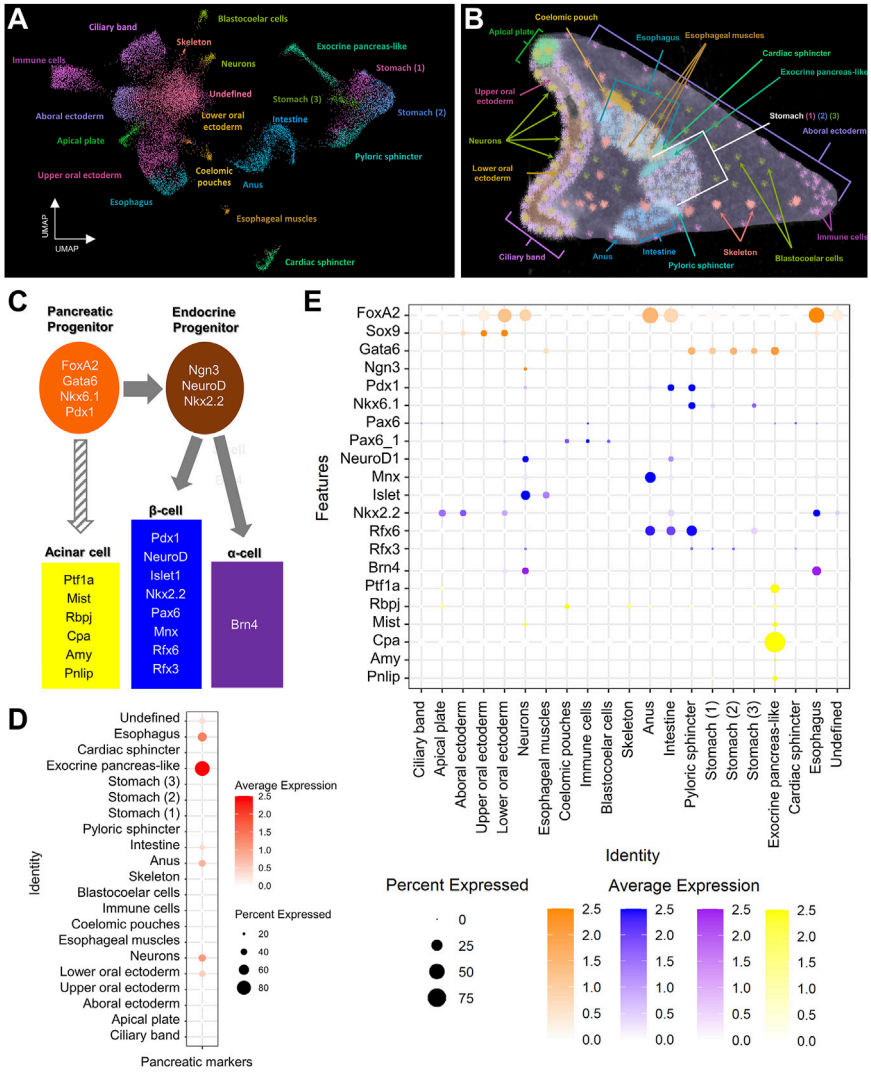

FIGURE 1
Pancreatic-like molecular signature of the *S. purpuratus* larva cell type families. **(A)** Uniform Manifold Approximation and Projection (UMAP) showing the 3 dpf *S. purpuratus* cell type families (modified from Paganos et al., 2021). **(B)** X-ray Microtomography (MicroCT) of the 3 dpf *S. purpuratus* pluteus larva, placed in lateral view, in which the different cell type families are labelled with pseudo-coloring. Color code is the same as the one used in **(A)**. **(C)** Simplified schematic representation of pancreatic gene markers known to be present in specific stages of pancreatic development and distinct pancreatic lineages. **(D)** Dotplot showing the average score of the sea urchin pancreatic marker orthologs shown in **(C)** across the larval cell type families. **(E)** Dotplot showing the average expression of the pancreatic markers across the larval cell type families. Color code in **(E)** is the same as the one used in **(C)**.

mesodermally-derived lineage of pigment cells and were therefore annotated as immune cells. Sea urchin pigment cells are immune cells known to migrate from the tip of the archenteron to the ectoderm during gastrulation and from the ectoderm to the digestive tract later on in development and the presence of pigment cells in the anal domain have been validated by previous studies (Buckley and Rast, 2017; Perillo et al., 2020). Whether the cells we find in our digestive tract subclustering correspond to transfated pigment cells, that employ an endodermal genetic program after migration to the anal region or endodermally derived pigment cells needs further investigation.

Once the identity of the subclusters was validated, we set out to explore the expression of specific pancreatic markers in the different digestive tract-associated cell types. Plotting for the average expression of these genes validated our initial assessment of a broad endocrine-like signature in a plethora of digestive tract clusters and the confined expression of exocrine pancreas genes in only two very similar subclusters (Figure 2B). Specifically,

The validation of the single cell predictions was done through the use of FISH and using specific antisense mRNA probes against the sea urchin orthologs of several key pancreatic markers. The FISH data confirmed the shared expression of

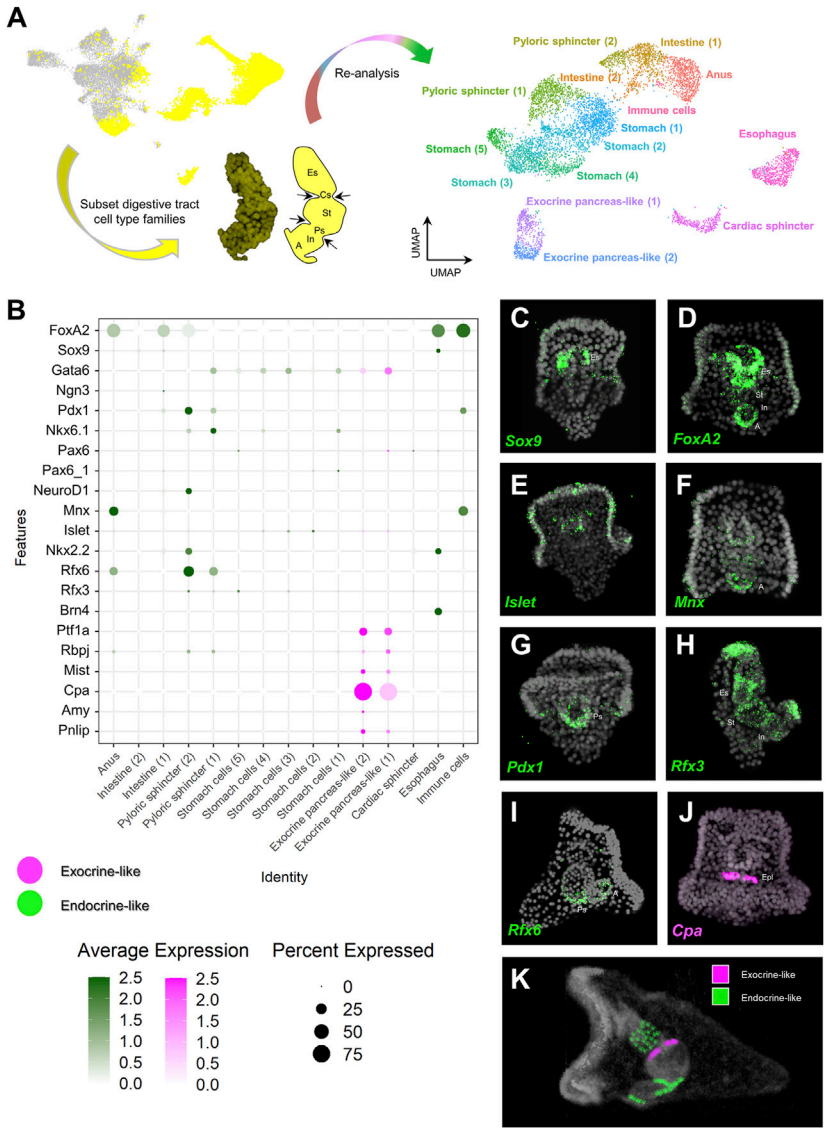

FIGURE 2
Distribution of endocrine and exocrine pancreas-like markers across the digestive tract. **(A)** Summary of the pipeline used to increase the resolution of the digestive tract cell type composition. Digestive tract related cell type families are highlighted in yellow (left), subsetted and subclustered resulting in the generation of 15 clusters (right). **(B)** Dotplot showing the average expression of pancreatic gene markers across the digestive tract subclustered dataset. Colored boxes are used to highlight endocrine-like (green) and exocrine-like (magenta) molecular signatures. **(C–J)** FISH using antisense probes designed against several of the pancreatic markers used in **(B)**. Color code of the signal is the same as in **(B)**. DAPI was used to label the nuclei (gray). **(K)** MicroCT of the 3 dpf *S. purpuratus* pluteus larva, placed in lateral view, in which the different pancreatic-like molecular fingerprints found in the digestive tract are labelled with pseudo-coloring. Color code is the same as the one using in **(B)**. A, Anus; Es, Esophagus; Cs, Cardiac sphincter; Epl: Exocrine pancreas-like; In, Intestine; Ps, Pyloric sphincter; St, stomach.

the sea urchin orthologs of *Sox9* and *FoxA2* (Figures 2C,D) in the esophageal region, the neuronal expression of *Islet* (Figure 2E), the cell type specific expression of *Cpa* (*Sp-Cpa2L*) in the upper part of the midgut region (Figure 2J), the broad expression of *Rfx3* across the digestive tract cell types (Figure 2H) and the enrichment of *Mnx*, *Pdx1* and *Rfx6* in cell populations of the posterior gut (Figures 2F,G,I, respectively). The results of this analysis are summarized in Figure 2K.

Molecular characterization of the sea urchin exocrine pancreas-like cells

Once the mapping of the pancreatic-like cell types in the different parts of the digestive tract was established, we set out to characterize in detail the exocrine pancreas-like cells, which was the primary goal of our study. Previous studies from our group demonstrated that a unique population of cells producing

10.3389/fcell.2022.991664

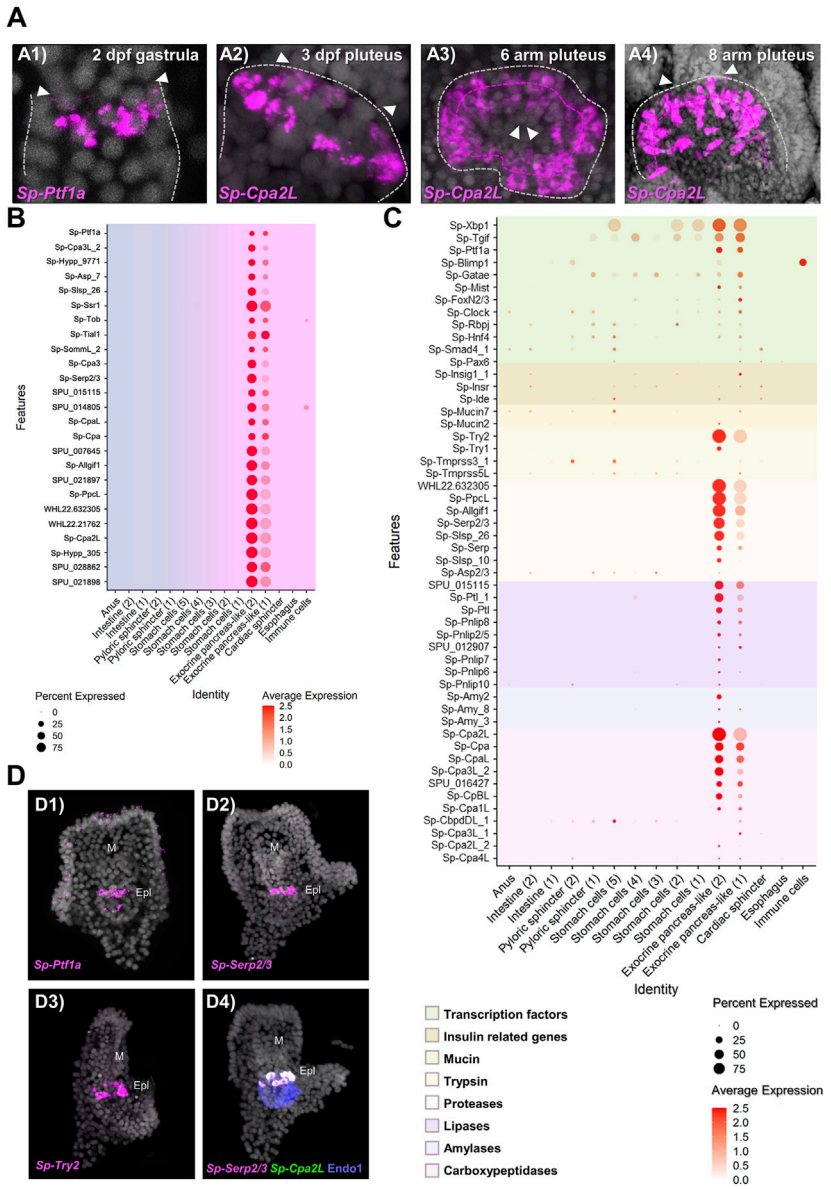

FIGURE 3
Molecular characterization of the *S. purpuratus* larva exocrine pancreas-like cells. **(A)** FISH using antisense probes against *Sp-Ptf1a* (A1) and *Sp-Cpa2L* (A2–4) at gastrula and various larval stages, respectively. Contour of the digestive tract compartment (gray) and the double belt row structure (magenta) are shown in dotted lines. Arrowheads indicate the position of the presumptive (A1) and the actual cardiac sphincter (A2–4). Specimens in A1, A2, and A4 are oriented in lateral view and the larva in A3 is viewed from the cardiac sphincter. **(B)** Dotplot showing the average expression of the top 25 exocrine pancreas-like marker genes. **(C)** Dotplot showing the average expression of sea urchin orthologous genes encoding for proteins found in mammalian acinar cells. **(D)** FISH validations of gene predictions shown in **(C)** using antisense mRNA probes for *Sp-Ptf1a* (D1), *Sp-Serp2/3* (D2, D4), *Sp-Trypsin2* (D3) and *Cpa2L* (D4). FISH shown in D4 was paired with IHC for the midgut and posterior gut marker Endo1. DAPI was used to label the nuclei (gray). Epl, Exocrine pancreas-like; M, Mouth.

digestive enzymes and located in the upper part of the larval midgut. These cells use a pancreatic-like regulatory circuit that is activated by the Notch signaling and includes the sea urchin homologs of the transcription factors *Hnf1a* and *Ptf1a*, that in mammals is controlling the specification and differentiation of pancreatic acinar cells (Perillo et al., 2016). The subclustering analysis reported in this study revealed the presence of two extremely diversified clusters within the digestive tract that correspond to exocrine pancreas-like cells, as suggested by the expression of the transcription factors *Sp-Ptf1a*, *Sp-Rbpj*, plus the presence of the enzymes carboxypeptidase (*Cpa*), amylase (*Amy*) and pancreatic lipase coding genes (*Pnlip*). *In situ* hybridization

using antisense probes for *Sp-Ptf1a* and *Sp-Cpa2L* corroborated our previous observations that there is a continuous increase of the number of cells constituting the exocrine cell type over time (Figure 3A). These exocrine cells originate at late gastrula stage (2 dpf) as two *Sp-Ptf1a* positive cells in the midgut domain (Figure 3, A1); at 3 dpf pluteus larva, these adopt the shape of a belt-like structure consisting of five to seven cells (Figure 3, A2) located in the upper part of the stomach. As larval development continues, a second tier of exocrine-like cells arises right next to the first one (Figure 3, A3) and the double rowed belt structure is retained up to the end of the larval development, at the competent 8 arm pluteus stage (Figure 3, A4).

Based on the above results, we explored the system to understand to what extent the molecular signature of the sea urchin exocrine pancreas-like cells is similar to the one of the mammalian acinar cells. For this reason, we next investigated whether the genes encoding for proteins involved in the exocrine function in vertebrates are also expressed in the exocrine pancreas-like cells of the sea urchin. It is well known that the exocrine process depends on the coordinated function of trafficking proteins including members of the syntaxin and synaptotagmin families, proteins which promote exocytosis of cargo-loaded vesicles (Messenger et al., 2014). Here we found that the exocrine pancreas-like cell type family expressed mRNAs related to vesicle trafficking such as *Sp-Nsf, Sp-Trappc2, Sp-Sec22*, various syntaxins (*Sp-Stx5, Sp-Stx6, Sp-Stx7, Sp-Stx12, Sp-Stx18*) and synaptotagmins (*Sp-Syt6, Sp-Syt7, Sp-Syt15*), coating such as mRNAs encoding for clathrin heavy and light chains and exocytosis mRNAs encoding for different exocyst complex component proteins (Supplementary Figure S2; Supplementary File 1). The expression pattern of all of them appears to be highly restricted to this cell type family since no co-localization of these mRNAs could be observed in any other cell type family of the larva (Supplementary Figure S2; Supplementary File 1). However, traces of this molecular signature were detected in neighboring cell types such as stomach cells and the cardiac sphincter as well as the neuronal cell type family suggesting the use of a similar but not identical vesicle trafficking toolkit between neuroendocrine and exocrine cells.

To better understand how similar the exocrine cells are to the mammalian acinar cells we looked for the presence of diverse gene families including transcription factors and terminal differentiation genes that are typically expressed in pancreatic acinar cells. Regarding transcription factors, we found a cell type specific expression of a module that includes the transcription factors *Sp-Xbp1, Sp-Tgif. Sp-Ptf1a, Sp-Blimp1, Sp-Gatae, Sp-Mist, Sp-Fox2/3, Sp-Clock, Sp-Rbpj, Sp-Hnf4, Sp-Smad4* and *Sp-Pax6* (Figure 3C, D1) typical of pancreatic cells. Pancreatic acinar cells have a complex physiology and their proper function to produce and secrete zymogens is controlled by signals originating from neighboring pancreatic cell types. Plotting for genes related to one of the most important pancreatic hormones, the insulin, we found the presence of insulin related genes such as insulin receptor (*Sp-Insr*) and insulin degrading enzyme (*Sp-Ide*) in the exocrine clusters as well as two mucin genes (*Sp-Mucin2* and *Sp-Mucin7*) known to encode for mucin proteins used for protective and lubricative role in acinar cells (Figure 3C). The presence of transcriptional regulators and effector proteins supports, with confidence, the presence of acinar-type cells in the sea urchin. However, what really differentiates pancreatic acinar cells from the rest of the pancreatic lineages is their ability to produce zymogens involved in food digestion. Typical pancreatic zymogens include proteases, lipases, amylases and carboxypeptidases. Previous studies in our laboratory demonstrated the presence of at least one carboxypeptidase (*Sp-Cpa2L*), one amylase (*Amy3*) and one pancreatic lipase (*Pnlip2/5*) gene expressed in the exocrine domain of the sea urchin larva (Perillo et al., 2016). A further characterization of these genes' domains of expression would provide evidence for the co-expression of those and additional members of the exocrine pancreatic gene families (Figure 3C,D). Based on our analysis presented in this study, *Sp-Trypsin1 (Try1)* and *Sp-Trypsin2 (Try2)* were predicted to be specifically expressed in the two exocrine populations, and here the expression of the latter was also confirmed by FISH (Figure 3, D3). Similarly, we extended our analysis to least eight additional members of the protease family and those were found to be marking specifically the exocrine cells as is the case of the protease *Sp-Serp2/3*, which was found to be expressed within those cells and co-localized with *Sp-Cpa2L* transcripts (Figure 3; D2, D4). Moreover, members of the ribonuclease and deoxyribonucleases protein families were also found to be differentially expressed in the exocrine cells (Supplementary Files 2 and 3). Overall, we were able to expand our knowledge regarding the exocrine cells specific expression of carboxypeptidases, amylases and lipases by adding the expression of 10, 2 and 8 new members, respectively (Figure 3C), while also discovering the presence of proteases and (deoxy)ribonucleases in sea urchin exocrine cells.

Next, we set out to explore how unique is the molecular signature of the two exocrine putative cell types in respect to the rest of the digestive tract cell types. Plotting of the top 25 exocrine marker genes (Figure 3B) showed a well-confined expression of these genes only in the exocrine pancreas-like clusters suggesting that: 1) a highly diversified genetic program operates in these cells; 2) cells in these two clusters express similar genes but at different expression levels, which is indicative of the presence of diverse developmental exocrine states. To further understand the nature of the two exocrine clusters we compared their transcriptomic profile. This analysis showed that the two exocrine clusters are very similar to each other and distinct from the rest of the digestive tract cell types. However, their mutual comparison revealed fine transcriptomic differences (Supplementary Figure S3A). Looking carefully into the genes

10.3389/fcell.2022.991664

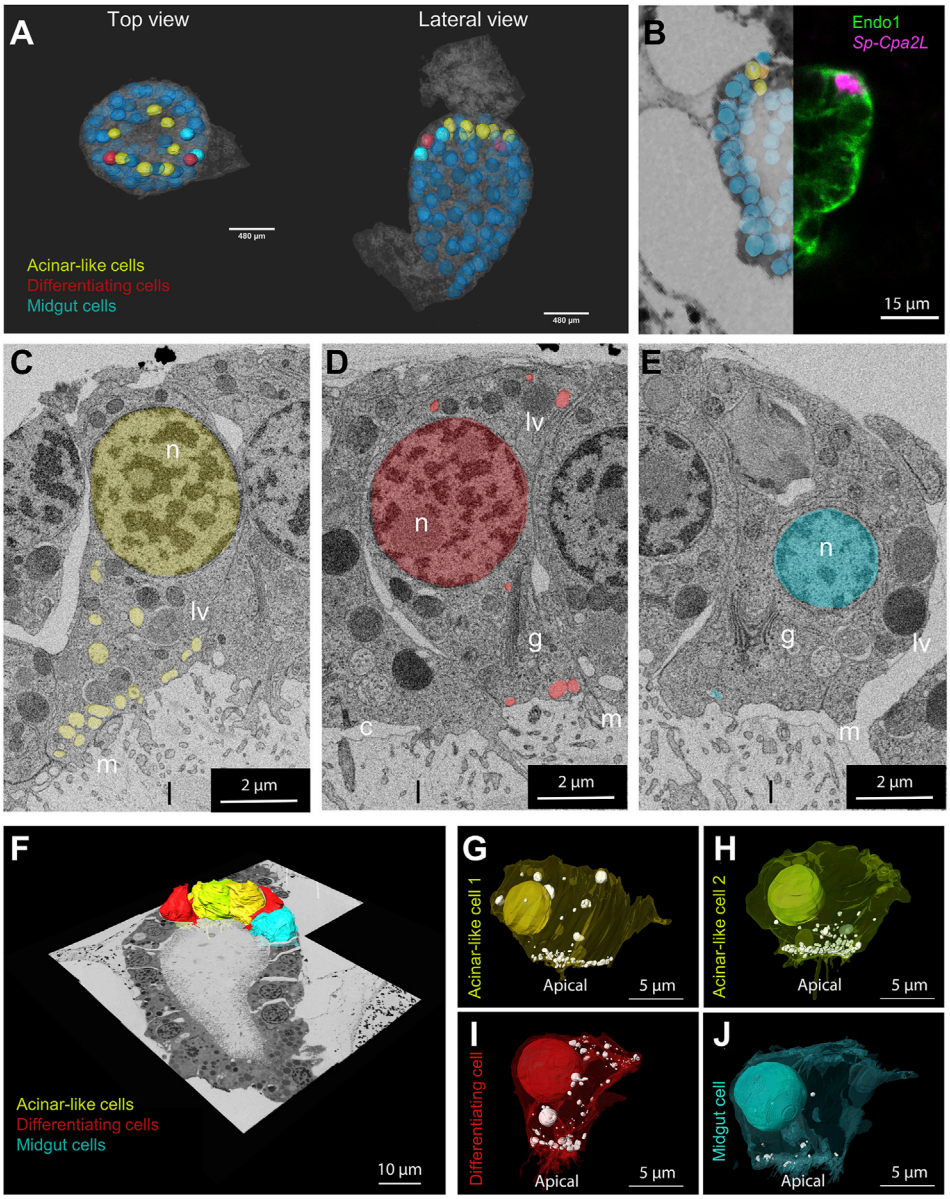

FIGURE 4
Morphological characterization of the *S. purpuratus* larva exocrine pancreas-like cells. **(A)** Nuclei segmentation of the entire midgut region in which cell membranes are visible (semitransparent). Midgut (blue), differentiating (red) and exocrine pancreas-like nuclei (yellow) are shown. The nuclei shown with lower transparency are the ones segmented and used for the analysis. Cell membranes are semi-transparent. **(B)** Overlay and stitching of the FISH for Sp-Cpa2L (magenta), IMH for endo1 and the vEM dataset. **(C–E)** Isolated slices showing an example of the vesicle relative number and polarization per cell type identified. 3D reconstruction of the cells located in the upper part of the midgut region. Plasma membranes of cell types analyzed were segmented and shown projected on the stitched EM dataset. **(F–J)** Individual 3D reconstructions of the segmented cell types of interest. The plasma membranes visible in a semi-transparent manner, revealing the nuclei and vesicle number and position. Yellow and lime, exocrine cell; Red, differentiating cell; cyan; main stomach cell. c, cilium; g, golgi; n, nucleus; l, lumen; lv, larger vesicles; m, microvilli.

that were found differentially expressed in the two clusters we found that genes that are related to a midgut cell fate such as *Sp-ManrC1A* were enriched in the exocrine pancreas-like cluster-1 (Supplementary Figure S3B). On the other hand, exocrine cells markers expressed in fully differentiated exocrine pancreas-like cells such as *Sp-Cpa2L*, *Sp-Cpa3* and *Sp-Serp2/3* were detected among the top 25 marker genes of the exocrine pancreas-like cluster-2 (Supplementary Figure S3C). Taken together, our data

suggest the existence of distinct developmental states of the exocrine cells that could potentially give rise to a unique fully differentiated exocrine cell type.

Morphological characterization of the sea urchin exocrine pancreas-like cells

The assessment of cell type evolution relies on the identification of evolutionary conserved regulatory programs that in case of homologous cell types give rise to distinct cell morphologies. Our scRNA-seq analysis applied on the 3 dpf *S. purpuratus* pluteus larva has revealed a high degree of molecular conservation between the sea urchin exocrine pancreas-like cells and the mammalian pancreatic acinar cells. Next, we pondered on the question whether their gene expression similarities are also reflected at a cellular phenotypic level. To address this question, we performed a 3D ultrastructural analysis of a 3 dpf larva using volume electron microscopy (vEM). To this aim, larvae were high pressure frozen, freeze substituted and embedded in an epoxy resin. The full volume of a characteristic larva (as judged by X-ray microCT) was finally imaged by serial block face electron microscopy (SBEM) at a resolution of 15 × 15 × 50 nm^3 and the resulting images were computationally aligned in order to reconstruct the 3D organization of the midgut region (Figure 4A).

Manual image alignment with the FISH analysis allowed us to predict the location of the exocrine pancreatic cells in the first layer of midgut, immediately below the cardiac sphincter domain (Figure 4B). Examining the vEM dataset, we checked whether we could identify in this region cells that showed a distinct morphological signature. Interestingly, the ultrastructural analysis revealed the presence of a cluster of seven cells with specific characteristics. Because of their location and of their distinct morphological signature, we could identify them as exocrine pancreatic-like cells. Comparing them with other cells located in the midgut region, we could identify common features, as well as specific traits (Figures 4C–E). All midgut cells are polarized, with the Golgi apparatus present in the apical side, where they present a cilium and several villi protruding in the gut lumen. Moreover, they all contain a few large (~1 μm) vesicles filled with electrondense content, which we speculate could be digested endocytosed material. However, the cluster of cells adjacent to the cardiac sphincter, are characterized by a large number of vesicles (~300 nm in diameter) with non-electron-scattering content accumulated near the apical plasma membrane (Figure 4C). Interestingly, we also found two cells, next to the exocrine cells, in which more vesicles are present with respect to the other midgut cell, but these are less apically polarized (Figure 4D). Due to the intermediate phenotype of these cells, we believe they may be potentially differentiating cell. To confirm the characteristics of the different cell types as seen in the 2D images, we selected examples of different individuals for each class, performed a 3D segmentation and quantified the number and polarization of the light vesicles (Figures 4F–J). This analysis confirmed that the exocrine pancreas-like cells, as well as the putative differentiating cells, contain at least three times more vesicles than a typical main stomach cell (Supplementary Figure S4). Moreover, the localization of these vesicles is highly polarized towards the apical plasma membrane in exocrine cells (>75% of vesicles present between the basis of the nucleus and the apical membrane), but it is not for the putative differentiating cells (<50%; Supplementary Figure S4).

This analysis confirmed that all the exocrine pancreas-like cells contain vesicles localized in the apical part of the plasma membrane towards the lumen and that they contain at least three times more vesicles than a main stomach cell (Supplementary Figure S4). Regarding the putative differentiating cell type, we confirmed that they contain similar number of vesicles when compared to the exocrine pancreas-like cells, while they lack specific localization (Supplementary Figure S4).

Discussion

Pancreatic-like cells in sea urchin revealed a fundamental step in pancreas evolution

Exploring the scRNA-seq dataset of the 3 dpf *S. purpuratus* pluteus larva (Paganos et al., 2021) for a pancreatic-like molecular fingerprint resulted in the identification, and validation, of the presence of previously proposed pancreatic-like cell types in echinoderms. As previously suggested (Perillo et al., 2018; Paganos et al., 2021), the sea urchin larva nervous system utilizes a large amount of pancreatic transcription factors, which is also supported by the data of the present study. According to our analysis, the sea urchin neurons score the highest outside the endodermally-derived cell type families and utilize transcription factor orthologous to those used in most of the mammalian pancreas cell lineages, with an enrichment of the β endocrine transcription factors *Pdx1*, *NeuroD1*, *Mnx*, *Islet* and *Rfx3*, suggesting once more the tight evolutionary (and/or phenotypic) link between neural and pancreatic cells. In addition to the evolutionary conserved program between these two distal cell type families, the data suggest that sea urchin larva could potentially be an ideal candidate to address the evolution of endocrine systems.

According to our single cell data, the digestive tract of the sea urchin larva contains two major categories of pancreatic like cells: endocrine and exocrine-like. Endocrine cell markers are found in cell clusters scattered across the digestive tract, the exocrine ones, are confined in two distinct clusters of the digestive tract dataset and thus suggesting a highly diversified signature and role of the two systems. Cells of the anal, intestinal, pyloric sphincter and esophageal domains appear to have a strong endocrine signature, which is in agreement with

previous data showing the expression of an insulin-like peptide that structurally is related to the cephalochordate insulin in the posterior gut of the late pluteus larva (Perillo and Arnone 2014). Exploring our data of the 3 dpf larva for the expression of the insulin gene did not produce any obvious results, in line with its known expression restricted to late stages and suggesting that the endocrine-like cells found in the posterior gut of the 3 dpf larva are probably immature. Nonetheless future studies are needed to distinguish whether these intestinal and pyloric sphincter cells reflect a distinct developmental state of the insulin producing cells or mature cells arise from cell progenitors altogether specified later during development. Overall, our analysis revealed the presence, at a single cell resolution, of endocrine and exocrine-like molecular signatures scattered in distinct cell types of the *S. purpuratus* larva. These findings are in line with previously proposed hypothesis that the emergence of pancreatic cell types happened in distinct steps during evolution and that such cell types are all present in the sea urchin.

Homology between sea urchin and vertebrate pancreatic acinar cells

Our analysis confirms that the sea urchin exocrine cells utilize a pancreatic gene regulatory program including orthologs of the transcription factors *Ptf1a, Mist, Xbp1, Tgif, Blimp1, Gata6. Pax6, Rbpj* and *Hnf4*, all of which are well known pancreatic gene markers and most of them regulators of pancreas development (St-Onge et al., 1997; Huang et al., 2008; Husain and Thrower, 2009; Hess et al., 2011; Martinelli et al., 2013; Chiou et al., 2017). For instance, *Rbpj* is a transcription factor known to partner with *Ptf1a* to execute its regulatory function (Masui et al., 2007), while the transcription factor *Xbp1* is shown to be required for the homeostasis of acinar cells since its depletion in mice results in extensive apoptosis of those cells (Hess et al., 2011). Furthermore, we report here that sea urchin exocrine pancreas-like cells are able to synthetize proteins of the protease and trypsin families and also use an expanded set of carboxypeptidases, amylases and pancreatic lipases.

One unique characteristic of pancreatic acinar cells from different species is that they present a morphology that is highly polarized, with the secretory vesicles concentrated at the apical side of their plasma membrane, facing the lumen (Husain and Thrower, 2009). Here, using volume EM, we showed that sea urchin exocrine, pancreas-like cells contain a larger number of vesicles when compared to the rest of the midgut cells, with a similar accumulation of vesicles at the apical side of the plasma membrane, reminiscent of what is found in mammalian acinar cells. Interestingly, our integrated approach allowed us to identify, with a high degree of confidence, a population of not fully differentiated exocrine pancreas-like cells located next to the exocrine cells. The potentially undifferentiated state of these cells is suggested by: 1) the expression of more transcription factors in one [exocrine pancreas-like (1)] of the two recognized exocrine pancreas-like cell subclusters, in combination with the reduced expression of terminal differentiation genes, 2) the greater transcriptional similarity of this subcluster to the midgut domain, 3) the comparable number of vesicles to the exocrine-like cells, which are lacking subcellular polarization and 4) the demonstrated increase in sea urchin exocrine pancreas-like cell numbers and complexity during development, compatible with a continuous cellular differentiation of newly specified exocrine cells along development.

Taken together, our results demonstrate that the sea urchin larva possesses exocrine pancreatic-like cells that we interpret as homologous to the mammalian acinar cells (Figure 5). Their homology is supported by both molecular and morphological characters, including the evolutionary conservation of the: 1) ontogenesis program, both deriving from the endoderm, 2) molecular specification pathways, 3) molecular fingerprint, 4) spatial organization, with sea urchin acinar-like cells being grouped together forming belt-like structures 5) and cells' morphology. These lines of evidence suggest that those cell types in sea urchins and vertebrates are, thus, homologous, sharing a common ancestry. Whether this homology can be extended outside the deuterostome clade remains an open question that needs further analysis. However, we envision such a possibility since digestive cells with similar gene expression profiles have been reported in sponges and cnidarians (Steinmetz et al., 2017; Sebe-Pedros et al., 2018; Musser et al., 2021). In the latter cases we are still lacking the precise molecular and morphological data to support such an evolutionary link.

Coalescence of cell types in a single organ (pancreas) is necessary for the efficient crosstalk between the exocrine and endocrine fractions

In conclusion, we show that the integration of different approaches is sufficient and essential for the thorough characterization of a give cell type and the assessment of its evolution. Our study provides molecular data confirming and expanding the hypothesis that the sea urchin larva contains cell types with a pancreatic-like molecular wiring among which neurons are endocrine-like, while the digestive tract contains both a broad spectrum of endocrine-like and well-defined populations of exocrine-like cells. Using single cell transcriptomics and volume EM we demonstrate that both from molecular and morphological perspectives acinar-like cells are homologous to the mammalian exocrine pancreas cells. The validation of the presence of acinar-like cells in a "pancreas-less" non-chordate deuterostome strengthens the hypothesis that the cellular building blocks of pancreas

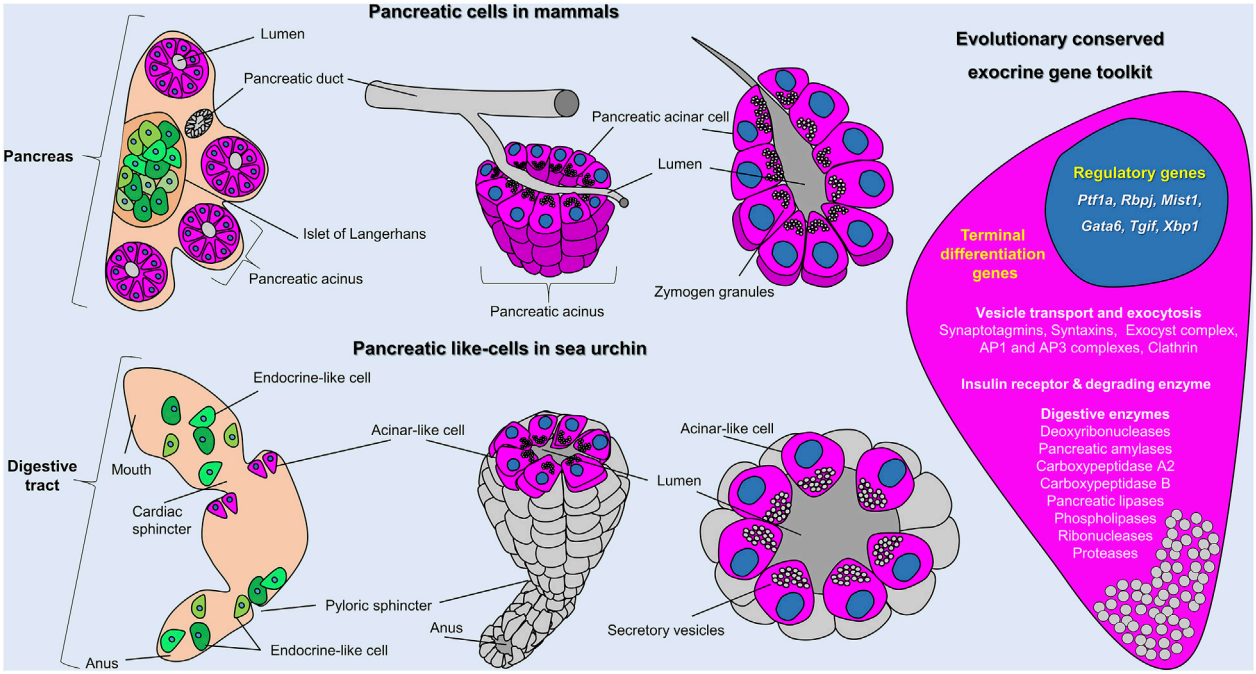

FIGURE 5
Sea urchin acinar-like cells. Schematic representation summarizing the molecular and morphological conserved features of vertebrate acinar and invertebrate acinar-like cells as shown in this study. Cartoons show the distribution and organization of pancreatic cells in mammals (top row) and sea urchin (bottom row) and (on the right) an overview of the evolutionary conserved gene toolkit shared between sea urchin and mammalian exocrine pancreatic cells. In mammals, exocrine (magenta) and endocrine (green) cells coalesce into a single organ; the pancreas. In sea urchins, acinar-like (magenta) and endocrine pancreas–like (green) cells are scattered within the digestive tract. The cartoon on the right represents an overview of the evolutionary conserved regulatory and terminal differentiation genes found both in mammalian and sea urchin exocrine cells. A full gene list of the sea urchin transcripts found in the acinar-like cell type family can be found in Supplementary Files 2 and 3.

predate the formation of pancreas as a distinct organ in the vertebrate lineage. What were the evolutionary forces that shaped the coalescence of the pancreatic cells into a distinct organ in mammals still remains an open question and needs further investigation. Of great interest is our finding that sea urchin acinar cells express insulin pathway-related genes, such as insulin receptor (*Insr*) and insulin degrading enzyme (*Ide*), suggesting the interaction between endocrine and exocrine cells in sea urchins. Furthermore, both populations are in close connection within the sea urchin stomach region, a feature which is also found in mammalian acinar cells, suggesting a possible evolutionary conserved crosstalk between the insulinergic cells and pancreatic exocrine cells, a phenomenon that would take place later during development when insulin is produced by the posterior gut cells.

As postulated in the past by different authors, tissue level organization enables the coordination of functions between different cells and division of labor. One possibility is that the increase of organismal complexity and physical distances of the different cell types as well as the subsequent increase in homeostatic control and energy costs balance, created the need for inventing a more efficient system in which cells are able to perform their individual tasks in a coordinated and finely controlled manner as is the case of pancreas. The creation of such a system could have been eased by the existence of an already established primitive crosstalk of the individual pancreatic cells, something we believe to be possible, since we found that sea urchin acinar-like cells express genes that could potentially allow them to respond to insulin produced by different endocrine cell types of the digestive tract. In fact, such a crosstalk between endocrine and exocrine pancreas has been demonstrated as early as in 1882, with more recent studies suggesting an intimate regulation of the exocrine pancreas by insulin and potentially other islet cell products (Kühne and Lea, 1882; Czakó et al., 2009; Overton and Mastracci, 2022). Similarly, it has been shown that also the exocrine pancreas is able to control the differentiation of the endocrine β-cells (Overton and Mastracci, 2022). Demonstrating such an interaction was already present in an early branched deuterostome would be of great interest, since it would suggest a crosstalk between the exocrine and endocrine pancreatic cells that would predates (evolutionarily speaking) their spatial co-localization in a distinct organ. Another possibility is that this machinery is, in fact, used to interact with the neighboring sea urchin esophageal cells known to produce a derived insulin-like peptide (Perillo and Arnone 2014).

Taken together we hypothesize that the increase of the distances among the vertebrate digestive tract cell types, a feature directly tied to its increase in cell type content, created the need for diversification of the different functions by specific tissue autonomous units, in this case the pancreas. As a result, pancreatic cell types were brought together to form a distinct organ versus being scattered within the digestive tract of animals to reduce the physical distance of the individual pancreatic cells and to allow a tissue autonomous regulation through paracrine signaling resulting to a precise coordination of cell activities, a faster response and novel functions. A snapshot of this evolutionary process is reflected by the shift of pancreatic cells organization from being scattered within the digestive tract in invertebrates such as echinoderms, cephalochordates and tunicates (Reinecke and Collet, 1998; Olinski et al., 2006; Arda et al., 2013; Lecroisey et al., 2015), to forming simple pancreatic organs with distinct endocrine and exocrine domains in early branching vertebrates such as teleost fish (Falkmer et al., 1985; Yui and Fujita, 1986; Youson et al., 2006), leading to their final interconnection and embedding of the endocrine and exocrine tissues to form a proper pancreas in mammals.

Data availability statement

The datasets presented in this study can be found in online repositories. The names of the repository/repositories and accession number(s) can be found below: https://datadryad.org/stash, https://doi.org/10.5061/dryad.n5tb2rbvz.

Author contributions

Conceptualization, PP, PM, GB, and MIA; methodology, PP, PR, JC, GM, and GB; validation, PP, PR, JC, GM, and GB; writing—original draft preparation, PP; writing—review and editing, PP, PR, JC, GM, PM. GB and MIA; visualization, PP, PR, JC, and GM; supervision, MIA.

Funding

PP was supported by Marie Curie ITN EvoCELL (H2020 Grant Number: 766053 to MIA) and by a Research Grant from the Human Frontiers Science Program (Ref.-No:RGP0002/2019 to MIA). PM visited the laboratory of MIA with an Assemble Plus (310) Grant.

Acknowledgments

The authors would like to thank Davide Caramiello for taking care of the adult sea urchins at Stazione Zoologica Anton Dohrn and Erica Riccio for her assistance in spawning the animals. The authors are also grateful to Margherita Perillo for critically reading the manuscript and providing insightful feedback.

Conflict of interest

The authors declare that the research was conducted in the absence of any commercial or financial relationships that could be construed as a potential conflict of interest.

Publisher's note

Supplementary material

The Supplementary Material for this article can be found online at: https://www.frontiersin.org/articles/10.3389/fcell.2022.991664/full#supplementary-material

References

Afelik, S., Chen, Y., and Pieler, T. (2006). Combined ectopic expression of Pdx1 and Ptf1a/p48 results in the stable conversion of posterior endoderm into endocrine and exocrine pancreatic tissue. *Genes Dev.* 20, 1441–1446. doi:10.1101/gad.378706

Ahlgren, U., Jonsson, J., and Edlund, H. (1996). The morphogenesis of the pancreatic mesenchyme is uncoupled from that of the pancreatic epithelium in IPF1/PDX1-deficient mice. *Development* 122, 1409–1416. doi:10.1242/dev.122.5.1409

Ait-Lounis, A., Bonal, C., Seguin-Estevez, Q., Schmid, C. D., Bucher, P., Herrera, P. L., et al. (2010). The transcription factor Rfx3 regulates beta-cell differentiation, function, and glucokinase expression. *Diabetes* 59, 1674–1685. doi:10.2337/db09-0986

Andrikou, C., Pai, C. Y., Su, Y. H., and Arnone, M. I. (2015). Logics and properties of a genetic regulatory program that drives embryonic muscle development in an echinoderm. *Elife* 4. doi:10.7554/eLife.07343

Annunziata, R., and Arnone, M. I. (2014). A dynamic regulatory network explains ParaHox gene control of gut patterning in the sea urchin. *Development* 141, 2462–2472. doi:10.1242/dev.105775

Annunziata, R., Perillo, M., Andrikou, C., Cole, A. G., Martinez, P., and Arnone, M. I. (2014). Pattern and process during sea urchin gut morphogenesis: The regulatory landscape. *Genesis* 52, 251–268. doi:10.1002/dvg.22738

Arda, H. E., Benitez, C. M., and Kim, S. K. (2013). Gene regulatory networks governing pancreas development. *Dev. Cell* 25, 5–13. doi:10.1016/j.devcel.2013.03.016

Arntfield, M. E., and van der Kooy, D. (2011). β-Cell evolution: How the pancreas borrowed from the brain: The shared toolbox of genes expressed by neural and pancreatic endocrine cells may reflect their evolutionary relationship. *Bioessays.* 33, 582–587. doi:10.1002/bies.201100015

Buckley, K. M., and Rast, J. P. (2017). An organismal model for gene regulatory networks in the gut-associated immune response. *Front. Immunol.* 8, 1297. doi:10.3389/fimmu.2017.01297

Burlison, J. S., Long, Q., Fujitani, Y., Wright, C. V., and Magnuson, M. A. (2008). Pdx-1 and Ptf1a concurrently determine fate specification of pancreatic multipotent progenitor cells. *Dev. Biol.* 316, 74–86. doi:10.1016/j.ydbio.2008.01.011

Butler, A., Hoffman, P., Smibert, P., Papalexi, E., and Satija, R. (2018). Integrating single-cell transcriptomic data across different conditions, technologies, and species. *Nat. Biotechnol.* 36, 411–420. doi:10.1038/nbt.4096

Cao, C., Lemaire, L. A., Wang, W., Yoon, P. H., Choi, Y. A., Parsons, L. R., et al. (2019). Comprehensive single-cell transcriptome lineages of a proto-vertebrate. *Nature* 571, 349–354. doi:10.1038/s41586-019-1385-y

Cardona, A., Saalfeld, S., Schindelin, J., Arganda-Carreras, I., Preibisch, S., Longair, M., et al. (2012). TrakEM2 software for neural circuit reconstruction. *PLoS One* 7, e38011. doi:10.1371/journal.pone.0038011

Chari, T., Weissbourd, B., Gehring, J., Ferraioli, A., Leclere, L., Herl, M., et al. (2021). Whole-animal multiplexed single-cell RNA-seq reveals transcriptional shifts across Clytia medusa cell types. *Sci. Adv.* 7, eabh1683. doi:10.1126/sciadv.abh1683

Chiou, S. H., Risca, V. I., Wang, G. X., Yang, D., Gruner, B. M., Kathiria, A. S., et al. (2017). BLIMP1 induces transient metastatic heterogeneity in pancreatic cancer. *Cancer Discov.* 7, 1184–1199. doi:10.1158/2159-8290.CD-17-0250

Cole, A. G., Rizzo, F., Martinez, P., Fernandez-Serra, M., and Arnone, M. I. (2009). Two ParaHox genes, SpLox and SpCdx, interact to partition the posterior endoderm in the formation of a functional gut. *Development* 136, 541–549. doi:10.1242/dev.029959

Czakó, L., Hegyi, P., Rakonczay, Z., Wittmann, T., and Otsuki, M. (2009). Interactions between the endocrine and exocrine pancreas and their clinical relevance. *Pancreatology* 9, 351–359. doi:10.1159/000181169

Ediger, B. N., Du, A., Liu, J., Hunter, C. S., Walp, E. R., Schug, J., et al. (2014). Islet-1 Is essential for pancreatic beta-cell function. *Diabetes* 63, 4206–4217. doi:10.2337/db14-0096

Falkmer, S., Dafgard, E., El-Salhy, M., Engstrom, W., Grimelius, L., and Zetterberg, A. (1985). Phylogenetical aspects on islet hormone families: A minireview with particular reference to insulin as a growth factor and to the phylogeny of PYY and NPY immunoreactive cells and nerves in the endocrine and exocrine pancreas. *Peptides* 6 (3), 315–320. doi:10.1016/0196-9781(85)90391-2

Fincher, C. T., Wurtzel, O., De Hoog, T., Kravarik, K. M., and Reddien, P. W. (2018). Cell type transcriptome atlas for the planarian Schmidtea mediterranea. *Science* 360, eaaq1736. doi:10.1126/science.aaq1736

Fujikura, J., Hosoda, K., Kawaguchi, Y., Noguchi, M., Iwakura, H., Odori, S., et al. (2007). Rbp-j regulates expansion of pancreatic epithelial cells and their differentiation into exocrine cells during mouse development. *Dev. Dyn.* 236, 2779–2791. doi:10.1002/dvdy.21310

Gosmain, Y., Katz, L. S., Masson, M. H., Cheyssac, C., Poisson, C., and Philippe, J. (2012). Pax6 is crucial for beta-cell function, insulin biosynthesis, and glucose-induced insulin secretion. *Mol. Endocrinol.* 26, 696–709. doi:10.1210/me.2011-1256

Gu, C., Stein, G. H., Pan, N., Goebbels, S., Hornberg, H., Nave, K. A., et al. (2010). Pancreatic beta cells require NeuroD to achieve and maintain functional maturity. *Cell Metab.* 11, 298–310. doi:10.1016/j.cmet.2010.03.006

Gutierrez, G. D., Bender, A. S., Cirulli, V., Mastracci, T. L., Kelly, S. M., Tsirigos, A., et al. (2017). Pancreatic beta cell identity requires continual repression of non-beta cell programs. *J. Clin. Invest.* 127, 244–259. doi:10.1172/JCI88017

Hess, D. A., Humphrey, S. E., Ishibashi, J., Damsz, B., Lee, A. H., Glimcher, L. H., et al. (2011). Extensive pancreas regeneration following acinar-specific disruption of Xbp1 in mice. *Gastroenterology* 141, 1463–1472. doi:10.1053/j.gastro.2011.06.045

Huang, J., Karakucuk, V., Levitsky, L. L., and Rhoads, D. B. (2008). Expression of HNF4alpha variants in pancreatic islets and Ins-1 beta cells. *Diabetes. Metab. Res. Rev.* 24, 533–543. doi:10.1002/dmrr.870

Husain, S., and Thrower, E. (2009). Molecular and cellular regulation of pancreatic acinar cell function. *Curr. Opin. Gastroenterol.* 25, 466–471. doi:10.1097/MOG.0b013e32832ebfac

Hussain, M. A., Miller, C. P., and Habener, J. F. (2002). Brn-4 transcription factor expression targeted to the early developing mouse pancreas induces ectopic glucagon gene expression in insulin-producing beta cells. *J. Biol. Chem.* 277, 16028–16032. doi:10.1074/jbc.M107124200

Karpińska, M., and Czauderna, M. (2022). Pancreas—its functions, disorders, and physiological impact on the mammals' organism. *Front. Physiol.* 13, 807632. doi:10.3389/fphys.2022.807632

Kawaguchi, Y., Cooper, B., Gannon, M., Ray, M., Macdonald, R. J., and Wright, C. V. (2002). The role of the transcriptional regulator Ptf1a in converting intestinal to pancreatic progenitors. *Nat. Genet.* 32, 128–134. doi:10.1038/ng959

Kühne, W., and Lea, A. S. (1882). *Beobachtungen über die Absonderung des Pankreas*. Heidelberg, Germany: Carl Winter's Universitätsbuchhandlung.

Lecroisey, C., Le Petillon, Y., Escriva, H., Lammert, E., and Laudet, V. (2015). Identification, evolution and expression of an insulin-like peptide in the cephalochordate *Branchiostoma lanceolatum*. *PLoS One* 10, e0119461. doi:10.1371/journal.pone.0119461

Macfarlane, W. M., Mckinnon, C. M., Felton-Edkins, Z. A., Cragg, H., James, R. F., and Docherty, K. (1999). Glucose stimulates translocation of the homeodomain transcription factor PDX1 from the cytoplasm to the nucleus in pancreatic beta-cells. *J. Biol. Chem.* 274, 1011–1016. doi:10.1074/jbc.274.2.1011

Martinelli, P., Cañamero, M., Del Pozo, N., Madriles, F., Zapata, A., and Real, F. X. (2013). Gata6 is required for complete acinar differentiation and maintenance of the exocrine pancreas in adult mice. *Gut* 62, 1481–1488. doi:10.1136/gutjnl-2012-303328

Marty-Santos, L., and Cleaver, O. (2016). Pdx1 regulates pancreas tubulogenesis and E-cadherin expression. *Development* 143, 1056. doi:10.1242/dev.135806

Massri, A. J., Greenstreet, L., Afanassiev, A., Berrio, A., Wray, G. A., Schiebinger, G., et al. (2021). Developmental single-cell transcriptomics in the *Lytechinus variegatus* sea urchin embryo. *Development* 148, dev198614. doi:10.1242/dev.198614

Mastracci, T. L., and Sussel, L. (2012). The endocrine pancreas: Insights into development, differentiation and diabetes. *Wiley Interdiscip. Rev. Membr. Transp. Signal* 1, 609–628. doi:10.1002/wdev.44

Masui, T., Long, Q., Beres, T. M., Magnuson, M. A., and Macdonald, R. J. (2007). Early pancreatic development requires the vertebrate Suppressor of Hairless (RBPJ) in the PTF1 bHLH complex. *Genes Dev.* 21, 2629–2643. doi:10.1101/gad.1575207

Messenger, S. W., Falkowski, M. A., and Groblewski, G. E. (2014). Ca^{2+}-regulated secretory granule exocytosis in pancreatic and parotid acinar cells. *Cell Calcium* 55, 369–375. doi:10.1016/j.ceca.2014.03.003

Musser, J. M., Schippers, K. J., Nickel, M., Mizzon, G., Kohn, A. B., Pape, C., et al. (2021). Profiling cellular diversity in sponges informs animal cell type and nervous system evolution. *Science* 374, 717–723. doi:10.1126/science.abj2949

Olinski, R. P., Dahlberg, C., Thorndyke, M., and Hallbook, F. (2006). Three insulin-relaxin-like genes in *Ciona intestinalis*. *Peptides* 27, 2535–2546. doi:10.1016/j.peptides.2006.06.008

Overton, D. L., and Mastracci, T. L. (2022). Exocrine-endocrine crosstalk: The influence of pancreatic cellular communications on organ growth, function and disease. *Front. Endocrinol.* 13, 904004. doi:10.3389/fendo.2022.904004

Paganos, P., Caccavale, F., La Vecchia, C., D'Aniello, E., D'Aniello, S., and Arnone, M. I. (2022). FISH for all: A fast and efficient fluorescent *in situ* hybridization (FISH) protocol for marine embryos and larvae. *Front. Physiol.* 13, 878062. doi:10.3389/fphys.2022.878062

Paganos, P., Voronov, D., Musser, J. M., Arendt, D., and Arnone, M. I. (2021). Single-cell RNA sequencing of the *Strongylocentrotus purpuratus* larva reveals the blueprint of major cell types and nervous system of a non-chordate deuterostome. *Elife* 10, e70416. doi:10.7554/eLife.70416

Pan, F. C., Brissova, M., Powers, A. C., Pfaff, S., and Wright, C. V. (2015). Inactivating the permanent neonatal diabetes gene Mnx1 switches insulin-producing beta-cells to a delta-like fate and reveals a facultative proliferative capacity in aged beta-cells. *Development* 142, 3637–3648. doi:10.1242/dev.126011

Perillo, M., and Arnone, M. I. (2014). Characterization of insulin-like peptides (ILPs) in the sea urchin *Strongylocentrotus purpuratus*: Insights on the evolution of the insulin family. *Gen. Comp. Endocrinol.* 205, 68–79. doi:10.1016/j.ygcen.2014.06.014

Perillo, M., Oulhen, N., Foster, S., Spurrell, M., Calestani, C., and Wessel, G. (2020). Regulation of dynamic pigment cell states at single-cell resolution. *Elife* 9, e60388. doi:10.7554/eLife.60388

Perillo, M., Paganos, P., Mattiello, T., Cocurullo, M., Oliveri, P., and Arnone, M. I. (2018). New neuronal subtypes with a "Pre-Pancreatic" signature in the sea urchin stongylocentrotus purpuratus. *Front. Endocrinol.* 9, 650. doi:10.3389/fendo.2018.00650

Perillo, M., Paganos, P., Spurrell, M., Arnone, M. I., and Wessel, G. M. (2021). Methodology for whole mount and fluorescent RNA *in situ* hybridization in echinoderms: Single, double, and beyond. *Methods Mol. Biol.* 2219, 195–216. doi:10.1007/978-1-0716-0974-3_12

Perillo, M., Wang, Y. J., Leach, S. D., and Arnone, M. I. (2016). A pancreatic exocrine-like cell regulatory circuit operating in the upper stomach of the sea urchin *Strongylocentrotus purpuratus* larva. *BMC Evol. Biol.* 16, 117. doi:10.1186/s12862-016-0686-0

Piccand, J., Strasser, P., Hodson, D. J., Meunier, A., Ye, T., Keime, C., et al. (2014). Rfx6 maintains the functional identity of adult pancreatic beta cells. *Cell Rep.* 9, 2219–2232. doi:10.1016/j.celrep.2014.11.033

Pin, C. L., Rukstalis, J. M., Johnson, C., and Konieczny, S. F. (2001). The bHLH transcription factor Mist1 is required to maintain exocrine pancreas cell organization and acinar cell identity. *J. Cell Biol.* 155, 519–530. doi:10.1083/jcb.200105060

Reinecke, M., and Collet, C. (1998). The phylogeny of the insulin-like growth factors. *Int. Rev. Cytol.* 183, 1–94. doi:10.1016/s0074-7696(08)60142-4

Salamanca-Díaz, D. A., Schulreich, S. M., Cole, A. G., and Wanninger, A. (2022). Single-cell RNA sequencing atlas from a bivalve larva enhances classical cell lineage studies. *Front. Ecol. Evol.* 9. doi:10.3389/fevo.2021.783984

Sebe-Pedros, A., Saudemont, B., Chomsky, E., Plessier, F., Mailhe, M. P., Renno, J., et al. (2018). Cnidarian cell type diversity and regulation revealed by whole-organism single-cell RNA-seq. *Cell* 173, 1520–1534. doi:10.1016/j.cell.2018.05.019

Slack, J. M. (1995). Developmental biology of the pancreas. *Development* 121, 1569–1580. doi:10.1242/dev.121.6.1569

St-Onge, L., Sosa-Pineda, B., Chowdhury, K., Mansouri, A., and Gruss, P. (1997). Pax6 is required for differentiation of glucagon-producing alpha-cells in mouse pancreas. *Nature* 387, 406–409. doi:10.1038/387406a0

Steinmetz, P. R. H., Aman, A., Kraus, J. E. M., and Technau, U. (2017). Gut-like ectodermal tissue in a sea anemone challenges germ layer homology. *Nat. Ecol. Evol.* 1, 1535–1542. doi:10.1038/s41559-017-0285-5

Stuart, T., Butler, A., Hoffman, P., Hafemeister, C., Papalexi, E., Mauck, W. M., et al. (2019). Comprehensive integration of single-cell data. *Cell* 177, 1888–1902. doi:10.1016/j.cell.2019.05.031

Tabula Muris, C. (2020). A single-cell transcriptomic atlas characterizes ageing tissues in the mouse. *Nature* 583, 590–595. doi:10.1038/s41586-020-2496-1

Tarashansky, A. J., Musser, J. M., Khariton, M., Li, P., Arendt, D., Quake, S. R., et al. (2021). Mapping single-cell atlases throughout Metazoa unravels cell type evolution. *Elife* 10, e66747. doi:10.7554/eLife.66747

Titze, B., Genoud, C., and Friedrich, R. W. (2018). SBEMimage: Versatile acquisition control software for serial block-face electron microscopy. *Front. Neural Circuits* 12, 54. doi:10.3389/fncir.2018.00054

Youson, J. H., Al-Mahrouki, A. A., Amemiya, Y., Graham, L. C., Montpetit, C. J., and Irwin, D. M. (2006). The fish endocrine pancreas: Review, new data, and future research directions in ontogeny and phylogeny. *Gen. Comp. Endocrinol.* 148, 105–115. doi:10.1016/j.ygcen.2005.12.005

Yui, R., and Fujita, T. (1986). Immunocytochemical studies on the pancreatic islets of the ratfish Chimaera monstrosa. *Arch. Histol. Jpn.* 49, 369–377. doi:10.1679/aohc.49.369

Zecchin, E., Mavropoulos, A., Devos, N., Filippi, A., Tiso, N., Meyer, D., et al. (2004). Evolutionary conserved role of ptf1a in the specification of exocrine pancreatic fates. *Dev. Biol.* 268, 174–184. doi:10.1016/j.ydbio.2003.12.016

frontiers | Frontiers in Cell and Developmental Biology

TYPE Perspective
PUBLISHED 23 December 2022
DOI 10.3389/fcell.2022.1071961

OPEN ACCESS

EDITED BY
Pedro Martinez,
University of Barcelona, Spain

REVIEWED BY
Mike Paulin,
University of Otago, New Zealand
Volker Hartenstein,
University of California, United States

*CORRESPONDENCE
Leonid L. Moroz,
moroz@whitney.ufl.edu
Daria Y. Romanova,
darjaromanova@gmail.com

SPECIALTY SECTION
This article was submitted to Evolutionary Developmental Biology, a section of the journal Frontiers in Cell and Developmental Biology

RECEIVED 17 October 2022
ACCEPTED 13 December 2022
PUBLISHED 23 December 2022

CITATION
Moroz LL and Romanova DY (2022), Alternative neural systems: What is a neuron? (Ctenophores, sponges and placozoans).
Front. Cell Dev. Biol. 10:1071961.
doi: 10.3389/fcell.2022.1071961

Alternative neural systems: What is a neuron? (Ctenophores, sponges and placozoans)

Leonid L. Moroz[1,2]* and Daria Y. Romanova[3]*

[1]Departments of Neuroscience and McKnight Brain Institute, University of Florida, Gainesville, FL, United States, [2]Whitney Laboratory for Marine Bioscience, University of Florida, St. Augustine, FL, United States, [3]Institute of Higher Nervous Activity and Neurophysiology of RAS, 5A Butlerova, Moscow, Russia

How to make a neuron, a synapse, and a neural circuit? Is there only one 'design' for a neural architecture with a universally shared genomic blueprint across species? The brief answer is "No." Four early divergent lineages from the nerveless common ancestor of all animals independently evolved distinct neuroid-type integrative systems. One of these is a subset of neural nets in comb jellies with unique synapses; the second lineage is the well-known Cnidaria + Bilateria; the two others are non-synaptic neuroid systems in sponges and placozoans. By integrating scRNA-seq and microscopy data, we revise the definition of neurons as synaptically-coupled polarized and highly heterogenous secretory cells at the top of behavioral hierarchies with learning capabilities. This physiological (not phylogenetic) definition separates 'true' neurons from non-synaptically and gap junction-coupled integrative systems executing more stereotyped behaviors. Growing evidence supports the hypothesis of multiple origins of neurons and synapses. Thus, many non-bilaterian and bilaterian neuronal classes, circuits or systems are considered functional rather than genetic categories, composed of non-homologous cell types. In summary, little-explored examples of convergent neuronal evolution in representatives of early branching metazoans provide conceptually novel microanatomical and physiological architectures of behavioral controls in animals with prospects of neuro-engineering and synthetic biology.

KEYWORDS

ctenophora, placozoa, porifera, nervous system evolution, synapse, innexins, neurotransmitters, homology

Introduction

> "The current definition of a nervous system has negative consequences in the field of evolutionary biology that preclude discussing the processes of convergent evolution in multicellular organisms. A phylogenetic definition of an organism's biological system prevents us from considering whether that system has emerged in other organisms outside that definition."- Miguel-Tome and Llinas (2021).

The origins and rise of neuronal complexity are among the rarest yet globally impactful life transitions, and these events likely occurred over 570–530 million years ago near the Cambrian boundary. Despite more than a century of comparative research, the mechanisms and pathways of nervous system evoluton among 30 + animal phyla are elusive (Moroz, 2018). From broad genomic and comparative viewpoints, we still do not have an agreed definition of a neuron. As a result, understanding astonishing neuronal diversity is a critical experimental endeavor and theoretical challenge by itself.

All studied extant neural systems contain highly heterogeneous neuronal populations with multiple cell types, which is the hallmark of any neural organization. Every neuron in a given nervous system can be unique regarding its connectivity, functions, morphology, and gene expression patterns. But, the rules underlying the neuronal heterogeneity and the entire scope of the neuronal diversity across phyla remain unknown, calling for novel unbiassed NeuroSystematics and/or Periodic System of Neurons with predictive power (Moroz, 2018).

How different are neurons, and more importantly, *why* are they so different? The evolutionary hypothesis can be as follows. Neurons are different not only because they have different functions but also because neurons, as evolutionary units (Arendt, 2008; Arendt et al., 2016), have different genealogies with distinct gene regulatory programs and signal molecules (neurotransmitters) reflecting their parallel evolution at the broadest evolutionary scale (Moroz, 2009). Studied by scRNA-seq vertebrate [e.g., (Raj et al., 2018; Armand et al., 2021; Bandler et al., 2022; Delgado et al., 2022)] and invertebrate neuronal cell types [e.g., (Corrales et al., 2022; Dillon et al., 2022)] are organized in hierarchical trees but with unknown principles and uncertain criteria for homologization across phyla. How this diversity evolved in the first place is also unknown because strategies to probe ancestral neuronal specification events are limited.

Pre-bilaterian metazoans as essential reference species for fundamental neuroscience

Here, we must stress the need to study *reference* species (vs. '*model*' organisms) as taxonomically diverse evolutionary groups with a wide-ranging spectrum of ecological adaptations and novelties in neural architecture (Striedter et al., 2014). Representatives of three early branching metazoans lineages, placozoans (the phylum Placozoa), sponges (Porifera), and comb jellies (Ctenophora) are the most critical reference species to reconstruct the origins of animal innovations, which led to the formation of neural systems (Figure 1 and Figure 2). Regrettably, these pre-bilaterians belong to the most enigmatic animals in neuroscience; they are often viewed as less relevant for biomedical questions with noticeable underfunding.

The position of comb jellies as the sister lineage to all Metazoa (Figure 2B) has been supported by independent large-scale phylogenomic studies: this is the Ctenophora-first hypothesis (Whelan et al., 2015; Halanych et al., 2016; Whelan et al., 2017; Laumer et al., 2019; Fernandez and Gabaldon, 2020; Li et al., 2021). Other evolution models challenge this topology of the animal tree of life and place nerveless sponges as the earliest diverged lineage (Sponge-first hypothesis), followed by ctenophores with developed neural systems, and then again nerveless placozoans (Telford et al., 2016; Kapli and Telford, 2020; Redmond and McLysaght, 2021; Giacomelli et al., 2022). Morphological and hydrodynamic views of animal evolution also emphasize the sponge-first hypothesis (Nielsen, 2019, 2022). However, "Systematic and standardized testing of diverse phylogenetic models suggests that we should be skeptical of Porifera-sister results both because they are recovered under such narrow conditions and because the models in these conditions fit the data no better than other models that recover Ctenophora-sister" (Li et al., 2021).

Regardless of these two conflicting phylogenetic hypotheses, the unique architecture of extant neural systems in ctenophores strongly supports the hypothesis of independent origins of neurons and synapses over 550 million years of animal evolution (Moroz, 2014b; Moroz et al., 2014; Moroz, 2015; Moroz and Kohn, 2016). According to this scenario, a nerveless organism was the last common ancestor of all extant animals (LCAA or the urmetazoan). Ancestors of ctenophores evolved a distinct neuronal organization to control complex ciliated locomotion (by multiple comb plates) and other behaviors in these predatory animals. Sponges and placozoans *remained* nerveless by occupying different ecological niches (Nielsen, 2022; Romanova et al., 2022), with unique adaptations based on orchestrating cilia beating and expanding non-muscular contractivity (Leys, 2015; Smith et al., 2015; Armon et al., 2018; Leys et al., 2019; Kornder et al., 2022; Nielsen, 2022). The common ancestors of cnidarians and bilaterians also evolved neural cell types to integrate the operation of multiple muscular, ciliated, and secretory effectors as adaptations that might accompany the increased body sizes of early animals and complex movements. Nevertheless, *four* early divergent lineages from the LCAA *independently* evolved alternative neuroid-type integrative systems (as summarized in Figure 1 and Figure 2).

This hypothesis implies dissimilar gene regulatory programs with unique combinations of transcription factors and other regulators controlling terminal specifications of neurons in ctenophores, cnidarians and bilaterians, respectively, as well as parallel recruitment of neurotransmitters and other signal molecules. For example, serotonin, dopamine, noradrenaline, octopamine, histamine, and acetylcholine act as neurotransmitters in bilaterians but not in ctenophores or

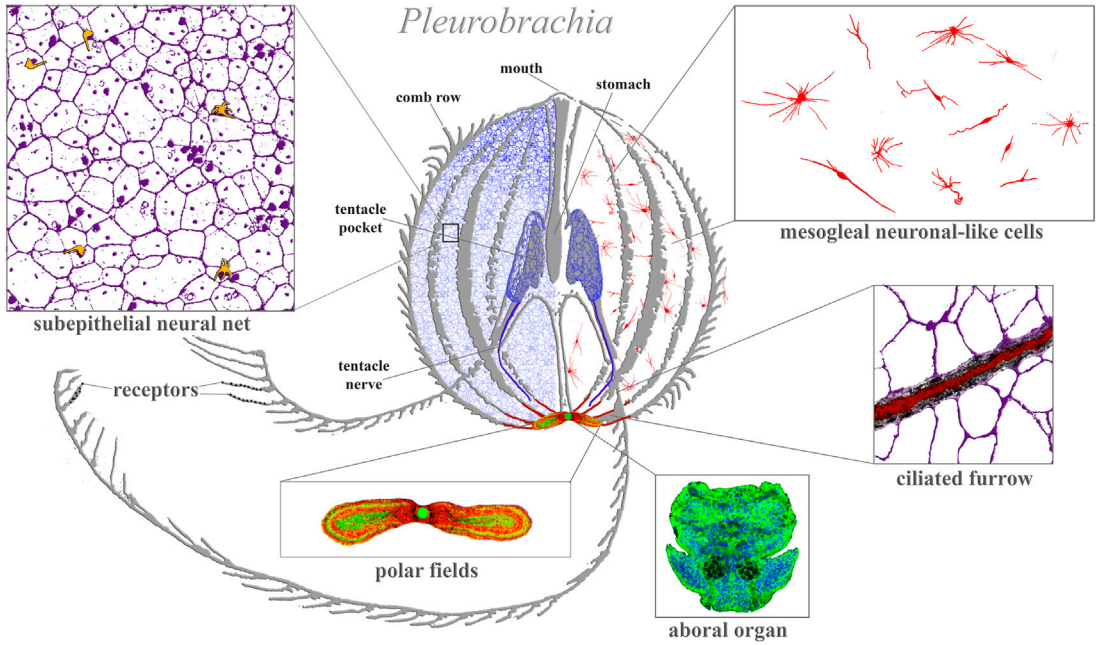

FIGURE 1
Ctenophore neural systems. As an illustrated example, the schematic diagram is based on the recent study of the cydippid *Pleurobrachia bachei* (Norekian and Moroz, 2016; 2019b). Different colors indicate different cellular populations. Most neurons and receptors (yellow) are located within the subepithelial neural net in the skin (blue, magenta) and tentacle shields with two tentacular nerves (dark blue). There are two concentrations of neural elements: one in the aboral organ (green) with densely packed neurons and other cell types (the elementary brain?); and the second in the polar fields putative chemosensory structures (yellow/green, red marks phalloidin-labeled elements). The mesoglea has a diffuse population of neuron-like cells (red). Eight ciliated furrows (conductive ciliated cells—red lines) connect the aboral organ with comb plates. The ciliated furrows are closely associated with neural net elements (insert) and are possible under neuronal control.

cnidarians (Moroz et al., 2014; Moroz et al., 2021b). None of the ctenophore (neuro) peptide homologs are found in any other animal phylum (Moroz et al., 2014; Moroz and Kohn, 2016; Sachkova et al., 2021; Hayakawa et al., 2022). Furthermore, known bilaterian neuronal markers and many relevant transcription factors either absent in ctenophores or if present were not expressed in neurons (Moroz et al., 2014; Moroz and Kohn, 2015). This line of evidence can be further experimentally tested to falsify or support the hypothesis of the independent origins of neurons. The initial functional genomic/transcriptomic analyses of sequenced from 30 + species (Whelan et al., 2017) revealed distinct molecular toolkits associated with ctenophores' neuromuscular and synaptic organizations (Moroz et al., 2014; Moroz and Kohn, 2016; Moroz et al., 2020b).

Several authors argue for a single origin of neurons and subsequent loss of neuronal and muscle cell types in placozoans and sponges (Rokas, 2013; Ryan, 2014; Ryan and Chiodin, 2015), irrespective of any modern phylogeny. The functional reasons for such 'neuronal' losses in free-living (non-parasitic) animals are unclear, and in our opinion, this hypothesis lacks sufficient rationale and support. A few selected genes involved in the excitability, secretion, or reception of some eukaryotic signal molecules cannot be used for the homologization of neural structures across metazoans. Moreover, the absence of pan-neuronal gene-/molecular markers (Moroz and Kohn, 2015) and shared gene regulatory programs leading to neuronal specification favor independent origins of neurons in ctenophores and the common ancestor of cnidarians + bilaterians (Moroz et al., 2014; Moroz and Kohn, 2016). Because cnidarians have both endoderm- and ectoderm-derived neuronal populations, there is also a possibility of cnidarian-specific neuronal cell types (Arendt, 2019).

Predictably, one or few neuronal cell-type lineages could be more evolutionarily ancient than others, but comparative data are lacking. Therefore, all hypotheses and evolutionary scenarios outlined above should be rigorously tested by the broadest sampling and molecular/physiological characterizations of all cell types across major taxonomical groups of extant animals. Ideally, this goal should include analysis of all about 100 animal classes and even orders, with extensive scRNA-seq profiling and cell-type homology testing, focusing on non-bilaterian metazoans as a start. This monumental task requires decades of research. The actual outcomes will lead to the unbiased phylogenomic classification of neuronal and other cell types across metazoans (=NeuroSystematics). NeuroSystematic

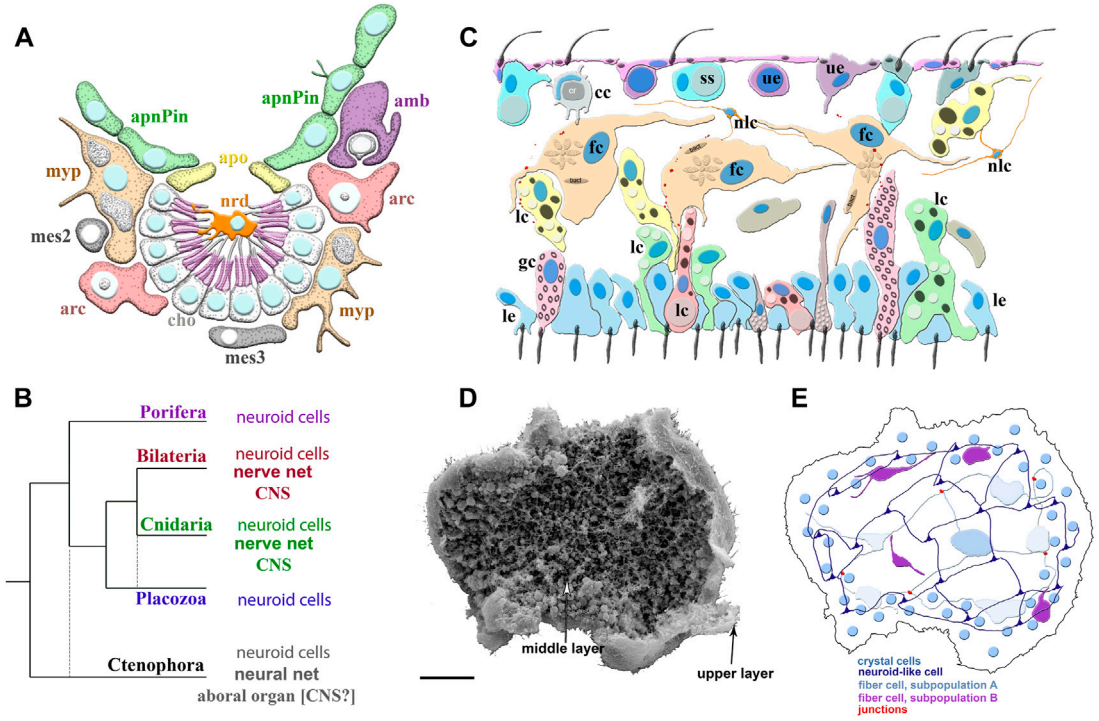

FIGURE 2
Poriferan and Placozoan neuroid systems. **(A)** Different cell types (different colors) were identified using scRNA-seq in the demosponge *Spongilla lacustris* (Musser et al., 2021): apnPin—apendopinacocytes; apo—apopylar cells; amb—amoebocytes; arc—archeocytes; cho—choanocytes; mes2 and mes3—mesocytes; myp—myopeptidocytes; nrd—neuroid cells (orange). The neuroid cells are located in the center of the choanocyte chamber, make connections to choanocytes, and might be involved in their control as neuronal-like elements. These neuroid cells contain secretory apparatus and vesicles. However, the transcriptome profiles of these neuroid cells are remarkably different subset from other known neural/neuroid-type cells in metazoans (Nakanishi et al., 2015; Musser et al., 2021), suggesting that these are sponge-specific innovations with no apparent homologs in other animals. The nature of these cellular interactions is unknown. **(B)** The emerging diversity of cell types in the placozoans. The diagram is based on recent ultrastructural studies (Smith et al., 2014; Smith et al., 2015; Mayorova et al., 2018; Mayorova et al., 2019; Romanova et al., 2021). Several morphologically distinct cell types were identified: cc—crystal cells; fc—fiber cells; gc—gland cells; lc—lipophil cells; le—lower epithelial cells; nlc-neuroid-like cells, which were previously labeled as stellate-like cells (Romanova et al., 2021); ss—shiny spheres; ue—upper epithelial cells. **(C1)** Scanning electron microscopy of *Trichoplax*—an animal without an upper cell layer. The photo shows the spatial organization of a complex meshwork formed by elements above the middle layer and the upper layers of the animal. Distributed net-like structures were formed by processes of different subtypes of fiber cells and stellate-like cells, which we also named neuroid-like cells. Some heterogeneity of fiber and neuroid-like cells is anticipated from recent ultrastructural studies (Romanova et al., 2021). **(C2)** Schematics of the spatial distribution of different subtypes of fiber, neuroid-like cells, and their processes. All these cells might form in a net-like structure above the upper layer with crystal cells as a distributed integrative system. This reconstruction is based on (Romanova et al., 2021; Romanova et al., 2022) and unpublished data. Scale: 20 μm.

would be the foundation to unravel genomic bases controlling neuronal identity and neuronal circuit evolution with the predictive power of novel cell phenotypes—a hypothetical Periodic System of Neurons (Moroz, 2018). Promising approaches include scRNA-seq, tools of statistical geometry (Liang et al., 2015) and novel algorithms (Tarashansky et al., 2021) to find conservative Character Identity Networks (Wagner, 2007; Wagner, 2014) defining homologous cell types (Musser et al., 2021; Li et al., 2022); eventually targeting reconstructions of neuronal ancestry (Moroz, 2009; 2014a; Arendt et al., 2015).

Admittedly, the cellular and molecular bases of behaviors in sponges, placozoans, and ctenophores are so remarkably distinct compared to the rest of the animals that it would be advantageous to explore the concept of 3 separate 'designs' for neuroid architectures (Figure 1 and Figure 2) that evolved in parallel from the late Precambrian time.

Indeed, placozoans show remarkable complex and highly integrated behaviors of numerous cellular populations without any recognizable synaptic organization or gap junctions, implying highly coordinated paracrine secretion and volume transmission. For example, during *Trichoplax* feeding, hundreds of cells and cilia reversible change their behaviors, and some of these cells could also be chemosensory such as gland cells in the rim (Smith et al., 2015); perhaps co-acting together with a meshwork of fiber and other neuroid cells and forming one type of the alternative integrative system (Figures 2C–E).

Relatively complex behaviors present in the demosponge (*Amphimedon*) larvae eventually leading to settlement and

metamorphosis. Sensing environmental cues can be mediated by specialized epithelial secretory flask cells, which possess a cilium and F-actin-rich protrusion, secretory vesicles, and neurite-like processes (Nakanishi et al., 2015). These cells share similar structural features with sensory-neurosecretory cells in cnidarian and bilaterian larvae, implying the hypothesis of their shared ancestry with eumetazoans (Nakanishi et al., 2015). It is intriguing to view these flask-like cells as evolutionary predecessors of some neuronal types or, more likely, analogs of such predecessors. Early diverged ancestral animal lineages might share some homologous molecular components of the sensory and secretory machinery. On the other hand, the equally feasible scenario can be co-options of functionally similar molecular complexes for similar chemoreceptive tasks forming a case for convergent evolution based on the modular organization of eukaryotic signaling systems (Arendt, 2020).

After the metamorphosis, the larval flask cells can be transdifferentiated into stem-like archeocytes and, subsequentially to other cell types such as choanocytes and others (Nakanishi et al., 2014). Interestingly, recently discovered, by scRNA-seq, adult neuroid cells in *Spongilla* (Figure 2A) also belong to the broad archeocyte/amoebocyte family (Musser et al., 2021). Although these correlations might hint at the common ancestry of both types of neuroid cells in two species of sponges, we need reliable evidence for their homologization using future molecular/scRNA-seq data.

Similarly, there are no reliable molecular markers for placozoan fiber or other neuroid-like cells (Figures 2C,E). Moreover, sponge flask cells and placozoan fiber/gland cells likely utilize species-/lineage-specific secretory molecules, absent in ctenophores, cnidarians or bilaterians (Srivastava et al., 2008; Srivastava et al., 2010; Moroz et al., 2014; Nakanishi et al., 2015; Smith et al., 2015; Musser et al., 2021). As a result, for these two groups of nerveless animals, we use the term alternative integrative systems, considering the hypothesis of their parallel evolution. At the same time, the control of metamorphosis in ancestral larvae by different types of sensory-secretory cells or conceptually similar control of feeding and digestion in early animals could be universal exaptations underlying the origins of true neural signaling and nervous systems.

Equally important to this goal would be revisiting the terminology and definition of neurons, nervous systems, and synapses. There are two options in this endeavor. The first is broadening the definition of neural systems to include plants (Baluska, 2009; Baluska and Mancuso, 2009b; a;c; Baluska et al., 2009; Baluska, 2010; Baluska et al., 2010; Baluska and Mancuso, 2021) and, perhaps, other eukaryotes, as was recently proposed (Miguel-Tome and Llinas, 2021). The second option is narrowing the physiological definition of neural systems to animals only, but with the concept of non-homologous (to bilaterians) neuronal cell type lineages and extensive convergent evolution. More generally, the entire spectrum of alternative integrative systems in organisms should include (a) 'true' neuronal systems across Metazoa, considering examples of their convergent evolution as in Ctenophora (Figure 1) or distinct set of synaptic ensembles in Cnidaria (Anderson, 1985; Anderson and Grunert, 1988; Anderson and Spencer, 1989); (b) different neuroid-type conductive, (chemo) sensory and secretory cells in non-bilaterian animals (Mackie, 1970; Anderson, 1980; Anderson and Schwab, 1982; Mackie, 1990; Tamm, 2014a; Nakanishi et al., 2015; Smith et al., 2015; Moroz et al., 2021b; Musser et al., 2021; Romanova et al., 2021), Figure 2; and (c) physically or chemical coupled cell populations in non-animal groups (Miguel-Tome and Llinas, 2021).

This manuscript explores a broader definition of neurons as functional rather than genetic traits using examples of alternative neural/integrative systems in basal metazoan lineages. Here, we are paying more attention to the nervous systems of ctenophores, as the most unique from all known of neuroid-type organizations.

What is a neuron? Chemical synapses as the hallmark of the neuronal organization?

Practical and conceptual challenges. Due to specific microanatomical criteria, there are no problems recognizing neurons in vertebrates, arthropods, mollusks, or worms. However, identifying diverse neuronal cell types in basal deuterostomes (e.g., hemichordates or *Xenoturbella*) and across non-bilaterians is challenging. Researchers frequently use a location by *in situ* hybridization with various markers in comparative studies. However, most mRNAs are usually not transported to neuronal processes hiding specific cell morphology such as branched neurites, characteristics for many neurons (Puthanveettil et al., 2013). Immunohistochemistry helps at a limited scale for transmitter markers since many signal molecules also operate in non-neuronal cells. And we, *a priori*, do not know that any given transmitter candidate is a neurotransmitter, i.e., a signal molecule released from neurons for information transmission. In fact, such rigorous proof of identity is absent for most neurotransmitter candidates in ctenophores and cnidarians. The unbiased identification of neurons in developmental stages and neural nets is more complicated. Plus, there are multiple non-neuronal polarized secretory cells with numerous processes.

The lack of universal pan-neuronal markers (Moroz and Kohn, 2015) adds extra challenges for identifying neuronal types in early-branched metazoans. Physiological and functional definitions of biological systems and even individual cells are widely used in textbooks and experimental biology (secretory, digestive, immune, skeletal, contractive, respiratory, circulatory, locomotory, *etc.*), but not so often in evolutionary neuroscience.

Function-based terminology does not always imply homologization and direct phylogenetic relationships among respiratory or circulatory systems, for example. In contrast, it opens to multiple convergent/independent/parallel evolution instances, including the origins and diversifications of nervous systems (Moroz, 2009; Miguel-Tome and Llinas, 2021).

It is interesting to reread the 60 years old debate of two influential thinkers in evolutionary neuroscience—how to recognize and determine neurons in ctenophores.

- "G. O. Mackie: I am interested in the two types of cells in the ciliated groove. Both appear to conduct but you call one of them nerves and you say that the other conducts in a 'neuroid" fashion. Where do you draw the line between nerve cells and 'neuroid' conducting cells?
- G. A. Horridge: The epithelial cells have grown elongated and parallel. They conduct over long distances and resemble nerve cells but happen to be ciliated. I would call this an independent origin of a nerve cell, but the whole definition of nerves is in question. As soon as you trace the origin of any category down to its simplest limits, you find that your definitions become arbitrary. If you remove stones from a heap until you have four left, is that still a heap? If you remove another and you have 3, is that a heap? When you have only two left, that is probably not a heap. Similarly, when you discover progressively more elementary nervous system or follow any structure in the animal kingdom down to its simplest limits you find that your definitions are no longer simple."—cited from (Horridge, 1966).

Morphological and molecular data over the last decade added new layers of complexities to the organization of 'simpler' neural systems in ctenophores. The overall neuromuscular architecture has been characterized in 11 ctenophore species representing major phyletic lineages within this group: *Euplokamis*, *Pleurobrachia*, benthic ctenophores, lobates (*Mnemiopsis* and *Bolinopsis*), *Beroe*, *Dryodora* and even unnamed species (Norekian and Moroz, 2016; 2019a; b;2020; 2021).

Figure 1 illustrates the neural organization of the cydippid *Pleurobrachia* as an example. This species has about 10,000–15,000 neurons, which form four distinct subsystems, each with unique molecular and microanatomical organization: 1) epithelial neural net with neurons arranged in specific orthogonal fashion and their branches to tentacles; 2) compact neural-like cells in the aboral organ with the gravity sensor (Tamm, 2014b) and a putative integrative center (Tamm, 1982) (=elementary brain?); 3) distinct populations of neural-type cells in the polar fields (putative chemoreceptor structures); and 4) diffuse mesogleal neuroid-like net of cells with unknown functions. There are apparent connections (including synaptic) within four subsystems (Hernandez-Nicaise, 1991). This type of organization is well-preserved across 11 studied ctenophore species with novel *lineage-specific neuronal populations*, such as those found in the feeding lobes of lobates (*Mnemiopsis* and *Bolinopsis* (Norekian and Moroz, 2021) or independently evolved giant axonal systems and striated muscles in *Euplokamis* (Norekian and Moroz, 2020). We can now distinguish more than 20 morphologically different populations of neurons and five types of receptors in each studied species (Norekian and Moroz, 2019a; b;2020).

Surprisingly, at least five neurons in the early post-hatching stages of *Mnemiopsis* can form a syncitium with fused plasma membranes (Sachkova et al., 2021; Burkhardt et al., 2022). Such syncytial-type of networks are relatively rare in nature. Notable exemptions include neurons of the cephalopod stellate ganglion, where their processes are fused to form giant axons (Young, 1939), syncytial neural nets in the colonial polyp *Velella* (Mackie, 1960; Mackie et al., 1988), cell-cell fusion in leech, gastropod molluscs, nematodes, mammals (Oren-Suissa et al., 2010; Giordano-Santini et al., 2016; Giordano-Santini et al., 2020). Neurite and synaptic fusion and pruning occurred during neural development and neuroplasticity in *Drosophila* (Yu and Schuldiner, 2014) and mammals (Faust et al., 2021) and might be mechanisms of adaptations for the propagation of signals. By summarizing the Neuron Doctrine, Raymon y Cajal 'wisely considered that "neuronal discontinuity . . . could sustain *some exceptions*" (Cajal, 1995; Bullock et al., 2005). Coupling cells and neurites into functional syncytia might occur with and without electrical synapses (see also below). Ctenophores present the exceptional opportunity to readdress 100 years-old reticular concepts of neuronal architectures.

Whether the syncytial organization of some ctenophore larval neurons is primarily, or secondary traits remain to be determined. Does it exist in adults or other ctenophores species? In summary, the syncytial type organization, unique tripartite synapses, unique molecular toolkits, unique expression of transcription factors, and diversity of unique, ctenophore-specific neuropeptides, plus lack of majority known low molecular weight transmitters are arguments for the hypothesis of independent origins of these neural systems, as proposed earlier (Moroz, 2009; 2014a; Moroz et al., 2014; Moroz, 2021). However, in addition to neuronal systems, the ctenophore contained several neuroid conductive systems in the ciliated furrows and some mesoglea muscle-like and star-like cells (Hernandez-Nicaise, 1968; Tamm, 1973; Tamm, 1982; Tamm, 1984; Tamm and Moss, 1985; Hernandez-Nicaise, 1991; Tamm and Tamm, 2002; Tamm, 2014a; Norekian and Moroz, 2020). These cell populations return us to the 60-year Mackie-Horridge discussion of separating neurons from other neuroid-like cells.

Establishing universal criteria to define neurons is vital in analyzing the origin and evolution of nervous systems. Are there any such universal criteria? Is there a universal molecular toolkit that makes a neuron? What is a neuron from the genomic viewpoint? Available scRNA-seq data alone did not provide practical markers to recognize neurons (Sebe-Pedros et al.,

2018). Neither action potentials nor exocytosis/receptive molecular components of synapses are absolute prerequisites of neurons, as they were found in sponges and placozoans (Leys et al., 1999; Sakarya et al., 2007; Kosik, 2009; Srivastava et al., 2010; Leys, 2015; Varoqueaux and Fasshauer, 2017; Wong et al., 2019; Romanova et al., 2020). Historically, there can be many transition stages within the same evolutionary cell lineage, from a simple secretory cell without well-defined processes to a highly polarized neuron with hundreds of specialized neurites and thousands of synapses.

Regarding the definition of neurons, the combination of the following features of neurons should be considered. Still, they need to be carefully validated in a broad comparative survey that includes representatives of all basal metazoan lineages.

(1) Neurons are asymmetrical, highly polarized secretory cells, which persistently maintain one or multiple cellular processes (neurites) as well as distinct compartments specialized for directed information processing to other cell types and demonstrate experience-dependent plasticity and *elaborated integrative* functions. In our opinion, the presence of short and long-term plasticity features are essential features of neurons and, perhaps, many proneuronal cells.
(2) Neurons can make polarized and specialized connections (synapses) but do not necessarily do so in all their neurites and nervous circuits, as documented in basal metazoans and various bilaterians. Hormonal-like volume transmission in some cells (or neurites) can support many integrative functions without a specialized synapse and synaptic cleft. This happens if targets are localized within a few micrometers from transmitter release points or if fast chemical transmission is not required (e.g., for many small or sessile animals with limited motor reactions or for regulation of visceral/regenerative processes).
(3) Neurons are cells specialized for *integrating numerous signals* and information transmission functions. It was suggested that a neuron could express more genes, gene products, and especially ligand-gated receptors to support its integrative operations than other cell types (Moroz, 2009). Many homeostatic and signaling pathways in neurons can be redundant, and such expanded redundancy might also be a characteristic feature of neurons enabling greater plasticity and adaptability neural circuits. This is the easily testable hypothesis when one can directly quantify all genes expressed in given neurons (vs. other cell types) using next-generation sequencing technologies. Moreover, ensembles of neurons revealed novel emerging properties absent in other cell populations. Such emerging properties can form so-called neural syntax and endogenous self-maintaining oscillations and rhythms (Buzsaki, 2010; Hanson, 2021), which often separate 'true' neural systems from others.

Thus, we define neurons as a hierarchical ensemble of polarized heterogenous secretory cells *with synapses*, evolved for generation, integration, and directional propagation of electrochemical signals leading to the release of extracellular messengers—features that enable them to transmit information, primarily chemical in nature, beyond their immediate neighbors (at useful speed) and without affecting all intervening cells en route. Systemic decision-making, short- and long-term neuroplasticity as parts of learning and memory mechanisms are inherent components of any neural organization.

We do not know if all extant neurons have plasticity properties, but the development of phenotypic plasticity in terms of strength of synaptic transmission or (hyper) excitability might be an important trait for the evolution of nervous systems (Walters and Moroz, 2009). It would be intriguing to test whether ctenophores, placozoans, or sponges learn and remember. What kinds of non-associated and associated memory mechanisms exist in these lineages? In summary, not a single character, but a combination of features can be a better definition of neurons. Four components are critical to elaborate and clarify the used terms.

First, we emphasize the definition of neurotransmitters as signaling chemical messengers *not involved directly in nutrition* and related metabolic pathways (Miguel-Tome and Llinas, 2021). In such cases as glutamate and ATP, these presynaptically released molecules act on specific ligand-gated receptors in target cells. Only secondary, these molecules can contribute to cellular metabolism *via* uptake or transfer through other supportive/glia-type cells. This comment does not contradict the view that ancient usages of these molecules in cellular metabolism was the vital exaptation predating neuronal origins, which subsequentially led to neofunctionalizations and selection of such abundant metabolites as neurotransmitters (Moroz et al., 2021a; Moroz et al., 2021b).

Second, when metabolites 'become' signaling molecules, transmitters, and neurotransmitters, it tune natural selection processes toward their spatial distribution and novel functions in intracellular communications as rich information carriers. Indeed, in contrast to nutrients, *the receiver* (=postsynaptic cell) *does not 'know'* what the signal value would be from the information standpoint (Miguel-Tome and Llinas, 2021). However, the selection of neurotransmitters includes chemical and past evolutionary history and bioenergetic constraints for preserving, eliminating, or expanding selected messengers in particular neural circuits and species (Moroz et al., 2021b; Moroz and Romanova, 2021).

Third, compartmentalizing hundreds of chemical communications enriches *the speed of decision-making* by neuronal ensembles (as a separate system with emerging properties) and communications to virtually *all* other systems within an organism. In other words, neurons extensively communicate *via* multiple receptors to 'determine' which signal to send or not to send to

other cell types (Miguel-Tome and Llinas, 2021). Thus, the *elaborated integrative activity* (thousands of rapid communications between neurons) is the second hallmark of nervous systems, which separates them from other tissues and organs. In contrast to computers, the elaborated integrative activity of nervous systems is primarily based on the elaborated heterogeneity of its units (neurons) and a broad spectrum of chemically different intercellular messengers (rather than the usage of one excitatory and one inhibitory transmitters, for example).

The systemic exaptation leading to the origin of the neuronal organization was the ancestral recruitment of dozens and even hundreds of signal molecules in early animals. The *primordial transmitter diversity* scenario explains why even simpler extant nervous systems always have multiple neurotransmitters (rather than one or a few for depolarization or hyperpolarization responses in postsynaptic cells), as discussed elsewhere (Moroz et al., 2021b). Any nervous system comprises numerous neurotransmitter systems because neurons evolved from a broad diversity of functionally and genetically different secretory cells (Moroz, 2009; 2014a, 2021). Multiple transmitters and synapses physically and functionally 'brought protoneurons together'. Transmitters and synapses 'made and shaped' nervous systems as we know them today in animals. The corollary of this hypothesis is the prediction that neural circuits in virtually unexplored ctenophores or integrative systems in nerveless animals such as placozoans composed of multiple polarized secretory cell types with dozens and even hundreds of transmitters. These predictions can be experimentally tested.

Fourth, *neurons evolved to learn and store information*, primarily by changing synaptic strength, wiring, and excitability. These features put neuroplasticity and memory mechanisms at the crossroad of animal adaptations supporting dynamic changes in stereotyped and learned behaviors to find new ecological niches and protection. The diversity of chemical transmission and synapses is an ideal playground to tune and further develop different forms of memory from the earliest stages of neuronal evolution. It is well-established that learning and memory mechanisms include biochemical and structural changes in synapses and excitability. There are multichemical cross-talks from pre- and postsynaptic cells using retrograde messengers (Kandel, 2001).

Furthermore, a complex dialog between synapses and the nucleus of a neuron leads to dramatic changes in gene expression programs and long-term (epigenetic) modification of the genome operation as the fundamentals of long-term memory (Kandel, 2001, 2009; Kandel et al., 2014; Asok et al., 2019). As a result, the combination of multi-transmitter and synaptic organizations, coupled with genome operation, provides the most exceptional communication, information transmission, and storage capabilities with the potential for countless emerging properties of neural systems in general. The rise of elementary intelligence and cognitive features are inherently coupled with synaptic wiring and evolved in parallel across many phyla.

Thus, we think the presence of chemical synapses is the most crucial feature of any extant neural/neuronal system. This criterion can separate canonical neuronal systems from other integrative systems in animals and beyond. For practical reasons, the criterion of the presence of chemical synapses taxonomically restricts the term neurons as an animal-specific innovation only. It contrasts and prevents confusions with different terminologies, like arguments for the existence of neural systems in plants and other eukaryotes [extensively reviewed in (Miguel-Tome and Llinas, 2021)]. We do not discuss artificial networks and systems, although we accept the hypothesis that cells with the function of neurons and synapse analogs can be discovered in other taxons (Miguel-Tome and Llinas, 2021) and potentially in other extraterrestrial life forms. See the appendix for some different definitions of neurons.

Again, on a practical note, the proposed incorporation of synapses in the definition of a neuron can also be a critical criterion that separates 'true' neurons/nervous systems from the so-called neuroid cells/neuroid systems in non-bilaterians (Figure 1, and Figure 2). Even considering the presence of syncytial organization within some neuronal elements in ctenophores (Sachkova et al., 2021), the past and recent electron microscopy reconstructions revealed the presence of numerous synapses with different secretory vesicles (Horridge and Mackay, 1964; Horridge, 1965; Hernandez-Nicaise, 1968; 1973b; a;c; 1974; Hernandez-Nicaise, 1991; Sachkova et al., 2021) reflecting the use of multiple transmitters.

The synapse-centered definition of neurons and nervous systems does not conflict with the presence of pure neurosecretory cells (without classical synapses like bag cells in the sea slug, *Aplysia* (Kupfermann, 1967, 1970) in nervous systems as the evolutionary conserved and the most ancient mode of integration. In earlier animals, (neuro) peptide/transmitter volume secretion was a remarkable proto-neuronal exaptation, and it is perfectly preserved and fully functional in all modern nervous systems (Moroz et al., 2021b). Many neurons have synaptic (highly localized) terminals and non-synaptic sites at different neurites, like in serotonergic metacerebral interneurons of Euthyneural gastropods (Weiss and Kupfermann, 1976; Gillette and Davis, 1977; Fuller et al., 1998; Sudlow et al., 1998), further stressing the importance of volume transmission for systemic integration of behaviors.

The participation of other cell types, including glia, in neuronal computations does not conflict with the definition of neurons proposed here. Indeed, vertebrate glial cells can communicate with each other through complex chemical signaling, cell adhesion molecules, and gap junctions (Bergles et al., 2000; Fields and Stevens-Graham, 2002; Bergles et al., 2010), but mammalian neurons and glia share the same path during neurogenesis, and neurons can be derived from glia (Noctor et al., 2001).

The origin of chemical synapses with a narrow synaptic cleft and adhesive highly localized molecules might be a dividing

rubicon for the formation and rapid diversification of what we call canonical nervous systems today. We consider various secretory cells and volume transmission as the predecessor of neurons (Moroz, 2009, 2021). Still, all extant neural systems contain chemical synapses, at least in some parts, which is critical for more rapid, localized, and directional transmission. The evolution of synapses was based on combinatorics of the evolutionary conserved molecular modules (Ryan et al., 2008; Ryan and Grant, 2009; Arendt, 2020, 2021) involved in exocytosis and transmitter's sensing with recruitments of diverse adhesive molecules evolved in unicellular and colonial eukaryotes for other functions (as exaptations). The presence of unique synapses and neurons in ctenophores suggests that the formation of the synaptic organization evolved more than once (Moroz and Kohn, 2016); see below.

Finally, the evolutionary making of the chemical synapse involved a dramatic reorganization of the endoplasmic reticulum, lipid diversifications, and compartmentalization within intracellular membranes, further promoting the rise of a neuronal organization (Moroz and Romanova, 2021). Molecular and functional classification of synapses, as performed in mammals (Emes et al., 2008; Grant, 2009; Masch et al., 2018; Roy et al., 2018; Zhu et al., 2018; Cizeron et al., 2020; Grant and Fransen, 2020; Bulovaite et al., 2022), is the most perspective direction to uncover the principles of neural 'designs' in basal metazoans.

Electrical synapses in neural systems are less prominent compared to chemical transmission

Both canonical gap junction proteins and recently discovered tunneling nanotubes mediate a long-range junctional communication to coordinate metabolic coupling and signaling in a broad diversity of cells and tissues (Ariazi et al., 2017; Abudara et al., 2018; Guiza et al., 2018; Mayorquin et al., 2018). The electrical synapses or gap junctions also occur between neurons and might co-evolve with neurons (Ovsepian and Vesselkin, 2014; Ovsepian, 2017; Ovsepian et al., 2020). However, their fraction and contribution to the overall neuronal wiring are less prominent and often reflect no directional coupling. For example, in human brains, only about 1%–10% of connections are electrical (and mediated by connexins); the rest are chemical synapses. The same distribution is found in the model nematode (*C. elegans*), with about 10% of electrical synapses (mediated by innexins); the rest are chemical synapses.

Of note, invertebrate gap junctions were discovered first—since the name—innexins. Later, Panchin and others also discovered innexins in humans and other vertebrates (Panchin et al., 2000). Yuri Panchin proposed the new name, pannexins for this superfamily to unify both invertebrate and vertebrate innexins [from the Latin *pan*—all, throughout and *nexus* - connection, bond (Panchin et al., 2000)]. Although these two terms are synonymous, some distinct features of vertebrate pannexins (see below) lead to more often usage of this term for humans and mammals, while innexins continue to be broadly used for invertebrates.

Non-homologous classes of proteins (connexins and innexins/ = pannexins) make gap junctions (Baranova et al., 2004; Panchin, 2005; Abascal and Zardoya, 2013; Guiza et al., 2018) with the same membrane topology (Maeda et al., 2009; Oshima et al., 2016; Deng et al., 2020; Michalski et al., 2020; Qu et al., 2020; Ruan et al., 2020), reflecting their convergent evolution. Each hemichannel consists of six subunits for connexins and eight for innexins, and they are localized at opposite sides of two interacting cells (Oshima et al., 2016; Skerrett and Williams, 2017; Villanelo et al., 2017). Each hemichannel can be both homomeric (consisting of identical subunits) or heteromeric (different subunits), providing enormous combinatorial diversity of gap junctions: N^6 for connexins and N^8 for innexins (N = number of genes/isoforms).

In contrast to pannexins (Panchin, 2005), connexins were found only in tunicates and vertebrates (an apomorphy). The amphioxus genome encodes only one pannexin/innexin gene. This comparative distribution suggests that connexins evolved after early chordates lost innexins diversity (Welzel and Schuster, 2022). Three pannexins genes are present in mammals. Even so, they do not make electrical synapses because N-glycosylation in extracellular loops prevents interactions of hemichannels and the formation of functional junctions (Penuela et al., 2007; Sanchez-Pupo et al., 2018; Ruan et al., 2020; Welzel and Schuster, 2022). Pannexins hemichannels release various metabolites and signal molecules (such as ATP) from cell types (non-only neurons) with multiple functions (Panchin, 2005; Ransford et al., 2009; Scemes et al., 2009; D'Hondt et al., 2011; Sosinsky et al., 2011; Deng et al., 2020).

The best-studied system for the systemic neurobiology of innexins is the nematode *Caenorhabditis elegans*. According to its neuronal connectome reconstructions, 302 neurons can make 8693 synapses, but only 890 (10.2%) are electrical and formed by innexins. The *C. elegans* genome encodes 25 innexins, and 20 might contribute to neuronal wiring (Starich et al., 2001; Simonsen et al., 2014; Hall, 2017; Bhattacharya et al., 2019). The connectome of 282 somatic neurons contains 6393 interneuronal chemical synapses, 1410 neuromuscular chemical synapses, and 890 gap junctions (Varshney et al., 2011). Electrical synapses might have functional directionality and plasticity but at a limited scale. Thus, a reduced directionally of majority of studied electrical synapses might be one of the significant constraints, limiting their "expansions' across neuronal populations within all phyla.

Quantitative analyses of two numerically similar networks in *C. elegans* further demonstrate relationships between electrical and chemical synapses in the nervous system. Chklovskii and others (Varshney et al., 2011) analyzed the gap junction network of

279 neurons that make 514 junction connections consisting of one or more junctions. This electrical circuit has about 2-fold more gap junctions than neurons, however, finding directionality and *heterogenous* postsynaptic targets was challenging. In contrast, the chemically wired network in the same species also consists of 279 neurons and 2194 directed connections implemented by one or more chemical synapses. This network contained about one order of magnitude extent of chemical synapses, which were directional, with more transmitters and receptors providing significantly more computational capability and communication flexibility. It might be why chemical synapses are the hallmark of the nervous system from the very beginning.

Complex directionality with localized wiring could be the features that enhanced speed and computational power in expanded neural circuits of larger animals vs. anticipated dominance of pure volume transmission in early/potentially smaller animals. 3D spatial information transmission in neural assemblies (Moroz et al., 2021b) is inherent for chemical synapses, even at potentially higher bioenergetic costs to the nervous system.

In addition to simpler forms of electrical coupling (de-/and hyperpolarization) mediated by gap junctions; electric fields can also mediate inhibitory synaptic action as in the Mauthner cell network (Faber and Pereda, 2018). However, chemical synapses execute significantly more complex excitatory and inhibitory actions, with unprecedented capability to amplify signals and recruit different signaling pathways. These features further increase information capabilities supporting more complex behavioral controls, learning and memory. Finally, chemical synapses provide greater redundancy and adaptability within neuronal circuits and systemic integration of visceral and somatic functions by adding functional and evolutionary robustness to neuronal architectures.

Admittedly, electrical and true chemical synapses co-evolved due to increased animal and behavioral complexities (Ovsepian, 2017; Ovsepian et al., 2020), with extraordinary phylum-specific diversification across the animal tree. During synaptogenesis, electrical synapses might be established first and promote the formation of chemical synapses in development (Ovsepian and Vesselkin, 2014).

Bioenergetic studies indicated that the nervous system is very costly. As a result, a preferential selection of some groups of transmitters vs. others might occur [i.e., favoring the preservation of neuropeptide signaling machinery and some low molecular weight transmitters such as glutamate (Moroz et al., 2021a; Moroz et al., 2021b)]. The adaptability of chemical synapses overcomes the higher bioenergetic cost of information processing.

Origin and diversification of innexins

Innexins/pannexins-based junctions are not found in colonial and unicellular eukaryotes; therefore, they are metazoan but not neuron-specific synapomorphy. Phylogenomics survey pointed out that pannexins evolved in the common ancestor of all metazoans (Moroz et al., 2014) and intensely diversified in virtually every studied animal phylum, including ctenophores (Moroz and Kohn, 2016), cnidarians, and most protostome lineages (Moroz et al., 2014; Welzel and Schuster, 2022). These numerous events of *independent innexin radiation* correlate with the respective increases in tissue/organ differentiation and needs for physical/metabolic cell coupling *unrelated* to neuronal functions. The simpler bodyplans in placozoans and sponges are associated with the absence/loss of innexins and 'needs' of direct intercellular connections.

Gap junctions, recruited in the evolution of early animals, address the dramatic increase in the number of cell types (compared to colonial organisms), by coupling similar cell populations to mediate more stereotyped functions: secretion, contractility, coordinating cilia beating, exchange macromolecules and mRNAs during embryogenesis, regeneration, contribution to mechanistic tissue biology, *etc.* Thus, gap junctions are much more widespread across cell types and tissues (e.g., practically every cell in *C. elegans* expresses gap junctions) and broadly used to communicate between other cell types rather than neurons, including the integrative functions during development.

In ctenophores, innexins are very diverse and involved in numerous functions, from embryogenesis to behavioral control. Moroz and Kohn found that the genomes of both *Pleurobrachia bachei* and *Mnemiopsis leidyi* encode 12 innexins each (Moroz et al., 2014; Moroz and Kohn, 2016), potentially creating 429,981,696 combinations (12^8). Analysis of ten ctenophore transcriptomes and two genomes showed that independent diversification of innexins occurred early in ctenophore evolution with several ctenophore-lineage-specific innovations (Moroz et al., 2014; Moroz and Kohn, 2016; Welzel and Schuster, 2022). This phylogeny suggests that ongoing adaptive radiation of gap junction proteins is associated with the profound diversification of the bodyplans within Ctenophora [pelagic vs. benthic species, active vs. passive predators, *etc.* (Whelan et al., 2017)]. Equally interesting is the finding that 67% of ctenophore innexins have N-glycosylation sites, potentially preventing the formation of gap junctions between cells as in chordates. These N-glycosylation sites also evolved independently in ctenophores because they are not conserved in all species within the phylum (Welzel and Schuster, 2022).

Moroz et al. (2014) compared the gene expression profiles of *Pleurobrachia* innexins during development and across all major adult tissues. Remarkable innexins' expression was shown in early and later embryos and larvae of *Pleurobrachia* when the nervous system was not formed, but with the burst of expression for all 12 innexin genes in adults, including co-expression of several genes in the aboral organ, combs and tentacles (Moroz et al., 2014). Ctenophore gap junctions are likely responsible for

communications in alternative conductive pathways, including combs (Satterlie and Case, 1978) and ciliated furrows (Figure 1), which G. A. Horridge originally called the neuroid cells. The aboral organ and distributed neural nets control and integrate alternative conducting pathways. Although jap junction-mediated interactions have not been studied in detail, the nervous system with chemical synapses occupies the top of a hierarchical organization of behaviors in ctenophores.

Convergent evolution of synapses

Generalized extant neurons are cells that make chemical synapses among themselves and other cell types, with few exceptions. The first neural-like integrative systems were non-synaptic with volume transmission (Moroz, 2009; Moroz et al., 2021b; Jekely, 2021). Comparative data from nerveless animals and choanoflagellates support this hypothesis. All major components of presynaptic (secretory part) and postsynaptic (receptive part) modular machinery predate animals. (Sakarya et al., 2007; Kosik, 2009; Ryan and Grant, 2009; Conaco et al., 2012; Moroz and Kohn, 2015; Wong et al., 2019; Arendt, 2020; Ovsepian et al., 2020; Gohde et al., 2021). There are no pan-synaptic genes (Moroz and Kohn, 2015). A subset of evolutionarily conserved proteins is common to all neurons and synapses (exocytosis components, receptors, channels, transporters, *etc.*). Still, they are not unique neurons or synapses and are often co-opted for multiple functions. Genes encoding most of these proteins are broadly expressed across other non-neuronal cells and tissues; therefore, they have limited use as specific neuronal or synaptic markers, particularly in the analysis of non-bilaterian systems. This notion suggests: different adhesive molecules (e.g., cadherins, neuroligins, neurexins, *etc.*) and chaperons could subsequentially or in parallel scaffold individual protein modules to form chemical synapses with a defined synaptic cleft and its components.

The corollary of the neuronal polyphyly hypothesis is the scenario of independent origins of synapses (Moroz, 2009; 2014a). This scenario is supported by data about the distinct structural and presumed molecular organization of ctenophore synapses derived from genomic studies (Moroz and Kohn, 2016). However, the molecular composition of ctenophore synapses, their neurotransmitters, and signal molecules, in general, are largely unknown. The initial evidence exists for transmitter roles of glutamate (Moroz et al., 2014; Moroz and Kohn, 2015; Moroz et al., 2020b), nitric oxide (Moroz et al., 2020a), and ctenophore-specific neuropeptides in *Pleurobrachia*, *Mnemiopsis*, *Bolinopsis*, and kin (Moroz et al., 2014; Moroz and Kohn, 2015; Sachkova et al., 2021). Nevertheless, not a single synapse has been physiologically or molecularly characterized in ctenophores.

Earlier ultrastructural data revealed an unusual tripartite synaptic organization—the 'presynaptic triad' (Hernandez-Nicaise, 1973c, 1974; Hernandez-Nicaise, 1991). Each presynaptic region contains three layers of organelles: a layer of synaptic vesicles lining the presynaptic membrane, a cistern of agranular endoplasmic reticulum just above the row of vesicles, followed by one or several mitochondria. The non-polarized organization with the apparent ability to form synapses everywhere and symmetrical synapses was also demonstrated (Hernandez-Nicaise, 1973c; Hernandez-Nicaise, 1991) and confirmed by recent reconstruction (Sachkova et al., 2021; Burkhardt et al., 2022).

Synaptic systems in cnidarians and bilaterians are also quite different (Anderson, 1985; Anderson and Grunert, 1988; Anderson and Spencer, 1989; Anderson and Trapido-Rosenthal, 2009), with only partially overlapping subsets of neurotransmitters, receptors, and components of the synaptic cleft (Moroz and Kohn, 2015; Moroz et al., 2021b). Again, not a single synapse has been molecularly characterized in cnidarians, basal bilaterians, or any basal deuterostome. Thus, targeting synaptic systems in a taxonomically broad array of reference species would be both a discovery-driven enterprise and an opportunity to ask many intriguing questions, particularly about the directionality in information processing, learning and memory, and cellular bases of behavior across pre-bilaterians.

Considering more than one billion years of separate evolutionary paths for every phylum, we predict discoveries of fundamental differences across phyla regarding molecular diversity and the operation of synapses. Equally important would be the characterization of the volume transmission dynamic and its relationships with chemical synapses and other integrative systems in basal metazoans. The deciphering hierarchy within (neuro) transmitter systems and neural circuits is also a new direction of comparative research across all non-bilaterian lineages. It is an exciting time to unite multiple disciplines in such an endeavor.

In summary, little-explored examples of convergent neuronal evolution in early branching metazoans are essential to discover novel molecular and cellular toolkits controlling stereotyped and learned behaviors with prospects of neuro-engineering and synthetic biology. We also predict a greater diversity of neuroid and other systems in prebilaterian metazoans, including sponges and placozoans (Figure 2), than in Bilateria.

Concluding remarks

We agree with the recent statement: "to advance our knowledge of the nervous system, we should adopt a physiological definition (Miguel-Tome and Llinas, 2021). From this perspective, we stress several significant points and testable hypotheses:

(1) Neurons (and nervous systems) are functional but not a genetic category.

(2) Any given neural system is not a single character; it includes different cell lineages with different genealogies and origins.
(3) Both centralized and distributed nervous systems could be chimeric and composed of highly heterogenous cell populations, perhaps with unrelated origins.
(4) There are no pan-neuronal/pan-synaptic genes, and synapses evolved more than once with different neurotransmitter systems and adhesion molecules forming the synaptic cleft.
(5) Neurons with different transmitters evolved independently from different secretory neuroid-like, digestive and/or immune-type cells that might already have these (or similar) transmitters (e.g., secretory peptides, GABA, monoamines, *etc.*) or components of relevant transmitter synthetic pathways. However, transmitter phenotype could be changed in development (Spitzer, 2017; Bertuzzi et al., 2018; Meng et al., 2018; Ferrarelli, 2020; Li et al., 2020) and evolution with co-option of peptide-type and low molecular weight neurotransmitters.
(6) Novel signaling molecules and neurotransmitter systems should exist in non-bilaterians, and their diversity might exceed the diversity of neurotransmitter systems in bilaterians. In other words, neural systems in early-branching metazoans are molecularly/genetically more heterogenous than more derived bilaterian neural ensembles, which could secondarily lose the primordial diversity of molecular players in the LCAA or the urbilaterian.
(7) Phylogeny of systemic memory is based on the early evolution of the synaptic organization; by characterizing neuroplasticity mechanisms in representatives of all four non-bilaterian lineages, it would be reconstructed. Some learning and memory mechanisms might be different in non-bilaterians expanding the scope of neuroplasticity.
(8) Degrees of emerging properties across nervous systems and neuronal ensembles significantly differ in basal metazoans, especially in ctenophores vs. bilaterians.
(9) Multiple alternative neuroid-like integrative systems are present in all early-branched metazoan lineages with distinct hierarchical organizations, contributing to these species' learning and memory mechanisms.
(10) The role of neuroid-like integrative systems in cognition and behavior of bilaterians may be under-appreciated. (i.e., we may be overstating the role of neurons because of a misleading analogy between electronic computers and brains). (This comment was suggested by the reviewer, and we fully agree with this statement).

Considering minimal information about neural systems in ctenophores and alternative, integrative systems in sponges and placozoans, many fundamental questions about neuronal identity, plasticity and neuronal homology remained controversial. Based on expression data in sponges (Musser et al., 2021), their neuroid cells express a different subset of genes, which are distinct from other known neural cells in other animals. Thus, we implement a hypothesis of their independent origins and propose the terminology of alternative integrative/neural systems.

Given these proposed generalized features of neurons, it is reasonable to address the question: what is the molecular/genomic foundation that lets a cell be or not be a neuron?

The neural system evolved as a primary integrative system in organisms and considering the extreme diversity of microchemical microenvironments, the presence of multiple signal molecules, and numerous external signals; it would be reasonable to predict that most neurons are tuned to process multiple signals. Co-options of numerous (even redundant) signaling pathways might provide a versatile molecular playground for processing interneuronal communications and functions.

Evidence from some vertebrate and molluscan neurons, where deep single-cell sequencing were performed indicated the presence of several dozens of receptors within the same cell. However, as correctly indicated by one of the reviewers, "simpler" mechanoreceptive sensory neurons or specialized olfactory cells can be specialized to process a single signal. But such neurons do not exist alone, and they transmit information to interneurons and other cell types, which integrate numerous signals.

One of us earlier proposed that a complex and coordinated transcriptome/epigenomic response in a cell with co-expression of multiple genes (or even a majority of genes in a genome) at any given time is the primary requirement to be a neuron in the first place (Moroz, 2009). It might also be a significant component in developing the logic of gene regulation that drives neural evolution and the origin of various cell types in nervous and other integrative systems. What factors could initiate such a generalized, integrative, and adaptive transcriptome/epigenome response in earlier cells and promote the emergence of neuronal-like properties? The neurogenic role of injury in evolution can be one of these universal factors (Moroz, 2009; Moroz et al., 2021b). The memory of injury could be the earliest form of memory in evolution (Walters and Moroz, 2009). Similarly, defense/immune-type signaling involved in regenerative and morphogenic responses could be exaptations for early neurogenesis (Moroz, 2009; Fields et al., 2020; Moroz et al., 2021b). These and other hypotheses are testable by implementing comparative approaches with modern single-cell 'omic' technologies.

Data availability statement

The original contributions presented in the study are included in the article, further inquiries can be directed to the corresponding authors.

Author contributions

LM and DR designed the study; DR prepared illustrations; DR and LM wrote the draft of the paper; and all authors reviewed, commented on, and edited the manuscript.

Funding

This work was supported in part by the Human Frontiers Science Program (RGP0060/2017), and National Science Foundation (1146575,1557923,1548121,1645219) grants to LM.

Acknowledgments

We would like to thank the reviewers of this manuscript for critical and highly valuable suggestions, and references.

Conflict of interest

The authors declare that the research was conducted in the absence of any commercial or financial relationships that could be construed as a potential conflict of interest.

Publisher's note

References

Abascal, F., and Zardoya, R. (2013). Evolutionary analyses of gap junction protein families. *Biochim. Biophys. Acta* 1828, 4–14. doi:10.1016/j.bbamem.2012.02.007

Abudara, V., Retamal, M. A., Del Rio, R., and Orellana, J. A. (2018). Synaptic functions of hemichannels and pannexons: A double-edged sword. *Front. Mol. Neurosci.* 11, 435. doi:10.3389/fnmol.2018.00435

Anderson, P. A., and Grunert, U. (1988). Three-dimensional structure of bidirectional, excitatory chemical synapses in the jellyfish *Cyanea capillata*. *Synapse* 2, 606–613. doi:10.1002/syn.890020605

Anderson, P. A. (1985). Physiology of a bidirectional, excitatory, chemical synapse. *J. Neurophysiol.* 53, 821–835. doi:10.1152/jn.1985.53.3.821

Anderson, P. A., and Schwab, W. E. (1982). Recent advances and model systems in coelenterate neurobiology. *Prog. Neurobiol.* 19, 213–236. doi:10.1016/0301-0082(82)90007-7

Anderson, P. A., and Spencer, A. N. (1989). The importance of cnidarian synapses for neurobiology. *J. Neurobiol.* 20, 435–457. doi:10.1002/neu.480200513

Anderson, P. A., and Trapido-Rosenthal, H. G. (2009). Physiological and chemical analysis of neurotransmitter candidates at a fast excitatory synapse in the jellyfish Cyanea capillata (Cnidaria, Scyphozoa). *Invert. Neurosci.* 9, 167–173. doi:10.1007/s10158-009-0095-9

Anderson, P. (1980). Epithelial conduction: Its properties and function. *Prog. Neurobiol.* 15, 161–203. doi:10.1016/0301-0082(80)90022-2

Arendt, D., Benito-Gutierrez, E., Brunet, T., and Marlow, H. (2015). Gastric pouches and the mucociliary sole: Setting the stage for nervous system evolution. *Philos. Trans. R. Soc. Lond B Biol. Sci.* 370, 20150286. doi:10.1098/rstb.2015.0286

Arendt, D. (2021). Elementary nervous systems. *Philos. Trans. R. Soc. Lond B Biol. Sci.* 376, 20200347. doi:10.1098/rstb.2020.0347

Arendt, D. (2019). Many ways to build a polyp. *Trends Genet.* 35, 885–887. doi:10.1016/j.tig.2019.09.003

Arendt, D., Musser, J. M., Baker, C. V. H., Bergman, A., Cepko, C., Erwin, D. H., et al. (2016). The origin and evolution of cell types. *Nat. Rev. Genet.* 17, 744–757. doi:10.1038/nrg.2016.127

Arendt, D. (2008). The evolution of cell types in animals: Emerging principles from molecular studies. *Nat. Rev. Genet.* 9, 868–882. doi:10.1038/nrg2416

Arendt, D. (2020). The evolutionary assembly of neuronal machinery. *Curr. Biol.* 30, R603–R616. doi:10.1016/j.cub.2020.04.008

Ariazi, J., Benowitz, A., De Biasi, V., Den Boer, M. L., Cherqui, S., Cui, H., et al. (2017). Tunneling nanotubes and gap junctions-their role in long-range intercellular communication during development, health, and disease conditions. *Front. Mol. Neurosci.* 10, 333. doi:10.3389/fnmol.2017.00333

Armand, E. J., Li, J., Xie, F., Luo, C., and Mukamel, E. A. (2021). Single-cell sequencing of brain cell transcriptomes and epigenomes. *Neuron* 109, 11–26. doi:10.1016/j.neuron.2020.12.010

Armon, S., Bull, M. S., Aranda-Diaz, A., and Prakash, M. (2018). Ultrafast epithelial contractions provide insights into contraction speed limits and tissue integrity. *Proc. Natl. Acad. Sci. U. S. A.* 115, E10333–E10341. doi:10.1073/pnas.1802934115

Asok, A., Leroy, F., Rayman, J. B., and Kandel, E. R. (2019). Molecular mechanisms of the memory trace. *Trends Neurosci.* 42, 14–22. doi:10.1016/j.tins.2018.10.005

Baluska, F. (2009). Cell-cell channels, viruses, and evolution: Via infection, parasitism, and symbiosis toward higher levels of biological complexity. *Ann. N. Y. Acad. Sci.* 1178, 106–119. doi:10.1111/j.1749-6632.2009.04995.x

Baluska, F., Lev-Yadun, S., and Mancuso, S. (2010). Swarm intelligence in plant roots. *Trends Ecol. Evol.* 25, 682–683. doi:10.1016/j.tree.2010.09.003

Baluska, F., and Mancuso, S. (2009a). Deep evolutionary origins of neurobiology: Turning the essence of 'neural' upside-down. *Commun. Integr. Biol.* 2, 60–65. doi:10.4161/cib.2.1.7620

Baluska, F., and Mancuso, S. (2021). Individuality, self and sociality of vascular plants. *Philos. Trans. R. Soc. Lond B Biol. Sci.* 376, 20190760. doi:10.1098/rstb.2019.0760

Baluska, F., and Mancuso, S. (2009b). Plant neurobiology: From sensory biology, via plant communication, to social plant behavior. *Cogn. Process* 10, S3–S7. doi:10.1007/s10339-008-0239-6

Baluska, F., and Mancuso, S. (2009c). Plant neurobiology: From stimulus perception to adaptive behavior of plants, via integrated chemical and electrical signaling. *Plant Signal Behav.* 4, 475–476. doi:10.4161/psb.4.6.8870

Baluska, F., Mancuso, S., Volkmann, D., and Barlow, P. W. (2009). The 'root-brain' hypothesis of Charles and Francis Darwin: Revival after more than 125 years. *Plant Signal Behav.* 4, 1121–1127. doi:10.4161/psb.4.12.10574

Baluska, F. (2010). Recent surprising similarities between plant cells and neurons. *Plant Signal Behav.* 5, 87–89. doi:10.4161/psb.5.2.11237

Bandler, R. C., Vitali, I., Delgado, R. N., Ho, M. C., Dvoretskova, E., Ibarra Molinas, J. S., et al. (2022). Single-cell delineation of lineage and genetic identity in the mouse brain. *Nature* 601, 404–409. doi:10.1038/s41586-021-04237-0

Baranova, A., Ivanov, D., Petrash, N., Pestova, A., Skoblov, M., Kelmanson, I., et al. (2004). The mammalian pannexin family is homologous to the invertebrate innexin gap junction proteins. *Genomics* 83, 706–716. doi:10.1016/j.ygeno.2003.09.025

Bergles, D. E., Jabs, R., and Steinhauser, C. (2010). Neuron-glia synapses in the brain. *Brain Res. Rev.* 63, 130–137. doi:10.1016/j.brainresrev.2009.12.003

Bergles, D. E., Roberts, J. D., Somogyi, P., and Jahr, C. E. (2000). Glutamatergic synapses on oligodendrocyte precursor cells in the hippocampus. *Nature* 405, 187–191. doi:10.1038/35012083

Bertuzzi, M., Chang, W., and Ampatzis, K. (2018). Adult spinal motoneurons change their neurotransmitter phenotype to control locomotion. *Proc. Natl. Acad. Sci. U. S. A.* 115, E9926–E9933. doi:10.1073/pnas.1809050115

Bhattacharya, A., Aghayeva, U., Berghoff, E. G., and Hobert, O. (2019). Plasticity of the electrical connectome of *C. elegans*. *Cell* 176, 1174–1189. doi:10.1016/j.cell.2018.12.024

Bullock, T. H., Bennett, M. V., Johnston, D., Josephson, R., Marder, E., and Fields, R. D. (2005). Neuroscience. The neuron doctrine, redux. *Science* 310, 791–793. doi:10.1126/science.1114394

Bullock, T. H., and Horridge, G. A. (1965). *Structure and function in the nervous systems of invertebrates*. Illinois, United States: University of Chicago Press.

Bullock, T. H., Okrkand, R., and Alan, G. (1977). *Introduction to nervous systems*. San Francisco: W.H. Freeman and Company.

Bulovaite, E., Qiu, Z., Kratschke, M., Zgraj, A., Fricker, D. G., Tuck, E. J., et al. (2022). A brain atlas of synapse protein lifetime across the mouse lifespan. *Neuron*. doi:10.1016/j.neuron.2022.09.009

Burkhardt, P., Digel, L., Naumann, B., Soto-Àngel, J. J., Nordmann, E.-L., Sachkova, M. Y., et al. (2022). Syncytial nerve net in a ctenophore sheds new light on the early evolution of nervous systems. bioRxiv preprint doi:10.1101/2022.08.14.503905

Buzsaki, G. (2010). Neural syntax: Cell assemblies, synapsembles, and readers. *Neuron* 68, 362–385. doi:10.1016/j.neuron.2010.09.023

Cajal, S. R. (1995). "Histology of the nervous system of man and vertebrates," in *History of neuroscience*. Editors N. Swanson and L. W. Swanson (New York: Oxford Univ. Press).

Cizeron, M., Qiu, Z., Koniaris, B., Gokhale, R., Komiyama, N. H., Fransen, E., et al. (2020). A brainwide atlas of synapses across the mouse life span. *Science* 369, 270–275. doi:10.1126/science.aba3163

Conaco, C., Bassett, D. S., Zhou, H., Arcila, M. L., Degnan, S. M., Degnan, B. M., et al. (2012). Functionalization of a protosynaptic gene expression network. *Proc. Natl. Acad. Sci. U. S. A.* 109, 10612–10618. doi:10.1073/pnas.1201890109

Corrales, M., Cocanougher, B. T., Kohn, A. B., Wittenbach, J. D., Long, X. S., Lemire, A., et al. (2022). A single-cell transcriptomic atlas of complete insect nervous systems across multiple life stages. *Neural Dev.* 17, 8. doi:10.1186/s13064-022-00164-6

D'hondt, C., Ponsaerts, R., De Smedt, H., Vinken, M., De Vuyst, E., De Bock, M., et al. (2011). Pannexin channels in ATP release and beyond: An unexpected rendezvous at the endoplasmic reticulum. *Cell Signal* 23, 305–316. doi:10.1016/j.cellsig.2010.07.018

Delgado, R. N., Allen, D. E., Keefe, M. G., Mancia Leon, W. R., Ziffra, R. S., Crouch, E. E., et al. (2022). Individual human cortical progenitors can produce excitatory and inhibitory neurons. *Nature* 601, 397–403. doi:10.1038/s41586-021-04230-7

Deng, Z., He, Z., Maksaev, G., Bitter, R. M., Rau, M., Fitzpatrick, J. a. J., et al. (2020). Cryo-EM structures of the ATP release channel pannexin 1. *Nat. Struct. Mol. Biol.* 27, 373–381. doi:10.1038/s41594-020-0401-0

Dillon, N., Cocanougher, B., Sood, C., Yuan, X., Kohn, A. B., Moroz, L. L., et al. (2022). Single cell RNA-seq analysis reveals temporally-regulated and quiescence-regulated gene expression in Drosophila larval neuroblasts. *Neural Dev.* 17, 7. doi:10.1186/s13064-022-00163-7

Emes, R. D., Pocklington, A. J., Anderson, C. N., Bayes, A., Collins, M. O., Vickers, C. A., et al. (2008). Evolutionary expansion and anatomical specialization of synapse proteome complexity. *Nat. Neurosci.* 11, 799–806. doi:10.1038/nn.2135

Faber, D. S., and Pereda, A. E. (2018). Two forms of electrical transmission between neurons. *Front. Mol. Neurosci.* 11, 427. doi:10.3389/fnmol.2018.00427

Faust, T. E., Gunner, G., and Schafer, D. P. (2021). Mechanisms governing activity-dependent synaptic pruning in the developing mammalian CNS. *Nat. Rev. Neurosci.* 22, 657–673. doi:10.1038/s41583-021-00507-y

Fernandez, R., and Gabaldon, T. (2020). Gene gain and loss across the metazoan tree of life. *Nat. Ecol. Evol.* 4, 524–533. doi:10.1038/s41559-019-1069-x

Ferrarelli, L. K., and Wong, W. (2020). Focus issue: Signaling in neuronal development, function, and disease. *Sci. Signal.* 13, eg4. doi:10.1126/scisignal.aaa0836

Fields, C., Bischof, J., and Levin, M. (2020). Morphological coordination: A common ancestral function unifying neural and non-neural signaling. *Physiol. (Bethesda)* 35, 16–30. doi:10.1152/physiol.00027.2019

Fields, C., Glazebrook, J. F., and Levin, M. (2022). Neurons as hierarchies of quantum reference frames. *arXiv:2201.00921v1 [q-bio.NC]*.

Fields, R. D., and Stevens-Graham, B. (2002). New insights into neuron-glia communication. *Science* 298, 556–562. doi:10.1126/science.298.5593.556

Fuller, R. R., Moroz, L. L., Gillette, R., and Sweedler, J. V. (1998). Single neuron analysis by capillary electrophoresis with fluorescence spectroscopy. *Neuron* 20, 173–181. doi:10.1016/s0896-6273(00)80446-8

Giacomelli, M., Rossi, M. E., Lozano-Fernandez, J., Feuda, R., and Pisani, D. (2022). Resolving tricky nodes in the tree of life through amino acid recoding. bioRxiv preprint doi:10.1101/2022.02.24.479670

Gillette, R., and Davis, W. (1977). The role of the metacerebral giant neuron in the feeding behavior of *Pleurobranchaea*. *J. Comp. Physiology* 116, 129–159. doi:10.1007/bf00605400

Giordano-Santini, R., Kaulich, E., Galbraith, K. M., Ritchie, F. K., Wang, W., Li, Z., et al. (2020). Fusogen-mediated neuron-neuron fusion disrupts neural circuit connectivity and alters animal behavior. *Proc. Natl. Acad. Sci. U. S. A.* 117, 23054–23065. doi:10.1073/pnas.1919063117

Giordano-Santini, R., Linton, C., and Hilliard, M. A. (2016). Cell-cell fusion in the nervous system: Alternative mechanisms of development, injury, and repair. *Semin. Cell Dev. Biol.* 60, 146–154. doi:10.1016/j.semcdb.2016.06.019

Gohde, R., Naumann, B., Laundon, D., Imig, C., Mcdonald, K., Cooper, B. H., et al. (2021). Choanoflagellates and the ancestry of neurosecretory vesicles. *Philos. Trans. R. Soc. Lond B Biol. Sci.* 376, 20190759. doi:10.1098/rstb.2019.0759

Grant, S. G. (2009). A general basis for cognition in the evolution of synapse signaling complexes. *Cold Spring Harb. Symp. Quant. Biol.* 74, 249–257. doi:10.1101/sqb.2009.74.033

Grant, S. G. N., and Fransen, E. (2020). The synapse diversity dilemma: Molecular heterogeneity confounds studies of synapse function. *Front. Synaptic Neurosci.* 12, 590403. doi:10.3389/fnsyn.2020.590403

Guiza, J., Barria, I., Saez, J. C., and Vega, J. L. (2018). Innexins: Expression, regulation, and functions. *Front. Physiol.* 9, 1414. doi:10.3389/fphys.2018.01414

Halanych, K. M., Whelan, N. V., Kocot, K. M., Kohn, A. B., and Moroz, L. L. (2016). Miscues misplace sponges. *Proc. Natl. Acad. Sci. U. S. A.* 113, E946–E947. doi:10.1073/pnas.1525332113

Hall, D. H. (2017). Gap junctions in *C. elegans*: Their roles in behavior and development. *Dev. Neurobiol.* 77, 587–596. doi:10.1002/dneu.22408

Hanson, A. (2021). Spontaneous electrical low-frequency oscillations: A possible role in Hydra and all living systems. *Philos. Trans. R. Soc. Lond B Biol. Sci.* 376, 20190763. doi:10.1098/rstb.2019.0763

Hayakawa, E., Guzman, C., Horiguchi, O., Kawano, C., Shiraishi, A., Mohri, K., et al. (2022). Mass spectrometry of short peptides reveals common features of metazoan peptidergic neurons. *Nat. Ecol. Evol.* 6, 1438–1448. doi:10.1038/s41559-022-01835-7

Hernandez-Nicaise, M.-L. (1991). "Ctenophora," in *Microscopic anatomy of invertebrates: Placozoa, Porifera, Cnidaria, and Ctenophora*. Editors F. W. F. W. Harrison and J. A. Westfall (New York: Wiley), 359–418.

Hernandez-Nicaise, M. L. (1968). Specialized connexions between nerve cells and mesenchymal cells in ctenophores. *Nature* 217, 1075–1076. doi:10.1038/2171075a0

Hernandez-Nicaise, M. L. (1973c). The nervous system of ctenophores. III. Ultrastructure of synapses. *J. Neurocytol.* 2, 249–263. doi:10.1007/BF01104029

Hernandez-Nicaise, M. L. (1973b). [The nervous system of ctenophores. II. The nervous elements of the mesoglea of beroids and cydippids (author's transl)]. *Z Zellforsch Mikrosk Anat.* 143, 117–133. doi:10.1007/bf00307455

Hernandez-Nicaise, M. L. (1973a). [The nervous system of ctenophores. I. Structure and ultrastructure of the epithelial nerve-nets]. *Z Zellforsch Mikrosk Anat.* 137, 223–250. doi:10.1007/bf00307432

Hernandez-Nicaise, M. L. (1974). Ultrastructural evidence for a sensory-motor neuron in Ctenophora. *Tissue Cell* 6, 43–47. doi:10.1016/0040-8166(74)90021-4

Hobert, O. (2013). The neuronal genome of *Caenorhabditis elegans*. *WormBook* 13, 1–106. doi:10.1895/wormbook.1.161.1

Horridge, G. A., and Mackay, B. (1964). Neurociliary synapses in *Pleurobrachia* (Ctenophora). *Q. J. Microsc. Sci.* 105, 163–174. doi:10.1242/jcs.s3-105.70.163

Horridge, G. A. (1965). Non-motile sensory cilia and neuromuscular junctions in a ctenophore independent effector organ. *Proc. R. Soc. Lond. [Biol.]* 162, 333–350. doi:10.1098/rspb.1965.0042

Horridge, G. A. (1966). "Pathways of co-ordination in ctenophores," in *The Cnidaria and their evolution*. Editor J. V. Rees (London, New York: Academic Press Inc. (London) Ltd), 247–266.

Jekely, G. (2021). The chemical brain hypothesis for the origin of nervous systems. *Philos. Trans. R. Soc. Lond B Biol. Sci.* 376, 20190761. doi:10.1098/rstb.2019.0761

Kandel, E. R., Dudai, Y., and Mayford, M. R. (2014). The molecular and systems biology of memory. *Cell* 157, 163–186. doi:10.1016/j.cell.2014.03.001

Kandel, E. R., Schwartz, J. H., Jessel, T. M., Siegelbaum, S. A., and Hudspeth, A. J. (2000). *Principles of neural science*. New York, United States: McGraw-Hill Professional.

Kandel, E. R. (2009). The biology of memory: A forty-year perspective. *J. Neurosci.* 29, 12748–12756. doi:10.1523/JNEUROSCI.3958-09.2009

Kandel, E. R. (2001). The molecular biology of memory storage: A dialogue between genes and synapses. *Science* 294, 1030–1038. doi:10.1126/science.1067020

Kapli, P., and Telford, M. J. (2020). Topology-dependent asymmetry in systematic errors affects phylogenetic placement of Ctenophora and Xenacoelomorpha. *Sci. Adv.* 6, eabc5162. doi:10.1126/sciadv.abc5162

Kornder, N. A., Esser, Y., Stoupin, D., Leys, S. P., Mueller, B., Vermeij, M. J. A., et al. (2022). Sponges sneeze mucus to shed particulate waste from their seawater inlet pores. *Curr. Biol.* 32, 3855–3861. e3. doi:10.1016/j.cub.2022.07.017

Kosik, K. S. (2009). Exploring the early origins of the synapse by comparative genomics. *Biol. Lett.* 5, 108–111. doi:10.1098/rsbl.2008.0594

Kupfermann, I. (1970). Stimulation of egg laying by extracts of neuroendocrine cells (bag cells) of abdominal ganglion of *Aplysia*. *J. Neurophysiol.* 33, 877–881. doi:10.1152/jn.1970.33.6.877

Kupfermann, I. (1967). Stimulation of egg laying: Possible neuroendocrine function of bag cells of abdominal ganglion of *Aplysia californica*. *Nature* 216, 814–815. doi:10.1038/216814a0

Laumer, C. E., Fernandez, R., Lemer, S., Combosch, D., Kocot, K. M., Riesgo, A., et al. (2019). Revisiting metazoan phylogeny with genomic sampling of all phyla. *Proc. Biol. Sci.* 286, 20190831. doi:10.1098/rspb.2019.0831

Lentz, T. L. (1968). *Primitive nervous systems*. New Haven and London: Yale University Press.

Leys, S. P. (2015). Elements of a 'nervous system' in sponges. *J. Exp. Biol.* 218, 581–591. doi:10.1242/jeb.110817

Leys, S. P., Mackie, G. O., and Meech, R. W. (1999). Impulse conduction in a sponge. *J. Exp. Biol.* 202, 1139–1150. doi:10.1242/jeb.202.9.1139

Leys, S. P., Mah, J. L., Mcgill, P. R., Hamonic, L., De Leo, F. C., and Kahn, A. S. (2019). Sponge behavior and the chemical basis of responses: A post-genomic view. *Integr. Comp. Biol.* 59, 751–764. doi:10.1093/icb/icz122

Li, H. Q., Pratelli, M., Godavarthi, S., Zambetti, S., and Spitzer, N. C. (2020). Decoding neurotransmitter switching: The road forward. *J. Neurosci.* 40, 4078–4089. doi:10.1523/JNEUROSCI.0005-20.2020

Li, J., Wang, J., Zhang, P., Wang, R., Mei, Y., Sun, Z., et al. (2022). Deep learning of cross-species single-cell landscapes identifies conserved regulatory programs underlying cell types. *Nat. Genet.* 54, 1711–1720. doi:10.1038/s41588-022-01197-7

Li, Y., Shen, X. X., Evans, B., Dunn, C. W., and Rokas, A. (2021). Rooting the animal tree of life. *Mol. Biol. Evol.* 38, 4322–4333. doi:10.1093/molbev/msab170

Liang, C., Forrest, A. R., and Wagner, G. P. (2015). The statistical geometry of transcriptome divergence in cell-type evolution and cancer. *Nat. Commun.* 6, 6066. doi:10.1038/ncomms7066

Mackie, G. O. (1970). Neuroid conduction and the evolution of conducting tissues. *Q. Rev. Biol.* 45, 319–332. doi:10.1086/406645

Mackie, G. O., Singla, C. L., and Arkett, S. A. (1988). On the nervous system of *Velella* (Hydrozoa: Chondrophora). *J. Morphol.* 198, 15–23. doi:10.1002/jmor.1051980103

Mackie, G. O. (1990). The elementary nervous system revisited. *Am. Zoologist* 30, 907–920. doi:10.1093/icb/30.4.907

Mackie, G. O. (1960). The structure of the nervous system in *Velella*. *J. Cell Sci.* s3-101, 119–131. doi:10.1242/jcs.s3-101.54.119

Maeda, S., Nakagawa, S., Suga, M., Yamashita, E., Oshima, A., Fujiyoshi, Y., et al. (2009). Structure of the connexin 26 gap junction channel at 3.5 A resolution. *Nature* 458, 597–602. doi:10.1038/nature07869

Masch, J. M., Steffens, H., Fischer, J., Engelhardt, J., Hubrich, J., Keller-Findeisen, J., et al. (2018). Robust nanoscopy of a synaptic protein in living mice by organic-fluorophore labeling. *Proc. Natl. Acad. Sci. U. S. A.* 115, E8047–E8056. doi:10.1073/pnas.1807104115

Mayorova, T. D., Hammar, K., Winters, C. A., Reese, T. S., and Smith, C. L. (2019). The ventral epithelium of *Trichoplax adhaerens* deploys in distinct patterns cells that secrete digestive enzymes, mucus or diverse neuropeptides. *Biol. Open* 8, bio045674. doi:10.1242/bio.045674

Mayorova, T. D., Smith, C. L., Hammar, K., Winters, C. A., Pivovarova, N. B., Aronova, M. A., et al. (2018). Cells containing aragonite crystals mediate responses to gravity in *Trichoplax adhaerens* (Placozoa), an animal lacking neurons and synapses. *PLoS One* 13, e0190905. doi:10.1371/journal.pone.0190905

Mayorquin, L. C., Rodriguez, A. V., Sutachan, J. J., and Albarracin, S. L. (2018). Connexin-mediated functional and metabolic coupling between astrocytes and neurons. *Front. Mol. Neurosci.* 11, 118. doi:10.3389/fnmol.2018.00118

Meng, D., Li, H. Q., Deisseroth, K., Leutgeb, S., and Spitzer, N. C. (2018). Neuronal activity regulates neurotransmitter switching in the adult brain following light-induced stress. *Proc. Natl. Acad. Sci. U. S. A.* 115, 5064–5071. doi:10.1073/pnas.1801598115

Michalski, K., Syrjanen, J. L., Henze, E., Kumpf, J., Furukawa, H., and Kawate, T. (2020). The Cryo-EM structure of pannexin 1 reveals unique motifs for ion selection and inhibition. *Elife* 9, e54670. doi:10.7554/eLife.54670

Miguel-Tome, S., and Llinas, R. R. (2021). Broadening the definition of a nervous system to better understand the evolution of plants and animals. *Plant Signal Behav.* 16, 1927562. doi:10.1080/15592324.2021.1927562

Moroz, L. L. (2015). Convergent evolution of neural systems in ctenophores. *J. Exp. Biol.* 218, 598–611. doi:10.1242/jeb.110692

Moroz, L. L. (2014b). Genealogy of genealogy of neurons. *Commun. Integr. Biol.* 7, 1–6.

Moroz, L. L., Kocot, K. M., Citarella, M. R., Dosung, S., Norekian, T. P., Povolotskaya, I. S., et al. (2014). The ctenophore genome and the evolutionary origins of neural systems. *Nature* 510, 109–114. doi:10.1038/nature13400

Moroz, L. L., and Kohn, A. B. (2016). Independent origins of neurons and synapses: Insights from ctenophores. *Philos. Trans. R. Soc. Lond B Biol. Sci.* 371, 20150041. doi:10.1098/rstb.2015.0041

Moroz, L. L., and Kohn, A. B. (2015). Unbiased view of synaptic and neuronal gene complement in ctenophores: Are there pan-neuronal and pan-synaptic genes across Metazoa? *Integr. Comp. Biol.* 55, 1028–1049. doi:10.1093/icb/icv104

Moroz, L. L. (2021). Multiple origins of neurons from secretory cells. *Front. Cell Dev. Biol.* 9, 669087. doi:10.3389/fcell.2021.669087

Moroz, L. L. (2018). NeuroSystematics and periodic system of neurons: Model vs reference species at single-cell resolution. *ACS Chem. Neurosci.* 9, 1884–1903. doi:10.1021/acschemneuro.8b00100

Moroz, L. L., Nikitin, M. A., Policar, P. G., Kohn, A. B., and Romanova, D. Y. (2021a). Evolution of glutamatergic signaling and synapses. *Neuropharmacology* 199, 108740. doi:10.1016/j.neuropharm.2021.108740

Moroz, L. L. (2009). On the independent origins of complex brains and neurons. *Brain Behav. Evol.* 74, 177–190. doi:10.1159/000258665

Moroz, L. L., Romanova, D. Y., and Kohn, A. B. (2021b). Neural versus alternative integrative systems: Molecular insights into origins of neurotransmitters. *Philos. Trans. R. Soc. Lond B Biol. Sci.* 376, 20190762. doi:10.1098/rstb.2019.0762

Moroz, L. L., Romanova, D. Y., Nikitin, M. A., Sohn, D., Kohn, A. B., Neveu, E., et al. (2020a). The diversification and lineage-specific expansion of nitric oxide signaling in placozoa: Insights in the evolution of gaseous transmission. *Sci. Rep.* 10, 13020. doi:10.1038/s41598-020-69851-w

Moroz, L. L., and Romanova, D. Y. (2021). Selective advantages of synapses in evolution. *Front. Cell Dev. Biol.* 9, 726563. doi:10.3389/fcell.2021.726563

Moroz, L. L., Sohn, D., Romanova, D. Y., and Kohn, A. B. (2020b). Microchemical identification of enantiomers in early-branching animals: Lineage-specific diversification in the usage of D-glutamate and D-aspartate. *Biochem. Biophys. Res. Commun.* 527, 947–952. doi:10.1016/j.bbrc.2020.04.135

Moroz, L. L. (2014a). The genealogy of genealogy of neurons. *Commun. Integr. Biol.* 7, e993269. doi:10.4161/19420889.2014.993269

Musser, J. M., Schippers, K. J., Nickel, M., Mizzon, G., Kohn, A. B., Pape, C., et al. (2021). Profiling cellular diversity in sponges informs animal cell type and nervous system evolution. *Science* 374, 717–723. doi:10.1126/science.abj2949

Nakanishi, N., Sogabe, S., and Degnan, B. M. (2014). Evolutionary origin of gastrulation: Insights from sponge development. *BMC Biol.* 12, 26. doi:10.1186/1741-7007-12-26

Nakanishi, N., Stoupin, D., Degnan, S. M., and Degnan, B. M. (2015). Sensory flask cells in sponge larvae regulate metamorphosis via calcium signaling. *Integr. Comp. Biol.* 55, 1018–1027. doi:10.1093/icb/icv014

Nielsen, C. (2019). Early animal evolution: A morphologist's view. *R. Soc. Open Sci.* 6, 190638. doi:10.1098/rsos.190638

Nielsen, C. (2022). Hydrodynamics in early animal evolution. *Biol. Rev. Camb Philos. Soc.* doi:10.1111/brv.12909

Noctor, S. C., Flint, A. C., Weissman, T. A., Dammerman, R. S., and Kriegstein, A. R. (2001). Neurons derived from radial glial cells establish radial units in neocortex. *Nature* 409, 714–720. doi:10.1038/35055553

Norekian, T. P., and Moroz, L. L. (2020). Comparative neuroanatomy of ctenophores: Neural and muscular systems in Euplokamis dunlapae and related species. *J. Comp. Neurol.* 528, 481–501. doi:10.1002/cne.24770

Norekian, T. P., and Moroz, L. L. (2016). Development of neuromuscular organization in the ctenophore Pleurobrachia bachei. *J. Comp. Neurol.* 524, 136–151. doi:10.1002/cne.23830

Norekian, T. P., and Moroz, L. L. (2021). Development of the nervous system in the early hatching larvae of the ctenophore *Mnemiopsis leidyi*. *J. Morphol.* 282, 1466–1477. doi:10.1002/jmor.21398

Norekian, T. P., and Moroz, L. L. (2019a). Neural system and receptor diversity in the ctenophore Beroe abyssicola. *J. Comp. Neurol.* 527, 1986–2008. doi:10.1002/cne.24633

Norekian, T. P., and Moroz, L. L. (2019b). Neuromuscular organization of the ctenophore Pleurobrachia bachei. *J. Comp. Neurol.* 527, 406–436. doi:10.1002/cne.24546

Oren-Suissa, M., Hall, D. H., Treinin, M., Shemer, G., and Podbilewicz, B. (2010). The fusogen EFF-1 controls sculpting of mechanosensory dendrites. *Science* 328, 1285–1288. doi:10.1126/science.1189095

Oshima, A., Tani, K., and Fujiyoshi, Y. (2016). Atomic structure of the innexin-6 gap junction channel determined by cryo-EM. *Nat. Commun.* 7, 13681. doi:10.1038/ncomms13681

Ovsepian, S. V., O'leary, V. B., and Vesselkin, N. P. (2020). Evolutionary origins of chemical synapses. *Vitam. Horm.* 114, 1–21. doi:10.1016/bs.vh.2020.04.009

Ovsepian, S. V. (2017). The birth of the synapse. *Brain Struct. Funct.* 222, 3369–3374. doi:10.1007/s00429-017-1459-2

Ovsepian, S. V., and Vesselkin, N. P. (2014). Wiring prior to firing: The evolutionary rise of electrical and chemical modes of synaptic transmission. *Rev. Neurosci.* 25, 821–832. doi:10.1515/revneuro-2014-0037

Panchin, Y., Kelmanson, I., Matz, M., Lukyanov, K., Usman, N., and Lukyanov, S. (2000). A ubiquitous family of putative gap junction molecules. *Curr. Biol.* 10, R473–R474. doi:10.1016/s0960-9822(00)00576-5

Panchin, Y. V. (2005). Evolution of gap junction proteins--the pannexin alternative. *J. Exp. Biol.* 208, 1415–1419. doi:10.1242/jeb.01547

Penuela, S., Bhalla, R., Gong, X. Q., Cowan, K. N., Celetti, S. J., Cowan, B. J., et al. (2007). Pannexin 1 and pannexin 3 are glycoproteins that exhibit many distinct characteristics from the connexin family of gap junction proteins. *J. Cell Sci.* 120, 3772–3783. doi:10.1242/jcs.009514

Puthanveettil, S. V., Antonov, I., Kalachikov, S., Rajasethupathy, P., Choi, Y. B., Kohn, A. B., et al. (2013). A strategy to capture and characterize the synaptic transcriptome. *Proc. Natl. Acad. Sci. U. S. A.* 110, 7464–7469. doi:10.1073/pnas.1304422110

Qu, R., Dong, L., Zhang, J., Yu, X., Wang, L., and Zhu, S. (2020). Cryo-EM structure of human heptameric Pannexin 1 channel. *Cell Res.* 30, 446–448. doi:10.1038/s41422-020-0298-5

Raj, B., Wagner, D. E., Mckenna, A., Pandey, S., Klein, A. M., Shendure, J., et al. (2018). Simultaneous single-cell profiling of lineages and cell types in the vertebrate brain. *Nat. Biotechnol.* 36, 442–450. doi:10.1038/nbt.4103

Ransford, G. A., Fregien, N., Qiu, F., Dahl, G., Conner, G. E., and Salathe, M. (2009). Pannexin 1 contributes to ATP release in airway epithelia. *Am. J. Respir. Cell Mol. Biol.* 41, 525–534. doi:10.1165/rcmb.2008-0367OC

Redmond, A. K., and Mclysaght, A. (2021). Author Correction: Evidence for sponges as sister to all other animals from partitioned phylogenomics with mixture models and recoding. *Nat. Commun.* 12, 6639. doi:10.1038/s41467-022-33707-w

Rokas, A. (2013). Genetics. My oldest sister is a sea walnut? *Science* 342, 1327–1329. doi:10.1126/science.1248424

Romanova, D. Y., Nikitin, M. A., Shchenkov, S. V., and Moroz, L. L. (2022). Expanding of life strategies in placozoa: Insights from long-term culturing of Trichoplax and hoilungia. *Front. Cell Dev. Biol.* 10, 823283. doi:10.3389/fcell.2022.823283

Romanova, D. Y., Smirnov, I. V., Nikitin, M. A., Kohn, A. B., Borman, A. I., Malyshev, A. Y., et al. (2020). Sodium action potentials in placozoa: Insights into behavioral integration and evolution of nerveless animals. *Biochem. Biophys. Res. Commun.* 532, 120–126. doi:10.1016/j.bbrc.2020.08.020

Romanova, D. Y., Varoqueaux, F., Daraspe, J., Nikitin, M. A., Eitel, M., Fasshauer, D., et al. (2021). Hidden cell diversity in placozoa: Ultrastructural insights from hoilungia hongkongensis. *Cell Tissue Res.* 385, 623–637. doi:10.1007/s00441-021-03459-y

Roy, M., Sorokina, O., Skene, N., Simonnet, C., Mazzo, F., Zwart, R., et al. (2018). Proteomic analysis of postsynaptic proteins in regions of the human neocortex. *Nat. Neurosci.* 21, 130–138. doi:10.1038/s41593-017-0025-9

Ruan, Z., Orozco, I. J., Du, J., and Lu, W. (2020). Structures of human pannexin 1 reveal ion pathways and mechanism of gating. *Nature* 584, 646–651. doi:10.1038/s41586-020-2357-y

Ryan, J. F., and Chiodin, M. (2015). Where is my mind? How sponges and placozoans may have lost neural cell types. *Philos. Trans. R. Soc. Lond B Biol. Sci.* 370, 20150059. doi:10.1098/rstb.2015.0059

Ryan, J. F. (2014). Did the ctenophore nervous system evolve independently? *Zool. (Jena)* 117, 225–226. doi:10.1016/j.zool.2014.06.001

Ryan, T. J., Emes, R. D., Grant, S. G., and Komiyama, N. H. (2008). Evolution of NMDA receptor cytoplasmic interaction domains: Implications for organisation of synaptic signalling complexes. *BMC Neurosci.* 9, 6. doi:10.1186/1471-2202-9-6

Ryan, T. J., and Grant, S. G. (2009). The origin and evolution of synapses. *Nat. Rev. Neurosci.* 10, 701–712. doi:10.1038/nrn2717

Sachkova, M. Y., Nordmann, E. L., Soto-Angel, J. J., Meeda, Y., Gorski, B., Naumann, B., et al. (2021). Neuropeptide repertoire and 3D anatomy of the ctenophore nervous system. *Curr. Biol.* 31, 5274–5285.e6. doi:10.1016/j.cub.2021.09.005

Sakarya, O., Armstrong, K. A., Adamska, M., Adamski, M., Wang, I. F., Tidor, B., et al. (2007). A post-synaptic scaffold at the origin of the animal kingdom. *PLoS One* 2, e506. doi:10.1371/journal.pone.0000506

Sanchez-Pupo, R. E., Johnston, D., and Penuela, S. (2018). N-glycosylation regulates pannexin 2 localization but is not required for interacting with pannexin 1. *Int. J. Mol. Sci.* 19, 1837. doi:10.3390/ijms19071837

Satterlie, R. A., and Case, J. F. (1978). Gap junctions suggest epithelial conduction within the comb plates of the ctenophore *Pleurobrachia bachei*. *Cell Tissue Res.* 193, 87–91. doi:10.1007/BF00221603

Scemes, E., Spray, D. C., and Meda, P. (2009). Connexins, pannexins, innexins: Novel roles of "hemi-channels. *Pflugers Arch.* 457, 1207–1226. doi:10.1007/s00424-008-0591-5

Sebe-Pedros, A., Chomsky, E., Pang, K., Lara-Astiaso, D., Gaiti, F., Mukamel, Z., et al. (2018). Early metazoan cell type diversity and the evolution of multicellular gene regulation. *Nat. Ecol. Evol.* 2, 1176–1188. doi:10.1038/s41559-018-0575-6

Simonsen, K. T., Moerman, D. G., and Naus, C. C. (2014). Gap junctions in *C. elegans*. *Front. Physiol.* 5, 40. doi:10.3389/fphys.2014.00040

Skerrett, I. M., and Williams, J. B. (2017). A structural and functional comparison of gap junction channels composed of connexins and innexins. *Dev. Neurobiol.* 77, 522–547. doi:10.1002/dneu.22447

Smith, C. L., Pivovarova, N., and Reese, T. S. (2015). Coordinated feeding behavior in Trichoplax, an animal without synapses. *PLoS One* 10, e0136098. doi:10.1371/journal.pone.0136098

Smith, C. L., Varoqueaux, F., Kittelmann, M., Azzam, R. N., Cooper, B., Winters, C. A., et al. (2014). Novel cell types, neurosecretory cells, and body plan of the early-diverging metazoan Trichoplax adhaerens. *Curr. Biol.* 24, 1565–1572. doi:10.1016/j.cub.2014.05.046

Sosinsky, G. E., Boassa, D., Dermietzel, R., Duffy, H. S., Laird, D. W., Macvicar, B., et al. (2011). Pannexin channels are not gap junction hemichannels. *Channels (Austin)* 5, 193–197. doi:10.4161/chan.5.3.15765

Spitzer, N. C. (2017). Neurotransmitter switching in the developing and adult brain. *Annu. Rev. Neurosci.* 40, 1–19. doi:10.1146/annurev-neuro-072116-031204

Squire, L., Berg, D., Bloom, F. E., Du Lac, S., Ghosh, A., and C, N. S. (2013). *Fundamental neuroscience ansterdam*. Amsterdam, Netherlands: Elsevier.

Srivastava, M., Begovic, E., Chapman, J., Putnam, N. H., Hellsten, U., Kawashima, T., et al. (2008). The *Trichoplax* genome and the nature of placozoans. *Nature* 454, 955–960. doi:10.1038/nature07191

Srivastava, M., Simakov, O., Chapman, J., Fahey, B., Gauthier, M. E., Mitros, T., et al. (2010). The Amphimedon queenslandica genome and the evolution of animal complexity. *Nature* 466, 720–726. doi:10.1038/nature09201

Starich, T., Sheehan, M., Jadrich, J., and Shaw, J. (2001). Innexins in *C. elegans*. *Cell Commun. Adhes.* 8, 311–314. doi:10.3109/15419060109080744

Striedter, G. F., Belgard, T. G., Chen, C. C., Davis, F. P., Finlay, B. L., Gunturkun, O., et al. (2014). NSF workshop report: Discovering general principles of nervous system organization by comparing brain maps across species. *J. Comp. Neurol.* 522, 1445–1453. doi:10.1002/cne.23568

Sudlow, L. C., Jing, J., Moroz, L. L., and Gillette, R. (1998). Serotonin immunoreactivity in the central nervous system of the marine molluscs

Pleurobranchaea californica and *Tritonia diomedea*. *J. Comp. Neurol.* 395, 466–480. doi:10.1002/(sici)1096-9861(19980615)395:4<466::aid-cne4>3.0.co;2-#

Tamm, S. L. (2014a). Cilia and the life of ctenophores. *Invertebr. Biol.* 133, 1–46. doi:10.1111/ivb.12042

Tamm, S. L. (1982). "Ctenophora," in *Electrical conduction and behavior in "simple" invertebrates* (Oxford: Clarendon Press), 266–358.

Tamm, S. L. (2014b). Formation of the statolith in the ctenophore *Mnemiopsis leidyi*. *Biol. Bull.* 227, 7–18. doi:10.1086/BBLv227n1p7

Tamm, S. L. (1984). Mechanical synchronization of ciliary beating within comb plates of ctenophores. *J. Exp. Biol.* 113, 401–408. doi:10.1242/jeb.113.1.401

Tamm, S. L., and Moss, A. G. (1985). Unilateral ciliary reversal and motor responses during prey capture by the ctenophore *Pleurobrachia*. *J. Exp. Biol.* 114, 443–461. doi:10.1242/jeb.114.1.443

Tamm, S. L., and Tamm, S. (2002). Novel bridge of axon-like processes of epithelial cells in the aboral sense organ of ctenophores. *J. Morphol.* 254, 99–120. doi:10.1002/jmor.10019

Tamm, S. (1973). Mechanisms of ciliary Co-ordination in ctenophores. *J. Exp. Biol.* 59, 231–245. doi:10.1242/jeb.59.1.231

Tarashansky, A. J., Musser, J. M., Khariton, M., Li, P., Arendt, D., Quake, S. R., et al. (2021). Mapping single-cell atlases throughout Metazoa unravels cell type evolution. *Elife* 10, e66747. doi:10.7554/eLife.66747

Telford, M. J., Moroz, L. L., and Halanych, K. M. (2016). Evolution: A sisterly dispute. *Nature* 529, 286–287. doi:10.1038/529286a

Varoqueaux, F., and Fasshauer, D. (2017). Getting nervous: An evolutionary overhaul for communication. *Annu. Rev. Genet.* 51, 455–476. doi:10.1146/annurev-genet-120116-024648

Varshney, L. R., Chen, B. L., Paniagua, E., Hall, D. H., and Chklovskii, D. B. (2011). Structural properties of the *Caenorhabditis elegans* neuronal network. *PLoS Comput. Biol.* 7, e1001066. doi:10.1371/journal.pcbi.1001066

Villanelo, F., Escalona, Y., Pareja-Barrueto, C., Garate, J. A., Skerrett, I. M., and Perez-Acle, T. (2017). Accessing gap-junction channel structure-function relationships through molecular modeling and simulations. *BMC Cell Biol.* 18, 5. doi:10.1186/s12860-016-0121-9

Wagner, G. P. (2014). *Homology, genes, and evolutionary innovation*. Princenton and Oxford: Princenton University Press.

Wagner, G. P. (2007). The developmental genetics of homology. *Nat. Rev. Genet.* 8, 473–479. doi:10.1038/nrg2099

Walters, E. T., and Moroz, L. L. (2009). Molluscan memory of injury: Evolutionary insights into chronic pain and neurological disorders. *Brain Behav. Evol.* 74, 206–218. doi:10.1159/000258667

Weiss, K. R., and Kupfermann, I. (1976). Homology of the giant serotonergic neurons (metacerebral cells) in *Aplysia* and pulmonate molluscs. *Brain Res.* 117, 33–49. doi:10.1016/0006-8993(76)90554-0

Welzel, G., and Schuster, S. (2022). Connexins evolved after early chordates lost innexin diversity. *Elife* 11, e74422. doi:10.7554/eLife.74422

Whelan, N. V., Kocot, K. M., Moroz, L. L., and Halanych, K. M. (2015). Error, signal, and the placement of Ctenophora sister to all other animals. *Proc. Natl. Acad. Sci. U. S. A.* 112, 5773–5778. doi:10.1073/pnas.1503453112

Whelan, N. V., Kocot, K. M., Moroz, T. P., Mukherjee, K., Williams, P., Paulay, G., et al. (2017). Ctenophore relationships and their placement as the sister group to all other animals. *Nat. Ecol. Evol.* 1, 1737–1746. doi:10.1038/s41559-017-0331-3

Wong, E., Molter, J., Anggono, V., Degnan, S. M., and Degnan, B. M. (2019). Co-expression of synaptic genes in the sponge Amphimedon queenslandica uncovers ancient neural submodules. *Sci. Rep.* 9, 15781. doi:10.1038/s41598-019-51282-x

Young, Z. Y. (1939). Fused neurons and synaptic contacts in the giant nerve fibres of cephalopods. *Philos. Trans. R. Soc. Lond. B. Biol. Sci.* 229, 465–503. doi:10.1098/rstb.1939.0003

Yu, F., and Schuldiner, O. (2014). Axon and dendrite pruning in Drosophila. *Curr. Opin. Neurobiol.* 27, 192–198. doi:10.1016/j.conb.2014.04.005

Zhu, F., Cizeron, M., Qiu, Z., Benavides-Piccione, R., Kopanitsa, M. V., Skene, N. G., et al. (2018). Architecture of the mouse brain synaptome. *Neuron* 99, 781–799. doi:10.1016/j.neuron.2018.07.007

Appendix: Selected examples of definitions of neurons and nervous systems

"By means of nerves, the pathways of the senses are distributed like the roots and fibers of a tree." --Alessandro Benedetti, 1497. https://web.stanford.edu/class/history13/earlysciencelab/body/nervespages/nerves.html

Here, we provide diverse illustrations of particular neuronal features with some of our comments (all highlights are ours).

1) "nervous system, organized group of cells specialized for the conduction of electrochemical stimuli from sensory receptors through a network to the site at which a response occurs"—Britannica https://www.britannica.com/science/nervous-system - by Thomas L. Lentz, the author of *Primitive Nervous Systems* (Lentz, 1968).

More expanded the same definition: 'In animals, in addition to chemical regulation *via* the endocrine system, there is another integrative system called the nervous system. A nervous system can be defined as an organized group of cells, called neurons, specialized for the conduction of an impulse—an *excited* state—from a sensory receptor through a nerve network to an effector, the site at which the response occurs.' https://www.britannica.com/science/nervous-system

2) "the bodily system that in vertebrates is made up of the brain and spinal cord, nerves, ganglia, and parts of the receptor organs and that receives and *interprets* stimuli and transmits impulses to the effector organs" https://www.merriam-webster.com/dictionary/nervous-system
3) "A nervous system might be defined as an organized constellation of cells (neurons) specialized for the *repeated* conduction of an *excited* state from receptor sites or from neurons to effectors or other neurons" (Bullock and Horridge, 1965).

- Inhibition and endogenous rhythmics are equally important information/signaling components.

4) "A nervous system might be defined as an organized constellation of nerve cells *and associated non-nervous cells*; it includes receptors, but not most effector cells. A corollary of the definition of nervous is that they differ both quantitatively and qualitatively from other organ systems, *because they deal only incidentally with material and energy*. Their function and specialization is to *process information*, and their organizational complexity *greatly exceeds* that of any other system." (Bullock et al., 1977)

- Here, the critical note was added, which separates the usage of signal molecules for informational processing from the use of released other molecules for nutrition and bioenergetic purposes.

5) "Nerve cells—which we shell hereafter synonymously call neurons—may be defined as cells specialized for generation, integration, and conduction of *excited* states, including most sensory but not effector cells. A corollary of this definition of nerve cells is that they derive their excitation intrinsically or from the environment, from special sense cells, or from other neurons and deliver it to other excitable or to effectors such as muscle cells." (Bullock et al., 1977).

- Inhibition and endogenous rhythmics are equally important information/signaling components.

6) "Neurons are heterogeneously shaped, highly active secretory cells." (Squire et al., 2013)

- This definition stresses one of the essential features of neurons but is also applicable to some endocrine and other secretory [e.g., mucus or digestive-related secretion].

7) "Neurons are information processing devices that receive, integrate and transmit signals to induce specific patterns of behavior." (Hobert, 2013)

- All of these functions can be applied to many cell types of nerveless animals. Even in nerveless animals such as *Trichoplax*, we can find cells that fulfill this definition of neurons (Figure 2). It would be necessary to stress that the remarkable chemical and secretory heterogeneity of cell types is the key to neural organization

8) The nervous system is defined by the presence of a special type of cell—the neuron (sometimes called "neurone" or "nerve cell"). Neurons can be distinguished from other cells in a number of ways, but their most fundamental property is that *they communicate with other cells via synapses*, which are membrane-to-membrane junctions containing molecular machinery that allows rapid transmission of signals, either electrical or chemical.—Wikipedia (https://en.wikipedia.org/wiki/Nervous_system#cite_note-KandelCh2-10) with reference to (Kandel et al., 2000) *"Ch. 2: Nerve cells and behavior"*.

9) Past and present views of neurons and research perspectives within frameworks of the Cajal Neuron Doctrine have been elegantly summarized in 2005 (Bullock et al., 2005). We provide three quotes relevant to the present discussion. "A

neuron is an anatomically and functionally distinct cellular unit that arises through the differentiation of a precursor neuroblast cell. What has evolved is a modern view of the neuron that allows a more broad and intricate perspective of *how information is processed in the nervous system.*" " . . .axon-glial communication violates the Neuron Doctrine in two ways. Information is communicated between cells at sites far removed from chemical synapses, and it propagates in a transduced form through cells that are not neurons".

- The raised questions are fundamental to studying neural systems in invertebrates and basal metazoans, particularly where identifying glia-type cells is elusive. Equally, important would be the characterization of alternative integrative systems within the broad spectrum of organisms, as discussed in this manuscript.

10) 'A nervous system is the system of a multicellular organism that 1) contains a group or groups of cells that are specialized in transmitting, generating or processing information, 2) sends signals to other systems, allowing the organism to react to or act upon exogenous and endogenous states by controlling those systems' activity, and 3) generates and sends signals to other systems as the result of communication among multiple specialized cells of the system.' (Miguel-Tome and Llinas, 2021)

- This is the conceptually broadest definition of nervous system from a physiological standpoint rather than a phylogenetic perspective, as stressed by these authors (Miguel-Tome and Llinas, 2021). It incorporates plants and might become elusive since specific molecular and functional modules would be difficult to formalize. In any case, it stresses extensive parallel evolution and functional convergence of my integrative systems across all domains of life.

11) "Neurons as hierarchies of quantum reference frames" (Fieldsa et al., 2022)—This is an intriguing systemic definition of neurons to be further explored from physical and information viewpoints.

frontiers in Ecology and Evolution

ORIGINAL RESEARCH
published: 15 February 2022
doi: 10.3389/fevo.2022.769433

Ancestral Stem Cell Reprogramming Genes Active in Hemichordate Regeneration

*Tom Humphreys[1†], Keith Weiser[1], Asuka Arimoto[2], Akane Sasaki[2], Gene Uenishi[1], Brent Fujimoto[1], Takeshi Kawashima[3], Kekoa Taparra[1], Janos Molnar[1], Noriyuki Satoh[3], Yusuke Marikawa[1] and Kuni Tagawa[2]**

[1] Institute for Biogenesis Research, University of Hawai'i at Mānoa, Honolulu, HI, United States, [2] Marine Biological Laboratory, Graduate School of Integrated Sciences for Life, Hiroshima University, Hiroshima, Japan, [3] Marine Genomics Unit, Okinawa Institute of Science and Technology Graduate University, Okinawa, Japan

Hemichordate enteropneust worms regenerate extensively in a manner that resembles the regeneration for which planaria and hydra are well known. Although hemichordates are often classified as an extant phylogenetic group that may hold ancestral deuterostome body plans at the base of the deuterostome evolutionary line leading to chordates, mammals, and humans, extensive regeneration is not known in any of these more advanced groups. Here we investigated whether hemichordates deploy functional homologs of canonical Yamanaka stem cell reprogramming factors, *Oct4*, *Sox2*, *Nanog*, and *Klf4*, as they regenerate. These reprogramming factors are not expressed during regeneration of limbs, fins, eyes or other structures that represent the best examples of regeneration in chordates. We first examined *Ptychodera flava* EST libraries and identified *Pf-Pou3, Pf-SoxB1*, *Pf-Msxlx,* and *Pf-Klf1/2/4* as most closely related to the Yamanaka factors, respectively. *In situ* hybridization analyses revealed that all these homologs are expressed in a distinct manner during head regeneration. Furthermore, *Pf-Pou3* partially rescued the loss of endogenous Oct4 in mouse embryonic stem cells in maintaining the pluripotency gene expression program. Based on these results, we propose that hemichordates may have co-opted these reprogramming factors for their extensive regeneration or that chordates may have lost the ability to mobilize these factors in response to damage. The robustness of these pluripotency gene circuits in the inner cell mass and in formation of induced pluripotent stem cells from mammalian somatic cells shows that these programs are intact in humans and other mammals and that these circuits may respond to as yet unknown gene regulatory signals, mobilizing full regeneration in hemichordates.

Keywords: hemichordates, regeneration, stem-cell reprogramming genes, *Pou3*, *SoxB1*, *Msxlx*, *Klf1/2/4*

OPEN ACCESS

Edited by:
Pedro Martinez,
University of Barcelona, Spain

Reviewed by:
Thomas Stach,
Humboldt University of Berlin, Germany
Christopher John Lowe,
Stanford University, United States

***Correspondence:**
Kuni Tagawa
kuni@hiroshima-u.ac.jp

[†]*Deceased*
Passed away on February 7th, 2014

Specialty section:
This article was submitted to Evolutionary Developmental Biology, a section of the journal Frontiers in Ecology and Evolution

Received: *02 September 2021*
Accepted: *24 January 2022*
Published: *15 February 2022*

Citation:
Humphreys T, Weiser K, Arimoto A, Sasaki A, Uenishi G, Fujimoto B, Kawashima T, Taparra K, Molnar J, Satoh N, Marikawa Y and Tagawa K (2022) Ancestral Stem Cell Reprogramming Genes Active in Hemichordate Regeneration. Front. Ecol. Evol. 10:769433. doi: 10.3389/fevo.2022.769433

INTRODUCTION

The robust regeneration capacity of hemichordates, though known since the 19th century, has only recently received much attention as a model for studying regenerative processes (Humphreys et al., 2010; Miyamoto and Saito, 2010; Luttrell et al., 2016; Arimoto and Tagawa, 2018). Hemichordates, like planaria and hydra, can regenerate the whole body from relatively small pieces. A recent review suggests that very few other animal groups exhibit complete regeneration. Most are restricted to modest damage repair, such as severed appendages or eye damage (Agata and Inoue, 2012). On

the other hand, mammalian reprogramming factors are not expressed in the modest examples of regeneration known in vertebrates, limb regeneration, for example. Although full regeneration in hemichordates can occur after a multitude of injuries, producing many different portions of their bodies (Humphreys et al., 2010; Miyamoto and Saito, 2010; Luttrell et al., 2016; Arimoto and Tagawa, 2018), we have focused on anterior regeneration after decapitation just posterior to the branchial basket to show that homologs of canonical reprogramming factors that produce mammalian induced pluripotent stem cells (iPSCs) (Takahashi and Yamanaka, 2006) function in regeneration of the acorn worm, *Ptychodera flava*.

The first frame of **Figure 1** shows an uncut animal with its original head, which includes the proboscis and collar, corresponding to the prosome and mesosome of the worm, respectively (Lacalli, 2005). Arrowheads mark the site where decapitation will occur (**Figure 1A**). The next six frames of **Figure 1** show regeneration of this same animal over the next 11 days when an almost full-sized head has regrown on the cut stump. After the cut at 0 time, the body cavity and gut are a gaping wound to the outside environment (**Figure 1B**). By 2 days post-amputation (dpa), the edge of the wound becomes swollen, apparently from inflammation processes, and begins to pull closed (**Figure 1C**). At 3 dpa, the wound is closed and a cellular blastema has formed at the dorsal edge of the healed cut (shown with an arrow in **Figure 1D**). This blastema grows rapidly and by 5 dpa has the outline of a nascent head with a proboscis and collar surrounding a newly opened pharyngeal mouth (**Figure 1E**). The head continues to grow and differentiate on the stump of original tissue. Normal behavior of the animal is regained by day 9 or 10. By 11–14 dpa the new head, attached directly to the relatively unchanged stump of old tissue, approaches the diameter of the original body and stops growing (**Figure 1G**). Head regeneration is epimorphic on the stump of old tissue with little evidence of tissue reorganization.

In planaria, regeneration is based on neoblasts, a unique population of continuously dividing pluripotent stem cells that produce new cells in the planarian and form a regeneration blastema when part of the animal is removed (Morgan, 1900; Stephan-Dubois and Kolmayer, 1959; Elliott and Sánchez-Alvarado, 2013). In amphibian limb regeneration, a blastema forms, not from pluripotent stem cells, but apparently by dedifferentiation of limb tissue cells to multipotent stem cells (Kragl et al., 2009). Stem cells of various potency have been described in regeneration of other animals, such as crinoid echinoderms and colonial ascidians (Ferrario et al., 2020), but for most animals that show some regeneration, the role of stem cells is not well established. The role of stem cells or of dedifferentiation in hemichordate regeneration was unknown. Therefore, the present study examined the mode of regeneration with molecular probes.

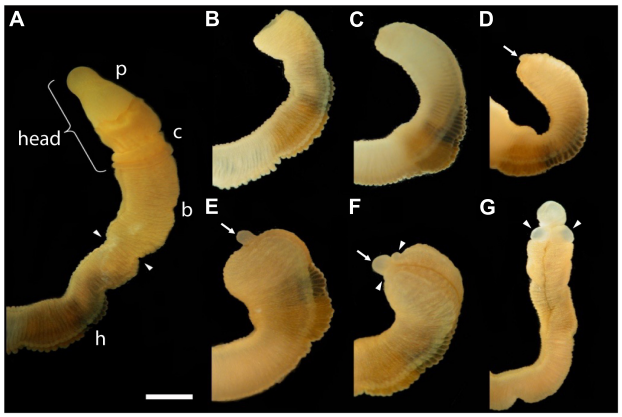

FIGURE 1 | The time sequence of head regeneration of an individual *Ptychodera flava*. Note that *P. flava* worms are very hydraulic and the same animal may be extended and thin one moment and contracted and thick the next. **(A)** The uncut, intact animal. Arrowheads mark the site at posterior end of the gill basket where the animal was severed. Scale bar = 2 mm in all frames. **(B)** 0 days post-amputation (dpa); gaping anterior wound where the body wall has been severed. **(C)** 1 dpa; edges of the severed body wall are slightly swollen and smoothened and the wound has begun to close. **(D)** 3 dpa; wound has closed and a tiny blastema can be detected dorsal to the closure site (arrow). **(E)** 5 dpa; the blastema is growing rapidly (arrow). **(F)** 7 dpa; the blastema is shaped into a nascent proboscis (arrow) with a collar (arrowheads). **(G)** 11 dpa, the new head, approaching final size to match the original body, is attached to the original anterior cut stump. All views of the left side, except **(G)**, which is more ventral. Arrowheads show the newly regenerating collar. p, proboscis; c, collar; b, branchial region; h, hepatic region.

MATERIALS AND METHODS

Animals and Regeneration Experiments

Specimens of *Ptychodera flava* were collected from areas of fine to coarse, clean sand on the extensive flat shallow reef at Paiko, Oahu, Hawaii, where tidal depths range from 0 to 0.7 m. Worms were exposed by disturbing the sand to a depth of 4–10 cm with a wave of the hand in the water over the sand. Worms ranged from 2 to 20 cm in length. About 2% of the worms collected exhibited signs of recent anterior regeneration irrespective of the season. Animals were maintained in the laboratory in 60-liter seawater aquaria filled with reconstituted sea water (Instant Ocean) at 26°C and 3 cm of coarse (1–3-mm grains) coral gravel on the bottom filter driven by aeration. The aquaria were kept clean, and 50% of the water was changed every 2 weeks.

Intact animals or anterior pieces with heads that had posterior parts removed by transection were kept in closed plastic boxes with tops and bottoms of heavy 1-mm mesh screen, covered with a layer of fine, clean sand (2–5 mm). Recently transected posterior bodies were kept in clean glass bowls in the aquaria until about 12 days of regeneration, at which point the animals regained burrowing behavior and could crawl out of the bowls. They were then moved to the closed plastic boxes with mesh tops and bottoms and a layer of fine sand. In all experiments, freshly collected animals were severed at various body levels with an orthogonal cut using sharp surgical scissors.

5-Bromo-2′-Deoxyuridine and 5-Ethynyl-2′-Deoxyuridine Labeling

5-bromo-2′-deoxyuridine (BrdU) was incorporated into developing blastemas by incubating *P. flava* at the specified regenerative day in individual 5-cm dishes containing 2 mL

salinized water with 100 μM BrdU for 16 h at room temp. Severed blastema samples were fixed in 4% paraformaldehyde with 0.5 M NaCl, 0.1 M MOPS, pH 7.5 for 2 h on ice. Blastema samples were then washed sequentially in 30% EtOH, twice in 50% EtOH, and three times in 80% EtOH, for 5 min each at room temperature (RT), and stored in 80% EtOH at −80°C until they were used for paraffin embedding. On the day of embedding, samples were washed 3 × 10 min in 100% EtOH at RT, then 2 × 30 min in 100% xylene at RT, then once in 50% xylene 50% paraffin for 1 h at 60°C. Finally, samples were transferred to molds and washed 2 × 2 h in paraffin at 60°C, before allowing them to set in fresh paraffin, with the sample oriented for sectioning at 20 μm. Slides were rehydrated by washing sequentially 2 × 10 min in xylene at RT, 2 × 10 min in 100% EtOH at RT, in 75% EtOH for 5 min at RT, in 50% EtOH for 5 min at RT, and in 100% H_2O for 5 min at RT. For antigen retrieval, samples were incubated in 10 mM citrate pH 6.0 for 35 min at 100°C. After cooling to RT for 20 min, samples were processed for immunohistochemistry (IHC). Samples were washed in PBS with 0.2% gelatin and 0.05% sodium azide and processed for IHC. The anti-BrdU antibody (OBT0030, Oxford Biotech) was used at a 1:200 dilution, while the secondary antibody was used at a 1:500 dilution. DAPI was used to visualize all nuclei.

Ptychodera flava were incubated with 100 μM 5-ethynyl-2′-deoxyuridine (EdU) in seawater to perform a pulse-chase reaction. EdU labeled cells were visualized following instructions supplied with the Click-iT EdU Alexa Fluor 594 Imaging Kit (Life Technologies, New York, NY, United States). To examine whether dividing cells moved or not, uninjured animals were pulsed for 24 h with 100 μM EdU in seawater. Animals were then decapitated and allowed to regenerate for 48 h. Moreover, animals were pulsed for 6 h at 3 days after decapitation and chased for 24 h.

Samples were fixed in 4% paraformaldehyde overnight and dehydrated in EtOH. Then, samples were rehydrated and embedded in 4% agarose and sectioned at 50 μm. Sections were blocked with 3% BSA for 30 min, permeabilized with 0.5% Triton X-100, and then washed twice with 3% BSA for 30 min. Finally, sections were incubated with Click-iT reaction buffer ($CuSO_4$, Alexa Fluor 594 azide, ascorbic acid) for 2 h.

In situ Hybridization

Fixation of samples and *in situ* hybridization were carried out as previously described for hemichordate embryos and larvae (Tagawa et al., 1998; Lowe et al., 2004) using probes for *Pf-SoxB1* (Taguchi et al., 2002), *Pf-Pou3*, *Pf-Msxlx*, *Pf-Klf1/2/4*, *Pf-Gsc* (our present study), and *Pf-F*oxA (Taguchi et al., 2000). Orthology of *Pf-Pou3*, *Pf-Msxlx* and *Pf-klf1/2/4,* newly isolated genes in this study, was determined using neighbor joining and maximum likelihood methods (details in the **Supplementary Material**). The sequence of *Pf-Gsc* was identical to that previously reported by Su et al. (2019). Nucleotide sequence data reported here are available in the DDBJ/EMBL/GenBank database under the following accession numbers: LC622252 for *Pf-Pou3*, LC622253 for *Pf-Msxlx*, LC622254 for *Pf-Klf1/2/4*, LC622255 for *Pf-Gsc*, AB894822 for *Pf-SoxB1,* and AB023019 for *Pf-F*oxA. Sources of sequences are also available in the **Supplementary Material**.

Functional Assay of *Pf-Pou3*

A mouse ES cell line ZHBTc4 (Niwa et al., 2000), a gift from Dr. Hitoshi Niwa (RIKEN Center for Developmental Biology, Kobe, Japan) was cultured in ESGRO Complete Clonal Grade Medium (Millipore, Billerica, MA, United States) without feeder cells on gelatin-coated dishes. In the ZHBTc4 cell line, the *Oct4* gene promoter was engineered to respond to TetR (tetracycline-dependent transcriptional repressor), so that endogenous *Oct4* expression could be suppressed by addition of tetracycline to the culture medium (Niwa et al., 2000). cDNA encoding *Pf-Pou3* was inserted in the multiple cloning site of the pCAG-IP vector (a gift from Dr. Niwa), which contains the CAG promoter, the internal ribosome entry site, and the puromycin resistance gene. The CAG promoter consists of the cytomegalovirus early enhancer element and the chicken beta-actin gene promoter, and its activity is not affected by tetracycline. For transfection, 5×10^4 cells were seeded in each well of 24-well plates, and plasmids (800 ng per well) were transfected the following day using Lipofectamine 2000 (Invitrogen, Carlsbad, CA, United States) according to manufacturer instructions, followed by antibiotic selection (puromycin) for over 2 weeks to obtain stably transfected cell lines. Endogenous *Oct4* expression in ZHBTc4 cells was suppressed by addition of tetracycline at 10 ng/mL for 24 h. Cells were then harvested for gene expression analyses by quantitative RT-PCR. Total RNA was extracted using TRI reagent (Invitrogen) and used for cDNA synthesis with oligo dT primer and M-MLV Reverse Transcriptase (Promega). Real-time PCR was performed using iCycler Thermal Cycler with MyiQ Single Color Real-Time PCR Detection System (Bio-Rad, Hercules, CA, United States) with iQ SYBR Green Supermix (Bio-Rad). *GAPDH* levels were used to normalize expression levels of *Oct4*-dependent genes, namely *Rex1, Fgf4*, and *Klf4*. Experiments were repeated four times, and data are presented as means ± SD.

RESULTS

Where Do Blastema Cells Originate?

To determine the provenance of dividing cells in hemichordate regeneration, we first employed BrdU labeling at various times of regeneration. By 48 h, cell division is apparent in the dorsal epidermis proximal to the decapitation cut and by 72 h the population of dividing cells is even more prominent in the blastema that has formed and in the dorsal epidermis proximal to the original cut (data not shown). As shown in **Figure 2**, at 6 dpa of regeneration, there is a prominent population of dividing cells in the dorsal epidermis, about 3–4 mm proximal to the regenerating proboscis and in the regenerating portion itself. At this point, most dividing cells in the original tissue appear to be in epidermal ectoderm (see arrow in **Figure 2B**), but some are below the basement membrane among the mesodermal cells (see arrowheads in **Figure 2B**).

Then we employed EdU labeling at earlier stages of regeneration. When intact animals are labeled with EdU, virtually all labeled cells appear in the gut epithelium (**Figure 3A**). If EdU was pulsed and removed from intact animals and then the animals were decapitated and allowed to regenerate,

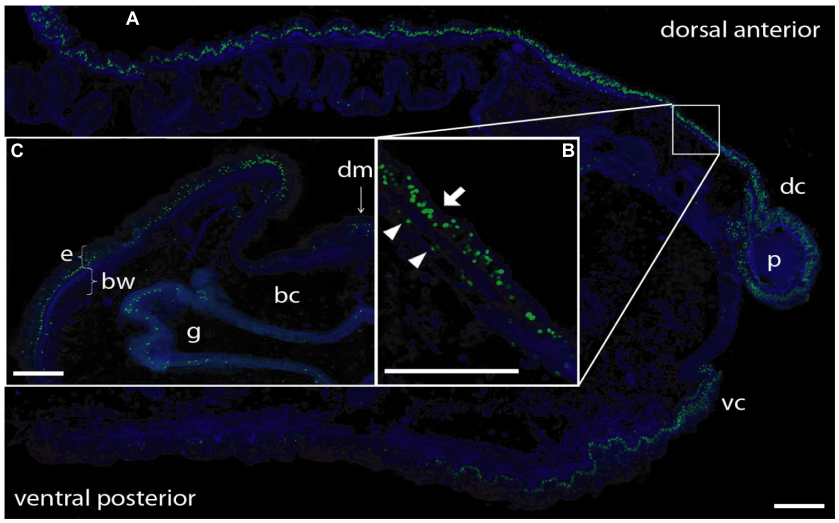

FIGURE 2 | BrdU labeling of nuclei during anterior regeneration. Green indicates BrdU-labeled nuclei. Blue is DAPI staining for all nuclei. Scale bars = 0.3 mm. **(A)** Anterior sagittal section of an animal with a regenerating proboscis at 6 days post-amputation (dpa). Many nuclei synthesizing DNA are distributed in the blastema/regenerating proboscis and in cells of the ectodermal columnar epithelium around the blastema, extending considerably more posterior in the dorsal epithelium. **(B)** Inset: Enlargement of the area from the small square in **(A)**. Most labeled nuclei are in the epithelium (arrow), but there is a small set of mesenchymal-labeled nuclei (arrowheads) below the basement membrane of the epithelium (staining of basement membrane not shown in this image). **(C)** Lateral dorsal quadrant of a body cross section posterior to a regenerating blastema at 5 dpa. Nuclei incorporating BrdU are distributed in the dorsal lateral epithelium from the dorsal midline to the lateral edge. The ventral epithelium (not shown) contains few labeled nuclei. Labeling in the gut wall is the same as in non-regenerating animals. Acquired microscopic data were composed into a single image for each sample. bc, body cavity; bw, body wall (mesodermal); dc, dorsal collar; dm, dorsal mesentery; e, epithelium (ectodermal); g, gut cavity; p, proboscis; vc, ventral collar.

these previously labeled cells remain mostly in the gut and do not appear to contribute to subsequent blastema formation (**Figure 3B**). In contrast, if EdU was pulsed and removed from the animal at 3 dpa, labeled cells were mainly detected in regenerating epithelium and its vicinity, not in the gut epithelium (**Figure 3C**). After 24 h, labeled cells appeared to remain in the anterior portion of regenerating tissues and the mass of labeled cells enlarged especially in the nascent proboscis (**Figure 3D**; arrow), although labeled cells increased in gut epithelium compared to the earlier stage of regeneration (**Figures 3C,D**). These observations of dividing cells during anterior regeneration suggest that cells contributing to hemichordate regeneration come predominantly from dorsal ectodermal epithelium and ventral ectodermal epithelium in the vicinity of the original amputation.

Do Blastema Cells Express Reprogramming Factors?

Hemichordate Homologs of Mammalian Reprogramming Factors

A full set of functional reprogramming factor genes, *Sox2, Klf4, Oct4,* and *Nanog*, has not been identified in any group except mammals, even though orthologs of *Oct4* and *Nanog* have been identified in the ancestral line of vertebrates (Theunissen et al., 2011; Onichtchouk, 2012). Although hints of the basics of a pluripotent gene program have been suggested in planaria and hydra, it seems that an *Oct4*-centric program is not present in these animals (Eisenhoffer et al., 2008). As the crucial lineage in the evolutionary line leading to mammals, it may be possible that hemichordates carry comparable gene programs. To identify and characterize hemichordate homologs of the four mammalian reprogramming factor genes, we carried out BLAST searches of *P. flava* EST libraries with approximately 160,000 independent sequences (Tagawa et al., 2014). When we found candidate genes, we confirmed them by molecular phylogenetic analysis (Takahashi et al., 2007; see **Supplementary Material**). First, together with results of previous studies (Taguchi et al., 2002; Zhong et al., 2011), the orthology of *Pf-SoxB1* with mammalian *Sox2* is evident. Second, molecular phylogenetic analysis demonstrated the orthology of *Pf-Klf1/2/4* with mouse and human *Klf4* (**Supplementary Figures 1, 2**).

On the other hand, the presence of *Oct4* and *Nanog* orthologs in invertebrates requires careful characterization, since no studies have identified *Oct4* nor *Nanog* sequences except in vertebrates, not even in invertebrate chordates. As to *Oct4,* an ancient trait of Oct4 and Pou proteins has been suggested (Holland et al., 2007; Tapia et al., 2012). Of the six classes of Pou transcription factors, classes I, III, IV, and VI were already present in the last common ancestor of metazoan and the PouII class was recovered only from bilaterians and the PouV class only from vertebrates (Gold et al., 2014). Both PouII and PouV class genes are most likely evolved from PouIII (Onichtchouk, 2016). We found that the *P. flava* genome contains members of classes II, III, IV, and VI. We named a hemichordate gene in the Pou3 subclass, *Pf-Pou3* (**Supplementary Figures 3, 4**). Mammalian *Oct4* (*Pou5f1*) has a sequence that is most closely related to the human and mouse *Pou3* genes, since Pou3 and Pou5 formed a clade in the molecular phylogenetic tree (**Supplementary Figures 3, 4**).

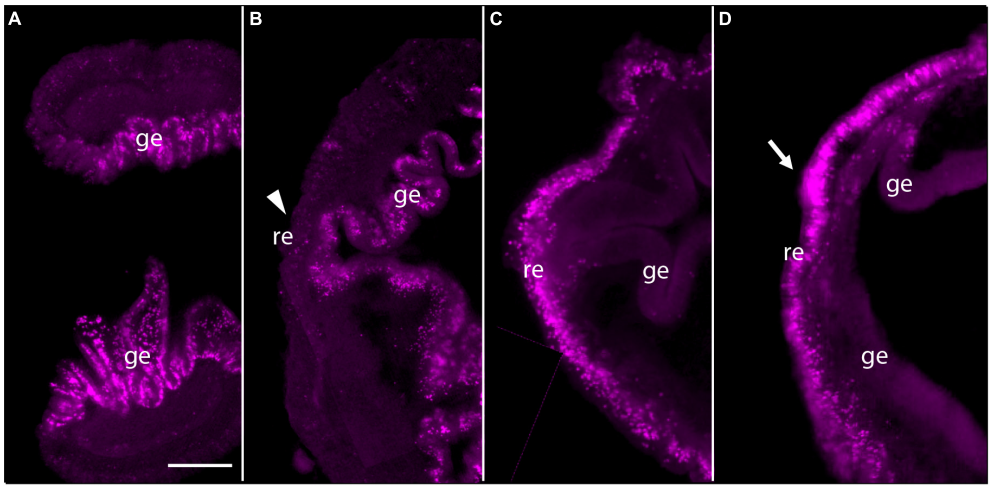

FIGURE 3 | Pulse-Chace experiments using EdU. **(A)** Uninjured animals were incubated with EdU and dividing cells were detected. Most dividing cells were observed in the gut epithelium. **(B)** Uninjured animals were incubated with EdU, then cut and allowed to regenerate for 48 h. There were very few labeled cells in anterior regenerating tissue (arrowhead), but many labeled cells in the gut epithelium. **(C)** Animals were labeled with EdU at 3 days post-amputation (dpa) and dividing cells were detected. Labeled cells were detected in and around the epithelium of regenerating tissues. **(D)** Animals were labeled with EdU at 3 dpa and allowed to regenerate for 24 h. Labeled cells appeared to remain in the anterior portion of the regenerating tissue after 24 h. The mass of labeled cells enlarged, and the regenerating blastema appeared to start forming a small proboscis (arrow). The left side is the anterior portion of regenerating tissues in all panels. Scale bar = 0.3 mm and all samples are 3–4 mm in size. Acquired microscopic data were composed into a single image for each sample. ge, gut epithelium; re, regenerating epithelium.

That is, the characterization of *Pou* homeobox genes among all human homeobox genes suggests that *Pou5* (*Pou5f1* or *Oct4*) and *Pou3* evolved from a shared ancestral gene (Holland et al., 2007; Tapia et al., 2012). Therefore, we conclude that *Pf-Pou3* is a homolog of mammalian *Oct4*. This homology was supported by a functional assay of *Pf-Pou3*, as will be described later (see section "Functional Assay of *Pf-Pou3 in vitro*").

The aforementioned sequences orthologous to *Nanog* have not been found outside of vertebrates. Our previous study demonstrated that highly significant matches of *Nanog* were found only in homeodomains. The seven best matches encoded genes containing NK-subclass homeodomain sequences (Molnar et al., unpublished data). Further phylogenetic analysis indicated that these sequences represent *P. flava* orthologs of the NKL-subclass genes, *Msxlx, Msx, Dlx, NK2.1, NK2.3, NK5,* and *Tlx*. Of them, *P. flava Msxlx* was shown in phylogenetic trees to be most closely related to human *Nanog*. Since *Nanog* is not present in invertebrates, we carried out molecular phylogeny of invertebrate *Msxlx* genes and found that *Pf-Msxlx* is a hemichordate member of *Msxlx* genes (see **Supplementary Figures 5, 6**). In summary, *Pf-SoxB1*, *Pf-Klf1/2/4*, *Pf-Pou3,* and *Pf-Msxlx* comprise a homologous set of mammalian reprogramming factor genes, *Sox2*, *Klf4*, *Oct4,* and *Nanog*.

Expression of *Pf-Pou3*, *Pf-Msxlx*, *Pf-SoxB1*, and *Pf-Klf1/2/4* During Regeneration

To answer the question of whether these genes are expressed in acorn worm regeneration, we made antisense probes for whole mount *in situ* hybridization from each of the *P. flava* sequences and reacted these probes with fixed tissue from regenerating individuals at various days following body transection, using *in situ* protocols developed for embryonic tissue (Tagawa et al., 1998; Humphreys et al., 2010). Sense probes were made for control reactions in all cases and as expected, did not produce a signal. *In situ* hybridization of tissue at the site of transection, 0 or 24 h after surgery, produced no signal in the cut stump from any of these probes or at 0 dpa for *Pf-Pou3* (**Figure 4A**) or at 0 dpa and 1 dpa for *Pf-SoxB1* (**Figures 5A,B**). From 2 - 4 dpa, while wound closure is occurring and a blastema is established, all probes began to produce signals, but in two distinct patterns. Before a signal is evident in the blastema, signals from *Pf-Pou3* and *Pf-Msxlx* appear in the original tissue along the dorsal midline, just posterior to the site of the original transection (**Figures 4B,C**). As described above, the dorsal epidermis is the location of early dividing cells when regeneration begins (**Figures 2**, **3**). As regeneration proceeds, initial expression of *Pf-Pou3* in the medial dorsal tissue of the old body wall posterior to the cut extends anteriorly and becomes prominent at the dorsal base of the blastema (**Figures 4C,D**). This expression in the dorsal base of the blastema continues during growth and differentiation of the blastema and head (**Figure 4E**). Although the most prominent expression of *Pf-Pou3* occurs in the dorsal surface of the original body wall and in the base of the blastema, there may be slight signal throughout the blastema and regenerating head during the course of regeneration (**Figures 4D,E**). The initial dorsal midline signal from the *Pf-Msxlx* probe also becomes more prominent, extends up to the dorsal base of the blastema, and spreads a bit laterally at the base of the blastema (**Figures 4F–H**), but only a small signal-positive region is evident in the dorsal base of the blastema and does not extend into the regenerating head (**Figures 4G,H**).

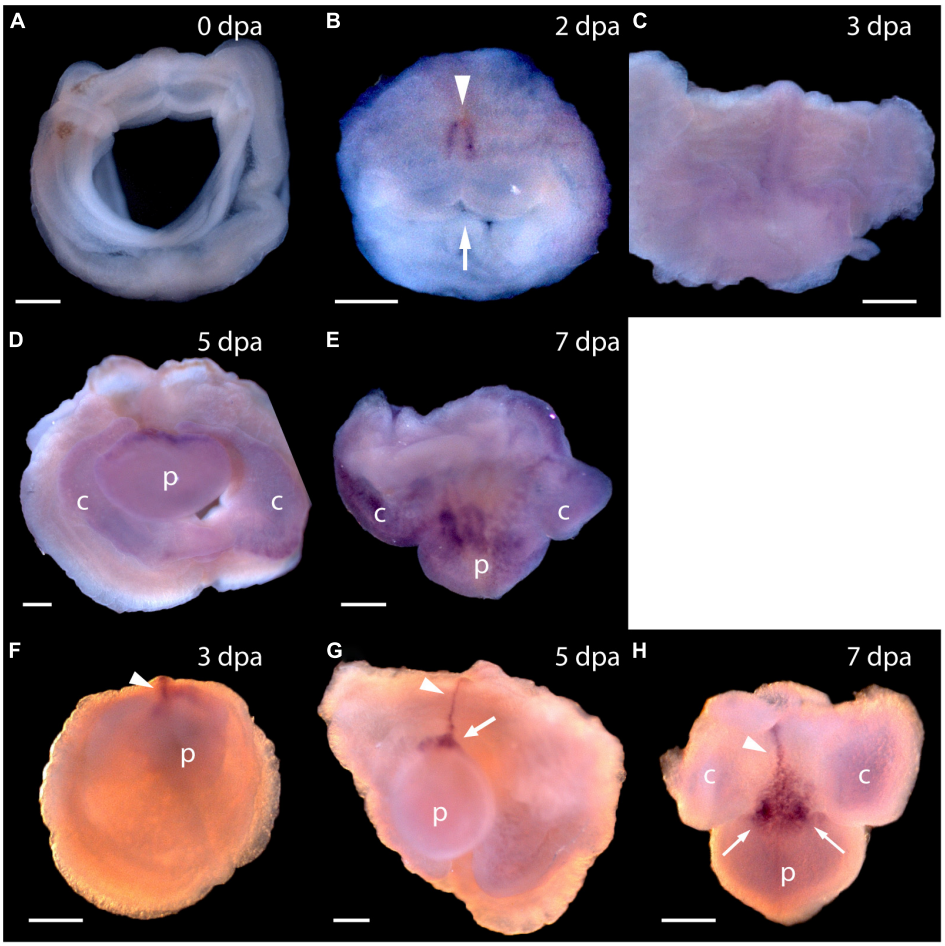

FIGURE 4 | Expression of *Pf-Pou3* and *Pf-Msxlx* during head regeneration. **(A–E)** Whole mount *in situ* hybridization of *Pf-Pou3*. **(A)** At 0 days post-amputation (dpa), no signal is detected in the tissue at the site of transection. **(B)** At 2 dpa, signal is first detected along the dorsal mid-line (arrowhead) just posterior to the site of transection. Note that at 2 dpa the wound edges are swollen and the wound is still open to the gut (arrow). **(C)** At 3 dpa, the wound has closed and signal along the dorsal midline has extended anteriorly into the base of the nascent blastema. **(D)** At 5 dpa and **(E)** at 7 dpa (dorsal view), a strong signal at the base of the blastema and forming head continues during the course of regeneration. At this time, a weak signal appears throughout the blastema and forming head. **(F–H)** *In situ* hybridization of *Pf-Msxl*x. **(F)** At 3 dpa, signal is evident along the dorsal nerve track (arrowhead). **(G)** At 5 dpa and **(H)** at 7 dpa (dorsal view), signal has extended along the dorsal mid-line to the base of the blastema where it widens into a triangle (arrows). This pattern of expression continues as the new head develops. p, nascent proboscis; c, nascent collar. Dorsal is up in all frames, unless noted. Scale bars = 0.25 mm.

As soon as the blastema is evident, signals from *Pf-SoxB1* and *Pf-Klf1/2/4* show as general signals throughout the blastema (**Figure 5D** for *Pf-SoxB1* and **Figure 5H** for *Pf-Klf1/2/4*). Some *Pf-SoxB1* signal may appear at 2 dpa in a reticulated pattern around the swollen edges of the cut body wall (**Figure 5C**) contracting together to close the wound. As soon as the wound opening has sealed and a blastema is evident, *Pf-SoxB1* gives a strong signal distributed throughout the blastema, and only in the blastema (**Figures 5D–G**). Although the *Pf-SoxB1* signal is very bright in the blastema, *Pf-SoxB1* produces no evident signal along the dorsal midline where *Pf-Pou3* and *Pf-Msxlx* signals are prominent (see **Figures 4B–E** for *Pf-Pou3* and **Figures 4F–H** for *Pf-Msxlx,* which are oriented to prominently display the dorsal midline of the preparation). As with *Pf-SoxB1*, the *Pf-Klf1/2/4* signal is distributed throughout the blastema and regenerating tissue at all times from the time when the blastema can first be recognized until head formation approaches completion (**Figures 5H–J**). In our hands, the *Pf-SoxB1* signal is always much brighter than the *Pf-Klf1/2/4* signal (compare **Figures 5A–G** with **Figures 5H–J**).

Functional Assay of *Pf-Pou3 in vitro*

Examination of the ancestral origin of *Oct4* and its role in mammalian pluripotency has shown that homologs of the *Oct4* gene occur among all classes of vertebrates. These genes from lower vertebrates function in mouse embryonic stem (ES) cells to replace the function of the mouse *Oct4* gene when the latter is silenced (Tapia et al., 2012). We took the same approach, asking if *Pf-Pou3* could replace the function of mouse *Oct4* gene in mouse ES cells. We used mouse ZHBTc4 stem cells in which the endogenous *Oct4* gene was deleted, but that contain a mouse *Oct4* transgene that can be suppressed with tetracycline

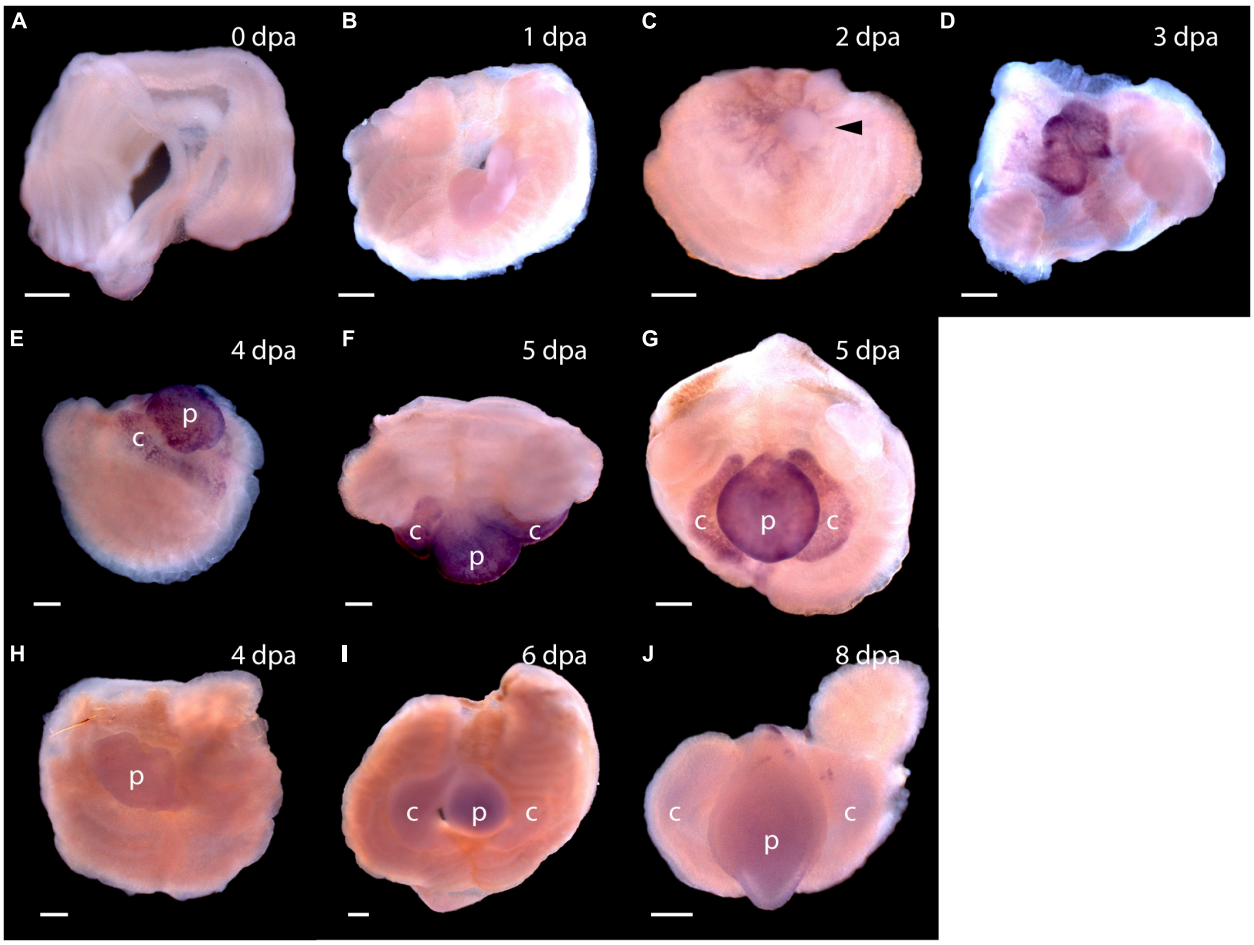

FIGURE 5 | Expression of stem cell genes *Pf-SoxB1* and *Pf-Klf1/2/4* during head regeneration. **(A–G)** Whole mount *in situ* hybridization of *Pf-SoxB1*. At 0 days post-amputation (dpa) **(A)** and at 1 dpa **(B)**, no signal is detected. **(C)** At 2 dpa, a fine, reticulated signal appears at the swollen edges of the cut body wall being pulled into the closing wound. The arrowhead marks an unlabeled, rounded bleb of swollen body wall not yet pulled into the wound. **(D)** At 3 dpa, a strong signal appears only in the blastema. This blastema appears as two parts. These parts usually merge into one as they grow. **(E)** At 4 dpa, signal appears only in blastema with signal showing in the nascent collar as well as in the proboscis. **(F)** At 5 dpa, dorsal view, signal appears only in the blastema with no signal along the dorsal midline where *Pf-Pou3* and *Pf-Msxlx* signals are prominent (see **Figures 4A–G** for *Pf-Pou3* and **Figures 4F–H** for *Pf-Msxlx*). **(G)** At 5 dpa, there is signal throughout the blastema, but no signal in the dorsal trunk. Dorsal is up in all frames except **(F)** where the dorsal surface is facing the viewer. **(H–J)** *In situ* hybridization of *Pf-Klf1/2/4*. **(H)** At 4 dpa, **(I)** at 6 dpa, and **(J)** at 8 dpa, definite, but weak signal spread generally throughout the blastema and regenerating tissue. p, nascent proboscis; c, nascent collar. Scale bars = 0.25 mm.

(Niwa et al., 2000). Cells were transfected with a hemagglutinin (HA)-tagged *Pf-Pou3* gene under control of a CAG promoter.

Immunohistochemistry with HA antibody showed that *Pf-Pou3* protein is expressed in these cells and is localized to the nucleus (data not shown). As shown in **Figure 6**, *Pf-Pou3* supports short-term expression of several *Oct4*-dependent genes that otherwise are not expressed when the endogenous mouse *Oct4* is turned off with tetracycline. Expression of three *Oct4*-dependent genes, *Rex1*, *Fgf4*, and *Klf4* as measured by qPCR, was decreased considerably when *Oct4* expression was turned off, but was maintained for 24 h upon expression of *Pf-Pou3*. This result indicates a functional conservation between *Pf-Pou3* and *Oct4*, supporting homology of the hemichordate and vertebrate genes.

Are Hemichordate Blastema Cells Pluripotent?

Expression of *Pou3*, *Msxlx*, *SoxB,* and *Klf1/2/4,* homologs of mammalian reprogramming factors, in the regeneration blastema of *P. flava* suggests these cells may be pluripotent. How might we begin to test this idea? We thought it is possible that as cells of the *P. flava* head blastema initiate differentiation, they express sets of genes similar to what pluripotent mouse epiblast cells express as they initiate development. Two of the first genes expressed in the inner cell mass as the primitive streak and head fold form at the beginning of mouse embryo development are *goosecoid* and *Foxa2* (Tam and Behringer, 1997). We applied a *Pf-FoxA* sequence from our previous study (Taguchi et al., 2000) and isolated *Pf-Gsc* sequences from our EST libraries

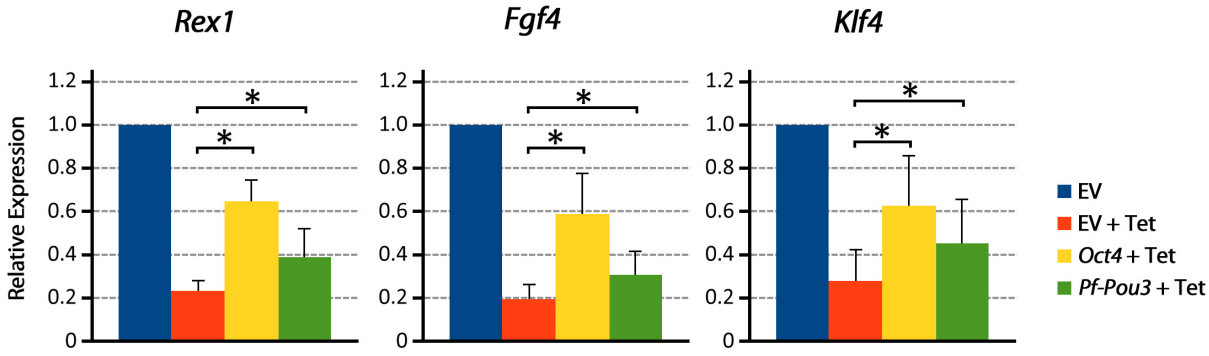

FIGURE 6 | *Pf-Pou3* maintains expression of stem cell genes on loss of *Oct4* in mouse embryonic stem cells. ZHBTc4 cells were stably transfected with vectors constitutively expressing mouse *Oct4*, *P. flava Pou3 (Pf-Pou3)*, or empty vector negative control (EV). Stable cell lines were then grown for 24 h in the presence or absence of tetracycline (Tet). The graph shows the results of qPCR on cDNA generated from these cells measuring *Oct 4*-associated stem cell genes *Rex1* (*Zfp42*), *Fgf4*, and *Klf4*, displayed as quantities relative to negative control (EV). Asterisks represents statistical significance determined with the Mann–Whitney *U* test ($p < 0.05$). Expression of target genes was significantly reduced in the absence of *Oct4* and *Pf-Pou3*, but expression of all *Oct4*-associated genes tested was significantly recovered by stable transfection of mouse *Oct4* or hemichordate *Pf-Pou3*.

(Tagawa et al., 2014) and asked, using *in situ* hybridization to mRNA, if and when these genes are expressed in developing blastema. We observed no signals in tissue before the blastema formed at 3 dpa. Signals from both *Pf-Gsc* and *Pf-FoxA* then appear in the antero-ventral margin of the blastema in a subset of the tissue expressing *Pf-SoxB1* and *Pf-Klf1/2/4* (**Figure 7**). Signals for the organizer genes were in the ventral blastema, opposite the dorsal *Pf-Pou3* and *Pf-Msxlx* signals (compare **Figures 4B,C** and **Figures 4F–H** with **Figures 7A–H**). These results indicate that differentiation in the blastema for head regeneration in *P. flava* begins by expression of the same genes as are expressed in pluripotent mouse epiblast cells, as the primitive streak forms and development begins. This result supports the idea that cells establishing the blastema may be pluripotent, like mouse epiblast cells.

DISCUSSION

Although hemichordates are marine invertebrates, closely related to chordates, including humans, they possess a remarkable regeneration capability, similar to that of planarians. We have shown here that dividing cells in intact animals are mainly those of the gut epithelium, probably because intestinal tissues are continuously being replaced as part of normal homeostasis. The dividing cells do not seem to be stem-like cells that contribute to wound healing or regeneration in hemichordates (**Figures 2**, **3**). We find no evidence to suggest that acorn worms with a primordial deuterostome body plan have a stem-cell-like system resembling that of planaria. Decapitation, followed by initiation of head regrowth appears to activate and mobilize cell division in a population of cells that experience few cell-divisions in intact worms (**Figure 3C**). These slowly dividing or possibly non-dividing cells are mobilized and contribute as rapidly dividing cells. They are found in the epithelium, blastema and regenerating tissue in decapitated worms (**Figures 3C,D**). If these cells are a variety of stem-like cells, as seems likely, they do not constitute a prominent portion of regularly dividing cells, although other possibilities for the origin of dividing cells remain to be examined.

The discoveries of mouse and human pluripotent stem cells have engendered much optimism concerning their possible contribution to reparative medicine (Takahashi and Yamanaka, 2006; Takahashi et al., 2007). Very exciting advances establishing the gene programs that determine the pluripotent cell state and the ability to use the key genes as reprogramming factors have raised hopes of making almost any cell become pluripotent. However, to date little success has been achieved in using pluripotent stem cells in regenerative medicine. Studies of modest examples of regeneration in vertebrates, amphibian limb regeneration, zebra fish brain or tail regeneration, etc., find that pluripotent cells are not involved in these processes, and key genes controlling the pluripotent state are not expressed there (Kragl et al., 2009; Onichtchouk, 2012; Tapia et al., 2012). Although the blastema or regeneration blastema, a zone of undifferentiated progenitors, of vertebrates had been thought to contain a homogeneous group of cells and viewed as a single cell-type with multipotency or pluripotency, current studies have demonstrated that the blastema is a population of heterogeneous lineage-restricted progenitor cells (Kragl et al., 2009; Johnson et al., 2020).

In tunicates, invertebrate chordates, the closest relative of vertebrates, whole-body regeneration has been reported in association with asexual reproduction (Ferrario et al., 2020). Although recently, a new model system for solitary ascidians has just emerged and has shown a novel example of whole-body regeneration (Gordon et al., 2019), its molecular mechanism is unclear. In cephalochordates, the earliest diverging invertebrate chordates, however, whole-body regeneration has not been reported, although limited regeneration capabilities have been reported (Ferrario et al., 2020). In echinoderms, another invertebrate deuterostome taxon, whole-body regeneration has been reported in sea stars in relation to axial patterning (Cary et al., 2019), in addition to extensive regeneration

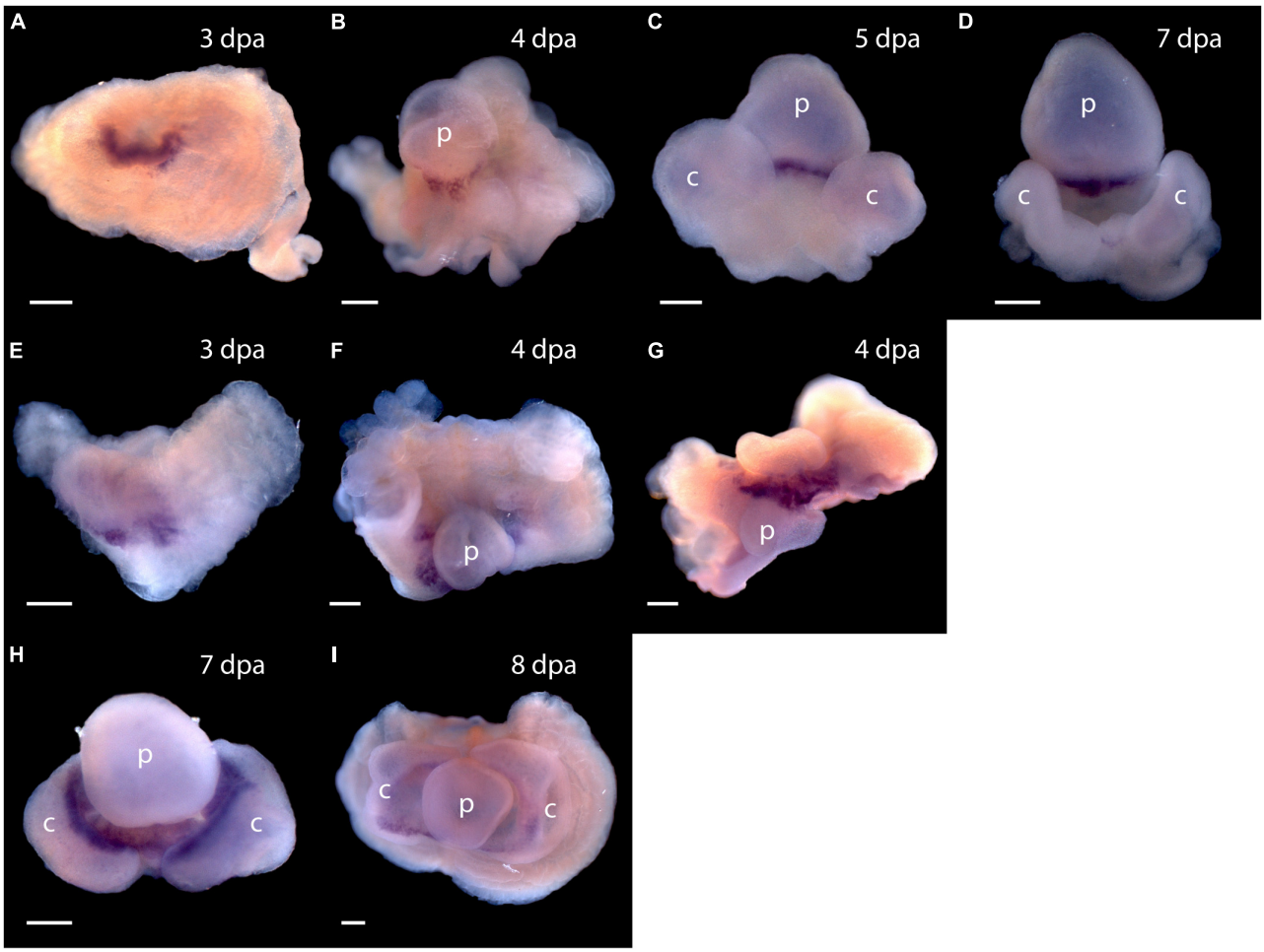

FIGURE 7 | Expression of organizer genes *Pf-Gsc* and *Pf-FoxA*. **(A–D)** Whole mount *in situ* hybridization of *Pf-Gsc* at **(A)** 3 days post-amputation (dpa), **(B)** 4 dpa, **(C)** 5 dpa, and **(D)** 7 dpa of regeneration, respectively. *Pf-Gsc* marks the ventral base of the blastema, which become the base of the proboscis in all samples stained. **(E–I)** Whole mount *in situ* hybridization of *Pf-FoxA* at 3–8 dpa of regeneration. **(E)** *Pf-FoxA* is expressed at the ventral margin of the blastema, lateral to the *Pf-Gsc* signal, which becomes the edge of collar at 3 dpa. **(F)** At 4 dpa, dorsal view **(G)** at 4 dpa, **(H)** at 7 dpa, **(I)** at 8 dpa, ventral view. Ventral is facing the viewer in all figures except **(F,G)** in which the proboscis is facing the viewer. p, nascent proboscis; c, nascent collar. Dorsal is up in all panels except panel **(G)**. Scale bars = 0.25 mm.

reported in all echinoderm classes. However, there are no reports focusing on reprogramming context in whole-body regeneration, except organ regeneration of holothurian echinoderms (Mashanov et al., 2015).

Here we show that hemichordates, kin to chordates, carry functional homologs of key genes in the mammalian reprogramming factor gene network and express these genes during regeneration. Two of the four reprogramming factors, *Oct4* and *Nanog*, are vertebrate-specific genes and are not found even in invertebrate chordates. Since these genes have evolved more rapidly than other genes in mammalian genomes (Holland et al., 2007), as shown by long branch lengths of molecular trees, careful examination is required to discuss orthology or homology between vertebrate and invertebrate counterparts. Furthermore, interspecific conservation among vertebrate homeodomains of the *Nanog* gene is very low, only 28 of 60 amino acid sequences being conserved (Molnar et al., unpublished data). This contrasts to other NKL subclasses of homeobox genes, such as *Msx,* in which 46 of 60 are conserved. In classification of human homeobox genes (Holland et al., 2007), *Nanog* is related to the human *Msx* genes, but there are no *Msxlx* genes found in vertebrates. Invertebrates have both *Msx* and *Msxlx* in their genomes and vertebrate *Nanog* may have been derived from *Msx* in the NKL families just as invertebrate *Msxlx* may have been derived from *Msx*. In the *P. flava* genomes, *Msxlx* is the one most closely related to human *Nanog*. Therefore, hemichordate *Msxlx* might be a functional substitute of vertebrate *Nanog*. *Pf-Msxlx* expression during regeneration overlaps with *Pf-Pou3* at the dorsal midline of regenerating worms where cell division remains active. This supports *Pf-Msxlx* as a hemichordate homolog of mammalian *Nanog*, although this conclusion should be examined in future functional studies.

On the relationship between hemichordate *Pou3* and vertebrate *Oct4*, our search showed that the *P. flava* genome

contains members of classes II, III, IV, and VI of Pou transcription factors, and the class III *Pf-Pou3* is the most closely related sequence to mammalian class V, to which *Oct4* belongs (**Supplementary Figures 3, 4**). A recent study on evolution of Pou class genes suggests that both class II and class V Pou genes were most likely derived from class III Pou (Gold et al., 2014; Onichtchouk, 2016). A member of class III Pou called Brn4 (Pou3f4) is unable to generate iPSCs when introduced into mouse embryonic fibroblasts. However, Velychko et al. (2020) demonstrated that Brn4 (Pou3f4) modified by swapping domains with those of Oct4 was able to generate iPSCs, although the efficiency was low compared to wild-type Oct4 (Velychko et al., 2020). In the present study, we showed that *Pf-Pou3* could replace the function of intrinsic mouse *Oct4* in ES cells. Therefore, the *Pf-Pou3* gene is very likely a functional homolog, as well as a sequence homolog of mouse *Oct4*. This suggests that the *P. flava* genome may have a pluripotency reprogramming gene program related to that of mammals. It would be interesting to examine in the future whether other invertebrate class III Pou homologs can replace *Oct4*, as in the case of *Pf-Pou3*.

The most likely interpretation of our results is that hemichordates possess a signaling system that activates a pluripotent reprogramming-like gene network and utilizes this system as part of its wound healing response. This may account for the very vigorous regenerative capabilities of hemichordates. If this is the case, it supports the very optimistic projections that knowing how *P. flava* makes and controls pluripotent cells could be a key to understanding in regenerative biology and improving regenerative medicine. Nevertheless, why do vertebrates other than mammals not use their well-developed pluripotency reprogramming capabilities for regeneration? One interpretation is that the hemichordate situation is probably ancestral in deuterostomes, and that the vertebrate evolutionary line, for currently unfathomable reasons, lost the capability to activate this program in wound responses. The alternative is that hemichordates independently developed signaling pathways to activate pluripotent reprogramming during wound healing responses and to use pluripotent cells to regenerate effectively. Since our results indicate that a great deal of functional homology of reprogramming factors has been conserved during the considerable evolutionary time between hemichordates and mice, either of the above scenarios suggest that the signaling system now present in hemichordates could inform approaches to activate reprogramming and regeneration in human injuries. Further expression analyses of these genes during normal head development and comparisons of expression patterns between normal and regenerating heads may disclose clearer molecular mechanisms underlying potential functions of these genes in evolution of animal regeneration.

DATA AVAILABILITY STATEMENT

The datasets presented in this study can be found in online repositories. The names of the repository/repositories and accession number(s) can be found in the article/ **Supplementary Material**.

AUTHOR CONTRIBUTIONS

TH and KuT conceived the study. KeT, GU, and BF collected *P. flava* and performed regeneration experiments. GU and BF performed BrdU and EdU labeling experiments, respectively. GU, AA, AS, and KuT performed *in situ* hybridization. JM and TK analyzed the sequences of *P. flava* reprogramming factors. KW and YM analyzed the functional assays of the *P. flava* homolog of vertebrate *Oct4* (*Pf-Pou3*). TH prepared the original draft of the manuscript. NS and KuT reviewed and edited the manuscript. NS acquired funding. All authors have read and agreed to the published version of the manuscript.

FUNDING

This research was funded by a KAKENHI (Grant-in-Aid for Scientific Research) on Priority Areas "Comparative Genomics" from the Ministry of Education, Culture, Sports, Science and Technology of Japan to NS (No. 17018018).

ACKNOWLEDGMENTS

We thank Asao Fujiyama and Yuji Kohara at the National Institute of Genetics, Japan for the *Ptychodera flava* EST analysis. We also thank Frederic Mercier at the University of Hawai'i at Mānoa for technical support on EdU staining and sectioning of *P. flava*. Special thanks go to Hitoshi Niwa for kindly providing the mouse ES cell line ZHBTc4 and pCAG-IP vector. Computations were partially performed on the NIG supercomputer at ROIS National Institute of Genetics, Japan. The IBBP (Interuniversity Bio-Backup Project for Basic Biology) at the National Institute for Basic Biology, supported our work in maintaining the cDNA samples in this study (ID: Kyushu 0004).

SUPPLEMENTARY MATERIAL

The Supplementary Material for this article can be found online at: https://www.frontiersin.org/articles/10.3389/fevo.2022.769433/full#supplementary-material

REFERENCES

Agata, K., and Inoue, T. (2012). Survey of the differences between regenerative and non-regenerative animals. *Dev. Growth Differ.* 54, 143–152. doi: 10.1111/j.1440-169X.2011.01323.x

Arimoto, A., and Tagawa, K. (2018). Regeration in the entropneust hemichordate, *Ptychodera flava,* and its evolutionary implication. *Dev. Growth Differ.* 60, 400–408.

Cary, G. A., Wolff, A., Zueva, O., Pattinato, J., and Hinman, V. F. (2019). Analysis of sea star larval regeneration reveals conserved processes of whole-body

regeneration across the metazoan. *BMC Biol.* 17:16. doi: 10.1186/s12915-019-0633-9

Eisenhoffer, G. T., Kang, H., and Sánchez-Alvarado, A. (2008). Molecular analysis of stem cells and their descendants during cell turnover and regeneration in the planarian *Schmidtea mediterranea*. *Cell Stem Cell* 3, 327–339. doi: 10.1016/j.stem.2008.07.002

Elliott, S. A., and Sánchez-Alvarado, A. (2013). The history and enduring contributions of planarians to the study of animal regeneration. *Wiley Interdiscip. Rev. Dev. Biol.* 2, 301–326. doi: 10.1002/wdev.82

Ferrario, C., Sugni, M., Somorjai, I. M. L., and Ballarin, L. (2020). Beyond Adult Stem Cells: dedifferentiation as a Unifying Mechanism Underlying Regeneration in Invertebrate Deuterostomes. *Front. Cell Dev. Biol.* 8:587320. doi: 10.3389/fcell.2020.587320

Gold, D. A., Gates, R. D., and Jacobs, D. K. (2014). The early expansion and evolutionary dynamics of POU class genes. *Mol. Biol. Evol.* 31, 3136–3147. doi: 10.1093/molbev/msu243

Gordon, T., Manni, L., and Shenker, N. (2019). Regeneration ability in four stolidobranch ascidians: ecological and evolutionary implications. *J. Exp. Mar. Biol. Ecol.* 519:151184. doi: 10.1016/j.jembe.2019.151184

Holland, P. W. H., Booth, H. A. F., and Bruford, E. A. (2007). Classification and nomenclature of all human homeobox genes. *BMC Biol.* 5:47. doi: 10.1186/1741-7007-5-47

Humphreys, T., Sasaki, A., Uenishi, G., Taparra, K., Arimoto, A., and Tagawa, K. (2010). Regeneration in the hemichordate *Ptychodera flava*. *Zool. Sci.* 27, 91–95.

Johnson, G. L., Masias, E. J., and Lehoczky, J. A. (2020). Cellular heterogeneity and lineage restriction during mouse digit tip regeneration at single-cell resolution. *Dev. Cell* 52, 525–540. doi: 10.1016/j.devcel.2020.01.026

Kragl, M., Knapp, D., Nacu, E., Khattak, S., Maden, M., Epperlein, H. H., et al. (2009). Cells keep a memory of their tissue origin during axolotl limb regeneration. *Nature* 460, 60–65. doi: 10.1038/nature08152

Lacalli, T. C. (2005). Protochordate body plan and the evolutionary role of larvae: old controversies resolved?. *Can. J. Zool.* 83, 216–224.

Lowe, C. J., Tagawa, K., Humphreys, T., Kirschner, M., and Gerhart, J. (2004). "Hemichordate embryos: procurement, culture, and basic methods," in *Methods Cell Biol*, eds C. A. Ettensohn, G. A. Wray, and G. M. Wessel (Amsterdam: Elsevier), 171–194. doi: 10.1016/s0091-679x(04)74008-x

Luttrell, S. M., Gotting, K., Ross, E., Alvarado, A. S., and Swalla, B. J. (2016). Head regeneration in hemichordates is not a strict recapitulation of development. *Dev. Dyn.* 245, 1159–1175. doi: 10.1002/dvdy.24457

Mashanov, V. S., Zueva, O. R., and Garcia-Arraras, J. E. (2015). Expression of pluripotency factors in echinoderm regeneration. *Cell Tissue Res.* 359, 521–536. doi: 10.1007/s00441-014-2040-4

Miyamoto, N., and Saito, Y. (2010). Morphological characterization of the asexual reproduction in the acorn worm *Balanoglossus simodensis*. *Dev. Growth Differ.* 52, 615–627. doi: 10.1111/j.1440-169X.2010.01197.x

Morgan, T. H. (1900). Regeneration in Planarians. *Arch. Mikrosk. Anat.* 10, 58–119.

Niwa, H., Miyazaki, J., and Smith, A. G. (2000). Quantitative expression of Oct-3/4 defines differentiation, dedifferentiation or self-renewal of ES cells. *Nat. Genet.* 24, 372–376. doi: 10.1038/74199

Onichtchouk, D. (2012). Pou5f1/Oct4 in pluripotency control: insights from zebrafish. *Genesis* 50, 75–85. doi: 10.1002/dvg.20800

Onichtchouk, D. (2016). Evolution and functions of Oct4 homologs in non-mammalian vertebrates. *Biochim. Biophys. Acta* 1859, 770–779. doi: 10.1016/j.bbagrm.2016.03.013

Stephan-Dubois, F., and Kolmayer, S. (1959). Migration and differentiation of the cells of regeneration in the planarian *Dendrocoelum lacteum*. *C. R. Soc. Biol.* 153, 1856–1858.

Su, Y. H., Chen, Y. C., Ting, H. C., Fan, T. P., Lin, C. Y., Wang, K. T., et al. (2019). BMP controls dorsoventral and neural patterning in indirect-developing hemichordates providing insight into a possible origin of chordates. *Proc. Natl. Acad. Sci. U. S. A.* 116, 12925–12932. doi: 10.1073/pnas.1901919116

Tagawa, K., Arimoto, A., Sasaki, A., Izumi, M., Fujita, S., Humphreys, T., et al. (2014). A cDNA resource for gene expression studies of a hemichordate *Ptychodera flava*. *Zool. Sci.* 31, 414–420. doi: 10.2108/zs130262

Tagawa, K., Humphreys, T., and Satoh, N. (1998). Novel pattern of *Brachyury* gene expression in hemichordate embryos. *Mech. Dev.* 75, 139–143. doi: 10.1016/s0925-4773(98)00078-1

Taguchi, S., Tagawa, K., Humphreys, T., Nishino, A., Satoh, N., and Harada, Y. (2000). Characterization of a hemichordate *fork head/HNF-3* gene expression. *Dev. Genes Evol.* 210, 11–17. doi: 10.1007/pl00008181

Taguchi, S., Tagawa, K., Humphreys, T., and Satoh, N. (2002). Group B *Sox* genes that contribute to specifications of the vertebrate brain are expressed in the apical organ and ciliary bands of hemichordate larvae. *Zool. Sci.* 19, 57–66. doi: 10.2108/zsj.19.57

Takahashi, K., Tanabe, K., Ohnuki, M., Narita, M., Ichisaka, T., Tomoda, K., et al. (2007). Induction of pluripotent stem cells from adult human fibroblasts by defined factors. *Cell* 131, 861–872. doi: 10.1016/j.cell.2007.11.019

Takahashi, K., and Yamanaka, S. (2006). Induction of pluripotent stem cells from mouse embryonic and adult fibroblast cultures by defined factors. *Cell* 126, 663–676. doi: 10.1016/j.cell.2006.07.024

Tam, P. P., and Behringer, R. R. (1997). Mouse gastrulation: the formation of a mammalian body plan. *Mech. Dev.* 68, 3–25. doi: 10.1016/s0925-4773(97)00123-8

Tapia, N., Reinhardt, P., Duemmler, A., Wu, G., Arauzo-Bravo, M. J., Esch, D., et al. (2012). Reprogramming to pluripotency is an ancient trait of vertebrate Oct4 and Pou2 proteins. *Nat. Commun.* 3:1279. doi: 10.1038/ncomms2229

Theunissen, T. W., Costa, Y., Radzisheuskaya, A., van Oosten, A. L., Lavial, F., Pain, B., et al. (2011). Reprogramming capacity of Nanog is functionally conserved in vertebrates and resides in a unique homeodomain. *Development* 138, 4853–4865. doi: 10.1242/dev.068775

Velychko, S., Kang, K., Kim, S. M., Kwak, T. H., Kim, K. P., and Park, C. (2020). Fusion of reprogramming factors alters the trajectory of somatic lineage conversion. *Cell Rep.* 27, 30–39. doi: 10.1016/j.celrep.2019.03.023

Zhong, L., Wang, D., Xiaoni Gan, X., Yang, T., and He, S. (2011). Parallel expansions of Sox transcription factor group B predating the diversifications of the arthropods and jawed vertebrates. *PLoS One* 6:e16570. doi: 10.1371/journal.pone.0016570

Conflict of Interest: The authors declare that the research was conducted in the absence of any commercial or financial relationships that could be construed as a potential conflict of interest.

Publisher's Note: All claims expressed in this article are solely those of the authors and do not necessarily represent those of their affiliated organizations, or those of the publisher, the editors and the reviewers. Any product that may be evaluated in this article, or claim that may be made by its manufacturer, is not guaranteed or endorsed by the publisher.

frontiers in Ecology and Evolution

ORIGINAL RESEARCH
published: 26 January 2022
doi: 10.3389/fevo.2021.783984

Single-Cell RNA Sequencing Atlas From a Bivalve Larva Enhances Classical Cell Lineage Studies

David A. Salamanca-Díaz[1†], Stephan M. Schulreich[1†], Alison G. Cole[2†] and Andreas Wanninger[1†]*

[1] Unit for Integrative Zoology, Department of Evolutionary Biology, University of Vienna, Vienna, Austria, [2] Division of Molecular Evolution and Development, Department of Neuroscience and Developmental Biology, University of Vienna, Vienna, Austria

Ciliated trochophore-type larvae are widespread among protostome animals with spiral cleavage. The respective phyla are often united into the superclade Spiralia or Lophotrochozoa that includes, for example, mollusks, annelids, and platyhelminths. Mollusks (bivalves, gastropods, cephalopods, polyplacophorans, and their kin) in particular are known for their morphological innovations and lineage-specific plasticity of homologous characters (e.g., radula, shell, foot, neuromuscular systems), raising questions concerning the cell types and the molecular toolkit that underlie this variation. Here, we report on the gene expression profile of individual cells of the trochophore larva of the invasive freshwater bivalve *Dreissena rostriformis* as inferred from single cell RNA sequencing. We generated transcriptomes of 632 individual cells and identified seven transcriptionally distinct cell populations. Developmental trajectory analyses identify cell populations that, for example, share an ectodermal origin such as the nervous system, the shell field, and the prototroch. To annotate these cell populations, we examined ontology terms from the gene sets that characterize each individual cluster. These were compared to gene expression data previously reported from other lophotrochozoans. Genes expected to be specific to certain tissues, such as *Hox1* (in the shell field), *Caveolin* (in prototrochal cells), or *FoxJ* (in other cillia-bearing cells) provide evidence that the recovered cell populations contribute to various distinct tissues and organs known from morphological studies. This dataset provides the first molecular atlas of gene expression underlying bivalve organogenesis and generates an important framework for future comparative studies into cell and tissue type development in Mollusca and Metazoa as a whole.

Keywords: Bivalvia, development, *Dreissena*, evo-devo, trochophore, evolution, cell type

OPEN ACCESS

Edited by:
Maria Ina Arnone, Stazione Zoologica Anton Dohrn, Italy

Reviewed by:
Jose Maria Martin-Duran, Queen Mary University of London, United Kingdom
Nathan Kenny, University of Otago, New Zealand

***Correspondence:**
Andreas Wanninger
andreas.wanninger@univie.ac.at

***ORCID:**
David A. Salamanca-Díaz
orcid.org/0000-0003-2082-3939
Stephan M. Schulreich
orcid.org/0000-0002-5309-0228
Alison G. Cole
orcid.org/0000-0002-7515-7489
Andreas Wanninger
orcid.org/0000-0002-3266-5838

Specialty section:
This article was submitted to Evolutionary Developmental Biology, a section of the journal Frontiers in Ecology and Evolution

Received: *27 September 2021*
Accepted: *16 December 2021*
Published: *26 January 2022*

Citation:
Salamanca-Díaz DA, Schulreich SM, Cole AG and Wanninger A (2022) Single-Cell RNA Sequencing Atlas From a Bivalve Larva Enhances Classical Cell Lineage Studies. Front. Ecol. Evol. 9:783984. doi: 10.3389/fevo.2021.783984

INTRODUCTION

The organization and diversity of cell types constitute key features during the ontogenetic establishment of animal body plans. Distinct transcriptional profiles of cell populations are an important prerequisite for the formation of cell types, and, ultimately, tissues, of multicellular animals (Shapiro et al., 2013; Stegle et al., 2015; Arendt et al., 2016). Accordingly, deciphering the transcriptomic code underlying the ontogeny of these cell types is crucial for sound inferences of the shared evolutionary history of cells and tissues across the animal kingdom. Among the multicellular animals, adult mollusks exhibit a particularly high morphological diversity that has resulted in a number of autapomorphic characters on various phylogenetic levels

[e.g., radula, shell(s), foot, neuromuscular systems] (Smith et al., 2011; Wanninger and Wollesen, 2019). However, despite their unique innovations in the adult body plan, numerous mollusks display a conserved, ciliated, trochophore-type larva that is also found in other lophotrochozoans including annelids and platyhelminths (Nielsen, 2018). The molecular pathways underlying the morphological diversification from this common larval type into clade-specific features remains largely unresolved.

Traditional studies have focused on the ontogeny of different tissues by tracing the mitotic history of a cell and generating so-called fate maps, resulting in the reconstruction of so-called cell lineages (Lillie, 1895; Meisenheimer, 1900; Luetjens and Dorresteijn, 1995; Dictus and Damen, 1997; Render, 1997; Henry et al., 2004; Hejnol et al., 2007; Lyons et al., 2017; Farrell et al., 2018). While cell lineages for certain putative homologous structures (e.g., the prototroch) have been identified, striking differences in mitotic history details are evident even between closely related taxa, particularly within Mollusca (Wanninger and Wollesen, 2015). Moreover, some lineage diagrams do not assign fates to all terminal ends of the cell lineage tree, hindering broad comparisons across taxa (Meisenheimer, 1900; Luetjens and Dorresteijn, 1995). For more detailed insights into differences and shared features on the ontogeny of tissues and organ systems, gene expression analyses using *in situ* hybridization has been widely used on a variety of molluscan taxa (e.g., Hinman et al., 2003; Lee et al., 2003; Wollesen et al., 2015a,b, 2018; Redl et al., 2016; Wang et al., 2017; Salamanca-Díaz et al., 2021). These studies represent a framework for comparative analyses of genes underlying the formation of features such as the shell field, nervous system, foot, sensory structures, and others (Wanninger and Wollesen, 2019). However, this approach is hampered by the fact that only a fraction of genes are known to be active in certain regions and developmental stages of the respective target species. Novel approaches of sequencing live, dissociated cells (single-cell RNA sequencing, scRNA-seq) followed by *in silico* methods using fine-grained computational pipelines have allowed for characterization of transcriptomic profiles related to cell types and cell states based on their distinct, relative gene expression levels. Such studies have resulted in comprehensive lists of genes that are expressed during ontogeny (Tang et al., 2010; Trapnell et al., 2014; Achim et al., 2015; Satija et al., 2015; Trapnell, 2015; Vergara et al., 2017; Svensson et al., 2018; Zhong et al., 2018). Accordingly, recent studies have uncovered the presence of previously uncharacterized cell types and an unexpected transcriptomic heterogeneity amongst cell populations and have revealed numerous genes with hitherto unknown function (Karaiskos et al., 2017; Achim et al., 2018; Briggs et al., 2018; Farrell et al., 2018; Fincher et al., 2018; Plass et al., 2018; Sebé-Pedrós et al., 2018; Wagner et al., 2018; Foster et al., 2019, 2020; Siebert et al., 2019; Duruz et al., 2020; Wendt et al., 2020; García-Castro et al., 2021; Paganos et al., 2021; Sur and Meyer, 2021).

The quagga mussel *Dreissena rostriformis*, native to the Dnieper drainage of the Ukrainian Black Sea region (Nalepa and Schloesser, 2019), has managed to rapidly spread across European and North American freshwater bodies (Mills et al., 1993; Heiler et al., 2013; Aldridge et al., 2014; Karatayev et al., 2014; Wakida-Kusunoki et al., 2015; Nalepa and Schloesser, 2019). Together with its congener, the zebra mussel *Dreissena polymorpha*, they build dense populations which consume large amounts of phytoplankton with often damaging impact on native invertebrate and fish populations (Raikow, 2004; Strayer et al., 2004; McNickle et al., 2006; Karatayev et al., 2014; Nalepa and Schloesser, 2019). This makes the quagga and zebra mussel one of the most prevalent and successful invasive mollusks (Karatayev et al., 2007). Efforts to understand and manipulate the rate of colonization and dispersal for these species have mainly focused on the adult stage when the population is already established, while data on the dispersive larval stages, the trochophore and the veliger, are still lacking (McCartney et al., 2019).

Here, we present the first comprehensive scRNA-seq study on the trochophore larva of any mollusk, the quagga mussel *Dreissena rostriformis*. We generated a scRNA-seq library from dissociated cells of entire larvae. Using this dataset, we define distinct cell types present in this larval type. We assign identities to identified cell populations based on characterization of distinct transcriptomic signatures and predict relationships between cell types by modeling developmental trajectories within the dataset. We analyze ciliary, neuronal, muscle, and other cell types with potential importance to environment sensing and larval spreading. Through this work, we also provide a comprehensive molecular atlas of gene expression underlying *Dreissena rostriformis* development, thereby laying the foundation for further research into understanding the features that allow quagga mussel larvae to rapidly conquer new freshwater habitats.

MATERIALS AND METHODS

Animal Collection and Cultures

Sexually mature individuals of *Dreissena rostriformis* were collected in the Danube River in Vienna, Austria (N 48°14′45.812″, O 16°23′38.145″) between April and September, 2019. Adults were gathered from underneath stones and transferred to the laboratory where they were cleaned and maintained in aquaria with filtered river water (FRW) at 19°C.

Spawning of animals was induced by exposing sexually mature specimens for 15 min to a 10^{-3} M solution of serotonin (#H9523, Sigma-Aldrich, Darmstadt, Germany), followed by one wash and subsequent maintenance in FRW. Individuals were kept isolated in FRW inside 50 mL glass beakers and after approximately 30 min, up to 50% of the treated specimens started to spawn. Oocytes and motile sperm were then collected separately from the water column. Fertilization rates were high when three to four drops of sperm-containing water were added to 50 ml glass beakers with oocytes. The cultures were maintained at 23°C. After fertilization, water was changed every half an hour for the first 3 h and then every 6 h to remove excess sperm and avoid bacterial or fungal infection.

10X Single-Cell 3′ RNA-Seq

Sample Preparation

Cell dissociations of *Dreissena* larvae were generated by first washing 13 h post fertilization (hpf) trochophore larvae over a 20 μm mesh with sterile autoclaved fresh river water (AFRW).

Larvae were concentrated into 1.5 mL tubes by centrifugation (1rcf) for 5 min and AFRW was replaced with a pronase enzyme in AFRW (8 mg/mL) (#10165921001, Roche Diagnostics, Mannheim, Germany) and the tubes were subsequently placed in gentle agitation for 30 min on a rocker at the slowest setting in order to keep the cells and reagents in suspension. Larvae were dissociated by first passing them through a syringe with a hypodermic needle with 0.4 mm diameter. This procedure was repeated and monitored until a uniform single cell solution was visible under the microscope. Cell viability was assessed by adding an acridine orange/propidium iodide (AO/PI) staining solution (#CS2-0106; Nexcelom Bioscience, Lawrence, MA, United States) to stain live and dead cells, respectively (Cellometer K2; Nexcelom Bioscience). A single cell suspension measuring 76.8% viability with a concentration of 1000 cells/μL was loaded into a 10x Chromium Controller using Chromium Single Cell 3′ Kit v2 reagents (#120237, 10x Genomics, United States). cDNA synthesis and library construction were made according to specifications from the manufacturer. Library quantification was performed on a Bioanalyzer (#5067-4626, High Sensitivity DNA reagents, Agilent Technology; Agilent 2100 Bioanalyzer) and sequenced on the Illumina platform.

Mapping Tool Preparation and Cell Clustering

The transcriptomes used for creating the mapping tool, together with the reference genome to map the reads against, were previously generated (Calcino et al., 2019). Gene models were elongated 2 kilobases in the 3′direction to account for poorly annotated three-prime ends (Levin et al., 2016). To annotate the transcriptome, we performed a BLASTX search in each individual gene sequence against the human and the Pacific giant oyster (*Crassostrea gigas*) genomes. For each transcript, the BLAST hit with the highest *E*-value was selected for annotation. We utilized InterProScan v5.46-81.0 (Jones et al., 2014) to search for gene ontology and allocate domains on the reference genome by surveying publicly available databases such as GO terms, Pfam, and PANTHER (**Supplementary Table 1**). The reference database was generated using CellRanger MakeRef v3.1.0 with default settings. Afterward, sample libraries were demultiplexed using CellRanger Makefastq v3.1.0 with default settings and filtered according to cell barcode and Unique Molecular Markers (UMIs) using CellRanger Count v3.1.0 with parameters of –force-cells = 1000 –chemistry = SC3Pv2. The resulting cell count gene expression matrix was analyzed in R v3.6.1 (R Developement Core Team, 2015) with the Seurat v4.0.1 package (Satija et al., 2015). Samples were considered to represent a single cell transcriptome if it contained at least 150 genes. Samples with more than 4,000 sequenced genes were removed as these represent multiplets. The count matrix was processed through a standard Seurat pipeline using default parameters as follows: counts were first normalized, and log scaled (NormalizeData and ScaleData functions) and principal component analysis was performed (RunPCA) using only highly variable features (FindVariableFeatures). We visually inspected an elbow plot of standard deviation of the principal components (**Supplementary Figure 1**) and selected the top 30 principal components for clustering. We then generated a KNN graph based on the Euclidean distance in PCA space following the Louvain algorithm [FindNeighbors (k.param = 10, nn.method = "annoy," annoy.metric = "cosine")] and clustered the data [FindClusters (random.seed = 0, res = 0.5)]. For data visualization, we projected all single cell transcriptomes into a uniform space of 2 dimensions [Uniform Manifold Approximation and Projection (UMAP): RunUMAP (n.neighbors = 10 L, spread = 0.45, min.dist = 0.1, local.connectivity = 100)]. Marker genes were identified with the FindAllMarkers function (random.seed = 0), which considers only genes that were enriched and expressed in at least 10% of the cells in each population (min.pct = 0.1) and with a log fold difference larger than 0.6 (logfc.threshold = 0.6). Later, a filter was performed for the top 10 genes with the higher average logarithmic fold change values (**Supplementary Tables 2, 3**). Additional cutoff thresholds were explored and the whole pipeline was applied to observe how they affect the remaining cells in the dataset (**Supplementary Figure 2** and **Supplementary Table 5**). We applied a graph imputation algorithm with the R package MAGIC (van Dijk et al., 2018) on single cells for de-noising the count matrix and fill in missing transcripts. The R package topGO (Alexa et al., 2006) was implemented to perform a GO terms enrichment analysis on genes from each cluster, determining statistically the molecular activity of a gene (molecular function), the place in the cell where the gene produces an effect (cellular component), and the physiological process influenced by a gene (biological process). Following this, expression of orthologous marker genes from distinct cell types were examined in this dataset to validate cluster identification assigned by GO term results.

Pseudotime Trajectory Analysis

In order to root the pseudotime trajectories in a single place and to calculate the number of transcriptomic changes of each population, we implemented the R package StemID to predict developmentally uncommitted cell populations from maximum transcriptome entropy calculations (Grün et al., 2016). This one cell population, which clustered together based upon the lack of differentially expressed genes compared with the other clusters in the dataset, also received the lowest entropy calculation. This suggests that these cells represent a pool of uncommitted cells within the embryo (Hemmrich et al., 2012; Fincher et al., 2018; Siebert et al., 2019). Cells were ordered along a calculated similarity trajectory with this population defined as the starting point using the Monocle3 R package (Cao et al., 2019), imported from Seurat with the package SeuratWrappers v0.3. Cells were re-clustered using the "cluster_cells" function (resolution = 0.02). The "learn_graph" function was implemented to model the cell differentiation paths throughout development. This principal graph was used to order cells in pseudotime using the "orderCells" function with undifferentiated cells defined as the root. Monocle interprets multiple ends to a trajectory as cellular decisions.

Gene Cloning

A first-strand cDNA Synthesis Kit for RT-PCR (#11483188001, Roche Diagnostics, Mannheim, Germany) was used for cDNA

synthesis from the pooled RNA. PCR products were size fractioned by gel electrophoresis and purified with a QIAquick Gel Extraction Kit (#28706, Qiagen, Hilden, Germany). PCR products were cloned in pGEM-T Easy Vectors (#A1380, Promega, Mannheim, Germany). Plasmid minipreps were grown overnight, purified with a QIAprep Spin Miniprep Kit (#27106, Qiagen), and sequenced for verification. Forward and reverse primers for each gene sequence can be found in **Supplementary Table 4**.

Probe Synthesis and Whole Mount *in situ* Hybridization

To provide spatial information associated with the transcriptomic signatures and further validate cell type annotations, whole mount *in situ* hybridization analysis of some of the highly expressed cell population-specific genes were performed on trochophore larvae aged 13–15 hpf. Plasmid products were linearized by PCR amplification using M13 primers as described previously (Wollesen et al., 2015b). Antisense riboprobes were synthesized using digoxigenin-UTP (#11175025910, DIG RNA Labeling Kit, Roche Diagnostics) and SP6/ T7 polymerase (#10810274001, #1088176001, Roche Diagnostics).

Larvae were fixed for 1 h in 4% paraformaldehyde (PFA) (20% PFA + 10x PBS; DEPC- treated H_2O), followed by three washes of 15 min each in Phosphate Buffer Solution (PBS). For long-term storage of samples, subsequent washing steps for at least 15 min each were performed in different concentrations of methanol (25, 50, and 75%) in 1x PBS. For whole mount *in situ* hybridization, larvae stored in 100% methanol were rehydrated in 0.1 M PBS and decalcified with PPE (20% PFA + 10x PBS + 0.5 M EGTA at pH 8.0 + diethyl pyrocarbonate; DEPC-treated H_2O). Afterward, samples were treated with proteinase-K at 37°C for 10 min (10 μg/mL in PTw: 1x PBS + 0.1% Tween-20). Samples were washed in PTw and post-fixed for 45 min in 4% PFA. Subsequently, samples were washed and transferred to hybridization buffer (50% formamide, 5X SSC, 50 μg/ml heparin, 500 μg/ml yeast tRNA, 0.1% Tween-20, pH 6.0) for 8–10 h at 56–60°C. Probe hybridization was performed at the same temperature with probe concentrations ranging between 1 and 2 ng/μL for 30–48 h. Washing steps after hybridization were done using the following solutions: 75% hybridization buffer + 25% of SSC (3 M NaCl + 0.3 M saline-sodium citrate; SSC buffer + DEPC H_2O) for three times 10 min each, then 50% hybridization buffer + 50% SSC twice for 10 min each, 25% hybridization buffer + 75% SSC for 7 min (once) and 1X SSC + 0.1% Tween-20 for three times for 5 min each. Next, three washes in 0.1 M maleic acid buffer (MAB) were performed. A digoxigenin (DIG)-labeled alkaline phosphatase (AP) antibody (#11093274910, Roche Diagnostics) was used at a dilution of 1:5000 in blocking solution (#11096176001, 10x blocking reagent; Roche Diagnostics + 0.1 M MAB) at 4°C overnight. Samples were then washed in PTw three times for 20 min each and twice for 10 min each. Development of the color reaction was done in a NBT/BCIP solution (#11383213001, #11383221001, Roche Diagnostics) diluted in 1x alkaline phosphatase buffer (0.5 M NaCl + 0.5 M Tris at pH 9.5 + 50 mM $MgCl_2$ + 0.1% Tween-20 + DEPC H_2O) at 4°C with constant buffer replacement until signal was detected. Color reactions were stopped by washing five times for 10 min each with PTw.

Immunocytochemistry

Trochophore larvae (13 hpf) were fixed in 4% PFA for 1 h, then washed and stored at 4°C in 1x PBS with 0.1% sodium azide added. Afterward, samples were permeabilized by three washing steps of 15 min in 1x PBS + 0.2% Triton X-100 + 0.1% NaN_3 (PTA). Blocking was performed in PTA + 6% normal goat serum (NGS) overnight at 4°C. Primary antibody incubation was performed over night at 4°C with anti-acetylated α-tubulin (raised in mouse, monoclonal, #T6793, Sigma-Aldrich) at a concentration of 1:400 diluted in PTA + 6% NGS. Two washes with PTA of 15 min each followed. For the secondary antibody, goat anti-mouse Alexa 568 (#A-11004, Thermo Fisher Scientific, Waltham, MA, United States) was added and the samples were incubated overnight at 4°C. This was followed by two washes with PBS for 15 min each. After that, a mix of CellMask Green Stain (#H32714, Invitrogen, Carlsbad, CA, United States; 1:100) and DAPI (#D1306, Sigma-Aldrich, 1:2000) in PBS was added for 1 h. Then, the samples were washed thrice with PBS for 15 min each and mounted on glass slides with Fluoromount-G (#0100-01, SouthernBiotech, Birmingham, AL, United States) and stored at 4°C for a few days prior to image collection.

Image Collection and Figure Processing

Trochophore larvae (13 hpf) used for *in situ* hybridization were mounted in 100% glycerol and documented with an Olympus BX53 Microscope (Olympus, Hamburg, Germany). Immunofluorescent antibody preparations were scanned with a Leica TCS SP5 II confocal microscope (Leica Microsystems GmbH, Wetzlar, Germany). FIJI (Schindelin et al., 2012) was used for image analysis and further processing to estimate cell number in a larva through nuclei counting, employing the 3D Object Counter v2 with a threshold of 75. All figures, light micrographs, and graphical representations were prepared, compiled, and adjusted for contrast and brightness using Inkscape version 0.92.4-4 (Inkscape Project, 2020).

RESULTS

De novo Cell Cluster Annotation and Marker Gene Identification in a Bivalve Trochophore Larva

Based on nuclei counts from immunostainings, we estimated that the trochophore larva of the quagga mussel *Dreissena rostriformis* is composed of approximately 110 cells. Therefore, we aimed to sequence ∼1000 cells with the 10x Genomics platform. In total we sequenced 41325580 reads and 84.9% of these reads mapped to the reference genome, i.e., the remaining percentage could not be mapped to either exonic, intronic, intergenic regions or antisense genes. After filtering out cells with less than 150 molecules and with more than 4000 sequenced molecules, a total of 632

cells were captured, corresponding to around five individuals (**Figures 1A,B**). The number of genes detected in a cell (nFeatures) have a median of 1054.5 and a mean of 1141.8, while the number of molecules detected within a cell (nCount) have a median of 3253 and a mean value of 4172.8. After processing the cell count matrix with the Seurat pipeline, the heterogeneity of cell states in the trochophore larvae was assessed. Graph-based clustering revealed seven transcriptionally distinct cell populations (**Figures 2A–G**). Analysis of the genes underlying this clustering, as described below, identified cell populations corresponding to "ciliary/prototroch," "neuronal," "endoderm," "muscle," "epidermal," "shell field," and "undifferentiated" identities (**Figures 3A, 4A**).

Transcriptional Domains Confirm Cell Type Identity in the Larva

Ciliary cells in *Dreissena* start to develop early in the gastrula stage. GO terms analysis revealed one cluster of cells with a statistically significant enrichment in genes involved in processes related to cilia assembly, movement and cell motility, and microtubule-based processes (**Figures 2A–A″**), thus identifying a "ciliary/prototroch" cell population within the dataset. Moreover, further sub-structure within this group is exhibited when the clustering resolution parameter is increased (**Supplementary Figures 1I–K** and **Supplementary Table 3**). In the larva, there are several subtypes of ciliated cells such as prototroch, telotroch, and apical tuft cells (Meisenheimer, 1900; Pavlicek et al., 2018). The structure seen in this cluster could reflect the different subtypes of ciliary cells in the live animal.

Cells identified as "neuronal" present highly expressed genes where there is an enrichment of neurogenesis-related processes such as neuropeptide signaling pathway, proton transmembrane transport (iron ion transport), and acetylcholine receptor regulator activity (**Figures 2B–B″** and **Supplementary Tables 1, 2**). When increasing the resolution for finding clusters, results revealed subclusters within this population (**Supplementary Figures 1I–K** and **Supplementary Tables 2, 3**). Even though the two resulting subclusters have equal enrichment for neuronal processes, they have differential expression of markers setting them apart from each other (**Supplementary Tables 2, 3**). For example, while the red subcluster has predominant expression of *FMRFamide receptor,* the turquoise one on the right presents high expression of *neuronal acetylcholine receptor subunit alpha-6* (**Supplementary Figures 1I, 4C,D**). Annotations from transcriptomic signatures in the cluster "neuronal" indicate that neuropeptides are secreted from these cells. Accordingly, in-depth analysis of gene expression signatures of this cluster appears particularly promising for characterizing the gene regulatory networks responsible for the differentiation of neuronal cells.

The cluster "endoderm" shows all related cells share gene annotations from human and *Crassostrea* orthologs related to enzymatic reactions that are likely to occur in the developing digestive system, e.g., *arginase-1* (Gene.72022), *cathepsin K preproprotein* (Gene.17238), *neutral cholesterol ester hydrolase-1* (Gene.4751) (Kirschke et al., 1995; Duruz et al., 2020), but also included immune response-related genes, e.g., *galectin-8* (Gene.117090) (Vasta et al., 2015). Moreover, GO terms for processes related to ribosome biogenesis, RNA processing, translation, and ATP synthesis-coupled proton transport show enrichment in this cluster (**Figures 2C–C″**). Since all these activities are crucial for cell survival, one could assume the enriched processes are crucial for all cell states at this stage and some of the genes are expressed in other clusters. However, the annotations from the top differentially expressed genes identified in this cluster suggest that these cells are involved in endoderm development and immune responses (**Supplementary Figure 4**). Altogether, cells in this cluster are highly likely to have endodermal fates in the quagga mussel larva.

Bivalves have two predominant adductor muscles of which the anterior adductor and some larval retractor systems already start to form in the trochophore larva (unpublished observation). We identified cells with muscle identity in our dataset on the "muscle" cluster where there is gene ontology enrichment with processes associated with muscle system formation such as calcium ion binding, actin filament depolymerization, and protein peptidyl-prolyl isomerization (protein folding) (**Figures 2D–D″** and **Supplementary Table 1**). In addition, the commonly expressed marker during animal myogenesis, *myosin heavy chain (mhc*; Castellani and Cohen, 1987; Ladurner and Rieger, 2000; Dyachuk and Odintsova, 2009; Li et al., 2019), is expressed in this cluster. In the *Dreissena* trochophore, transcripts of *mhc* are found in the anterior mesoderm. They form spot-like expression domains in the anterior region between the developing digestive tract and the shell field (**Figures 3B–B″,E**). Hence, *in silico* annotations and *in situ* hybridization data support the identity of muscle cells for this cluster.

Cells with an "epidermal" identity formed a cluster with GO terms enrichment in processes that play a role as integral components of the membrane, such as epidermis morphogenesis and homophilic cell adhesion via plasma membrane (**Figures 2E–E″** and **Supplementary Table 1**). To visualize these cells in the larva, *in situ* hybridization of one of the top marker genes was performed. The gene *teashirt* (*tsh*) has an expression domain in cell populations adjacent to the anterior and posterior margins of the cells forming the shell gland (**Figures 3D–D″,G**). This gene expression domain and GO term annotations suggest that this cluster contributes to the formation of various types of epithelia and epidermal tissue in the trochophore larva of *Dreissena*.

Dreissena trochophores exhibit a developing shell field which grows and envelops the visceral region in later stages. We identified cells belonging to the cluster "shell field," which express several genes with unknown ontology term or ortholog match. Cells belonging to this cluster express numerous short-numbered-kilobases genes, which match hitherto uncharacterized molluscan genes (**Supplementary Table 1**). Nevertheless, the few GO terms collected show enrichment in processes that interact with the extracellular matrix, such as integrin-mediated signaling pathway and positive regulation of cell cycle G2/M phase progress (**Figures 2F–F″**

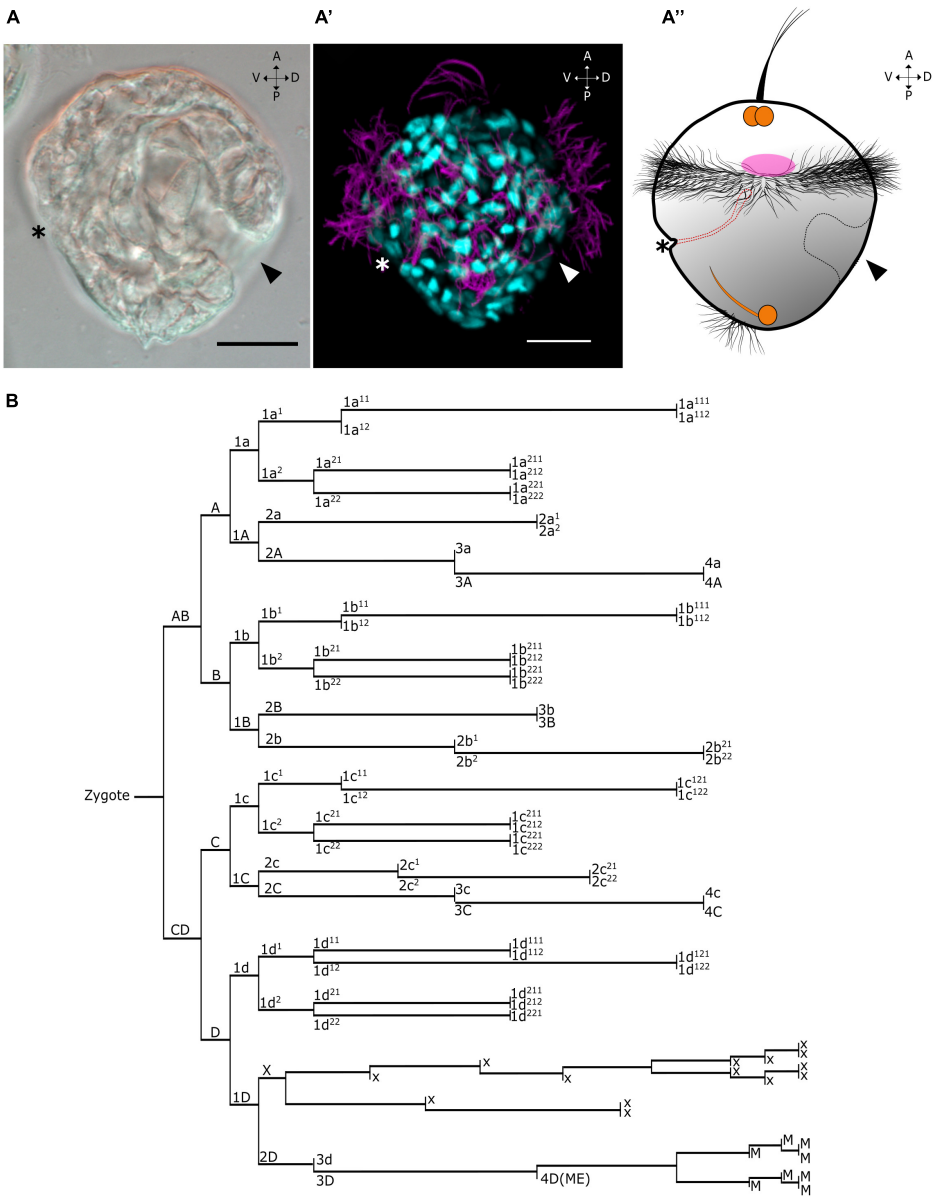

FIGURE 1 | Single-cell transcriptomics of *Dreissena rostriformis* larvae. Age of larvae is 13 hpf. **(A–A")** Lateral view of differential interference contrast (left), alpha-acetylated tubulin/ DAPI immunostained trochophores (center), and scheme illustrating the overall morphology of the trochophore larva (right). Asterisk on the larvae indicates the mouth opening. Arrowhead points to the shell field on the right side. Orange marked areas denote the developing nervous system based on data from Pavlicek et al. (2018). Pink marked area denotes the developing muscular system. Dotted black lines highlight shell field cells. Dotted red lines highlight the developing digestive system. Anterior (A), posterior (P), ventral (V), and dorsal (D). Scale bars equal 20 μm. **(B)** Cell lineage tree of *Dreissena* modified from Meisenheimer (1900) and Luetjens and Dorresteijn (1995).

and **Supplementary Table 1**). From the set of highly expressed genes forming the transcriptomic signature in this cluster, *hic31* was chosen to visualize the cluster in the *Dreissena* larva because it was previously shown to be involved in establishing the protein matrix prior to shell secretion (Liu et al., 2015, 2018). In *Dreissena* trochophores, *hic31* expression is present around the margin of the shell field (**Figures 3C–C″,F**). Thus, gene annotations and *in situ* hybridization data support the identity of shell field cells for this cluster.

We identified one cluster devoid of a unique transcriptional signature (**Figure 2G**). These cells were considered "undifferentiated" because their GO term annotations showed that they have significant levels of regulation of DNA replication, protein synthesis, and translational initiation in the *Dreissena* trochophore (**Figures 2G–G″**). The predominant expression of such "housekeeping genes" as well as the shared expression signatures of these genes with all clusters, in combination with a lack of distinct expression of marker genes

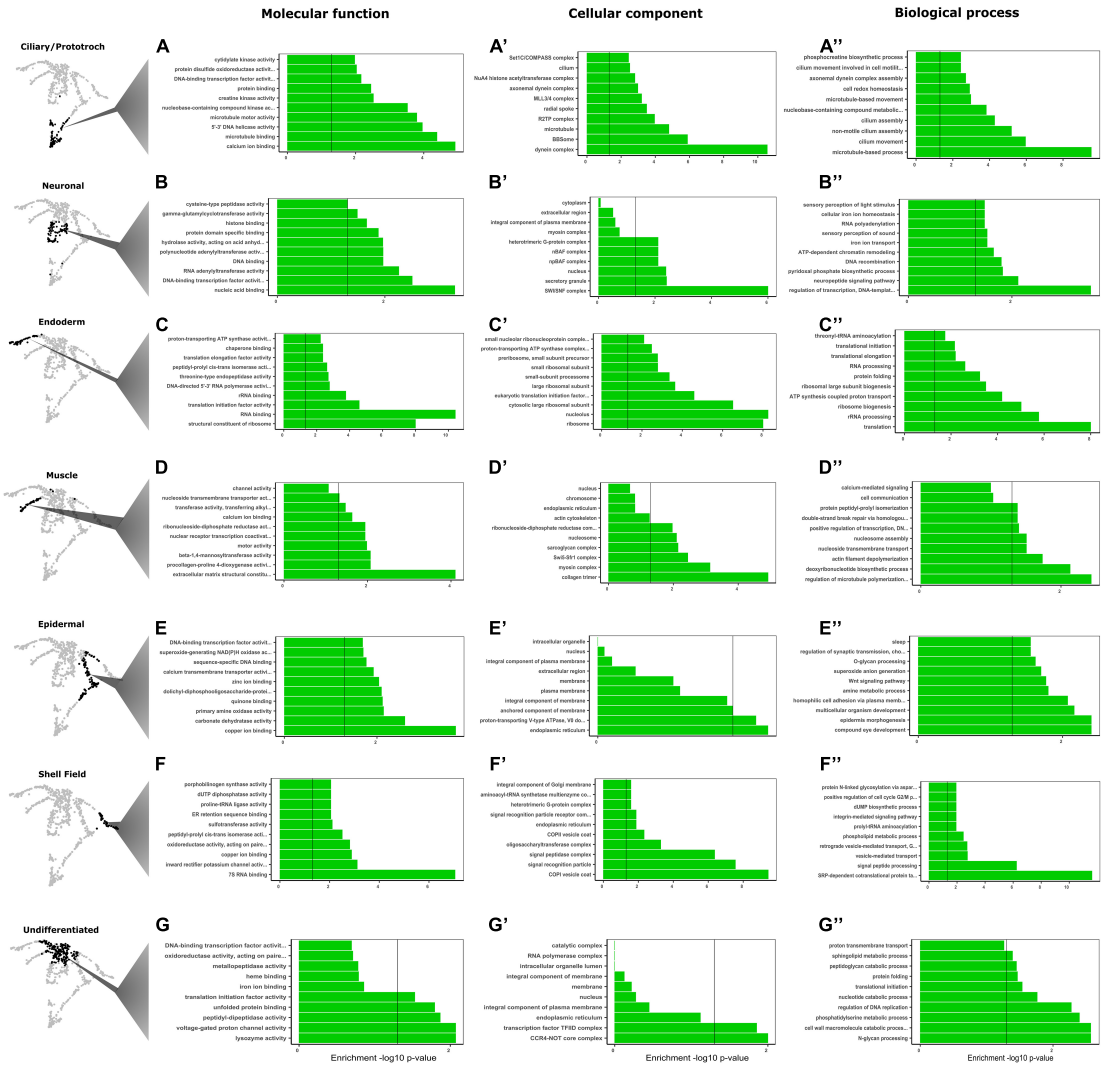

FIGURE 2 | Gene ontology (GO) analyses leads to identification and validation of clusters of differentially expressed genes. **(A–G")** GO terms associated with molecular function, cellular component, and biological processes. Classification of the corresponding GO terms form each highlighted cluster on the left side of the panel. Each row represents a cluster with significant transcriptomic signature and each column shows the categories of enrichment by molecular function, cellular component, and biological processes. Vertical black line (*p*-value = 0.05) in each graph represents statistical significance threshold set after performing a Fisher's exact test.

(**Supplementary Figure 4** and **Supplementary Tables 1–3**), is a typical feature of animal cells that have not yet undergone differentiation into developmental fates and is often observed in whole-organism single cell RNA-seq datasets (Hemmrich et al., 2012; Fincher et al., 2018; Siebert et al., 2019; Duruz et al., 2020). This cluster is composed of cells with low gene counts (151–1332), suggesting that these cells lack sufficient information to robustly cluster with similar cell populations and thus could represent a clustering artifact. In this case, this cell population would be expected to disappear with more stringent filtering (min. 500 detected genes), allowing for more robust clustering of the remaining cell populations. However, removing these low information cells does not improve clustering but rather shifts the cluster boundary, resulting in a cluster of cells with less information (**Supplementary Data 2**). Although this may represent a technical artifact, it could also be interpreted as a real biological signal at this stage of development wherein many of the embryonic cells are in a permissive cell state prior to activating cell differentiation pathways. In addition, results from StemID, an algorithm for predicting multipotent cell identities (Grün, 2020), suggest a statistically supported link of all clusters to these cells in the trochophore stage and indicate there is a starting point for differentiation trajectories in this cluster (**Supplementary Figure 3**). Altogether, *in silico* analyses support the notion that this cluster is composed of cells which have not yet developed a unique transcriptomic signature and thus the identified developmental trajectories are differentiated from this cluster.

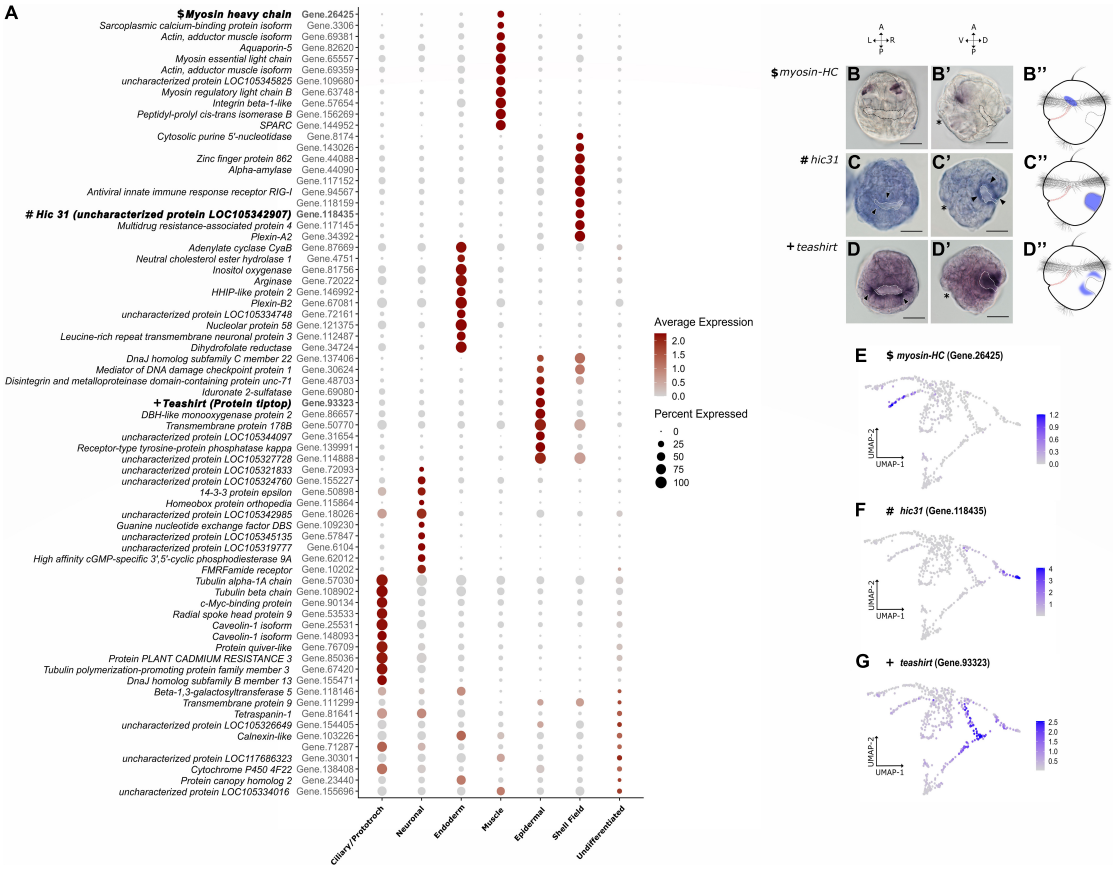

FIGURE 3 | Mapping cell state markers on the trochophore larva. **(A)** Top 10 highly expressed genes per cluster. On the left side of each gene is the putative ortholog match from *Crassostrea gigas*. Color intensity represents the average gene expression while circle size is the percentage of cells expressing a certain gene. In bold are the IDs of the genes used for cluster validation through *in situ* hybridization in **(B–D)**. **(B–D")** Expression domains of randomly sampled marker genes from a dorsal **(B–D)** and a lateral point of view **(B'–D')**. **(B–B")** *Mhc* expression located in cells from the anterior region between the developing digestive tract and the shell field. Dotted lines highlight the secreted shell field. **(C–C")** *Hic31* expression located in cells belonging to the outer margin of the shell field (arrowheads). **(D–D")** *Tsh* expression is found in the epidermal cells limiting the outline of the shell field. Asterisk indicates the mouth opening on the left side. Anterior (A), posterior (P), ventral (V), dorsal (D), left (L), and right (R). Scale bars are 20 μm. **(E–G)** Feature plots of each respective gene used for *in situ* hybridization and after running the gene imputation algorithm with MAGIC.

Pseudotime Trajectories Infer Relationships Between Cell Populations

We aimed to identify trajectories and reconstruct lineages from the cell clusters of *Dreissena rostriformis* trochophore larvae. While running the Monocle3 algorithm without any assumptions *a priori*, eight major trajectory ends could be recovered to model a differentiation tree with all cell populations and relate them to one single root, the "undifferentiated" cluster (**Figure 4B**). Two trajectory ends correspond to the clusters enriched with processes related to muscle development, endoderm development, and ribosomal activity (**Figures 2C–D′**, **3B**). "Muscle" and "endoderm" originate from a common cell lineage, the corresponding cell division can be observed on the node linking these two cell types (**Figure 4C**). The remaining trajectories show terminal ends in neuronal and ciliary clusters (**Figure 4B**). The presence of multiple differentiation pathways in these clusters supports further structure within the respective cell groups. There is one trajectory linking shell field and several epidermal cells (**Figure 4B**). This suggests a specification pathway that employs a subset of epithelial cells destined to contribute to the shell field. To assign putative terminal fates on the lineage tree of *Dreissena* and link them to our annotated clusters, we analyzed defined fate maps from other mollusks and made an estimation on the expected cell types per individual (**Figure 4C**). We then compared the number of expected clusters from the revised lineage tree of *Dreissena* to the actual number of cells obtained in our dataset (**Figure 4E**). Thereby, the "expected" cluster cells were counted from a developmental stage that was approximately one cell division cycle younger (67 cells) than that of the "outcome" cluster (110 cells). This was done to assess whether the same cell types described in classical cell lineage studies were also recovered by our single cell RNA-seq approach. While the proportions of expected versus outcome match well for the "neuronal," "ciliary," and "endoderm," the proportion of "shell field" and "muscle" cells show a higher proportion in the expected than in the

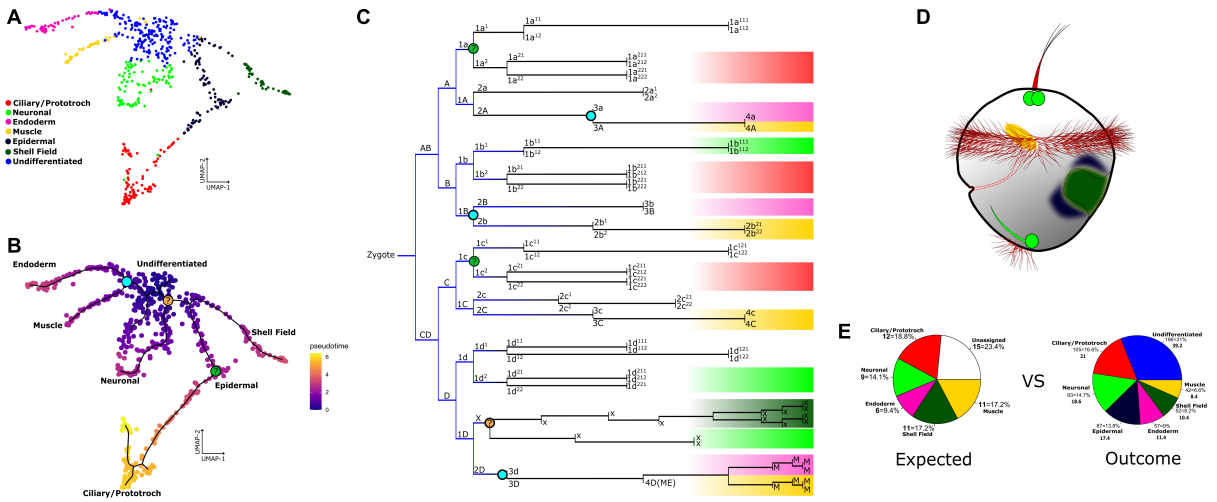

FIGURE 4 | Cell clusters mapped onto the *Dreissena* cell lineage tree and their location in the trochophore larva. **(A)** Resulting UMAP graph with cluster identification result of our annotation pipeline. Identified cell clusters are named and color-coded. **(B)** Calculated pseudotime showing recovered differentiation trajectories among extant clusters. Black lines represent the learned pseudotime trajectories. Colored nodes marked in the trajectory pathways and in the cell lineage tree represent the possible developmental decisions inferred from pseudotime and are drawn into the cell lineage map. The aquamarine node represents the developmental decision between endodermal and muscle cells. Light orange and light green represent the nodes that do not have a certain position on the fate map. **(C)** Cell lineage tree of *Dreissena* modified from Meisenheimer (1900) and Luetjens and Dorresteijn (1995). Highlighted are the putative terminal cell identities with the same color code from the UMAP projection. Blue gradient on the lines of early cell lineages represents the multipotency of the cells, which is lost in further cell divisions to acquire identity and could still be present in some lineages. Cell lineages not colored here mean the fate of these cell lineages was not identified in the fate map of *Dreissena*. **(D)** Putative location of clusters on the larva based on annotation methods described here. **(E)** Pie charts showing the percentage of cell types based on counts from cell lineage studies for one single larva (left, "expected") vs. the percentage of cell types based on counts of this study from five larvae (right, "outcome").

actual outcome analysis. This could be due to the annotation of previously unrecognized cell types on the lineage tree from *Dreissena* that might affect the cluster proportions of the "outcome" (**Figure 4E**). For example, concerning the shell field and epidermal cells, that both derive from the ectoderm, these might not yet have undergone fate specification in the analyzed developmental stage and thus might all fall in one category (here: shell field) in the "expected" analysis. The higher value for "muscle" cells in the "expected" chart relative to the "outcome" one might be because considerably fewer cells have undergone differentiation into muscle cells, a situation that is congruent with morphological analyses that showed a strikingly simple myoanatomy of *Dreissena* trochophores (Meisenheimer, 1900; Pavlicek et al., 2018, unpublished observations). Overall, the trajectories traced across the whole dataset position extant clusters uniformly along each respective path. This shows that developmental trajectories are well sampled in our dataset. In addition, it confirms that our cluster annotations recover the correct proportions of expected cell types from the lineage tree and that the pseudotime analysis is a good indicator of differentiation paths in the live larva.

DISCUSSION

Verification of Cluster Identity by Ortholog Comparison Across Metazoa

The trochophore larva of the quagga mussel is comprised of well-defined features such as a shell field, a ciliated prototroch, telotroch and apical tuft, a simply-built nervous system, and a developing digestive tract (Pavlicek et al., 2018; Salamanca-Díaz et al., 2021). Our single cell transcriptomic atlas of the *Dreissena* trochophore provides the first detailed analysis of the transcriptomic toolkit of a larval bivalve mollusk at single cell resolution, capturing cells corresponding to each of these morphological features (**Figures 4A,D**). Overall, our transcriptomic annotations in the quagga mussel *Dreissena rostriformis* confirm that key molecular factors expressed in all clusters are comparable to other species. As such, the cells identified as "ciliary/prototroch" are enriched in genes involved in ciliogenesis and cilia movement and the development of the dynein complex known to be a crucial part of locomotion in many metazoans (King, 2012). Ciliated cells found in the annelids *Platynereis dumerilii*, *Hydroides elegans*, and *Capitella teleta* similarly express orthologs of *Caveolin, Forkhead box J (foxJ)*, *rshp4*, *dynein heavy chain 9 (DNAH9)*, *tubulin polymerization-promoting family member 3*, and *tektin4* (**Supplementary Figure 4** and **Supplementary Tables 1–3**; Arenas-Mena et al., 2007; Achim et al., 2018; Sur and Meyer, 2021). Furthermore, genes expressed in ciliary cells of *Dreissena* are also present in motor cilia of more distantly related organisms such as the acoel *Isodiametra pulchra* (i.e., *Dynein heavy chain* and *tubulin* homologs) and in ciliary band cells of the sea urchin *Strongylocentrotus purpuratus* (e.g., *foxJ*) (Duruz et al., 2020; Paganos et al., 2021). This shows that the "ciliary/prototroch" cells in our data possess a distinct transcriptomic signature indicative of the ability to produce cilia, and that at least some of this molecular program was present in

the last common ancestor of bivalves, annelids, sea urchins, and xenacoelomorphs.

We identified cells that have ontology enrichment of neuroreceptors crucial for peptide signaling and factors related to mechanosensation and photosensation (**Figures 2B–B″**). Additionally, this cluster shows high expression of orthologs that play a role in the differentiation of the anlagen for the developing larval neurosecretory cells, e.g., *FMRFamide receptor, neuronal acetylcholine receptor subunit alpha-6* and *neuregulin 2*, in the bivalves *Macrocallista nimbosa*, *Mizuhopecten yessoensis*, and *Mytilus galloprovincialis* (**Supplementary Figure 4** and **Supplementary Tables 1–3**; Price and Greenberg, 1977; Wang et al., 2017; Gerdol et al., 2020). This indicates the presence of a neurosecretory center in this cluster that contains the key machinery for neuronal differentiation and suggests that the neuroanatomy of *Dreissena* trochophore larvae may be more complex than currently appreciated by morphological data using fluorescence-coupled antibody staining (Pavlicek et al., 2018).

Cells identified as "endoderm" expresses orthologs linked to protein breakdown processes and catalytic reactions which take place in the digestive system (**Figures 2C–C″**; Kirschke et al., 1995; Duruz et al., 2020). This is supported by the expression of crucial functional orthologs such as *hepatocyte nuclear factor 4 (hnf4), hematopoietically expressed homeobox gene* (*hhex*), and *galectin*. *Galectin* has been reported to promote phagocytosis of pathogens as a defense mechanism present in all cells and in hemocytes in adult stages, playing a role in innate immune responses and intracellular digestion in aquatic mollusks (Vasta et al., 2015). *Hnf4* is considered a marker of developing endoderm since its expression has been found in gut stem cells in several metazoans (Achim et al., 2018; Wendt et al., 2020; Paganos et al., 2021; Sur and Meyer, 2021) and was highly expressed exclusively in this cluster (in a limited number of cells only). *Hhex* is considered a regulator of hepatocyte development in deuterostomes (Wallace et al., 2001; Evseeva et al., 2021; Paganos et al., 2021) and was also found to be expressed in cells of this cluster (**Supplementary Figure 4** and **Supplementary Tables 1–3**). Although detection of these transcriptional markers is restricted to few cells, this is not uncommon for transcription factors, and overall the molecular fingerprint of this cluster is coherent with the developing gastrodermis.

Dreissena muscle progenitor cells consistently express common muscle and mesodermal markers. Among the gene orthologs identified in the "muscle" cluster, expression of *twist, Hand*, *Mox*, and *myosin heavy chain (mhc)* were detected (**Figures 3A,E** and **Supplementary Figure 4**). These genes are typically involved in mesoderm and/or muscle formation across metazoan clades (Castellani and Cohen, 1987; Ladurner and Rieger, 2000; Nederbragt et al., 2002; Dyachuk and Odintsova, 2009; Dobi et al., 2015; Achim et al., 2018; Li et al., 2019). In addition, there is gene ontology enrichment of several processes associated with muscle differentiation such as calcium ion binding and actin filament depolymerization (**Figures 2D–D″**).

The cluster "epidermal" shows enrichment of epidermis-related processes such as its morphogenesis and cell adhesion (**Figures 2E–E″**). Moreover, this cluster expresses orthologs of epidermal cells from the acoel *Isodiametra pulchra* and the annelid *Capitella teleta* that are associated with extracellular matrix factors and tight junctions such as *annexin,* cadherins, and claudin family members (**Supplementary Figure 4** and **Supplementary Tables 1–3**; Duruz et al., 2020; Sur and Meyer, 2021). Claudin is a transmembrane protein that is a crucial component of tight junctions in cells and cadherins are a type of cell adhesion molecules important for epithelium formation (Broders and Thiery, 1995; Krause et al., 2008; Piontek et al., 2008; Shapiro, 2016). For *annexin*, while playing a role in calcium-dependent membrane-binding and constituting an ectodermal marker in several metazoans (Meyer and Seaver, 2009; Duruz et al., 2020; Sur and Meyer, 2021), our results find this gene expressed also in ciliary and shell field cells (**Supplementary Figure 4** and **Supplementary Tables 1–3**). Hence, these shared transcriptomic signatures suggest that the precursor for both clusters have an ectodermal origin. Overall, the ortholog search supports the identity of this cluster by allowing one to one comparisons of cluster markers from different animals.

Orthologs of genes expressed in the shell field cluster that are known to play a role in early molluscan shell formation include *Hox1, chitin binding protein*, and *hic31* (**Supplementary Figure 4** and **Supplementary Tables 1–3**; Kakoi et al., 2008; Kin et al., 2009; Tan et al., 2017; Wollesen et al., 2018; Zhao et al., 2018; Liu et al., 2020; Salamanca-Díaz et al., 2021). Transcripts expressed here show ontology enrichment in processes such as peptide signaling and plasma membrane interactions, linking the activity of these cells to shell building mechanisms (**Figures 2F–F″**). However, most of the upregulated genes in this cluster do not have a known ontology term or an ortholog match with other metazoans (**Supplementary Tables 1–3**). Previous studies analyzing gene products expressed in shell secreting mantle tissues of various bivalves and gastropods found that, despite having a common biomineralization toolbox, the shell matrix expresses many novel, duplicated, and reorganized genes. These features have led to the conclusion that molluscan shells are "rapidly evolving" (Jackson et al., 2006; Aguilera et al., 2017; Zhao et al., 2018). This opens the possibility for further analyses in *Dreissena* shell field cells and to test whether these markers constitute hitherto unknown genes.

Enhancing the Cell Fate Map of *Dreissena*

Cell groups were linked together by tracing pseudotime trajectories across our dataset (**Figure 4B**). As these trajectories are represented in function of pseudotime, they can be used as a bioinformatical approximation of developmental decisions. By comparing terminal fates from other molluscan lineage trees to our results, we were able to link scRNA-seq data to the cellular lineage tree of *Dreissena* (Meisenheimer, 1900; **Figure 1B**). The "muscle" and "endoderm" clusters are separated here by a node in the scRNA-seq dataset (**Figure 4B**). According to cell fate maps from *Dreissena* and other mollusks, there is a significant portion of the endoderm that originates from mesodermal lineages

(Nielsen, 2005; Kurita et al., 2009; Chan and Lambert, 2011; Gharbiah et al., 2013; Lyons et al., 2017). Therefore, since these clusters have an origin in a common cell lineage, the node between these two groups may mark the corresponding cell division visualized in the cell fate map (**Figure 4C**). On the other hand, the clusters seen in the rest of the built trajectories, i.e., shell field and epidermal, neuronal and ciliary/prototroch (**Figures 4B,C**), have their origin in macromeres composed mainly of the ectodermal germ layer (Nielsen, 2005; Kurita et al., 2009; Chan and Lambert, 2011; Gharbiah et al., 2013; Lyons et al., 2017). Furthermore, after increasing cluster resolution and analyzing ortholog gene expression in both, ciliary and neuronal cells, there was occurrence of more than one subtype in each cluster (**Supplementary Figures 1I–K**). This was supported by the trajectory analyses that display multiple ends in both ciliary and neuronal cells (**Figure 4B**). We suggest that this diversity within a cluster could represent the different subtypes of ciliary and neuronal cells seen in the live larva, i.e., apical tuft, prototroch, telotroch, *FMFRamide receptor*-positive and *neuronal acetylcholine receptor subunit alpha-6*-positive cells, respectively (**Supplementary Figure 4** and **Supplementary Tables 1–3**). Similar cluster diversity in neuronal cell types is found in single cell datasets from other metazoans such as the annelid *Capitella teleta* and the sea urchin *Strongylocentrotus purpuratus*. All neuronal cell types of these species share a baseline transcriptomic signature, with only enough differences in expression to subdivide the overall cluster into different categories, e.g., 12 neuronal subtypes in the sea urchin and four neural subgroups in *C. teleta* (Achim et al., 2018; Foster et al., 2020; Paganos et al., 2021). Moreover, when analyzing the cell lineage tree of *Dreissena*, our data highlights that the underlying transcriptomic signature is similar across lineages that give rise to the same fate (**Figure 3C**).

CONCLUSION

Our analyses identified all expected major cell populations in the trochophore larva of the quagga mussel, *Dreissena rostriformis* (**Figure 4E**). When comparing our results to studies on other metazoans, we were able to support previous morphological annotations from cell groups such as "ciliary," "neuronal," "muscle," "endoderm," and "shell field." Our cluster validations, such as the BLASTX search, GO term annotations, and *in situ* hybridization identified marker genes for each of these cell types. Moreover, we were able to gain a first glimpse into developmental decisions, e.g., "endoderm" + "muscle," and cluster structure within already known cell lineages, e.g., "ciliary/prototroch" and "neuronal." Our data demonstrate that the levels of differentially expressed genes can be used as markers to identify clusters of cells in early developmental (larval) stages of (bivalve) mollusks, thus adding these animals to the suite of taxa that can now be accessed for comparative evolutionary studies on cell type level using scRNA-seq techniques. This should ultimately lead to a better understanding as to how animals form and which genes and cell types are involved in shaping larval and adult life cycle stages across Metazoa.

DATA AVAILABILITY STATEMENT

The data presented in this study are deposited in NCBI's Gene Expression Omnibus and are accessible through the GEO series accession number GSE192624 (https://www.ncbi.nlm.nih.gov/geo/query/acc.cgi?acc=GSE192624).

AUTHOR CONTRIBUTIONS

DS-D, AC, and AW designed the research and contributed to interpretation of data. DS-D performed the experiments, generated data with contribution of AC, performed the data analysis with assistance of AC, and drafted the manuscript with input from AW and AC. AC generated the sequencing library from cell suspensions provided by DS-D. SS contributed to gene annotation from the muscle cluster and performed *in situ* hybridization of *myosin heavy chain*. All authors read and approved the final version of the manuscript.

FUNDING

This work was supported by a completion grant of the Vienna Doctoral School of Ecology and Evolution (VDSEE) to DS-D and by the Austrian Science Fund (FWF) (grant P29455-B29 to AW and P31018-B29 to AC).

ACKNOWLEDGMENTS

The authors thank Julia Steger and Oliver Link (Vienna) for their support and valuable input when developing the dissociation suspension and assisting the first experimental trials, and Hannah Schmidbaur and Elena A. Ritschard (Vienna) for bioinformatics advice on the gene annotations. The authors also thank Uli Technau for hosting DS-D during this work.

SUPPLEMENTARY MATERIAL

The Supplementary Material for this article can be found online at: https://www.frontiersin.org/articles/10.3389/fevo.2021.783984/full#supplementary-material

Supplementary Figure 1 | (A) Barcode plot showing the cumulative distribution of UMIs in function of barcodes. Violin plots show feature distribution for the overall data before **(B)** and after **(C)** setting thresholds to the data, and in every cluster **(D)** from the dataset. **(E)** Scatter plot showing the correlation between features, Pearson correlation is shown on top of the plot. **(F)** Top 2000 most variably expressed genes used for further calculation of significant principal components. Cells were filtered out based on less than 150 and more than 4000 features. **(G)** Elbow plot showing the standard deviations of the calculated principal components. **(H)** Statistics table on the single cell transcriptome libraries showing sequencing, mapping, and cell metrics summary for this study. **(I–K)**

UMAP graphs result of an increased cluster-finding algorithm resolution with 0.7, 1, and 2 as resolution threshold, respectively.

Supplementary Figure 2 | Dataset exploration on different filtering thresholds. **(A,C,D,G,H,K)** Represent the data after filtering out cells with less than 300 and more than 4000 genes, resulting in 490 cells. **(B,E,F,I,J,L)** Represent the data after filtering out cells with less than 500 and more than 4000 genes, resulting in 430 cells. **(A,B)** Violin plots showing feature and count distribution for the filtered data, with more than 300 and 500 genes, respectively. **(C,E)** Original clustering highlighted in the filtered data, with more than 300 and 500 genes, respectively. **(D–J)** UMAP graphs result of an increased cluster-finding algorithm resolution in filter settings of more than 300 and 500 genes, with 0.5, 1, and 5 as resolution threshold, respectively. **(K,L)** Pseudotime trajectory calculations for each respective filtered data threshold.

Supplementary Figure 3 | Prediction of a stem cell-like cluster at the root of the differentiation pathways based on the initial clustering. The entropy values are shown as color of the vertices. The color of the link represents the $-\log_{10}$ *p*-value. Thickness of the link indicates the score, reflecting cell density coverage on a link.

Supplementary Figure 4 | (A) Orthologs known to be stem cell markers identified in our dataset, expressed across all clusters. **(B)** Dot plot of ortholog gene expression per cluster. **(C)** Orthologs identified in the dataset used to annotate cluster identities. **(D)** Dot plot of ortholog gene expression per cluster. Color intensity represents the average gene expression while circle size is the percentage of cells expressing a certain gene.

Supplementary Figure 5 | Negative controls (sense riboprobes) of *in situ* hybridization experiments for each randomly sampled marker gene used for cluster annotation. **(A–C)** Lateral views of *mhc, hic31,* and *tsh,* respectively. Anterior (A), posterior (P), ventral (V), and dorsal (D). Scale bars are 20 μm. Dotted lines indicate the outline of the shell field. Asterisk indicates the mouth opening on the left side.

Supplementary Table 1 | Gene annotations of the transcriptome used for this dataset. Annotations from Pfam, PANTHER, GO terms, and BLASTX hit from human and *Crassostrea gigas* orthologs are indicated in each column accordingly.

Supplementary Table 2 | Differentially expressed markers per cluster result from the output FindAllMarkers function with a cluster threshold set up to 0.5.

Supplementary Table 3 | Top 10 differentially expressed markers per cluster result from the output FindAllMarkers function with a cluster threshold set up to 0.7.

Supplementary Table 4 | List of primers and nucleotide sequence for each gene used for cloning. Forward and reverse primers used for amplifying each gene by PCR are indicated.

Supplementary Table 5 | Explored cutoffs in the dataset and the number of remaining cells of each cluster after each filtering. Thresholds were set from more than 100 genes and less than 4000 to more than 500 genes and less than 2500, respectively. Dotted lines indicate the outline of the shell field and the symbol * indicates the mouth opening on the left side.

REFERENCES

Achim, K., Eling, N., Vergara, H. M., Bertucci, P. Y., Musser, J., Vopalensky, P., et al. (2018). Whole-body single-cell sequencing reveals transcriptional domains in the annelid larval body. *Mol. Biol. Evol.* 35, 1047–1062. doi: 10.1093/molbev/msx336

Achim, K., Pettit, J.-B., Saraiva, L. R., Gavriouchkina, D., Larsson, T., Arendt, D., et al. (2015). High-throughput spatial mapping of single-cell RNA-seq data to tissue of origin. *Nat. Biotechnol.* 33, 503–509.

Aguilera, F., McDougall, C., Degnan, B. M., and Irwin, D. (2017). Co-option and de novo gene evolution underlie molluscan shell diversity. *Mol. Biol. Evol.* 34, 779–792. doi: 10.1093/molbev/msw294

Aldridge, D. C., Ho, S., and Froufe, E. (2014). The ponto-caspian quagga mussel, *Dreissena rostriformis* bugensis (Andrusov, 1897), invades Great Britain. *Aquat. Invasions* 9, 529–535.

Alexa, A., Rahnenführer, J., and Lengauer, T. (2006). Improved scoring of functional groups from gene expression data by decorrelating GO graph structure. *Bioinformatics* 22, 1600–1607. doi: 10.1093/bioinformatics/btl140

Arenas-Mena, C., Wong, K. S.-Y., and Arandi-Forosani, N. (2007). Ciliary band gene expression patterns in the embryo and trochophore larva of an indirectly developing polychaete. *Gene Expr. Patterns* 7, 544–549. doi: 10.1016/j.modgep.2007.01.007

Arendt, D., Musser, J. M., Baker, C. V. H., Bergman, A., Cepko, C., Erwin, D. H., et al. (2016). The origin and evolution of cell types. *Nat. Rev. Genet.* 17, 744–757. doi: 10.1038/nrg.2016.127

Briggs, J. A., Weinreb, C., Wagner, D. E., Megason, S., Peshkin, L., Kirschner, M. W., et al. (2018). The dynamics of gene expression in vertebrate embryogenesis at single-cell resolution. *Science* 360:eaar5780. doi: 10.1126/science.aar5780

Broders, F., and Thiery, J. P. (1995). "Structure and function of cadherins BT," in *Organization of the Early Vertebrate Embryo*, eds N. Zagris, A. M. Duprat, and A. Durston (Berlin: Springer), 183–208. doi: 10.1007/978-1-4899-1618-1_16

Calcino, A. D., de Oliveira, A. L., Simakov, O., Schwaha, T., Zieger, E., Wollesen, T., et al. (2019). The quagga mussel genome and the evolution of freshwater tolerance. *DNA Res.* 26, 411–422. doi: 10.1093/dnares/dsz019

Cao, J., Spielmann, M., Qiu, X., Huang, X., Ibrahim, D. M., Hill, A. J., et al. (2019). The single-cell transcriptional landscape of mammalian organogenesis. *Nature* 566, 496–502. doi: 10.1038/s41586-019-0969-x

Castellani, L., and Cohen, C. (1987). Myosin rod phosphorylation and the catch state of molluscan-muscles. *Science (New York, N.Y.)* 235, 334–337. doi: 10.1126/science.3026049

Chan, X. Y., and Lambert, J. (2011). Patterning a spiralian embryo: a segregated RNA for a Tis11 ortholog is required in the 3a and 3b cells of the *Ilyanassa embryo*. *Dev. Biol.* 349, 102–112. doi: 10.1016/j.ydbio.2010.10.001

Dictus, W. J. A. G., and Damen, P. (1997). Cell-lineage and clonal-contribution map of the trochophore larva of *Patella vulgata* (Mollusca)1Both authors contributed equally to this work.1. *Mech. Dev.* 62, 213–226. doi: 10.1016/S0925-4773(97)00666-7

Dobi, K. C., Schulman, V. K., and Baylies, M. K. (2015). Specification of the somatic musculature in *Drosophila*. *Wires Dev. Biol.* 4, 357–375. doi: 10.1002/wdev.182

Duruz, J., Kaltenrieder, C., Ladurner, P., Bruggmann, R., Martìnez, P., and Sprecher, S. G. (2020). Acoel single-cell transcriptomics: cell-type analysis of a deep branching bilaterian. *BioRxiv* [Preprint]. doi: 10.1101/2020.07.10.196782 BioRxiv 2020.07.10.196782,

Dyachuk, V., and Odintsova, N. (2009). Development of the larval muscle system in the mussel *Mytilus trossulus* (Mollusca, Bivalvia): original article. *Dev. Growth Differ.* 51, 69–79. doi: 10.1111/j.1440-169X.2008.01081.x

Evseeva, M. N., Dyikanov, D. T., Karagyaur, M. N., Prikazchikova, T. A., Sheptulina, A. F., Balashova, M. S., et al. (2021). Hematopoietically-expressed homeobox protein HHEX regulates adipogenesis in preadipocytes. *Biochimie* 185, 68–77. doi: 10.1016/j.biochi.2021.02.011

Farrell, J. A., Wang, Y., Riesenfeld, S. J., Shekhar, K., Regev, A., and Schier, A. F. (2018). Single-cell reconstruction of developmental trajectories during zebrafish embryogenesis. *Science* 360:eaar3131. doi: 10.1126/science.aar3131

Fincher, C. T., Wurtzel, O., de Hoog, T., Kravarik, K. M., and Reddien, P. W. (2018). Cell type transcriptome atlas for the planarian *Schmidtea mediterranea*. *Science* 360:eaaq1736. doi: 10.1126/science.aaq1736

Foster, S., Oulhen, N., and Wessel, G. (2020). A single cell RNA sequencing resource for early sea urchin development. *Development* 147:dev191528. doi: 10.1242/dev.191528

Foster, S., Teo, Y. V., Neretti, N., Oulhen, N., and Wessel, G. M. (2019). Single cell RNA-seq in the sea urchin embryo show marked cell-type specificity in the Delta/Notch pathway. *Mol. Reproduct. Dev.* 86, 931–934. doi: 10.1002/mrd.23181

García-Castro, H., Kenny, N. J., Iglesias, M., Álvarez-Campos, P., Mason, V., Elek, A., et al. (2021). ACME dissociation: a versatile cell fixation-dissociation method for single-cell transcriptomics. *Genome Biol.* 22:89. doi: 10.1186/s13059-021-02302-5

Gerdol, M., Moreira, R., Cruz, F., Gómez-Garrido, J., Vlasova, A., Rosani, U., et al. (2020). Massive gene presence-absence variation shapes an open pan-genome in the Mediterranean mussel. *Genome Biol.* 21:275. doi: 10.1186/s13059-020-02180-3

Gharbiah, M., Nakamoto, A., and Nagy, L. M. (2013). Analysis of ciliary band formation in the mollusc *Ilyanassa obsoleta*. *Dev. Genes Evol.* 223, 225–235. doi: 10.1007/s00427-013-0440-1

Grün, D. (2020). Revealing dynamics of gene expression variability in cell state space. *Nat. Methods* 17, 45–49. doi: 10.1038/s41592-019-0632-3

Grün, D., Muraro, M. J., Boisset, J.-C., Wiebrands, K., Lyubimova, A., Dharmadhikari, G., et al. (2016). De novo prediction of stem cell identity using single-cell transcriptome data. *Cell Stem Cell* 19, 266–277. doi: 10.1016/j.stem.2016.05.010

Heiler, K. C. M., Bij de Vaate, A., Ekschmitt, K., von Oheimb, P. V., Albrecht, C., and Wilke, T. (2013). Reconstruction of the early invasion history of the quagga mussel (Dreissena rostriformis bugensis) in Western Europe. *Aquat. Invasions* 8, 53–57.

Hejnol, A., Martindale, M. Q., and Henry, J. Q. (2007). High-resolution fate map of the snail *Crepidula fornicata*: The origins of ciliary bands, nervous system, and muscular elements. *Dev. Biol.* 305, 63–76. doi: 10.1016/j.ydbio.2007.01.044

Hemmrich, G., Khalturin, K., Boehm, A.-M., Puchert, M., Anton-Erxleben, F., Wittlieb, J., et al. (2012). Molecular signatures of the three stem cell lineages in hydra and the emergence of stem cell function at the base of multicellularity. *Mol. Biol. Evol.* 29, 3267–3280. doi: 10.1093/molbev/mss134

Henry, J. Q., Okusu, A., and Martindale, M. Q. (2004). The cell lineage of the polyplacophoran, *Chaetopleura apiculata*: variation in the spiralian program and implications for molluscan evolution. *Deve. Biol.* 272, 145–160. doi: 10.1016/j.ydbio.2004.04.027

Hinman, V. F., O'Brien, E. K., Richards, G. S., and Degnan, B. M. (2003). Expression of anterior Hox genes during larval development of the gastropod *Haliotis asinina*. *Evol. Dev.* 5, 508–521.

Inkscape Project (2020). *Inkscape*. Available online at: https://inkscape.org (accessed March 3, 2021).

Jackson, D. J., McDougall, C., Green, K., Simpson, F., Wörheide, G., and Degnan, B. M. (2006). A rapidly evolving secretome builds and patterns a sea shell. *BMC Biol.* 4:40. doi: 10.1186/1741-7007-4-40

Jones, P., Binns, D., Chang, H.-Y., Fraser, M., Li, W., McAnulla, C., et al. (2014). InterProScan 5: genome-scale protein function classification. *Bioinformatics (Oxford, England)* 30, 1236–1240. doi: 10.1093/bioinformatics/btu031

Kakoi, S., Kin, K., Miyazaki, K., and Wada, H. (2008). Early development of the japanese spiny oyster (*Saccostrea kegaki*): characterization of some genetic markers. *Zool. Sci.* 25, 455–464. doi: 10.2108/zsj.25.455

Karaiskos, N., Wahle, P., Alles, J., Boltengagen, A., Ayoub, S., Kipar, C., et al. (2017). The *Drosophila embryo* at single-cell transcriptome resolution. *Science* 358, 194–199. doi: 10.1126/science.aan3235

Karatayev, A. Y., Burlakova, L. E., Pennuto, C., Ciborowski, J., Karatayev, V. A., Juette, P., et al. (2014). Twenty five years of changes in *Dreissena* spp. populations in Lake Erie. *J. Great Lakes Res.* 40, 550–559.

Karatayev, A. Y., Padilla, D. K., Minchin, D., Boltovskoy, D., and Burlakova, L. E. (2007). Changes in global economies and trade: the potential spread of exotic freshwater bivalves. *Biol. Invasions* 9, 161–180. doi: 10.1007/s10530-006-9013-9

Kin, K., Kakoi, S., and Wada, H. (2009). A novel role for dpp in the shaping of bivalve shells revealed in a conserved molluscan developmental program. *Dev. Biol.* 329, 152–166. doi: 10.1016/j.ydbio.2009.01.021

King, S. M. (2012). Integrated control of axonemal dynein AAA+ motors. *J. Struct. Biol.* 179, 222–228. doi: 10.1016/j.jsb.2012.02.013

Kirschke, H., Barrett, A. J., and Rawlings, N. D. (1995). Proteinases 1: lysosomal cysteine proteinases. *Protein Profile* 2, 1581–1643.

Krause, G., Winkler, L., Mueller, S. L., Haseloff, R. F., Piontek, J., and Blasig, I. E. (2008). Structure and function of claudins. *Biochim. Biophys. Acta* 1778, 631–645. doi: 10.1016/j.bbamem.2007.10.018

Kurita, Y., Deguchi, R., and Wada, H. (2009). Early development and cleavage pattern of the Japanese Purple Mussel, *Septifer virgatus*. *Zool. Sci.* 26, 814–820. doi: 10.2108/zsj.26.814

Ladurner, P., and Rieger, R. (2000). Embryonic muscle development of *Convoluta pulchra* (Turbellaria–Acoelomorpha, Platyhelminthes). *Dev. Biol.* 222, 359–375.

Lee, P. N., Callaerts, P., De Couet, H. G., and Martindale, M. Q. (2003). Cephalopod Hox genes and the origin of morphological novelties. *Nature* 424, 1061–1065. doi: 10.1038/nature01872

Levin, M., Anavy, L., Cole, A. G., Winter, E., Mostov, N., Khair, S., et al. (2016). The mid-developmental transition and the evolution of animal body plans. *Nature* 531, 637–641. doi: 10.1038/nature16994

Li, H., Li, Q., Yu, H., and Du, S. (2019). Developmental dynamics of myogenesis in Pacific oyster *Crassostrea gigas*. *Comp. Biochem. Physiol. Part B* 227, 21–30.

Lillie, F. R. (1895). The embryology of the unionidae. A study in cell-lineage. *J. Morphol.* 10, 1–100. doi: 10.1002/jmor.1050100102

Liu, G., Huan, P., and Liu, B. (2020). Identification of three cell populations from the shell gland of a bivalve mollusc. *Dev. Genes Evol.* 230, 39–45. doi: 10.1007/s00427-020-00646-9

Liu, X., Jin, C., Li, H., Bai, Z., and Li, J. (2018). Morphological structure of shell and expression patterns of five matrix protein genes during the shell regeneration process in *Hyriopsis cumingii*. *Aquacult. Fish.* 3, 225–231. doi: 10.1016/j.aaf.2018.09.005

Liu, X., Zeng, S., Dong, S., Jin, C., and Li, J. (2015). A novel matrix protein hic31 from the prismatic layer of hyriopsis cumingii displays a collagen-like structure. *PLoS One* 10:e0135123. doi: 10.1371/journal.pone.0135123

Luetjens, C. M., and Dorresteijn, A. W. C. (1995). Multiple, alternative cleavage patterns precede uniform larval morphology during normal development of *Dreissena polymorpha* (Mollusca, Lamellibranchia). *Rouxs Arch. Dev. Biol.* 205, 138–149. doi: 10.1007/BF00357760

Lyons, D. C., Perry, K. J., and Henry, J. Q. (2017). Morphogenesis along the animal-vegetal axis: fates of primary quartet micromere daughters in the gastropod *Crepidula fornicata*. *BMC Evol. Biol.* 17:217. doi: 10.1186/s12862-017-1057-1

McCartney, M. A., Auch, B., Kono, T., Mallez, S., Zhang, Y., Obille, A., et al. (2019). The genome of the Zebra Mussel, *Dreissena polymorpha*: a resource for invasive species research. *BioRxiv* [Preprint]. doi: 10.1101/696732 BioRxiv 696732,

McNickle, G. G., Rennie, M. D., and Sprules, W. G. (2006). Changes in benthic invertebrate communities of South Bay, Lake Huron following invasion by zebra mussels (*Dreissena polymorpha*), and potential effects on lake whitefish (*Coregonus clupeaformis*) diet and growth. *J. Great Lakes Res.* 32, 180–193.

Meisenheimer, J. (1900). *Entwicklungsgeschichte von Dreissensia polymorpha Pall*. Leipzig: Wilhelm Engelmann.

Meyer, N. P., and Seaver, E. C. (2009). Neurogenesis in an annelid: Characterization of brain neural precursors in the polychaete *Capitella* sp. *Dev. Biol.* 335, 237–252. doi: 10.1016/j.ydbio.2009.06.017

Mills, E. L., Dermott, R. M., Roseman, E. F., Dustin, D., Mellina, E., Conn, D. B., et al. (1993). Colonization, ecology, and population structure of the "quagga"mussel (Bivalvia: Dreissenidae) in the lower Great Lakes. *Can. J. Fish. Aquat. Sci.* 50, 2305–2314.

Nalepa, T. F., and Schloesser, D. W. (2019). *Quagga and Zebra Mussels: Biology, Impacts, and Control*. Boca Raton, FL: CRC Press.

Nederbragt, A. J., Lespinet, O., Van Wageningen, S., Van Loon, A. E., Adoutte, A., and Dictus, W. J. A. G. (2002). A lophotrochozoan twist gene is expressed in the ectomesoderm of the gastropod mollusk *Patella vulgata*. *Evol. Dev.* 4, 334–343. doi: 10.1046/j.1525-142X.2002.02020.x

Nielsen, C. (2005). Trochophora larvae: cell-lineages, ciliary bands and body regions. 2. Other groups and general discussion. *J. Exp. Zool. Part B* 304, 401–447. doi: 10.1002/jez.b.21050

Nielsen, C. (2018). Origin of the trochophora larva. *R. Soc. Open Sci.* 5:180042. doi: 10.1098/rsos.180042

Paganos, P., Voronov, D., Musser, J., Arendt, D., and Arnone, M. I. (2021). Single cell RNA sequencing of the *Strongylocentrotus purpuratus* larva reveals the blueprint of major cell types and nervous system of a non-chordate deuterostome. *Elife* 10:e70416. doi: 10.7554/eLife.70416

Pavlicek, A., Schwaha, T., and Wanninger, A. (2018). Towards a ground pattern reconstruction of bivalve nervous systems: neurogenesis in the zebra mussel *Dreissena polymorpha*. *Organ. Divers. Evol.* 18, 101–114. doi: 10.1007/s13127-017-0356-0

Piontek, J., Winkler, L., Wolburg, H., Müller, S. L., Zuleger, N., Piehl, C., et al. (2008). Formation of tight junction: determinants of homophilic interaction between classic claudins. *FASEB J.* 22, 146–158. doi: 10.1096/fj.07-8319com

Plass, M., Solana, J., Wolf, F. A., Ayoub, S., Misios, A., Glažar, P., et al. (2018). Cell type atlas and lineage tree of a whole complex animal by single-cell transcriptomics. *Science* 360:eaaq1723. doi: 10.1126/science.aaq1723

Price, D. A., and Greenberg, M. J. (1977). Purification and characterization of a cardioexcitatory neuropeptide from the central ganglia of a bivalve mollusc. *Prep. Biochem.* 7, 261–281. doi: 10.1080/00327487708061643

R Developement Core Team (2015). *R: A Language and Environment for Statistical Computing*, Vol. 1. Vienna: R Foundation for Statistical Computing, 409. doi: 10.1007/978-3-540-74686-7

Raikow, D. F. (2004). Food web interactions between larval bluegill (*Lepomis macrochirus*) and exotic zebra mussels (*Dreissena polymorpha*). *Can. J. Fish. Aquat. Sci.* 61, 497–504.

Redl, E., Scherholz, M., Wollesen, T., Todt, C., and Wanninger, A. (2016). Cell proliferation pattern and twist expression in an aplacophoran mollusk argue against segmented ancestry of mollusca. *J. Exp. Zool. Part B* 326, 422–436. doi: 10.1002/jez.b.22714

Render, J. (1997). Cell Fate Maps in theIlyanassa obsoleta Embryo beyond the Third Division. *Dev. Biol.* 189, 301–310. doi: 10.1006/dbio.1997.8654

Salamanca-Díaz, D. A., Calcino, A. D., de Oliveira, A. L., and Wanninger, A. (2021). Non-collinear Hox gene expression in bivalves and the evolution of morphological novelties in mollusks. *Sci. Rep.* 11:3575. doi: 10.1038/s41598-021-82122-6

Satija, R., Farrell, J. A., Gennert, D., Schier, A. F., and Regev, A. (2015). Spatial reconstruction of single-cell gene expression data. *Nat. Biotechnol.* 33, 495–502. doi: 10.1038/nbt.3192

Schindelin, J., Arganda-Carreras, I., Frise, E., Kaynig, V., Longair, M., Pietzsch, T., et al. (2012). Fiji: an open-source platform for biological-image analysis. *Nat. Methods* 9, 676–682. doi: 10.1038/nmeth.2019

Sebé-Pedrós, A., Saudemont, B., Chomsky, E., Plessier, F., Mailhé, M.-P., Renno, J., et al. (2018). Cnidarian cell type diversity and regulation revealed by whole-organism single-cell RNA-seq. *Cell* 173, 1520–1534.e20. doi: 10.1016/j.cell.2018.05.019

Shapiro, E., Biezuner, T., and Linnarsson, S. (2013). Single-cell sequencing-based technologies will revolutionize whole-organism science. *Nat. Rev. Genet.* 14, 618–630. doi: 10.1038/nrg3542

Shapiro, L. (2016). "Structure and function of cadherin extracellular regions BT," in *The Cadherin Superfamily: Key Regulators of Animal Development and Physiology*, eds S. T. Suzuki and S. Hirano (Berlin: Springer), 71–91. doi: 10.1007/978-4-431-56033-3_4

Siebert, S., Farrell, J. A., Cazet, J. F., Abeykoon, Y., Primack, A. S., Schnitzler, C. E., et al. (2019). Stem cell differentiation trajectories in Hydra resolved at single-cell resolution. *Science* 365:eaav9314. doi: 10.1126/science.aav9314

Smith, S. A., Wilson, N. G., Goetz, F. E., Feehery, C., Andrade, S. C. S., Rouse, G. W., et al. (2011). Resolving the evolutionary relationships of molluscs with phylogenomic tools. *Nature* 480, 364–367. doi: 10.1038/nature10526

Stegle, O., Teichmann, S. A., and Marioni, J. C. (2015). Computational and analytical challenges in single-cell transcriptomics. *Nat. Rev. Genet.* 16, 133–145. doi: 10.1038/nrg3833

Strayer, D. L., Hattala, K. A., and Kahnle, A. W. (2004). Effects of an invasive bivalve (*Dreissena polymorpha*) on fish in the Hudson River estuary. *Can. J. Fish. Aquat. Sci.* 61, 924–941.

Sur, A., and Meyer, N. P. (2021). Resolving transcriptional states and predicting lineages in the annelid capitella teleta using single-Cell RNAseq. *Front. Ecol. Evol.* 8:523.

Svensson, V., Vento-Tormo, R., and Teichmann, S. A. (2018). Exponential scaling of single-cell RNA-seq in the past decade. *Nat. Protoc.* 13, 599–604.

Tan, S., Huan, P., and Liu, B. (2017). Expression patterns indicate that BMP2/4 and Chordin, not BMP5-8 and Gremlin, mediate dorsal–ventral patterning in the mollusk *Crassostrea gigas*. *Dev. Genes Evol.* 227, 75–84. doi: 10.1007/s00427-016-0570-3

Tang, F., Barbacioru, C., Bao, S., Lee, C., Nordman, E., Wang, X., et al. (2010). Tracing the derivation of embryonic stem cells from the inner cell mass by single-cell RNA-Seq analysis. *Cell Stem Cell* 6, 468–478.

Trapnell, C. (2015). Defining cell types and states with single-cell genomics. *Genome Res.* 25, 1491–1498.

Trapnell, C., Cacchiarelli, D., Grimsby, J., Pokharel, P., Li, S., Morse, M., et al. (2014). The dynamics and regulators of cell fate decisions are revealed by pseudotemporal ordering of single cells. *Nat. Biotechnol.* 32:381.

van Dijk, D., Sharma, R., Nainys, J., Yim, K., Kathail, P., Carr, A. J., et al. (2018). Recovering gene interactions from single-cell data using data diffusion. *Cell* 174, 716–729.e27. doi: 10.1016/j.cell.2018.05.061

Vasta, G. R., Feng, C., Bianchet, M. A., Bachvaroff, T. R., and Tasumi, S. (2015). Structural, functional, and evolutionary aspects of galectins in aquatic mollusks: From a sweet tooth to the Trojan horse. *Fish Shellfish Immunol.* 46, 94–106. doi: 10.1016/j.fsi.2015.05.012

Vergara, H. M., Bertucci, P. Y., Hantz, P., Tosches, M. A., Achim, K., Vopalensky, P., et al. (2017). Whole-organism cellular gene-expression atlas reveals conserved cell types in the ventral nerve cord of Platynereis dumerilii. *Proc. Natl. Acad. Sci. U.S.A.* 114, 5878–5885.

Wagner, D. E., Weinreb, C., Collins, Z. M., Briggs, J. A., Megason, S. G., and Klein, A. M. (2018). Single-cell mapping of gene expression landscapes and lineage in the zebrafish embryo. *Science* 360, 981–987. doi: 10.1126/science.aar4362

Wakida-Kusunoki, A. T., Wakida, F. T., and De Leon-Sandoval, J. M. (2015). First record of quagga mussel *Dreissena rostriformis* bugensis (Andrusov, 1897) (Bivalvia, Dreissenidae) from Mexico. *BioInvasions Rec.* 4, 31–36.

Wallace, K. N., Yusuff, S., Sonntag, J. M., Chin, A. J., and Pack, M. (2001). Zebrafish hhex regulates liver development and digestive organ chirality. *Genesis* 30, 141–143. doi: 10.1002/gene.1050

Wang, S., Zhang, J., Jiao, W., Li, J., Xun, X., Sun, Y., et al. (2017). Scallop genome provides insights into evolution of bilaterian karyotype and development. *Nat. Ecol. Evol.* 1:0120. doi: 10.1038/s41559-017-0120

Wanninger, A., and Wollesen, T. (2015). "Evolutionary developmental biology of invertebrates 2: lophotrochozoa (Spiralia)," in *Evolutionary Developmental Biology of Invertebrates 2: Lophotrochozoa (Spiralia)*, ed. A. Wanninger (Berlin: Springer-Verlag), 103–154. doi: 10.1007/978-3-7091-1871-9

Wanninger, A., and Wollesen, T. (2019). The evolution of molluscs. *Biol. Rev.* 94, 102–115. doi: 10.1111/brv.12439

Wendt, G., Zhao, L., Chen, R., Liu, C., O'Donoghue, A. J., Caffrey, C. R., et al. (2020). A single-cell RNA-seq atlas of andlt;emandgt;Schistosoma mansoniandlt;/emandgt; identifies a key regulator of blood feeding. *Science* 369, 1644–1649. doi: 10.1126/science.abb7709

Wollesen, T., Rodriguez Monje, S. V., de Oliveira, A. L., and Wanninger, A. (2018). Staggered Hox expression is more widespread among molluscs than previously appreciated. *Proc. R. Soc. B* 285:20181513. doi: 10.1098/rspb.2018.1513

Wollesen, T., Rodríguez Monje, S. V., McDougall, C., Degnan, B. M., and Wanninger, A. (2015a). The ParaHox gene Gsx patterns the apical organ and central nervous system but not the foregut in scaphopod and cephalopod mollusks. *EvoDevo* 6:41. doi: 10.1186/s13227-015-0037-z

Wollesen, T., Rodríguez Monje, S. V., Todt, C., Degnan, B. M., and Wanninger, A. (2015b). Ancestral role of Pax2/5/8 in molluscan brain and multimodal sensory system development. *BMC Evol. Biol.* 15:231. doi: 10.1186/s12862-015-0505-z

Zhao, R., Takeuchi, T., Luo, Y.-J., Ishikawa, A., Kobayashi, T., Koyanagi, R., et al. (2018). Dual gene repertoires for larval and adult shells reveal molecules essential for molluscan shell formation. *Mol. Biol. Evol.* 35, 2751–2761. doi: 10.1093/molbev/msy172

Zhong, S., Zhang, S., Fan, X., Wu, Q., Yan, L., Dong, J., et al. (2018). A single-cell RNA-seq survey of the developmental landscape of the human prefrontal cortex. *Nature* 555, 524–528.

Conflict of Interest: The authors declare that the research was conducted in the absence of any commercial or financial relationships that could be construed as a potential conflict of interest.

Publisher's Note: All claims expressed in this article are solely those of the authors and do not necessarily represent those of their affiliated organizations, or those of the publisher, the editors and the reviewers. Any product that may be evaluated in this article, or claim that may be made by its manufacturer, is not guaranteed or endorsed by the publisher.

frontiers | Frontiers in Cell and Developmental Biology

TYPE Brief Research Report
PUBLISHED 12 September 2022
DOI 10.3389/fcell.2022.999511

OPEN ACCESS

EDITED BY
Neva P. Meyer,
Clark University, United States

REVIEWED BY
William Smith,
University of California, United States
Takeo Horie,
Osaka University, Japan
Tian Yuan,
Wake Forest School of Medicine,
United States

*CORRESPONDENCE
Alberto Stolfi,
alberto.stolfi@biosci.gatech.edu

SPECIALTY SECTION
This article was submitted to Evolutionary Developmental Biology, a section of the journal Frontiers in Cell and Developmental Biology

RECEIVED 21 July 2022
ACCEPTED 24 August 2022
PUBLISHED 12 September 2022

CITATION
Kim K, Orvis J and Stolfi A (2022), Pax3/7 regulates neural tube closure and patterning in a non-vertebrate chordate.
Front. Cell Dev. Biol. 10:999511.
doi: 10.3389/fcell.2022.999511

Pax3/7 regulates neural tube closure and patterning in a non-vertebrate chordate

Kwantae Kim, Jameson Orvis and Alberto Stolfi*

School of Biological Sciences, Georgia Institute of Technology, Atlanta, GA, United States

Pax3/7 factors play numerous roles in the development of the dorsal nervous system of vertebrates. From specifying neural crest at the neural plate borders, to regulating neural tube closure and patterning of the resulting neural tube. However, it is unclear which of these roles are conserved in non-vertebrate chordates. Here we investigate the expression and function of Pax3/7 in the model tunicate *Ciona*. Pax3/7 is expressed in neural plate border cells during neurulation, and in central nervous system progenitors shortly after neural tube closure. We find that separate *cis*-regulatory elements control the expression in these two distinct lineages. Using CRISPR/Cas9-mediated mutagenesis, we knocked out *Pax3/7* in F0 embryos specifically in these two separate territories. *Pax3/7* knockout in the neural plate borders resulted in neural tube closure defects, suggesting an ancient role for Pax3/7 in this chordate-specific process. Furthermore, knocking out *Pax3/7* in the neural impaired Motor Ganglion neuron specification, confirming a conserved role for this gene in patterning the neural tube as well. Taken together, these results suggests that key functions of Pax3/7 in neural tube development are evolutionarily ancient, dating back at least to the last common ancestor of vertebrates and tunicates.

KEYWORDS

Pax3/7, pax3, pax7, ciona, tunicate, neural tube closure, neural plate borders

Introduction

Tunicates are marine non-vertebrate chordates and comprise the sister group to the vertebrates (Delsuc et al., 2006; Putnam et al., 2008). Work on diverse tunicate species such as *Ciona* spp. have contributed to our understanding of chordate evolution and the evolutionary origins of many vertebrate innovations (Lemaire, 2011; Satoh, 2013). In vertebrates, the lateral borders of the neural plate give rise to some of these important vertebrate innovations, such as neural crest cells and placodes. Given their importance to vertebrate development, the evolutionary origins of vertebrate neural crest and placodes have been the subject of much interest (Baker and Bronner-Fraser, 1997; Wada, 2001; Rothstein and Simoes-Costa, 2022). In cephalochordates and tunicates, a dorsal neural plate also gives rise to a hollow neural tube in a process that is similar to vertebrate neurulation (Nicol and Meinertzhagen, 1988; Albuixech-Crespo et al., 2017) (Figure 1A). The lateral borders of the neural plate (and later the dorsal part of the neural tube) in these non-vertebrate chordates also give rise to putative homologs of certain cell types that are

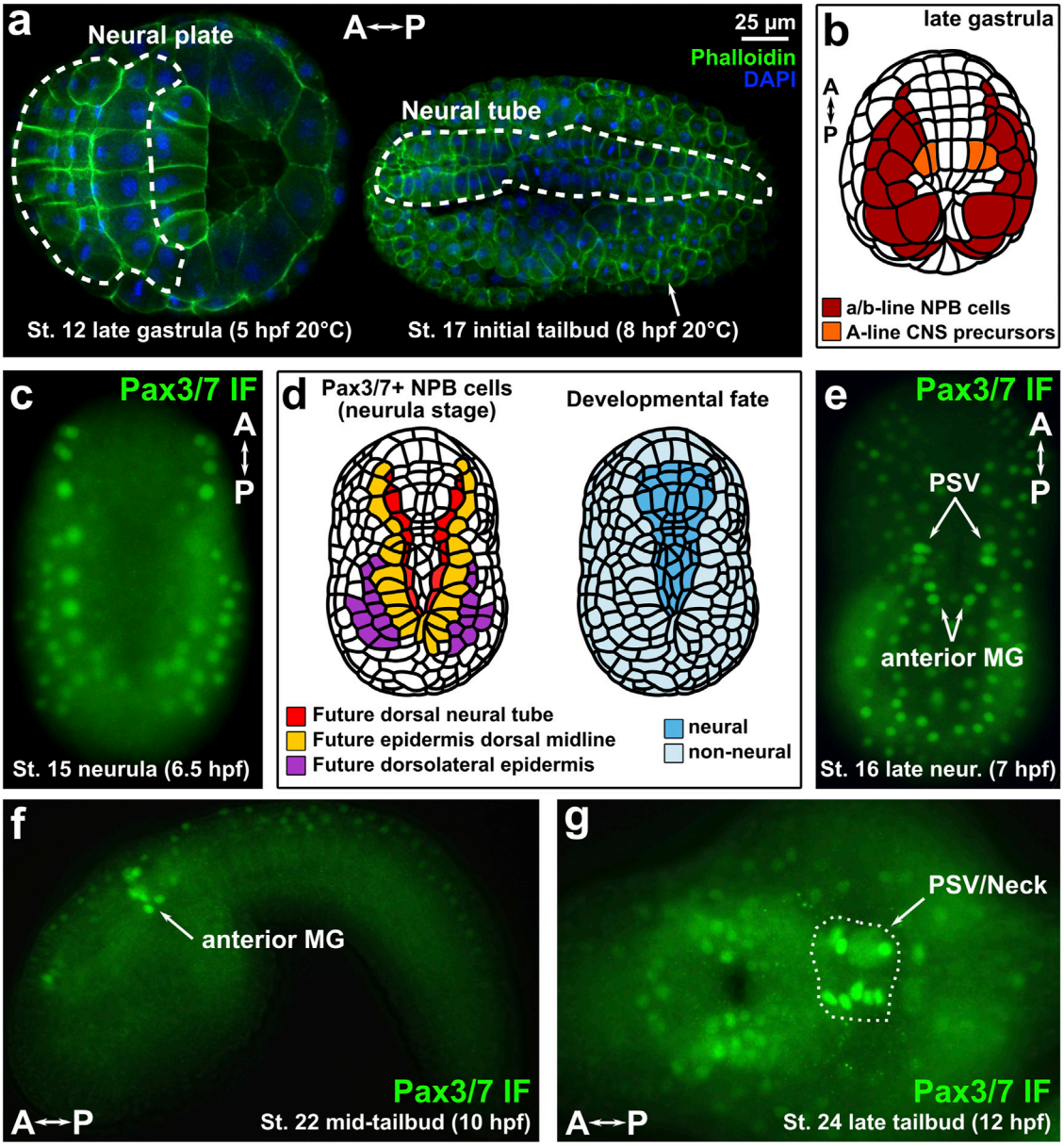

FIGURE 1
Immunofluorescence of Pax3/7 in Ciona embryos. **(A)** Ciona robusta (intestinalis type A) embryos showing neural plate and neural tube cells. **(B)** Diagram of late gastrula Ciona embryo showing Pax3/7-expressing territories examined in this study. NPB: Neural Plate Borders. CNS: Central Nervous System. **(C)** Immunofluorescence (IF) of Pax3/7 (DP312 antibody) showing expression in lateral borders of the neural plate. **(D)** Diagram of Pax3/7 + cells in the neural plate borders, indicating their ultimate contribution tothree different dorsal derivatives of the neural/non-neural boundary region of the ectoderm: dorsal neural tube, dorsal midline epidermis, and dorsolateral epidermis. **(E)** IF of Pax3/7 at the late neurula/initial tailbud stage in which specific Motor Ganglion (MG) and Posterior Sensory Vesicle (PSV) neural progenitors are labelled by anti-Pax3/7 DP312 antibody. **(F)** IF of Pax3/7 in the anterior MG of the mid-tailbud embryo. **(G)** IF of Pax3/7 at late tailbud stage, showing expression in the brain and "Neck" regions of the CNS (circled by dashed line). A–P: anterior-posterior axis.

derived from placodes and/or neural crest in vertebrates, like for instance melanin-containing pigment cells and sensory neurons (Holland et al., 1999; Yu et al., 2008; Abitua et al., 2012; Stolfi et al., 2015). A more recent model has been proposed wherein the olfactorian ancestor (last common ancestor of tunicates and vertebrates) had a placode-like embryonic territory flanking the neural plate giving rise to sensory neurons (Horie et al., 2018; Papadogiannis et al., 2022). Later elaboration of the neural plate borders would have resulted in more specialized neural crest and placodes in vertebrates.

Whatever the exact evolutionary history of neural crest and placodes, it has become clear that the lateral borders of the neural plate has been an important source of evolutionary novelties in chordate evolution. Several transcription factors show conserved, overlapping expression patterns that define these borders, among them Zic, Tfap2, Msx, and Pax3/7 (Thawani and Groves, 2020). Of these, Pax3/7 factors are arguably the most specific to the neural plate borders themselves. In vertebrates, Pax3 and Pax7 play diverse roles in the specification of neural crest cells and placodes (Maczkowiak et al., 2010; Milet and Monsoro-Burq, 2012). They are also required for neural tube closure and patterning of the dorsal neural tube, which arises from the neural plate borders in vertebrates (Epstein et al., 1991; Mansouri and Gruss, 1998). Thus, Pax3/7 factors are indispensable for neural plate border specification and later development of diverse neural crest-, placode-, and neural tube-derived cell types in vertebrates.

Given the importance of Pax3/7 factors in neural plate border specification in vertebrates, we sought to study its potentially conserved functions in *Ciona*. Understanding the role of Pax3/7 in *Ciona* might shed light on the potentially ancestral functions of this important factor in the last common chordate ancestor, predating the origins of vertebrate neural crest and placodes. In tunicates, a conserved *Pax3/7* ortholog is expressed in the neural plate borders of the embryo (Wada et al., 1997; Mazet et al., 2005; Stolfi et al., 2015). In the stereotyped, miniature embryos of *Ciona* and *Halocynthia roretzi,* this means that Pax3/7 expression is observed at the neurula stage as invariant anterior-posterior rows of cells fated to form the dorsal row of the neural tube and the dorsal and dorsolateral cells of the epidermis, prior to neural tube closure. Additionally, Pax3/7 is also expressed in progenitor cells located in the lateral rows of the neural tube after its closure. More specifically, this includes the anterior part of the Motor Ganglion (MG), which was proposed to be homologous to dorsal parts of the rhombospinal regions of the vertebrate nervous system (Stolfi et al., 2011). Although in vertebrates the dorsal neural tube is derived from the neural plate borders, this is not the case in *Ciona,* in which Pax3/7+ MG precursors are not derived from Pax3/7+ neural plate border cells but rather from an entirely different lineage altogether (Nicol and Meinertzhagen, 1988; Cole and Meinertzhagen, 2004; Imai et al., 2009) (Figure 1B). Thus, while Pax3/7+ neural plate border cells are derived from the animal pole of the *Ciona* embryo (a/b-lineages), Pax3/7+ MG cells are derived from the vegetal pole (A-lineage).

Here we use tissue-specific CRISPR/Cas9 to investigate the function of *Pax3/7* in these different cell lineages that are evolutionarily linked to the vertebrate neural plate border and its derivatives. We show that knocking out *Pax3/7* in the neural plate borders impairs neural tube closure, as well as specific gene expression. *Pax3/7* knockout in the MG also confirmed its crucial role in patterning this compartment and specifying commissural neurons similar to its role in the vertebrate dorsal spinal cord. These results show that, although tunicates lack conventional neural crest and cranial placodes, conserved Pax3/7-dependent programs for neural plate border specification, neural tube closure, and motor circuit patterning likely predate the origin of vertebrates.

Methods

Immunofluorescence of Pax3/7

Monoclonal antibodies DP311 and DP312, raised against *Drosophila* Prd (Davis et al., 2005) were kindly provided by Nipam Patel. Embryos were fixed in MEM-FA (3.7% formaldehyde, 0.1 M MOPS pH7.4, 0.5 M NaCl, 1 mM EGTA, 2 mM MgSO4, 0.05% Triton X-100), washed/quenched in 1X PBS, 0.35% Triton X-100, 50 mM NH4Cl, and washed in 1X PBS, 0.05% Triton X-100. Embryos were then blocked for 30 min at room temperature in "Blocker" Buffer (1X PBS, 0.05% Triton X-100, 1% Thermo Scientific "Blocker" BSA). Embryos were incubated in antibodies 1:100 in "Blocker" Buffer overnight at 4°C. Embryos were washed three times in 1X PBS, 0.05% Triton X-100 (rocking 15 min at room temperature, each time). Samples were incubated in AlexaFluor-488 anti-mouse IgG secondary antibody 1: 500 in Blocker buffer for 1 h at room temperature. Washes were performed as in the previous step before mounting and imaging.

Embryo electroporations

Gravid adult *Ciona robusta (intestinalis Type A)* were collected and shipped by M-REP from San Diego, CA. Embryo dechorionation and electroporation was performed as previously established (Christiaen et al., 2009a, Christiaen et al., 2009b). Fluorescent reporter plasmids were electroporated at concentrations of 10–35 μg/700 μl electroporation volume for histone fusions, and 70–100 μg/700 μl for other reporters. Leech H2B::mCherry and Unc-76::GFP/YFP reporter plasmid backbones have been previously published (Gline et al., 2009; Imai et al., 2009). *Tyrp. a>2XGFP* was a kind gift from Filomena Ristoratore (Racioppi et al., 2014). Embryos were fixed and washed as for immunofluorescence above, without blocking or incubating. Embryos were mounted in Mounting Solution (1X PBS, 2% DABCO, 50% Glycerol) and imaged on compound epifluorescence or scanning-point confocal microscopes. All relevant sequences can be found in Supplementary Material S1.

CRISPR/Cas9

Pax3/7 sgRNA expression cassettes on the "F + E" optimized scaffold (Chen et al., 2013; Stolfi et al., 2014) were designed by

CRISPOR (Haeussler et al., 2016) and cloned together with the U6 promoter (Nishiyama and Fujiwara, 2008) by One-Step Overlap PCR (OSO-PCR) as previously described (Gandhi et al., 2017; Gandhi et al., 2018). OSO-PCR cassettes were individually tested for mutagenesis efficacy by the "peakshift" method (Gandhi et al., 2018) before cloning into plasmids, by electroporating 25 µl of unpurified PCR product and 25 µg of Eef1α>Cas9 (Sasakura et al., 2010; Stolfi et al., 2014) per 700 µl volume (Supplementary Table S1). Amplicons representing alleles from pools of embryos were PCR amplified and Sanger-sequenced as detailed in Gandhi et al., 2018. All sgRNA, Cas9 vector, and primer sequences and electroporation recipes are in Supplementary Material S1.

Results

Immunofluorescence of Pax3/7

To visualize Pax3/7 expression in the neural plate borders of *C. robusta* (also known as *intestinalis Type A*), we performed immunofluorescence (IF) staining of neurula- and tailbud-stage embryos using monoclonal antibodies raised against the *Drosophila* Pax3/7 ortholog (Paired), which show broad specificity for pan-metazoan Pax3/7 proteins (Davis et al., 2005). Both antibody clones DP311 and DP312 showed staining of nuclearly-localized Pax3/7 expressed in anterior-posterior rows of cells at the mid-neurula stage, which will contribute to dorsal neural tube and dorsal midline/dorsolateral epidermis later on (Figures 1C,D, Supplementary Figure S1) (St. 15; 6.5 h post-fertilization or hpf at 20˚C), consistent with its expression by mRNA *in situ* hybridization as previously reported in *Ciona* (Stolfi et al., 2015) and in the nearly identical embryos of another tunicate species, *Halocynthia roretzi* (Ohtsuka et al., 2014). Although DP311 showed qualitatively less background, DP312 staining was brighter overall, so we proceeded with the latter clone. At late neurula stage (St. 16; 7 hpf at 20˚C), staining started to appear in the progenitors of the posterior sensory vesicle (PSV) region of the brain, and anterior MG (Figure 1E). At mid-tailbud stage (St. 22; 10 hpf at 20˚C), Pax3/7 IF signal was observed in the lateral rows of the anterior MG (Figure 1F), while slightly later at St. 24 (12 hpf, 20˚C) signal was stronger in the PSV and "neck", which are neural progenitors situated between the neurons of the brain and the MG (Figure 1G). These patterns are also consistent with those detected by *Pax3/7 in situ* hybridization previously (Imai et al., 2009; Stolfi et al., 2011).

Cis-regulatory modules controlling *Pax3/7* expression

Because the early (neurula) and late (tailbud) domains of Pax3/7 expression are not connected by descent, arising from distinct blastomeres of the 8-cell stage embryo, we hypothesized that separate *cis*-regulatory modules might control their activation in the different lineages. Previously, a ~3.5 kb sequence immediately upstream of the *Pax3/7* transcription start site had been shown to drive reporter gene expression in the neural plate borders (Horie et al., 2018) (Figure 2A). We tested a longer sequence stretching further upstream, comprising -5877 bp upstream of the Pax3/7 start codon, alongside the *Fgf8/17/18* reporter which labels the A9.30 lineage that gives rise to most of the MG (Imai et al., 2009) The extended fragment was sufficient to drive GFP reporter gene expression in both the neural plate border derivatives and the lateral rows of the neural tube in the brain, neck, and anterior MG (Figure 2B). Expression in the Neck was often not as bright as in the brain or MG, reflecting perhaps the apparent downregulation in this compartment as observed by *in situ* previously (Imai et al., 2009). When we isolated just the -5877 to -4121 fragment and placed this in front of the basal promoter of the *Friend of GATA* gene (bpFOG), which is routinely used in *Ciona* as a minimal promoter, (Rothbächer et al., 2007), this was sufficient to drive GFP expression in the brain/neck/MG but not in the neural plate borders (Figure 2C). Expression was seen in both A11.120 and A11.119 left/right pairs of neural progenitor cells in the MG. Although expression of *Pax3/7* in A11.119 appears to be downregulated when observed by *in situ* hybridization (Stolfi et al., 2011), it has been reported as initiating in the mother cell (A10.60). Thus, this likely represents GFP protein accumulation, and is consistent with the IF staining observed at 10 hpf (Figure 1E).

We also identified separate *cis*-regulatory elements in introns 1 and 4 that were also sufficient to drive expression in neural plate border derivatives (Figures 2D,E), hinting at complex regulatory control of *Pax3/7* expression through partially overlapping "shadow enhancers" (Hong et al., 2008). Taken together, our results suggest that the different domains of *Pax3/7* expression in the neurectoderm (neural plate borders and lateral rows of the brain/neck/MG) are largely regulated by distinct *cis*-regulatory elements (Figure 2F).

CRISPR/Cas9-mediated knockout of *Pax3/7*

To study the functions of *Pax3/7* in neural development in the tunicate embryo, we sought to use tissue-specific CRISPR/Cas9 as previously adapted to *Ciona* (Sasaki et al., 2014; Stolfi et al., 2014; Gandhi et al., 2017). We tested two candidate single-chain guide RNA (sgRNA) constructs (Pax3/7.2.1 and Pax3/7.4.1), targeting exons 2 and 4 respectively (Figure 3A). We validated their mutagenesis efficacies following the "peakshift" method of Sanger-sequencing PCR amplicons of targeted sequences (Gandhi et al., 2018). Efficacies for Pax3/7.2.1 and Pax3/7.4.1 were 17% and 34% mutagenesis, respectively (Figure 3B) (Supplementary Table S1).

We next tested the ability of these sgRNAs, when combined, in eliminating Pax3/7 expression from the neural plate borders.

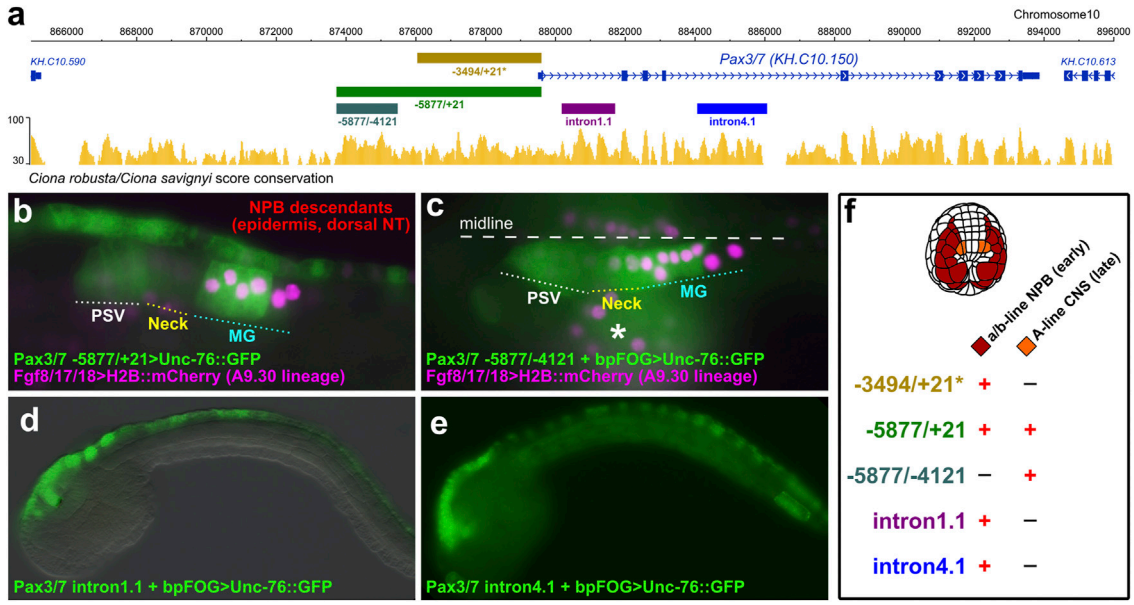

FIGURE 2
Pax3/7 reporter plasmids. **(A)** Diagram from ANISEED genome browser (Dardaillon et al., 2020), showing location of *cis*-regulatory sequences and conservation between *Ciona robusta/savignyi*. Asterisk denotes -3494 upstream fragment previously published (Horie et al., 2018). **(B)** Late tailbud (St. 23) embryo electroporated with *Pax3/7–5877/+21>Unc-76::GFP* and *Fgf8/17/18>H2B::mCherry* (which labels the A9.30 lineage that gives rise to most of the MG), showing expression in neural plate border (NPB) descendants in the dorsal midline of the epidermis and neural tube, and in compartments of the central nervous system (CNS) including Posterior Sensory Vesicle (PSV) and Motor Ganglion (MG). **(C)** St. 23 embryo electroporated with *Pax3/7–5877/-4121 + bpFOG>Unc-76::GFP* and *Fgf8/17/18>H2B::mCherry,* showing expression only in the CNS, not in the NPB descendants. Asterisk indicates mesenchyme, which shows leaky expression of reporters. **(D)** Embryo electroporated with *Pax3/7 intron1.1 + bpFOG>Unc-76::GFP*. This partial intronic fragment drives reporter gene expression in the descendants of the NPBs. **(E)** Embryo electroporated with *Pax3/7 intron4.1 + bpFOG>Unc-76::GFP*. This partial intronic fragment also drives expression in part of the NPB descendants. **(F)** Summary of expression observed with the different *Pax3/7* reporter constructs, indicating expression in a/b-line and A-line cells. bpFOG = basal promoter of *FOG*, which is used as a minimal promoter to test isolated *cis*-regulatory elements in *Ciona*. Unc-76::GFP = GFP tagged with an Unc-76 fragment used to exclude GFP from the nucleus and to completely fill axons, routinely used in *Ciona*.

To do this, we co-electroporated the sgRNAs with *FOG>Cas9*, which drives Cas9 expression in all animal pole-derived cells including the neural plate borders. A *FOG>CD4::mCherry* reporter plasmid was also co-electroporated to reveal transfected cells' outlines, and DP312 antibody IF was used to assay Pax3/7 expression. Pax3/7 sgRNAs were compared to a negative control sgRNA ("Control") that does not target any sequence in the *Ciona* genome (Stolfi et al., 2014). While in the negative control neurula embryos (St. 16) the Pax3/7 antibody clearly labeled the nuclei of both transfected and non-transfected cells (Figure 3C), we detected substantial loss of Pax3/7 IF signal in cells transfected with *Pax3/7* CRISPR constructs. Non-transfected cells in the same embryos served as a clean internal control for Pax3/7 IF, showing that the loss of Pax3/7 was visibly confined to only transfected cells. In some embryos, no Pax3/7+ cells were seen at all in the transfected half, suggesting biallelic knockout of *Pax3/7*.

To score this, we performed Pax3/7 IF on *Pax3/7* CRISPR and negative control embryos co-electroporated *FOG>H2B::mCherry* to visualize the nuclei of transfected cells at stage 16 (Figure 3D; Supplementary Figure S2). Cells were scored for H2B::mCherry expression and Pax3/7 IF signal, independently on either left or right borders of the neural plate to account for mosaicism (Figure 3E). Embryos with no H2B::mCherry expression in the neural plate borders (untransfected) were not included, as were embryos oriented in a way that obscured the view of the neural plate borders. In 52 such *Pax3/7* CRISPR embryo halves, 40 were H2B::mCherry+, but only 7 of those were also positive for Pax3/7 while 33 were negative, indicating loss of Pax3/7 in 82% of transfected neural plate borders. In negative control embryos, 42 of 43 H2B::mCherry + halves were positive for Pax3/7. Pax3/7 was observed in 100% of untransfected (H2B::mCherry-negative) neural plate border cells in both *Pax3/7* CRISPR (12/12) and negative control embryos (10/10). In sum, these results confirmed the specificity and high efficacy of *Pax3/7* CRISPR knockout in this system.

Knockout of *Pax3/7* in the neural plate borders impairs neural tube closure

In *Ciona* and vertebrates, neural tube closure is driven in part by epithelial "zippering" involving the formation of

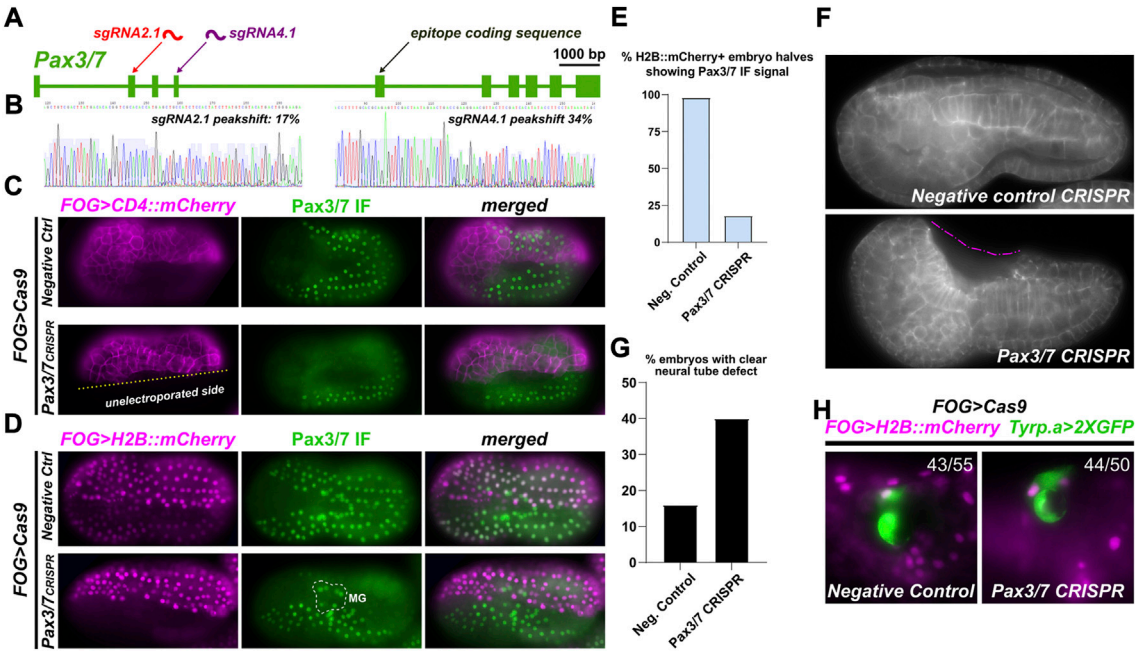

FIGURE 3
Pax3/7 CRISPR in the neural plate borders. **(A)** Diagram of *Pax3/7* locus and location of sgRNA targets, relative to epitope sequence recognized by DP312 antbody. **(B)** Peakshift sequencing traces indicating presence of indels resulting from CRISPR/Cas9-mediated double-stranded DNA breaks. **(C)** Tissue-specific CRISPR/Cas9-mediated knockout of *Pax3/7*, performed in a/b-line cells using the *FOG>Cas9* plasmid and assayed by DP312 immunofluorescence at stage 16. *FOG>CD4::mCherry* counterstains cell membranes, demonstrating the specificity and efficacy of *Pax3/7* knockout. **(D)** *Pax3/7* CRISPR and negative control embryos generated as above (same stage also), but using *FOG>H2B::mCherry* to score proportion of CRISPR knockouts. Motor Ganglion (MG) cells are not derived from a/b lineages, and therefore Cas9 is never expressed in their lineage. Thus, Pax3/7 signal is not lost from the MG, only NPBs. **(E)** Embryos scored for loss of Pax3/7 immunofluorescent signal (from panel d), showing substantial loss of staining in *Pax3/7* CRISPR H2B::mCherry+ NPB cells (n = 40 embryo halves) compared to negative control (n = 43 halves). **(F)** *Pax3/7* CRISPR and negative control (U6>DenhT2) embryos stained with fluorescent phalloidin conjugate to reveal cell outlines after neural tube closure, at stage 20. Dashed pink line denotes a large cavity as a result of failed neural tube closure. **(G)** Embryos above were scored for incomplete neural tube closure defect (n = 100 embryos each condition). Embryos with inconclusive neural tube closure phenotype were not scored as defective. **(H)** *Pax3/7* CRISPR does not affect the specification of neural plate border-derived pigment cells. Ratios indicate number of FOG>H2B::mCherry+ larvae (19 hpf, 20°C) showing *Tyrp.a>2XGFP* reporter expression (43 of 55 larvae in negative control, 44 of 50 larvae in *Pax3/7* CRISPR).

cellular "rosettes" in which cells undergo sequential apical contraction and cell junction exchange (Hashimoto et al., 2015; Hashimoto and Munro, 2019; Mole et al., 2020). In some of our CRISPants, we noticed a lack of such rosettes and epithelial zippering, implying that perhaps loss of *Pax3/7* might impair this process (Figure 3C; Supplementary Figure S3). In vertebrates, Pax3/7 factors are essential for neural tube closure (Epstein et al., 1991). Thus, we sought to determine if CRISPR knockout of *Pax3/7* might induce similar neural tube defects in *Ciona*.

We carried out tissue-specific knockout of *Pax3/7* as described above, targeting Cas9 and therefore CRISPR activity to the animal pole (neural plate borders, not brain/neck/MG). We then imaged early tailbud embryos (St. 20) looking for any neural tube closure defects, not differentiating between mild or severe defects (Figure 3F). When we scored *Pax3/7* CRISPR embryos (Figure 3G), we observed defects in 40% of embryos (n = 100). 36% had seemingly normal neural tube closure, while 22% of embryos were "unclear" due to orientation of embryo on the slide. In contrast, in embryos electroporated with the same components except a negative control sgRNA ("DenhT2") in the place of *Pax3/7*-specific sgRNAs, only 16% embryos showed a neural tube defect of any severity, likely due to non-specific effects of dechorionation/electroporation. 59% of negative control embryos were normal, while 25% were unclear. These data suggest that, as in vertebrates, Pax3/7 is required in the neural plate borders for normal neural tube closure.

To test whether Pax3/7 regulates conserved gene expression and/or specifies conserved cell types derived from the neural plate borders in *Ciona*, we focused on the melanin-containing pigment cells that give rise to the ocellus and otolith pigment cells. These two cells arise from the neural plate borders and might be evolutionarily linked to neural crest-derived melanocytes in vertebrates (Abitua et al., 2012; Olivo et al., 2021). However, *Pax3/7* CRISPR did not significantly affect their specification, as

10.3389/fcell.2022.999511

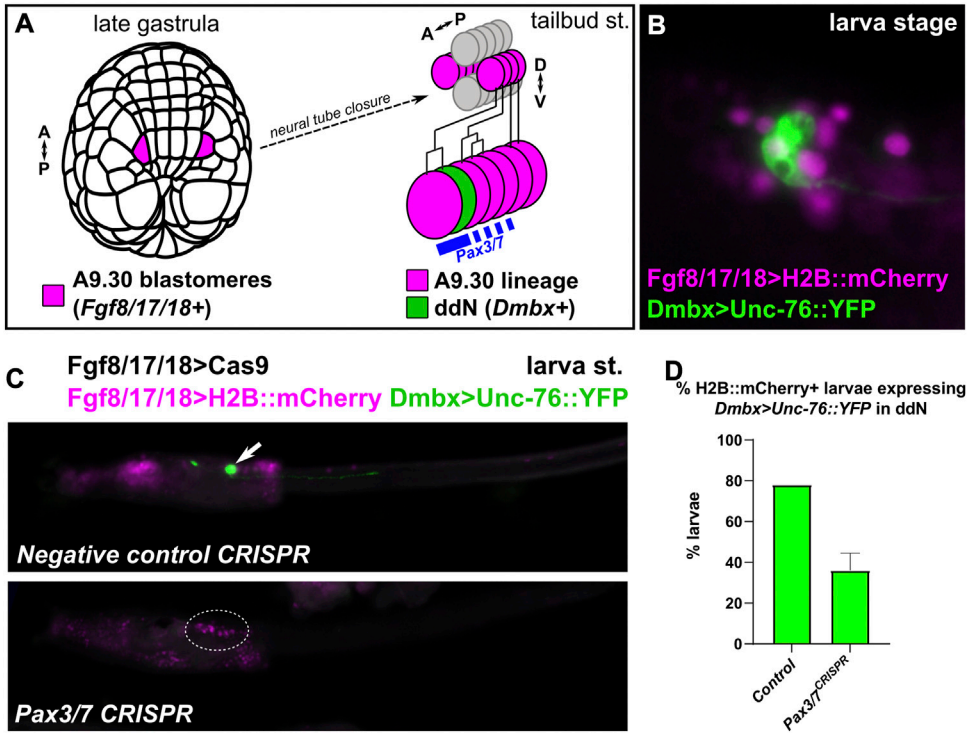

FIGURE 4
Pax3/7 CRISPR in the Motor Ganglion. **(A)** Diagram indicating the descent of the A9.30 pair of blastomeres which give rise to the Pax3/7+ cells of the anterior Motor Ganglion (MG), including the *Dmbx*-expressing descending decussating neuron (ddN). A–P: anterior-posterior, D–V: dorsal-ventral. **(B)** Larva electroporated with *Fgf8/17/18>H2B::mCherry* and *Dmbx > Unc-76::YFP*, showing the Dmbx+ ddN cell. **(C)** A9.30 lineage-specific CRISPR/Cas9-mediated knockout of *Pax3/7* using *Fgf8/17/18>Cas9* to limit CRISPR activity to the A9.30 lineage, avoiding other territories (e.g. neural plate borders). *Dmbx* reporter plasmid labels ddNs (arrow) in negative control larvae, but this labeling is eliminated (dotted outline) in a large proportion of *Pax3/7* CRISPR larvae. **(D)** Larvae at left were scored for presence/absence of *Dmbx* reporter expression in the ddNs. Experiment was performed in duplicate, n = 50 for each condition per replicate. Error bars indicate range.

assayed by expression of the *Tyrp.a>2XGFP* reporter (Racioppi et al., 2014). Therefore, we cannot conclude whether Pax3/7 is required or not for the specification and differentiation of neural plate border-derived cell types in *Ciona*.

MG-specific knockout of *Pax3/7* blocks ddN specification

Although its role in specifying cells derived from the animal pole-derived lineages of the neural plate borders of *Ciona* remains unclear, Pax3/7 was previously shown to specify anterior MG fates derived from more medial cells of the neural plate. Pax3/7 is required for the specification of a single pair of descending decussating neurons (ddNs, A12.239 cell pair), which was shown through a combination of morpholino knockdown (Imai et al., 2009), overexpression of full-length Pax3/7 and dominant-repressor (Pax3/7::WRPW) as well as *cis*-regulatory analyses (Stolfi et al., 2011). However, a genetic knockout of *Pax3/7* was never attempted in the *Ciona* MG. We used the *Fgf8/17/18* promoter (Imai et al., 2009) to drive expression of Cas9 in the A9.30 lineage, which gives rise to most of the core MG including the ddNs (Figure 4A). *Fgf8/17/18>Cas9* was co-electroporated with *Pax3/7*-targeting sgRNAs and a *Dmbx* reporter plasmid (Figure 4B) (Stolfi and Levine, 2011), and larvae were assayed for reporter gene expression in ddNs. As predicted, an average of 36% of *Pax3/7* CRISPR larvae showed *Dmbx* reporter expression across two replicates, compared to an average of 78% of negative control CRISPR larvae (Figures 4C,D). These results further confirm the requirement of Pax3/7 in the regulation of *Dmbx* expression and ddN specification in the *Ciona* MG.

Discussion

Here we show that the main ortholog of vertebrate *Pax3* and *Pax7* in tunicates, *Pax3/7,* plays conserved roles in neural development. In vertebrates, *Pax3* and *Pax7* have overlapping expression patterns and functions, which evolved following duplication of a single ancestral *Pax3/7* gene (Wada et al., 1997). While *Ciona* also has a divergent, tunicate-specific *Pax3/7* paralog which has been named *Pax3/7-related* (ANISEED gene ID: Cirobu.g00006874), that lacks the paired box domain and is not significantly expressed during embryogenesis (Imai et al., 2004). Expression of *Pax3/7* in the neural plate borders of tunicates is interesting as it implies specific ancestral functions that predate the emergence of neural crest in vertebrates, which arise from this territory and depend on Pax3/7 for their specification (Monsoro-Burq, 2015).

We have shown that *Pax3/7* is expressed in the lateral borders of the neural plate in *Ciona* and is required there for proper neural tube closure of *Ciona*, as shown by our CRISPR/Cas9-mediated knockout. Nodal signaling has been previously implicated in neural tube closure in *Ciona* (Mita and Fujiwara, 2007). One of the direct transcriptional targets of the Nodal pathway in the neural plate borders is *Pax3/7* (Mita et al., 2010). Therefore, the effects of Nodal perturbation on neural tube closure observed might be effected in part by Pax3/7 function. Pax3 mouse mutants show frequent neural tube defects (Epstein et al., 1991; Greene et al., 2009; Sudiwala et al., 2019), and mutations in the human *PAX3* gene have been found in a small number of individuals with neural tube defects (Hart and Miriyala, 2017). In mouse, supplementation of folic acid suppresses the incidence of neural tube defects in Pax3 mutants, suggesting that understanding Pax3 function is key to understanding how folic acid works to prevent neural tube defects in human development (Burren et al., 2008). However, little is known about how the transcriptional targets of Pax3 contribute to neural tube closure. *Ciona* embryos have been shown to be a powerful model for studying the cellular dynamics of neural tube closure, especially the process for epithelial zippering (Hashimoto et al., 2015; Hashimoto and Munro, 2019). Given the defects observed in this process upon CRISPR/Cas9-mediated knockout of *Pax3/7,* we propose that *Ciona* might also be a good model in which to study potentially conserved effectors of neural tube closure.

We were not able to answer whether or not Pax3/7 is required for the specification of conserved cell types arising from the neural plate borders in *Ciona,* nor what its transcriptional targets might be in this territory. In *Halocynthia,* injected *Pax3/7* mRNA was previously shown to be sufficient to activate ectopic pigment cell gene expression (Wada et al., 1997). This discrepancy might be due to species differences, or might point to Pax3/7 being sufficient, but not necessary, for pigment cell specification in tunicates. Future studies will be required to identify the targets of Pax3/7 in the tunicate neural plate borders and compare them to Pax3/7 targets in vertebrates, especially genes required for the specification of cell types derived from neural crest. One possibility is that role of Pax3/7 in the development of neural crest-derived cell types (e.g. melanocytes) is a vertebrate innovation, even if their developmental origins from the neural plate borders might predate the appearance of neural crest and vertebrates themselves.

Finally, we show that *Ciona* Pax3/7 is required later on for the specification of neurons in the anterior MG, which is proposed to be homologous to vertebrate dorsal spinal cord and hindbrain (Stolfi et al., 2011; Ryan et al., 2017). In vertebrates, there is lineage continuity between the neural plate borders and the dorsal neurons of the spinal cord and hindbrain. It was shown that separate *cis*-regulatory elements control the onset and maintenance of *Pax3* expression in the vertebrate neural plate borders/dorsal neural tube (Moore et al., 2013), and it was proposed that these separate elements control onset and maintenance in the same cell lineage (Moore et al., 2013). In contrast, the *Pax3/7*-expressing cells of the neural plate border (a/b-lineage) do not give rise to later *Pax3/7*-expressing MG neurons (A-lineage) in *Ciona* (Imai et al., 2009). We propose that the physical and ontological separation between rhombospinal neural progenitors and neural plate borders is a tunicate-specific innovation. *Pax3/7* expression would have been split into these two separate lineages through the elaboration of two separate *cis*-regulatory elements. It is possible that the last common ancestor had separate elements for onset and maintenance of *Pax3/7* expression, and that in tunicates the "onset" element became dedicated exclusively to earlier neural plate border expression, while the "maintentance" element became dedicated to later neural tube expression. Further analysis of these different *cis*-regulatory elements will be needed to refine this evolutionary model.

Data availability statement

The original contributions presented in the study are included in the article/Supplementary Materials, further inquiries can be directed to the corresponding author.

Author contributions

This study was conceived by AS, KK, and JO. Experiments were performed and data collected by AS, KK, and JO Data was analyzed by AS, KK, and JO. Initial draft was written by AS. AS and KK edited the draft.

Funding

This study was funded by NSF IOS grant 1940743 to AS.

Acknowledgments

The authors would like to thank Florian Razy-Krajka and Susanne Gibboney for technical support. The authors also thank Katarzyna Piekarz for feedback and helpful suggestions. We are grateful to Nipam Patel and Gabrielle Jerz for sending the DP311 and DP312 antibodies.

Conflict of interest

The authors declare that the research was conducted in the absence of any commercial or financial relationships that could be construed as a potential conflict of interest.

Publisher's note

Supplementary material

The Supplementary Material for this article can be found online at: https://www.frontiersin.org/articles/10.3389/fcell.2022.999511/full#supplementary-material

References

Abitua, P. B., Wagner, E., Navarrete, I. A., and Levine, M. (2012). Identification of a rudimentary neural crest in a non-vertebrate chordate. *Nature* 492, 104–107. doi:10.1038/nature11589

Albuixech-Crespo, B., Herrera-Ubeda, C., Marfany, G., Irimia, M., and Garcia-Fernandez, J. (2017). Origin and evolution of the chordate central nervous system: Insights from amphioxus genoarchitecture. *Int. J. Dev. Biol.* 61, 655–664. doi:10.1387/ijdb.170258jg

Baker, C. V. H., and Bronner-Fraser, M. (1997). The origins of the neural crest. Part II: An evolutionary perspective. *Mech. Dev.* 69, 13–29. doi:10.1016/s0925-4773(97)00129-9

Burren, K. A., Savery, D., Massa, V., Kok, R. M., Scott, J. M., Blom, H. J., et al. (2008). Gene–environment interactions in the causation of neural tube defects: Folate deficiency increases susceptibility conferred by loss of Pax3 function. *Hum. Mol. Genet.* 17, 3675–3685. doi:10.1093/hmg/ddn262

Chen, B., Gilbert, L. A., Cimini, B. A., Schnitzbauer, J., Zhang, W., Li, G.-W., et al. (2013). Dynamic imaging of genomic loci in living human cells by an optimized CRISPR/Cas system. *Cell* 155, 1479–1491. doi:10.1016/j.cell.2013.12.001

Christiaen, L., Wagner, E., Shi, W., and Levine, M. (2009a). Electroporation of transgenic DNAs in the sea squirt Ciona. *Cold Spring Harb. Protoc.* 2009, pdb.prot5345. doi:10.1101/pdb.prot5345

Christiaen, L., Wagner, E., Shi, W., and Levine, M. (2009b). Isolation of sea squirt (Ciona) gametes, fertilization, dechorionation, and development. *Cold Spring Harb. Protoc.* 2009, pdb.prot5344. doi:10.1101/pdb.prot5344

Cole, A. G., and Meinertzhagen, I. A. (2004). The central nervous system of the ascidian larva: Mitotic history of cells forming the neural tube in late embryonic *Ciona intestinalis*. *Dev. Biol.* 271, 239–262. doi:10.1016/j.ydbio.2004.04.001

Dardaillon, J., Dauga, D., Simion, P., Faure, E., Onuma, T. A., DeBiasse, M. B., et al. (2020). Aniseed 2019: 4D exploration of genetic data for an extended range of tunicates. *Nucleic Acids Res.* 48, D668–D675. doi:10.1093/nar/gkz955

Davis, G. K., D'Alessio, J. A., and Patel, N. H. (2005). Pax3/7 genes reveal conservation and divergence in the arthropod segmentation hierarchy. *Dev. Biol.* 285, 169–184. doi:10.1016/j.ydbio.2005.06.014

Delsuc, F., Brinkmann, H., Chourrout, D., and Philippe, H. (2006). Tunicates and not cephalochordates are the closest living relatives of vertebrates. *Nature* 439, 965–968. doi:10.1038/nature04336

Epstein, D. J., Vekemans, M., and Gros, P. (1991). Splotch (Sp2H), a mutation affecting development of the mouse neural tube, shows a deletion within the paired homeodomain of Pax-3. *Cell* 67, 767–774. doi:10.1016/0092-8674(91)90071-6

Gandhi, S., Haeussler, M., Razy-Krajka, F., Christiaen, L., and Stolfi, A. (2017). Evaluation and rational design of guide RNAs for efficient CRISPR/Cas9-mediated mutagenesis in Ciona. *Dev. Biol.* 425, 8–20. doi:10.1016/j.ydbio.2017.03.003

Gandhi, S., Razy-Krajka, F., Christiaen, L., and Stolfi, A. (2018). *CRISPR knockouts in Ciona embryos, transgenic ascidians*. Berlin, Germany: Springer, 141–152.

Gline, S. E., Kuo, D. H., Stolfi, A., and Weisblat, D. A. (2009). High resolution cell lineage tracing reveals developmental variability in leech. *Dev. Dyn.* 238, 3139–3151. doi:10.1002/dvdy.22158

Greene, N. D. E., Massa, V., and Copp, A. J. (2009). Understanding the causes and prevention of neural tube defects: Insights from the splotch mouse model. *Birth Defects Res. A Clin. Mol. Teratol.* 85, 322–330. doi:10.1002/bdra.20539

Haeussler, M., Schönig, K., Eckert, H., Eschstruth, A., Mianné, J., Renaud, J.-B., et al. (2016). Evaluation of off-target and on-target scoring algorithms and integration into the guide RNA selection tool CRISPOR. *Genome Biol.* 17, 148. doi:10.1186/s13059-016-1012-2

Hart, J., and Miriyala, K. (2017). Neural tube defects in waardenburg syndrome: A case report and review of the literature. *Am. J. Med. Genet. A* 173, 2472–2477. doi:10.1002/ajmg.a.38325

Hashimoto, H., and Munro, E. (2019). Differential expression of a classic cadherin directs tissue-level contractile asymmetry during neural tube closure. *Dev. Cell* 51, 158–172. e154. doi:10.1016/j.devcel.2019.10.001

Hashimoto, H., Robin, F. B., Sherrard, K. M., and Munro, E. M. (2015). Sequential contraction and exchange of apical junctions drives zippering and neural tube closure in a simple chordate. *Dev. Cell* 32, 241–255. doi:10.1016/j.devcel.2014.12.017

Holland, L. Z., Schubert, M., Kozmik, Z., and Holland, N. D. (1999). AmphiPax3/7, an amphioxus paired box gene: Insights into chordate myogenesis, neurogenesis, and the possible evolutionary precursor of definitive vertebrate neural crest. *Evol. Dev.* 1, 153–165. doi:10.1046/j.1525-142x.1999.99019.x

Hong, J.-W., Hendrix, D. A., and Levine, M. S. (2008). Shadow enhancers as a source of evolutionary novelty. *Science* 321, 1314. doi:10.1126/science.1160631

Horie, R., Hazbun, A., Chen, K., Cao, C., Levine, M., and Horie, T. (2018). Shared evolutionary origin of vertebrate neural crest and cranial placodes. *Nature* 560, 228–232. doi:10.1038/s41586-018-0385-7

Imai, K. S., Hino, K., Yagi, K., Satoh, N., and Satou, Y. (2004). Gene expression profiles of transcription factors and signaling molecules in the ascidian embryo: Towards a comprehensive understanding of gene networks. *Development* 131, 4047–4058. doi:10.1242/dev.01270

Imai, K. S., Stolfi, A., Levine, M., and Satou, Y. (2009). Gene regulatory networks underlying the compartmentalization of the Ciona central nervous system. *Development* 136, 285–293. doi:10.1242/dev.026419

Lemaire, P. (2011). Evolutionary crossroads in developmental biology: The tunicates. *Development* 138, 2143–2152. doi:10.1242/dev.048975

Maczkowiak, F., Matéos, S., Wang, E., Roche, D., Harland, R., and Monsoro-Burq, A. H. (2010). The Pax3 and Pax7 paralogs cooperate in neural and neural crest patterning using distinct molecular mechanisms, in *Xenopus laevis* embryos. *Dev. Biol.* 340, 381–396. doi:10.1016/j.ydbio.2010.01.022

Mansouri, A., and Gruss, P. (1998). Pax3 and Pax7 are expressed in commissural neurons and restrict ventral neuronal identity in the spinal cord. *Mech. Dev.* 78, 171–178. doi:10.1016/s0925-4773(98)00168-3

Mazet, F., Hutt, J. A., Milloz, J., Millard, J., Graham, A., and Shimeld, S. M. (2005). Molecular evidence from *Ciona intestinalis* for the evolutionary origin of vertebrate sensory placodes. *Dev. Biol.* 282, 494–508. doi:10.1016/j.ydbio.2005.02.021

Milet, C., and Monsoro-Burq, A. H. (2012). Neural crest induction at the neural plate border in vertebrates. *Dev. Biol.* 366, 22–33. doi:10.1016/j.ydbio.2012.01.013

Mita, K., and Fujiwara, S. (2007). Nodal regulates neural tube formation in the *Ciona intestinalis* embryo. *Dev. Genes Evol.* 217, 593–601. doi:10.1007/s00427-007-0168-x

Mita, K., Koyanagi, R., Azumi, K., Sabau, S. V., and Fujiwara, S. (2010). Identification of genes downstream of nodal in the *Ciona intestinalis* embryo. *Zool. Sci.* 27, 69–75. doi:10.2108/zsj.27.69

Mole, M. A., Galea, G. L., Rolo, A., Weberling, A., Nychyk, O., De Castro, S. C., et al. (2020). Integrin-mediated focal anchorage drives epithelial zippering during mouse neural tube closure. *Dev. Cell* 52, 321–334. doi:10.1016/j.devcel.2020.01.012

Monsoro-Burq, A. H. (2015). PAX transcription factors in neural crest development. *Semin. Cell Dev. Biol.* 44, 87–96. doi:10.1016/j.semcdb.2015.09.015

Moore, S., Ribes, V., Terriente, J., Wilkinson, D., Relaix, F., and Briscoe, J. (2013). Distinct regulatory mechanisms act to establish and maintain Pax3 expression in the developing neural tube. *PLoS Genet.* 9, e1003811. doi:10.1371/journal.pgen.1003811

Nicol, D., and Meinertzhagen, I. A. (1988). Development of the central nervous system of the larva of the ascidian, *Ciona intestinalis* L: II. Neural plate morphogenesis and cell lineages during neurulation. *Dev. Biol.* 130, 737–766. doi:10.1016/0012-1606(88)90364-8

Nishiyama, A., and Fujiwara, S. (2008). RNA interference by expressing short hairpin RNA in the *Ciona intestinalis* embryo. *Dev. Growth Differ.* 50, 521–529. doi:10.1111/j.1440-169X.2008.01039.x

Ohtsuka, Y., Matsumoto, J., Katsuyama, Y., and Okamura, Y. (2014). Nodal signaling regulates specification of ascidian peripheral neurons through control of the BMP signal. *Development* 141, 3889–3899. doi:10.1242/dev.110213

Olivo, P., Palladino, A., Ristoratore, F., and Spagnuolo, A. (2021). Brain sensory organs of the Ascidian Ciona robusta: Structure, function and developmental mechanisms. *Front. Cell Dev. Biol.* 2435, 701779. doi:10.3389/fcell.2021.701779

Papadogiannis, V., Pennati, A., Parker, H. J., Rothbächer, U., Patthey, C., Bronner, M. E., et al. (2022). Hmx gene conservation identifies the origin of vertebrate cranial ganglia. *Nature* 605, 701–705. doi:10.1038/s41586-022-04742-w

Putnam, N. H., Butts, T., Ferrier, D. E. K., Furlong, R. F., Hellsten, U., Kawashima, T., et al. (2008). The amphioxus genome and the evolution of the chordate karyotype. *Nature* 453, 1064–1071. doi:10.1038/nature06967

Racioppi, C., Kamal, A. K., Razy-Krajka, F., Gambardella, G., Zanetti, L., Di Bernardo, D., et al. (2014). Fibroblast growth factor signalling controls nervous system patterning and pigment cell formation in *Ciona intestinalis*. *Nat. Commun.* 5, 4830. doi:10.1038/ncomms5830

Rothbächer, U., Bertrand, V., Lamy, C., and Lemaire, P. (2007). A combinatorial code of maternal GATA, Ets and β-catenin-TCF transcription factors specifies and patterns the early ascidian ectoderm. *Development* 134, 4023–4032. doi:10.1242/dev.010850

Rothstein, M., and Simoes-Costa, M. (2022). On the evolutionary origins and regionalization of the neural crest. *Seminars Cell & Dev. Biol.* 2022. doi:10.1016/j.semcdb.2022.06.008

Ryan, K., Lu, Z., and Meinertzhagen, I. A. (2017). Circuit homology between decussating pathways in the Ciona larval CNS and the vertebrate startle-response pathway. *Curr. Biol.* 27, 721–728. doi:10.1016/j.cub.2017.01.026

Sasaki, H., Yoshida, K., Hozumi, A., and Sasakura, Y. (2014). CRISPR/C as9-mediated gene knockout in the ascidian C iona intestinalis. *Dev. Growth Differ.* 56, 499–510. doi:10.1111/dgd.12149

Sasakura, Y., Suzuki, M. M., Hozumi, A., Inaba, K., and Satoh, N. (2010). Maternal factor-mediated epigenetic gene silencing in the ascidian *Ciona intestinalis*. *Mol. Genet. Genomics* 283, 99–110. doi:10.1007/s00438-009-0500-4

Satoh, N. (2013). *Developmental genomics of ascidians*. New Jersey, US: John Wiley & Sons.

Stolfi, A., Gandhi, S., Salek, F., and Christiaen, L. (2014). Tissue-specific genome editing in Ciona embryos by CRISPR/Cas9. *Development* 141, 4115–4120. doi:10.1242/dev.114488

Stolfi, A., and Levine, M. (2011). Neuronal subtype specification in the spinal cord of a protovertebrate. *Development* 138, 995–1004. doi:10.1242/dev.061507

Stolfi, A., Ryan, K., Meinertzhagen, I. A., and Christiaen, L. (2015). Migratory neuronal progenitors arise from the neural plate borders in tunicates. *Nature* 527, 371–374. doi:10.1038/nature15758

Stolfi, A., Wagner, E., Taliaferro, J. M., Chou, S., and Levine, M. (2011). Neural tube patterning by Ephrin, FGF and Notch signaling relays. *Development* 138, 5429–5439. doi:10.1242/dev.072108

Sudiwala, S., Palmer, A., Massa, V., Burns, A. J., Dunlevy, L. P. E., De Castro, S. C. P., et al. (2019). Cellular mechanisms underlying Pax3-related neural tube defects and their prevention by folic acid. *Dis. Model. Mech.* 12, dmm042234. doi:10.1242/dmm.042234

Thawani, A., and Groves, A. K. (2020). Building the border: Development of the chordate neural plate border region and its derivatives. *Front. Physiol.* 11, 608880. doi:10.3389/fphys.2020.608880

Wada, H., Holland, P. W., Sato, S., Yamamoto, H., and Satoh, N. (1997). Neural tube is partially dorsalized by overexpression ofHrPax-37: The ascidian homologue ofPax-3andPax-7. *Dev. Biol.* 187, 240–252. doi:10.1006/dbio.1997.8626

Wada, H. (2001). Origin and evolution of the neural crest: A hypothetical reconstruction of its evolutionary history. *Dev. Growth Differ.* 43, 509–520. doi:10.1046/j.1440-169x.2001.00600.x

Yu, J.-K., Meulemans, D., McKeown, S. J., and Bronner-Fraser, M. (2008). Insights from the amphioxus genome on the origin of vertebrate neural crest. *Genome Res.* 18, 1127–1132. doi:10.1101/gr.076208.108

frontiers | Frontiers in Cell and Developmental Biology

PERSPECTIVE
published: 23 June 2022
doi: 10.3389/fcell.2022.941168

Marsupials and Multi-Omics: Establishing New Comparative Models of Neural Crest Patterning and Craniofacial Development

Axel H. Newton *†

The School of BioSciences, University of Melbourne, Parkville, VIC, Australia

Studies across vertebrates have revealed significant insights into the processes that drive craniofacial morphogenesis, yet we still know little about how distinct facial morphologies are patterned during development. Studies largely point to evolution in GRNs of cranial progenitor cell types such as neural crest cells, as the major driver underlying adaptive cranial shapes. However, this hypothesis requires further validation, particularly within suitable models amenable to manipulation. By utilizing comparative models between related species, we can begin to disentangle complex developmental systems and identify the origin of species-specific patterning. Mammals present excellent evolutionary examples to scrutinize how these differences arise, as sister clades of eutherians and marsupials possess suitable divergence times, conserved cranial anatomies, modular evolutionary patterns, and distinct developmental heterochrony in their NCC behaviours and craniofacial patterning. In this review, I lend perspectives into the current state of mammalian craniofacial biology and discuss the importance of establishing a new marsupial model, the fat-tailed dunnart, for comparative research. Through detailed comparisons with the mouse, we can begin to decipher mammalian conserved, and species-specific processes and their contribution to craniofacial patterning and shape disparity. Recent advances in single-cell multi-omics allow high-resolution investigations into the cellular and molecular basis of key developmental processes. As such, I discuss how comparative evolutionary application of these tools can provide detailed insights into complex cellular behaviours and expression dynamics underlying adaptive craniofacial evolution. Though in its infancy, the field of "comparative evo-devo-omics" presents unparalleled opportunities to precisely uncover how phenotypic differences arise during development.

Keywords: NCC, mammal, heterochrony, constraint, evolution, GRN, skull

OPEN ACCESS

Edited by:
Neva P. Meyer,
Clark University, United States

Reviewed by:
Shunsuke Suzuki,
Shinshu University, Japan
Anna Keyte,
The Rockefeller University,
United States

****Correspondence:***
Axel H. Newton
axel.newton@unimelb.edu.au

†ORCID:
Axel H. Newton
orcid.org/0000-0001-7175-5978

Specialty section:
This article was submitted to Evolutionary Developmental Biology, a section of the journal Frontiers in Cell and Developmental Biology

Received: *11 May 2022*
Accepted: *06 June 2022*
Published: *23 June 2022*

Citation:
Newton AH (2022) Marsupials and Multi-Omics: Establishing New Comparative Models of Neural Crest Patterning and Craniofacial Development. Front. Cell Dev. Biol. 10:941168. doi: 10.3389/fcell.2022.941168

1 INTRODUCTION

One of the most remarkable, yet enigmatic aspects of the vertebrate skull is the broad diversity of craniofacial shapes observed between species. While our understanding of craniofacial biology has been significantly enhanced through investigations across several vertebrate models, we still know very little about the processes that drive the development of distinct craniofacial adaptations. Comparative embryology and developmental biology in jawed and jawless vertebrates have revealed

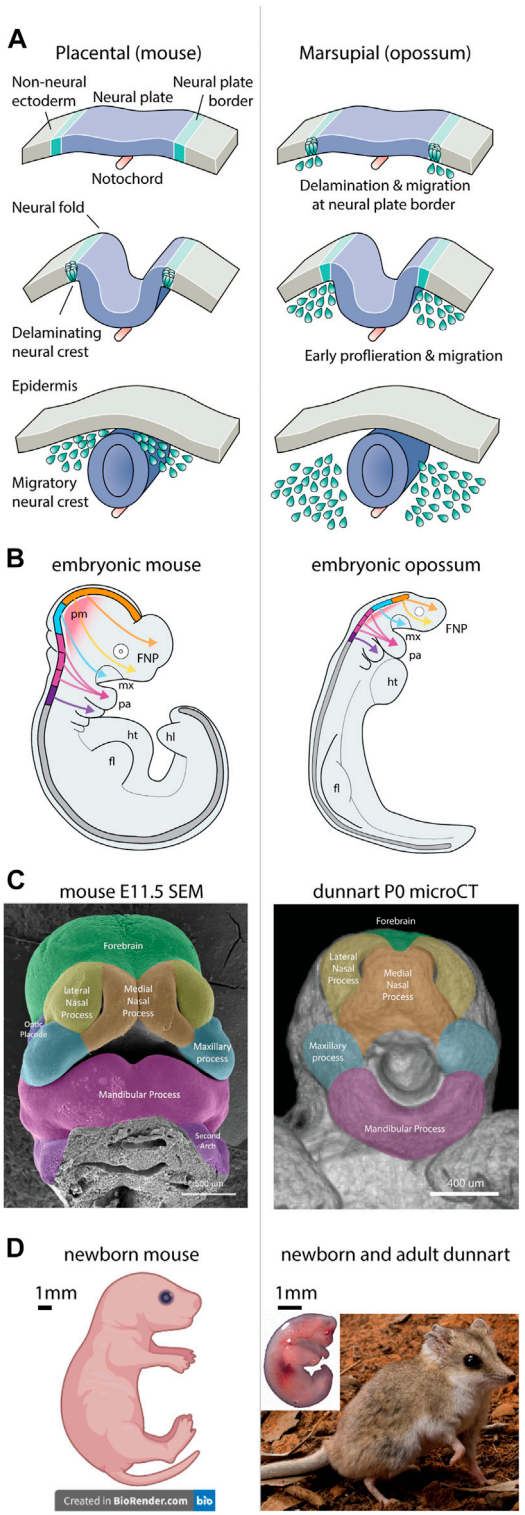

FIGURE 1 | Neural crest and craniofacial development between therian mammals. Craniofacial heterochrony between therian mammals arises from altered neural crest cell behaviours. **(A)** In placental mammals, the neural crest forms in the neural folds and delaminates from the neural tube to migrate throughout the embryo. In marsupials however, the neural crest forms and delaminates from the neural plate border, leading to accelerated migration in (*Continued*)

FIGURE 1 | the early embryo—redrawn from (Martik and Bronner, 2021). **(B)** Neural crest migration pathways are shared between therian mammals, though are accelerated in marsupials relative to developmental stage. Note marsupials display rapid development of the facial complex and forelimbs, while the CNS and hindlimbs are rudimentary. **(C)** The facial prominences of newborn marsupials resemble those observed in an embryonic mouse (credit FaceBase.org) (Samuels, B. D., 2020). **(D)** Comparative images of newborn mouse and dunnart, demonstrating the altriciality of the dunnart at birth. The adult dunnart superficially resembles a mouse. Image credits: dunnart newborn—Laura Cook; Dunnart Adult—David Paul—Museums Victoria; mouse pup—created with BioRender.com. Abbreviations: fl, forelimb; FNP, frontonasal process; hl, hindlimb; ht, heart; md, mandibular process; mx, maxillary process; pa, pharyngeal arch; pm, paraxial (head) mesoderm.

that craniofacial morphogenesis is driven by a transient population of embryonic progenitors called the neural crest (Kuratani et al., 2018; Fish, 2019). Multipotent neural crest cells (NCCs) direct patterning and development of the head and neck, amongst other structures, and are controlled by deeply conserved gene regulatory networks (GRNs) constituting a species-generic program (Green et al., 2015; Martik and Bronner, 2021). The combination of these developmental and evolutionary observations, with forward genetics and human clinical models of craniofacial disease, have provided a holistic understanding of how the craniofacial prominences are patterned and skull bones develop (Wilkie and Morriss-Kay, 2001; Szabo-rogers et al., 2010; Murillo-Rincón and Kaucka, 2020). However, despite this fundamental understanding of craniofacial biology across vertebrates, we still know remarkably little about how species-specific diversity arises and is patterned during development.

One way we can begin to address this phenomenon is by utilizing comparative models to quantitatively examine how disparities or similarities arise during development. These models need to be suitably chosen depending on the hypothesis being tested. i.e., examining closely related species with unique skull morphologies (disparity), versus distantly related species with similar skull morphologies (convergence). Mammals provide excellent examples to address these hypotheses, owing to their conserved anatomy yet remarkable craniofacial disparity or convergence, shared developmental patterns, heterochrony and lineage-specific constraints, and appropriate divergence times, e.g., within orders or across clades. Through application of these models, we can begin to tease apart how facial morphogenesis and shape diversity is regulated at the cellular and molecular level (Newton et al., 2017; Usui and Tokita, 2018; Newton and Pask, 2020), informing new models of development.

In this article, I outline my perspectives on establishing new comparative mammalian models for investigations into the developmental basis of craniofacial patterning. I discuss the underlying biology of craniofacial morphogenesis, including NCC biology, its influence on patterning, and heterochrony between therian mammals. I emphasize the importance of establishing an appropriate marsupial model for comparative investigations with the eutherian laboratory mouse, including

the establishment and utilization of transgenic approaches. Finally, I discuss how single-cell multi-omic approaches, regularly utilized in developmental biology, should be applied to comparative craniofacial models to scrutinize differential cell and molecular behaviours underlying mammalian craniofacial patterning and shape diversity. Establishing a marsupial model for comparative mammalian biology will strengthen our understanding of craniofacial development and how morphological diversity is generated throughout evolution.

2 Neural Crest Cells and Patterning of the Head

Development of the vertebrate head and craniofacial skeleton is achieved largely through the contribution of migratory NCCs. NCC specification is regulated through a deeply-conserved GRN comprised of shared suites of core transcriptional regulators, constituting a species-generic program (Green et al., 2015; Martik and Bronner, 2021). During early embryogenesis, NCCs arise within the neuroectoderm at the neural plate border (**Figure 1A**). Initially, WNT, FGF, and BMP signalling pathways define the border and initiate pre-migratory NCC specification in response to activation of *SOX9* (Cheung and Briscoe, 2003). Committed NCCs undergo activation of epithelial-to-mesenchymal transcription factors, *SOX10, SNAIL* and *SLUG*, and other NCC-specific transcription factors such as *MSX1* and *TFAP2A* (Martik and Bronner, 2021), causing the cells to delaminate and migrate away from the forming neural tube (**Figure 1A**). The spatial location of NCCs along the anterior-posterior axis of the embryo predefine their paths of migration. The anterior-most cranial NCCs of the forebrain and hindbrain populate the frontonasal process and maxillary arch (**Figures 1B,C**), contributing to development of the facial skeleton, whereas more posterior cranial NCCs populate the pharyngeal arches to form the musculoskeletal elements of the lower jaw and neck (**Figures 1B,C**). NCC migration into their target primordia occur in response to cues within the local extracellular environment. Here, as NCCs populate the developing prominences, reciprocal FGF, BMP, SHH, and retinoic acid signalling interactions between mesenchymal NCCs and the epithelial ectoderm and endoderm direct their spatial organization and activate GRNs responsible for proliferation, outgrowth and differentiation of the craniofacial skeleton [(Creuzet et al., 2004; Minoux and Rijli, 2010; Dash and Trainor, 2020; Murillo-Rincón and Kaucka, 2020) and references within].

2.1 The Origin of Species-Specific Pattern

The specific influence of NCCs patterning the vertebrate head has been showcased through cross-species transplantations and xenografts. These experiments have revealed that NCCs possess intrinsic programming and autonomous behaviours which drive species-specific patterning (Schneider, 2018). NCC transplantation chimeras in avian embryos see recipient species develop donor-specific patterning, bone formation and craniofacial morphology (Schneider and Helms, 2003; Chen et al., 2012; Hall et al., 2014; Ealba et al., 2015). Such morphological outcomes are driven *via* intrinsic NCC behaviours, including donor-specific regulation of the cell-cycle and distinct expression of transcriptional regulators and signalling factors (Hall et al., 2014). These unique NCC behaviours are further suggested to influence their local environment to produce distinct morphological outcomes. Here, NCC-derived signals modulate activation of reciprocal signalling pathways to the surrounding ectoderm and endoderm which determine gene expression and spatiotemporal patterning of the facial primordia (Schneider, 2018). In agreement with this, while shared (species-generic) genes and patterning factors are active in the developing facial prominences, each species displays distinct expression profiles during beak outgrowth and development (Wu et al., 2004; Wu et al., 2006; Brugmann et al., 2010). Together, these data suggest that intrinsic species-specific NCC programming influences interactions with their local environment, regulating differentiation of craniofacial cells and tissues and the development of distinct morphological identities.

2.2 Marsupial Heterochrony, Accelerated Neural Crest Cell Specification and Migration

The mechanisms underlying mammalian neural crest patterning and craniofacial development have been largely ascertained from studies in mouse. However, while these findings may be relevant for eutherian mammals, comparative studies in marsupials have revealed pronounced heterochrony in their NCC behaviours. During specification at the neural plate border, marsupial NCCs undergo rapid delamination and migration prior to neural plate folding (**Figure 1A**) (Smith, 1997; Smith, 2001; Smith, 2020; Vaglia and Smith, 2003; Wakamatsu et al., 2014), leading to large accumulations of NCCs within the forming facial prominences at an earlier equivalent developmental stage to that seen in eutherians (**Figure 1B**) (Smith, 2001). Remarkably, very little is known about the molecular regulation of marsupial NCCs during development. Two related studies revealed that in the opossum embryo, NCC specification and delamination is accelerated as a result of sequence alteration in a *SOX9* enhancer which drives early activation of *SOX9* in the neural plate border (Wakamatsu et al., 2014; Wakamatsu and Suzuki, 2019). This accelerated activation likely influences the heterochronic migration, proliferation, and ossification observed in marsupials, though no other studies have interrogated these processes or drawn comparisons with eutherians. This represents a large gap in our understanding of how NCC behaviours influence development and differ between distinct mammalian clades. Future studies should address the genetic underpinning of these behavioural differences and their contribution to craniofacial patterning. Curiously, it remains to be seen whether transplantation of marsupial NCCs into recipient mouse embryos (or vice versa) would retain their heterochronic behaviours and promote differential establishment of the facial prominences and skeleton. As such, observations into marsupial NCC biology and comparative heterochrony between eutherians are required

for a complete understanding of mammalian NCC patterning and craniofacial development.

3 Craniofacial Patterning, Disparity, and Convergence in Therian Mammals

Mammals have evolved unique cranial adaptations which distinguish them from other vertebrates. Evolutionary novelties such as a hinged jaw, middle ear bones and muzzle or semi-motile snout (Higashiyama et al., 2021) have allowed mammals to adapt to a diverse range of ecological niches. However, since diverging ~160 million years ago (Bininda-Emonds et al., 2007), therian mammals (marsupials and eutherians) have evolved distinct reproductive and developmental strategies, resulting in heterochrony and lineage-specific constraints (Smith, 1997). The marsupial mode of reproduction requires well-developed jaws and forelimbs at a comparatively early stage to allow the altricial neonate to crawl from the birth canal into pouch and attach to the teat for an extended period of suckling. These distinct functional requirements require differences in the onset of development of the olfactory and central nervous system, and musculoskeletal element of the head body and limbs (Smith, 1997; Nunn and Smith, 1998; Weisbecker et al., 2008; Sears, 2009; Keyte and Smith, 2010; Keyte and Smith, 2012; Chew et al., 2014). Particularly, during craniofacial development, ossification and suture closure of the facial bones are advanced to meet the functional requirements associated with suckling (Sánchez-Villagra et al., 2008; Rager et al., 2014; Spiekman and Werneburg, 2017; Cook et al., 2021). Overall, these constraints imposed on the marsupial orofacial bones are suggested to limit evolvability of their cranial anatomy.

Marsupials have evolved altered patterns of cranial modularity (Goswami, 2006; Goswami, 2007; Goswami et al., 2009; Goswami et al., 2012; Goswami et al., 2016) which are thought to reduce their overall skull shape diversity compared to eutherians (Bennett and Goswami, 2013; Fabre et al., 2021). For example, the marsupial jaws form a functionally constrained module, while the frontonasal bones and neurocranium are under relaxed constraint and can evolve more freely (Goswami et al., 2016). On the other hand, eutherian mammals largely lack these constraints during development, thus their cranial bone groups are free to evolve independently producing a greater range of morphological adaptations. Importantly, these frontonasal, jaw and neurocranium bone groups (anatomical modules) possess distinct embryonic origins, arising from the cranial NC, first arch NC, or head mesoderm, respectively (developmental modules) (Couly et al., 1993; Jiang et al., 2002; Yoshida et al., 2008). These semi-independent origins, known as mosaicism, allow flexibility in how different cranial morphologies can evolve and change (Felice and Goswami, 2018), even in the presence of functional constraints. Importantly, the combination of cranial mosaicism with cell-autonomous programming of NCCs provide clues as to how particular cranial adaptations can arise during evolution. Specifically, it can be hypothesized that evolution within GRNs associated with cranial progenitor cell types can produce adaptive morphological outcomes.

These evolutionary hypotheses have been recently applied, investigating the origins of the remarkable craniofacial convergence observed between the marsupial thylacine and eutherian wolf (Goswami et al., 2011; Feigin et al., 2018). During postnatal ontogeny, the thylacine and wolf frontonasal and neurocranial bones develop with strong shape convergence, whilst the thylacine's maxillary bones (upper jaw) possess constrained shape shared with other marsupials and disparate patterns to that seen in the wolf (Newton et al., 2021). This supports the notion that adaptive evolution (similarity and disparity) of the mammalian skull is modular (Goswami, 2006; Goswami and Polly, 2010), facilitated by mosaic evolution of select bone groups. Furthermore, the distinct embryological origins of the convergent bone groups observed between the thylacine and wolf suggest their underlying GRNs may be convergently targeted by selection. Indeed, comparative genomic investigations of the loci underlying the thylacine and wolf's cranial convergence revealed enrichment of homoplasy in GRNs associated with cranial mesenchyme migration, differentiation, and ossification (Feigin et al., 2019). Taken together, these studies support the hypothesis that evolution within GRNs of embryonic cranial precursors may specify species-specific patterning of the facial primordia, ultimately influencing craniofacial shape. However, this hypothesis requires further validation, particularly into the role of mammalian NCC heterochrony during early facial development and patterning. As such, establishing a marsupial model of NCC patterning and craniofacial biology that is amenable to manipulation is essential to our understanding of how evolutionary adaptations are produced during development.

4 A Marsupial Model to Investigate Mammalian Heterochrony

Modern studies of NCC development and craniofacial patterning in mammals have leveraged the mouse Cre-Lox system, with several transgenic reporter lines established to target various stages of the NCC or skull developmental pathway (Zhang et al., 2002; Rodda and McMahon, 2006; Yoshida et al., 2008; Stine et al., 2009; Rauch et al., 2010; Lewis et al., 2013). Of these, the *Wnt1-cre* strain has been widely utilized for NCC developmental biology to uncover the spatiotemporal decisions underlying NCC differentiation (Soldatov et al., 2019), defining tissue boundaries between NCC and non NCC-derived cranial structures (Jiang et al., 2002; Hu et al., 2004; Lewis et al., 2013), as well as a multipotent NCC line to define models of differentiation (Ishii et al., 2012; Nguyen et al., 2018). In addition, chromatin profiling of mouse NCCs and craniofacial prominences have annotated the regulatory landscape of craniofacial enhancers and putative GRNs (Visel et al., 2009a; Visel et al., 2009b; Attanasio et al., 2013; Pennacchio et al., 2018). Yet while these tools provide powerful and valuable outcomes, they are scarcely utilized outside murine models, limiting comparative mammalian research. Recently however, several new marsupial

resources are actively being established, including a pioneering study to generate the first genetically modified marsupials—founder lines of tyrosinase knockout opossums (Kiyonari et al., 2021). Though marsupial transgenic resources are still in their infancy, these advances have primed the generation of new marsupial Cre-Lox resources for developmental investigations. Of note, the generation of a marsupial orthologous *WNT1-cre* line would allow targeted labelling of neural crest cells and their craniofacial derivatives, opening the door for comparative developmental studies and investigations into mammalian heterochrony.

4.1 The Dunnart as the Gold-Standard Marsupial Model

In the past, several marsupial species have provided insights to various aspects of mammalian biology, reproduction, and development (Selwood and Coulson, 2006), with the American opossum (*Monodelphis domestica*) informing models of NCC and limb development (Martin and Mackay, 2003; Vaglia and Smith, 2003; Goswami et al., 2012; Beiriger and Sears, 2014). However, *Monodelphis* are basal American marsupials (superorder Ameridelphia) possessing an 80-million-year divergence from Australian marsupials, similar to times shared between human and mouse. Therefore, an Australian laboratory-based marsupial model with similar easy husbandry, year-round breeding and experimental manipulation is still required for a more complete understanding of mammalian (and marsupial) biology. Dunnarts (*Sminthopsis* sp.; superorder Australidelphia) are small, carnivorous, mouse-like marsupials that are easy to maintain, possess simple husbandry and are polyovular, poly-oestrous and spontaneous ovulators which produce multiple litters of up to 10 pouch young year round (Frigo and Woolley, 1996; Frigo and Woolley, 1997; Suárez et al., 2017; Cook et al., 2021). Owing to this, several new resources are being established for the fat-tailed dunnart (*S. crassicaudata*, hereafter referred to as the dunnart) as the gold-standard model for next-gen marsupial biology. These include a chromosome level assembly, transcriptomic and gene regulatory datasets, induced pluripotent cells, inbred strains, and transgenic laboratory lines (Eldridge et al., 2020). Furthermore, like other marsupials, the dunnart possesses significant heterochrony in development of its head, brain and limbs compared with eutherian species, making it an excellent model for comparative mammalian research.

One of the most remarkable features of dunnart biology is its rapid gestation and ultra-altricial state at birth (Suárez et al., 2017; Cook et al., 2021). Dasyurid marsupials, including the dunnart, represent some of the most altricial of all extant mammals. Dunnart neonates are born after a rapid 13.5-day gestation, compared to ~20 days in mouse (**Figure 1D**), and superficially resemble a eutherian foetus. At birth, the dunnart orofacial region appears as rudimentary facial prominences akin to an embryonic day 11.5–12 mouse (**Figure 1C**), despite being functional to accommodate suckling. The newborn dunnart lacks a developed brain and has paddle-like hindlimbs, but possesses highly developed, muscularized forelimbs with claws to accommodate crawling (**Figure 1D**) (Suárez et al., 2017; Cook et al., 2021). Remarkably, newborn dunnarts lack mineralized bone in the facial skeleton and forelimbs, which rapidly ossify within the first 24 h, while the hindlimbs do not start to ossify until ~D5 (Cook et al., 2021). This extreme heterochrony and altriciality at birth allows direct manipulations of these developmental systems *ex utero*, at equivalent eutherian embryonic stages (Paolino et al., 2018). Critically, the ultra-altricial birth of dasyurids demand additional acceleration of the onset of NCC specification, migration and proliferation, compared to the opossum (Smith, 2020). These features distinguish the dunnart as an exceptional mammalian model to investigate NCC-derived craniofacial patterning and ossification. However, detailed analyses which substantiate these early NCC behaviours in *Sminthopsis* have yet to be performed, representing an important first step to understand their NCC biology and thus heterochrony in mammals. Nevertheless, the dunnart is well positioned to determine how altered developmental timing influences ontogeny and craniofacial morphogenesis, providing new insights into the origin of species-specific pattern.

5 A Look to the Future: Comparative Evo-Devo-Omics

The age of comparative and functional genomics has accelerated investigations into the molecular basis of mammalian trait evolution. Comparative genomics has allowed identification of genes and regulatory regions under selection within and between lineages (Capra et al., 2013; Parker et al., 2013; Foote et al., 2015; Feigin et al., 2018, 2019); comparative bulk RNA-seq has revealed differentially expressed genes between tissues or developing structures (Eckalbar et al., 2016; Cooper et al., 2020); and chromatin pulldown or accessibility assays (ChIP, HiC, or ATAC-seq) define the gene regulatory landscape associated with these tissues or developing structures (Visel et al., 2009a; Attanasio et al., 2013). However, though powerful, individually these analyses are static and may overlook dynamic processes that contribute to development of complex traits. For example, while identification of differentially expressed genes or enhancers active in the embryonic orofacial region may constitute components that contribute to mammalian facial shape diversity (species-generic), such analyses are unable to capture dynamic regulation of these and the GRNs that influence development of unique anatomical features (species-specific) (Schneider, 2018)—as exemplified in avian models (Schneider and Helms, 2003; Chen et al., 2012; Hall et al., 2014; Ealba et al., 2015). As such, alternative approaches are required to disentangle the complex landscape of craniofacial development between disparate species.

The advent of single-cell omics has revolutionized developmental biology, producing high-resolution atlases of diverse developmental processes (Cao et al., 2019). To date, single-cell studies have been applied to multiple aspects of neural crest patterning and craniofacial development (Li et al., 2019; Soldatov et al., 2019; Farmer et al., 2021; Morrison et al., 2021; Pagella et al., 2021; Tatarakis et al., 2021), providing unique insights into how these complex developmental processes are regulated. Single-cell transcriptomics (scRNA-seq) allow detailed characterization of transcriptional profiles and cell-types present within developing structures, fate decisions and gene expression dynamics underlying differentiation of progenitors into mature

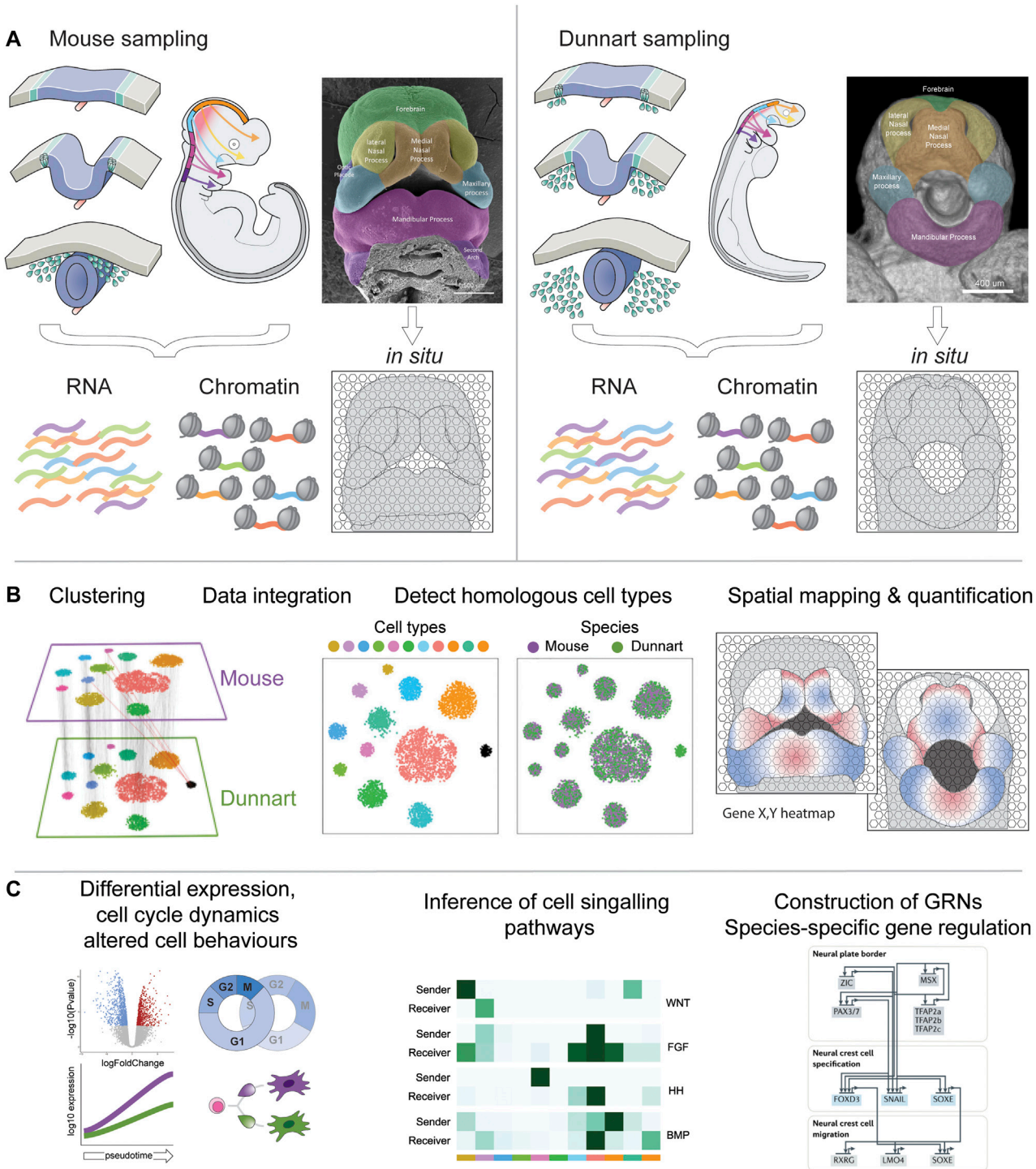

FIGURE 2 | Workflow for comparative craniofacial single-cell multiomics. **(A)** Single cells can be isolated from dunnart and mouse NCCs and developing craniofacial prominences for multiplexed isolation and sequencing of RNA and open chromatin. Facial tissue sections can be processed for *in situ* spatial transcriptomics or MERFISH (Xia et al., 2019). Single-cell RNA and ATAC-seq data can be readily integrated using pipelines such as Seurat (Butler et al., 2018). **(B)** Dunnart and mouse datasets can be individually clustered or integrated to generate an atlas of homologous cell type populations—adapted from (Stuart et al., 2019). Cell transcriptomic and epigenetic profiles can be further mapped back to their spatial organization in the embryo. **(C)** The combination of these methods allows sophisticated downstream workflows to examine differential expression between species-specific clusters (pseudobulk) or cell lineage differentiation (pseudotime), inference of cell-cell signalling relationships (Jin et al., 2021), or construction of GRNs and species-specific patterns of gene regulation (Martik and Bronner, 2021).

cell types (Trapnell et al., 2014), and cell-cell signalling interactions between adjacent tissues (Jin et al., 2021). Importantly, scRNA-seq data can be integrated with genome-wide assays for Transposase-Accessible Chromatin (ATAC-seq) to define regulatory elements active within their underlying cell types (Buenrostro et al., 2015; Cao et al., 2018; Stuart et al., 2019), or spatial transcriptomics to resolve cellular gene expression profiles in individual cells (Xia et al., 2019) or developing tissues *in situ* (Marx, 2021). Used in combination, these techniques provide powerful methods to integrate developmental biology with gene expression dynamics and construction of species-specific GRNs.

Despite their potential, single-cell multi-omic approaches have been scarcely applied in comparative evolutionary biology. Such studies of "comparative evo-devo-omics" between taxa are becoming rapidly viable to investigate the molecular mechanisms underlying convergence, constraint, or innovation in specific developmental processes (Shafer, 2019; Mahadevaiah et al., 2020). However, the lack of these applied studies are largely in response to significant technical limitations surrounding integration and batch correction of disparate datasets, specificity and stage-matching of tissues and homologous cell types between disparate species, and quality of the underlying genome and transcriptome—reviewed by (Shafer, 2019). Nevertheless, these limitations can be mitigated through application of tools aiding dataset integration, sequencing depth and batch correction, as well as issues with transcriptome quality and gene orthology (Butler et al., 2018; Haghverdi et al., 2018). Furthermore, new applied methodologies are being produced to better identify and match homologous cell and tissue types (Tosches et al., 2018; Welch et al., 2019; Feregrino and Tschopp, 2021) and their proportions between distantly related species and datasets (Phipson et al., 2021). Given the rapid rate by which these limitations are being resolved by the community, comparative evo-devo-omics presents a powerful platform to interrogate the cell, molecular and developmental mechanisms underlying heterochronic NCC specification and facial patterning between marsupial and eutherian mammals.

5.1 Mammalian Craniofacial Heterochrony at Single Cell Resolution

Using the above examples, I present a hypothetical workflow for detailed investigations into mammalian craniofacial heterochrony and evolution through a comparative lens. First, sampling of single-cell RNA, chromatin and spatial profiles of stage-matched dunnart and mouse embryos (**Figure 2A**) will allow generation of species-specific transcriptional atlases, building on existing datasets (Soldatov et al., 2019) and producing novel mammalian resources. The resulting transcriptomic, epigenetic and spatial profiles can be clustered and integrated for detection of homologous and novel cell types (Tosches et al., 2018; Welch et al., 2019), conserved and disparate gene co-expression modules (Feregrino and Tschopp, 2021), cell type proportions (Phipson et al., 2021) and spatial quantification of genes *in situ* (**Figure 2B**). From here, evolutionary hypotheses can be tested through identification of dynamic transcriptional, signalling, epigenetic and spatial relationships, revealing shared (species-generic) and unique (species-specific) processes underlying facial development and evolution (**Figure 2C**). Through application of these approaches, we can begin to determine how NCC gene regulatory architecture differs between therian mammals, and their influence on heterochronic craniofacial patterning. Ultimately, this will not only provide valuable data into how diverse facial shapes are produced during development, but also provide novel insights into how mammalian craniofacial diversity arises during evolution.

DATA AVAILABILITY STATEMENT

The original contributions presented in the study are included in the article/Supplementary Material, further inquiries can be directed to the corresponding author.

AUTHOR CONTRIBUTIONS

AN conceived the study and wrote the manuscript.

ACKNOWLEDGMENTS

I thank my mentors Andrew Pask, Christy Hipsley, Stephen Frankenberg, and Craig Smith for constructive discussions and guidance which led to the preparation of this manuscript.

REFERENCES

Attanasio, C., Nord, A. S., Zhu, Y., Blow, M. J., Li, Z., Liberton, D. K., et al. (2013). Fine Tuning of Craniofacial Morphology by Distant-Acting Enhancers. *Science* 342, 1–20. doi:10.1126/science.1241006

Beiriger, A., and Sears, K. E. (2014). Cellular Basis of Differential Limb Growth in Postnatal Gray Short-Tailed Opossums (Monodelphis Domestica). *J. Exp. Zool. Mol. Dev. Evol.)* 322, 221–229. doi:10.1002/jez.b.22556

Bennett, C. V., and Goswami, A. (2013). Statistical Support for the Hypothesis of Developmental Constraint in Marsupial Skull Evolution. *BMC Biol.* 11. doi:10.1186/1741-7007-11-52

Bininda-Emonds, O. R. P., Cardillo, M., Jones, K. E., MacPhee, R. D. E., Beck, R. M. D., Grenyer, R., et al. (2007). The Delayed Rise of Present-Day Mammals. *Nature* 446, 507–512. doi:10.1038/nature05634

Brugmann, S. A., Powder, K. E., Young, N. M., Goodnough, L. H., Hahn, S. M., James, A. W., et al. (2010). Comparative Gene Expression Analysis of Avian Embryonic Facial Structures Reveals New Candidates for Human Craniofacial Disorders. *Hum. Mol. Genet.* 19, 920–930. doi:10.1093/hmg/ddp559

Buenrostro, J. D., Wu, B., Litzenburger, U. M., Ruff, D., Gonzales, M. L., Snyder, M. P., et al. (2015). Single-cell Chromatin Accessibility Reveals Principles of Regulatory Variation. *Nature* 523, 486–490. doi:10.1038/nature14590

Butler, A., Hoffman, P., Smibert, P., Papalexi, E., and Satija, R. (2018). Integrating Single-Cell Transcriptomic Data across Different Conditions, Technologies, and Species. *Nat. Biotechnol.* 36, 411–420. doi:10.1038/nbt.4096

Cao, J., Cusanovich, D. A., Ramani, V., Aghamirzaie, D., Pliner, H. A., Hill, A. J., et al. (20182018). Joint Profiling of Chromatin Accessibility and Gene Expression in Thousands of Single Cells. *Science* 361, 1380–1385. doi:10.1126/science.aau0730

Cao, J., Spielmann, M., Qiu, X., Huang, X., Ibrahim, D. M., Hill, A. J., et al. (2019). The Single-Cell Transcriptional Landscape of Mammalian Organogenesis. *Nature* 566, 496–502. doi:10.1038/s41586-019-0969-x

Capra, J. A., Erwin, G. D., Mckinsey, G., Rubenstein, J. L. R., and Pollard, K. S. (2013). Many Human Accelerated Regions Are Developmental Enhancers. *Phil. Trans. R. Soc. B* 368, 20130025. doi:10.1098/rstb.2013.0025

Chen, C.-C., Balaban, E., and Jarvis, E. D. (2012). Interspecies Avian Brain Chimeras Reveal that Large Brain Size Differences Are Influenced by Cell-Interdependent Processes. *PLoS One* 7, e42477. doi:10.1371/journal.pone.0042477

Cheung, M., and Briscoe, J. (2003). Neural Crest Development Is Regulated by the Transcription Factor Sox9. *Development* 130, 5681–5693. doi:10.1242/dev.00808

Chew, K. Y., Shaw, G., Yu, H., Pask, A. J., and Renfree, M. B. (2014). Heterochrony in the Regulation of the Developing Marsupial Limb. *Dev. Dyn.* 243, 324–338. doi:10.1002/dvdy.24062

Cook, L. E., Newton, A. H., Hipsley, C. A., and Pask, A. J. (2021). Postnatal Development in a Marsupial Model, the Fat-Tailed Dunnart Sminthopsis crassicaudata; Dasyuromorphia: Dasyuridae. *Commun. Biol.* 4, 1–14. doi:10.1038/s42003-021-02506-2

Cooper, K., Saxena, A., Sharma, V., Neufeld, S., Tran, M., Gutierrez, H., et al. (2020). Interspecies Transcriptome Analyses Identify Genes that Control the Development and Evolution of Limb Skeletal Proportion. *FASEB J.* 34, 1–1. doi:10.1096/fasebj.2020.34.s1.00363

Couly, G. F., Coltey, P. M., and Le Douarin, N. M. (1993). The Triple Origin of Skull in Higher Vertebrates: a Study in Quail-Chick Chimeras. *Development* 117, 409–429. doi:10.1242/dev.117.2.409

Creuzet, S., Schuler, B., Couly, G., and Le Douarin, N. M. (2004). Reciprocal Relationships between Fgf8 and Neural Crest Cells in Facial and Forebrain Development. *Proc. Natl. Acad. Sci. U.S.A.* 101, 4843–4847. doi:10.1073/pnas.0400869101

Dash, S., and Trainor, P. A. (2020). The Development, Patterning and Evolution of Neural Crest Cell Differentiation into Cartilage and Bone. *Bone* 137, 115409. doi:10.1016/j.bone.2020.115409

Dickel, D. E., Ypsilanti, A. R., Pla, R., Zhu, Y., Barozzi, I., Mannion, B. J., et al. (2018). Ultraconserved Enhancers Are Required for Normal Development. *Cell* 172, 491–499. e15. doi:10.1016/j.cell.2017.12.017

Ealba, E. L., Jheon, A. H., Hall, J., Curantz, C., Butcher, K. D., and Schneider, R. A. (2015). Neural Crest-Mediated Bone Resorption Is a Determinant of Species-specific Jaw Length. *Dev. Biol.* 408, 151–163. doi:10.1016/j.ydbio.2015.10.001

Eckalbar, W. L., Schlebusch, S. A., Mason, M. K., Gill, Z., Parker, A. V., Booker, B. M., et al. (2016). Transcriptomic and Epigenomic Characterization of the Developing Bat Wing. *Nat. Genet.* 48, 528–536. doi:10.1038/ng.3537

Eldridge, M. D. B., Deakin, J. E., MacDonald, A. J., Byrne, M., Fitzgerald, A., Johnson, R. N., et al. (2020). The Oz Mammals Genomics (OMG) Initiative: Developing Genomic Resources for Mammal Conservation at a Continental Scale. *Aust. Zool.* 40, 505–509. doi:10.7882/AZ.2020.003

Fabre, A.-C., Dowling, C., Portela Miguez, R., Fernandez, V., Noirault, E., and Goswami, A. (2021). Functional Constraints during Development Limit Jaw Shape Evolution in Marsupials. *Proc. R. Soc. B* 288, 1–8. doi:10.1098/rspb.2021.0319

Farmer, D. J. T., Mlcochova, H., Zhou, Y., Koelling, N., Wang, G., Ashley, N., et al. (2021). The Developing Mouse Coronal Suture at Single-Cell Resolution. *Nat. Commun.* 12, 1–14. doi:10.1038/s41467-021-24917-9

Feigin, C. Y., Newton, A. H., Doronina, L., Schmitz, J., Hipsley, C. A., Mitchell, K. J., et al. (2018). Genome of the Tasmanian Tiger Provides Insights into the Evolution and Demography of an Extinct Marsupial Carnivore. *Nat. Ecol. Evol.* 2, 182–192. doi:10.1038/s41559-017-0417-y

Feigin, C. Y., Newton, A. H., and Pask, A. J. (2019). Widespread Cis-Regulatory Convergence between the Extinct Tasmanian Tiger and Gray Wolf. *Genome Res.* 29, 1648–1658. doi:10.1101/gr.244251.118

Felice, R. N., and Goswami, A. (2018). Developmental Origins of Mosaic Evolution in the Avian Cranium. *Proc. Natl. Acad. Sci. U.S.A.* 115, 555–560. doi:10.1073/pnas.1716437115

Feregrino, C., and Tschopp, P. (2021). Assessing Evolutionary and Developmental Transcriptome Dynamics in Homologous Cell Types. *Dev. Dyn.*, 1–18. doi:10.1002/dvdy.384

Fish, J. L. (2019). Evolvability of the Vertebrate Craniofacial Skeleton. *Seminars Cell & Dev. Biol.* 91, 13–22. doi:10.1016/j.semcdb.2017.12.004

Foote, A. D., Liu, Y., Thomas, G. W. C., Vinař, T., Alföldi, J., Deng, J., et al. (2015). Convergent Evolution of the Genomes of Marine Mammals. *Nat. Genet.* 47, 272–275. doi:10.1038/ng.3198

Frigo, L., and Woolley, P. A. (1997). Growth and Development of Pouch Young of the Stripe-Faced Dunnart, Sminthopsis Macroura (Marsupialia : Dasyuridae), in Captivity. *Aust. J. Zool.* 45, 157–170. doi:10.1071/ZO97002

Frigo, L., and Woolley, P. (1996). Development of the Skeleton of the Stripe-Faced Dunnart, Sminthopsis Macroura (Marsupialia: Dasyuridae). *Aust. J. Zool.* 44, 155–164. doi:10.1071/ZO9960155

Goswami, A. (2007). Cranial Modularity and Sequence Heterochrony in Mammals. *Evol. Dev.* 9, 290–298. doi:10.1111/j.1525-142X.2007.00161.x

Goswami, A. (2006). Cranial Modularity Shifts during Mammalian Evolution. *Am. Nat.* 168, 270–280. doi:10.1086/505758

Goswami, A., Milne, N., and Wroe, S. (2011). Biting through Constraints: Cranial Morphology, Disparity and Convergence across Living and Fossil Carnivorous Mammals. *Proc. R. Soc. B* 278, 1831–1839. doi:10.1098/rspb.2010.2031

Goswami, A., Polly, P. D., Mock, O. B., and Sánchez-villagra, M. R. (2012). Shape, Variance and Integration during Craniogenesis: Contrasting Marsupial and Placental Mammals. *J. Evol. Biol.* 25, 862–872. doi:10.1111/j.1420-9101.2012.02477.x

Goswami, A., and Polly, P. D. (2010). The Influence of Modularity on Cranial Morphological Disparity in Carnivora and Primates (Mammalia). *PLoS One* 5, e9517–8. doi:10.1371/journal.pone.0009517

Goswami, A., Randau, M., Polly, P. D., Weisbecker, V., Bennett, C. V., Hautier, L., et al. (2016). Do developmental Constraints and High Integration Limit the Evolution of the Marsupial Oral Apparatus? *Integr. Comp. Biol.* 56, 404–415. doi:10.1093/icb/icw039

Goswami, A., Weisbecker, V., and Sánchez-Villagra, M. R. (2009). Developmental Modularity and the Marsupial-Placental Dichotomy. *J. Exp. Zool.* 312B, 186–195. doi:10.1002/jez.b.21283

Green, S. A., Simoes-costa, M., and Bronner, M. E. (2015). Evolution of Vertebrates as Viewed from the Crest. *Nature* 520, 474–482. doi:10.1038/nature14436

Haghverdi, L., Lun, A. T. L., Morgan, M. D., and Marioni, J. C. (2018). Batch Effects in Single-Cell RNA-Sequencing Data Are Corrected by Matching Mutual Nearest Neighbors. *Nat. Biotechnol.* 36, 421–427. doi:10.1038/nbt.4091

Hall, J., Jheon, A. H., Ealba, E. L., Eames, B. F., Butcher, K. D., Mak, S.-S., et al. (2014). Evolution of a Developmental Mechanism: Species-specific Regulation of the Cell Cycle and the Timing of Events during Craniofacial Osteogenesis. *Dev. Biol.* 385, 380–395. doi:10.1016/j.ydbio.2013.11.011

Higashiyama, H., Koyabu, D., Hirasawa, T., Werneburg, I., Kuratani, S., and Kurihara, H. (2021). Mammalian Face as an Evolutionary Novelty. *Proc. Natl. Acad. Sci. U.S.A.* 118, 1–8. doi:10.1073/pnas.2111876118

Hu, Q., Ueno, N., and Behringer, R. R. (2004). Restriction of BMP4 Activity Domains in the Developing Neural Tube of the Mouse Embryo. *EMBO Rep.* 5, 734–739. doi:10.1038/sj.embor.7400184

Ishii, M., Arias, A. C., Liu, L., Chen, Y.-B., Bronner, M. E., and Maxson, R. E. (2012). A Stable Cranial Neural Crest Cell Line from Mouse. *Stem Cells Dev.* 21, 3069–3080. doi:10.1089/scd.2012.0155

Jiang, X., Iseki, S., Maxson, R. E., Sucov, H. M., and Morriss-Kay, G. M. (2002). Tissue Origins and Interactions in the Mammalian Skull Vault. *Dev. Biol.* 241, 106–116. doi:10.1006/dbio.2001.0487

Jin, S., Guerrero-Juarez, C. F., Zhang, L., Chang, I., Ramos, R., Kuan, C.-H., et al. (2021). Inference and Analysis of Cell-Cell Communication Using CellChat. *Nat. Commun.* 12, 1–20. doi:10.1038/s41467-021-21246-9

Keyte, A. L., and Smith, K. K. (2010). Developmental Origins of Precocial Forelimbs in Marsupial Neonates. *Development* 137, 4283–4294. doi:10.1242/dev.049445

Keyte, A., and Smith, K. K. (2012). Heterochrony in Somitogenesis Rate in a Model Marsupial,Monodelphis Domestica. *Evol. Dev.* 14, 93–103. doi:10.1111/j.1525-142X.2011.00524.x

Kiyonari, H., Kaneko, M., Abe, T., Shiraishi, A., Yoshimi, R., Inoue, K.-i., et al. (2021). Targeted Gene Disruption in a Marsupial, Monodelphis Domestica, by CRISPR/Cas9 Genome Editing. *Curr. Biol.* 31, 3956–3963. doi:10.1016/j.cub.2021.06.056

Kuratani, S., Kusakabe, R., and Hirasawa, T. (2018). The Neural Crest and Evolution of the Head/trunk Interface in Vertebrates. *Dev. Biol.* 444, S60–S66. doi:10.1016/j.ydbio.2018.01.017

Lewis, A. E., Vasudevan, H. N., O'Neill, A. K., Soriano, P., and Bush, J. O. (2013). The Widely Used Wnt1-Cre Transgene Causes Developmental Phenotypes by Ectopic Activation of Wnt Signaling. *Dev. Biol.* 379, 229–234. doi:10.1016/j.ydbio.2013.04.026

Li, H., Jones, K. L., Hooper, J. E., and Williams, T. (2019). The Molecular Anatomy of Mammalian Upper Lip and Primary Palate Fusion at Single Cell Resolution. *Dev* 146, dev174888. doi:10.1242/dev.174888

Mahadevaiah, S. K., Sangrithi, M. N., Hirota, T., and Turner, J. M. A. (2020). A Single-Cell Transcriptome Atlas of Marsupial Embryogenesis and X Inactivation. *Nature* 586, 612–617. doi:10.1038/s41586-020-2629-6

Martik, M. L., and Bronner, M. E. (2021). Riding the Crest to Get a Head: Neural Crest Evolution in Vertebrates. *Nat. Rev. Neurosci.* 22, 616–626. doi:10.1038/s41583-021-00503-2

Martin, K. E. A., and Mackay, S. (2003). Postnatal Development of the Fore- and Hindlimbs in the Grey Short-Tailed Opossum, Monodelphis Domestica. *J. Anat.* 202, 143–152. doi:10.1046/j.1469-7580.2003.00149.x

Marx, V. (2021). Method of the Year: Spatially Resolved Transcriptomics. *Nat. Methods* 18, 9–14. doi:10.1038/s41592-020-01033-y

Minoux, M., and Rijli, F. M. (2010). Molecular Mechanisms of Cranial Neural Crest Cell Migration and Patterning in Craniofacial Development. *Development* 137, 2605–2621. doi:10.1242/dev.040048

Morrison, J. A., McLennan, R., Teddy, J. M., Scott, A. R., Kasemeier-Kulesa, J. C., Gogol, M. M., et al. (2021). Single-cell Reconstruction with Spatial Context of Migrating Neural Crest Cells and Their Microenvironments during Vertebrate Head and Neck Formation. *Dev* 148, dev199468. doi:10.1242/dev.199468

Murillo-Rincón, A. P., and Kaucka, M. (2020). Insights Into the Complexity of Craniofacial Development From a Cellular Perspective. *Front. Cell Dev. Biol.* 8, 1–8. doi:10.3389/fcell.2020.620735

Newton, A. H., Feigin, C. Y., and Pask, A. J. (2017). RUNX2 Repeat Variation Does Not Drive Craniofacial Diversity in Marsupials. *BMC Evol. Biol.* 17, 1–9. doi:10.1186/s12862-017-0955-6–

Newton, A. H., and Pask, A. J. (2020). Evolution and Expansion of the RUNX2 QA Repeat Corresponds with the Emergence of Vertebrate Complexity. *Commun. Biol.* 3, 771. doi:10.1038/s42003-020-01501-3

Newton, A. H., Weisbecker, V., Pask, A. J., and Hipsley, C. A. (2021). Ontogenetic Origins of Cranial Convergence between the Extinct Marsupial Thylacine and Placental Gray Wolf. *Commun. Biol.* 4, 51. doi:10.1038/s42003-020-01569-x

Nguyen, B. H., Ishii, M., Maxson, R. E., and Wang, J. (2018). Culturing and Manipulation of O9-1 Neural Crest Cells. *J. Vis. Exp.* 9, 58346. doi:10.3791/58346

Nunn, C. L., and Smith, K. K. (1998). Statistical Analyses of Developmental Sequences: The Craniofacial Region in Marsupial and Placental Mammals. *Am. Nat.* 152, 82–101. doi:10.1086/286151

Pagella, P., de Vargas Roditi, L., Stadlinger, B., Moor, A. E., and Mitsiadis, T. A. (2021). A Single-Cell Atlas of Human Teeth. *iScience* 24, 102405. doi:10.1016/j.isci.2021.102405

Paolino, A., Fenlon, L. R., Kozulin, P., Richards, L. J., and Suárez, R. (2018). Multiple Events of Gene Manipulation via in Pouch Electroporation in a Marsupial Model of Mammalian Forebrain Development. *J. Neurosci. Methods* 293, 45–52. doi:10.1016/j.jneumeth.2017.09.004

Parker, J., Tsagkogeorga, G., Cotton, J. A., Liu, Y., Provero, P., Stupka, E., et al. (2013). Genome-wide Signatures of Convergent Evolution in Echolocating Mammals. *Nature* 502, 228–231. doi:10.1038/nature12511

Phipson, B., Sim, C. B., Porrello, E., Hewitt, A. W., Powell, J., and Oshlack, A. (2021). Propeller: Testing for Differences in Cell Type Proportions in Single Cell Data. *bioRxiv* 2021, 470236. doi:10.1101/2021.11.28.470236

Rager, L., Hautier, L., Forasiepi, A., Goswami, A., and Sánchez-Villagra, M. R. (2014). Timing of Cranial Suture Closure in Placental Mammals: Phylogenetic Patterns, Intraspecific Variation, and Comparison with Marsupials. *J. Morphol.* 275, 125–140. doi:10.1002/jmor.20203

Rauch, A., Seitz, S., Baschant, U., Schilling, A. F., Illing, A., Stride, B., et al. (2010). Glucocorticoids Suppress Bone Formation by Attenuating Osteoblast Differentiation via the Monomeric Glucocorticoid Receptor. *Cell Metab.* 11, 517–531. doi:10.1016/j.cmet.2010.05.005

Rodda, S. J., and McMahon, A. P. (2006). Distinct Roles for Hedgehog and Canonical Wnt Signaling in Specification,differentiation and Maintenance of Osteoblast Progenitors. *Development* 133, 3231–3244. doi:10.1242/dev.02480

Samuels, B. D., Aho, R., Brinkley, J. F., Bugacov, A., Feingold, E., Fisher, S., et al. (2020). FaceBase 3: Analytical Tools and FAIR Resources for Craniofacial and Dental Research. *Development (Cambridge, England)*, 147(18), dev191213. doi:10.1242/dev.191213

Sánchez-Villagra, M. R., Goswami, A., Weisbecker, V., Mock, O., and Kuratani, S. (2008). Conserved Relative Timing of Cranial Ossification Patterns in Early Mammalian Evolution. *Evol. Dev.* 10, 519–530. doi:10.1111/j.1525-142X.2008.00267.x

Schneider, R. A., and Helms, J. A. (2003). The Cellular and Molecular Origins of Beak Morphology. *Science* 299, 565–568. doi:10.1126/science.1077827

Schneider, R. A. (2018). Neural Crest and the Origin of Species-specific Pattern. *Genesis* 56, e23219–33. doi:10.1002/dvg.23219

Sears, K. E. (2009). Differences in the Timing of Prechondrogenic Limb Development in Mammals: The Marsupial-Placental Dichotomy Resolved. *Evol. (N. Y).* 63, 2193–2200. doi:10.1111/j.1558-5646.2009.00690.x

Selwood, L., and Coulson, G. (2006). Marsupials as Models for Research. *Aust. J. Zool.* 54, 137. doi:10.1071/ZOv54n3_IN

Shafer, M. E. R. (2019). Cross-Species Analysis of Single-Cell Transcriptomic Data. *Front. Cell Dev. Biol.* 7, 1–9. doi:10.3389/fcell.2019.00175

Smith, K. K. (1997). Comparative Patterns of Craniofacial Development in Eutherian and Metatherian Mammals. *Evolution* 51, 1663. doi:10.2307/2411218

Smith, K. K. (2001). Early Development of the Neural Plate, Neural Crest and Facial Region of Marsupials. *J. Anat.* 199, 121–131. doi:10.1017/S0021878201008202 10.1046/j.1469-7580.2001.19910121.x

Smith, K. K. (2020). J P Hill and Katherine Watson's Studies of the Neural Crest in Marsupials. *J. Morphol.* 281, 1567–1587. doi:10.1002/jmor.21270

Soldatov, R., Kaucka, M., Kastriti, M. E., Petersen, J., Chontorotzea, T., Englmaier, L., et al. (2019). Spatiotemporal Structure of Cell Fate Decisions in Murine Neural Crest. *Science* 364, eaas9536. doi:10.1126/science.aas9536

Spiekman, S. N. F., and Werneburg, I. (2017). Patterns in the Bony Skull Development of Marsupials: High Variation in Onset of Ossification and Conserved Regions of Bone Contact. *Sci. Rep.* 7, 1–11. doi:10.1038/srep43197

Stine, Z. E., Huynh, J. L., Loftus, S. K., Gorkin, D. U., Salmasi, A. H., Novak, T., et al. (2009). Oligodendroglial and Pan-Neural Crest Expression of Cre Recombinase Directed bySox10enhancer. *Genesis* 47, 765–770. doi:10.1002/dvg.20559

Stuart, T., Butler, A., Hoffman, P., Hafemeister, C., Papalexi, E., Mauck, W. M., et al. (2019). Comprehensive Integration of Single-Cell Data. *Cell* 177, 1888–1902. e21. doi:10.1016/j.cell.2019.05.031

Suárez, R., Paolino, A., Kozulin, P., Fenlon, L. R., Morcom, L. R., Englebright, R., et al. (2017). Development of Body, Head and Brain Features in the Australian Fat-Tailed Dunnart (Sminthopsis crassicaudata; Marsupialia: Dasyuridae); A Postnatal Model of Forebrain Formation. *PLoS One* 12, e0184450–18. doi:10.1371/journal.pone.0184450

Szabo-rogers, H. L., Smithers, L. E., Yakob, W., and Liu, K. J. (2010). New Directions in Craniofacial Morphogenesis. *Dev. Biol.* 341, 84–94. doi:10.1016/j.ydbio.2009.11.021

Tatarakis, D., Cang, Z., Wu, X., Sharma, P. P., Karikomi, M., MacLean, A. L., et al. (2021). Single-cell Transcriptomic Analysis of Zebrafish Cranial Neural Crest Reveals Spatiotemporal Regulation of Lineage Decisions during Development. *Cell Rep.* 37, 110140. doi:10.1016/j.celrep.2021.110140

Tosches, M. A., Yamawaki, T. M., Naumann, R. K., Jacobi, A. A., Tushev, G., and Laurent, G. (2018). Evolution of Pallium, hippocampus, and Cortical Cell Types Revealed by Single-Cell Transcriptomics in Reptiles. *Science.* 360, 881–888. doi:10.1126/science.aar4237

Trapnell, C., Cacchiarelli, D., Grimsby, J., Pokharel, P., Li, S., Morse, M., et al. (2014). The Dynamics and Regulators of Cell Fate Decisions Are Revealed by Pseudotemporal Ordering of Single Cells. *Nat. Biotechnol.* 32, 381–386. doi:10.1038/nbt.2859

Usui, K., and Tokita, M. (2018). Creating Diversity in Mammalian Facial Morphology: A Review of Potential Developmental Mechanisms. *Evodevo* 9, 1–17. doi:10.1186/s13227-018-0103-4

Vaglia, J. L., and Smith, K. K. (2003). Early Differentiation and Migration of Cranial Neural Crest in the Opossum, Monodelphis Domestica. *Evol. Dev.* 5, 121–135. doi:10.1046/j.1525-142X.2003.03019.x

Visel, A., Blow, M. J., Li, Z., Zhang, T., Akiyama, J. A., Holt, A., et al. (2009a). ChIP-seq Accurately Predicts Tissue-specific Activity of Enhancers. *Nature* 457, 854–858. doi:10.1038/nature07730

Visel, A., Rubin, E. M., and Pennacchio, L. A. (2009b). Genomic Views of Distant-Acting Enhancers. *Nature* 461, 199–205. doi:10.1038/nature08451

Wakamatsu, Y., Nomura, T., Osumi, N., and Suzuki, K. (2014). Comparative Gene Expression Analyses Reveal Heterochrony forSox9expression in the Cranial Neural Crest during Marsupial Development. *Evol. Dev.* 16, 197–206. doi:10.1111/ede.12083

Wakamatsu, Y., and Suzuki, K. (2019). Sequence Alteration in the Enhancer Contributes to the Heterochronic Sox9 Expression in Marsupial Cranial Neural Crest. *Dev. Biol.* 456, 31–39. doi:10.1016/j.ydbio.2019.08.010

Weisbecker, V., Goswami, A., Wroe, S., and Sánchez-Villagra, M. R. (2008). Ossification Heterochrony in the Therian Postcranial Skeleton and the Marsupial-Placental Dichotomy. *Evol. (N. Y).* 62, 2027–2041. doi:10.1111/j.1558-5646.2008.00424.x

Welch, J. D., Kozareva, V., Ferreira, A., Vanderburg, C., Martin, C., and Macosko, E. Z. (2019). Single-Cell Multi-Omic Integration Compares and Contrasts Features of Brain Cell Identity. *Cell* 177, 1873–1887. e17. doi:10.1016/j.cell.2019.05.006

Wilkie, A. O. M., and Morriss-Kay, G. M. (2001). Genetics of Craniofacial Development and Malformation. *Nat. Rev. Genet.* 2, 458–468. doi:10.1038/35076601

Wu, P., Jiang, T.-X., Shen, J.-Y., Widelitz, R. B., and Chuong, C.-M. (2006). Morphoregulation of Avian Beaks: Comparative Mapping of Growth Zone Activities and Morphological Evolution. *Dev. Dyn.* 235, 1400–1412. doi:10.1002/dvdy.20825

Wu, P., Jiang, T.-X., Suksaweang, S., Widelitz, R. B., and Chuong, C.-M. (2004). Molecular Shaping of the Beak. *Science* 305, 1465–1466. doi:10.1126/science.1098109

Xia, C., Fan, J., Emanuel, G., Hao, J., and Zhuang, X. (2019). Spatial Transcriptome Profiling by MERFISH Reveals Subcellular RNA Compartmentalization and Cell Cycle-dependent Gene Expression. *Proc. Natl. Acad. Sci. U.S.A.* 116, 19490–19499. doi:10.1073/pnas.1912459116

Yoshida, T., Vivatbutsiri, P., Morriss-Kay, G., Saga, Y., and Iseki, S. (2008). Cell Lineage in Mammalian Craniofacial Mesenchyme. *Mech. Dev.* 125, 797–808. doi:10.1016/j.mod.2008.06.007

Zhang, M., Xuan, S., Bouxsein, M. L., Von Stechow, D., Akeno, N., Faugere, M. C., et al. (2002). Osteoblast-specific Knockout of the Insulin-like Growth Factor (IGF) Receptor Gene Reveals an Essential Role of IGF Signaling in Bone Matrix Mineralization. *J. Biol. Chem.* 277, 44005–44012. doi:10.1074/jbc.M208265200

Conflict of Interest: The authors declare that the research was conducted in the absence of any commercial or financial relationships that could be construed as a potential conflict of interest.

Publisher's Note: All claims expressed in this article are solely those of the authors and do not necessarily represent those of their affiliated organizations, or those of the publisher, the editors and the reviewers. Any product that may be evaluated in this article, or claim that may be made by its manufacturer, is not guaranteed or endorsed by the publisher.

frontiers in Cell and Developmental Biology

ORIGINAL RESEARCH
published: 28 July 2020
doi: 10.3389/fcell.2020.00572

Polarized Sonic Hedgehog Protein Localization and a Shift in the Expression of Region-Specific Molecules Is Associated With the Secondary Palate Development in the Veiled Chameleon

*Marek Hampl[1,2], Jana Dumkova[3], Michaela Kavkova[4], Hana Dosedelova[1], Anna Bryjova[5], Oldrich Zahradnicek[6,7], Martin Pyszko[8], Milos Macholan[9], Tomas Zikmund[4], Jozef Kaiser[4] and Marcela Buchtova[1,2]**

[1] Laboratory of Molecular Morphogenesis, Institute of Animal Physiology and Genetics, Czech Academy of Sciences, Brno, Czechia, [2] Department of Experimental Biology, Faculty of Science, Masaryk University, Brno, Czechia, [3] Department of Histology and Embryology, Faculty of Medicine, Masaryk University, Brno, Czechia, [4] Laboratory of Computed Tomography, Central European Institute of Technology, Brno University of Technology, Brno, Czechia, [5] Institute of Vertebrate Biology, Czech Academy of Sciences, Brno, Czechia, [6] Department of Developmental Biology, Institute of Experimental Medicine, Czech Academy of Sciences, Prague, Czechia, [7] Department of Radiation Dosimetry, Nuclear Physics Institute, Czech Academy of Sciences, Prague, Czechia, [8] Department of Anatomy, Histology, and Embryology, Faculty of Veterinary Medicine, University of Veterinary and Pharmaceutical Sciences, Brno, Czechia, [9] Laboratory of Mammalian Evolutionary Genetics, Institute of Animal Physiology and Genetics, Czech Academy of Sciences, Brno, Czechia

OPEN ACCESS

Edited by:
Pedro Martinez, University of Barcelona, Spain

Reviewed by:
Kristin Artinger, University of Colorado Anschutz Medical Campus, United States
Raul Diaz, Southeastern Louisiana University, United States

***Correspondence:**
Marcela Buchtova
buchtova@iach.cz

Specialty section:
This article was submitted to Evolutionary Developmental Biology, a section of the journal Frontiers in Cell and Developmental Biology

Received: *20 February 2020*
Accepted: *15 June 2020*
Published: *28 July 2020*

Citation:
Hampl M, Dumkova J, Kavkova M, Dosedelova H, Bryjova A, Zahradnicek O, Pyszko M, Macholan M, Zikmund T, Kaiser J and Buchtova M (2020) Polarized Sonic Hedgehog Protein Localization and a Shift in the Expression of Region-Specific Molecules Is Associated With the Secondary Palate Development in the Veiled Chameleon. Front. Cell Dev. Biol. 8:572. doi: 10.3389/fcell.2020.00572

Secondary palate development is characterized by the formation of two palatal shelves on the maxillary prominences, which fuse in the midline in mammalian embryos. However, in reptilian species, such as turtles, crocodilians, and lizards, the palatal shelves of the secondary palate develop to a variable extent and morphology. While in most Squamates, the palate is widely open, crocodilians develop a fully closed secondary palate. Here, we analyzed developmental processes that underlie secondary palate formation in chameleons, where large palatal shelves extend horizontally toward the midline. The growth of the palatal shelves continued during post-hatching stages and closure of the secondary palate can be observed in several adult animals. The massive proliferation of a multilayered oral epithelium and mesenchymal cells in the dorsal part of the palatal shelves underlined the initiation of their horizontal outgrowth, and was decreased later in development. The polarized cellular localization of primary cilia and Sonic hedgehog protein was associated with horizontal growth of the palatal shelves. Moreover, the development of large palatal shelves, supported by the pterygoid and palatine bones, was coupled with the shift in *Meox2*, *Msx1,* and *Pax9* gene expression along the rostro-caudal axis. In conclusion, our results revealed distinctive developmental processes that contribute to the expansion and closure of the secondary palate in chameleons and highlighted divergences in palate formation across amniote species.

Keywords: secondary palate, SHH, primary cilia, skeletogenesis, chameleon, reptile

INTRODUCTION

The morphology of the dorsal area of the oral cavity varies among amniotic groups (Abramyan and Richman, 2015). Reptiles and birds form an incomplete secondary palate with either large openings that connect the oral and nasal cavities or narrow natural clefts, with the exception of crocodilians that develop a fully closed secondary palate (Abramyan et al., 2014). The hard palate is made up of several bones. In mammals, the most rostral part of the hard palate is formed by the premaxillary bone, the largest area is supported by palatal prominences of the maxillary bones, and only the most caudal part of the hard palate is supported by the palatine bones. Compared to mammals, the premaxillary bone in birds is significantly larger and represents the major upper beak forming bone. The largest bones are the palatines, while the maxillary bones are markedly reduced in size. The pterygoid bones in birds are located caudally behind the palatine bones (Richman et al., 2006). In some turtles that develop a secondary palate, the hard palate is formed by the premaxillary, maxillary, and palatine bones, and at the midline by the vomer. In some extinct turtle species, medial prominences of the jugal bones grow into the hard palate (Abramyan and Richman, 2015). In contrast, the arrangement of bones contributing to the hard palate in crocodilians is similar to mammals, except for the most caudal part, which is supported by the ectopterygoid and pterygoid bones.

In chameleons, the hard palate is rostrally formed by the palatine bones and caudally by the pterygoid bones (Romer, 1956). This pattern demonstrates a much larger role for the pterygoid bones in the formation of the palate in reptiles compared to mammals, where the pterygoid is localized caudally from the palatine bone and contributes to the formation of the soft palate (Mohamed, 2018). In comparison to mammals and crocodilians, the maxillary bones of chameleons support the palate only laterally. In the rostral portion of the chameleon palatal midline, the palate is supported by the vomer, which stiffens the nasal septum, and it is located dorsal to the palatal plane. The caudal part is partly formed by the ectopterygoid, which connects the pterygoid, maxillary, and jugal bones (Tolley and Herrel, 2015). Here, we will focus on the initiation of individual skeletal elements that support the hard palate in the chameleon as well as developmental processes that contribute to the formation of their large palatal shelves.

The palatal shelves form as bilateral outgrowth processes from the maxillary prominences during embryonic development in amniotes. They grow in the medial direction toward the midline to either incompletely or fully separate the oral and nasal cavities. During mammalian embryogenesis, the palatal shelves first grow vertically alongside the tongue; later, they are redirected into the horizontal plane to elongate toward each other. This process results in their contact at the midline and fusion with the opposite palatal shelf (Greene and Pratt, 1976; Ferguson, 1988). Crocodilians form a complete secondary palate similar to mammals, but a large proportion of the palatal shelves expands in the horizontal direction from the beginning of the development. Only the most caudal part of their palatal shelves is similar to the mammalian growth pattern, namely the initial vertical growth followed by horizontal course (Ferguson, 1981b). Solely horizontal growth is typical also for lizards and birds. Unlike crododillians, however, the palatal shelves never fuse together in these clades, forming the "physiological palatal cleft" (Ferguson, 1988; Richman et al., 2006; Abramyan et al., 2014).

Most adult chameleons possess open secondary palate with a narrow spacing between the palatal shelves in the midline. However, in some adult animals, the palatal shelves are in contact and form an enclosed secondary palate that resembles the crocodilian palate. Formation of the long palatal processes, which are almost in contact in midline can be caused by a combination of many different morphological aspects, e.g., relative skull dimensions, or tongue shape, as well as their altered size. These can arise as combination of many developmental processes such as enhanced cell proliferation/decreased apoptosis, alteration of cellular polarity etc. In this study, we evaluated in detail some of the developmental processes that contribute to the formation of unique features of the chameleon secondary palate. The macroscopic and microscopic structures of the chameleon palate were analyzed during pre- and post-hatching stages because the growth of the palatal shelves continues in chameleon also during post-hatching developmental period.

MATERIALS AND METHODS

Animals

Embryonic specimens of the veiled chameleon (*Chamaeleo calyptratus*) were obtained from private and commercial breeders. Sample of the Siamese crocodile (*Crocodylus siamensis*) was kindly provided from the collection of prof. Sedmera (Department of Anatomy, Faculty of Medicine, Charles University, Prague, Czech Republic). Specimens of the ocelot gecko (*Paroedura picta*) were obtained from Prof. Lukáš Kratochvíl (Department of Ecology, Faculty of Science, Charles University, Prague, Czech Republic).

Chameleon eggs were purchased from a private breeder (Prague, Czech Republic) and cultivated on moistened vermiculite substrate at 29°C. Each week, starting at week 10 after the oviposition, individuals were collected for immunohistochemistry, RNAScope, and whole-mount *in situ* hybridization (ISH) processing and skeleton staining.

Juvenile and adult reptiles including chameleons were obtained in the frozen state from the University of Veterinary and Pharmaceutical Sciences (Brno, Czech Republic). They were part of the collection at the Department of Anatomy, Histology and Embryology as a gift from Clinics of Small Animals.

The phylogenetic tree was adapted from Hedges (2012) and Zheng and Wiens (2016).

All procedures were performed according to the experimental protocols and rules established by the Laboratory Animal Science Committee of the Institute of Animal Physiology and Genetics (Liběchov, Czech Republic).

Micro-Computed Tomography (CT) Analysis

Frozen juvenile and adult individuals were measured, dissected to determine gender, and decapitated. We removed the mandible and fixed the head in 4% paraformaldehyde (PFA). The microCT measurements were performed using the GE Phoenix v|tome|x L 240 laboratory system equipped with a 180 kV/15 W nanofocus tube. The measurements were performed at an acceleration voltage of 60 kV and X-ray tube current of 200 μA. The acquisition time was 900 ms for every 2,000 images of a 360° rotation. The microCT data were obtained with a voxel resolution of 4.5 μm. Tomographic reconstruction was realized with the GE phoenix datos|x 2.0 software. Manual segmentation of microCT data and 3D model imaging were implemented in the VG Studio software MAX.

Alcian Blue and Sirius Red Staining on Slides

Transversal sections were stained with Alcian blue for cartilage and Sirius red for collagen fibers (010254, Diapath, Italy). Histological sections were deparaffinized with xylene and rehydrated through a descending alcohol series. Samples were stained with 1% Alcian blue in 3% acetic acid (10 min), Ehrlich hematoxylin (2 min), 2.5% phosphomolybdic acid (10 min), and 0.1% Sirius Red (1 h).

Skeleton Staining

Embryos were removed from eggs, decapitated, and the heads fixed in absolute ethanol. The heads were stained with an Alcian blue and Alizarin red solution, and then cleared in KOH/glycerol. Before fixation, the skin from heads was removed for better penetration of staining solution and for better final visualization.

Scanning Electron Microscopy

Chameleon embryos were fixed in 4% paraformaldehyde, washed in distilled water, and dehydrated through a graded ethanol series (30–100%). Subsequently, the samples were dried using the CPD 030 Critical Point Dryer (BAL-TEC) and shadowed by gold in a metal shadowing apparatus (Balzers SCD040). The samples were observed and photographed with the TESCAN Vega TS 5136 XM scanning electron microscope (Tescan, Czech Republic).

Transmission Electron Microscopy

The palatal shelves were removed and fixed in 3% glutaraldehyde for 24 h, washed three times in 0.1 M cacodylate buffer, and post-fixed in 1% OsO_4 solution for 1 h. After washing in cacodylate buffer, the samples were dehydrated in ethanol, followed by acetone, and embedded in Durcupan epoxy resin. Semithin sections were stained with Toluidine blue. Ultra-thin sections (∼60 nm thick) were cut using the Leica EM UC6 ultramicrotome (Leica Microsystems GmbH, Vienna, Austria) and placed on formvar-coated nickel grids. The selected sections, contrasted with lead citrate and uranyl acetate, were observed using the Morgagni^{TM} 268 transmission electron microscope (FEI Company, Eindhoven, Netherlands). Pictures were taken using the Veleta CCD camera (Olympus, Münster, Germany).

Immunofluorescence on Histological Slides

Embryos were removed from eggs, decapitated, and then fixed in 4% PFA overnight. For morphometry, the lower jaw was removed and the palate was photographed. Length and width of the palatal shelves, head widths, and gaps between the palatal shelves, were measured as labeled in **Figures 1H**, **6E**. The scatter plots were created using the Statistica 13.5.0.17 package (TIBCO Software Inc., 2018).

If necessary, the specimens were decalcified before further processing in 12.5% ethylenediaminetetraacetic acid (EDTA) either at room temperature or at 37°C for 1–3 weeks, depending on the calcification level. The specimens were then embedded in paraffin and sectioned (5 μm) in the transversal planes. For immunohistochemistry, the sections were deparaffinized in xylene and rehydrated through descending ethanol series. Antigen retrieval was performed either in 1% citrate buffer or in the DAKO antigen retrieval solution (S1699, DAKO Agilent, United States) at 97.5°C.

For protein localization, we incubated the sections with the primary antibody for 1 h at room temperature or overnight at 4°C. The following antibodies were used: PCNA (1:50, M0879, DAKO Agilent, United States), sonic hedgehog (SHH; 1:100, sc-9024, Santa Cruz, United States), and acetylated α-tubulin (1:200, 32–2700, Invitrogen, Thermo Fisher Scientific, United States). Subsequently, the sections were incubated with the following secondary antibodies (1:200) for 30 min at room temperature: anti-mouse Alexa Fluor 488 (A11001), anti-mouse Alexa Fluor 568 (A11004), anti-rabbit Alexa Fluor 488 (A11008), and anti-rabbit Alexa Fluor 594 (A11037, all Thermo Fisher Scientific, United States).

The sections were mounted with the Prolong Gold antifade mountant with DAPI (P36935, Thermo Fisher Scientific, United States) or Fluoroshield with DAPI (F6057, Sigma, Merck, Germany). If DRAQ5 (62251, Thermo Fisher Scientific, United States) was used for nuclei staining, the sections were mounted with Fluoroshield (F6182, Sigma, Merck, Germany). Pictures were obtained with the Leica DMLB2 fluorescence microscope (Leica, Germany) or Leica SP8 (Leica, Germany) and Zeiss LSM800 (Zeiss, Germany) confocal microscopes. Analysis of polarized localization of SHH ligand was performed using the CirkStat software (author Dr. Lucie Komolíková Burešová).

Terminal Deoxynucleotidyl Transferase dUTP Nick End Labeling (TUNEL) Assay

Apoptotic cells were detected using the TUNEL assay (ApopTag Peroxidase *In Situ* Apoptosis Detection Kit, Cat. No. S7101, Chemicon, Temecula, United States). Nuclei were counterstained with hematoxylin. The sections were photographed under bright-field illumination with the Leica DMLB2 compound microscope (Leica, Germany).

Polymerase Chain Reaction (PCR) and Gel Electrophoresis

Msx1, *Meox2, Pax9,* and *Hprt1* gene expression was analyzed in tissues isolated from chameleon embryonic bodies. Total

RNA was extracted using the RNeasy Plus Mini Kit (74136, Qiagen, Germany) according to the manufacturer's instructions. The total RNA concentration and purity was measured using the NanoDrop One (Thermo Fisher Scientific, United States). First-strand complementary DNA (cDNA) was synthesized using the gb Reverse Transcription Kit (3012, Generi Biotech, Czech Republic) according to the manufacturer's instructions. PCR was performed in 10 μl reactions that contained 10x PCR Buffer + $MgCl_2$, PCR Grade Nucleotide Mix, and Fast Start Taq DNA Polymerase (all Roche, Switzerland) mixed with forward and reverse primers for *Msx1*, *Meox2, Pax9,* and *Hprt1* (Generi Biotech, Czech Republic). PCR products were detected using gel electrophoresis in 1% agarose gel at voltage 120 V for 40 min. The primers were designed based on sequences from the veiled chameleon transcriptome (Pinto et al., 2019). Used chameleon sequences of assembled contigs corresponding to individual genes and table with all details are included in **Supplementary Material** based on published data (Pinto et al., 2019) (**Supplementary Material S1**).

Plasmid Purification and *in situ* Hybridization Probe Synthesis

Total RNA was isolated from embryonic chameleon tissues using the RNeasy Plus Mini Kit, according to the manufacturer's instructions. The total RNA concentration and purity was measured using the NanoDrop One. First-strand cDNA was synthesized using the gb Reverse Transcription Kit, according to the manufacturer's instructions. PCR was performed in a 50 μl reaction volume containing 10x PCR Buffer + $MgCl_2$, PCR Grade Nucleotide Mix, and Fast Start Taq DNA Polymerase mixed with forward and reverse primers for *Msx1* and *Meox2* (Generi Biotech, Czech Republic). The PCR products were isolated from agarose gels using the QIAquick Gel Extraction Kit (28706, Qiagen, Germany), according to the manufacturer's instructions. *Msx1* and *Meox2* PCR products were sequenced (Eurofins, Czech Republic) and used to transform the One Shot MAX efficiency DH5α Competent Cells (44-0097, Thermo Fisher Scientific, United States). The transformed cells were subsequently selected using the TOPO TA Cloning Kit (45-0640, Thermo Fisher Scientific, United States) on Luria-Bertani (LB) agar plates treated with X-gal. Plasmids were then purified using the QIAGEN Plasmid Midi Kit (12145, Qiagen, Germany), according to the manufacturer's instructions. DNA was sequenced using the endogenous M13F primer site (Eurofins, Czech Republic) and linearized by PCR using both M13 primers. Linearized PCR products were transcribed with the T7 polymerase for the antisense probe (10881767001, Roche, Switzerland) or Sp6 polymerase for the sense probe (10810274001, Roche, Switzerland).

Whole-Mount *in situ* Hybridization

Whole chameleon embryos or heads were fixed in 4% PFA overnight at 4°C. The tissues were dehydrated and rehydrated in a methanol series. Proteinase K (10 μg/ml) was applied for 45 min at room temperature, and the tissues were then post-fixed in a combination of 4% PFA and 25% glutaraldehyde for 20 min at room temperature. The tissues were incubated with the probe in a hybridization mix at 68°C for *Msx1* and at 60°C for *Meox2* overnight while rotating in a hybridization oven (Compact Line OV4, Biometra, Germany). Subsequently, the tissues were incubated in a hybridization mix, washed with maleic acid buffer containing Tween 20 (MABT), and incubated with anti-digoxigenin (DIG) conjugated to alkaline phosphatase (AP; 11093274910, Roche, Switzerland) overnight at 4°C while shaking. Finally, the signal was developed using the BM Purple (11442074001, Roche, Switzerland). Pictures were captured using the Leica M205 FA stereoscope (Leica, Germany).

RNAScope

The embryos were fixed in 4% PFA and fixation time differed based on the stage. The tissues were then dehydrated in an ethanol series, embedded in paraffin, and 5 μm transverse sections were obtained. The sections were deparaffinized in xylene and dehydrated in 100% ethanol. To detect gene expression, we used the RNAScope® Multiplex Fluorescent v2 Assay kit (323 110, ACD Bio, United States) for formalin-fixed paraffin embedded tissues according to the manufacturer's instructions. All reactions, which require 40°C incubation temperature, were performed in the HybEZ™ II Oven (ACD Bio, United States). The probes were designed based on sequences from the chameleon transcriptome (**Supplementary Material**); *Msx1* (805271, ACD Bio, United States) and *Meox2* (805281, ACD Bio, United States) probes were used. The hybridized probes were visualized using the TSA-Plus Cyanine 3 system (NEL744001KT, Perkin-Elmer, United States), according to the manufacturer's protocol. DAPI (323 108, ACD Bio, United States) was used to stain nuclei. Pictures were obtained with the Leica SP8 confocal microscope (Leica, Germany).

Real-Time PCR

Msx1, *Meox2,* and *Pax9* gene expression was analyzed in tissues isolated from the rostral and caudal parts of the palatal shelves and upper jaws. Rostral parts of the palatal shelves included the palatine bones and mesenchyme, caudal palatal shelves contained pterygoid and ectopterygoid bones and adjacent mesenchyme. Rostral parts of the upper jaw contained the maxillary bones and mesenchyme, caudal parts of the upper jaw contained caudal parts of the maxillary bones and rostral part of the jugal bones and adjacent mesenchyme. One sample was pooled from two or three embryos; six biological replicates were analyzed. RNA isolation, and first-strand cDNA synthesis were performed as described above. Real-time PCR reactions were performed using the SYBR Green (3005, Generi Biotech, Czech Republic) in 20-μl reactions on the LightCycler 480 (Roche, Switzerland). The comparative C_T method was used for analysis. The thermal conditions were as follows: preincubation at 95°C for 10 min, 45 cycles (denaturation at 95°C for 10 s, annealing at 57°C for 10 s, and extension at 72°C for 10 s), and melting at 95°C for 5 s and at 65°C for 1 min. *Hprt1* was used as a housekeeping gene.

RESULTS

The Palatal Shelves in Adult Chameleons Are Well Developed and Resemble the Crocodilian Secondary Palate Before Its Closure

Most adult chameleons possess open secondary palate with the large palatal shelves and small spacing between them in the midline. Therefore, the connection between the oral and nasal cavity remains open, similarly to other non-crocodilian reptiles. However, the macroscopic analysis of 53 juvenile and adult individuals of the veiled chameleon (**Figures 1A–D**), revealed that the lateral palatal shelves are well developed and significantly protruded horizontally toward the midline. The medial edge shape of the palatal shelves can vary from round to flat in both females and males (**Figures 1E–G**). We also observed that the growth of the palatal shelves continued even during post-hatching stages. This phenomenon can lead to contact or even enclosure of the contralateral shelves at the midline in some adult animals. Enclosure of the secondary palate was observed in several animals of both sexes and regardless of age, with more fused shelves observed in males (15% in males and 3% in females; **Figure 1G**). However, the majority of male adult animals possessed palatal shelves that did not approach each other (60% in males and 39% in females; **Figure 1E**). The secondary palate that featured a medial meeting of the palatal shelves was the major pattern for adult female animals (25% in males and 58% in females; **Figure 1F**).

Because of the diverse extent to which the palatal shelves have developed in individual adults, we tested the correlation (**Figures 1H–J**) between width of the palatal shelves and width of the head (**Figure 1I**), and the correlation between width of the gap between the palatal shelves and width of the head (**Figure 1J**). Indeed, the measurements were found to be highly correlated (R^2 = 97.6%; $p << 0.0001$; and R^2 = 33.7%; $p < 0.001$, respectively).

Palatal Shelves Are Supported by Skeletal Elements Contributing to Hard Palate Formation

We next used a microCT analysis to reveal, whether enclosure of the palatal shelves was only superficial, i.e., formed by soft tissues, or if bones forming the palatal shelves were in the direct contact (i.e., whether a suture between the bones was formed). We compared different post-hatching stages, from juvenile with largely opened palate (**Figure 2A**), through adults with large lateral palatal shelves with the initial contact of soft tissues (**Figure 2B**), to older animals with enclosed secondary palates (**Figure 2C**). This analysis revealed that the major palate-forming bones (palatine and pterygoid) expanded medially toward the midline during the post-hatching period (**Figure 2**). However, even in the apparently compact and sealed secondary palate of the oldest animals, the bones were neither fused nor in contact. Therefore, only the soft tissue contributed to palatal shelf fusion (**Figures 2F–F″**, arrows), a finding that is in contrast to suture formation in crocodiles and mammalian species.

Thickness of Palate-Forming Bones Changes During Post-hatching Development

To evaluate areas with the greatest thickness and expanded growth of bone matrix inside individual skeletal elements contributing to the secondary palate, we performed a wall thickness analysis on micro-CT 3D data (**Figure 3**). We expected that the bone mass will be remodeled depending on the load on individual skeletal elements during post-hatching development.

The analysis revealed the highest values in the ectopterygoid bone for all analyzed individuals (**Figures 3A–C**). In the maxillary bone, the thickest area was in the maxillary caudal zone in the juvenile (**Figure 3A**). The central areas of the maxillae, especially their interdental spaces, exhibited an enhanced wall thickness in older individuals (**Figure 3B**). In the oldest specimen, the pterygoid bone and the lateral portion of the palatine bone displayed higher values compared to other bones that contribute to the palatal region (**Figure 3C**).

The Main Palate-Forming Bones Are the First to Ossify in the Craniofacial Skeleton

To uncover the ossification sequence, we performed whole mount skeletal staining during pre-hatching development. Prior to bone mineralization, craniofacial cartilages were present (**Figures 4A–A″**). The first mineralized skeletal elements in the facial region were the palatine and pterygoid bones (**Figures 4B,B″** and **Supplementary Figure S1A–A″**), slightly followed by the jugal bone in the caudal region (**Figure 4B″**). Maxillary bones were mineralized later (**Figures 4C,C′** and **Supplementary Figures S1B,B′**) and ossification subsequently proceeded rostrally to connect with the premaxilla and caudally to the joint with the jugal bone (**Figure 4C**). The progress of bone mineralization resulted in medial contact between the maxillary and palatine bones and rostral contact with the ossifying premaxilla. Concurrent with premaxilla ossification, we observed the development of hard tissues in the egg tooth (**Figures 4C′,D′**) and the onset of vomer mineralization (**Figures 4C′,D′**). Caudally, the ossification of the ectopterygoids and the lateral contact of pterygoids and jugal bones was initiated at almost the same time as the ossification of rostral portion of the maxillary bone (**Figures 4C–C″**).

Simultaneously with ossification centers of the jugal, post-orbitofrontal, squamosal, and quadrate bones started to ossify (**Figure 4B**), bones of the most caudal craniofacial area, basisphenoid and basioccipital, formed via endochondral ossification. Their mineralization was established just after the ossification of the major palate-forming bones (**Figures 4C,D**). Their ossification progressed toward each other to form an enclosed basicranium later in development (**Figures 4E–H**). During this process, the surrounding craniofacial bones continuously mineralized, and the original cartilaginous articulation between them ossified (**Figure 4H**).

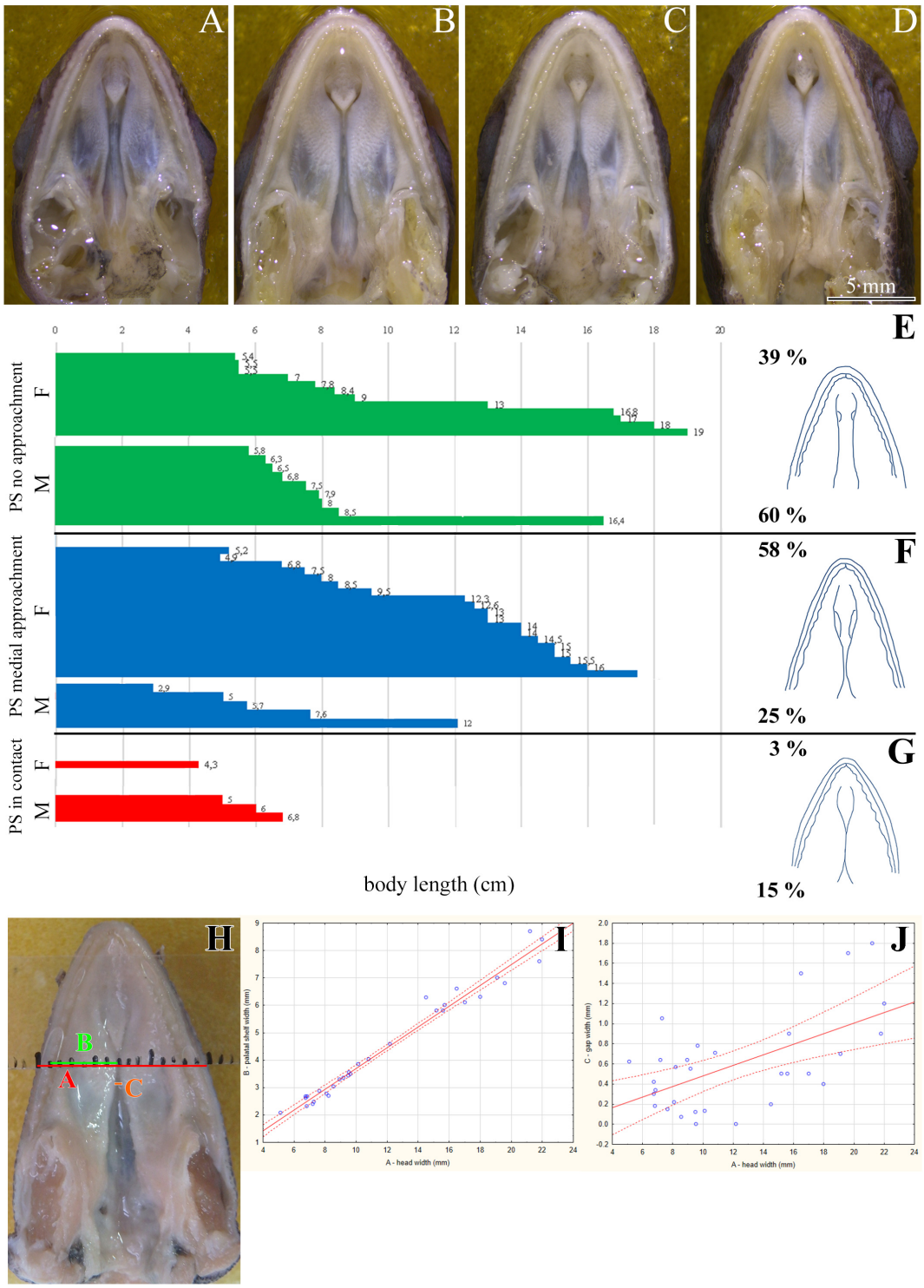

FIGURE 1 | Morphology of the secondary palate in post-hatching stages of the veiled chameleon. Macroscopic view on the palate exhibits different shape and approach state of the palatal shelves in individual chameleons of a similar size **(A–D)**. The graphs compare the distribution of different degrees of a closure of the gap between the palatal shelves in female and male chameleons **(E–G)**. For comparison, 33 female and 20 male adult and juvenile veiled chameleons of different size were used. Head width was measured in place where the distance between the palatal shelves was the smallest (distance **A**, red), and at the same place, width of the palatal shelves was measured from their medial edges to the tooth line (distance **B**, green). In the narrowest place between the palatal shelves the gap was measured (distance **C**, orange). Distance between small black lines in the schema is 1 mm **(H)**. A scatter plot of the palatal shelves width against head width of post-hatching stages **(I)**. Scatter plot of the gap between the palatal shelves against head width of post-hatching stages **(J)**. Thirty one animals were used for measuring the head and palatal shelves size. Ninety five percent confidence regression bands are shown as dashed curves. Scale bar **(A–D)**: 5 mm.

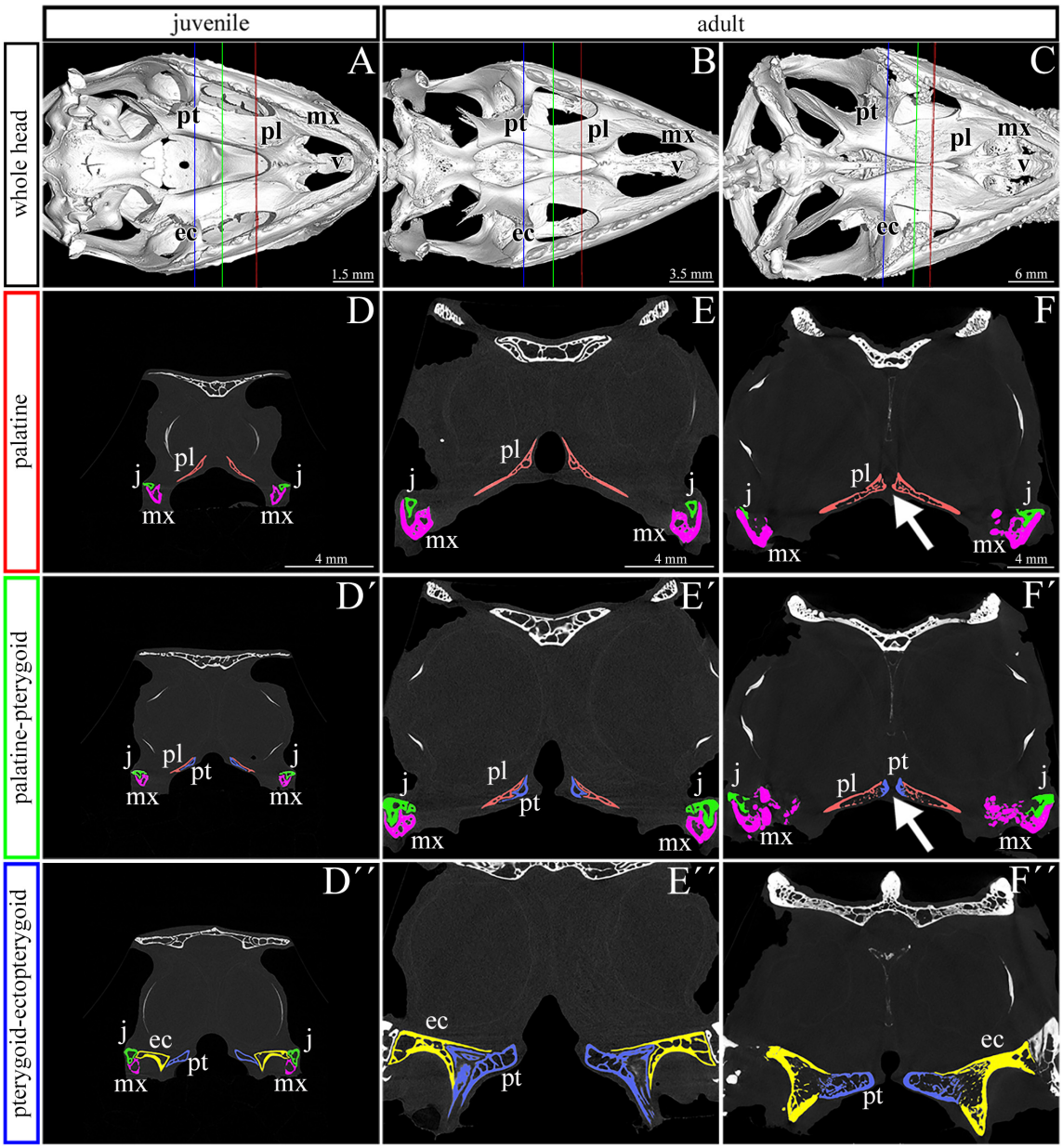

FIGURE 2 | Skeletal analysis of the secondary palate at post-hatching stages of chameleon by microCT. Whole mount cranial skeleton from palatal view displays post-hatching development of the palate-forming bones in chameleon **(A–C)**. Transversal sections of microCT scans reveal developmental and morphological changes of the palate-forming bones in three different planes during post-hatching development. Cross sections through the palatine bones (red lines in whole mount skulls) **(D–F)**. Cross sections of the junction between the palatine and pterygoid bones (green lines on whole mount skulls) **(D′–F′)**. Cross sections of the pterygoid, ectopterygoid, and jugal bones (blue lines on whole mount skulls) **(D″–F″)**. White arrows in **(F,F′)** show contact of soft palatal tissues. ec, ectopterygoid; j, jugal; mx, maxillary bone; pl, palatine bone; pt, pterygoid bone. Scale bar: cross sections 4 mm.

The Rostral Area of the Palatal Shelves Is Formed by Cartilage

The palatal shelves in birds and mammals are typically only supported by membranous bones (Richman et al., 2006). However, in chameleons, we observed cartilage in the rostral palatal area throughout both pre-hatching and post-hatching (adult) developmental stages. At the pre-hatching developmental stages (77 dpo and 112 dpo), rudimentary cartilage was present in the rostral area of the palatal shelves closely adjacent to the dorsal portion of the palatal shelves. This cartilage expanded into the most medial tips of the palatal shelves (**Figures 5A,B**) and formed the palatal part of the nasal cartilage. The cartilage protruded between the maxillary bones, located ventrolaterally, and the vomer, located dorsomedially (**Figures 5A′,B,B′**). At the later stage (112 dpo) at the interface of the vomer and

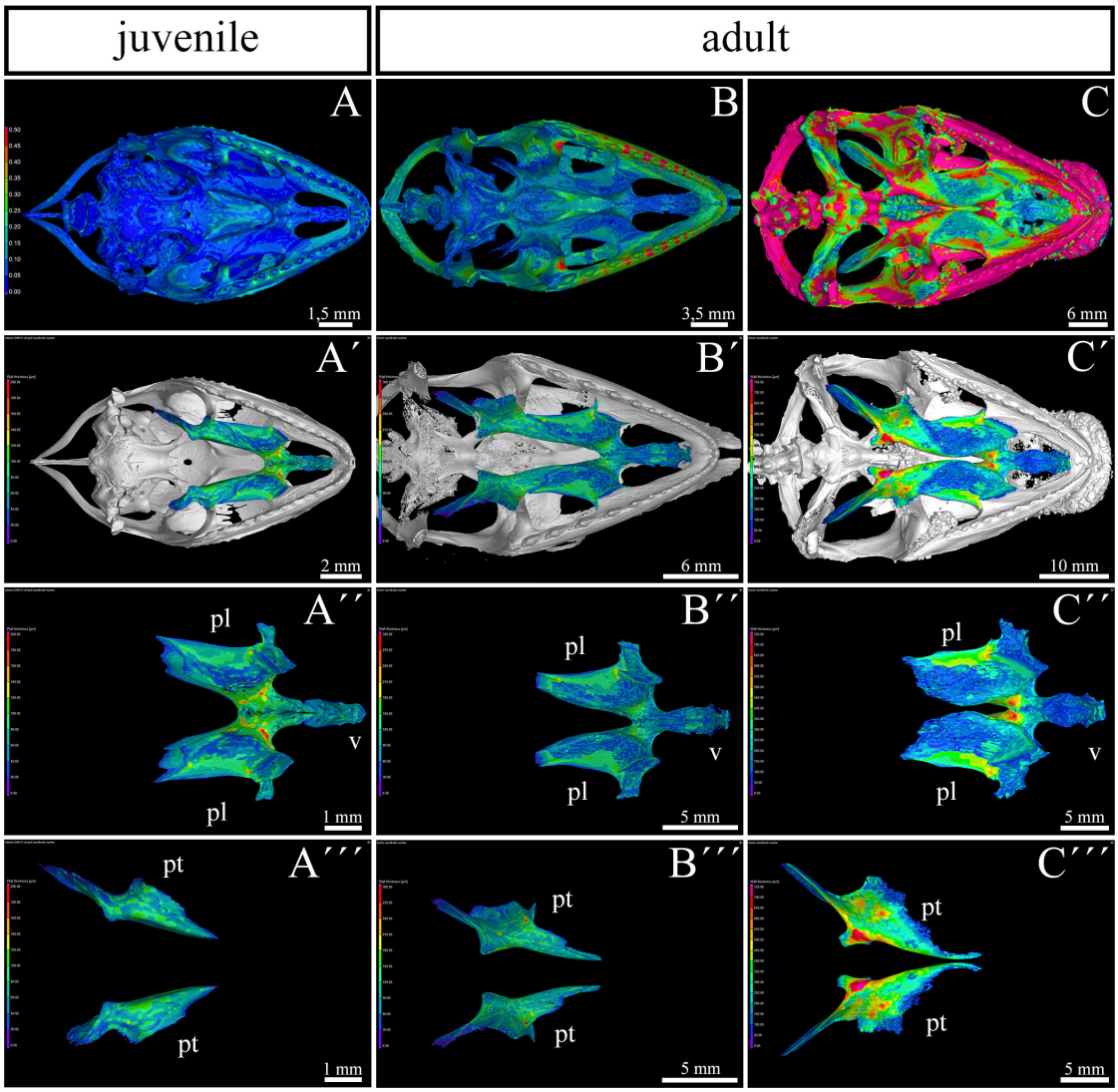

FIGURE 3 | Bone thickness skeletal analysis of individual bones at the post-hatching stages of chameleon by microCT. Bone thickness analysis of juvenile and two adult animals with palatal view on the skull. Same scales were used to reveal differences in ossification progress of individual skeletal elements with the age of animal **(A–C)**. Whole mount cranial skeleton from palatal view displays segmentation of the main palate-forming bones **(A′–C′)**. Detailed segmentation of the palatine bones and vomer in juvenile **(A′′)**, younger adult **(B′′)** and older adult **(C′′)** chameleons. Individually segmented pterygoid bones are shown on **(A′′′)** for juvenile, **(B′′′)** for younger adult, and **(C′′′)** for older adult. Notice that scales in the wall thickness analysis of individual bones **(A′–C′′′)** were set individually for each sample in order to describe the minute differences in bone thickness inside of individual skeletal elements. The main reason for setting the scales individually was that the images with unified scale lost some important detail in juvenile or in older adult. Bone thickness is displayed by a different colors from blue (the thinnest, 0 μm) to red (the thickest, up to 200 μm) demonstrated in colors legend. pl, palatine bone; pt, pterygoid bone; v, vomer. Scale bars are displayed individually for each picture.

palatine bones (**Figure 5E**, arrows), the cartilage divided into two parts and was covered by the epithelium (**Figure 5E′**). In this zone, the most rostral area of the palatal shelves protrusion was visible (**Figures 5D′,E′**), and the ventral part of the separated cartilage protruded medially to form the palatal shelves (**Figures 5D′,E′**, arrows).

In the caudal direction, the cartilage gradually retreated from the palatal shelves and was only preserved in the most distal tip (**Figures 5G,H**). At the earlier embryonic stage (77 dpo), the most caudal part of the cartilage (**Figure 5G′**, arrow) was located in the area of the palatine bones dilatation (**Figure 5G**, arrow). At 112 dpo, the cartilage in the tips of the palatal shelves terminated (**Figure 5H′**, arrow) at the anterior portion of the palatine bones (initial narrow part located medially posterior from vomer; **Figure 5H**). The same cartilage arrangement was visible in the adult chameleon (**Figures 5C–I′**).

Morphogenesis of the Palatal Shelves During Development

During early pre-hatching development (77 dpo), the palatal shelves were initiated as medial bulge-like protrusions of the

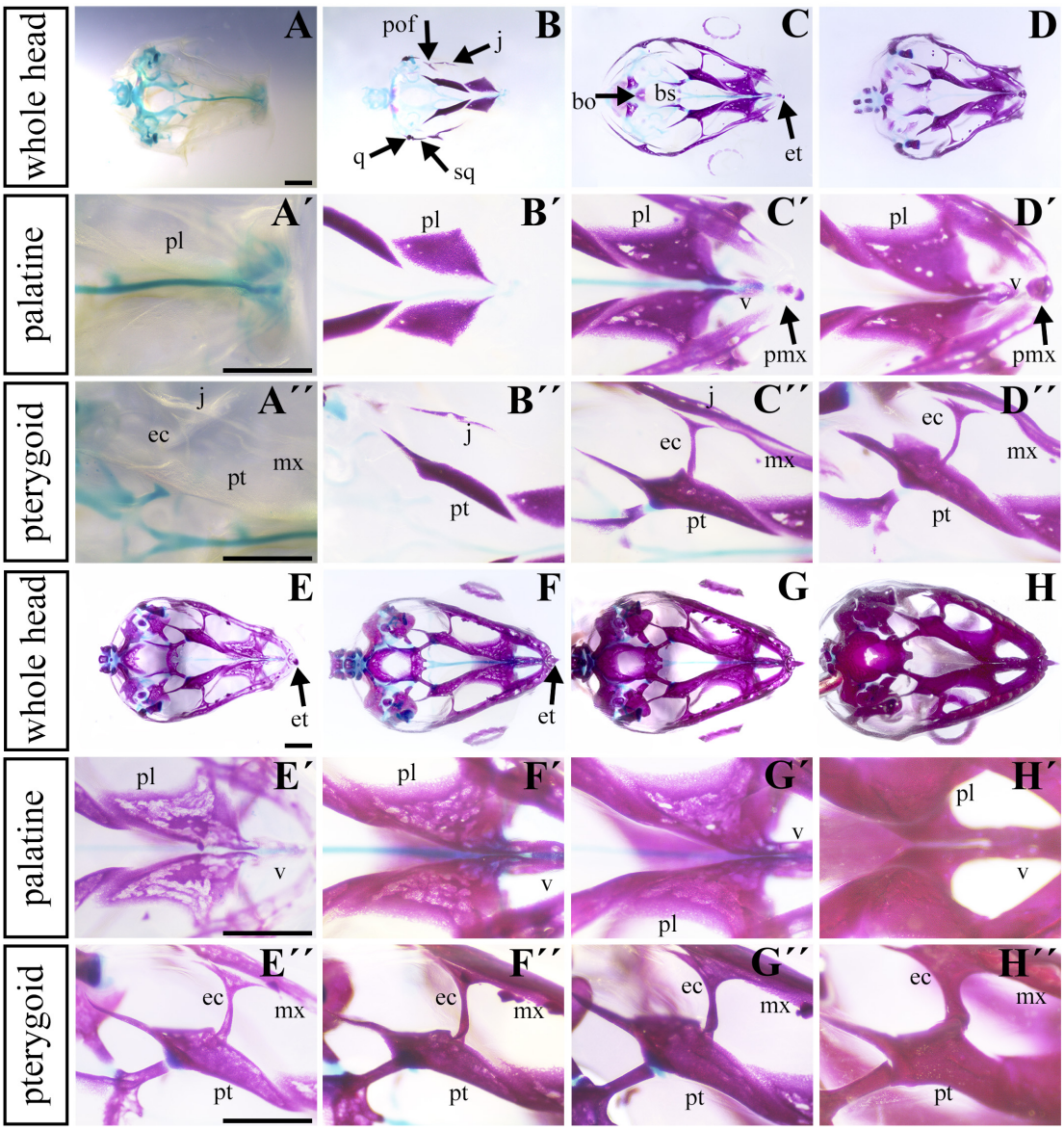

FIGURE 4 | Ossification of individual bones contributing to the secondary palate during pre-hatching stages. Lower power images **(A–D)** of palatal view of all bones and cartilages that contribute to formation of palate at earlier pre-hatching stages of chameleon embryos. Higher power images display either the palatine bones **(A′–D′)** or pterygoid bones **(A″–D″)** ossification during pre-hatching development of the veiled chameleon. The same arrangement of pictures for later stages of pre-hatching stages of chameleon embryos **(E–H″)**. Bones and cartilage were stained using Alcian blue and Alizarin red staining. bo, basioccipital bone; bs, basisphenoid bone; ec, ectopterygoid bone; et, egg tooth; j, jugal bone; mx, maxillary bone; pl, palatine bone; pmx, premaxillary bone; pof, post-orbitofrontal bone; pt, pterygoid bone; q, quadrate bone; sq, squamosal bone; v, vomer. Scale bar: 1 mm.

maxillary prominences (**Figures 5A,A′**, see also in **Figure 8**). The dorsal parts of these protrusions were then transformed into long and thin shelves that protruded dorsomedially (**Figures 5B,B′**). In pre-hatching stages, we did not observe any chameleon with the palatal shelves in direct contact in the midline or with the nasal septum. However, we observed this contact later in development, when the shelves significantly elongated in the dorsomedial direction to meet each other at the midline (**Figure 5I**).

Like in adults, the size and shape of the palatal structures were highly variable (**Figures 6A–D**). Nevertheless, individual measurements were strongly correlated (R^2 ranging from 51.8 to 64.4%; $p < 0.0001$; **Figures 6F–I**). However, a comparison between the gap width and the head width indicated slight, though insignificant, negative correlation ($R^2 = 4.5\%$; $p = 0.1466$; **Figure 6J**). As expected, the same negative (and marginally significant) correlation was found between the gap width and the palatal shelf width ($R^2 = 12.9\%$; $p = 0.0122$; not shown).

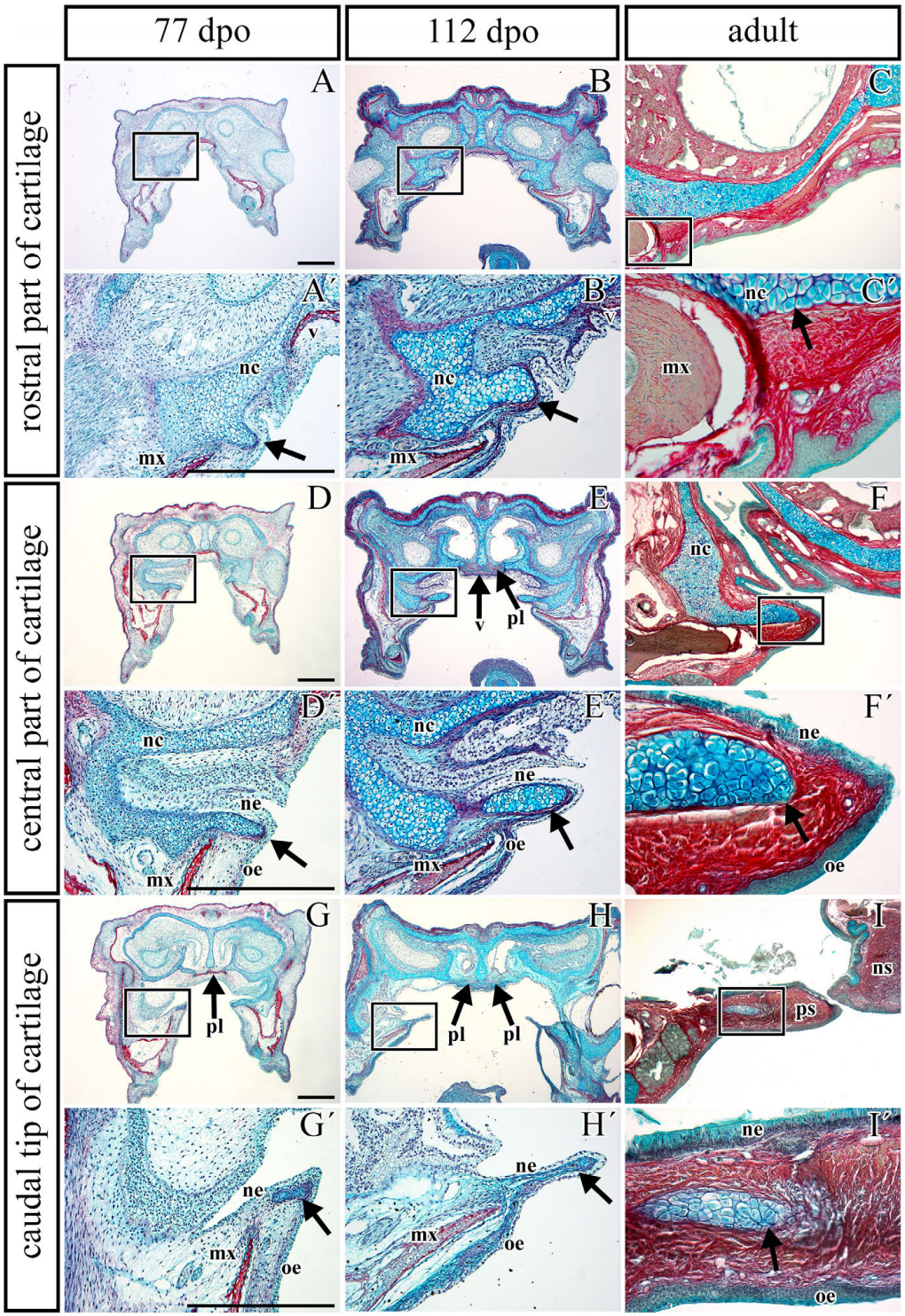

FIGURE 5 | Transversal microscopic sections through the rostral part of head in pre- and post-hatching chameleons with skeletal staining. Alcian blue, Green trichrome, and Sirius red staining on transversal sections display contribution of the palatal cartilage process to the secondary palate formation during pre-hatching development (77 and 112 dpo) and in adult chameleon. Palatal cartilage, as a part of the nasal capsule cartilage, penetrates the palatal shelves at their very rostral parts **(A,A′-C,C′)**, then supports the palatal shelves along the mediolateral axis **(D,D′–F,F′)**. Almost at the middle area of the palatine bones along the rostro-caudal axis, only rudiments of this cartilage are visible in the tip of the palatal shelves **(G,G–I,I′)**. Higher power pictures **(A′–I′)** show details from black rectangles in a lower power pictures **(A–I)**. mx, maxillary bone; nc, nasal cartilage; ne, nasal epithelium; ns, nasal septum; oe, oral epithelium; pl, palatine bone; ps, palatal shelf; v, vomer. Scale bar: 200 μm.

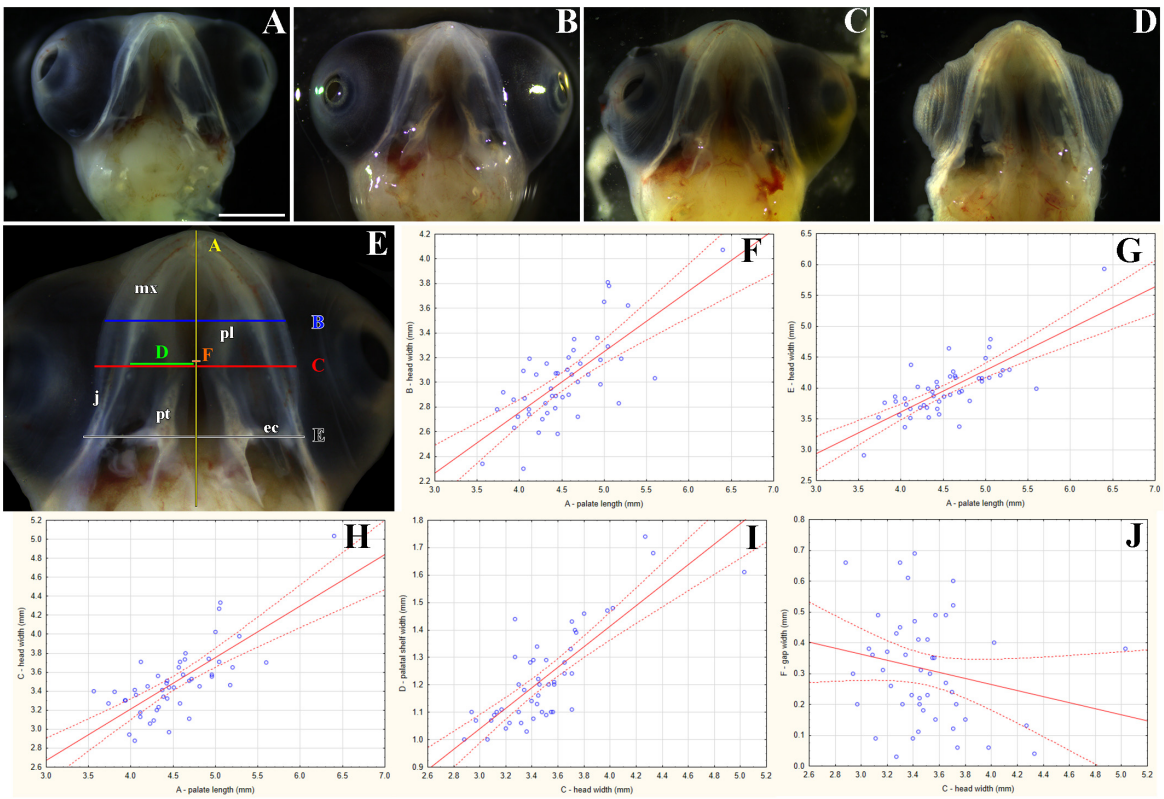

FIGURE 6 | Morphological variation of the palatal shelves in chameleon embryos. Variability of the palatal region in embryonic chameleons within 15th week of the pre-hatching development **(A–D)**. Embryonic heads are aligned from the smallest **(A)** to the largest **(D)**. Head lengths were measured from the tip of the rostrum to the most caudal part of the pterygoid bones (distance **A**); the measurements in panel **(E)** were used for correlation analyses between individual parameters **(F–J)**. Head width and palatal shelves width are shown in millimeters. 48 embryos were analyzed. Ninety five percent confidence regression bands are shown as dashed curves. ec, ectopterygoid; j, jugal bone; mx, maxillary bone; pl, palatine bone; pt, pterygoid bone. Scale bar **(A–D)**: 2 mm.

This suggests, again rather expectedly, that as the head and upper jaw increase, the gap between the two palatal shelves is progressively closing.

Scanning electron microscopy revealed a thickened structure at the edge of the palatal shelves that resembled the ectodermal ridge of an early limb. The ridge expanded up to half of the palatal shelves and was observed at all three analyzed pre-hatching developmental stages, which corresponded to the age between 17 and 20 weeks (**Supplementary Figure S2**). The most rostral area that surrounded the primary choanae was rough, with more distinct protuberances formed later in development (**Supplementary Figure S2**). Numerous microvilli and microplicae developed on the palatal surface (**Supplementary Figure S2**). In the most caudal area, we observed clusters of motile cilia (**Supplementary Figure S2**).

Epithelium of the Palatal Shelves Undergoes Region-Specific Differentiation During Pre-hatching Development

Transmission electron microscopy was used to further analyze the ultrastructure of epithelial cells in detail during development and to determine differences in individual area along the palatal shelves. Moreover, we focused on the ridge located in the tip of the palatal shelves, which we discovered by SEM (**Supplementary Figure S2**). Two distinct developmental stages (126 dpo and 161 dpo respectively) were selected.

Noticeable differences in epithelial lining of individual areas were already determined at the earlier analyzed stage (**Figures 7A–L**). The tip area corresponded to the future side of the attachment between the palatal shelves and nasal septum in the most rostral region (**Figure 7A**). This edge of the palatal shelves (medial edge) was covered with less differentiated rounded cells that distinctly protruded from the surface (**Figure 7B**). Numerous glycogen granules were present in all layers of the tip epithelium including in the most superficial layer (**Figure 7C**). The mesenchyme in the tip of the palatal shelves was almost free of collagen fibrils (**Figure 7D**), in contrast to other parts of the shelves.

The epithelial lining of the oral part of the palate (**Figures 7E–H**) comprised two layers of round or columnar basal cells, and two to four layers of squamous superficial cells covering them. Glycogen granules represented the major substance of the basal cells (**Figure 7E**), but they were rare in superficial flattened layers, which did not exhibit signs of keratinization. The basal part of

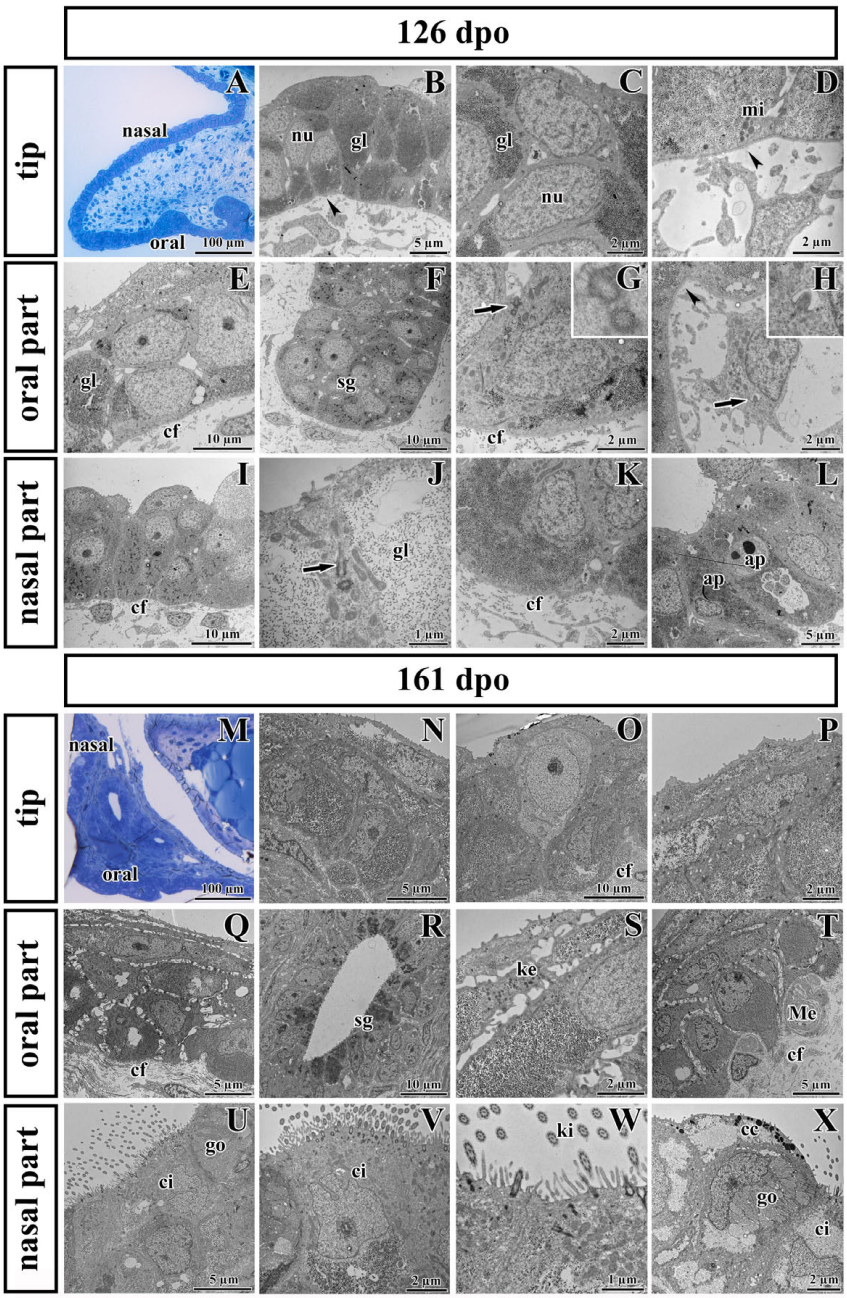

FIGURE 7 | Ultrastructural analysis of the palatal shelves at early and later stages of chameleon pre-hatching development. **(A)** Palatal overview of early developmental stage (126 dpo) stained with Toluidine Blue. **(B–D)** Epithelial cells on the tip of palate with nuclei (nu), high content of glycogen (gl), and mitochondria (mi). **(E–H)** Epithelial (OE) and mesenchymal cells in oral part of the palate. **(F)** The anlage of salivary gland (sg) invaginated from the OE. Primary cilium (arrow) in basal cell of salivary gland. **(H)** Primary cilium in mesenchymal cell (arrow). **(I–L)** Nasal part of palate with club-like cells and cells with high amount of glycogen (gl). **(J)** Primary cilium in epithelial cell (arrow). **(L)** Apoptotic bodies (ap) are present in cytoplasm of epithelial cells close to the nasal cavity. Collagen fibrils (cf) are abundant in mesenchyme with the exception of the tip of palate (arrowheads, **B,D**) and the area surrounding future salivary duct (arrowhead, **H**). **(M)** Palatal overview of later developmental stage (161 dpo) stained with Toluidine Blue. **(N–P)** Epithelial cells on the tip of the palatal shelf with high content of glycogen, collagen fibrils (cf) in mesenchyme present in high manner. **(Q–T)** Oral part of the palatal shelf with large intercellular spaces between epithelial cells (Q). **(R)** Epithelial protrusion of the salivary gland with luminal cell containing secretory granules (sg). **(S)** Keratohyalin granules are visible in the superficial layers of the oral part of epithelium. **(T)** Meissner corpuscles are surrounded by collagen fibrils (cf). **(U–X)** Nasal part of the palatal shelf with goblet cells (go), ciliated cells (ci) lined by motile cilia (kinocilia, ki) and club-like cells (cc).

the oral epithelium protruded into several epithelial thickenings, which formed primordia of the palatal gland (**Figure 7F**). Numerous collagen fibrils were found in the mesenchyme surrounding these glandular structures (**Figures 7F,G**), except of the angle between the oral epithelium and the beginning of future duct of salivary gland (**Figure 7H**).

The nasal portion of the palatal shelves (**Figures 7I–L**) exhibited noticeable morphological differences in comparison to the oral epithelium already at this developmental stage (126 dpo). The epithelium was formed by a basal cylindrical layer of cells with high amount of glycogen (**Figure 7J**). The superficial epithelial cells resembled immature club-like cells, which were covered by numerous microvilli (**Figures 7I, J**). Numerous collagen fibrils were present directly beneath the basement membrane (**Figures 7I, K**). Apoptotic bodies were located in the cytoplasm of epithelial cells in the basal angle of the nasal cavity (**Figure 7L**).

At the later stage, there were even more distinct differences between the oral and nasal parts of the palate (**Figures 7M–X**). The epithelium differentiated into dissimilar cell types. Squamous multilayered epithelium developed on the oral side of the palatal shelves (**Figures 7Q–T**) while motile cilia appeared in the nasal part (**Figures 7U–X**). Superficial cells facing to the oral cavity still did not exhibit signs of keratinization (**Figure 7Q**). Even at this late stage, the tip of the palatal shelves contained a population of less differentiated cells with reduced intercellular spaces and occasional large light cells penetrating through the epithelium (**Figure 7O**).

Proliferation of Mesenchymal Cells Decreases During the Growth of the Palatal Shelves in Pre-hatching Stages of the Veiled Chameleon

Based on the observation that the palatal shelves progressively extend toward the midline but do not reach each other, we wanted to uncover underlying cellular processes. To reveal possible dynamic changes in the proliferation pattern during growth of the palatal shelves, we used proliferating cell nuclear antigen (PCNA) labeling. At the earliest observed stage (77 dpo) in the rostral region (**Figures 8A–A′′**), we detected a large number of PCNA-positive cells in the dorsomedial mesenchyme of the developing maxillary prominence (**Figure 8A′′**, arrow). A large number of proliferating cells was also visible in the adjacent epithelium (**Figure 8A′′**). In the caudal part of the palate (**Figures 8D–D′′**), numerous PCNA-positive cells were located in the mesenchymal condensation of developing bones (**Figure 8D′′**, upper left arrow), and a few PCNA-positive cells were spread in the ventrolateral mesenchyme (**Figure 8D′′**, lower arrow). The epithelium was almost entirely free of proliferating cells; only a few positive cells were detected in the bend of the presumptive nasal epithelium (**Figure 8D′′**, upper right arrow).

During later development (98 dpo) in the rostral area of the developing palatal shelves (**Figures 8B–B′′**), a cluster of PCNA-positive cells was detected in the mesenchymal condensations of the developing palate-forming bones (**Figure 8B′′**, left arrow). The signal was also detected in the oral and nasal epithelium that covered the medial palatal protrusion (**Figure 8B′′**, upper and lower right arrows). In the caudal portion, only a few PCNA-positive cells were detected in the mesenchyme lateral from the mesenchymal condensation (**Figure 8E′′**, left arrow) and in the tip of the palatal shelf (**Figure 8E′′**, middle arrow). On the other hand, the epithelium in the oral and nasal areas was inhabited by a large number of proliferating cells (**Figure 8E′′**).

At the latest observed stage (105 dpo), (**Figures 8C–F′′**), the mesenchyme was almost free of PCNA-positive cells in both the rostral and caudal palatal areas. There were only few proliferating cells located in the oral part of the underlying mesenchyme in the caudal area; they were mostly associated with protruding palatal glands (**Figure 8F′′**, arrows). In contrast, there was still a small amount of PCNA-positive cells equally distributed in the oral and nasal epithelium covering the palatal shelves in both the rostral and caudal areas (**Figures 8C′′,F′′**).

Apoptosis Does Not Significantly Contribute to Palatogenesis in Chameleons

We detected only a small number of apoptotic cells in the palatal shelves during pre-hatching development using the TUNEL assay (**Supplementary Figures S3A–F**). At early stages, the apoptotic cells were detected in the mesenchymal condensations of the future palate-forming bones (**Supplementary Figures S3A′′,D′′**). During later stages, they were located in the mesenchyme surrounding the palatal region bones (**Supplementary Figures S3B′′,E′′**) or in the zones, where mesenchymal condensation split between two ossification centers of neighbor membranous bones. However, only a few apoptotic cells were distributed across the epithelium of the oral or nasal part of the palatal shelves or underlying mesenchyme (**Supplementary Figures S3C′′,F′′**).

Polarized SHH Protein Localization in the Mesenchymal Cells of the Palatal Shelves

Epithelial SHH is required for mesenchymal cell proliferation during palatogenesis in mammals (Mo et al., 1997; Zhang et al., 2002). In the mouse, *Shh* mRNA is mainly expressed in the palatal epithelium, while other members of the SHH pathway (the membrane receptors PTCH1 and SMO or the transcription factor GLI1-3) are expressed in the palatal mesenchyme and epithelium. *Shh* expression in the epithelium is reciprocally induced by signals from the mesenchyme and then it signals back to the mesenchyme (Rice et al., 2006).

Based on these facts, we asked whether the SHH signal is specifically located in the chameleon palatal shelves in order to stimulate cell proliferation in a specific pattern and direction. During growth of the chameleon palatal shelves, SHH protein was localized in the palatal epithelium and mesenchyme. At the earliest analyzed stage (77 dpo) of the rostral part (**Figures 9**, **10**) of the palatal epithelium, the strongest SHH signal was visible in the medial part of the palatal shelf protrusion (**Figures 9A–A^{d}**). Later (98 dpo), SHH was again detected in almost the entire epithelium that covered the developing palatal shelves, but there was apparently less SHH protein compared to the earlier stage

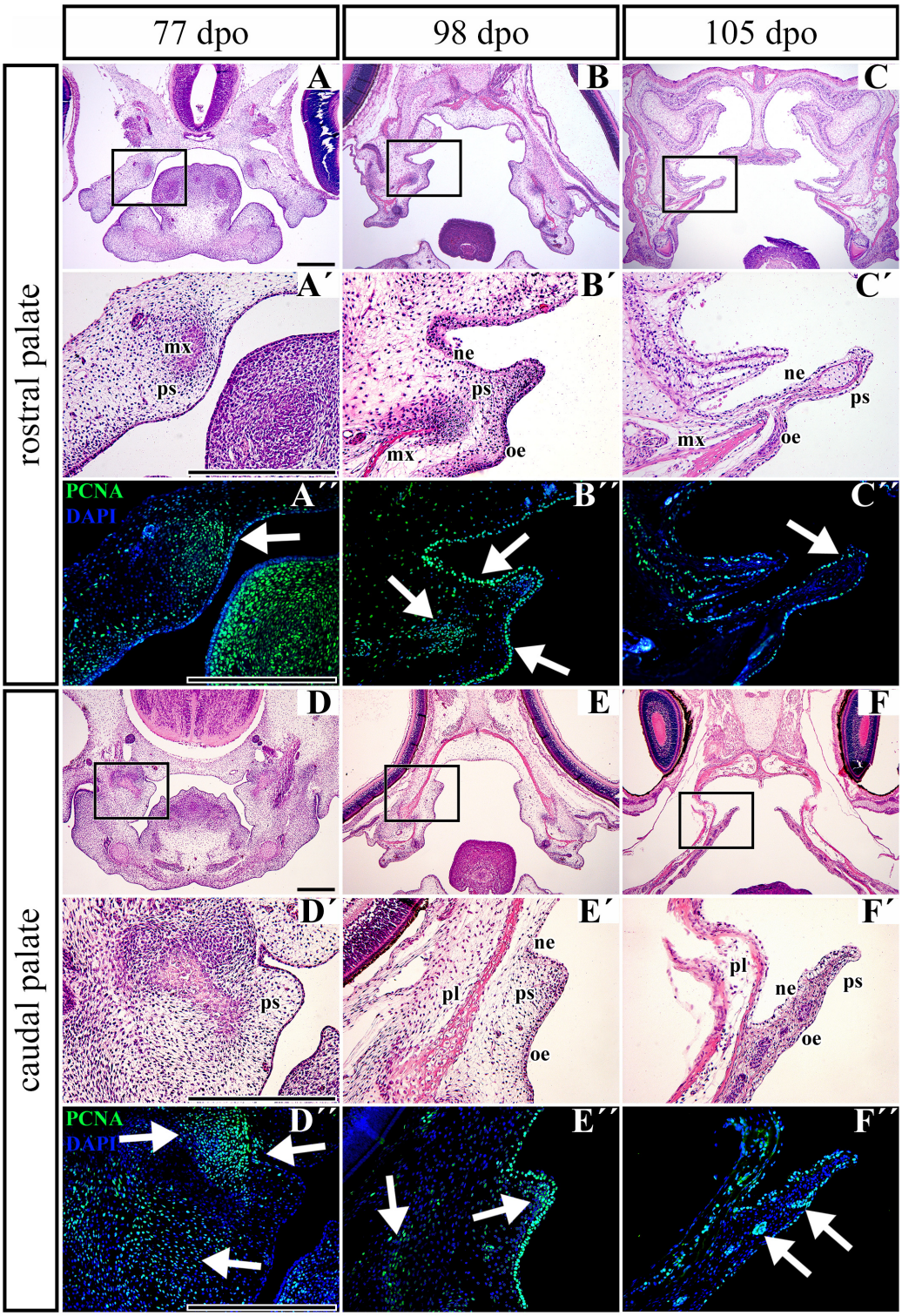

FIGURE 8 | Distribution of proliferating cells in the palatal shelves of chameleon embryos. Cell proliferation in the palatal shelves of 77 dpo **(A–D′′)**, 98 dpo **(B–E′′)**, and 105 dpo **(C–F′′)** stages of the veiled chameleon. Hematoxylin-Eosin staining on the frontal head sections in the lower power and higher power view from the rostral **(A,A′–C,C′)** and caudal **(D,D′–F,F′)** part of the palatal shelves. Immunohistochemical detection of PCNA-positive cells in the higher power view (details from black rectangles) from the rostral **(A′′–C′′)** and caudal **(D′′–F′′)** palatal shelves. PCNA-positive cells – green nuclei, PCNA-negative cells – blue nuclei (DAPI). White arrows point regions of PCNA-expressing cells in the forming palatal shelves. dpo, days post oviposition; mx, maxillary bone; ne, nasal epithelium; oe, oral epithelium; pl, palatine bone; ps, palatal shelf. Scale bar: 200 μm.

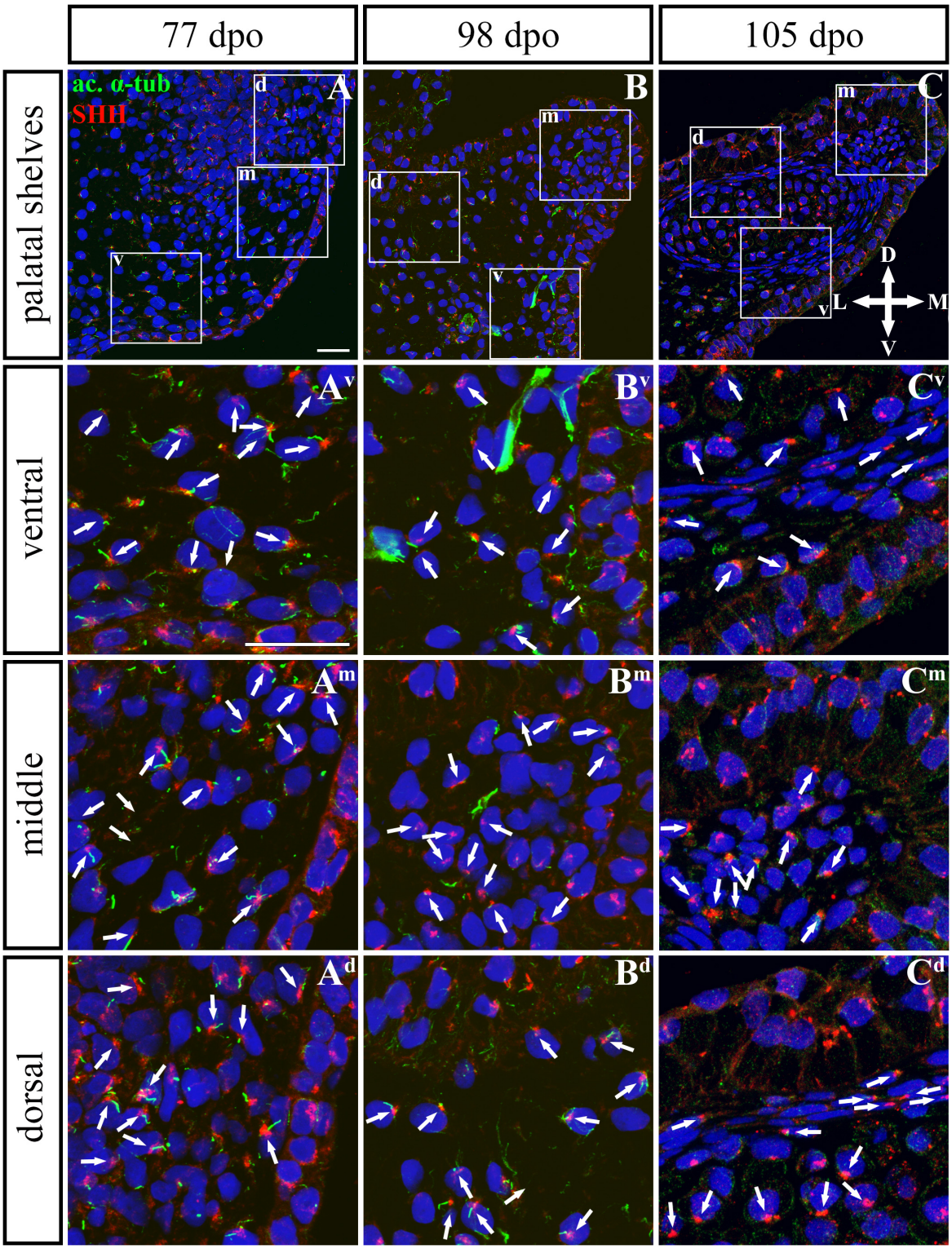

FIGURE 9 | SHH and acetylated α-tubulin protein localization in the rostral palatal shelves in pre-hatching chameleons. Immunodetection of SHH (red) and acetylated α-tubulin (green) proteins on transversal sections. Lower power pictures overview localization at 77 dpo **(A)**, 98 dpo **(B)**, and 105 dpo **(C)** during pre-hatching development. White rectangles define regions focused on ventral (v), middle (m) and dorsal (d) parts of the palatal shelves. Pictures **(A^v–C^d)** show higher power details from ventral, middle and dorsal regions. White arrowheads indicate polarized colocalization of SHH and primary cilium (detected using acetylated α-tubulin) on the same cellular side. Acetylated α-tubulin is present not only in primary cilia, but as well in microtubules of mitotic spindle, therefore there was signal in both structures detected in green. Nuclei are counterstained with DRAQ5. Scale bar: 20 μm.

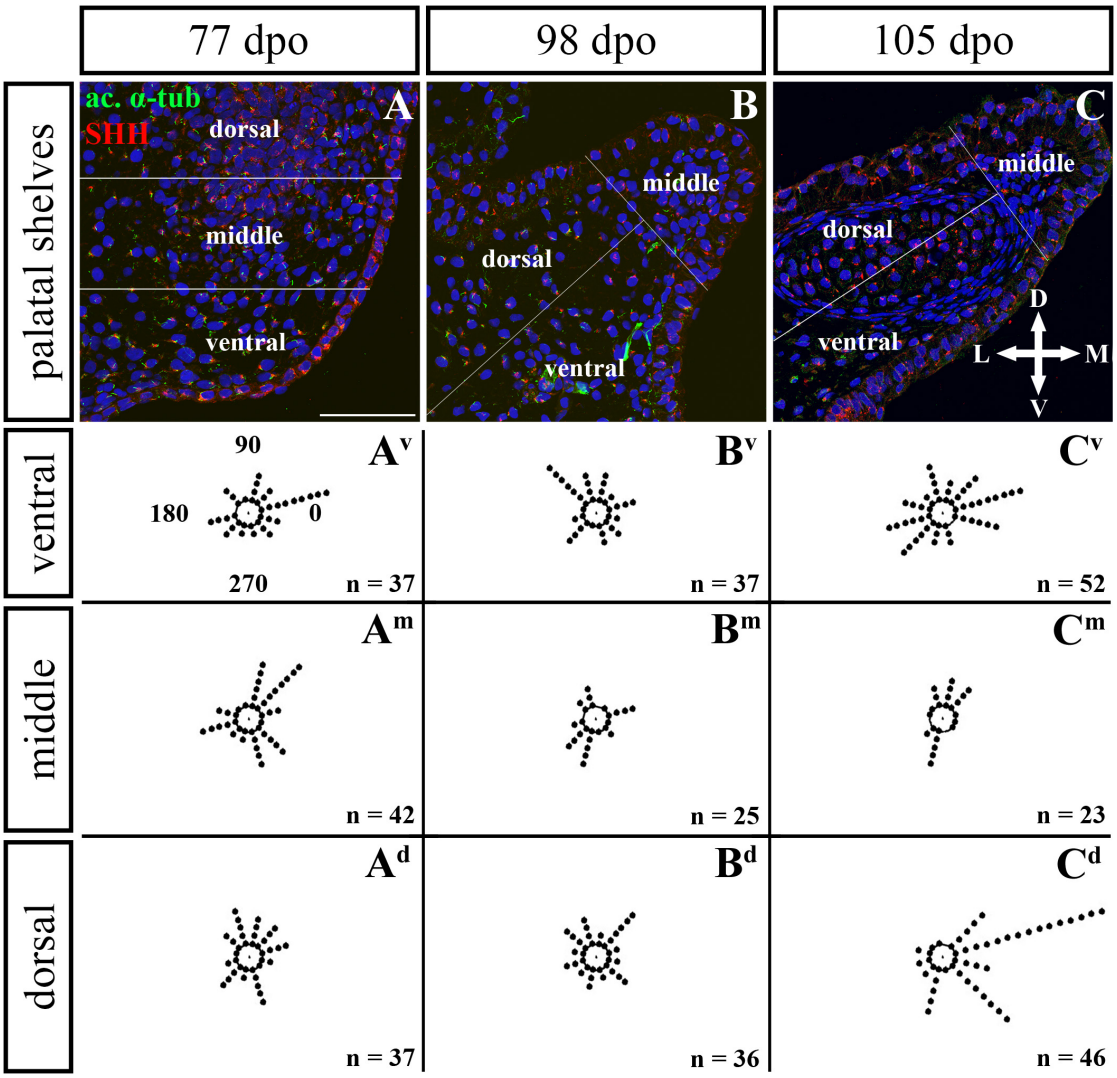

FIGURE 10 | Analysis of SHH ligand polarized localization in the rostral area of the palatal shelves during pre-hatching development. Immunohistochemical detection of SHH polarized localization in mesenchymal cells of the developing palatal shelves. Pictures **(A–C)** show transversal sections divided into ventral, middle and dorsal areas. Rose dot plots of 77 dpo **(A^v,A^m,A^d)**, 98 dpo **(B^v,B^m,B^d)**, and 105 dpo **(C^v,C^m,C^d)** stages show polarity of SHH in individual cells (each dot) according to the dorsoventral and mediolateral axes. The 360 degree circle was divided into 12 zones each with a 30 degree span. 0°, medial direction; 90°, dorsal direction; 180°, lateral direction; 270°, ventral direction. n, number of cells analyzed in each area. Scale bar: 50 μm.

(**Figures 9B–B^d**). However, amount of SHH protein was much reduced in the epithelium, especially in the palatal shelf tip at the oldest analyzed stage (105 dpo) (**Figures 9C–C^d**). In the rostral palatal mesenchyme at the 77 dpo stage, the SHH signal was located especially in the dorsal mesenchymal condensations (**Figures 9A,A^d**). Later in development (98 dpo), SHH was spread equally in all the mesenchymal cells (**Figure 9B**). However, at the 105 dpo stage, while there was some SHH signal in the mesenchymal cells, the amount of SHH protein was strongly reduced (**Figure 9C**).

In the caudal (**Figures 11**, **12**) epithelium, a strong SHH signal was detected at the early (92 dpo) (**Figures 11A–A^d**) and middle (113 dpo) (**Figures 11B–B^d**) analyzed stages. Only few SHH positive cells were detected in the epithelium at the latest observed stage (128 dpo) (**Figures 11C–C^d**). The SHH localization was similar in the mesenchyme of the caudal and rostral parts of the palatal shelves. SHH was visible in almost all mesenchymal cells at the 92 dpo stage, with the stronger signal detected in the ventrolateral region of the mesenchymal condensation (**Figure 11A**). At the 113 dpo stage, the SHH signal was slightly decreased (**Figure 11B**), whereas at the 128 dpo stage, there was only a trace amount of SHH (**Figure 9C**).

Given that SHH positivity was found in the mesenchymal cells in a specific polarized pattern, we analyzed the distribution of the oriented and localized SHH signal in the mesenchymal cells during outgrowth of the palatal shelves. The palatal shelves at the three developmental stages were divided into three distinct

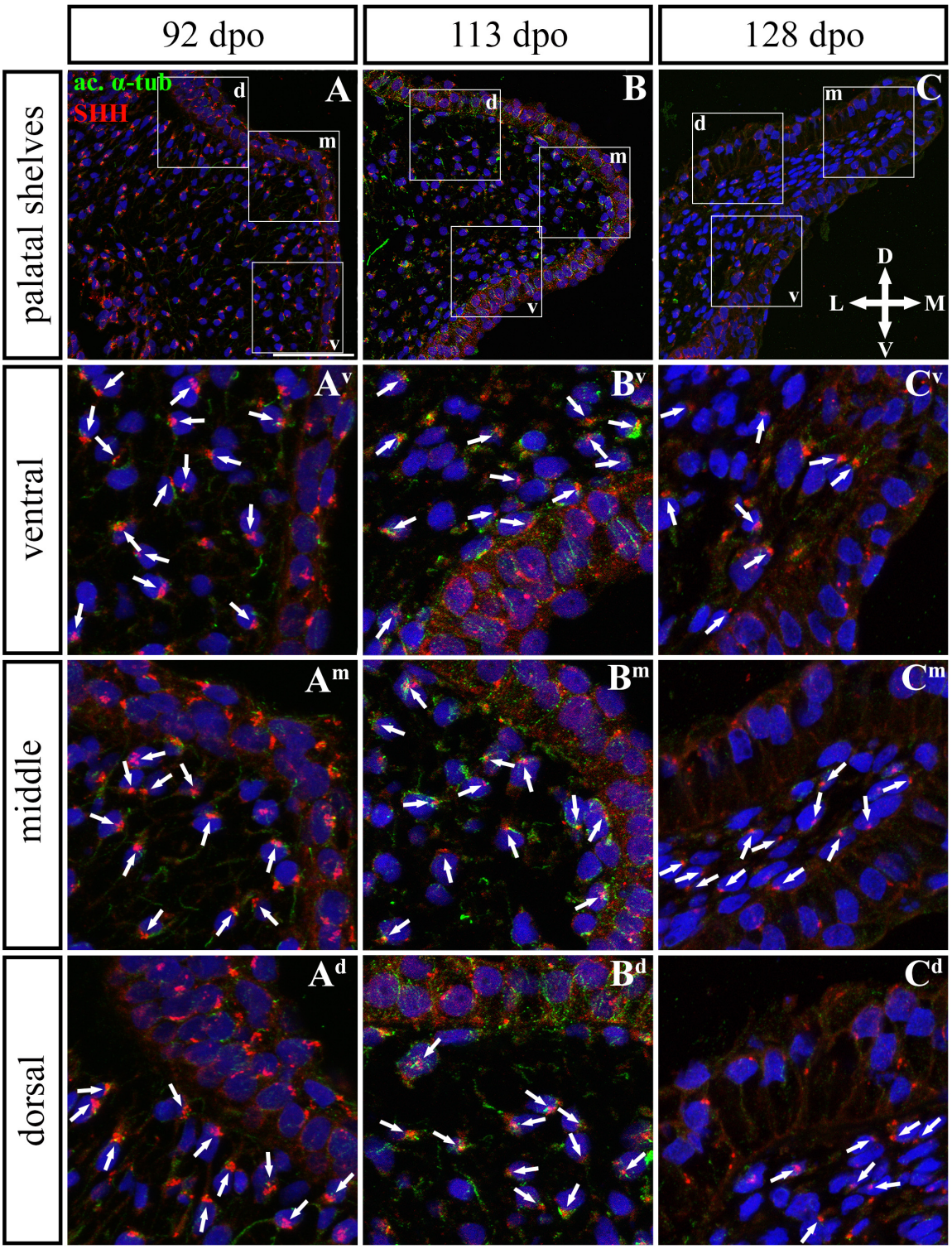

FIGURE 11 | SHH and acetylated α-tubulin protein localization in the caudal palatal shelves in pre-hatching chameleons. Immunodetection of SHH (red) and acetylated α-tubulin (green) proteins on transversal sections. Lower power pictures overview localization at 92 dpo **(A)**, 113 dpo **(B)**, and 128 dpo **(C)** during pre-hatching development. White rectangles define regions focused on ventral (v), middle (m) and dorsal (d) parts of the palatal shelves. Pictures **(A^v–C^d)** show higher power details from ventral, middle and dorsal regions. White arrowheads indicate polarized colocalization of SHH and primary cilium (detected using acetylated α-tubulin) on the same cellular side. Acetylated α-tubulin is present not only in primary cilia, but as well in microtubules of mitotic spindle, therefore there was signal from both detected in green. Nuclei are counterstained with DRAQ5. Scale bar: 20 μm.

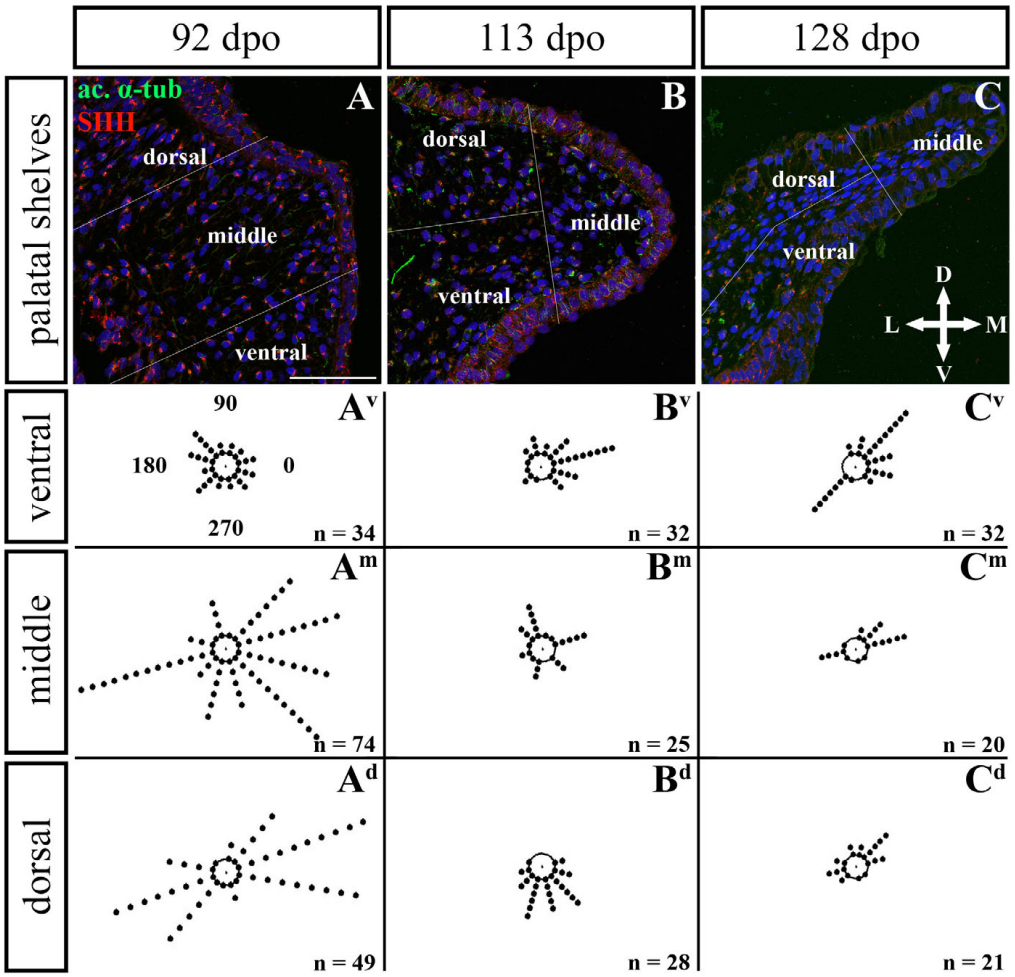

FIGURE 12 | Analysis of SHH ligand polarized localization in the caudal area of the palatal shelves during pre-hatching development. Immunohistochemical detection of SHH polarized localization in mesenchymal cells of the developing palatal shelves. Pictures **(A–C)** show transversal sections divided into ventral, middle and dorsal areas. Rose dot plots of 92 dpo **(A^v,A^m,A^d)**, 113 dpo **(B^v,B^m,B^d)** and 128 dpo **(C^v,C^m,C^d)** stages show polarity of SHH in individual cells (each dot) according to the dorsoventral and mediolateral axes. The 360 degree circle was divided into 12 zones each with a 30 degree span. 0°, medial direction; 90°, dorsal direction; 180°, lateral direction, 270°, ventral direction. n, number of cells analyzed in each area. Scale bar: 50 μm.

regions (dorsal, middle, and ventral) in both the rostral and caudal areas. SHH signal orientation was analyzed in relation to the position of the nucleus, and rose plots were used to reveal differences in the SHH localization pattern in different areas of the palatal shelves (**Figures 10**, **12**).

Although the analysis at the earliest analyzed stage revealed polarized but more or less random localization of the SHH protein in the mesenchymal cells in both the rostral (77 dpo) (**Figures 10A–A^d**) and caudal areas (92 dpo) (**Figures 12A–A^d**), there were some regional exceptions. The analysis in the ventral part of the rostral palatal shelves determined that the most of the cells exhibited SHH localization in medial direction (**Figures 10A^v**, close to 20° direction). In the caudal palatal shelves, a similar SHH localization pattern was detected in the middle and dorsal parts, where SHH of most of the cells was localized in the dorsomedial and ventromedial direction (**Figures 12A^m,A^d**, spans directions roughly from 315 to 45°). Moreover, there were many cells with SHH localized in a lateral direction opposite to the medial direction (**Figures 12A^m,A^d**, close to 200° direction). A similar situation was found in both later stages in the rostral (98 and 105 dpo) (**Figures 10B,C**) and caudal (113 and 128 dpo) (**Figures 12B,C**) areas. While in the rostral palatal shelves, polarized localization of the SHH protein was more random (**Figures 10B^v–B^d**) with respect to the growth direction, in caudal palatal shelves, SHH was localized in ventral mesenchymal cells more medially (**Figure 12B^v**, close to 20° direction) and in dorsal mesenchymal cells more ventrally (**Figure 12B^d**, spans directions roughly from 250 to 315°).

At the latest observed stage in both rostral (105 dpo) (**Figures 10C–C^d**) and caudal (128 dpo) (**Figures 12C–C^d**) regions, very similar SHH protein localization pattern of the mesenchymal cells was detected in the middle area. With respect to the direction of the most distal part of the palatal shelves, in the rostral region, SHH in most of the cells was localized

more in dorsal direction (**Figure 10C^{m}**, spans direction from 45 to 90°) and in the caudal region, it was particularly in medial direction (**Figure 12C^{m}**, spans direction from 20 to 45°). Most of the dorsal mesenchymal cells in the rostral palatal shelves had the SHH protein localized in the medial direction and this pattern resembled direction of the palatal shelf growth (**Figure 10C^{d}**, close to 20° direction). Dorsal mesenchymal cells in the caudal palatal shelves exhibited more random localization of SHH signal (**Figure 12C^{d}**). Similarly, random SHH localization was detected in the ventral mesenchymal cells of the rostral palatal shelves (**Figure 10C^{v}**), but in the caudal region, ventral mesenchymal cells demonstrated especially polarized localization of SHH (**Figure 12C^{v}**) corresponding to the prolonged shape of the palatal shelves in the dorsomedial direction (**Figure 12C**).

Colocalization of the Primary Cilia and the SHH Protein in the Mesenchymal Palatal Cells

As the hedgehog signaling was found to be polarized in the mesenchyme and it is well known to be regulated by primary cilia during development, we decided to further follow their appearance in the chameleon palatal shelves. Primary cilia have been observed in a large variety of mammalian cell types or numerous invertebrates (Wheatley et al., 1996; Huangfu et al., 2003; Haycraft et al., 2005; Huangfu and Anderson, 2005; Brugmann et al., 2010; Schock et al., 2016; Hampl et al., 2017), however, they have not yet been described in reptilian species. Therefore, we aimed to analyze the primary cilia structure in chameleon embryos and their possible association with the SHH protein during palatogenesis.

In chameleon embryos, the primary cilia were found in the epithelial and mesenchymal cells of the palatal shelves (**Figures 9**, **11**), including the palatal cartilage (**Supplementary Figure S4**). Ultrastructural analyses revealed the usual structure of primary cilia in the chameleon palatal shelves. The primary cilia comprised an axoneme that extended from a basal body, which is a modified version of the mother centriole (**Supplementary Figure S4**) and serves as a microtubule organizing center in the cell. The basal body had a "9 + 0" structure and was composed of nine microtubule triplets that displayed a radial symmetry. The second centriole was arranged orthogonally to the mother centriole. A microtubule-based axoneme consisted of nine doublet microtubules that lacked the central pair of microtubules (9 + 0) and was surrounded by a ciliary membrane (**Supplementary Figure S4**). In some cases, we observed an irregular arrangement of microtubules in the axoneme (**Supplementary Figure S4**). In chondrocytes, they were embosomed by numerous membranous structures of Golgi apparatuses and vesicles (**Supplementary Figure S4**). In epithelial and mesenchymal cells, the vesicles that surrounded the basal body of primary cilia were more random in comparison to chondrocytes (**Supplementary Figure S4**).

To further evaluate primary cilia distribution in palatal tissues, we used acetylated alpha-tubulin staining to visualize the ciliary axoneme (**Figures 10**, **12**). The primary cilia were associated with the SHH signal but not all SHH-positive cells possessed primary cilia on their surface (**Figures 10**, **12**). This inconsistency was probably associated with the actual cell cycle phase. The primary cilia were more frequent at both earlier observed stages in the rostral area (77 and 98 dpo, **Figures 10A,B**) as well as caudal area of the palatal shelves (92 and 113 dpo, **Figures 12A,B**). At the latest observed stages of both analyzed areas (105 dpo, **Figure 10C** and 128 dpo, **Figure 12C**), there were only a few primary cilia detected in the palatal shelves.

Msx1 and *Meox2* Expression Is Shifted Along the Rostro-Caudal Axis in the Craniofacial Region During Pre-hatching Development of the Veiled Chameleon

Although the molecular regulation of palatogenesis in mammals has been well studied, control of the secondary palate development in non-mammalian species, especially in reptiles, is almost unknown. Therefore, we decided to investigate the molecular mechanisms that contribute to the secondary palate development in chameleon embryos.

For further analyses, we selected three genes (*Msx1*, *Meox2*, and *Pax9*), all of which display a distinct expression pattern during mammalian palatogenesis. In mice, *Msx1* is typically expressed in the rostral part of the maxilla and premaxilla and in the rostral region of the palatal shelves (Zhou et al., 2013). On the contrary, *Meox2* is specific for the caudal zone of the palatal shelves (Jin and Ding, 2006). *Pax9* is expressed in both rostral and caudal parts of the palatal shelves, but the expression increases in the caudal direction (Zhou et al., 2013).

In chameleons, there is a different pattern of membranous bones that form the hard palate in comparison to mammals and other reptiles. While in mammals the secondary palate is formed by palatal processes of the maxilla and only the most caudal region is formed by the palatine bones, in chameleons the maxillary bones are shifted to lateral regions of the upper jaw. Since the main bones of the secondary palate in chameleons are palatines in the rostral region and pterygoids in the caudal region, we hypothesized that there would be a shift in gene expression of region-specific molecules (*Msx1, Meox2*) during chameleon palatogenesis.

First, we used whole-mount ISH to uncover the gene expression pattern of these molecules in the upper jaw and the palatal shelves of chameleon embryos at 106 dpo (**Figure 13**). Strong expression of *Msx1* was detected in the most rostral zone of the upper jaw (**Figure 13A′**) as well as in the very most caudal zone of the upper jaw (**Figure 13A**). It was also expressed very specifically in the developing teeth in the rostral part of the upper jaw (**Figure 13A′**). Expression of *Msx1* in the palatal shelves was localized only to the verymost rostral zone (**Figure 13A′**). A positive signal of *Msx1* was also detected around the medial, ventral and dorsal edges of the nasal pits (**Figures 13B,B′**).

In the upper jaw, *Meox2* was expressed from the rostral to caudal part with the strongest signal detected laterally in the rostral zone (**Figures 13C,C′**). The very rostral tip of the upper jaw was *Meox2*-negative (**Figure 13C′**). The whole rostral

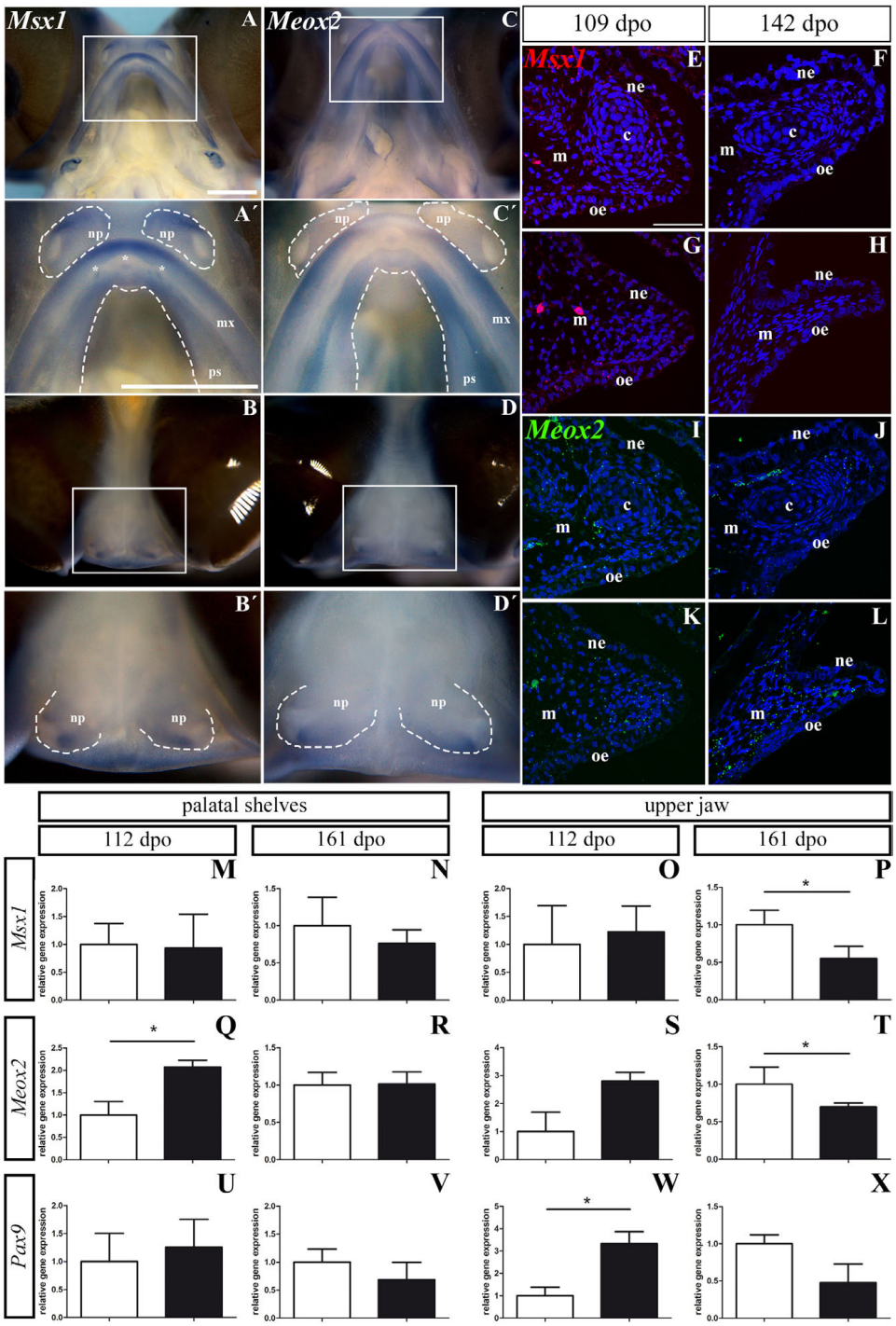

FIGURE 13 | *Msx1, Meox2*, and *Pax9* expression during pre-hatching development of chameleon. Whole mount *in situ* hybridization analysis of *Msx1* and *Meox2* expression on embryo at stage 106 dpo **(A–D′)**. Lower power pictures show overall view on expression of *Msx1* and *Meox2* in either ventral **(A,C)** or frontal **(B,D)** view. Higher power pictures display detail of *Msx1* and *Meox2* expression in the upper jaw region, palatal shelves and nasal pits, from ventral **(A′,C′)** and frontal **(B′,D′)** view. White rectangles define detailed area. The palatal shelves and nasal pits are highlighted with dashed line. Asterisks show expression of *Msx1* in developing teeth. np, nasal pit; mx, maxilla; ps, palatal shelf. Scale bars: 1 mm. RNAScope analysis of *Msx1* and *Meox2* expression **(E–L)**. Transversal sections with focus on the palatal shelves at 109 dpo **(E,G,I,K)** and 142 dpo **(F,H,J,L)** in rostral and caudal regions. Specific expression of *Msx1* in rostral **(E,F)** and caudal **(G,H)** region is shown as red dots. *Meox2* expression in rostral **(I,J)** and in caudal **(K,L)** regions is shown as green dots. Nuclei are counterstained with DAPI. ne, nasal epithelium; oe, oral epithelium; m, mesenchyme; c, cartilage. Scale bar: 50 μm. QPCR analysis of *Msx1, Meox2*, and *Pax9* expression **(M–X)**. Comparison of relative gene expression of *Msx1, Meox2*, and *Pax9* in the palatal shelves at earlier (112 dpo; **M,Q,U**) and later stage (161 dpo; **N,R,V**), and in the upper jaw at 112 dpo **(O,S,W)** and 161 dpo stage **(P,T,X)**, respectively. Gene expression is compared to the rostral region (white columns) and its gene expression level is displayed as value 1.0. The expression in the caudal region (black columns) is displayed as fold change to rostral area. *t*-test; $p^* < 0.05$.

part of the palatal shelves was *Meox2*-positive, while the caudal region of the palatal shelves was positive only in its lateral part close to the maxilla (**Figures 13C,C′**). In the nasal pits, we observed a *Meox2* expression pattern that was very similar to that of *Msx1* (**Figures 13D,D′**), only the signal of *Meox2* was much weaker compared to *Msx1* especially in the ventral view (**Figures 13A′,C′**).

Next, we wanted to detect expression of the palate-specific genes *Msx1* and *Meox2* in more detail on histological sections. Therefore, we used a fluorescent RNAScope assay for two developmental stages. At the early stage (109 dpo), there was relatively low expression of *Msx1* in the rostral and caudal palatal shelves. While the *Msx1* signal was dispersed within mesenchyme and palatal epithelium in the rostral region (**Figure 13E**), in the caudal region, there was higher expression in the ventral part of the palatal shelves and especially in the future oral epithelium (**Figure 13G**). At the later stage (142 dpo), *Msx1* expression was much lower. A weak signal was dispersed in the epithelium and mesenchyme in the rostral region (**Figure 13F**), but in the caudal region (**Figure 13H**) only few spots were detectable. *Meox2* was dispersed in the mesenchyme and epithelium of the rostral palatal region (**Figure 13I**), similar to *Msx1* (**Figure 13E**) at the earlier observed stage. In the caudal region, *Meox2* was expressed more in the mesenchyme close to the palatal shelf tip, and only a weak signal was detected in the palatal epithelium (**Figure 13K**). At the later stage, *Meox2* was almost omitted from the epithelium, and also much weaker signal was detected in the mesenchyme in the rostral zone (**Figure 13J**) compared to the earlier stage (**Figure 13I**). At the later stage in the caudal region of the palatal shelves, *Meox2* was strongly expressed in the mesenchyme, but the epithelium was almost free of any signal (**Figure 13L**).

Analysis of *Msx1, Meox2,* and *Pax9* Expression Levels Confirms the Altered Abundance of the Region-Specific Molecules During Craniofacial Development in Chameleons

To further quantify the observed gene expression pattern changes, we designed chameleon-specific primers for *Msx1*, *Meox2*, and *Pax9* and performed real-time PCR separately in tissues isolated from the rostral and caudal areas of the palatal shelves, as well as from more laterally situated tissues from the upper jaws. During pre-hatching development (112 dpo and 161 dpo) of the veiled chameleon, expression of these three genes varied along the rostro-caudal axis of the both palatal shelves as well as the upper jaws (**Figure 13** and **Supplementary Figure S5**).

In the palatal shelves, the level of *Msx1* expression was highly similar in the rostral (1.0 ± 0.3736) and caudal region (0.93 ± 0.6087, $p = 0.4494$) at the 112 dpo stage (**Figure 13M**), but at the 161 dpo stage, its expression was reduced in the caudal region (0.7617 ± 0.1860, $p = 0.2045$) relative to the rostral region (**Figure 13N**). In the upper jaw region, *Msx1* expression was slightly upregulated in the caudal (1.226 ± 0.4593, $p = 0.3788$) compared to the rostral area at 112 dpo (**Figure 13O**). However, at the 161 dpo stage, the *Msx1* signal was significantly reduced in the caudal region (0.55 ± 0.1629, $p = 0.0137$) compared to the rostral area (**Figure 13P**).

Significantly higher *Meox2* expression was detected in the caudal region (2.07 ± 0.1522, $p = 0.0244$) of the palatal shelves compared to the rostral region at 112 dpo (**Figure 13Q**). During later pre-hatching development, *Meox2* levels were comparable in both the rostral (1.00 ± 0.1692) and caudal regions (1.013 ± 0.1617, $p = 0.4680$) of the palatal shelves (**Figure 13R**). In the upper jaw region, *Meox2* was much highly expressed in the caudal region (2.81 ± 0.3105, $p = 0.0606$) when compared to the rostral area of 112 dpo stage (**Figure 13S**). Conversely, significantly lower expression was detected in the caudal region (0.69 ± 0.049, $p = 0.0460$) compared to the rostral area at 161 dpo stage (**Figure 13T**).

In the palatal shelves, *Pax9* expression was higher in the caudal area (1.256 ± 0.4985, $p = 0.3523$) compared to the rostral region at the 112 dpo stage (**Figure 13U**), but its expression was downregulated in the caudal area (0.687 ± 0.3111, $p = 0.2111$) relative to the rostral area at the 161 dpo stage (**Figure 13V**). The expression pattern in the upper jaw region was similar to the palatal shelves, with significantly higher expression in the caudal area (3.329 ± 0.5320, $p = 0.0286$) compared to rostral at 112 dpo stage (**Figure 13W**). Later in development, we again detected downregulated expression of *Pax9* in the caudal area (0.478 ± 0.2512, $p = 0.0763$) compared to the rostral area of the upper jaw region (**Figure 13X**).

DISCUSSION

Chameleons are well known for their colorful skin, ability to change skin pigmentation pattern, independently moving eyes, and their prey hunting strategy using a very quick, ballistic, and sticky tongue. Therefore, the veiled chameleon is one of the most frequent bred lizards as a pet. However, the veiled chameleon has recently gained the attention of developmental and experimental biologists. It has already been used to study gastrulation (Stower et al., 2015), neural crest migration (Diaz et al., 2019), limb patterning (Diaz and Trainor, 2015), jaw apparatus morphology (Iordansky, 2016), pigmentation, communication, embryonic diapause, and other aspects, including their development (reviewed in Diaz et al., 2015). Until now, research on a feeding apparatus in chameleons has focused mainly on their tongue (Anderson and Deban, 2010, 2012; Herrel et al., 2014) or teeth (Buchtová et al., 2013; Zahradnicek et al., 2014; Dosedělová et al., 2016). However, other craniofacial structures also exhibit interesting features, and thus we focused on the secondary palate formation, bones that support the secondary palate during both pre- and post-hatching developmental periods, and the mechanism involved in the growth of the palatal shelves. As the veiled chameleon develops large palatal shelves, which can reach the midline during post-hatching stages, it makes this model unique from the EVO-DEVO perspective.

Moreover, it is necessary to mention that the chameleon genome has not been fully sequenced and annotated yet, a factor that makes molecular studies more difficult in comparison to other common model animals. Molecular approaches can

be partially compensated by the recently published veiled chameleon transcriptome (Pinto et al., 2019). Another obstacle is the imbalance between developmental stages and difficulties in exact timing of pre-hatching development (Andrews and Donoghue, 2004; Andrews, 2007). This deficit is partly caused by the embryonic diapause, the duration of which can differ between egg clusters, as well as the large variability in the speed of developmental progress among individual embryos in dependence on conditions of external environment such as temperature or humidity during egg incubation.

Inter- and Intraspecies Morphological Variability of the Palatal Shelves

The secondary palate, develop in different species with variable degree from small processes located laterally on the maxillae to large palatal shelves meeting in the midline. Crocodilians exhibit typically fused palatal shelves and form an enclosed secondary palate as they live in an aquatic environment and need to completely separate the nasal and oral cavity. Similarly, mammals create the complete secondary palate, but it rather serves as an apparatus for suckling of milk and later in development for verbal communication (Kimmel et al., 2009; Abramyan and Richman, 2015). However, in most reptiles (**Figure 14**), very small palatal shelves are formed (e.g., geckos, iguana). In other reptiles, e.g., in snakes and turtles, the palatal shelves can be very rudimental with large communication between the oral and nasal cavity (**Figure 14**). On the other hand, birds develop the palatal shelves largely protruding into the midline, but they do not fuse with the opposite side leaving narrow spacing between them.

Interestingly, the macroscopic morphology of the chameleon palatal shelves varies in post-hatching animals and its appearance is not associated to sex or size of animals. We observed some individuals with large palatal shelves, which were in direct contact in the midline, but most of the animals exhibited a space between the shelves. This intraspecific variation in palate closure among chameleons can be caused by genetic variation but also by environmental causes. As all the juvenile and adult chameleons used in this study were obtained from several breeders and thus bred under different conditions, one of the aspects of the variability observed by us could be different feeding and environmental conditions under which the individuals grew. Other possibility is an influence of genetic variation. Unfortunately, we were not able to evaluate correlation of the palatal shelves expansion and genetic variation in *C. calyptratus*, however, the usage of support vector machine classification approaches, similar as was done for the testing of correlation between male color pattern variation in chameleon and molecular genetic population structure (Grbic et al., 2015) could help to uncover such associations in future.

Skeletal Bones That Form the Secondary Palate in Reptiles

The secondary palate of amniotes is composed of several membranous bones. Their pattern, size of individual skeletal elements, and the extent of their contribution to the secondary palate varies among amniote species (Hanken and Thorogood, 1993). In chameleons, the identity of bones in the palatal area is similar to other higher vertebrates with membranous bones that protrude into the large secondary palate. However, there are significant differences when comparing the pattern of these bones with other species that exhibit the palatal closure. In mammals and crocodilians, the most rostral part of the palate is formed by the premaxilla, and the largest part of the hard palate is supported by medial palatal protrusions of the maxillary bones joined together with a suture at the midline. Paired palatine bones are located caudally from the maxillary bones (**Figures 15A,B**). This location contrasts with chameleons, where the premaxilla comprises only a small proportion of the most rostral zone of the upper jaw. The maxilla is located generally laterally in the jaw and is the main tooth bearing bone (**Figure 15C**). The largest proportion of the chameleon palatal shelves is formed by the palatine bones expanding into their rostral area. In the caudal palatal area, the skeletal pattern in chameleons is similar to crocodilians, with a large and flattened pterygoid body. The pterygoid is also extensive and contributes to the secondary palate in fresh water turtles (Abramyan et al., 2014) and sea turtles (Jones et al., 2012). In contrast, mammalian pterygoid bones are reduced caudally either to small bones, e.g., in opossum (Mohamed, 2018), or as ventral processes of the sphenoid bone (pterygoid hamulus) in humans. These bones contribute to a proper function of the soft palate (Krmpotić-Nemanić et al., 2006).

A more comparable pattern of the palate-forming bones to chameleon can be observed in reptiles with open secondary palates, e.g., the geckos (**Figure 15D**). The premaxilla, maxilla, and vomer exhibit almost the same arrangement compared to chameleon. Similar to the chameleon, paired palatine bones are located in the middle of the palatal shelves: rostrally they are connected to the vomer, laterally to the maxilla and ectopterygoid, and caudally to the pterygoid (**Figure 15D**). The maxillary bones are shorter in the gecko and located more rostrally compared to the chameleon. The largest bone of the gecko skull, the pterygoid, is located caudally from the palatine bones (Daza et al., 2015). It was previously proposed that changes in pterygoid size and shape may be associated with differences in jaw movement during food processing or mastication (Crompton, 1995).

The caudal part of the chameleon palate is supported by the ectopterygoid that connects the maxillary, jugal, and pterygoid bones. The presence of the ectopterygoid in mammals is still controversial; it is most often considered to be a part of the pterygoid bone or pterygoid hamulus (Presley and Steel, 1978). In reptiles, however, the ectopterygoid represents an important bone that links the outer and inner rows of the upper jaw skeletal elements. The analysis of wall thickness also revealed that the ectopterygoid has one of the thickest bony trabecula in chameleon. This observation supports the idea of the ectopterygoid as the main bone that carries the pressure load.

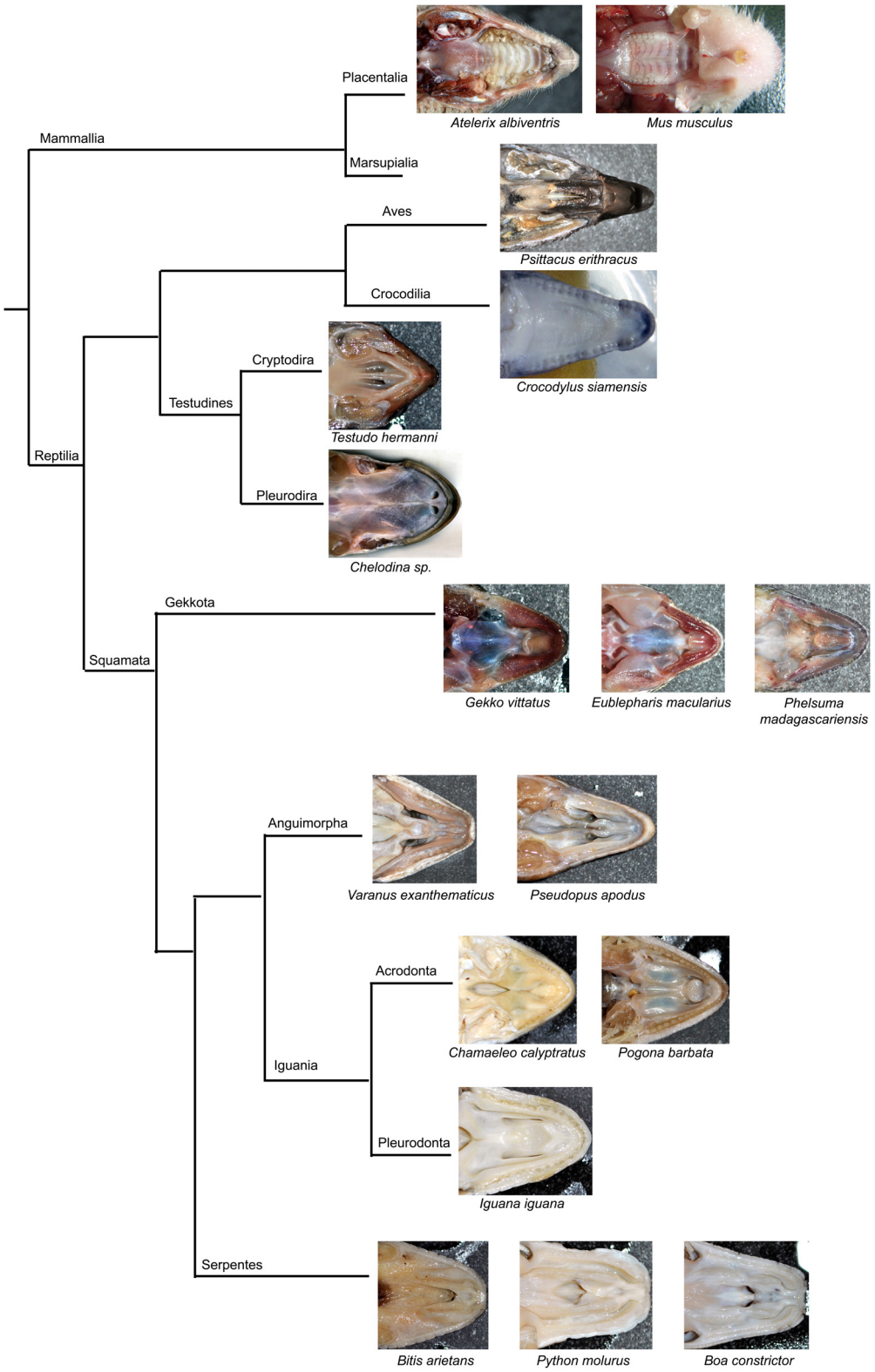

FIGURE 14 | Simplified phylogenetic tree with displayed secondary palate morphology.

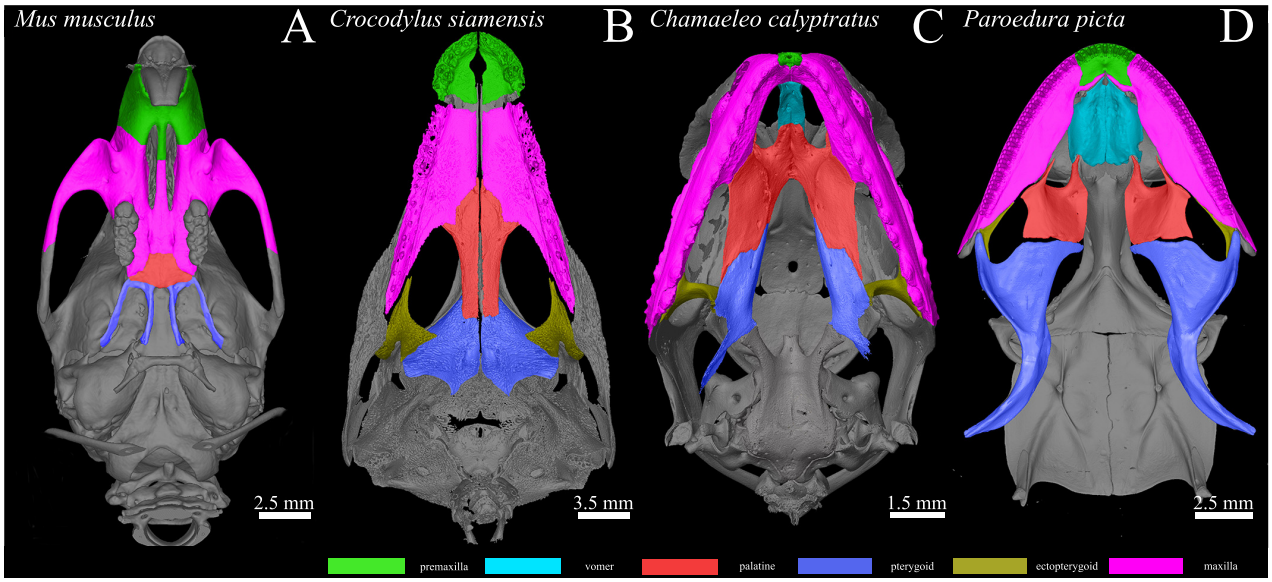

FIGURE 15 | Species-specific arrangement of skeleton contributing to the secondary palate. MicroCT analysis comparing the composition of the palate-forming bones on whole mount cranial skeletons of four different species: *Mus musculus* **(A)**, *Crocodylus siamensis* **(B)**, *Chamaeleo calyptratus* **(C)**, and *Paroedura picta* **(D)**. Individual bones are marked by different colors for better recognition. Each picture has its scale bar with value displayed.

Cartilaginous Structures Can Contribute to the Secondary Palate Formation

During ontogenetic development, the hard palate of birds and mammals is supported by membranous bones, but in the chameleon, we also observed a cartilaginous structure that invaded the palatal shelves. Interestingly, the cartilage protrudes into the palatal shelves also in mammals during their suckling period (Li et al., 2016). In this group, the palatal cartilage was described as a newly formed element that wholly develops in a membranous bone-forming tissue. In chameleons, the palatal cartilage develops as a part and protrusion of the chondrocranium. It separates from the nasal septum cartilage in the rostral palatal region, and its most caudal portion can reach almost the middle of the palatine bone. This cartilage is located in the palatal region from early pre-hatching development, through juvenile stages into adulthood. Although development of the chondrocranium was well described in several reptilian species (Hernández-Jaimes et al., 2012; Diaz and Trainor, 2019), to our knowledge, a similar structure for this palatal cartilage has not been described in other species.

The Main Palate-Forming Bones Are the First Bones to Ossify in the Craniofacial Skeleton in Species With an Enclosed Secondary Palate

Ossification centers of the craniofacial bones first appear in human around 6–7 weeks (40–42 days) post-conception in the developing mandibular, maxillary, and premaxillary bones. A week later (day 57), the vomer, palatine bones, pterygoid plates of the sphenoid bones, and zygomatic bones appear. Ossification centers of other craniofacial bones appear also during week 8 post-conception. Based on this information (Sperber et al., 2012), the main palate-forming bones – maxillary and premaxillary – are the first bones of the craniofacial skeleton to ossify in humans. Furthermore, in embryos of smaller mammals, such as the house mouse (*Mus musculus*) or golden hamster (*Mesocricetus auratus*), ossification centers for all the bones, that contribute to form the hard palate, appear during the initial phase of ossification: day 15 post-conception in mice (Johnson, 1933) and day 12 in hamsters (Kanazawa and Mochizuki, 1974).

The developmental sequences are similar in reptiles; ossification of the palate-forming bones is initiated first, but the order of the ossification of individual elements differs depending on their contribution to the palate. In the American alligator (*Alligator mississippiensis*), the first ossification is visible in the forming pterygoid and maxillary bones at 26 days post-oviposition (dpo). At 28 dpo, the ossification centers of premaxillary and jugal bones appear. At 35 dpo, the ectopterygoid, palatine, and vomer ossification centers are visible (Rieppel, 1993). In the bearded dragon lizard (*Pogona vitticeps*), the first ossification center appears in the forming pterygoid bone at 18 dpo, followed by the palatine, maxillary, and jugal bones at 24 dpo. Finally, at 28 dpo, the ossification centers emerge in the premaxillary, vomer, and ectopterygoid bones (Ollonen et al., 2018). In the Andean lizard (*Ptychoglossus bicolor*), the ossification timing is similar: the first ossification centers appear in the developing pterygoid, maxillary, jugal and prefrontal bones at 35 dpo, and the premaxillary, vomer and ectopterygoid centers are visible at 39 dpo (Hernández-Jaimes et al., 2012). Even in turtles, where the arrangement of the skeletal elements is altered in comparison to squamate reptiles, such as the alligator snapping

turtle (*Macrochelys temminckii*) representing freshwater turtles, the first ossification center appears in the maxilla at stage 17. The pterygoid ossification center is visible at stage 18, while the centers are visible at stage 20 for the premaxilla and at stage 21 for the vomer, palatine and jugal bones (Sheil, 2005). In this study, we determined, that the first bones ossified in the palatal region of the veiled chameleon were the pterygoid and palatine bones. Slightly later, ossification centers of the jugal bones appeared, followed by the maxillary and ectopterygoid bones. This sequential ossification is very similar to the bearded dragon lizard (*P. vitticeps*) with the only exception of timing of the maxillary bone ossification. The last bones ossified in the palatal region of chameleons are the vomer and premaxillary bones. Based on these few examples of reptilian and non-reptilian species, it is clear that the ossification of the palate-forming skeletal elements starts earlier during pre-hatching development to support developing palatal structures.

Outgrowth of the Palatal Shelves and Their Directionality

In mammals, medial bulge-like protrusions are formed on the lateral maxillary prominences at the beginning of the secondary palate development. These protrusions later grow and transform into the prolonged palatal shelves. First, the palatal shelves protrude vertically downward alongside the tongue and then they elongate in the horizontal direction. After reorientation into the horizontal plane, the palatal shelves grow toward the midline, where they finally fuse. The outgrowth of the palatal shelves from the paired maxillary prominences is a typical feature of amniote craniofacial development (Tamarin, 1982; Bush and Jiang, 2012). This phenomenon contrasts with more basal vertebrates, where the palatal shelves do not develop and the choanae open into the oral cavity (Jankowski, 2013). In amniotes, there is great variability in the intensity of the palatal shelves outgrowth or directionality of their initial outgrowth. In most lizards, snakes, and birds, the palatal shelves initially grow horizontally without fusion, and the spacing between them remains visible (Kimmel et al., 2009). In crocodilians, the palatal shelves expand also in the horizontal direction from the beginning of their development (Ferguson, 1981b). However, in the most caudal part of the palate, the shelves first protrude vertically and then they turn into horizontal position (Ferguson, 1981a,b, 1987), which is more similar to the mammalian developmental pattern, where the palatal shelves also first expand vertically and later turn horizontally (Bush and Jiang, 2012). In mammals, there are also differences in the morphology and outgrowth of the palatal shelves in the anterior and posterior areas of the secondary palate. In the anterior part, the shelves exhibit a finger-like shape that protrudes into the oral cavity. In the middle palatal zone, the palatal shelves have a more triangular shape while caudal parts have a rounded distal end (Bush and Jiang, 2012).

In this study, we revealed that the palatal shelves of chameleons do not grow strictly in the horizontal direction. They rather extend dorsomedially from the beginning of their initiation. Furthermore, these animals possess an open fissure between the palatal shelves when they hatch. However, the jaw and palate extensively develop and continue to grow even during post-hatching development. In fact, the palatal shelves directly contact in the midline of some adult animals. Certain rostro-caudal differences in the direction of the palatal shelves growth were observed already at the earliest analyzed embryonic stage. While in the rostral palatal region, there was medial round thickening of the future palatal shelf, in the caudal region, there was already a finger-like projection oriented into the horizontal plane. This shape resembles the palatal shelves of the caudal region at E14 in mice (Yu and Ornitz, 2011).

Specific Distribution of Proliferating Cells and Cellular Polarity Is Associated With the Directionality of the Palatal Shelves Outgrowth

The outgrowth of the palatal shelves is characterized by localized proliferation during early stages of development. As the result of this process, we observed differential outgrowth on one side of the palatal shelf. This conserved developmental mechanism was previously described for mammalian species (Iwabe et al., 2005), bird and reptilian (Abramyan et al., 2014) embryos. On the other hand, the loss of proliferation in certain areas was proposed to be the main cause of the palatal shelf outgrowth failure in turtles (Abramyan et al., 2014). In chameleons, we observed an unequal distribution of proliferating cells in the palatal shelves of pre-hatching embryos, with higher proliferation in the dorsal part of the maxillary protrusion resulting in formation of the large palatal shelves. On the other hand, as the animal aged, there was an apparent decrease in the number of proliferating cells, especially in the mesenchyme. This phenomenon seems to contribute to slowing down their outgrowth as the level of proliferation during critical early developmental stages is not effective enough in the palatal shelves for their reaching the midline even though their slow growth continues during post-hatching stages. Therefore, most adult chameleons have a gap between the collateral palatal shelves in the midline and the secondary palate thus remains open.

SHH and bone morphogenetic protein (BMP) signaling are key molecular pathways during the palatal shelves outgrowth (Zhang et al., 2002; Rice et al., 2006). In mammals, SHH expression is restricted to the lateral epithelium, especially to form the rugae palatinae. In chameleons, a stronger SHH signal was observed in both the epithelium and mesenchyme at early stages of development. During pre-hatching development, the amount of SHH protein visibly decreased in the mesenchyme and oral epithelium of the palatal shelves. This observed decrease of the SHH signal corresponded with decreased proliferation, which was followed by reduced growth of the palatal shelves in the dorsomedial direction in chameleons.

From the above mentioned observations, two questions emerge: Why do the palatal shelves not grow first vertically and then reorient to the horizontal direction in chameleons like in mammals? On the other hand, why do they not grow horizontally like in crocodilians, but rather extend in the dorsomedial direction toward each other and the nasal septum? It was

proposed that the growth direction of the palatal shelves during development is influenced by the presence of a large tongue, which functions as a physical barrier. During early mammalian development, the tongue fills almost the entire oronasal cavity, and thus there is no space for the palatal shelves to grow horizontally, and they have to extend first vertically along the tongue. Later, when the head grows along the dorsoventral axis, there is more space above the large tongue. At that time, the palatal shelves can reorient to the horizontal position and grow toward each other to form the complete palate. On the other hand, in crocodilians the tongue is more flattened, so there is no barrier that would impede direct horizontal growth of the palatal shelves. In line with this proposed hypothesis, the chameleon development lies somewhere between mammals and crocodilians. There is a relatively massive tongue in the oronasal cavity, but there is still some space left above it. This state is very similar to the late stage of mammalian palatogenesis during reorientation of the palatal shelves from a vertical to a horizontal position, when there is already free space for their horizontal growth. However, a slight developmental difference which we should mention is that the chameleon palatal shelves grow all along the jaw in dorsomedial direction in order to overgrow the tongue.

Another aspect of the palatal shelves' growth directionality could be polarized localization of the SHH protein and the localization of the primary cilia on the palatal mesenchymal cells. It has been previously reported during development of zebrafish craniofacial cartilages, that mesenchymal cells are oriented to the center of condensations based on expression of anti-gamma tubulin (labeling microtubule organizing center), which colocalized with the primary cilia (Le Pabic et al., 2014). The direction of the chameleon palatal shelves growth corresponds with the cellular localization of SHH protein and the primary cilia in several palatal regions during pre-hatching development, but not all of them. Based on our observations, specific SHH localization seems to be a consequence of mesenchymal cells polarization as SHH protein is bounded here to Hh receptors, which are enriched in the primary cilia and in the surrounding cellular membrane. Therefore, a combination of polarized localization of the primary cilia and associated SHH localization, and directed proliferation could be one of the causes resulting in outgrowth of the palatal shelves typical for pre-hatching chameleons. However, this phenomenon will be necessary to test experimentally in future.

On the other hand, it is necessary to mention, that alteration of the cell dynamics or cell polarity do not need to be only processes contributing to the palatal shelves' growth. The growth of bones and larger scale craniofacial architectural changes affect reciprocal position of the palatal shelves. As the skeletal architecture changes with age, the snout elongates, and the palatal shelves can be translocated to each other by their passive movement associated with narrowing of the midfacial structures. Such changes are common in embryonic and post embryonic ontogeny in reptiles, especially in chameleons that are known for their midline reduction (Rieppel and Crumly, 2009; Diaz and Trainor, 2019).

Expression of *Msx1*, *Meox2*, and *Pax9* During Palate Development in Non-mammalian Species

Palatogenesis is a highly regulated morphogenetic process; the speed and direction of outgrowths from the maxillary prominences must be precisely controlled. The complexity of the palatogenesis control is reflected by the common occurrence of a cleft palate in humans. While the regulation of mammalian palatogenesis has been well studied, knowledge about the genetic control of the secondary palate development in non-mammalian species, especially in reptiles, has been almost entirely omitted.

Msx1, Meox2, and Pax9 genes display distinct expression patterns during mammalian palatogenesis and mutations in these genes cause developmental defects, typically a cleft palate. In mouse, *Msx1* is typically expressed in the rostral palatal shelves (Zhou et al., 2013) while *Meox2* is rather expressed in the caudal palatal shelves (Jin and Ding, 2006). *Pax9* expression increases in the caudal direction in the palatal shelves (Zhou et al., 2013). An expression pattern similar to mouse embryos was observed in chicken with *Msx1* and *Pax9* genes expressed during early development in the maxillary prominences (Namkoong, 2015).

In chameleon, we detected expression of *Msx1* reduced in caudal parts of the palatal shelves and the upper jaw at the 161 dpo stage. Similarly in the chicken model at the HH26 stage, *Msx1* expression is also limited to the rostral part of the maxillary prominence (Namkoong, 2015). During embryonic development (stages 13, 15, and 17) of the Siamese crocodile (*Crocodylus siamensis*) and Chinese softshell turtle (*Pelodiscus sinensis*), *Msx1* expression was detected in the forming palate and maxillary prominences only at the stage 17 (rostro-caudal comparison not shown) (Tokita et al., 2013).

Here, we determined that expression pattern of *Meox2* in chameleon changes during embryonic development in the palatal shelves and the upper jaw region. While at an early stage (112 dpo), *Meox2* expression was much higher in the caudal areas, at later stage (161 dpo), its expression was the same in both regions of the palatal shelves and even higher in the rostral area of the upper jaw region. This pattern is similar to the expression pattern in mouse embryos (Jin and Ding, 2015).

At the early stage (112 dpo) in chameleon, *Pax9* expression was higher in the caudal region of the both palatal shelves and upper jaw region, which is in concert with the expression pattern in mouse embryos (Zhou et al., 2013). The same *Pax9* expression pattern (levels are higher in caudal region of the maxillary prominence) was shown in chicken at the HH24 stage (Namkoong, 2015). Conversely, in chameleon at the 161 dpo stage, *Pax9* was highly expressed in the rostral regions of the both palatal shelves and upper jaw region. In the Siamese crocodile, *Pax9* expression was detected in all three analyzed embryonic stages within forming upper jaw and surrounding tissues, with the strongest expression visible in the forming palatal shelves at stage 17. In the Chinese softshell turtle, *Pax9* was detected in the medial part of the maxillary prominences at stage 13, in the forming palatal shelves at stage 15, and in the medial part of the upper jaw at stage 17 (Tokita et al., 2013).

In this study, we found that all these analyzed genes were expressed during palate development also in a non-mammalian model, the veiled chameleon. Their expression levels differ along the rostro-caudal axis of the palatal shelves during embryonic development. While expression of the *Msx1* and *Pax9* genes was demonstrated during craniofacial embryonic development also in other reptiles, the Siamese crocodile and Chinese softshell turtle (Tokita et al., 2013), unfortunately, their analyzes was not focused on palatogenesis and the level of their expression could not be correlated with the rostro-caudal differences in the palatal shelves morphogenesis, which will be necessary to follow for possible comparisons in the future.

Primary Cilia in Non-mammalian Models

The primary cilia are essential cellular structures that are required for a proper function of several signaling pathways. Non-motile cilia should be present on almost all mammalian cells; they have also been detected in several non-mammalian species. The primary cilia were detected in the chicken, which is used as a model organism for human craniofacial ciliopathies (Schock et al., 2016). Furthermore, zebrafish have been used to model human ciliopathies with a craniofacial phenotype and defective SHH signaling (Duldulao et al., 2009). In *Xenopus*, primary cilia are important structures for signaling pathways and embryonic development (Shi et al., 2014). Although reptiles are becoming more popular among other classic model organism, there is no clear information about analysis or detection of the primary cilia in reptiles. This study is the first to display the primary cilia morphology in reptiles. Interestingly, we found an association of SHH polarity with the presence of the primary cilia in the palatal mesenchymal cells, which correlated with the growth direction of the palatal shelves of the veiled chameleon. However, the real significance of this association will require functional tests.

CONCLUSION

In conclusion, our results revealed several specific morphological features of the secondary palate formation in chameleons. However, there are some remaining developmental questions: Why are the palatal shelves so well developed in chameleons and why does the process of oral and nasal cavity separation continue during post-hatching development up to the complete closure of the palatal shelves in some adult chameleons? Based on the observed heterogenous morphology of the secondary palate in adult individuals, it is not clear if there is any functional advantage for the animals with separated cavities. One possibility is a mechanical need for closing the secondary palate to enable an effective tongue catapult to precisely control its direction. Moreover, the large palatal shelves can be developed just to keep food out of the nasal cavity, similarly to what has been described for birds (Jankowski, 2013). These functional causes of the secondary palate development in chameleons are not known and it will be interesting to uncover them in the future.

DATA AVAILABILITY STATEMENT

The raw data supporting the conclusions of this article will be made available by the authors, without undue reservation, to any qualified researcher.

ETHICS STATEMENT

All procedures were conducted following a protocol approved by the Laboratory Animal Science Committee of the Institute of Animal Physiology and Genetics, Academy of Sciences (licence no. CZ21760006, Liběchov, Czech Republic) under supervision of the Regional Veterinary Administration (Ústecký Region).

AUTHOR CONTRIBUTIONS

MH, JD, MK, HD, AB, OZ, MP, MM, and TZ performed the analysis. OZ, MP, and JK provided the material. MH, JD, MK, MM, JK, and MB drafted the manuscript. All authors contributed to the article writing and approved the submitted version.

FUNDING

This work was supported by the Czech Science Foundation (18-04859S) and by the MEYS CR (CZ.02.1.01/0.0/0.0/15_003/0000460).

ACKNOWLEDGMENTS

We would like to thank Prof. Lukáš Kratochvíl (Department of Ecology, Faculty of Science, Charles University in Prague, Czech Republic) for specimens of the ocelot gecko (*Paroedura picta*) and Prof. David Sedmera (Department of Anatomy, Faculty of Medicine, Charles University, Prague, Czech Republic) for specimens of the Siamese crocodile (*Crocodylus siamensis*). We also thank Dr. Lucie Komolíková Burešová, the author of the CirkStat software, which we used for the analysis of SHH polarized localization.

SUPPLEMENTARY MATERIAL

The Supplementary Material for this article can be found online at: https://www.frontiersin.org/articles/10.3389/fcell.2020.00572/full#supplementary-material

MATERIAL S1 | Chameleon sequences used for primer and probe design.

FIGURE S1 | Detailed palatal and lateral view on chameleon skull at pre-hatching stages. Palatal view on the chameleon head at earlier stage (98 dpo) and at later stage (112 dpo) **(A,B)**. Lateral view on the embryo at 98 dpo stage demonstrate ossification centers of maxillary bone (mx), jugal bone (j), and post-orbitofrontal (pfo) bone **(A′,A′′)**. Lateral view on the embryo of the 112 dpo old with focus ossification centers of maxillary bone (mx), jugal bone (j), and post-orbitofrontal

(pfo) bone **(B′)**. Pictures orientation: left (caudal, C), right (rostral, R). Scale bars: 1 mm.

FIGURE S2 | Palatal shelves morphology and surface structures arrangement of chameleon embryos in scanning electron microscope. Palatal view on prehatching stages of chameleon at age 17 weeks (weight of embryo 0.36 g), **(A–E)**, at age 18 weeks (weight of embryo 0.42 g), **(F–J)** and at age 20 weeks (weight of embryo 0.53 g) **(K–O)**. Low power view on the palatal shelves (ps) **(A,F,K)**. Higher magnification on the rostral areas of the palatal shelves with magnification on the palatal edge (pe), **(B,C,G,H,L,M)**. Higher magnification on the caudal areas of the palatal shelves with magnification on surface structures highlighting motile cilia in the oldest embryo (yellow arrow), **(D,E,I,J,N,O)**. Scale bars: **(A,F,K)** – 2 mm, **(B,G,L)** – 200 μm, **(C,H,M)** – 10 μm, **(D,I,N)** – 200 μm, **(E,J,O)** – 10 μm.

FIGURE S3 | Distribution of apoptotic cells in chameleon embryos. Cell death in the palatal shelves of three different pre-hatching stages of the veiled chameleon. HE stained frontal head sections in the lower power from rostral **(A–C)** and caudal **(D–F)** areas of the palatal shelves. Higher power view (details from black rectangles) of TUNEL-positive cells on transversal sections through head in rostral **(A′–C′)** and caudal **(D′–F′)** areas of the palatal shelves. Details of the palatal shelves with black arrows pointing on TUNEL-positive cells (brown) in either rostral **(A′′–C′′)** or caudal **(D′′–F′′)** regions of the palatal shelves. Nuclei (blue) are counterstained with Hematoxylin. Ps, palatal shelf. Scale bars: 200 μm, details: 100 μm.

FIGURE S4 | Ultrastructure of the palatal cartilage and primary cilia morphology in chameleon embryos. The rudiment of the palatal cartilage was present closely adjacent to nasal part of the palatal shelf and chondroblasts expanded into tip of the palatal shelf. Chondroblasts located on the cartilaginous periphery were flattened, centrally situated cells were oval or round-shaped. Primary cilia were frequently observed in the epithelium, mesenchyme or in the palatal cartilage (arrowheads). In chondrocytes, they were embosomed by membranous structures of Golgi apparatuses. Bb, basal body; cf, collagen fibrils type II; cp, ciliary pocket; ch, chondroblast; ecm, extracellular matrix; ga, Golgi apparatus; gl, glycogen; pe, perichondrium; re, rough endoplasmic reticulum.

FIGURE S5 | Gene expression analyses. Labeled areas from which tissues were collected for QPCR analyses **(A)**. Comparison of gene expression of *Msx1*, *Meox2*, and *Pax9* in the palatal shelves and in the upper jaw during pre-hatching development of the veiled chameleon. Gene expression comparison between individual genes in the palatal shelves of the earlier stage **(B)** and later stage **(C)**, and in the upper jaw of the earlier stage **(D)** and later stage **(E)**. Gene expression is shown as relative gene expression. In each group, gene expression of *Msx1* in the rostral tissue was used as a control for comparison.

TABLE S1 | List of contigs used for the primer and probe synthesis.

TABLE S2 | List of the primers for PCR and QPCR.

REFERENCES

Abramyan, J., Leung, K. J., and Richman, J. M. (2014). Divergent palate morphology in turtles and birds correlates with differences in proliferation and BMP2 expression during embryonic development. *J. Exp. Zool. B Mol. Dev. Evol.* 322, 73–85. doi: 10.1002/jez.b.22547

Abramyan, J., and Richman, J. M. (2015). Recent insights into the morphological diversity in the amniote primary and secondary palates. *Dev. Dyn.* 244, 1457–1468. doi: 10.1002/dvdy.24338

Anderson, C. V., and Deban, S. M. (2010). Ballistic tongue projection in chameleons maintains high performance at low temperature. *Proc. Natl. Acad. Sci. U.S.A.* 107, 5495–5499. doi: 10.1073/pnas.0910778107

Anderson, C. V., and Deban, S. M. (2012). Thermal effects on motor control and in vitro muscle dynamics of the ballistic tongue apparatus in chameleons. *J. Exp. Biol.* 215, 4345–4357. doi: 10.1242/jeb.078881

Andrews, R. M. (2007). Effects of temperature on embryonic development of the veiled chameleon, *Chamaeleo calyptratus*. *Comp. Biochem. Physiol. A. Mol. Integr. Physiol* 148, 698–706. doi: 10.1016/j.cbpa.2007.08.026

Andrews, R. M., and Donoghue, S. (2004). Effects of temperature and moisture on embryonic diapause of the veiled chameleon (*Chamaeleo calyptratus*). *J. Exp. Zool. A Comp. Exp. Biol.* 301, 629–635. doi: 10.1002/jez.a.56

Brugmann, S. A., Allen, N. C., James, A. W., Mekonnen, Z., Madan, E., and Helms, J. A. (2010). A primary cilia-dependent etiology for midline facial disorders. *Hum. Mol. Genet.* 19, 1577–1592. doi: 10.1093/hmg/ddq030

Buchtová, M., Zahradněček, O., Balková, S., and Tucker, A. S. (2013). Odontogenesis in the veiled chameleon (*Chamaeleo calyptratus*). *Arch. Oral. Biol.* 58, 118–133. doi: 10.1016/j.archoralbio.2012.10.019

Bush, J. O., and Jiang, R. (2012). Palatogenesis: morphogenetic and molecular mechanisms of secondary palate development. *Development* 139, 231–243. doi: 10.1242/dev.067082

Crompton, A. (1995). *Masticatory Function in Nonmammalian Cynodonts and Early Mammals. Functional Morphology in Vertebrate Paleontology*. Cambridge: Cambridge University Press.

Daza, J. D., Mapps, A. A., Lewis, P. J., Thies, M. L., and Bauer, A. M. (2015). Peramorphic traits in the tokay gecko skull. *J. Morphol.* 276, 915–928. doi: 10.1002/jmor.20389

Diaz, J. R. E., and Trainor, P. A. (2019). *An Integrative View of Lepidosaur Cranial Anatomy, Development and Diversification. Heads, Jaws and Muscles Anatomical, Functional and Developmental Diversity in Chordate Evolution*. Cham: Springer.

Diaz, R. E., Anderson, C. V., Baumann, D. P., Kupronis, R., Jewell, D., Piraquive, C., et al. (2015). The veiled chameleon (*Chamaeleo calyptratus* Duméril and Duméril 1851): a model for studying reptile body plan development and evolution. *Cold Spring Harb. Protoc.* 2015, 889–894.

Diaz, R. E., Shylo, N. A., Roellig, D., Bronner, M., and Trainor, P. A. (2019). Filling in the phylogenetic gaps: induction, migration, and differentiation of neural crest cells in a squamate reptile, the veiled chameleon (*Chamaeleo calyptratus*). *Dev. Dyn.* 248, 709–727. doi: 10.1002/dvdy.38

Diaz, R. E., and Trainor, P. A. (2015). Hand/foot splitting and the 're-evolution' of mesopodial skeletal elements during the evolution and radiation of chameleons. *BMC Evol. Biol.* 15:184. doi: 10.1186/s12862-015-0464-4

Dosedělová, H., Štěpánková, K., Zikmund, T., Lesot, H., Kaiser, J., Novotný, K., et al. (2016). Age-related changes in the tooth-bone interface area of acrodont dentition in the chameleon. *J. Anat.* 229, 356–368. doi: 10.1111/joa.12490

Duldulao, N. A., Lee, S., and Sun, Z. (2009). Cilia localization is essential for in vivo functions of the Joubert syndrome protein Arl13b/Scorpion. *Development* 136, 4033–4042. doi: 10.1242/dev.036350

Ferguson, M. W. (1981a). Review: the value of the American alligator (*Alligator mississippiensis*) as a model for research in craniofacial development. *J. Craniofac. Genet. Dev. Biol.* 1, 123–144.

Ferguson, M. W. (1981b). The structure and development of the palate in *Alligator mississippiensis*. *Arch. Oral. Biol.* 26, 427–443. doi: 10.1016/0003-9969(81)90041-8

Ferguson, M. W. (1987). Palate development: mechanisms and malformations. *Ir. J. Med. Sci.* 156, 309–315. doi: 10.1007/bf02951261

Ferguson, M. W. (1988). Palate development. *Development* 103(Suppl.), 41–60.

Grbic, D., Saenko, S. V., Randriamoria, T. M., Debry, A., Raselimanana, A. P., and Milinkovitch, M. C. (2015). Phylogeography and support vector machine classification of colour variation in panther chameleons. *Mol. Ecol.* 24, 3455–3466. doi: 10.1111/mec.13241

Greene, R. M., and Pratt, R. M. (1976). Developmental aspects of secondary palate formation. *J. Embryol. Exp. Morphol.* 36, 225–245.

Hampl, M., Cela, P., Szabo-Rogers, H. L., Bosakova, M. K., Dosedelova, H., Krejci, P., et al. (2017). Role of primary cilia in odontogenesis. *J. Dent. Res.* 96, 965–974. doi: 10.1177/0022034517713688

Hanken, J., and Thorogood, P. (1993). Evolution and development of the vertebrate skull: the role of pattern formation. *Trends Ecol. Evol.* 8, 9–15. doi: 10.1016/0169-5347(93)90124-8

Haycraft, C. J., Banizs, B., Aydin-Son, Y., Zhang, Q., Michaud, E. J., and Yoder, B. K. (2005). Gli2 and Gli3 localize to cilia and require the intraflagellar transport protein polaris for processing and function. *PLoS Genet.* 1:e53. doi: 10.1371/journal.pgen.0010053

Hedges, S. B. (2012). Amniote phylogeny and the position of turtles. *BMC Biol.* 10:64. doi: 10.1186/1741-7007-10-64

Hernández-Jaimes, C., Jerez, A., and Ramírez-Pinilla, M. P. (2012). Embryonic development of the skull of the Andean lizard *Ptychoglossus bicolor* (Squamata, Gymnophthalmidae). *J. Anat.* 221, 285–302. doi: 10.1111/j.1469-7580.2012.01549.x

Herrel, A., Redding, C. L., Meyers, J. J., and Nishikawa, K. C. (2014). The scaling of tongue projection in the veiled chameleon, *Chamaeleo calyptratus*. *Zoology* 117, 227–236. doi: 10.1016/j.zool.2014.01.001

Huangfu, D., and Anderson, K. V. (2005). Cilia and Hedgehog responsiveness in the mouse. *Proc. Natl. Acad. Sci. U.S.A.* 102, 11325–11330. doi: 10.1073/pnas.0505328102

Huangfu, D., Liu, A., Rakeman, A. S., Murcia, N. S., Niswander, L., and Anderson, K. V. (2003). Hedgehog signalling in the mouse requires intraflagellar transport proteins. *Nature* 426, 83–87. doi: 10.1038/nature02061

Iordansky, N. (2016). Functional relationships in the jaw apparatus of the chameleons and the evolution of adaptive complexes. *Zool. Z.* 95, 1173–1181.

Iwabe, N., Hara, Y., Kumazawa, Y., Shibamoto, K., Saito, Y., Miyata, T., et al. (2005). Sister group relationship of turtles to the bird-crocodilian clade revealed by nuclear DNA-coded proteins. *Mol. Biol. Evol.* 22, 810–813. doi: 10.1093/molbev/msi075

Jankowski, R. (2013). *The Complex Formation of the Secondary Palate and Nose in Evolution, The Evo-Devo Origin of the Nose, Anterior Skull Base and Midface*. Cham: Springer, 41–61.

Jin, J. Z., and Ding, J. (2006). Analysis of Meox-2 mutant mice reveals a novel postfusion-based cleft palate. *Dev. Dyn.* 235, 539–546. doi: 10.1002/dvdy.20641

Jin, J. Z., and Ding, J. (2015). Strain-dependent gene expression during mouse embryonic palate development. *J. Dev. Biol.* 3, 2–10. doi: 10.3390/jdb3010002

Johnson, M. L. (1933). The time and order of appearance of ossification centers in the albino mouse. *Am. J. Anat.* 52, 241–271. doi: 10.1002/aja.1000520203

Jones, M. E., Werneburg, I., Curtis, N., Penrose, R., O'higgins, P., Fagan, M. J., et al. (2012). The head and neck anatomy of sea turtles (Cryptodira: Chelonioidea) and skull shape in testudines. *PLoS One* 7:e47852. doi: 10.1371/journal.pone.0047852

Kanazawa, E., and Mochizuki, K. (1974). The time and order of appearance of ossification centers in the hamster before birth. *Jikken Dobutsu* 23, 113–122. doi: 10.1538/expanim1957.23.3_113

Kimmel, C. B., Sidlauskas, B., and Clack, J. A. (2009). Linked morphological changes during palate evolution in early tetrapods. *J. Anat.* 215, 91–109. doi: 10.1111/j.1469-7580.2009.01108.x

Krmpotić-Nemanić, J., Vinter, I., and Marusić, A. (2006). Relations of the pterygoid hamulus and hard palate in children and adults: anatomical implications for the function of the soft palate. *Ann. Anat.* 188, 69–74. doi: 10.1016/j.aanat.2005.05.005

Le Pabic, P., Ng, C., and Schilling, T. F. (2014). Fat-Dachsous signaling coordinates cartilage differentiation and polarity during craniofacial development. *PLoS Genet.* 10:e1004726. doi: 10.1371/journal.pgen.1004726

Li, J., Johnson, C. A., Smith, A. A., Hunter, D. J., Singh, G., Brunski, J. B., et al. (2016). Linking suckling biomechanics to the development of the palate. *Sci. Rep.* 6:20419.

Mo, R., Freer, A. M., Zinyk, D. L., Crackower, M. A., Michaud, J., Heng, H. H., et al. (1997). Specific and redundant functions of Gli2 and Gli3 zinc finger genes in skeletal patterning and development. *Development* 124, 113–123.

Mohamed, R. (2018). Anatomical and radiographic study on the skull and mandible of the common opossum. *Vet. Sci.* 5:44. doi: 10.3390/vetsci5020044

Namkoong, B. (2015). *The Molecular Determinants of Cranial Skeletal Development and Evolution*. Dissertation Thesis, Harvard University, Cambridge, MA.

Ollonen, J., Da Silva, F. O., Mahlow, K., and Di-Poï, N. (2018). Skull development, ossification pattern, and adult shape in the emerging lizard model organism. *Front. Physiol.* 9:278. doi: 10.3389/fphys.2018.00278

Pinto, B. J., Card, D. C., Castoe, T. A., Diaz, R. E., Nielsen, S. V., Trainor, P. A., et al. (2019). The transcriptome of the veiled chameleon (*Chamaeleo calyptratus*): a resource for studying the evolution and development of vertebrates. *Dev. Dyn.* 248, 702–708. doi: 10.1002/dvdy.20

Presley, R., and Steel, F. L. (1978). The pterygoid and ectopterygoid in mammals. *Anat. Embryol.* 154, 95–110. doi: 10.1007/bf00317957

Rice, R., Connor, E., and Rice, D. P. (2006). Expression patterns of Hedgehog signalling pathway members during mouse palate development. *Gene Expr. Patterns* 6, 206–212. doi: 10.1016/j.modgep.2005.06.005

Richman, J. M., Buchtová, M., and Boughner, J. C. (2006). Comparative ontogeny and phylogeny of the upper jaw skeleton in amniotes. *Dev. Dyn.* 235, 1230–1243. doi: 10.1002/dvdy.20716

Rieppel, O. (1993). Studies on skeleton formation in reptiles. v. Patterns of ossification in the skeleton of *Alligator mississippiensis* DAUDIN (Reptilia, Crocodylia). *Zool. J. Linn. Soc.* 109, 301–325. doi: 10.1111/j.1096-3642.1993.tb02537.x

Rieppel, O., and Crumly, C. (2009). Paedomorphosis and skull structure in *Malagasy chamaeleons* (Reptilia: Chamaeleoninae). *J. Zool.* 243, 351–380. doi: 10.1111/j.1469-7998.1997.tb02788.x

Romer, A. S. (1956). *Osteology of the Reptiles*. Chicago, IL: University of Chicago Press.

Schock, E. N., Chang, C. F., Youngworth, I. A., Davey, M. G., Delany, M. E., and Brugmann, S. A. (2016). Utilizing the chicken as an animal model for human craniofacial ciliopathies. *Dev. Biol.* 415, 326–337. doi: 10.1016/j.ydbio.2015.10.024

Sheil, C. A. (2005). Skeletal development of *Macrochelys temminckii* (Reptilia: Testudines: Chelydridae). *J. Morphol.* 263, 71–106. doi: 10.1002/jmor.10290

Shi, J., Zhao, Y., Galati, D., Winey, M., and Klymkowsky, M. W. (2014). Chibby functions in *Xenopus ciliary* assembly, embryonic development, and the regulation of gene expression. *Dev. Biol.* 395, 287–298. doi: 10.1016/j.ydbio.2014.09.008

Sperber, G. H., Sperber, S. M., and Guttmann, G. D. (eds) (2012). *Craniofacial Embryogenetics and Development*, 2nd Edn. Shelton: PMPH USA Ltd.

Stower, M. J., Diaz, R. E., Fernandez, L. C., Crother, M. W., Crother, B., Marco, A., et al. (2015). Bi-modal strategy of gastrulation in reptiles. *Dev. Dyn.* 29, 1144–1157. doi: 10.1002/dvdy.24300

Tamarin, A. (1982). The formation of the primitive choanae and the junction of the primary and secondary palates in the mouse. *Am. J. Anat.* 165, 319–337. doi: 10.1002/aja.1001650308

Tokita, M., Chaeychomsri, W., and Siruntawineti, J. (2013). Developmental basis of toothlessness in turtles: insight into convergent evolution of vertebrate morphology. *Evolution* 67, 260–273. doi: 10.1111/j.1558-5646.2012.01752.x

Tolley, K. A., and Herrel, A. (2015). *The Biology of Chameleons*. Berkeley, CA: University of California Press.

Wheatley, D. N., Wang, A. M., and Strugnell, G. E. (1996). Expression of primary cilia in mammalian cells. *Cell Biol. Int.* 20, 73–81. doi: 10.1006/cbir.1996.0011

Yu, K., and Ornitz, D. M. (2011). Histomorphological study of palatal shelf elevation during murine secondary palate formation. *Dev. Dyn.* 240, 1737–1744. doi: 10.1002/dvdy.22670

Zahradnicek, O., Buchtova, M., Dosedelova, H., and Tucker, A. S. (2014). The development of complex tooth shape in reptiles. *Front. Physiol.* 5:74. doi: 10.3389/fphys.2014.00074

Zhang, Z., Song, Y., Zhao, X., Zhang, X., Fermin, C., and Chen, Y. (2002). Rescue of cleft palate in Msx1-deficient mice by transgenic Bmp4 reveals a network of BMP and Shh signaling in the regulation of mammalian palatogenesis. *Development* 129, 4135–4146.

Zheng, Y., and Wiens, J. J. (2016). Combining phylogenomic and supermatrix approaches, and a time-calibrated phylogeny for squamate reptiles (lizards and snakes) based on 52 genes and 4162 species. *Mol. Phylogenet. Evol.* 94, 537–547. doi: 10.1016/j.ympev.2015.10.009

Zhou, J., Gao, Y., Lan, Y., Jia, S., and Jiang, R. (2013). Pax9 regulates a molecular network involving Bmp4, Fgf10, Shh signaling and the Osr2 transcription factor to control palate morphogenesis. *Development* 140, 4709–4718. doi: 10.1242/dev.099028

Conflict of Interest: The authors declare that the research was conducted in the absence of any commercial or financial relationships that could be construed as a potential conflict of interest.

frontiers in Cell and Developmental Biology

ORIGINAL RESEARCH
published: 22 October 2020
doi: 10.3389/fcell.2020.593377

Heterochronic Developmental Shifts Underlying Squamate Cerebellar Diversity Unveil the Key Features of Amniote Cerebellogenesis

*Simone Macrì and Nicolas Di-Poï**

Program in Developmental Biology, Institute of Biotechnology, University of Helsinki, Helsinki, Finland

Despite a remarkable conservation of architecture and function, the cerebellum of vertebrates shows extensive variation in morphology, size, and foliation pattern. These features make this brain subdivision a powerful model to investigate the evolutionary developmental mechanisms underlying neuroanatomical complexity both within and between anamniote and amniote species. Here, we fill a major evolutionary gap by characterizing the developing cerebellum in two non-avian reptile species—bearded dragon lizard and African house snake—representative of extreme cerebellar morphologies and neuronal arrangement patterns found in squamates. Our data suggest that developmental strategies regarded as exclusive hallmark of birds and mammals, including transit amplification in an external granule layer (EGL) and Sonic hedgehog expression by underlying Purkinje cells (PCs), contribute to squamate cerebellogenesis independently from foliation pattern. Furthermore, direct comparison of our models suggests the key importance of spatiotemporal patterning and dynamic interaction between granule cells and PCs in defining cortical organization. Especially, the observed heterochronic shifts in early cerebellogenesis events, including upper rhombic lip progenitor activity and EGL maintenance, are strongly expected to affect the dynamics of molecular interaction between neuronal cell types in snakes. Altogether, these findings help clarifying some of the morphogenetic and molecular underpinnings of amniote cerebellar corticogenesis, but also suggest new potential molecular mechanisms underlying cerebellar complexity in squamates. Furthermore, squamate models analyzed here are revealed as key animal models to further understand mechanisms of brain organization.

Keywords: development, evolution, cerebellum, squamates, patterning

OPEN ACCESS

Edited by:
Pedro Martinez, University of Barcelona, Spain

Reviewed by:
José L Ferran, University of Murcia, Spain
Tadashi Nomura, Kyoto Prefectural University of Medicine, Japan

***Correspondence:**
Nicolas Di-Poï
nicolas.di-poi@helsinki.fi

Specialty section:
This article was submitted to Evolutionary Developmental Biology, a section of the journal Frontiers in Cell and Developmental Biology

Received: *10 August 2020*
Accepted: *25 September 2020*
Published: *22 October 2020*

Citation:
Macrì S and Di-Poï N (2020) Heterochronic Developmental Shifts Underlying Squamate Cerebellar Diversity Unveil the Key Features of Amniote Cerebellogenesis. Front. Cell Dev. Biol. 8:593377. doi: 10.3389/fcell.2020.593377

INTRODUCTION

The cerebellum is a prominent feature of the vertebrate hindbrain that varies extensively in terms of relative size and morphology not only across major vertebrate groups, but also in closely related species with distinct ecological and behavioral strategies (Voogd and Glickstein, 1998; Butler and Hodos, 2005; Striedter, 2005; Macrì et al., 2019). It reaches the highest level of morphological complexity in birds, mammals, and in some cartilaginous and bony fishes, in which a remarkable

volume increase parallels a profound surface area expansion leading to a highly foliated structure (Butler and Hodos, 2005; Puzdrowski and Gruber, 2009; Sukhum et al., 2018). Remarkably, despite the observed variation in overall morphology, the basic features of cerebellar cytoarchitecture are relatively well-conserved across vertebrates (Larsell, 1967, 1970; Voogd and Glickstein, 1998; Butler and Hodos, 2005). Particularly, the cerebellar cortex is composed of a relatively small number of neuronal types, which are classified according to their function as excitatory or inhibitory neurons (Hashimoto and Hibi, 2012). The most important excitatory neurons include granule cells (GCs) and unipolar brush cells, and the inhibitory neurons include GABAergic Purkinje cells (PCs), Golgi cells, basket cells, and stellate cells. These neurons are arranged in a dense but well-defined trilaminar organization consisting of an inner granule layer (GL), middle PC layer (PCL), and outer molecular layer (ML) where PC dendrites receive GC axons. The orderly cellular layout and extensive connectivity of the cerebellum give rise to a massive signal processing capability that plays a crucial role in motor control and coordination but also in higher cognitive functions such as attention, memory, and language (Strick et al., 2009; Balsters et al., 2013; Buckner, 2013; Koziol et al., 2014; Baumann et al., 2015; Schmahmann, 2019). Owing to its relatively simple laminar organization, the cerebellum has been an attractive model for studying developmental patterns and functions of the central nervous system in multiple vertebrates, including basal lineages such as cyclostomes (Sugahara et al., 2016). Importantly, variations have been reported in the topographic arrangement of major cell layers, number of neurons, foliation pattern, and neuronal connectivity among vertebrate cerebella. Notably, the distinct spatial distribution of GCs in lampreys, sharks, and sturgeons as well as the scattered arrangement of PCs in some cartilaginous fishes, lungfishes, and snakes differs from the stereotyped organization found in teleosts, amphibians, archosaurs, and mammals (Butts et al., 2011; Yopak et al., 2017; Macrì et al., 2019). Furthermore, different cerebellar compartmental organization, as reflected by the presence/absence or heterogenous arrangement of discrete longitudinal stripes of PCs expressing similar markers such as aldolase C (also known as zebrin II; Voogd, 1967; Hawkes and Leclerc, 1987; Brochu et al., 1990; Aspden et al., 2015; Wylie et al., 2017; Yopak et al., 2017), but also by specific projections that give some individual peculiarities to these longitudinal compartments (Biswas et al., 2019; Na et al., 2019), have been observed in vertebrates. Finally, different developmental innovations in cellular behavior and signaling have been described among teleosts, chondrichthyans, and amniotes for generating transverse lobules and elaborate foliated cerebellar morphologies. As a result, although cerebellar development is well-known to rely on the spatiotemporal activity patterns of several key signaling pathways, the exact molecular and evolutionary mechanisms that govern the generation and arrangement of major neuronal types and foliation pattern are only partially resolved.

Developmental studies in birds and more recently in mammals have shown that the major divisions of the cerebellum, including the two cerebellar hemispheres and the medial region called vermis, originate from both the rhombomere 1 and the isthmus (also referred as rhombomere 0) and require gradients of fibroblast growth factor (FGF) signaling such as FGF8 for survival and differential development (Martínez et al., 2013; Watson et al., 2017). Furthermore, cerebellar neurons in birds and mammals originate from different germinal zones and migrate to their destination using radial and/or tangential migratory pathways. PC precursors (PCPs) and other GABAergic cells expressing specific markers such as the basic helix-loop-helix (bHLH) proneural gene *Ptf1* (Hoshino et al., 2005) stem from the ventricular zone (VZ) and follow a highly directed movement upon maturation, including radial migration toward the cerebellar pial surface for PCs. In contrast, GC precursors (GCPs) emerge from an atonal bHLH transcription factor 1 (*Atoh1*) expressing domain, the upper rhombic lip (URL; Alder et al., 1996; Wingate and Hatten, 1999; Wingate, 2001; MacHold and Fishell, 2005; Wang et al., 2005), and follow first a subpial tangential movement before producing post-mitotic GCs that migrate radially toward the VZ to form the internal GL (IGL). Although the two principal cerebellar germinal zones VZ and URL appear conserved at least within gnathostomes, the developmental pattern of neuronal precursors diverge among taxa (Hibi et al., 2017). Especially, GC development in mammals and birds includes a unique phase of *Atoh1*-mediated transit amplification in an external GL (EGL) during the initial tangential migration phase (Alder et al., 1996; Wingate and Hatten, 1999). Transit amplification is a widespread strategy in neural development that allows the fine-tuning of cell numbers, and such process has been linked to the evolution of highly foliated cerebella in vertebrates. However, the absence of a typical EGL in chondrichthyans and teleosts (Chaplin et al., 2010; Kani et al., 2010), two groups that include species with hugely foliated cerebella (Yopak et al., 2007; Sukhum et al., 2018), and the presence of a distinct, non-proliferative EGL in amphibians (Gona, 1972; Butts et al., 2014a) suggest that this transient structure is in fact a key developmental innovation found in birds and mammals. In addition to the different proliferative strategies, the presence/absence or even variations in the timing and/or complexity of migration patterns taken by post-mitotic neuronal derivatives likely reflect divergence in cerebellar morphology and spatial arrangement of cerebellar neurons within and between vertebrate groups (Hibi et al., 2017; Rahimi-Balaei et al., 2018; Macrì et al., 2019).

Among key signaling factors involved in early cerebellar development, analyses of mouse models have highlighted the fundamental role of *Atoh1* in determining GCP proliferation within the EGL in response to Sonic hedgehog (SHH) secreted from underlying PCs (Ben-Arie et al., 1997; Lewis et al., 2004). The importance of SHH pathway in cerebellar histogenesis has been further underscored by genetic analyses demonstrating that its level of activation controls both the size and foliation pattern of the cerebellum (Dahmane and Ruiz, 1999; Wallace, 1999; Wechsler-Reya and Scott, 1999; Corrales, 2004, 2006; Lewis et al., 2004). Morphogens belonging to the bone morphogenetic protein (BMP) family such as BMP4, BMP6, BMP7, and GDF7 have also been shown to regulate the proliferation, specification, and survival of cerebellar GCPs (Lee et al., 1998; Alder et al., 1999; Krizhanovsky and Ben-Arie, 2006; Su et al., 2006;

Barneda-Zahonero et al., 2009; Tong and Kwan, 2013). Similarly, the pivotal role of retinoic acid receptor-related orphan receptor alpha (*Rora*) in the developing cerebellum has been thoroughly documented. Particularly, disruption of *Rora* in *staggerer* mutant mice (Sidman et al., 1962) leads to severe deficiencies in PC physiology, morphology, and survival (Sotelo and Changeux, 1974; Landis and Sidman, 1978; Herrup and Mullen, 1979), which negatively impact EGL persistence and proliferation and ultimately result in cerebellar hypoplasia (Sidman et al., 1962). In a reciprocal fashion, the EGL has been shown to be critical for the peculiar positioning of PCs in monolayer, indicating that cortical integrity relies on the correct development of URL generated cells (Miyata et al., 1997; Jensen et al., 2002; Jensen, 2004). Especially, many studies have evidenced the key role of the extracellular matrix molecule Reelin (RELN) produced by post-mitotic GCPs in PC spatial alignment, and complete deficiency of *Reln* gene or of components of the RELN signaling pathway such as RELN receptors [very-low-density-lipoprotein receptor (VLDLR) and apolipoprotein E receptor 2 (ApoER2)] or adapter protein disabled-1 (DAB1) causes similar defects in cerebellar architecture and function, including extensive PC disorganization and hypoplasia (Heckroth et al., 1989; D'Arcangelo et al., 1995; Sheldon et al., 1997; Ware et al., 1997; Gallagher et al., 1998; Trommsdorff et al., 1999). Importantly, although the relevance of these genes and cellular interactions are relatively well-conserved in mammals and birds, significant molecular differences exist in all anamniote species investigated so far, including chondrichthyans, non-teleost and teleost ray-finned fishes, as well as amphibians. Notably, the distinctions are primarily linked to the various strategies used to generate and amplify GCs, including the absence of proliferative *Atoh1*-positive EGL progenitors and/or *Shh*-dependent GCP expansion in the developing cerebellum of anamniotes (Chaplin et al., 2010; Kani et al., 2010), further suggesting that the transient, proliferative EGL is an amniote adaptation to increase cerebellar complexity. However, substantial gaps in the vertebrate phylogeny remain unexplored. Especially, the molecular underpinnings of early cerebellar development, including the status of the EGL and cortical layer interactions, are still unknown for non-avian reptiles such as squamates (lizards and snakes), which occupy a key phylogenetic position and represent a major portion of the amniote tree with over 10,000 species. Furthermore, although the general organization of the cerebellum, from local circuitry to broad connectivity, is highly conserved among mammals, birds, and reptiles (Nieuwenhuys, 1967; Nieuwenhuys et al., 1998), adult squamates exhibit a wide diversity of cerebellar shape, size, and neuronal pattern directly linked to their ecological behaviors (Larsell, 1926; Aspden et al., 2015; Macrì et al., 2019), thus representing an excellent model to understand the evolutionary origin, structure, function, development, and adaptation of the amniote cerebellum.

Here, we performed the first study assessing the morphological, cellular, and molecular characterization of the developing embryonic cerebellum in non-avian reptiles, using two "non-classical" model species—the bearded dragon lizard (*Pogona vitticeps*) and the African house snake (*Boaedon fuliginosus*)—representative of extreme cerebellar morphologies and neuronal arrangement patterns found in squamates (Macrì et al., 2019). Our analysis suggests that cellular and molecular mechanisms previously identified in the developing cerebellum of birds and mammals are likely well-conserved in all major amniote groups, including squamate reptiles. Particularly, our gene expression data indicate that the formation of a proliferating EGL is most probably a true amniote developmental adaptation, although independent from the cerebellar foliation pattern. Furthermore, direct comparison of our two models suggests the existence of variations from the common amniote developmental blueprint in terms of GC generation and PC patterning, thus enriching the multi-faceted strategies adopted in vertebrate cerebellar histogenesis. Especially, the observed heterochronic shifts in the timing and/or duration of URL activity and EGL maintenance in snakes is expected to alter the dynamics of molecular interaction between GCs and PCs. Most importantly, although further experimental demonstrations would be needed, our findings give new insights about the contribution of key signaling pathways, cellular spatiotemporal interactions, and histogenetic events in defining the number and arrangement of major cerebellar neurons in vertebrates. Altogether, this set of results indicate the importance of squamate models to further understand basic principles of brain organization and evolutionary mechanisms of cerebellar complexity, which, in turn, can inform us as to how brain evolution has enabled vertebrate ecological capability.

RESULTS

Comparative Architecture of Cerebellum in *P. vitticeps* and *B. fuliginosus*

Despite its high levels of functional conservation, the cerebellum displays a wide range of morphological variation across vertebrates (Larsell, 1923, 1926, 1932; Voogd and Glickstein, 1998; Butler and Hodos, 2005; Striedter, 2005). Among amniotes, mammals and birds exhibit highly convoluted cerebellar architectures, whereas non-avian reptiles such as lizards and snakes feature less elaborated, unfoliated structures (Larsell, 1926; Nieuwenhuys, 1967; Nieuwenhuys et al., 1998). Exceptions include crocodilians and a few lizard species, in which one or two transverse fissures that divide the cerebellum into different lobes were observed (Larsell, 1926, 1932). Past and recent studies (Larsell, 1926; Macrì et al., 2019), however, revealed an extraordinarily rich gamut of cerebellar morphologies and cortical organization in squamates paralleling their exceptional ecomorphological diversification, thus highlighting the potential of this model for elucidating key processes underlying vertebrate brain evolution and development. To compare the distinctive morphological characteristics of the cerebellum in two squamate species with different ecological behaviors—one lizard (*P. vitticeps*) and one snake (*B. fuliginosus*), we used high-definition 3D reconstructions of whole-brains and isolated cerebella based on contrast-enhanced computed tomography (CT; **Figures 1A,B**) as well as histological stainings of brain sections (**Figures 1C,D**). A substantial divergence

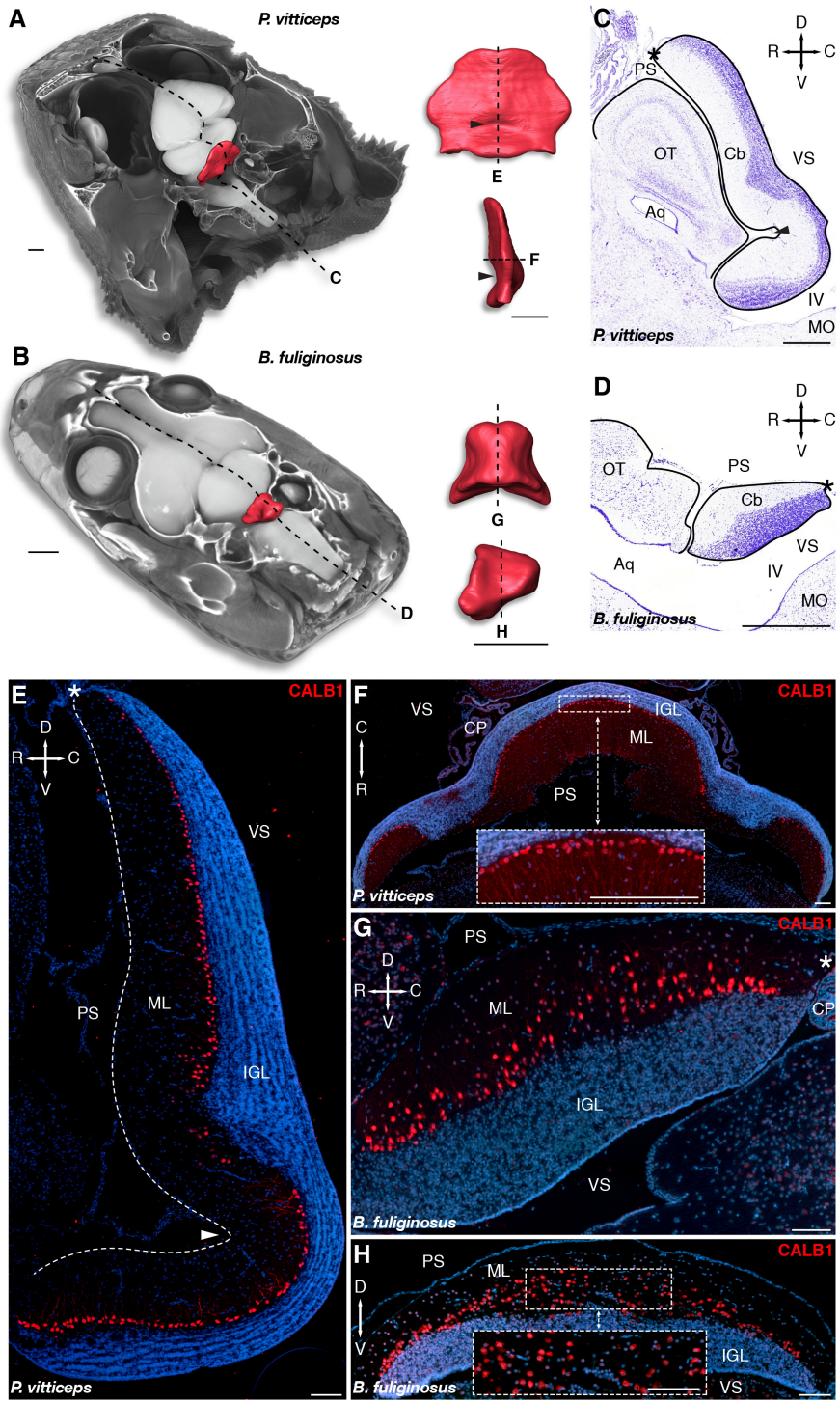

FIGURE 1 | Morphology and cellular arrangement of bearded dragon lizard (*P. vitticeps*) and African house snake (*B. fuliginosus*) cerebellum. **(A,B)** 3D-volume rendering and high-resolution whole-brain segmentation of iodine-stained juvenile heads of *P. vitticeps* **(A)** and *B. fuliginosus* **(B)** highlighting the cerebellum structure (red color). High magnifications of 3D-rendered cerebella of *P. vitticeps* **(A)** and *B. fuliginosus* **(B)** are shown in pial (top) and lateral (bottom) views in the right column. Arrowheads indicate the position of the incomplete fissure in *P. vitticeps* cerebellum. Dashed lines and letters mark the sectioning planes relative to the histological preparations and immunostaining experiments in panels **(C,D)** and **(E–H)**, respectively. **(C,D)** Nissl staining of the cerebellum and neighboring brain regions in *P. vitticeps* **(C)** and *B. fuliginosus* **(D)**. Black lines demarcate the contour of the cerebellum and adjacent brain regions. The arrowhead in panel **(C)** indicates the position of the incomplete fissure in *P. vitticeps* cerebellum, and asterisks in panels **(C,D)** indicate the position of the embryonic upper rhombic lip. Crossed arrows point toward rostral (R), caudal (C), dorsal (D), and ventral (V) directions. **(E–H)** Immunodetection of Purkinje cells (PCs) with CALB1 marker, using

(Continued)

FIGURE 1 | Continued
sagittal **(E)** or axial **(F)** sections of *P. vitticeps* and sagittal **(G)** or coronal **(H)** sections of *B. fuliginosus* juvenile cerebellum (red staining). Cell nuclei are counterstained with DAPI (blue staining). The arrowhead in panel **(E)** indicates the position of the incomplete fissure, and the white dashed line delimitates the cerebellar pial surface. Asterisks in panels **(E,G)** indicate the position of the embryonic upper rhombic lip. Insets in panels **(F,H)** show high magnifications of PC spatial organization. Crossed white arrows point toward rostral (R), caudal (C), dorsal (D), and ventral (V) directions. OT, optic tectum; Cb, cerebellum; Aq, aqueduct; MO, medulla oblongata; IV, fourth ventricle; PS, pial surface; ML, molecular layer; IGL, internal granule layer; VS, ventricular surface; CP, choroid plexus. Scale bars: 1 mm **(A,B)**, 500 μm **(C,D)**, 100 μm **(E–H)**.

of cerebellar shape, size, and spatial relationships with other brain subdivisions is evident between the two model species. Especially, besides the three-fold reduction in cerebellum volume observed in *B. fuliginosus* when compared to *P. vitticeps*, the snake exhibits a relatively small trapezoidal cerebellum, in contrast to the lizard leaf-shaped structure (**Figures 1A–D**). Furthermore, the presence of an incomplete fissure on the pial surface in *P. vitticeps* imparts a marked inversion in cerebellar tilting relative to the brain anatomical planes (**Figures 1A,C,E**). Consequently, *B. fuliginosus* cerebellum lies almost completely embedded in the 4th ventricle, whereas the lizard counterpart is dorsally elongated and bends over the tectal hemispheres, toward the rostral edge of the brain (**Figures 1A–D**). At the cellular level, our characterization of major cerebellar neuron types such as PCs and GCs confirms alternative spatial arrangement of PCs in the two species (Macrì et al., 2019), as revealed here by immunodetection of PC marker such as calbindin 1 (CALB1; **Figures 1E–H**). The lizard cortex shows a well-defined trilaminar organization, including a clearly distinguishable PC layer composed of cells neatly distributed along the outer border of the IGL (**Figures 1E,F**), as described for birds and mammals. In contrast, *B. fuliginosus* PCs appear scattered due to their arrangement in radially oriented columns, each containing a varying number of cells and protruding with different extent in the ML (**Figures 1G,H**). Altogether, these observations corroborate previous qualitative and quantitative descriptions of squamate cerebella, including heterogeneity in morphological features and PC spatial layouts among lizard and snake species (Larsell, 1926; Aspden et al., 2015; Wylie et al., 2017; Hoops et al., 2018; Macrì et al., 2019), and confirm the unique neuroanatomical landscape of this structure in squamates.

Generation and Patterning of Cerebellar PCs in *P. vitticeps*

The distinct neuron types of vertebrate cerebellum have well-defined, conserved developmental origins, including the URL and VZ germinal zones, and migrate to their destination using radial and/or tangential migratory pathways (Butts et al., 2011). The initial GABAergic progenitors giving rise to PCs emerge from the proliferative VZ epithelium (Altman and Bayer, 1997; Sotelo, 2004; Hoshino et al., 2005), and migrate radially toward the cerebellar pial surface as they mature, eventually acquiring both their physiological and morphological features as well as their monolayer arrangement typical of most amniote cerebella. To investigate PC developmental program in squamates, we first analyzed the lizard model, which shows a canonical spatial alignment of PCs at postnatal stages (**Figures 1E,F**). Immunolabelings of developing cerebella were performed at various post-ovipositional embryonic stages, using the PC lineage marker LIM homeobox protein 1 (LHX1; Zhao et al., 2007) in combination with proliferating cell nuclear antigen (PCNA) to get insights on the proliferative potential of the VZ epithelium. At 20 days post-oviposition (dpo), the earliest stage at which the developing cerebellar primordium can be clearly distinguished in our lizard model, LHX1-positive post-mitotic PCPs exit a highly proliferative VZ and migrate in a radially oriented fashion toward the outer pial surface (**Figure 2A**). Ten embryonic days later (30 dpo; **Figure 2B**), the VZ is still actively proliferating, and immature PCs aggregate as multi-layered sigmoidal PC clusters (PCCs) lying in an intermediate position along the ventricular-pial axis of the cerebellum. At this stage, the cerebellum appears elongated and thickened, and a second proliferative, pluristratified domain lines the entire length of pial surface in continuation with the URL (**Figure 2B**). At 40 dpo, proliferation attenuates on the ventricular surface, while both the URL and pial surface are still sites of sustained PCNA labeling (**Figure 2C**). PCs are more evenly spaced than in previous stages, and PCCs start dispersing to acquire a less stratified appearance (compare insets in **Figures 2B,C**). Furthermore, as noticed in juvenile lizards (**Figures 1C,E**), the 40 dpo stage features the formation of an incomplete and shallow fissure on the medial pial surface. As development proceeds, PCs continue their alignment process (**Figure 2D**), and by the time of hatching (60 dpo), they reach an almost continuous monolayer configuration (**Figure 2E**). Although the ventricular epithelium has exhausted its proliferative potential at 60 dpo, proliferation is still active on the pial cerebellar surface (**Figure 2E**), and a PCNA-positive domain of progressively reducing thickness is detected at least until two weeks post-hatching (**Figure 2E** and **Supplementary Figure 1A**). Together, these results indicate that PC patterning in our lizard model largely occurs at embryonic stages according to a similar ground plan than described in other amniotes.

Developmental Patterning of Cerebellar GCs and EGL Formation in *P. vitticeps*

Cerebellar GCs, the most abundant neurons of the vertebrate brain, differentiate from precursors generated in a highly germinative region—the URL, situated at the junction between the posterior rim of the developing cerebellar primordium and the roof plate (RP) of the fourth ventricle (Hallonet and Le Douarin, 1993; Ryder and Cepko, 1994; Alder et al., 1996; Hatten et al., 1997; Wingate, 2001). In amniotes, GCPs produced by the URL follow an elaborated migratory program, before settling in the IGL as terminally differentiated GCs. In their first, tangential translocation phase, GCPs migrate along the entire extent of the cerebellar pial surface to form a

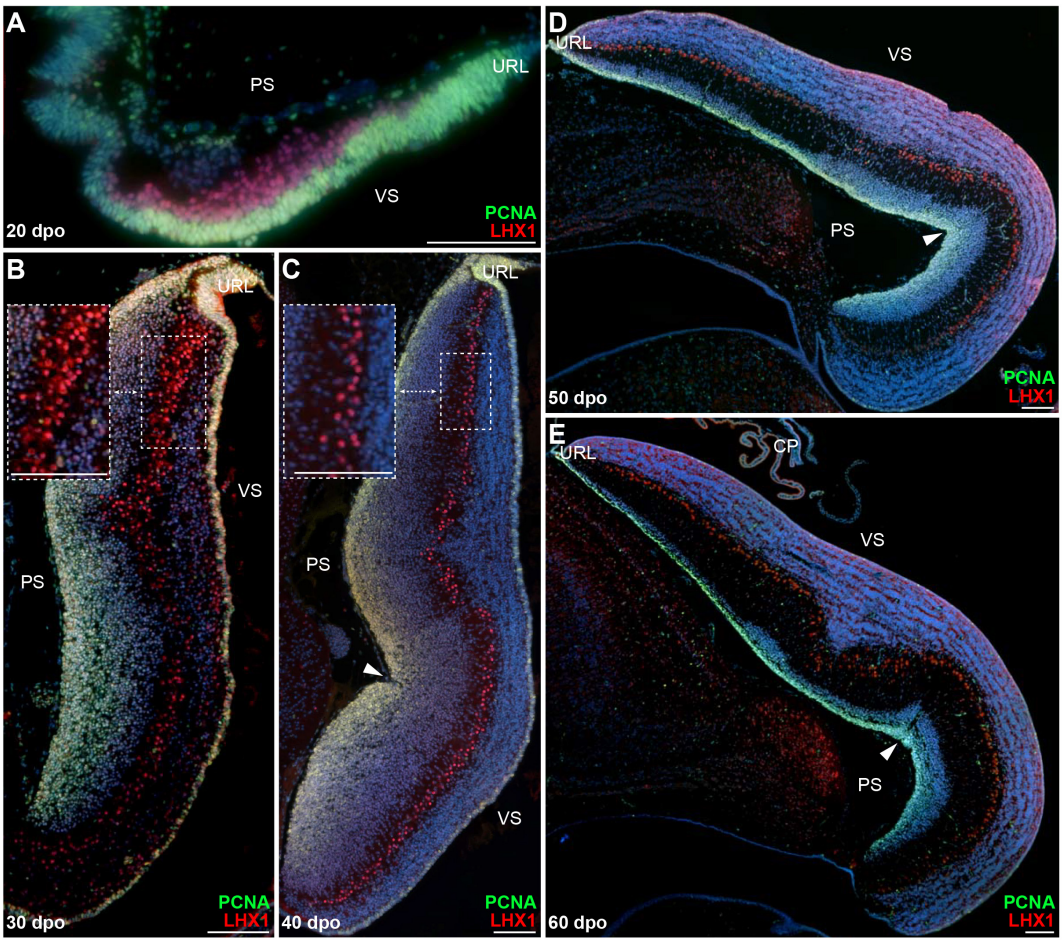

FIGURE 2 | Proliferation pattern and PC development in embryonic *P. vitticeps* cerebellum. **(A–E)** Double immunohistochemistry (IHC) staining for PCNA (green staining) and LHX1 (red) markers at various developmental stages, indicated as embryonic days post-oviposition (dpo), in the cerebellum of *P. vitticeps*. Arrowheads in panels **(C–E)** indicate the position of the incomplete fissure on the cerebellar pial surface. Insets in panels **(B,C)** show high magnifications of PC spatial organization. PS, pial surface; VS, ventricular surface; URL, upper rhombic lip. Scale bars: 100 μm.

pluristratified domain—the EGL, before undertaking a second, radially oriented, migratory step along the pial-to-ventricular cerebellar axis. The EGL is a highly proliferative, transient germinal zone responsible for the exponential amplification of GCPs, but its formation has only been documented in birds and mammals so far (Gona, 1972; Alder et al., 1996; Wingate and Hatten, 1999; Chaplin et al., 2010). Consequently, whether a proliferative EGL is an exclusive hallmark of some vertebrate groups or a feature shared by all amniotes remains unknown. To clarify this issue, we explored the patterns of GC generation in our lizard model, with a particular focus on the EGL-like features of the highly proliferating layer detected on cerebellar pial surface. We first immunostained *P. vitticeps* embryonic cerebella at representative stages (see **Figure 2**), using markers of GC lineage such as Zic family member 1/2/3 (ZIC1/2/3; Aruga et al., 1994, 1998) in combination with PCNA. From 20 to 30 dpo, a rapid expansion of PCNA-positive cells occurs on the pial surface of developing cerebellum, with ZIC1/2/3-positive post-mitotic GCPs starting to delaminate and migrate radially out from this zone as early as 25 dpo (**Figures 3A,B**). As development proceeds, GCs steadily accumulate on the opposite (ventricular) side of the cerebellum, resulting in the formation of a more delineated IGL, and the two proliferating URL and pial domains gradually thin out (**Figures 3B,C**). By the time of hatching (60 dpo), although a reduced proliferative activity remains on pial surface until early postnatal stages (**Supplementary Figure 1A**), the IGL already consists of a multilayered arrangement of tightly packed GCs, and its thickness has dramatically increased (**Figure 3C**). Importantly, these data clearly connotate the transient proliferative domain on pial surface as a genuine EGL, thus suggesting striking analogies in GC developmental strategies between squamates, birds, and mammals. Furthermore, the observed persistence of proliferation beyond hatching stage in *P. vitticeps* indicate finalization of cerebellar architecture at early postnatal life, thus resembling mouse cerebellogenesis.

To further confirm the presence of a proliferative EGL in squamates, we assessed the expression pattern of additional

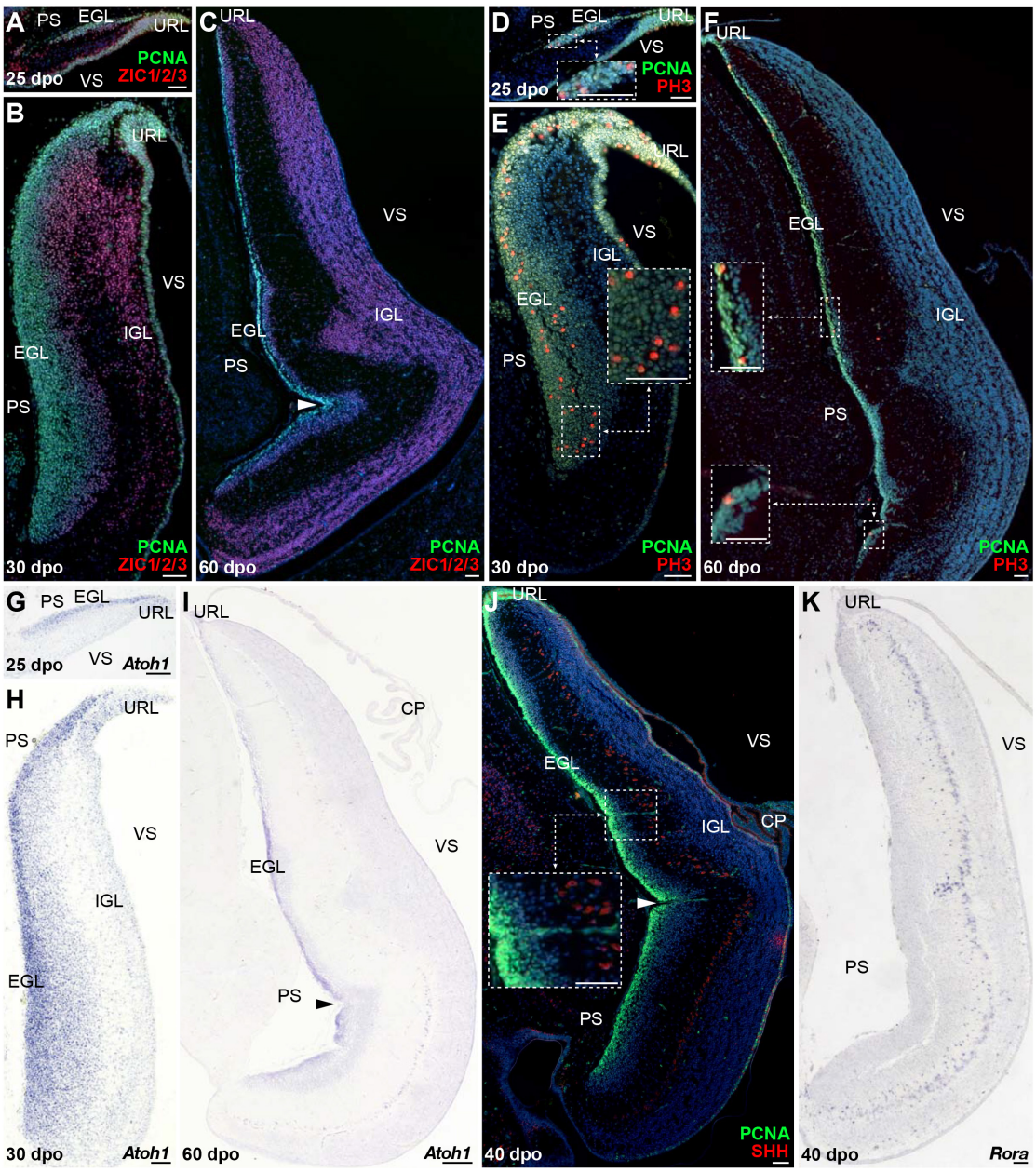

FIGURE 3 | Molecular characterization of GC patterning in *P. vitticeps*. **(A–F)** Double IHC for PCNA (green staining) with ZIC1/2/3 [**(A–C)**; red] or PH3 [**(D–F)**; red] markers at various indicated embryonic developmental stages (25, 30, and 60 dpo) in the cerebellum of *P. vitticeps*. Insets in panels **(D–F)** show high magnifications of mitotic progenitors on the pial surface. **(G–I)** *In situ* hybridization (ISH) showing the expression of *Atoh1* at various indicated embryonic developmental stages (25, 30, and 60 dpo). **(J,K)** Double IHC for PCNA (green) and SHH [**(J)**; red] or ISH for *Rora* **(K)** at 40 dpo. The inset in panel **(J)** shows high magnification of SHH-positive PCs. Arrowheads in **(C,I,J)** indicate the position of the incomplete fissure on the cerebellar pial surface. PS, pial surface; EGL, external granule layer; IGL, internal granule layer; VS, ventricular surface; URL, upper rhombic lip; CP, choroid plexus. Scale bars: 50 μm.

proliferative and molecular markers well-known to play a critical role in both EGL formation and maintenance in birds and mammals. Especially, the EGL is defined not only by its active, transient mitotic activity, but also by the expression of *Atoh1* (Akazawa et al., 1995; Ben-Arie et al., 1996, 1997) that is absolutely required both for GCP amplification and identity (Flora et al., 2009; Klisch et al., 2011). Furthermore, EGL precursors require SHH supplied by the underlying PCs to expand the GC population and achieve the correct cerebellar size and extent of foliation (Dahmane and Ruiz, 1999; Wallace, 1999; Wechsler-Reya and Scott, 1999; Corrales, 2004, 2006; Lewis et al., 2004). As revealed by co-immunodetection of PCNA with the phosphorylated form of histone H3 (PH3), a specific marker for cells undergoing mitosis, the lizard EGL displays

PCNA/PH3 double-positive cells indicative of mitotic events both in regions close to the URL as well as along the subpial stream of GC precursors (**Figures 3D–F**). In particular, at 25 dpo mitotic cells are found at different levels along the rostro-caudal EGL extent, including its rostral edge (**Figure 3D**). As cerebellum develops, cell divisions become more prominent and, like recently observed in chicken (Hanzel et al., 2019), also occur in more internal EGL regions (**Figure 3E**). Moreover, actively dividing cells are still detected even far from the URL region by 60 dpo (**Figure 3F**). Similarly to the situation in other amniotes, *in situ* hybridization (ISH) staining against *Atoh1* strongly labels *P. vitticeps* URL and EGL at all embryonic stages investigated, with an expression profile that precisely overlaps the spatiotemporal evolution of these two domains (**Figures 3G–I**). Furthermore, SHH protein expression is detected in PCs starting from 40 dpo, a stage where the EGL contains three to five layers of cells (**Figure 3J**). To corroborate SHH detection timing, we analyzed by ISH the expression pattern of the transcription factor *Rora*, one direct *Shh* modulator involved PC maturation, survival, and lifelong morpho-functional integrity (Sidman et al., 1962; Hamilton et al., 1996; Dussault et al., 1998; Gold et al., 2003, 2007; Chen et al., 2013; Takeo et al., 2015). As anticipated, *Rora* expression pattern perfectly matches SHH immunostaining in PCs, being detected from 40 dpo till adulthood in *P. vitticeps* (**Figure 3K** and **Supplementary Figure 1B**), thus confirming SHH spatiotemporal pattern. Altogether, our results strongly suggest the formation of a proliferative EGL structure on the pial surface of lizard cerebellum, likely yielding the generation of a vast number of GCs through a secondary transit-amplifying phase, thus indicating that squamates feature developmental milestones thought to be exclusive of birds and mammals.

Patterning and Generation of Cerebellar Neurons in *B. fuliginosus*

Owing to the divergent architecture and size of postnatal cerebellum in our two squamate models (see **Figure 1**), we then explored the cellular and molecular dynamics of *B. fuliginosus* neuronal development to identify possible mechanisms that could explain their peculiar organization. At early embryonic stages, although a cerebellar primordium showing a highly proliferative VZ can be distinguished at 12 dpo, PCNA-positive cells are only found on both cerebellar surfaces at 15 dpo, a stage when groups of LHX1-positive PCs have started to migrate out from the ventricular epithelium (**Figure 4A**). It is worth noting that the overall cerebellogenesis was anticipated to initiate earlier in *B. fuliginosus* than in *P. vitticeps* because of the relative advanced development of snake embryos at oviposition (Boback et al., 2012; Ollonen et al., 2018). At 25 dpo, PCs aggregate to form pluristratified PCCs in the middle of the developing cerebellum along the ventricular-pial axis, similarly to the situation observed in *P. vitticeps* at mid-embryonic stage, and the ventricular surface display less proliferative activity (**Figure 4B**). As cerebellum morphogenesis progresses, clear differences emerge in the snake PC developmental program when compared to the lizard counterpart. *B. fuliginosus* PCs fail to disperse and to undergo the complex spatial rearrangement observed during the last third of post-ovipositional development in *P. vitticeps*, but rather maintain a pluristratified, scattered configuration throughout embryogenesis (**Figures 4C–F**), a phenotype coherent with the observed juvenile situation (**Figures 1G,H**). The slight modifications observed in PC layout after 30 dpo (**Figures 4D–F**) are likely to be ascribed to consolidation of cerebellar neural wiring rather than to PC-autonomous dynamics. Compared to *P. vitticeps*, remarkable differences are also evident in the proliferative activity occurring on the pial surface. Especially, the number of PCNA-positive cells on the rostral half of this cerebellar side has already strongly reduced by 25 dpo, becoming almost entirely confined to the caudal third and URL of the cerebellum at 30 dpo (**Figure 4C**), and no proliferating cells are detected by 40 dpo (**Figures 4D–F**). This comparative analysis of neuron patterning indicates that, while the initial steps of PC radial migration and PCC formation appear conserved in our two squamate models, the alternative cortical organization in snakes is already determined during embryogenesis by a different PC capability to uniformly disperse from the multilayered cluster configuration.

When compared to *P. vitticeps*, the observed changes in the timing of PCNA labeling along the snake pial surface suggest variations in embryonic cerebellogenesis and EGL maintenance among squamate species. To confirm this hypothesis, we next assessed the status of GC patterning and EGL formation in snakes, using proliferative and molecular markers described above for lizards. Our immunohistochemistry (IHC) and ISH experiments suggest that the same molecular framework underlies lizard and snake GC generation but, as expected, remarkable differences in the timing of major cerebellogenesis events differentiate the two models. As observed in *P. vitticeps,* a multilayered *Atoh1*-positive, proliferative EGL, featuring mitotic cells both at its rostralmost edge and in more internal layers, is found in the snake starting from 15 dpo (**Figures 5A,B**). As cerebellogenesis continues, however, a progressive reduction in both EGL thickness and rostrocaudal extent is accompanied by a decrease in the number of mitotic cells that becomes gradually confined to the caudal edge immediately adjacent to the URL (20-30 dpo; **Figures 5C–E**), and no proliferative activity is detected on the pial surface as well as in the URL by 40 dpo (**Figure 5F**). The EGL germinative potential in the snake, thus, significantly differs from the proliferative pattern of *P. vitticeps* that persists for a much longer embryonic period and even beyond (**Supplementary Figure 1A**). Surprisingly, however, the 40 dpo stage features the initial detection of both SHH and *Rora* in snake PCs, regardless of EGL complete disappearance, indicating that similar molecular events than in *P. vitticeps* occur during PC maturation in snakes (**Figures 5F,G** and **Supplementary Figure 1C**). Furthermore, despite the initial shift in embryonic timing of early neuron patterning in terms of dpo, these observations suggest that cerebellum development is synchronized in terms of PC maturation stage at 40 dpo. Altogether, these findings further indicate that cellular and molecular mechanisms such as EGL formation and SHH expression by PCs are not an exclusive trait of birds and mammals but also a prominent feature of squamate cerebellogenesis. Interestingly, however, the absence of EGL at

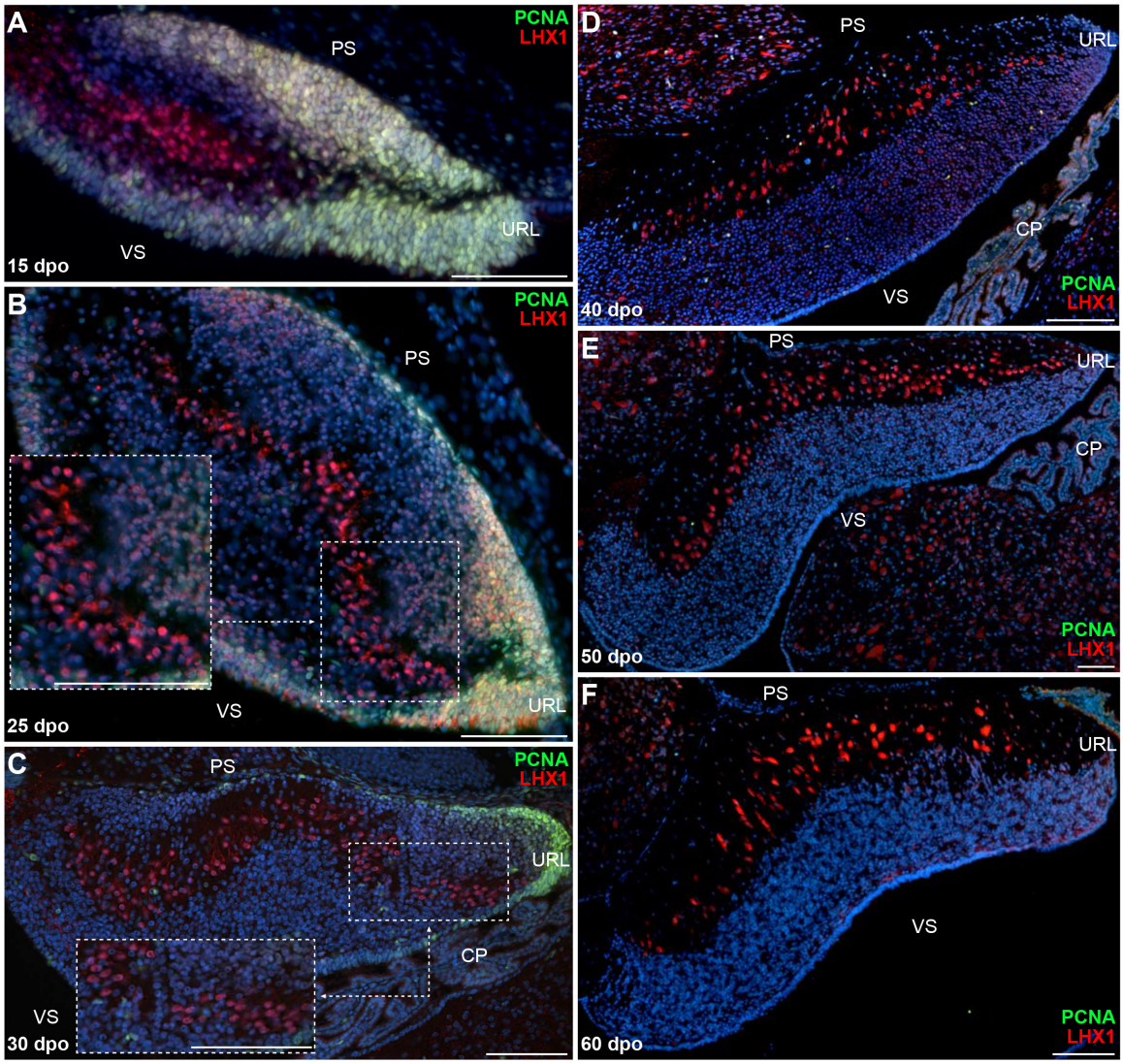

FIGURE 4 | Proliferation pattern and PC development in embryonic *B. fuliginosus* cerebellum. **(A–F)** Double IHC for PCNA (green staining) and LHX1 (red) markers at various developmental embryonic stages between 15 and 60 dpo in the cerebellum of *B. fuliginosus*. Insets in panels **(B,C)** show high magnifications of PC spatial organization. PS, pial surface; VS, ventricular surface; URL, upper rhombic lip; CP, choroid plexus. Scale bars: 100 μm.

the onset of SHH expression indicates the absence of secondary, PC-induced transit-amplifying phase in snakes, a phenotype already observed in mutant mice with complete abrogation of SHH signaling (Corrales, 2006) and coherent with the rapid decline of EGL structure.

Molecular Mechanisms Regulating Initial Formation and Maintenance of EGL in Squamates

We next aimed at assessing the molecular mechanisms that could explain the observed changes in URL proliferation activity and EGL formation between our two squamate species. Early cerebellar development relies on signaling molecules secreted by bordering non-neural tissues, including the choroid plexus (CP) and RP of the fourth ventricle (Yamamoto et al., 1996; Liu and Joyner, 2001; Wurst et al., 2001; Chizhikov et al., 2006; Krizhanovsky and Ben-Arie, 2006). In the context of GC development, BMP signaling from these non-neural areas plays a critical role in URL induction and generation of GCPs that migrate toward the EGL (Chizhikov et al., 2006; Krizhanovsky and Ben-Arie, 2006; Qin et al., 2006; Tong et al., 2015), and the potential of BMP ligands such as BMP7, GDF7, and BMP4 to regulate GCP proliferation and specification has been thoroughly documented both in cell/tissue culture assays and *in vivo* (Alder et al., 1996, 1999; Lee et al., 1998; Krizhanovsky and Ben-Arie, 2006; Su et al., 2006; Salero and Hatten, 2007). Additionally, activation of BMP canonical signaling through SMAD proteins has been reported in embryonic URL and EGL (Fernandes et al., 2012;

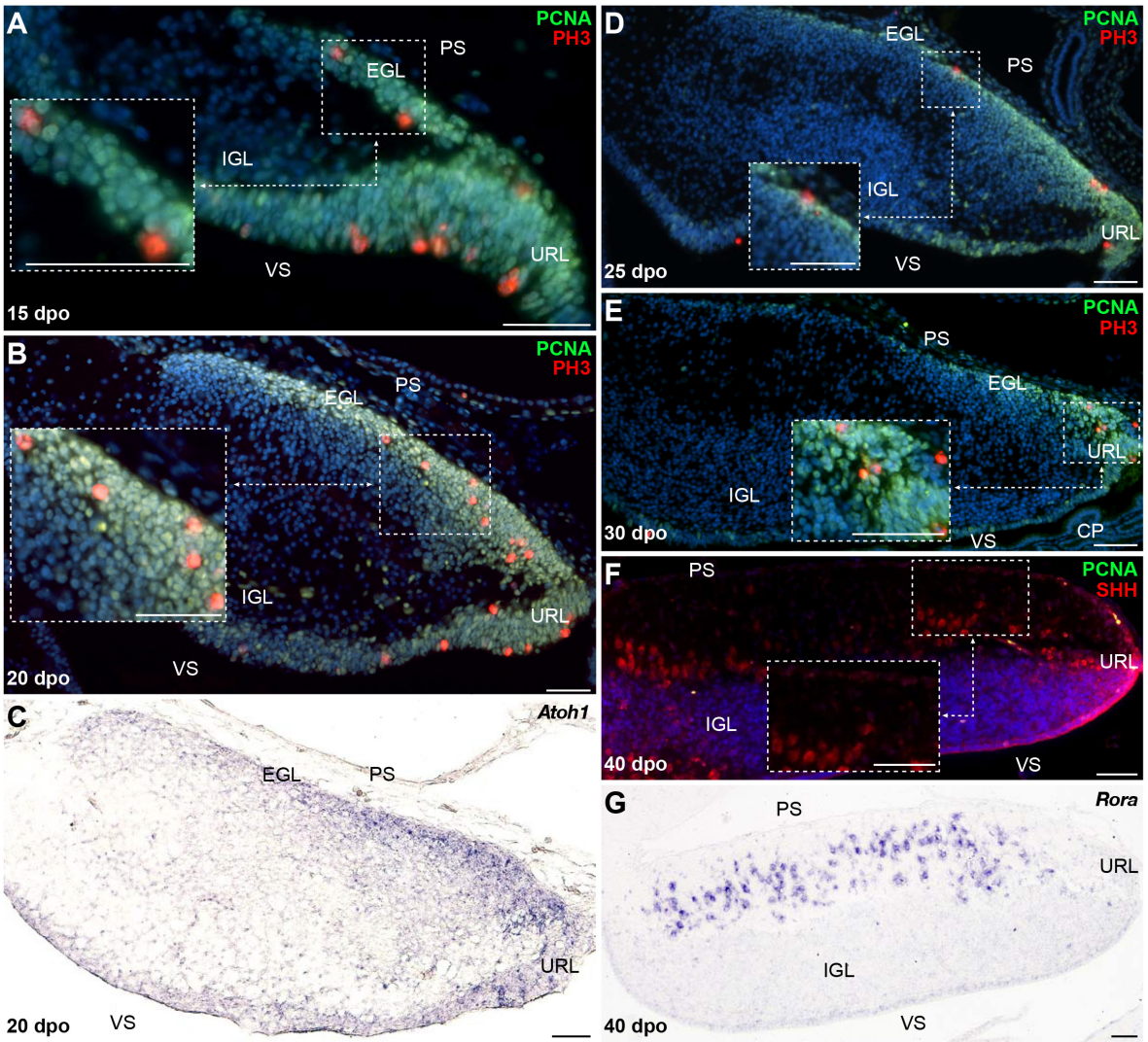

FIGURE 5 | Molecular characterization of GC patterning in *B. fuliginosus*. **(A–E)** Double IHC for PCNA (green staining) and PH3 (red) markers **(A,B,D,E)** or ISH for *Atoh1* **(C)** at various indicated embryonic developmental stages between 15 and 30 dpo in the cerebellum of *B. fuliginosus*. Insets in panels **(A,B,D,E)** show high magnifications of mitotic progenitors on the pial surface. **(F,G)** Double IHC for PCNA (green) and SHH [**(F)**; red] or ISH for *Rora* **(G)** at 40 dpo. The inset in panel **(F)** shows high magnification of SHH-positive PCs. PS, pial surface; EGL, external granule layer; IGL, internal granule layer; VS, ventricular surface; URL, upper rhombic lip; CP, choroid plexus. Scale bars: 50 μm.

Owa et al., 2018), and SMAD1/5 double-mutant mice display defects in URL development as well as a reduced EGL accompanied by PC spatial disorganization (Tong and Kwan, 2013). In light of these data, we tested whether the altered proliferative patterns in both URL and EGL of our snake model could derive from modifications in the temporal and/or spatial expression pattern of BMP ligands (**Figures 6A–K**). Strikingly, while *Bmp4* and *Bmp7* transcripts are initially found concomitantly with URL activation in the CP of both species (**Figures 6A,B,F,H**), our ISH experiments indicate a precocious downregulation of these genes in the latter region during *B. fuliginosus* cerebellogenesis. In contrast to *P. vitticeps* that still maintains expression of *Bmp* genes by 40 dpo (**Figures 6C,D**), only a barely detectable level is noticed beyond initial PCC formation in snakes (**Figures 6G-J**). Importantly, these differences in *Bmp* expression parallel variations in phosphorylated forms of SMAD1/5/9, reflecting activity of canonical BMP signaling, which are only faintly detected and rapidly restricted to the shrinking EGL and URL domains in snakes when compared to the broad, abundant expression pattern in lizards (**Figures 6E,K**). These data suggest a tight link between BMP secretion by extra-cerebellar, non-neural tissues and both URL and EGL spatiotemporal dynamics in squamates. While the overall gene expression and activation domains in *P. vitticeps* resemble the situation described in other amniotes, a heterochronic shift in the timing and/or duration of URL activity is likely linked to the disappearance of EGL structure before PC maturation in snakes, eventually leading to absence

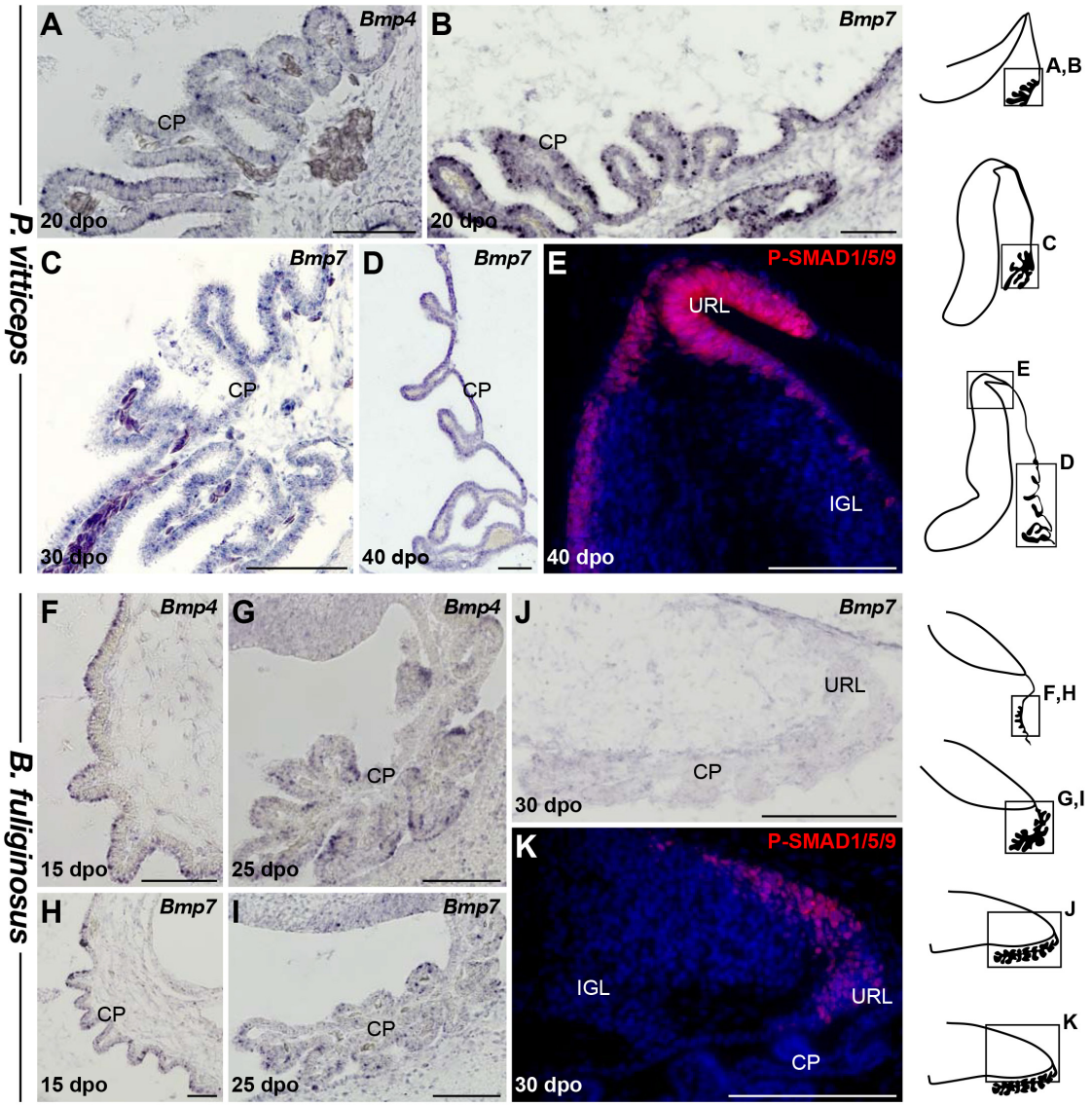

FIGURE 6 | Characterization of BMP signaling pathway during early cerebellogenesis in *P. vitticeps* and *B. fuliginosus*. **(A–D)** ISH showing the expression of *Bmp4* **(A)** or *Bmp7* **(B–D)** at various indicated embryonic developmental stages in non-neural tissues bordering the cerebellum of *P. vitticeps*. **(E)** IHC for P-SMAD1/5/9 in the dorsal part and URL region of *P. vitticeps* cerebellum at 40 dpo. **(F–I)** ISH showing the expression of *Bmp4* **(F–J)** or *Bmp7* **(H–J)** at various indicated embryonic developmental stages in non-neural tissues bordering the cerebellum of *B. fuliginosus*. **(K)** IHC for P-SMAD1/5/9 (red staining) in the caudal part and URL region of *B. fuliginosus* cerebellum at 30 dpo. IGL, internal granule layer; URL, upper rhombic lip; CP, choroid plexus. Scale bars: 100 μm.

of PC-induced transit-amplifying phase and EGL maintenance at subsequent developmental stages.

Molecular Mechanisms Regulating Cerebellar Cortex Lamination in *P. vitticeps* and *B. fuliginosus*

Although PCs and GCs arise from separate progenitor zones, complex interactions between these two cell types play pivotal roles during cerebellar morphogenesis. Therefore, our results suggest that the divergent EGL developmental states featured by our models could be, at least in part, associated with the final differential distribution of PCs. The acquisition of the stereotypic monolayer configuration by bird and mammalian PCs relies on a well-characterized molecular cascade triggered by the molecule RELN, a large glycoprotein secreted by radially migrating post-mitotic GCPs in the developing ML as well as by terminally differentiated GCs already settled in the IGL (Caviness and Rakic, 1978; D'Arcangelo et al., 1995; Miyata et al., 1997; Pesold et al., 1998; Jensen et al., 2002). Based on genetic and biochemical studies, two RELN receptors have been identified, including VLDLR that is particularly highly expressed in cerebellar PCs (D'Arcangelo, 2014). Upon RELN binding, these receptors mediate the phosphorylation of the adaptor

protein DAB1 that drives cytoskeletal rearrangements in PCs, eventually leading to the peculiar amniote PC pattern along the outer IGL border. Impairment at any level of this pathway leads to similar defects in cerebellar architecture, including severe alteration of PC topographic organization, and major locomotor deficits (D'Arcangelo et al., 1995; Sheldon et al., 1997; Ware et al., 1997; Gallagher et al., 1998; Trommsdorff et al., 1999). We then combined IHC and ISH experiments to identify potential variations in RELN signaling network that could determine the alternative cortical PC layout featured by our models. In *P. vitticeps*, *Reln* transcripts are initially particularly abundant in sparse post-mitotic GCPs delaminating from the EGL and then in a larger number of radially migrating post-mitotic GCPs (30 dpo), reflecting the massive progenitor expansion within EGL at early stages of cerebellum development (**Figure 7A** and data not shown). At 30 dpo, a faint staining is also detected on the ventricular side where early generated GCs start to colonize the presumptive IGL. As cerebellogenesis progresses, the *Reln* pattern

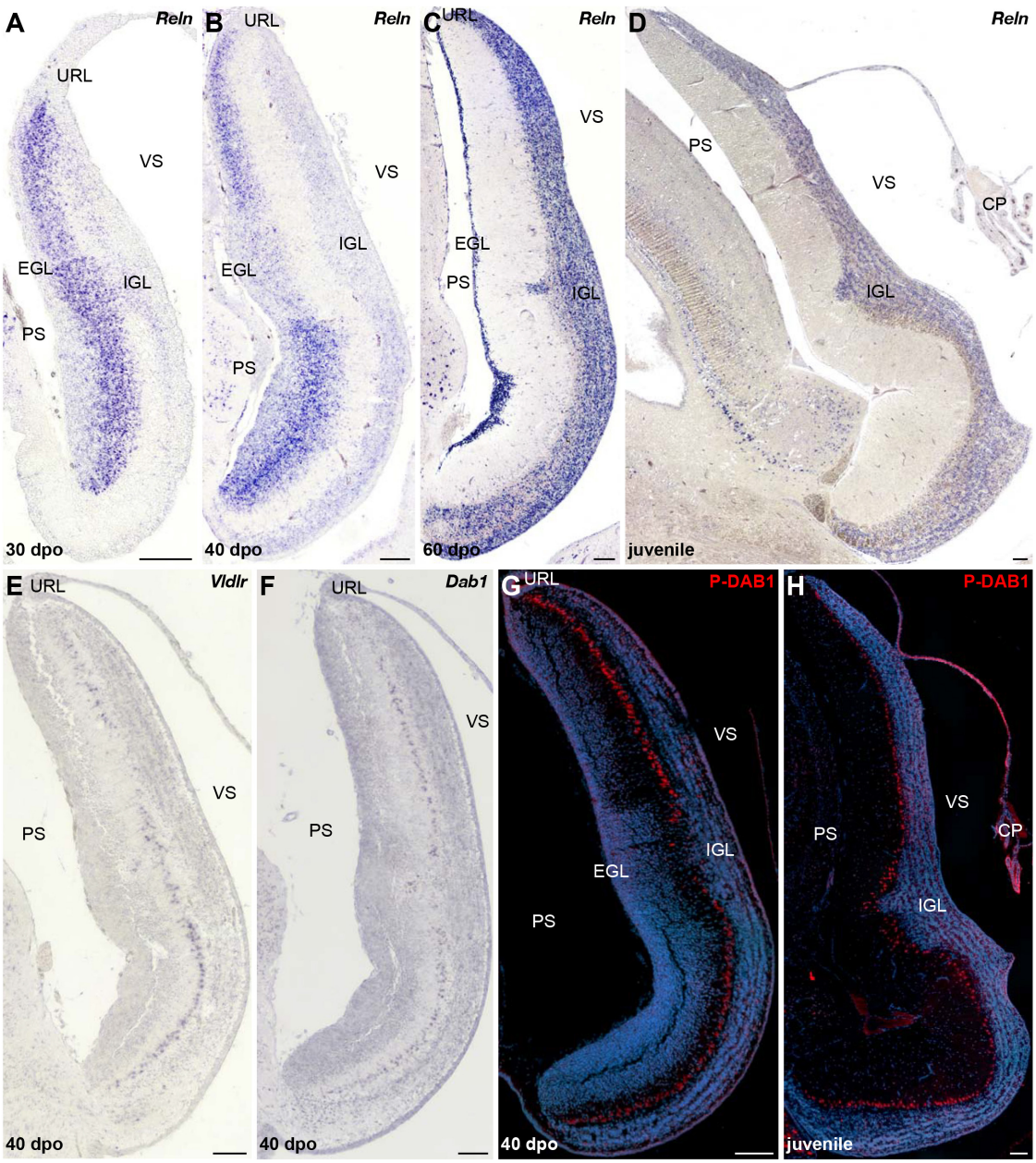

FIGURE 7 | Characterization of RELN signaling pathway in the developing cerebellum of *P. vitticeps*. **(A–D)** ISH for *Reln* at various indicated embryonic (30, 40, and 60 dpo) and juvenile stages in the cerebellum of *P. vitticeps*. **(E,F)** ISH for *Vldlr* **(E)** or *Dab1* **(F)** at 40 dpo. **(G,H)** IHC for P-DAB1 (red staining) at 40 dpo **(G)** and juvenile **(H)** stages. PS, pial surface; EGL, external granule layer; IGL, internal granule layer; VS, ventricular surface; URL, upper rhombic lip; CP, choroid plexus. Scale bars: 100 μm.

strictly follows both EGL shrinking and continuous accumulation of GCs in the IGL (**Figures 7B,C**). Like in mammals, *Reln* expression persists in the IGL of juvenile lizards (**Figure 7D**), where it likely promotes synaptic plasticity and modulates neurotransmitter release in a similar fashion of neuronal subsets residing in adult neocortex and hippocampus (Beffert et al., 2005; Herz and Chen, 2006; Hellwig et al., 2011). However, in contrast to the expression of components of the RELN pathway that initiates at early stage of EGL formation in rodent models (Rice et al., 1998; Trommsdorff et al., 1999), the expression pattern of *Vldlr* and *Dab1* appears relatively delayed in *P. vitticeps*, being only detected in migrating PCs beyond initial lizard PCC formation, from 40 dpo onward (**Figures 7E,F**). Coherent with that, the phosphorylated form of DAB1 (P-DAB1), a molecular read-out of RELN signaling activity, perfectly matches *Vldlr* and *Dab1* expression in lizards (**Figures 7G,H**). Interestingly, the gene expression profile of RELN pathway in *B. fuliginosus* matches the asynchronous pattern featured by the lizard, with strong *Reln* labeling being detected in GCPs delaminating from EGL at early developmental stages as well as in GCs already settled in the IGL from later stages till adulthood (**Figures 8A–C** and **Supplementary Figure 1D**). Furthermore, both *Dab1* mRNA and P-DAB1 are detected starting from 40 dpo in snake PCs, confirming the synchronized expression profile of squamate PCs at this stage, and their expression is further maintained at postnatal stages (**Figures 8D–F**).

Despite the observed activation of DAB1 at similar embryonic stage in both squamate models, the onset of PC response to RELN signals occurs in a radically divergent morphogenetic context in the two species. At 40 dpo, GCP generation from URL and EGL is still sustained in *P. vitticeps*, and the relatively high level of *Reln* expression observed in delaminating and migrating GCPs likely provides a permissive environment for PC spatial rearrangement (**Figure 7B**). On the opposite cerebellar ventricular surface, the forming lizard IGL rather shows a reduced level of *Reln* at 40 dpo, indicating that RELN-responding PCs at this stage are exposed to a gradient of gene expression with its highest level on the pial side. At subsequent stages, *Reln* expression becomes progressively exclusive to the IGL, in correlation with EGL shrinking and ML thickening (**Figures 7C,D**). In contrast, the snake EGL already disappeared from developing cerebellum by 40 dpo when PCs start expressing *Dab1*, and a clear cerebellar lamination featuring both a compact IGL and thick ML is established at this stage (**Figure 8C**). With respect to lizards, responding PCs in snakes are thus only exposed to one source of *Reln* produced by IGL GCs (**Figure 8C**). The asymmetry in cortical maturation at the onset of DAB1 activation, exposing PC to remarkably divergent molecular and spatial environment, might thus be responsible for alternative PC spatial layouts in our models. This hypothesis is coherent with the intact mature glial fiber organization and arrangement of PCs in radially oriented columns observed in the cerebellum of *B. fuliginosus* (**Figures 8G,H**), suggesting the presence of a proper guidance system supporting PC migration. Furthermore, previous observations on the asymmetric, fluctuating concentration of RELN during post-mitotic GCP migration in mice (Miyata et al., 1996) further suggest that RELN signaling emanating from GCPs is likely a major player in the positioning of PCs. Finally, the key importance of temporal and spatial patterning of GCs and PCs during cerebellar development have been demonstrated using transplantation experiments in rodents (Sotelo and Alvarado-Mallart, 1986, 1987a,b; Carletti et al., 2008), which showed that embryonic PCs transplanted in embryos at different developmental stages trigger variable ratios of PC misplacement in recipient ML, a phenotype related to host cortical maturation progression and EGL reduction (Carletti et al., 2008).

DISCUSSION

The generation, migration, and maturation of major cerebellar cell types are complex phenomena that impact whole-cerebellum morphogenesis, integrity, and function. Despite the overall conserved progenitor domains and salient physiological and morphological features of cerebellar GCs and PCs across vertebrates (Altman and Bayer, 1997), modifications in their developmental programs have been linked to the remarkable degree of cerebellar complexity achieved during vertebrate radiation in terms of both magnitude and spatial arrangement of neurons and foliation pattern. In this perspective, the absence of a typical EGL—defined as a distinct progenitor population covering the cerebellar pial surface and expressing *Atoh1*—in chondrichthyans and teleosts, but also the presence of a distinct, non-proliferative EGL in amphibians, indicate that the SHH-induced transit-amplifying phase in GCPs constitutes a hallmark of birds and mammals (Rodríguez-Moldes et al., 2008; Chaplin et al., 2010; Butts et al., 2014a; Pose-Méndez et al., 2016; Iulianella et al., 2019), likely allowing a massive GC production in a restricted developmental time window (Chaplin et al., 2010; Iulianella et al., 2019). In contrast, owing to the undetermined growth that characterizes the brain of anamniotes, some bony fishes and most likely chondrichthyans achieve extremely folded structures through continuous addition of GCs from stem progenitor pools throughout life (Candal et al., 2005; Zupanc et al., 2005; Rodríguez-Moldes et al., 2008; Chaplin et al., 2010; Kaslin et al., 2013; Butts et al., 2014b). Here, we show that squamate reptiles provide a new model system to examine both the role and evolutionary importance of EGL structure, neuronal arrangement patterns, but also signaling pathways in cerebellar morphogenesis (**Figure 9**). First, our data suggest that both the formation of a proliferative EGL and the expression of SHH by underlying PCs contribute to squamate cerebellogenesis, indicating that these processes are key developmental features of the amniote cerebellum. Furthermore, the direct comparison of our lizard and snake models strongly suggests the critical importance of spatiotemporal neuronal patterning and interaction between GCPs and PCs in defining cortical organization within amniotes. Indeed, the observed heterochronic shifts in URL activity and EGL maintenance in snakes is strongly expected to affect the dynamics of molecular interaction between these two cell types in snakes. Finally, although further experimental demonstrations would be needed, our data suggest the influence of key signaling

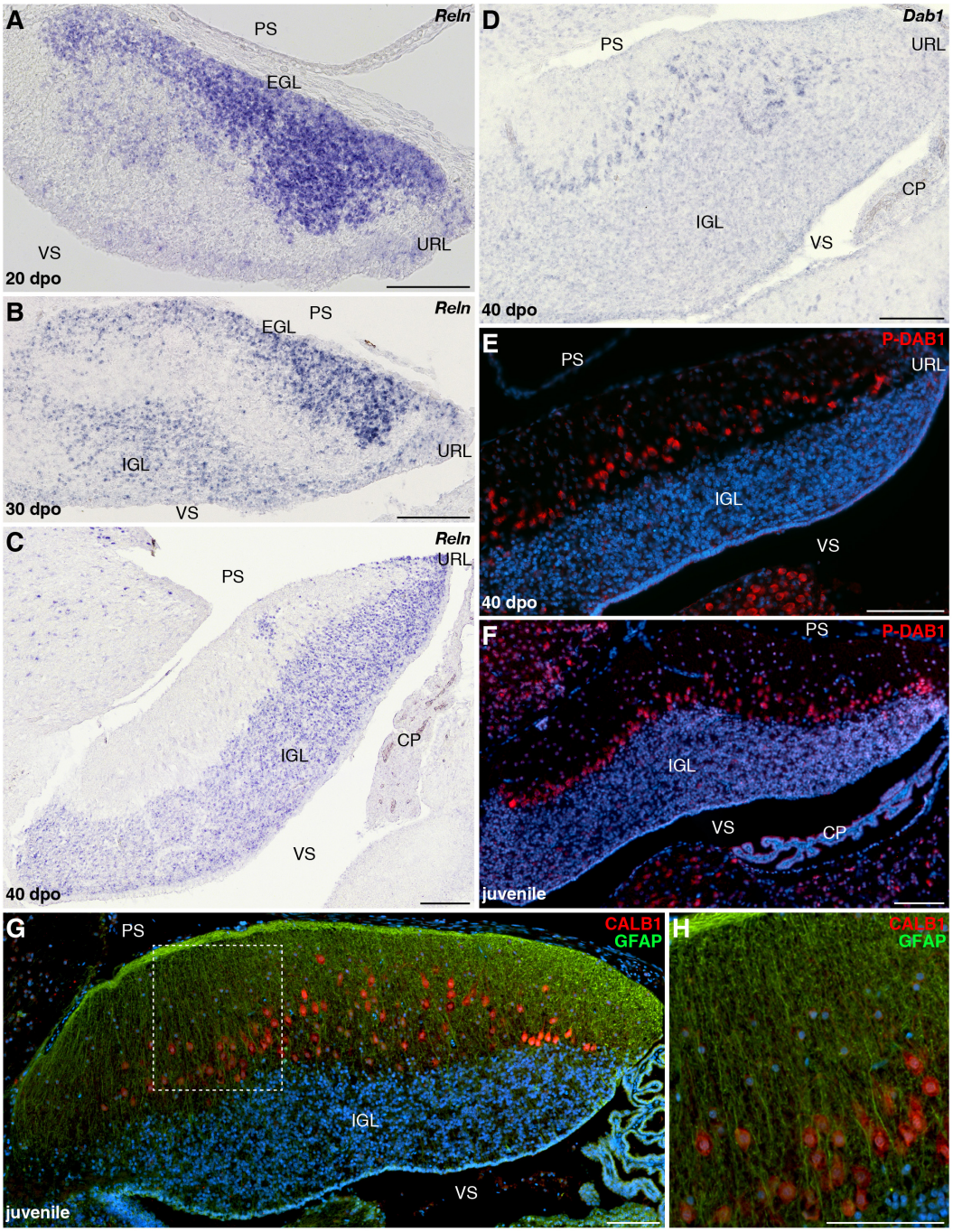

FIGURE 8 | Developmental characterization of RELN signaling pathway and mature glial fiber organization in the cerebellum of *B. fuliginosus*. **(A–D)** ISH for *Reln* **(A–C)** or *Dab1* **(D)** at various indicated embryonic stages (20, 30, and/or 40 dpo) in the cerebellum of *B. fuliginosus*. **(E,F)** IHC for P-DAB1 (red staining) at 40 dpo **(E)** and juvenile **(F)** stages. **(G,H)** Double IHC for CALB1 (red) and GFAP (green) in the cerebellum of juvenile *B. fuliginosus*. A high magnification view of the area contained in the dashed rectangle in panel **(G)** is shown in panel **(H)**. PS, pial surface; EGL, external granule layer; IGL, internal granule layer; VS, ventricular surface; URL, upper rhombic lip; CP, choroid plexus. Scale bars: 100 μm.

pathways such as RELN on the behavior and spatial positioning of PCs in vertebrate cerebella. Altogether, our study provides new insights into the developmental origins of diversity in cerebellar cortical architecture and foliation pattern found in amniotes, including the remarkable array of PC spatial layouts identified in squamate reptiles, thus helping to complete our evolutionary understanding of vertebrate phenotypical diversification.

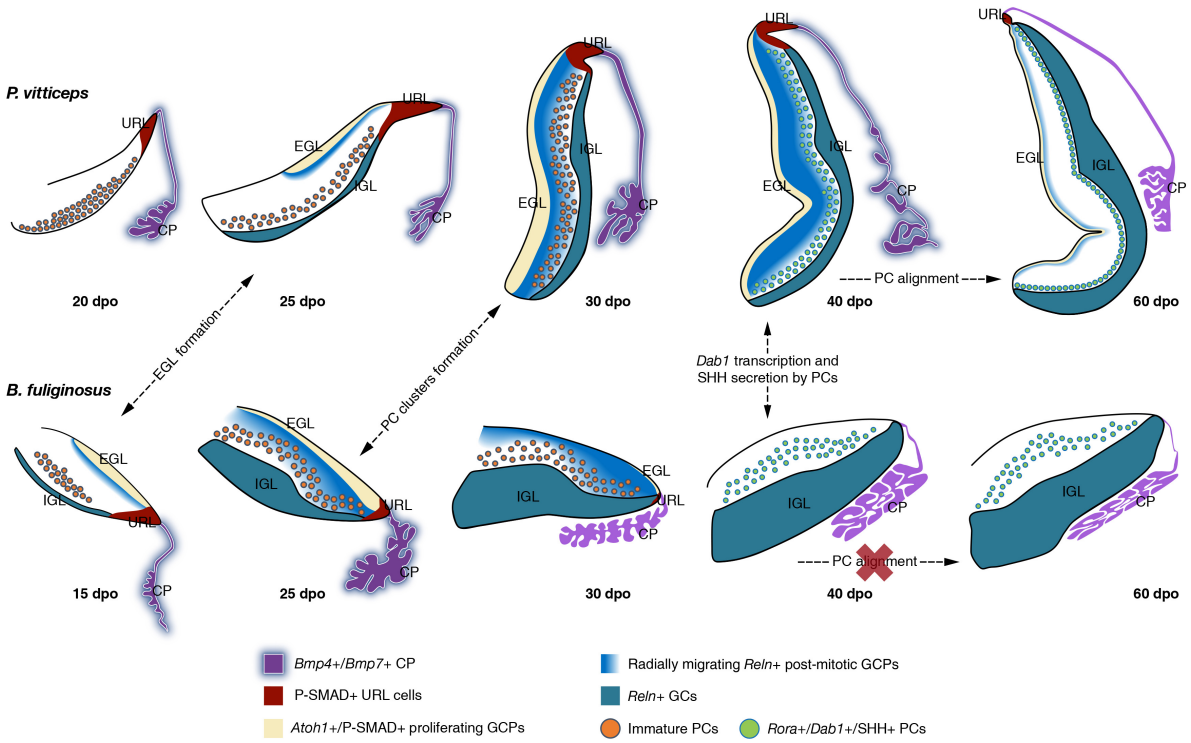

FIGURE 9 | Overview of cerebellar development in squamate models. Schematic representation of the main molecular and cellular events at the origin of the divergent cortical lamination in *P. vitticeps* **(top row)** and *B. fuliginosus* **(bottom row)** cerebellum. The presence or absence (red cross) of major developmental processes at indicated embryonic stages are shown by dashed arrows. Key gene expression patterns in cerebellar regions and/or cell types identified in this study are indicated by different colors (see color code and symbols in bottom row). EGL, external granule layer; IGL, internal granule layer; URL, upper rhombic lip; CP, choroid plexus; GCP, granule cell progenitor; GC, granule cell; PC, Purkinje cell.

Temporal Coupling Between EGL Formation and SHH Expression by Underlying PCs Regulates Squamate Cerebellar Complexity

The acute proliferation patterns of *Atoh1*-positive GCPs observed on the pial surface of the developing lizard and snake cerebellum unequivocally indicate the existence of a typical EGL in squamates, as previously identified in birds and mammals (**Figure 9**). In contrast, such secondary germinative zone has not been observed in a multitude of anamniote species (Rodríguez-Moldes et al., 2008; Chaplin et al., 2010; Butts et al., 2014b), including in metamorphic frogs where a subpial layer of cell migrating from the URL, resembling a non-proliferative EGL, has been described (Gona, 1972; Butts et al., 2014a). Our results, thus, document for the first-time that the EGL is a true amniote evolutionary novelty and not a distinctive feature of avian and mammalian cerebellogenesis. Importantly, however, we show that the EGL temporal dynamics differs considerably in our squamate models, the snake showing a precocious EGL decline and termination soon after its initial expansion, paralleling BMP expression pattern and activity in the adjacent CP and URL (**Figure 9**). In addition to differences in the timing of initial EGL formation, the heterogeneity in EGL duration between *P. vitticeps* and *B. fuliginosus* is expected to reside in the level of SHH signaling emanating from underlying PCs. Elegant experiments employing conditional mouse mutants have shown that the extent and complexity of cerebellar foliation is proportional to the intensity of SHH signaling (Corrales, 2006). A complete signal abrogation produces a precocious termination of GCP proliferation in the EGL, leading to the absence of foliation in the mutant cerebella, while more elaborated foliation patterns, resulting from EGL duration lengthening, parallel increase in SHH pathway activity. In a similar manner, the cerebella of our squamate models can be interpreted as phenotypic variants resulting from SHH signaling intensity modulation. Indeed, the complete decoupling between SHH pathway activation and EGL formation in the developing snake cerebellum recapitulates the situation occurring in mice totally depleted of SHH signaling after cerebellar primordium initiation. In such mutants, cerebellar foliation is inhibited because of a rapid depletion of GCPs from the EGL, and cerebella exhibit a dramatic reduction along the anteroposterior axis and lack any fissure. Likewise, the snake cerebellum is smooth and displays a significantly shorter pial surface extension (corresponding to mouse anteroposterior axis), when compared to the lizard counterpart that exhibits a more elaborated morphology. Furthermore, while both lizard and snake cerebella undergo an initial growth phase characterized by the lengthening and thickening of their cerebellar primordium, a second transit-amplifying phase of GCPs, featuring the formation

of an incomplete and shallow fissure on the medial pial surface, occurs only in the lizard and is concurrent with SHH pathway activation and maintenance of proliferative EGL until postnatal stages. Although one or two transverse fissures dividing the cerebellum into different lobes have been previously reported in crocodilians and in some lizard species (Larsell, 1926, 1932), it is however unclear if the fissure observed in *P. vitticeps* is equivalent to the fissura prima, the first fissure to appear in the mammalian cerebellum, or simply linked to the inverted tilting of the lizard cerebellum. Moreover, the absence of foliation pattern in *P. vitticeps* despite the prolonged EGL maintenance suggests an overall low level of SHH signaling activity originating from lizard PCs (Corrales, 2006), which might be directly associated with the relatively reduced number of cerebellar PCs in squamates when compared to mammals (Wetts and Herrup, 1982; Bakalian et al., 1991, 1995; Frederic et al., 1992; Zanjani et al., 1992, 2004; and personal observations). Nevertheless, the persistence of EGL in lizards is also coherent with the formation of a more compact IGL as well as with the overall increase in cerebellum size, when compared to snakes.

Together, our findings provide new insights into the mechanisms determining cerebellar complexity in amniote lineages, including within squamate reptiles, thus suggesting an expanded role of SHH signaling in orchestrating cerebellum morphological complexity toward a broader evolutionary scope. In this perspective, it will be of great interest to functionally validate *in ovo* the hypothesis of a SHH-mediated transition between the unfoliated morphologies exhibited by squamates and the sophisticated architectures of birds and mammals once overcome the technical limitations posed by the use of non-canonical models. Furthermore, the maintenance of SHH signaling by *B. fuliginosus* PCs at both embryonic and postnatal stages could be an excellent experimental framework to assess the additional functions of this protein. In addition to cerebellar GCP proliferation enhancement, SHH has been shown to exert a fundamental role in expanding and maintaining an heterogeneous progenitor pool in the developing prospective cerebellar white matter in mice (Fleming et al., 2013). Moreover, its detection in adult mouse and rat PCs (Traiffort et al., 2002; Corrales, 2004; Lewis et al., 2004; Okuda et al., 2016), and its capability to regulate glutamate and ATP secretion from adult cerebellar astrocytes *in vitro* (Okuda et al., 2016), suggest the key importance of this protein in the adult cerebellum, likely in synaptic plasticity modulation.

Importance of *Reln* Distribution Pattern in Cortical Maturation

A number of descriptive works on the cerebellar cortex of squamate species have emphasized the remarkable variation in PC spatial layouts, ranging from the almost regular monolayer exhibited by lizards to the scattered pattern featured by snakes (Larsell, 1926; ten Donkelaar and Bangma, 1992; Aspden et al., 2015; Wylie et al., 2017; Hoops et al., 2018). However, our recent quantitative work assessing PC topological distribution in a large squamate dataset depicted a much more complex scenario (Macrì et al., 2019). We revealed that a wide spectrum of PC spatial layouts is present both in snakes and lizards and parallels locomotor specialization, independently of phylogenetic relationships, likely reflecting different kinds of cerebellar mediated coordination. Our new data presented here unveil the developmental basis underlying such a wide variety of arrangements. We show that molecular markers expressed during early generation and maturation of PCs are conserved in both our models and coincide with the general PC developmental program described in other amniotes. No substantial difference is also evident between snakes and lizards during the initial radial migratory phase of post-mitotic PCPs, a process that, like in mice (Yuasa et al., 1993), is anticipated to occur in a RELN-independent fashion, as evidenced here by the lack of *Dab1*-positive PCs at early cerebellogenesis (**Figure 9**). However, despite the similar expression profile of both GCPs and PCs in our models, our findings outline that the dynamics of molecular interaction between these two cell types is altered in snakes. Especially, the rapid decline of radially migrating post-mitotic GCPs expressing *Reln*, a phenotype coherent with the observed heterochronic shifts in the timing and/or duration of URL activity and EGL maintenance, is expected to hamper the spatial reorganization of PCs at the end of their radial migratory phase in snakes (**Figure 9**). Although the exact mechanisms regulating the dispersal of PCs from PCC stage to monolayer organization are still unclear in mouse models (Rahimi-Balaei et al., 2018), our data corroborate previous studies proposing that post-mitotic GCPs are a major player in the positioning of PCs (Miyata et al., 1997; Jensen et al., 2002). More specifically, comparisons of our two models upon *Dab1* expression and activation indicate that either post-mitotic GCPs delaminating from the EGL and migrating across the PCCs or a combination of both EGL GCPs and IGL GCs are required for PC spatial reorganization in *P. vitticeps* (40 dpo; **Figure 9**). Coherent with these hypotheses, previous *in vitro* studies corroborated by *in vivo* observations have suggested that RELN is highly concentrated on the somata of GCPs as they move away from the EGL and contact the underlying PCCs, while the extracellular localization of the glycoprotein decreases and becomes only restricted to parallel fibers once GCs settle in the IGL (Miyata et al., 1996). Such switch in RELN concentration and localization might be associated to the transition from its positional instructive function during early cerebellogenesis to a role in PC position consolidation and dendritic maturation at later stages (Miyata et al., 1996). In such context, as the IGL GCs are the only source of *Reln* at the time of *Dab1* activation in snakes (40 dpo; **Figure 9**), the ML is likely permeated by a low concentration of RELN signals which accumulates on PC dendrites rather than somata, triggering only local responses that may favor synaptic plasticity but not cell body relocation. An additional obstacle to PCC dispersion in snakes could derive from a non-permissive spatial micro-environment. At 40 dpo, in fact, while lizard cortical segregation is only barely outlined, a clear lamination is already established in *B. fuliginosus* cerebellum, featuring a thick ML densely populated by GC parallel fibers that might constitute a physical barrier to PC repositioning.

Altogether, our observations further suggest a major role of the RELN pathway in controlling PC positioning in vertebrates

(Caviness and Rakic, 1978; D'Arcangelo et al., 1995; Miyata et al., 1997; Jensen et al., 2002). However, despite the similarities in ectopic arrangement of PCs noticed between the adult cerebellum of snakes (this study and Macrì et al., 2019) and vertebrate mutants affecting the RELN pathway (Heckroth et al., 1989; D'Arcangelo et al., 1995; Sheldon et al., 1997; Ware et al., 1997; Gallagher et al., 1998; Trommsdorff et al., 1999; Nimura et al., 2019), significant phenotypic differences in cortical organization are noticeable. Especially, snake PCs are not found amassed in clusters or trapped in the IGL, as shown in mouse and zebrafish mutants with movement or behavioral defects (Inoue et al., 1990; Nimura et al., 2019). Instead, our developmental data in *B. fuliginosus* indicate that PCs are arranged in radially oriented columns, each consisting of a different number of cells protruding in the ML, likely reflecting the presence of a proper guidance system provided by an organized radial glia scaffold supporting their migration. This also contrasts with the aberrant and distorted organization of cerebellar radial glia, along with other types of glia located in different brain areas, observed in *reeler* mice (Bignami and Dahl, 1974; Terashima et al., 1985; Yuasa et al., 1991; Yuasa, 1996; Hartfuss et al., 2003; Weiss et al., 2003) and *Reln* knockout zebrafish (Nimura et al., 2019). These differences suggest that *Reln* expression initiating at early stages of cerebellogenesis in differentiating GCPs, a distribution pattern similar among squamate models (**Figure 9**) but also in mice (Miyata et al., 1996; Rice et al., 1998), could be important for the maturation and migration of other cerebellar cell types, most likely developing glia.

In conclusion, our characterization of squamate cerebellogenesis indicates a complex and dynamic crosstalk between developing cerebellar neurons in a new major group of vertebrates, and strongly suggests the existence of variations from a common amniote developmental blueprint for cerebellar histogenesis. Furthermore, our comparative gene expression analysis, conducted on species featuring extremely divergent cortical arrangements, supports a pivotal role of heterochrony in generating phenotypic variation, but also give new insights into the morphogenetic and molecular underpinnings at the base of squamate cerebellar cortex diversification. Altogether, these findings provide a new perspective on the complex evolutionary processes and morphogenetic dynamics underlying increased complexity of the amniote cerebellum, highlighting the potential offered by squamate models to expand our understanding of such unique neurodevelopmental landscape.

MATERIALS AND METHODS

Sample Collection

P. vitticeps and *B. fuliginosus* embryonic series as well as hatchlings and juveniles (2–6 months after hatching) were obtained from our animal facility at the University of Helsinki. Fertilized eggs were incubated on a moistened vermiculite substrate at 29.5°C, as previously described (Ollonen et al., 2018). Embryos were collected at regular intervals spanning the entire post-ovipositional period (about 60 days in both species), and embryonic staging was performed on the basis of external morphology according to developmental tables available for the two species (Boback et al., 2012; Ollonen et al., 2018). A minimum of three biological replicates were analyzed for each developmental time point in the different experiments.

Micro-CT Scan and 3D Brain Reconstructions

High-resolution 3D CT-scans of *P. vitticeps* and *B. fuliginosus* heads were performed at the University of Helsinki imaging facility using Skyscan 1272 (Brucker, Belgium). Prior to micro-CT scanning, to allow reptile brain tissue visualization, samples were treated with 1% iodine solution as previously described (Metscher, 2009; Macrì et al., 2019). The following scan parameters were used: filter: Al 0.25 mm; source voltage: 60 kV; source current: 166 μA; voxel size: 12 μm; rotation steps: 0,2°; frame averaging: 8. Scans were reconstructed using NRecon 1.7.0.4 software (Bruker) and 3D volume rendering as well as segmentation were performed using the software Amira 5.5.0 (Thermo Fisher Scientific, United States). Both the whole-brain and isolated cerebellum were segmented, thus allowing assessment of volumetric measurements of these structures. The accuracy of all generated 3D models was carefully controlled along the three anatomical planes, as described (Macrì et al., 2019).

Nissl Staining and Immunohistochemistry

Embryonic heads were fixed overnight in 4% paraformaldehyde (PFA) at 4°C and dehydrated through a series of washes in PBS containing increasing methanol concentrations (25, 50, 75, and 100%). For optimal sectioning, the brains of both juvenile individuals and embryos presenting an advanced degree of skull ossification were dissected from the braincase before fixation. After dehydration, samples were paraffin-embedded and microtome-sectioned at 9 μm. For Nissl staining, sections were deparaffinized in xylene, rehydrated in decreasing ethanol concentration solutions (100, 95, 70%), and rinsed first in running tap water and successively in distilled water. Staining was performed in 0.1% (w/v) cresyl violet solution (cresyl violet acetate, Sigma-Aldrich, Cat# C5042) in distilled water, at 37°C. Once stained, sections were rinsed in distilled water and immersed in differentiating solution (95% ethanol in distilled water) for 10 min, dehydrated in 100% ethanol and cleared in xylene before mounting slides with DPX medium (Sigma-Aldrich, Cat# 06522). IHC on sections was conducted as previously described (Salomies et al., 2019), utilizing the following primary antibodies: PCNA (1:500, mouse monoclonal, BioLegend, Cat# 307901, RRID: AB_314691), CALB1 (1:300, rabbit polyclonal, Swant, Cat# CB38, RRID: AB_10000340), phospho histone H3 Ser10 (PH3, 1:500, rabbit polyclonal, Abcam, Cat# ab5176, RRID: AB_304763), SHH (1:400, rabbit polyclonal, LifeSpan Cat# LS-C40460, RRID:AB_2285962), LHX1 (1:400, rabbit polyclonal, LifeSpan, Cat# LS-C16214, RRID: AB_2135639), ZIC1/2/3 (1:300, rabbit polyclonal, LifeSpan, Cat# LS-C118695), phospho SMAD1/5/9 (P-SMAD1/5/9; 1:500, rabbit polyclonal, Cell

TABLE 1 | Details on nucleotide sequences used to obtain riboprobes in ISH experiments.

Gene name	Species	Sequence length (bp)	Sequence accession number (NCBI)	Nucleotide sequence position
Bmp4	*P. vitticeps*	670	XM_020813026	1…670
Bmp7	*P. vitticeps*	584	XM_020797472	50…633
Atoh1	*P. vitticeps*	966	CEMB01011076	706854…707819
Rora	*P. vitticeps*	942	XM_020784749	184…1125
Vldlr	*P. vitticeps*	830	XM_020801543	4592…5421
Reln	*P. vitticeps*	1237	XM_020790001	7804…9040
Dab1	*P. vitticeps*	848	XM_020789863	1064…1911
Bmp4	*P. guttatus*	785	XM_034433399	646…1430
Bmp7	*P. guttatus*	784	XM_034433071	502…1285
Atoh1	*B. fuliginosus*	623	MT993473	1…623
Rora	*B. fuliginosus*	907	MT993472	1…907
Reln	*B. fuliginosus*	927	MT993475	1…927
Dab1	*B. fuliginosus*	612	MT993474	1…612

Signaling Technology, Cat# 13820, RRID: AB_2493181), P-DAB1 (1:400, rabbit polyclonal, Biorbyt, Cat# orb156526), and glial fibrillary acidic protein (GFAP, 1:200, mouse monoclonal, Lifespan, Cat # LS-C357895). Alexa Fluor−488 (1:500-1:1000, goat anti−mouse IgG, Thermo Fisher Scientific, Cat# A-11001, RRID: AB_2534069) and Alexa Fluor−568 (1:500-1:1000, goat anti−rabbit IgG, Thermo Fisher Scientific, Cat# A−11011, RRID: AB_143157) were used as secondary antibodies. Slide mounting and nuclear counterstaining were carried out with Fluoroshield mounting medium (Sigma−Aldrich) containing 4′, 6′−diamidino−2−phenylindole (DAPI).

In situ Hybridization

In situ hybridization on paraffin sections was performed as previously described (Eymann et al., 2019), using digoxigenin (DIG)-labeled antisense riboprobes corresponding to atonal bHLH transcription factor 1 (*Atoh1*), retinoic acid receptor-related orphan receptor alpha (*Rora*), very-low-density-lipoprotein receptor (*vldlr*), Reelin (*Reln*), disabled-1 (*Dab1*), bone morphogenetic protein 4 (*Bmp4*), and bone morphogenetic protein 7 (*Bmp7*). Riboprobes were generated based on publicly available cDNA and/or genome sequences available for lizards and snakes, including *P. vitticeps* (Georges et al., 2015) and *Pantherophis guttatus* (*P. guttatus*; Ullate-Agote et al., 2014), as well as on newly produced nucleotide sequences for *B. fuliginosus* (**Table 1**). *In situ* hybridization was performed on paraffin sections as described previously (Eymann et al., 2019), using a hybridization temperature of 65°C. Following overnight hybridization, sections were washed and incubated with alkaline phosphatase-conjugated anti-DIG antibodies (1:2500, sheep polyclonal, Sigma-Aldrich, cat# 11093274910, RRID:AB_2734716). For colorimetric visualization of hybridization, sections were stained with a solution containing 5-bromo-4-chloro-3-indolyl phosphate and nitro blue tetrazolium.

Image Acquisition and Processing

Histological preparations as well as IHC and ISH slides were imaged using a Nikon Eclipse 90i microscope. Nikon DS−Fi U3 and Hamamatsu Flash4.0 cameras were used for capturing bright field and fluorescence images, respectively. Images larger than the microscope field of view were acquired as partially overlapping tiles and successively stitched together in Adobe Photoshop CC (RRID:SCR_014199) using the photomerge function. To improve visualization, linear levels were adjusted in Adobe Photoshop CC.

DATA AVAILABILITY STATEMENT

The datasets presented in this study can be found in online repositories. The names of the repository/repositories and accession number(s) can be found below: https://www.ncbi.nlm.nih.gov/genbank/, MT993472; https://www.ncbi.nlm.nih.gov/genbank/, MT993473; https://www.ncbi.nlm.nih.gov/genbank/, MT993474; https://www.ncbi.nlm.nih.gov/genbank/.

ETHICS STATEMENT

The animal study was reviewed and approved by Laboratory Animal Centre (LAC) of the University of Helsinki and/or National Animal Experiment Board (ELLA) in Finland (license numbers ESLH-2007-07445/ym-23, ESAVI/7484/04.10.07/2016, and ESAVI/13139/04.10.05/2017).

AUTHOR CONTRIBUTIONS

SM performed all the experiments. All authors designed the experimental approach, collected and prepared the samples, analyzed the data, wrote the manuscript, and read and approved the final manuscript.

FUNDING

This work was supported by funds from the Doctoral Program Brain & Mind (SM), University of Helsinki (ND-P),

Institute of Biotechnology (ND-P), and Academy of Finland (grant decisions 277301, 283727, and 312587 to ND-P).

ACKNOWLEDGMENTS

We thank Ann-Christine Aho and Maria Partanen for technical assistance in captive breeding and animal care; Heikki Suhonen (University of Helsinki, Finland) for access to X-ray computed tomography facility; the HiLAPS platform (University of Helsinki, Finland) for access to histology facility; Juha Partanen, Robert Vignali, and members of the Di-Poï laboratory for helpful discussions.

SUPPLEMENTARY MATERIAL

The Supplementary Material for this article can be found online at: https://www.frontiersin.org/articles/10.3389/fcell.2020.593377/full#supplementary-material

Supplementary Figure 1 | Molecular characterization of postnatal squamate cerebellum. **(A,B)** Double IHC for PCNA (green staining) and SHH (red) markers at 15 days post-hatching (dph) **(A)** or ISH for *Rora* at juvenile stage **(B)** in the cerebellum of *P. vitticeps*. The arrowhead in panel **(A)** indicates the position of the incomplete fissure on the cerebellar pial surface. Insets in **(A)** show high magnifications of proliferating GCPs (green) or SHH-positive PCs (red). **(C,D)** ISH for *Rora* **(C)** or *Reln* **(D)** in the cerebellum of juvenile *B. fuliginosus*. PS, pial surface; IGL, internal granule layer; VS, ventricular surface. Scale bars: 50 μm.

REFERENCES

Akazawa, C., Ishibashi, M., Shimizu, C., Nakanishi, S., and Kageyama, R. (1995). A mammalian helix-loop-helix factor structurally related to the product of *Drosophila* proneural gene *atonal* is a positive transcriptional regulator expressed in the developing nervous system. *J. Biol. Chem.* 270, 8730–8738. doi: 10.1074/jbc.270.15.8730

Alder, J., Cho, N. K., and Hatten, M. E. (1996). Embryonic precursor cells from the rhombic lip are specified to a cerebellar granule neuron identity. *Neuron* 17, 389–399. doi: 10.1016/s0896-6273(00)80172-5

Alder, J., Lee, K. J., Jessell, T. M., and Hatten, M. E. (1999). Generation of cerebellar granule neurons in vivo by transplantation of BMP-treated neural progenitor cells. *Nat. Neurosci.* 2, 535–540. doi: 10.1038/9189

Altman, J., and Bayer, S. A. (eds). (1997). "Development of the cerebellar system," in *Relation to Its Evolution, Structure, and Function*, (Boca Raton, FL: CRC Press).

Aruga, J., Minowa, O., Yaginuma, H., Kuno, J., Nagai, T., Noda, T., et al. (1998). Mouse Zic1 is involved in cerebellar development. *J. Neurosci.* 18, 284–293. doi: 10.1523/JNEUROSCI.18-01-00284.1998

Aruga, J., Yokota, N., Hashimoto, M., Furuichi, T., Fukuda, M., and Mikoshiba, K. (1994). A novel zinc finger protein, Zic, is involved in neurogenesis, especially in the cell lineage of cerebellar granule cells. *J. Neurochem.* 63, 1880–1890. doi: 10.1046/j.1471-4159.1994.63051880.x

Aspden, J. W., Armstrong, C. L., Gutierrez-Ibanez, C. I., Hawkes, R., Iwaniuk, A. N., Kohl, T., et al. (2015). Zebrin II/aldolase C expression in the cerebellum of the western diamondback rattlesnake (*Crotalus atrox*). *PLoS One* 10:e0117539. doi: 10.1371/journal.pone.0117539

Bakalian, A., Corman, B., Delhaye-Bouchaud, N., and Mariani, J. (1991). Quantitative analysis of the Purkinje cell population during extreme ageing in the cerebellum of the Wistar/Louvain rat. *Neurobiol. Aging* 12, 425–430. doi: 10.1016/0197-4580(91)90068-u

Bakalian, A., Delhaye-Bouchaud, N., and Mariani, J. (1995). Quantitative analysis of the purkinje cell and the granule cell populations in the cerebellum of nude mice. *J. Neurogenet.* 9, 207–218. doi: 10.3109/01677069509084157

Balsters, J. H., Whelan, C. D., Robertson, I. H., and Ramnani, N. (2013). Cerebellum and cognition: evidence for the encoding of higher order rules. *Cereb. Cortex* 23, 1433–1443. doi: 10.1093/cercor/bhs127

Barneda-Zahonero, B., Miñano-Molina, A., Badiola, N., Fadó, R., Xifró, X., Saura, C. A., et al. (2009). Bone morphogenetic protein-6 promotes cerebellar granule neurons survival by activation of the MEK/ERK/CREB pathway. *Mol. Biol. Cell* 20, 5051–5063. doi: 10.1091/mbc.e09-05-0424

Baumann, O., Borra, R. J., Bower, J. M., Cullen, K. E., Habas, C., Ivry, R. B., et al. (2015). Consensus paper: the role of the cerebellum in perceptual processes. *Cerebellum* 14, 197–220. doi: 10.1007/s12311-014-0627-7

Beffert, U., Weeber, E. J., Durudas, A., Qiu, S., Masiulis, I., Sweatt, J. D., et al. (2005). Modulation of synaptic plasticity and memory by Reelin involves differential splicing of the lipoprotein receptor Apoer2. *Neuron* 47, 567–579. doi: 10.1016/j.neuron.2005.07.007

Ben-Arie, N., McCall, A. E., Berkman, S., Eichele, G., Bellen, H. J., and Zoghbi, H. Y. (1996). Evolutionary conservation of sequence and expression of the bHLH protein Atonal suggests a conserved role in neurogenesis. *Hum. Mol. Genet.* 5, 1207–1216. doi: 10.1093/hmg/5.9.1207

Ben-Arie, N., Zoghbi, H. Y., Bellen, H. J., Armstrong, D. L., McCall, A. E., Gordadze, P. R., et al. (1997). Math1 is essential for genesis of cerebellar granule neurons. *Nature* 390, 169–172. doi: 10.1038/36579

Bignami, A., and Dahl, D. (1974). The development of Bergmann glia in mutant mice with cerebellar malformations: reeler, staggerer and weaver. Immunofluorescence study with antibodies to the glial fibrillary acidic protein. *J. Comp. Neurol.* 155, 219–229. doi: 10.1002/cne.901550207

Biswas, M. S., Luo, Y., Sarpong, G. A., and Sugihara, I. (2019). Divergent projections of single pontocerebellar axons to multiple cerebellar lobules in the mouse. *J. Comp. Neurol.* 527, 1966–1985. doi: 10.1002/cne.24662

Boback, S. M., Dichter, E. K., and Mistry, H. L. (2012). A developmental staging series for the African house snake, *Boaedon* (*Lamprophis*) *fuliginosus*. *Zoology* 115, 38–46. doi: 10.1016/j.zool.2011.09.001

Brochu, G., Maler, L., and Hawkes, R. (1990). Zebrin II: a polypeptide antigen expressed selectively by purkinje cells reveals compartments in rat and fish cerebellum. *J. Comp. Neurol.* 291, 538–552. doi: 10.1002/cne.902910405

Buckner, R. L. (2013). The cerebellum and cognitive function: 25 years of insight from anatomy and neuroimaging. *Neuron* 80, 807–815. doi: 10.1016/j.neuron.2013.10.044

Butler, A. B., and Hodos, W. (2005). *Comparative Vertebrate Neuroanatomy*. Hoboken, NJ: John Wiley & Sons, Inc.

Butts, T., Chaplin, N., and Wingate, R. J. T. (2011). Can clues from evolution unlock the molecular development of the cerebellum? *Mol. Neurobiol.* 43, 67–76. doi: 10.1007/s12035-010-8160-2

Butts, T., Hanzel, M., and Wingate, R. J. T. (2014a). Transit amplification in the amniote cerebellum evolved via a heterochronic shift in NeuroD1 expression. *Development* 141, 2791–2795. doi: 10.1242/dev.101758

Butts, T., Modrell, M. S., Baker, C. V. H., and Wingate, R. J. T. (2014b). The evolution of the vertebrate cerebellum: absence of a proliferative external granule layer in a non-teleost ray-finned fish. *Evol. Dev.* 16, 92–100. doi: 10.1111/ede.12067

Candal, E., Anadón, R., Bourrat, F., and Rodríguez-Moldes, I. (2005). Cell proliferation in the developing and adult hindbrain and midbrain of trout and medaka (teleosts): a segmental approach. *Dev. Brain Res.* 160, 157–175. doi: 10.1016/j.devbrainres.2005.08.009

Carletti, B., Williams, I. M., Leto, K., Nakajima, K., Magrassi, L., and Rossi, F. (2008). Time constraints and positional cues in the developing cerebellum regulate Purkinje cell placement in the cortical architecture. *Dev. Biol.* 317, 147–160. doi: 10.1016/j.ydbio.2008.02.005

Caviness, V. S., and Rakic, P. (1978). Mechanisms of cortical development: a view from mutations in mice. *Annu. Rev. Neurosci.* 1, 297–326. doi: 10.1146/annurev.ne.01.030178.001501

Chaplin, N., Tendeng, C., and Wingate, R. J. T. (2010). Absence of an external germinal layer in zebrafish and shark reveals a distinct, anamniote ground plan of cerebellum development. *J. Neurosci.* 30, 3048–3057. doi: 10.1523/JNEUROSCI.6201-09.2010

Chen, X. R., Heck, N., Lohof, A. M., Rochefort, C., Morel, M.-P., Wehrle, R., et al. (2013). Mature Purkinje cells require the retinoic acid-related orphan

receptor-α (RORα) to maintain climbing fiber mono-innervation and other adult characteristics. *J. Neurosci.* 33, 9546–9562. doi: 10.1523/JNEUROSCI.2977-12.2013

Chizhikov, V. V., Lindgren, A. G., Currle, D. S., Rose, M. F., Monuki, E. S., and Millen, K. J. (2006). The roof plate regulates cerebellar cell-type specification and proliferation. *Development* 133, 2793–2804. doi: 10.1242/dev.02441

Corrales, J. D. (2004). Spatial pattern of sonic hedgehog signaling through Gli genes during cerebellum development. *Development* 131, 5581–5590. doi: 10.1242/dev.01438

Corrales, J. D. (2006). The level of sonic hedgehog signaling regulates the complexity of cerebellar foliation. *Development* 133, 1811–1821. doi: 10.1242/dev.02351

Dahmane, N., and Ruiz, A. (1999). Sonic hedgehog regulates the growth and patterning of the cerebellum. *Development* 126, 3089–3100.

D'Arcangelo, G. (2014). Reelin in the years: controlling neuronal migration and maturation in the mammalian brain. *Adv. Neurosci.* 2014:597395. doi: 10.1155/2014/597395

D'Arcangelo, G. G., Miao, G., Chen, S.-C., Scares, H. D., Morgan, J. I., and Curran, T. (1995). A protein related to extracellular matrix proteins deleted in the mouse mutant reeler. *Nature* 374, 719–723. doi: 10.1038/374719a0

Dussault, I., Fawcett, D., Matthyssen, A., Bader, J. A., and Giguère, V. (1998). Orphan nuclear receptor RORα-deficient mice display the cerebellar defects of staggerer. *Mech. Dev.* 70, 147–153. doi: 10.1016/s0925-4773(97)00187-1

Eymann, J., Salomies, L., Macrì, S., and Di-Poï, N. (2019). Variations in the proliferative activity of the peripheral retina correlate with postnatal ocular growth in squamate reptiles. *J. Comp. Neurol.* 527, 2356–2370. doi: 10.1002/cne.24677

Fernandes, M., Antoine, M., and Hébert, J. M. (2012). SMAD4 is essential for generating subtypes of neurons during cerebellar development. *Dev. Biol.* 365, 82–90. doi: 10.1016/j.ydbio.2012.02.017

Fleming, J. T., He, W., Hao, C., Ketova, T., Pan, F. C., Wright, C. C. V., et al. (2013). The Purkinje neuron acts as a central regulator of spatially and functionally distinct cerebellar precursors. *Dev. Cell* 27, 278–292. doi: 10.1016/j.devcel.2013.10.008

Flora, A., Klisch, T. J., Schuster, G., and Zoghbi, H. Y. (2009). Deletion of Atoh1 disrupts sonic hedgehog and prevents medulloblastoma. *Science* 326, 1424–1428. doi: 10.1126/science.1181453

Frederic, F., Hainaut, F., Thomasset, M., Guenet, J. L., Delhaye-Bouchaud, N., and Mariani, J. (1992). Cell counts of Purkinje and inferior olivary neurons in the 'hyperspiny purkinje cells' mutant mouse. *Eur. J. Neurosci.* 4, 127–135. doi: 10.1111/j.1460-9568.1992.tb00859.x

Gallagher, E., Howell, B. W., Soriano, P., Cooper, J. A., and Hawkes, R. (1998). Cerebellar abnormalities in the disabled (mdab1-1) mouse. *J. Comp. Neurol.* 402, 238–251. doi: 10.1002/(sici)1096-9861(19981214)402:2<238::aid-cne8>3.0.co;2-h

Georges, A., Li, Q., Lian, J., O'Meally, D., Deakin, J., Wang, Z., et al. (2015). High-coverage sequencing and annotated assembly of the genome of the Australian dragon lizard *Pogona vitticeps*. *Gigascience* 4:45. doi: 10.1186/s13742-015-0085-2

Gold, D. A., Baek, S. H., Schork, N. J., Rose, D. W., Larsen, D. L. D., Sachs, B. D., et al. (2003). RORα coordinates reciprocal signaling in cerebellar development through sonic hedgehog and calcium-dependent pathways. *Neuron* 40, 1119–1131. doi: 10.1016/s0896-6273(03)00769-4

Gold, D. A., Gent, P. M., and Hamilton, B. A. (2007). RORα in genetic control of cerebellum development: 50 staggering years. *Brain Res.* 1140, 19–25. doi: 10.1016/j.brainres.2005.11.080

Gona, A. G. (1972). Morphogenesis of the cerebellum of the frog tadpole during spontaneous metamorphosis. *J. Comp. Neurol.* 146, 133–142. doi: 10.1002/cne.901460202

Hallonet, M. E. R., and Le Douarin, N. M. (1993). Tracing neuroepithelial cells of the mesencephalic and metencephalic alar plates during cerebellar ontogeny in quail – chick chimaeras. *Eur. J. Neurosci.* 5, 1145–1155. doi: 10.1111/j.1460-9568.1993.tb00969.x

Hamilton, B. A., Frankel, W. N., Kerrebrock, A. W., Hawkins, T. L., FitzHugh, W., Kusumi, K., et al. (1996). Disruption of the nuclear hormone receptor RORα in staggerer mice. *Nature* 379, 736–739. doi: 10.1038/379736a0

Hanzel, M., Rook, V., and Wingate, R. J. T. (2019). Mitotic granule cell precursors undergo highly dynamic morphological transitions throughout the external germinal layer of the chick cerebellum. *Sci. Rep.* 9:15218. doi: 10.1038/s41598-019-51532-y

Hartfuss, E., Förster, E., Bock, H. H., Hack, M. A., Leprince, P., Lugue, J. M., et al. (2003). Reelin signaling directly affects radial glia morphology and biochemical maturation. *Development* 130, 4597–4609. doi: 10.1242/dev.00654

Hashimoto, M., and Hibi, M. (2012). Development and evolution of cerebellar neural circuits. *Dev. Growth Differ.* 54, 373–389. doi: 10.1111/j.1440-169X.2012.01348.x

Hatten, M. E., Alder, J., Zimmerman, K., and Heintz, N. (1997). Genes involved in cerebellar cell specification and differentiation. *Curr. Opin. Neurobiol.* 7, 40–47. doi: 10.1016/s0959-4388(97)80118-3

Hawkes, R., and Leclerc, N. (1987). Antigenic map of the rat cerebellar cortex: the distribution of parasagittal bands as revealed by monoclonal anti-Purkinje cell antibody mobA113. *J. Comp. Neurol.* 256, 29–41. doi: 10.1002/cne.902560104

Heckroth, J. A., Goldowitz, D., and Eisenman, L. M. (1989). Purkinje cell reduction in the reeler mutant mouse: a quantitative immunohistochemical study. *J. Comp. Neurol.* 279, 546–555. doi: 10.1002/cne.902790404

Hellwig, S., Hack, I., Kowalski, J., Brunne, B., Jarowyj, J., Unger, A., et al. (2011). Role for reelin in neurotransmitter release. *J. Neurosci.* 31, 2352–2360. doi: 10.1523/JNEUROSCI.3984-10.2011

Herrup, K., and Mullen, R. J. (1979). Staggerer chimeras: intrinsic nature of Purkinje cell defects and implications for normal cerebellar development. *Brain Res.* 178, 443–457. doi: 10.1016/0006-8993(79)90705-4

Herz, J., and Chen, Y. (2006). Reelin, lipoprotein receptors and synaptic plasticity. *Nat. Rev. Neurosci.* 7, 850–859. doi: 10.1038/nrn2009

Hibi, M., Matsuda, K., Takeuchi, M., Shimizu, T., and Murakami, Y. (2017). Evolutionary mechanisms that generate morphology and neural-circuit diversity of the cerebellum. *Dev. Growth Differ.* 59, 228–243. doi: 10.1111/dgd.12349

Hoops, D., Desfilis, E., Ullmann, J. F. P., Janke, A. L., Stait-Gardner, T., Devenyi, G. A., et al. (2018). A 3D MRI-based atlas of a lizard brain. *J. Comp. Neurol.* 526, 2511–2547. doi: 10.1002/cne.24480

Hoshino, M., Nakamura, S., Mori, K., Kawauchi, T., Terao, M., Nishimura, Y. V., et al. (2005). Ptf1a, a bHLH transcriptional gene, defines GABAergic neuronal fates in cerebellum. *Neuron* 47, 201–213. doi: 10.1016/j.neuron.2005.06.007

Inoue, Y., Maeda, N., Kokubun, T., Takayama, C., Inoue, K., Terashima, T., et al. (1990). Architecture of Purkinje cells of the reeler mutant mouse observed by immunohistochemistry for the inositol 1,4,5-trisphosphate receptor protein P400. *Neurosci. Res.* 8, 189–201. doi: 10.1016/0168-0102(90)90020-f

Iulianella, A., Wingate, R. J., Moens, C. B., and Capaldo, E. (2019). The generation of granule cells during the development and evolution of the cerebellum. *Dev. Dyn.* 248, 506–513. doi: 10.1002/dvdy.64

Jensen, P. (2004). Analysis of cerebellar development in math1 null embryos and chimeras. *J. Neurosci.* 24, 2202–2211. doi: 10.1523/JNEUROSCI.3427-03.2004

Jensen, P., Zoghbi, H. Y., and Goldowitz, D. (2002). Dissection of the cellular and molecular events that position cerebellar purkinje cells: a study of the math1 null-mutant mouse. *J. Neurosci.* 22, 8110–8116. doi: 10.1523/JNEUROSCI.22-18-08110.2002

Kani, S., Bae, Y. K., Shimizu, T., Tanabe, K., Satou, C., Parsons, M. J., et al. (2010). Proneural gene-linked neurogenesis in zebrafish cerebellum. *Dev. Biol.* 343, 1–17. doi: 10.1016/j.ydbio.2010.03.024

Kaslin, J., Kroehne, V., Benato, F., Argenton, F., and Brand, M. (2013). Development and specification of cerebellar stem and progenitor cells in zebrafish: from embryo to adult. *Neural Dev.* 8:9. doi: 10.1186/1749-8104-8-9

Klisch, T. J., Xi, Y., Flora, A., Wang, L., Li, W., and Zoghbi, H. Y. (2011). In vivo Atoh1 targetome reveals how a proneural transcription factor regulates cerebellar development. *Proc. Natl. Acad. Sci. U.S.A.* 108, 3288–3293. doi: 10.1073/pnas.1100230108

Koziol, L. F., Budding, D., Andreasen, N., D'Arrigo, S., Bulgheroni, S., Imamizu, H., et al. (2014). Consensus paper: the cerebellum's role in movement and cognition. *Cerebellum* 13, 151–177. doi: 10.1007/s12311-013-0511-x

Krizhanovsky, V., and Ben-Arie, N. (2006). A novel role for the choroid plexus in BMP-mediated inhibition of differentiation of cerebellar neural progenitors. *Mech. Dev.* 123, 67–75. doi: 10.1016/j.mod.2005.09.005

Landis, D. M. D., and Sidman, R. L. (1978). Electron microscopic analysis of postnatal histogenesis in the cerebellar cortex of staggerer mutant mice. *J. Comp. Neurol.* 179, 831–863. doi: 10.1002/cne.901790408

Larsell, O. (1923). The cerebellum of the frog. *J. Comp. Neurol.* 36, 89–112. doi: 10.1002/cne.900360202

Larsell, O. (1926). The cerebellum of reptiles: lizards and snake. *J. Comp. Neurol.* 41, 59–94. doi: 10.1002/cne.900410103

Larsell, O. (1932). The cerebellum of reptiles: chelonians and alligator. *J. Comp. Neurol.* 56, 299–345. doi: 10.1002/cne.900560204

Larsell, O. (1967). *The Comparative Anatomy and Histology of the Cerebellum from Myxinoids through Birds*. Minneapolis, MN: University of Minnesota Press.

Larsell, O. (1970). *The Comparative Anatomy and Histology of the Cerebellum from Monotremes through Apes*. Minneapolis, MN: University of Minnesota Press.

Lee, K. J., Mendelsohn, M., and Jessell, T. M. (1998). Neuronal patterning by BMPs: a requirement for GDF7 in the generation of a discrete class of commissural interneurons in the mouse spinal cord. *Genes Dev.* 12, 3394–3407. doi: 10.1101/gad.12.21.3394

Lewis, P. M., Gritli-Linde, A., Smeyne, R., Kottmann, A., and McMahon, A. P. (2004). Sonic hedgehog signaling is required for expansion of granule neuron precursors and patterning of the mouse cerebellum. *Dev. Biol.* 270, 393–410. doi: 10.1016/j.ydbio.2004.03.007

Liu, A., and Joyner, A. L. (2001). Early anterior/posterior patterning of the midbrain and cerebellum. *Annu. Rev. Neurosci.* 24, 869–896. doi: 10.1146/annurev.neuro.24.1.869

MacHold, R., and Fishell, G. (2005). Math1 is expressed in temporally discrete pools of cerebellar rhombic-lip neural progenitors. *Neuron* 48, 17–24. doi: 10.1016/j.neuron.2005.08.028

Macrì, S., Savriama, Y., Khan, I., and Di-Poï, N. (2019). Comparative analysis of squamate brains unveils multi-level variation in cerebellar architecture associated with locomotor specialization. *Nat. Commun.* 10:5560. doi: 10.1038/s41467-019-13405-w

Martínez, S., Andreu, A., Mecklenburg, N., and Echevarria, D. (2013). Cellular and molecular basis of cerebellar development. *Front. Neuroanat.* 7:18. doi: 10.3389/fnana.2013.00018

Metscher, B. D. (2009). MicroCT for developmental biology: a versatile tool for high-contrast 3D imaging at histological resolutions. *Dev. Dyn.* 238, 632–640. doi: 10.1002/dvdy.21857

Miyata, T., Nakajima, K., Aruga, J., Takahashi, S., Ikenaka, K., Mikoshiba, K., et al. (1996). Distribution of a reeler gene-related antigen in the developing cerebellum: an immunohistochemical study with an allogeneic antibody CR-50 on normal and reeler mice. *J. Comp. Neurol.* 372, 215–228.

Miyata, T., Nakajima, K., Mikoshiba, K., and Ogawa, M. (1997). Regulation of Purkinje cell alignment by Reelin as revealed with CR-50 antibody. *J. Neurosci.* 17, 3599–3609. doi: 10.1523/JNEUROSCI.17-10-03599.1997

Na, J., Sugihara, I., and Shinoda, Y. (2019). The entire trajectories of single pontocerebellar axons and their lobular and longitudinal terminal distribution patterns in multiple aldolase C positive compartments of the rat cerebellar cortex. *J. Comp. Neurol.* 527, 2488–2511.

Nieuwenhuys, R. (1967). "Comparative anatomy of the cerebellum," in *Progress in Brain Research*, Vol. 25, eds C. A. Fox and R. S. Snider (Amsterdam: Elsevier), 1–93.

Nieuwenhuys, R., ten Donkelaar, H. J., and Nicholson, C. (1998). *The Central Nervous System of Vertebrates*. Berlin: Springer-Verlag.

Nimura, T., Itoh, T., Hagio, H., Hayashi, T., Di Donato, V., Takeuchi, M., et al. (2019). Role of Reelin in cell positioning in the cerebellum and the cerebellum-like structure in zebrafish. *Dev. Biol.* 455, 393–408. doi: 10.1016/j.ydbio.2019.07.010

Okuda, H., Tatsumi, K., Morita-Takemura, S., Nakahara, K., Nochioka, K., Shinjo, T., et al. (2016). Hedgehog signaling modulates the release of gliotransmitters from cultured cerebellar astrocytes. *Neurochem. Res.* 41, 278–289. doi: 10.1007/s11064-015-1791-y

Ollonen, J., Da Silva, F. O., Mahlow, K., and Di-Poï, N. (2018). Skull development, ossification pattern, and adult shape in the emerging lizard model organism *Pogona vitticeps*: a comparative analysis with other squamates. *Front. Physiol.* 9:278. doi: 10.3389/fphys.2018.00278

Owa, T., Taya, S., Miyashita, S., Yamashita, M., Adachi, T., Yamada, K., et al. (2018). Meis1 coordinates cerebellar granule cell development by regulating pax6 transcription, BMP signaling and atoh1 degradation. *J. Neurosci.* 38, 1277–1294. doi: 10.1523/JNEUROSCI.1545-17.2017

Pesold, C., Impagnatiello, F., Pisu, M. G., Uzunov, D. P., Costa, E., Guidotti, A., et al. (1998). Reelin is preferentially expressed in neurons synthesizing γ-aminobutyric acid in cortex and hippocampus of adult rats. *Proc. Natl. Acad. Sci. U.S.A.* 95, 3221–3226. doi: 10.1073/pnas.95.6.3221

Pose-Méndez, S., Candal, E., Mazan, S., and Rodríguez-Moldes, I. (2016). Morphogenesis of the cerebellum and cerebellum-related structures in the shark *Scyliorhinus canicula*: insights on the ground pattern of the cerebellar ontogeny. *Brain Struct. Funct.* 221, 1691–1717. doi: 10.1007/s00429-015-0998-7

Puzdrowski, R. L., and Gruber, S. (2009). Morphologic features of the cerebellum of the Atlantic stingray, and their possible evolutionary significance. *Integr. Zool.* 4, 110–122. doi: 10.1111/j.1749-4877.2008.00127.x

Qin, L., Wine-Lee, L., Ahn, K. J., and Crenshaw, E. B. (2006). Genetic analyses demonstrate that bone morphogenetic protein signaling is required for embryonic cerebellar development. *J. Neurosci.* 26, 1896–1905. doi: 10.1523/JNEUROSCI.3202-05.2006

Rahimi-Balaei, M., Bergen, H., Kong, J., and Marzban, H. (2018). Neuronal migration during development of the cerebellum. *Front. Cell. Neurosci.* 12:484. doi: 10.3389/fncel.2018.00484

Rice, D. S., Sheldon, M., D'Arcangelo, G., Nakajima, K., Goldowitz, D., and Curran, T. (1998). Disabled-1 acts downstream of Reelin in a signaling pathway that controls laminar organization in the mammalian brain. *Development* 125, 3719–3729.

Rodríguez-Moldes, I., Ferreiro-Galve, S., Carrera, I., Sueiro, C., Candal, E., Mazan, S., et al. (2008). Development of the cerebellar body in sharks: spatiotemporal relations of Pax6 expression, cell proliferation and differentiation. *Neurosci. Lett.* 432, 105–110. doi: 10.1016/j.neulet.2007.11.059

Ryder, E. F., and Cepko, C. L. (1994). Migration patterns of clonally related granule cells and their progenitors in the developing chick cerebellum. *Neuron* 12, 1011–1029. doi: 10.1016/0896-6273(94)90310-7

Salero, E., and Hatten, M. E. (2007). Differentiation of ES cells into cerebellar neurons. *Proc. Natl. Acad. Sci. U.S.A.* 104, 2997–3002. doi: 10.1073/pnas.0610879104

Salomies, L., Eymann, J., Khan, I., and Di-Poï, N. (2019). The alternative regenerative strategy of bearded dragon unveils the key processes underlying vertebrate tooth renewal. *eLife* 8:e47702. doi: 10.7554/eLife.47702

Schmahmann, J. D. (2019). The cerebellum and cognition. *Neurosci. Lett.* 688, 62–75. doi: 10.1016/j.neulet.2018.07.005

Sheldon, M., Rice, D. S., D'Arcangelo, G., Yoneshima, H., Nakajima, K., Mikoshiba, K., et al. (1997). Scrambler and Yotari disrupt the disabled gene and produce a reeler -like phenotype in mice. *Nature* 389, 730–733. doi: 10.1038/39601

Sidman, R. L., Lane, P. W., and Dickie, M. M. (1962). Staggerer, a new mutation in the mouse affecting the cerebellum. *Science* 137, 610–612. doi: 10.1126/science.137.3530.610

Sotelo, C. (2004). Cellular and genetic regulation of the development of the cerebellar system. *Prog. Neurobiol.* 72, 295–339. doi: 10.1016/j.pneurobio.2004.03.004

Sotelo, C., and Alvarado-Mallart, R. M. (1986). Growth and differentiation of cerebellar suspensions transplanted into the adult cerebellum of mice with heredodegenerative ataxia. *Proc. Natl. Acad. Sci. U.S.A.* 83, 1135–1139. doi: 10.1073/pnas.83.4.1135

Sotelo, C., and Alvarado-Mallart, R. M. (1987a). Embryonic and adult neurons interact to allow Purkinje cell replacement in mutant cerebellum. *Nature* 327, 421–423. doi: 10.1038/327421a0

Sotelo, C., and Alvarado-Mallart, R. M. (1987b). Reconstruction of the defective cerebellar circuitry in adult purkinje cell degeneration mutant mice by Purkinje cell replacement through transplantation of solid embryonic implants. *Neuroscience* 20, 1–22. doi: 10.1016/0306-4522(87)90002-9

Sotelo, C., and Changeux, J. P. (1974). Transsynaptic degeneration "en cascade" in the cerebellar cortex of staggerer mutant rice. *Brain Res.* 67, 519–526. doi: 10.1016/0006-8993(74)90499-5

Strick, P. L., Dum, R. P., and Fiez, J. A. (2009). Cerebellum and nonmotor function. *Annu. Rev. Neurosci.* 32, 413–434. doi: 10.1146/annurev.neuro.31.060407.125606

Striedter, G. (2005). *Principles of Brain Evolution*. Sunderland, MA: Sinauer Associates.

Su, H. L., Muguruma, K., Matsuo-Takasaki, M., Kengaku, M., Watanabe, K., and Sasai, Y. (2006). Generation of cerebellar neuron precursors from embryonic stem cells. *Dev. Biol.* 290, 287–296. doi: 10.1016/j.ydbio.2005.11.010

Sugahara, F., Pascual-Anaya, J., Oisi, Y., Kuraku, S., Aota, S. I., Adachi, N., et al. (2016). Evidence from cyclostomes for complex regionalization of the ancestral vertebrate brain. *Nature* 531, 97–100. doi: 10.1038/nature16518

Sukhum, K. V., Shen, J., and Carlson, B. A. (2018). Extreme enlargement of the cerebellum in a clade of teleost fishes that evolved a novel active sensory system. *Curr. Biol.* 28, 3857–3863.e3. doi: 10.1016/j.cub.2018.10.038

Takeo, Y. H., Kakegawa, W., Miura, E., and Yuzaki, M. (2015). Rorα regulates multiple aspects of dendrite development in cerebellar Purkinje cells in vivo. *J. Neurosci.* 35, 12518–12534. doi: 10.1523/JNEUROSCI.0075-15.2015

ten Donkelaar, H. J., and Bangma, G. C. (1992). "The cerebellum," in *Sensorimotor Integration. Biology of the Reptilia, Neurology C*, Vol. 17, eds C. Gans and P. S. Ulinski (Chicago, IL: The University of Chicago Press), 496–586.

Terashima, T., Inoue, K., Inoue, Y., Mikoshiba, K., and Tsukada, Y. (1985). Observations on golgi epithelial cells and granule cells in the cerebellum of the reeler mutant mouse. *Dev. Brain Res.* 18, 103–112. doi: 10.1016/0165-3806(85)90254-8

Tong, K. K., and Kwan, K. M. (2013). Common Partner Smad-independent canonical bone morphogenetic protein signaling in the specification process of the anterior rhombic lip during cerebellum development. *Mol. Cell. Biol.* 33, 1925–1937. doi: 10.1128/MCB.01143-12

Tong, K. K., Ma, T. C., and Kwan, K. M. (2015). BMP/Smad signaling and embryonic cerebellum development: stem cell specification and heterogeneity of anterior rhombic lip. *Dev. Growth Differ.* 57, 121–134. doi: 10.1111/dgd.12198

Traiffort, E., Charytoniuk, D. A., Faure, H., and Ruat, M. (2002). Regional distribution of sonic hedgehog, patched, and smoothened mRNA in the adult rat brain. *J. Neurochem.* 70, 1327–1330. doi: 10.1046/j.1471-4159.1998.70031327.x

Trommsdorff, M., Gotthardt, M., Hiesberger, T., Shelton, J., Stockinger, W., Nimpf, J., et al. (1999). Reeler/disabled-like disruption of neuronal migration in knockout mice lacking the VLDL receptor and ApoE receptor 2. *Cell* 97, 689–701. doi: 10.1016/s0092-8674(00)80782-5

Ullate-Agote, A., Milinkovitch, M. C., and Tzika, A. C. (2014). The genome sequence of the corn snake (*Pantherophis guttatus*), a valuable resource for EvoDevo studies in squamates. *Int. J. Dev. Biol.* 58, 10–12. doi: 10.1387/ijdb.150060at

Voogd, J. (1967). Comparative aspects of the structure and fibre connexions of the mammalian cerebellum. *Prog. Brain Res.* 25, 94–135.

Voogd, J., and Glickstein, M. (1998). The anatomy of the cerebellum. *Trends Neurosci.* 21, 370–375. doi: 10.1016/s0166-2236(98)01318-6

Wallace, V. A. (1999). Purkinje-cell-derived sonic hedgehog regulates granule neuron precursor cell proliferation in the developing mouse cerebellum. *Curr. Biol.* 9, 445–448. doi: 10.1016/s0960-9822(99)80195-x

Wang, V. Y., Rose, M. F., and Zoghbi, H. Y. (2005). Math1 expression redefines the rhombic lip derivatives and reveals novel lineages within the brainstem and cerebellum. *Neuron* 48, 31–43. doi: 10.1016/j.neuron.2005.08.024

Ware, M. L., Fox, J. W., González, J. L., Davis, N. M., Lambert De Rouvroit, C., Russo, C. J., et al. (1997). Aberrant splicing of a mouse disabled homolog, mdab1, in the scrambler mouse. *Neuron* 19, 239–249. doi: 10.1016/s0896-6273(00)80936-8

Watson, C., Shimogori, T., and Puelles, L. (2017). Mouse Fgf8-Cre-LacZ lineage analysis defines the territory of the postnatal mammalian isthmus. *J. Comp. Neurol.* 525, 2782–2799. doi: 10.1002/cne.24242

Wechsler-Reya, R. J., and Scott, M. P. (1999). Control of neuronal precursor proliferation in the cerebellum by sonic hedgehog. *Neuron* 22, 103–114. doi: 10.1016/s0896-6273(00)80682-0

Weiss, K. H., Johanssen, C., Tielsch, A., Herz, J., Deller, T., Frotscher, M., et al. (2003). Malformation of the radial glial scaffold in the dentate gyrus of reeler mice, scrambler mice, and ApoER2/VLDLR-deficient mice. *J. Comp. Neurol.* 460, 56–65. doi: 10.1002/cne.10644

Wetts, R., and Herrup, K. (1982). Cerebellar Purkinje cells are descended from a small number of progenitors committed during early development: quantitative analysis of lurcher chimeric mice. *J. Neurosci.* 2, 1494–1498. doi: 10.1523/JNEUROSCI.02-10-01494.1982

Wingate, R. J., and Hatten, M. E. (1999). The role of the rhombic lip in avian cerebellum development. *Development* 126, 4395–4404.

Wingate, R. J. T. (2001). The rhombic lip and early cerebellar development. *Curr. Opin. Neurobiol.* 11, 82–88. doi: 10.1016/s0959-4388(00)00177-x

Wurst, W., Bally-Cuif, L., and Bally-Cuif, L. (2001). Neural plate patterning: upstream and downstream of the isthmic organizer. *Nat. Rev. Neurosci.* 2, 99–108. doi: 10.1038/35053516

Wylie, D. R., Hoops, D., Aspden, J. W., and Iwaniuk, A. N. (2017). Zebrin II is expressed in sagittal stripes in the cerebellum of dragon lizards (*Ctenophorus* sp.). *Brain Behav. Evol.* 88, 177–186. doi: 10.1159/000452857

Yamamoto, M., McCaffery, P., and Dräger, U. C. (1996). Influence of the choroid plexus on cerebellar development: analysis of retinoic acid synthesis. *Dev. Brain Res.* 93, 182–190. doi: 10.1016/0165-3806(96)00038-7

Yopak, K. E., Lisney, T. J., Collin, S. P., and Montgomery, J. C. (2007). Variation in brain organization and cerebellar foliation in chondrichthyans: sharks and holocephalans. *Brain Behav. Evol.* 69, 280–300. doi: 10.1159/000100037

Yopak, K. E., Pakan, J. M. P., and Wylie, D. (2017). "The cerebellum of nonmammalian vertebrates," in *Evolution of Nervous Systems*, Vol. 1, ed. J. Kaas (Oxford: Academic Press), 373–385. doi: 10.1016/B978-0-12-804042-3.00015-4

Yuasa, S. (1996). Bergmann glial development in the mouse cerebellum as revealed by tenascin expression. *Anat. Embryol.* 194, 223–234. doi: 10.1007/BF00187133

Yuasa, S., Kawamura, K., Ono, K., Yamakuni, T., and Takahashi, Y. (1991). Development and migration of Purkinje cells in the mouse cerebellar primordium. *Anat. Embryol.* 184, 195–212. doi: 10.1007/BF01673256

Yuasa, S., Kitoh, J., Oda, S., and Kawamura, K. (1993). Obstructed migration of Purkinje cells in the developing cerebellum of the reeler mutant mouse. *Anat. Embryol.* 188, 317–329. doi: 10.1007/BF00185941

Zanjani, H., Lemaigre-Dubreuil, Y., Tillakaratne, N. J. K., Blokhin, A., McMahon, R. P., Tobin, A. J., et al. (2004). Cerebellar Purkinje cell loss in aging Hu-Bcl-2 transgenic mice. *J. Comp. Neurol.* 475, 481–492. doi: 10.1002/cne.20196

Zanjani, H. S., Mariani, J., Delhaye-Bouchaud, N., and Herrup, K. (1992). Neuronal cell loss in heterozygous staggerer mutant mice: a model for genetic contributions to the aging process. *Dev. Brain Res.* 67, 153–160. doi: 10.1016/0165-3806(92)90216-j

Zhao, Y., Kwan, K. M., Mailloux, C. M., Lee, W. K., Grinberg, A., Wurst, W., et al. (2007). LIM-homeodomain proteins Lhx1 and Lhx5, and their cofactor Ldb1, control Purkinje cell differentiation in the developing cerebellum. *Proc. Natl. Acad. Sci. U.S.A.* 104, 13182–13186. doi: 10.1073/pnas.0705464104

Zupanc, G. K. H., Hinsch, K., and Gage, F. H. (2005). Proliferation, migration, neuronal differentiation, and long-term survival of new cells in the adult zebrafish brain. *J. Comp. Neurol.* 488, 290–319. doi: 10.1002/cne.20571

Conflict of Interest: The authors declare that the research was conducted in the absence of any commercial or financial relationships that could be construed as a potential conflict of interest.

frontiers in Ecology and Evolution

REVIEW
published: 27 March 2020
doi: 10.3389/fevo.2020.00082

Of Circuits and Brains: The Origin and Diversification of Neural Architectures

Pedro Martinez[1,2] and Simon G. Sprecher[3]**

[1] Departament de Genètica, Microbiologia i Estadística, Universitat de Barcelona, Barcelona, Spain, [2] Institut Català de Recerca I Estudis Avançats (ICREA), Barcelona, Spain, [3] Department of Biology, University of Fribourg, Fribourg, Switzerland

Nervous systems are complex cellular structures that allow animals to interact with their environment, which includes both the external and the internal milieu. The astonishing diversity of nervous system architectures present in all animal clades has prompted the idea that selective forces must have shaped them over evolutionary time. In most cases, neurons seem to coalesce into specific (centralized) structures that function as "central processing units" (CPU): "brains." Why did neural systems adopt this physical configuration? When did it first happen? What are the physiological, computational, and/or structural advantages of concentrating many neurons in a specific place within the body? Here we examine the concept of nervous system centralization and factors that might have contributed to the evolutionary success of this centralization strategy. In particular, we suggest a putative scenario for the evolution of neural system centralization that incorporates different strands of evidence. This scenario is based on some premises: (1) Receptors originated before neurons (sensors before transmitters) and there were deployed in the first organisms in an asymmetric fashion (deposited randomly in the outer layer); (2) Receptors were segregated in a preferential position in response to an anisotropic environment, (3) Neurons were born in association with this receptors and used to transmit signals distally; (4) Energetics preferentially selected the localization of neurons, and synapsis, close to the receptors (to minimize wire use, for instance); (5) The presence of condensed areas of neurons could have stimulated the proliferation of more receptors in the vicinity, increasing the repertoire of signals processed in an specific body domain (i.e., head) plus contributing to amplify the computational power of the neuronal aggregate; (6) The proliferation of receptors would have induced the proliferation of more neurons in the aggregate, with a further increase in its computational power (hence, diversifying the behavioral repertoire). These last two steps of proliferation and aggregation could have been sustained through a feedback loop, reiterated many times, generating distinct topologies in different lineages. Our main aim in this paper is to examine the brain as both a biological and a physical or computational device.

Keywords: brain, nerve net, neural wiring, CPU, evolution

The 'grading of rank in the animal scale will be nowhere more apparent than in the nervous system in its office as integrator of the individual'

(Sherrington, 1906)

OPEN ACCESS

Edited by:
Maria Ina Arnone, Stazione Zoologica Anton Dohrn, Italy

Reviewed by:
Frank Hirth, King's College London, United Kingdom
Ildiko M. L. Somorjai, University of St Andrews, United Kingdom

***Correspondence:**
Pedro Martinez
pedro.martinez@ub.edu
Simon G. Sprecher
simon.sprecher@unifr.ch

Specialty section:
This article was submitted to Evolutionary Developmental Biology, a section of the journal Frontiers in Ecology and Evolution

Received: *13 January 2020*
Accepted: *12 March 2020*
Published: *27 March 2020*

Citation:
Martinez P and Sprecher SG (2020) Of Circuits and Brains: The Origin and Diversification of Neural Architectures. Front. Ecol. Evol. 8:82. doi: 10.3389/fevo.2020.00082

INTRODUCTION

The brain comprises compact, internally wired groups of neurons that function as the "central processing unit" ("CPU") controlling the behaviors of most bilaterians. The brain of most invertebrates is histologically organized into two domains: an external cortex of cell bodies and an internal net of neurites, the processes of neurons consisting of axons and dendrites that comprise the brain neuropil. The vertebrate brain is constructed differently, with several domains elaborated to serve distinct roles and cell bodies placed among neurons. The basic architecture is shared between hagfishes (agnathans; they have skulls but lack vertebrae) and humans (Sugahara et al., 2017). This closely knit assembly of cells receives the incoming processes of the peripheral sensory organs and sends afferent processes to effector tissues (i.e., muscles or internal organs). Most brains are spatially organized in a highly stereotypical manner, such that individual-to-individual variations in major domains are minimal. These domains serve different purposes, as the neurons within each domain are devoted to specific functions. The ability of brains to interpret environmental conditions and program specific responses to external/internal inputs relies on a consolidated net of connections between the brain domains. Thus, the brain acts as a bona fide CPU. Recent advances in various fields of neuroscience, including brain histology mapping, the study of specific circuits using genetic or optogenetic tools, single-cell transcriptome profiling, and computer modeling, have provided us with an unprecedented view of how brains are organized and how they orchestrate physiological functions. The integration of several strands of evidence provides us with arguments to build a hypothetical scenario for the origin of compact (centralized) nervous systems. Our review will follow a different approach than others dealing with the evolutionary history of brains (Ryan and Chiodin, 2015; Moroz and Kohn, 2016; Martín-Durán and Hejnol, 2019). Here we focus on those mechanisms that may underlie the condensation of neural components into those compact, integrated, units that we call a brain. In this endeavor we will follow the construction of progressively complex units of neural systems, from neurons to circuits to brains. The evolutionary scenario in which the neuronal systems appears and generates higher order structures will set the background in which these events have taken place. We finish this review by analyzing the physiological and behavioral aspects of brain functions. Throughout the text we will use the metaphor of a CPU, which provides us with a mechanical image of how certain brain circuits maybe functionally "constructed" or how they perform their tasks.

TERMINOLOGY

Before developing our arguments for the origin of brains, as derived from nets of neurons, we should indicate what we understand by the terms/concepts "brain", "nerve net" and "neural network."

We use the term "brain" to signify the organ made of a conglomeration of nerve cells, highly interconnected, typically associated with sensory receptors, in the anterior (relative to direction of movement) part of the body. It controls and coordinates the activities of the body through the direct action of neural impulses or the secretion of hormones. This organ, in most animals, integrates sensory information from the environment and regulates motor actions. We should stress the use of the term brain as specifically an organ exerting a centralized control over the body's other organs.

As "nerve net" we consider a structure that consists of scattered, more or less evenly distributed neurons, interconnected by single neurites (rather than bundles).

A "neural network" is defined as a circuit of neurons (nodes) that are chemically or functionally associated. Biological neural networks are known to have structures such as feedbacks, dendritic trees and synapses. They can have a varied number of components and are organized in a hierarchical way, with higher levels of organization sustaining higher information processing capacities.

We use the term "cluster of neurons" for large groups of densely connected neurons, without any further qualification. No assumption is made on their topological organization or their biological functions.

"Isotropic vs. anisotropic" media are used here as follows. Anisotropic environments refer to the geomorphology of the benthic zone, where the presence of the boundary layer between sediment (with also putative variations in granularity) and water, determines differentially the capacity of movement of an organism in alternative directions (in 3D space). Alternatively, we assume that the pelagic zone (water column) doesn't pose these directional limitations and thus, is considered an isotropic medium.

NEURONS: THE BUILDING BLOCKS

Neurons are the fundamental cellular units of the nervous system (though functionally, circuits are considered the fundamental units). They are the cells responsible for receiving sensory input from the external world and the internal milieu. They also relay information to organ systems such as the muscles, the vascular system, and the gut. The important work of Arendt and collaborators (reviewed in: Arendt et al., 2019) has addressed some of the key issues related to the origin, single or multiple (see below), of neurons and how these have diversified over evolutionary time. Their genealogy of neuronal classes, based on single cell data, allows us to trace the evolutionary origins of neuronal types and their phylogenetic relationships. Recognizing the relevance of these studies, here we focus our attention on the origin of neurons as the building blocks of all neural systems.

Several features are shared among many neuron types, including the presence of axons and dendrites, the release of vesicular transmitters, and the presence of pre- and post-synaptic sites. However, for most of these cellular features there are some neuron types that lack them or non-neuronal

cells that possess them, making it challenging to generate an unambiguous generalizable definition of a neuron. That said, the most widely shared feature of neurons is the presence of pre-synaptic machinery. Thus, it has been speculated that neurons are likely derived from neurosecretory cells that were able to provide local information to neighboring cells. Said that, multiple origins of neurons and synapses from different classes of ancestral secretory cells might have occurred more than once during ∼600 million years of animal evolution. This issue has been a matter of intense discussion over the last few years, in good part fueled by the uncertainties in the placement of different clades at the base of the Metazoa (i.e., Porifera and Ctenophora; see Telford et al., 2016).

In one set of scenarios, in which Porifera is taken as the bearer of proto-neuronal cells, the presence of well-understood sets of postsynaptic structural proteins in flask cells (large ciliary cells present in the epithelia) has suggested a path toward the building of the synapse in later lineages (Sakarya et al., 2007). The additional presence of osmophilic septae as well as impulse conduction in hexactinellid sponges point to the possibility of the presence of protoneurons in Porifera (Leys et al., 1999). However, the report of Sakarya and collaborators wouldn't exclude the alternative scenario in which neurons had arisen before and through a process involving the loss of transmembrane receptors, with the flask cells originated anew (Sakarya et al., 2007). In this last case, flask cells will be relics from the protoneurons. Other scenarios for the origin of some neuron types have been proposed, for instance that of Brunet and Arendt (2016) in which neurons could have originated through a partition of functions associated with a primary mechanosensory receptor cell. The fact that sponges have lost action potentials, suggest that spreading of action potentials may have only been acquired after the sponge lineage diverged from other animals. This would assume a putative alternative origin of neurons not involving the flask cells. The scarcity of data in sponges precludes us from taking a firmer stand.

Beyond local communication, the specific and highly targeted communication to other, more distant cells, was a selective factor contributing to the origin of neurons; secretory cells with extended processes and the ability to transmit fast, electrically based signals (action potentials). Most neurons are characterized by the expression of neurotransmitters (chemical signals at the synapse) and a set of scaffolding proteins that provide the support for their activities. Moreover, during development, neurons typically share specific classes of differentiation factors, a series of transcription factors that control the specification of neurons in different contexts. The recent analysis of neurotransmitters and regulatory factors' complements in ctenophores genomes has raised an alternative scenario in which neurons may have originated twice independently (Moroz et al., 2014; Moroz, 2015). However, and since we currently know little about the ctenophore nervous system, it will be critical, in order to select between alternative scenarios, to gain further insight into similarities and differences between ctenophore and eumetazoan neurons, whether in their specification mechanisms or their physiological activities (Jékely et al., 2015).

Irrespective of the number of times neurons have arisen over evolutionary time, what seems clear is that once neuronal cells were born, the possibility of coordinating the actions of several cells, with the potential to "program" complex behaviors, would have provided a selective advantage in the ulterior birth and further elaboration of nervous systems.

WHEN DID BRAINS APPEAR IN EVOLUTIONARY TIME?

The most accepted time for the origin of the centralized nervous system is during the Ediacaran Period, when signs of burrowing substrates in the ocean appear, implying the directional movement and, thus, the control of body's maneuvrability. In fact, some clear signs of nervous system fossilization (not without associated polemics) have been revealed in exceptionally preserved biotas in Cambrian deposits (Strausfeld et al., 2016; Ortega-Hernández et al., 2019). In 2017, Budd and Jensen described the temporal and ecological context in which the early bilaterians arose, probably slightly later than 560 million years ago, at the Ediacaran-Cambrian boundary (Budd and Jensen, 2017). The event was marked by a drastic change of ecology that drastically changed the benthos, introducing considerable spatial heterogeneity. According to these authors: "the breaking of the uniformity of organic carbon availability would have signaled a decisive shift away from the essentially static and monotonous earlier Ediacaran world into the dynamic and burrowing world of the Cambrian" (the so-called *'Cambrian substrate revolution').*

Bilateral symmetry allowed directional movement and exploration, which in the surface-subsurface of the benthos meant movement in an anisotropic environment. The need to cope with anisotropies would have to be resolved with "focused" or anisotropic sensory information (plus a hydrostatic skeleton). This would have been achieved by the aggregation/polarization of some sensory systems/receptors and the subsequent origin of a "centralized" processing unit performing computations—the brain. Active locomotion would have been supported by the presence of a neuronal CPU in the major axis of the body. In fact, it has been demonstrated that "a symmetry that is streamlined in only one direction, while non-streamlined in other directions, is favorable for maneuvrable locomotion" and provided to the bearers a *"potentially enormous selective advantage over other body plans assuring faster changeovers and a more precisely directed locomotion"* (Holló and Novák, 2012). This is a particular selective advantage in a world of high Reynolds numbers. The use of Reynolds number helps us understanding the flow regimes under which any object (i.e., animal) moves. The calculation of Reynolds numbers depends on different parameters such as the diameter of the flow channel, the average velocity, density and viscosity of the fluid. Since it represents a ratio of inertial to viscous forces in a fluid at a particular time, it allows us to model the behavior of these objects in particular flowing conditions. Lower Reynolds numbers indicate laminar flow and higher ones a turbulent flow. In this context, the introduction of this rheological parameter in the models of Holló and Novak predicts that radial symmetry

could have evolved, and sustained, only in animals with slow locomotion. Interestingly, the transition from a pre-Ediacaran to a Cambrian world would have represented the change from one with low Reynolds numbers (where viscous forces predominate over inertial forces) that is sensitive to chemical gradients to one dominated by ecosystems with higher Reynolds numbers. In this new world, anisotropic sensory inputs and directional movement would have been dominated by bilaterians with effective neural processing capabilities (centralized control). Moreover, since available processing capacity is determined by the prior experience of the animal (Inglis, 1983), it becomes advantageous to the survival of the animal to increase cognitive capacity in response to a history of frequent and large variations in the environment (for instance, those encountered by an active moving animal).

It has been speculated that the origin of locomotion (and, thus, the nervous system) would have required the availability of stored energy. This question remains unresolved, largely because it has been demonstrated that the origin of bilaterian (or for that matter, metazoan) novelties was not accompanied by changes in metabolic rates. In fact, according to the extensive work of Makarieva and collaborators (Makarieva et al., 2008): "*there seems to be a metabolic optimum that hasn't changed much, from bacteria to humans, so major transitions can't be explained by changes in metabolic rates.*"

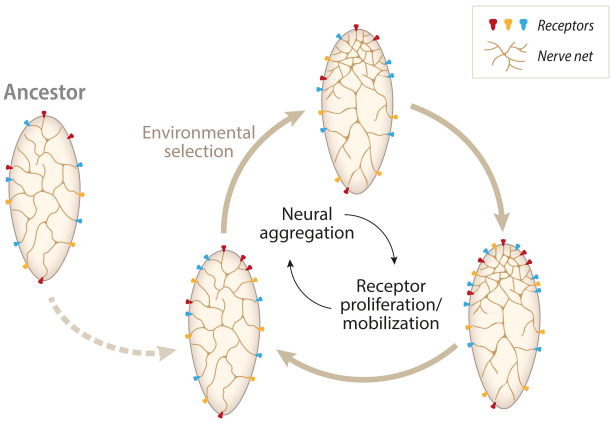

FIGURE 1 | A diagram representing one scenario for the evolution of centralized nervous systems from nerve-net precursors. The driving force is assumed to be a feedback loop between the number and diversity of receptors (sensory) and the neural aggregation in their vicinity. We called the hypothesis, the "Receptor and Neuronal Aggregation (RNA) Hypothesis." In summary, the hypothesis assumes an ancestor with few dispersed receptors in the body. The subsequent movement from an isotropic (benthic zone) to an anisotropic environment (the pelagic zone) would have selected the concentration of receptors at one specific location in the body (the head primordium). The presence of receptors will drag the neurons to the same body area, with the saving wire (neural processes length) as an energetic bonus. These aggregations of neurons would, eventually, interconnect, providing with a higher computing capacity to the ensemble. The whole process would gain by repeating itself many times, with more receptors accruing in the vicinity of the concentrated neural network followed by another round of neuronal mobilization or duplication/proliferation. These recurrent processes would be able to generate many, concentrated, neural architectures (brains). Adapted from Martinez et al. (2017).

DRIVING THE CONDENSATION PROCESS

As with any other evolutionary process, the centralization (condensation) of the nervous system must have represented a selective advantage in new environments, the origin of which may have changed to a subsequent stabilization of a more or less complex structure in different clades, always mediated by natural selection. Notably, for the function of a CPU discussed above, a condensation of the nervous system is not necessary; however, condensation may be beneficial for several reasons. Some models for the origin of an condensed brain have been put forward, with single or double condensation primary centers (see, for instance: Arendt et al., 2016). In this context, we had proposed also a scenario for brain evolution in a previous paper (Martinez et al., 2017; see also **Figure 1** for a diagram of the evolutionary process). The basic tenet of the paper is that neural condensation and circuit assembly might have been driven by the presence of sensory receptors in a particular location of the body (chiefly the anterior part). The presence of sensory receptors at the anterior end – defined by the direction of locomotion – allows an immediate perception of the novel environment when moving forward, including positive cues such as food as well as noxious and harmful stimuli. It is thus conceivable that sensory receptor accumulation might be more robust against selective pressure than another, more disperse architecture, especially when considering near-closed functional loops. This model rests on the assumption, now quite well accepted, that sensory cells evolved before neural (sensory) circuits. Cnidarian-bilaterian ancestors were probably already equipped with a simple repertoire of conserved photo-, chemo- and mechanoreceptors (Schlosser, 2015). Jékely and collaborators (Jékely et al., 2008; Marinković et al., 2019) have speculated that early circuits may have been devoted to control taxis, an essential factor in the Ediacaran-Cambrian origin of substrate mobility. Moreover, as perceptively stated by Tosches (2017): "*genes involved in sensory transduction or sensory cilium assembly, for example, are expressed nearly nowhere else, and mutations affecting these genes are not very likely to produce pleiotropic effects (Bendesky and Bargmann, 2011).*" This property of sensory systems would have provided a substrate for further receptor evolution through sensory tuning without affecting other body structures. The assembly of neurons around receptors might have contributed to the aggregation of proto-circuits, which would evolve into more complex architectures through mechanisms such as neuronal diversification and circuit duplications.

We shouldn't finish this section without a cautionary note. While discussing the process of condensation of the nervous system is our main objective in this manuscript, we should be aware that over evolutionary time, in some lineages, particularly those with a parasitic lifestyle, centralized nervous systems have gone through a process of secondary simplification [many examples are in the classical book of Bullock and Horridge, 1965; i.e., sessile tunicate urochordates, bryozoans, phoronids,

entoprocts, and parasitic cestode and trematode flatworms, plus "classical" vertebrate examples such the pedomorphic salamanders (Duellman and Trueb, 1986)]. These examples show that the centralization of the nervous system is not a unidirectional or irreversible process.

FROM NERVE NETS TO CENTRALIZED BRAINS: ISOTROPIC VS. ANISOTROPIC ENVIRONMENTS

Irrespective of the different models we have generated over the years on the structure of the nervous system for the last common protostome-deuterostome ancestor (PDA), it has been suggested several times (and seems the most plausible scenario) that centralized brains originated via the condensation of a nerve net in a specific location of the body (what we call the head). It has been speculated that this condensation happened only once, in the ancestor of all bilaterians (Balavoine and Adoutte, 2003; De Robertis, 2008), though this has also been challenged by other proposals assuming that centralization happened many times independently in different lineages (Moroz, 2012; Northcutt, 2012). We are not delving into this debate here. What we aim to understand is the basic arrangements of the nerve nets and centralized neural systems. The nets characterize the nervous system of cnidarians (though local concentrations of neurons are present) and some bilaterians (xenacoelomorphs or hemichordates, which have nets as an integral part of their neural architectures, though their neural systems are not exclusively organized as nets). Neural nets seem to be used in cnidarians due to the fact that they must deal with mostly isotropic environments (the pelagic zone), where signals come, essentially, from any direction. To sense these isotropic environments, it seems reasonable to use nets and sensors that are evenly distributed on the surface of the animal. This does not mean that the net does not have substructure; indeed, the substructure of neural nets has been illustrated by both immunostaining and transgenic lines (Nakanishi et al., 2012; Havrilak et al., 2017) and more recently by the detection of specific (and different) circuits involved in the various behaviours of Hydra (Dupre and Yuste, 2017). Thus, "simple nerve nets" seems to be an abuse of language. As has been seen in other contexts, superficial simplicity, in this case, hides organizational complexity. Moreover, it has been noted that the wiring diagrams and patterns of electrical activity still mask the dynamic changes in neurotransmitter diffusion gradients combined with spatially complex and tightly controlled patterns of receptor protein expression, which are very relevant at the nanoscale. This adds another, not-well-understood layer of complexity to the nervous systems [the "chemical connectome" (Bosch et al., 2017)]. As mentioned above, one might even argue that, at least for the purpose of locomotion, an apparently diffuse organization of the processing units may be best suited for radially symmetrical body plans.

Centralized nervous systems seem to have a much greater level of internal architectures, exemplified by the complex structural arrangements of some insects and vertebrates (plus the well-known case of cephalopods). Observing the patterns of neural activity of these organisms undergoing behavioral tests or inspecting neurotransmitter expression and domains within the nervous systems, not to mention the diversity of neuronal types, reveals an amazingly diverse internal substructure. This organizational complexity seems, with different degrees, to characterize most bilaterian clades. In fact, it might be the case that internal representations, memories of past events, and the coding of complex functions (social, etc.) are primarily achieved by the interaction of localized groups of neurons (circuits). It might be easier to store patterns in local circuits, where processing/computing is more efficient (in terms of time and energy spent). This would indicate that as these functions become more elaborate, it is better to compute in a complex but local group of neurons (brain) than to compute (and store) through a disperse net of neurons distributed throughout large portions of the body. It might be difficult to respond to external patterns through extended nets of neurons (as these would be too far apart); hence, an aggregated group of neurons locally interconnected may provide a good solution. This solution would have to conform to the limits of energy resources, processing speeds, and memory storage (see section below: "How do neural circuits use space and power so efficiently?").

An additional feature of complex brains (exemplified by the mammalian organ) is the fact that they have regional specialization, with different areas of the brain specialized for different functions (for a standard view of the regionalization in the mammalian brain see: Fodor, 1983). While the processing of different kinds of stimuli, or cognitive tasks, for that matter, is segregated into different parts of the brain, it is clear that this information should be functionally integrated (i.e., many different signals must be rapidly evaluated and coherently integrated to navigate safely in a complex environment) (Tononi et al., 1998). Functional integration benefits from the close clustering of processing centers; thus, a centralized neural system provides an ideal platform for multimodal sensory or cognitive information processing.

Before ending this section, a cautionary note: we must be aware that, in the end, it is the "network architecture" – not the anatomical appearance – that defines the function.

A USEFUL METAPHOR: THE BRAIN AS A COMPUTER

Neural systems process information and, as stated in previous sections, they do this by integrating internal and external (to the body) sensory information and sending a series of specific and targeted set of signals. In this context, the nervous system has been traditionally understood as a good system to explore with "information theory" [see von Neumann for an early treatment of the subject, though mostly dedicated to computer architecture (von Neumann, 1958)]. Neural systems compute and relay environmental information to the brain through a multi-layered path of cells, from sensory receptors to underlying neural circuits (Larderet et al., 2017). A schematic representation of the putative relationship

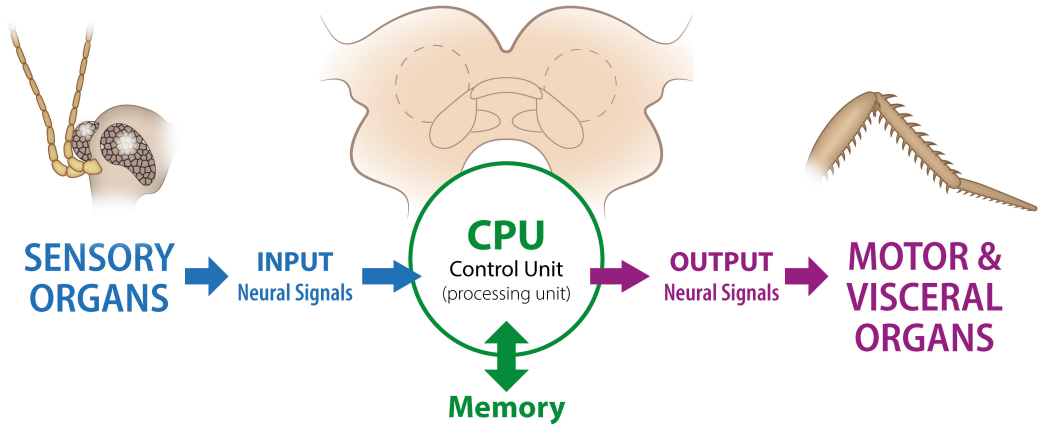

FIGURE 2 | Schematic representation of the "brain as a computer" concept. This diagram is based on the so-called "von Newman architecture scheme", which was originally proposed as a representation of a digital computer. While in the original formulation the "Processing" (with processor registers) and "Control" (with instruction registers) units were considered as independent components, for simplicity we have included both under the general name "Processing Unit." In most centralized nervous systems, the memory storage is also part of the anatomical structure holding the central computing unit (in the brain). In the diagram we show, in a very simplified way, the parallels between biological and computer structures. As an illustrative example we use a brain plus sensory and motor organs from a cockroach.

between biological and computer structures is presented in **Figure 2**.

In this context, it has become obvious that information processing in nervous systems and machines (computers) can be analyzed using a similar set of principles. Naturally, computers and brains are constructed following different principles, with computers (mostly) relying on sequential processing and brains using parallel processing. Moreover, and related to the previous observation, the speed of signal conduction/reaction time is vastly different in biological and artificial systems (neurons versus microprocessors), with electronic reaction times more than 10^4–10^5−-fold faster than those of neurons.

In this paper, our focus is on whether there is also some computational advantage in centralizing the neural arrangements, as opposed to organizing them in a distributed topology (i.e., nerve net). The main reason for using a compact structure is that a network topology with a core-periphery structure promotes effectively the integration of information in its central hub nodes (brain), and that this hub facilitates the sophisticated processing the animal brain uses in a complex world (Tononi et al., 1998; Shanahan et al., 2013). Processing of the information obtained from different stimuli is facilitated by a key feature of the organization of many brains: reciprocal and parallel connectivity among segregated groups of neurons. An argument for the need of this so-called functional clustering of brain regions is that such an structure allows maximizing the integration of information within the brain, "[t]he integrated information being formally defined as the information a system has besides the information that is available from the sum of its parts" (Deco et al., 2015). How functional specialization leads to integration into a coherent whole is now understood as the "neural complexity" of the system. In this context, complexity increases when a system is both highly integrated and highly specialized. The application of (quantitative) measures of complexity is becoming a central issue in the understanding of brains and their changes over evolutionary time from an information theoretical perspective. Though this research area is still in its infancy, further analysis of complexity in animal neural systems would provide us with additional clues on the organizational principles that constrain the organization of the different nervous systems.

Notably, the recent simulation experiments performed *in silico*:

"*demonstrate that adapted organisms possess a degree of integrated information reflecting the complexity of the habitats they have adapted to. As the diversity and richness of these niches grow, so do the nervous systems exploiting the attendant resources as well as their intrinsic causal powers. Commensurate with this increase in brain size is the growing ability of the species to learn to deal with novel situations*" (Koch, 2019).

The underlying principle is that richer networks of neurons are able to generate, comparatively, more potential alternative states than smaller ones; hence, and again according to Koch, "a large brain species is not only capable of more phenomenal distinctions that a smaller brained one but can also access more higher order distinctions or relations." In these models, fitness and complexity are related (at least within the limits of a small clade).

To sum up, fitness and computational power are linked through the modulation of component numbers and their functional integration. In fact, some parallels with integrated circuits are relevant here, for instance cost and performance. Packaged circuits use much less materials and with components in close proximity consume, comparatively to other non-compact arrangements, little power.

HOW DO THESE NEURAL CIRCUITS EVOLVE?

The mechanisms that organize (and reorganize) neural structures have been studied in different animals, and from these studies, some principles guiding neural systems' evolution have been defined. In the thorough review by Tosches (2017), she described some of the basic elements that guide nervous system evolution: changes in neuronal types, modifications of neuronal connections, reorganization of axonal paths (involving interactions between growth cones, surrounding tissues, and guidepost neurons), divergence and duplication of circuits, incorporation of neurons, and evolution of neuronal types through sub-functionalization of parental neurons. All these mechanisms of circuit evolution are explained by Tosches *in extenso*, so we do not need to further delve into their description here. However, what is important to point out in this context is that a combination of these mechanisms, at different organizational levels, should provide us with explanations for the many trajectories that neural systems have followed over evolutionary time. Understanding how these neural architectures and their changes are regulated at the gene, or gene network, level becomes now a pressing need. Interestingly, many of the principles that explain the evolution of neural circuits have parallels in the evolution of other network architectures (i.e., gene regulatory networks (Davidson and Peter, 2015), computer hardware and software design or in robotics (i.e., Fortuna et al., 2011).

A different approach to the evolutionary history of "brain condensation" is presented by Shigeno (2017). He describes the diverse patterns of information flow in the nervous systems of metazoans, recognizing four main types that arose at different evolutionary times (a schematic diagram is presented in **Figure 3**). The basic type is "diffused" (**Figure 3A**), which would correspond, for instance, to the net of cnidarians, with information processing occurring at the nodes in the net. This is a configuration used in some artificial networks (Kohonen, 1995). The "many to one" (**Figure 3B**) type are present in some early diverging clades (e.g., Acoela), in which sensory receptors in the body project to a point in space located in the anterior of the organism (brain). These nervous systems still keep, in part, the net (diffuse) arrangement of neurons. The type called "one to many" (**Figure 3C**) is characterized by the appearance of higher order intrinsic neuronal clusters. A central control connectivity centre (the brain) organizes the information processing. Numerous small intrinsic neurons with short neuronal processes and synapses are organized in the cortex (Shigeno, 2017). "One to many" topologies are seen in many protostome groups (arthropods, platyhelminths, annelids, etc.). Finally, the "many to one, one to many" type (**Figure 3D**) is characterized by the appearance of "interactive association centers for cognitive" function (i.e., Sherman and Guillery, 2013). The brain is organized internally with a rich structure of layers and loops (e.g., the mammalian thalamocortical relay loop). Cephalopods and mammals bear this type of information flow arrangements.

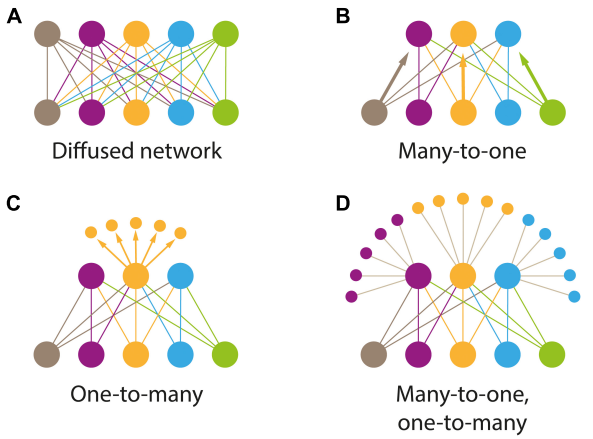

FIGURE 3 | Types of information flow patterns that were specialized during brain evolution and in different clades. A diagram showing the common blocks shared among various animals and used for the regulation of different cognitive tasks. Shigeno (2017) has proposed that the neuronal networks configuring the brains (Nervous Systems) of all animals can be classified into four basic types. **(A)** "Diffused type." Information processing occurs in simple elements called nodes (i.e., Cnidaria); **(B)** "Many to one" type. Present in the so-called primitive brains, a diffuse set of neuronal processes converge into an anterior structure (brain), located in the vicinity of sensory organs (i.e., Acoelomorpha); **(C)** "One to many" type. The connectivity pattern is organized in one centrally located processing unit (brain), and then processed in "many" small, higher order interneurons, generally called globuli in protostomes (i.e., polyclad flatworms or Annelida). In some clades, there is a feedback loop between the primary and other higher order centers. **(D)** "Many to one, one to many" type. They are organized in a hierarchical fashion (i.e., cortical to subcortical; with subcortical centers projecting back to cortical centers). This is the type of organization seen in mammalian or cephalopod brains. It is assumed that artificial neural networks use similar construction arrangements. Adapted from Shigeno (2017).

Ebbesson (1980) has also proposed a theory regarding the transition from nets to compact brains that relies on the changes in patterns of information flow in neural systems over evolutionary time described above. His theory is based on the idea of parcelation, in which neural nets progressively (or selectively) lose some of the diffuse connections and aggregate pre-existing subsystems.

It is important to point out that once brain architectures are established in the ancestors of a particular lineage, the process of selection continues modeling this architecture in order to accommodate different lifestyles. In fact, it has been shown in cases like the nematodes (Han et al., 2016) and the vertebrates (Gonda et al., 2013) that one salient characteristic of the brain is the variability of neuroanatomies between species, pointing to a continuous process of change.

Before ending this section, it is important to stress that the remodeling of neural architectures over evolutionary time follows alternative paths, with selective forces molding different aspects of the neural systems. Needless to say, some of these modifications are constrained by their previous evolutionary history, so as with any other biological structure, the nervous system in every animal is a product of historical constraints and adaptation (Wagner, 2014; for a recent treatment of the

subject). Two fundamental issues should be considered here: (1)- The elaboration of neural architectures in different clades on a common, shared, "substructure." This process has been illustrated rigorously in some cases (i.e., the arthropod central complex and vertebrate basal ganglia:

Strausfeld and Hirth, 2013a; or the arthropod mushroom bodies: Wolff et al., 2017), which is a clear example of the presence of deep neural circuitry homologies within bilaterian clades, (2)- The effect of constrains, imposed by different ecologies or lifestyles, on some neural architectures that lead them to adopt convergent features (i.e., as suggested for the cephalopod and vertebrate brains; Shigeno et al., 2018). While these modulatory effects on neural architectures seem to be pervasive, the arguments on which they are supported are not always solid. As a final cautionary note, it is important to mention that a more complete assessment of homologies should include structural, gene expression and functional data, otherwise our hypothesis of homology/convergence rests on shaky ground (see, also: Strausfeld and Hirth, 2013b; Lewitus, 2018).

HOW HAS THE BEHAVIOURAL REPERTOIRE CHANGED OVER EVOLUTIONARY TIME?

Does the emergence of centralized brains reflect the need to cope with a greater number of behavioral repertoires? Animals perform tasks that ensure their survival and reproduction, a fact that has been understood since Darwin. What is not clear is what kind of behaviors each major taxon is able to or needs to perform in their natural environment. Quantifying behavioral repertoires is not an easy endeavor, given the difficulty of simulating all putative conditions that any animal might face in their ecosystem. Moreover, if we add emotional behaviors (Anderson and Adolphs, 2014), those associated with internal states and instantiated (most likely) at the neural circuit level, the complexity of the challenge becomes astounding. However, different machine learning methodologies promise to quantify (to a large extent) the repertoire of behavioral states that a particular animal can perform. The information is still scant, but is interesting from a phylogenetic point of view. Based on the results of studies using machine learning, the fundamental repertoire of *Hydra vulgaris* (a cnidarian), independent of the experimental conditions and the individual, seems to coalesce into six basic behavioral states (elongation, tentacle swaying, body swaying, bending, contraction, and feeding; Han et al., 2018). However, this does not imply that *Hydra* has six types of behaviors, since these basic behavioral states may be combined in a plethora of different ecologically relevant behaviors. A similar project using the urochordate *Ciona intestinalis* shows that the larvae have eleven behavioral modes, including phototaxis, chemotaxis, mechanosensory but also some new ones such as thigmotaxis (movement induced by touching stimulus) or sensory arousal (Rudolf et al., 2019). Insects and nematodes have been well studied, but their behavioral modes are not quantified. However, a general agreement is that they are quite varied and extensive. Though this still qualifies as a very speculative assertion, one suggestion is that the transition to bilateralism would have resulted in a progressive enrichment of behavioral modes in ever more recent clades. This enrichment would imply the need for more sophisticated processing of information; hence, a complex CPU: the brain. Even without any specific quantification of repertoires, we know that some invertebrates, such as cephalopods and arthropods, display a higher-level psychological repertoire, with components such as cognition, emotion, planning, sleep, and consciousness. This indicates a substantial increase and sophistication of behaviors in more recent clades. A case in point is the striking richness of behaviors associated with vertebrate and mammalian systems. The meta-analysis performed in humans, for instance, shows the vast processing power of our brains (as measured through task-related neuroimaging; Smith et al., 2009).

Another important factor contributing to explain the rich behavioral repertoire of some animals is social life. New sensory modalities have evolved in different lineages to deal with kin recognition and to regulate parental care, aggression, mating, and imprinting. These sensory modalities become integrated in the nervous system, contributing to the growth in complexity, especially in the brain (the CPU). From the aggregative behavior of "simple" animals, such as some acoels (Franks et al., 2016), to the sophisticated social behavior of some insect and mammalian groups, the range and complexity of the structures involved have increased the complexity and internal connectivity of bilaterian brains. In addition, other behaviors such as mating have contributed further to this complexity in brain architecture.

HOW DO NEURAL CIRCUITS USE SPACE AND POWER SO EFFICIENTLY?

The function of neural systems depends heavily on the use of energy. Transmitting information through electrical signals is very expensive in terms of energy use. In the human body, roughly 20% of energy expenditure happens in the brain (though humans are at the upper end of the animal range), with most of it (estimated 75%) used at the synapses. Moreover, in the blowflies (*Calliphora vicina*), the retina alone consumes about 8% of the resting metabolic rate (Howard et al., 1987). One of the major implications of this expenditure is that brain architectures are using principles or architectures that minimize energy costs (Niven and Laughlin, 2008). The details of how the brain deals with energy and transmission efficiency are brilliantly exposed in the books by Sterling and Laughlin (2017) and by both, Niven and Laughlin, 2008 and Harris and collaborators (Harris et al., 2012). We have summarized some of the basic lessons described by these authors and added a few independent observations. The energetics of neural transmission are well known. Neural transmission (computation) is energetically expensive. The allocation of energy to the nervous system is disproportionally high when compared to the resting body's energy production. Most of this energy is spent in

synaptic transmission, where a large fraction of the energy expense is dedicated to the reversion of ion movements that generate postsynaptic responses. The source of energy is ATP, provided by the neurons or neighboring (glial) cells. Most of the energy used by neurons is related to the movement of ions across membranes. This energy is used mainly to pump Na^+ and K^+ ions, necessary to maintain resting potentials. This cost is canalized through the activity of the $3Na^+/2K^+$ ATPase. Electrical models of single fly photoreceptors have been used to estimate the energy cost of maintaining this ATPase activity. The values obtained suggest that this activity constitutes the major component of the energy cost in those cells (Niven et al., 2007). These results raise the problem of how synapses optimize their energy use. Strategies such as localizing mitochondria at the synapse, approximately one mitochondrion on either side of most synapses studied, provides a way to fuel synapses *in situ*. Over evolutionary time, nervous systems have optimized the ratio of information transmitted to energy consumption (Levy and Baxter, 1996). In fact, Harris and collaborators, as well as Sterling and Laughlin, have calculated that information transmission typically costs about 24,000 molecules of ATP per bit of information (Harris et al., 2012; Sterling and Laughlin, 2017). An additional factor contributing to the overall energetic expense of neural transmission is moving signals through the neural system. Neurons transmit signals to distant synapses. The speed of neural conduction (via action potentials) is proportional to the diameter of the fiber, so thicker axons (wires) provide faster conduction rates. In fact, conduction velocity in unmyelinated nerves has been shown to be proportionate to the square root of axonal diameter. This velocity always depends on biophysical properties of the membranes and is regulated through the combinations and densities of ion channels within the membrane (Hille, 2001). Saving time by sending signals at higher information rates and higher conduction velocities requires thicker axons, which involves higher energy costs and more of physical space. Nervous systems, in general, deal with this by shortening the wire length across all scales, from axon branching patterns to the overall layout. Thus, two general design principles explain the architectural arrangements of different brains: the so-called "saving wire" principle (a schematic wiring diagram is presented in **Figure 4**), in which total wire length is minimized throughout the entire individual, and the principle of homotypic interactions (when two regions A and B are well interconnected with a third, C, there is a high probability that A and B are also well connected). This principle might underlie the well-known "functional clustering" of brain regions (see above). These principles have been tested in several systems. Moreover, computational modeling of neuronal arrangements suggests that the most probable architecture for a given nervous system is one that follows these constructional principles (Cherniak, 1995). Needless to say, the principles that govern connections depend on the developmental parameters (i.e., where and when the neurons are born). Again, simulations that incorporate the timing of birth for neurons in a specific area corroborate that the architectures best preferred are those that use wire-saving and homotypic interactions as guiding principles (Lee et al., 2011). The lesson of these studies is that brains follow general layout principles that are also used in engineering and computational devices working in their optimal modes. Another related principle of design used in animal nervous systems is that of "local computation": wherever there is no need to coordinate the response over large areas of an animal (or a whole animal), local stimuli tend to be processed (computed) locally. This saves wire, energy consumption, and response time. More recent analysis has introduced a more nuanced view, suggesting that neural networks are more similar to network layouts that minimize the length of processing paths, rather than just wiring length. These findings suggest that neural systems are not exclusively optimized for minimal global wiring, but for a variety of factors, including the minimization of processing steps. These adaptations point in the same direction: *maximizing information-processing speed* (Kaiser and Hilgetag, 2006).

FIGURE 4 | A simple illustration of the "saving wire" principle. This principle states that in a neural circuit the placement of the different components is such that the addition of all internodes (between neuronal bodies) distances tends to be minimized. Experimental analysis of many neural circuits in different animals has shown that the principle if followed in most cases. The principle is here illustrated in a very simple circuit with only three components (neurons). When connection length among components is calculated, the placement of components in the left panel requires the greatest length. Adapted from Cherniak (1995).

Another feature of centralized systems is that the circuits involved in performing different tasks share neurons – that is, circuits are multiplexed. Many of the circuits most commonly studied are first-order circuits of sensory systems (for example, the olfactory bulb or the retina). These circuits are specialized and they serve as a counterexample: they are not multiplexed, even though the olfactory bulb, for example, integrates inputs from gustatory and temperature sensory neurons, which then alters how odors are perceived. Examples of multiplexed circuits are those of the spinal cord (or nerve cord in insects) for the control of movement (Harris et al., 2015). In this latter paper, Harris and collaborators show how different *Drosophila* neuronal hemilineages contribute to a range of evoked behaviors (walking, wing waving and buzz, uncoordinated leg movements and take off). The experiments are performed in a heat ramp with specific neurons being activated through the manipulation of temperature [using a temperature-sensitive channel (TRPA1) gene (Hamada et al., 2008)]. All of these behaviors can be traced to specific neuronal types, with most behavioral responses traced to few hemilineages (thus, multiplexing). Interestingly, these hemilineages appear to be organized in a modular fashion with cells in a module/group associated with a particular behavior.

Moreover, a related recent study carried out by Zarin and collaborators (Zarin et al., 2019) shows that, in the larva of *Drosophila*, the same premotor neurons (neurons that synapse onto motor neurons) participate in forward or backward locomotion, turning, etc. While some neurons are only active during specific locomotor modes, most neurons are active during many, indicating that the circuits are multiplex (a study that was made at synaptic resolution). In mice, for instance, a similar pattern is described for the sensorimotor cortical neurons, which are involved in co-representation of rewards and movement-related activities (Carus-Cadavieco et al., 2017). All in all, packing neurons and circuits seems to be a strategy for the efficient use of energetic resources in the brain. In complex environments, this should provide a selective advantage for the animals whose brains utilize this packing strategy.

CONCLUSION

The role of natural selection in shaping the brain over evolutionary time was stressed by Darwin in the different editions of *On the Origin of Species* (Jacyna, 2009). As with the mechanisms that underlie the origin/birth of new species, the mechanisms mediating the origin of novelties were obscure to him. This is understandable, given the state of knowledge during his time period. However, he was aware that structures (characters) have changed over time, in both their overall morphology and their internal structures. The brain also fascinated him. Currently, we take the origin and diversification of neural architectures as a problem that needs to be solved in the light of our current knowledge of phylogenetics, developmental biology, and physiology. We are equipped with tools that allow us to investigate the properties of the brain as a whole organ, operating under the constraints of chemical and physical laws. Moreover, as a computational system, the brain, in its many forms, has to conform to the limits of available energy resources, processing speed, and memory storage. This "internal" view of the brain system must be complemented with another, "external" perspective. Brains are functional organs that contribute to the survival of their bearers and hence, are adapted to the demands of the environments in which different animals live. In the previous sections, we outlined a putative scenario for the evolution of centralized nervous systems and, in doing so, we described the properties that might have been relevant in the construction of these systems. A further exploration of as many diverse neural systems as possible (Martinez, 2018) should prove especially fruitful in tracing the parallel "fates" of brains and behaviours over evolutionary time.

AUTHOR CONTRIBUTIONS

All authors listed have made a substantial, direct and intellectual contribution to the work, and approved it for publication.

FUNDING

The work is supported by the Swiss National Science Foundations (grant 310030_188471) to SS.

ACKNOWLEDGMENTS

We would like to thank the following people for helping us clarify some relevant points: Josep Abril (Barcelona), Albert Cardona (Cambridge, United Kingdom), and Murray Shanahan (London). Manuel Romera (Barcelona) helped us with the graphics. We would like to acknowledge the thorough work of the referees. They helped us to improve this manuscript.

REFERENCES

Anderson, D. J., and Adolphs, R. (2014). A framework for studying emotions across species. *Cell* 157, 187–200. doi: 10.1016/j.cell.2014.03.003

Arendt, D., Bertucci, P. Y., Achim, K., and Musser, J. M. (2019). Evolution of neuronal types and families. *Curr. Opin. Neurobiol* 56, 144–152. doi: 10.1016/j.conb.2019.01.022

Arendt, D., Tosches, M. A., and Marlow, H. (2016). From nerve net to nerve ring, nerve cord and brain–evolution of the nervous system. *Nat. Rev. Neurosci.* 17, 61–72. doi: 10.1038/nrn.2015.15

Balavoine, G., and Adoutte, A. (2003). The segmented Urbilateria: a testable scenario. *Integrat. Comp. Biol.*43, 137–147. doi: 10.1093/icb/43.1.137

Bendesky, A., and Bargmann, C. I. (2011). Genetic contributions to behavioural diversity at the gene-environment interface. *Nat. Rev. Genet.* 12, 809–820. doi: 10.1038/nrg3065

Bosch, T. C. G., Klimovich, A., Domazet-Lošo, T., Gründer, S., Holstein, T. W., Jékely, G., et al. (2017). Back to the basics: cnidarians start to fire. *Trends Neurosci.* 40, 92–105. doi: 10.1016/j.tins.2016.11.005

Brunet, T., and Arendt, D. (2016). From damage response to action potentials: early evolution of neural and contractile modules in stem eukaryotes. *Philos. Trans. R. Soc. Lond. B Biol. Sci.* 371, 20150043. doi: 10.1098/rstb.2015.0043

Budd, G. E., and Jensen, S. (2017). The origin of the animals and a 'Savannah' hypothesis for early bilaterian evolution. *Biol. Revi.* 92, 446–473. doi: 10.1111/brv.12239

Bullock, T. H., and Horridge, G. (1965). *Structure, and Function in the. (nervous)System of Invertebrates*. San Francisco, CA: Freeman.

Carus-Cadavieco, M., Gorbati, M., Ye, L., Bender, F., Van Der Veldt, S., Kosse, C., et al. (2017). Gamma oscillations organize top-down signalling to hypothalamus and enable food seeking. *Nature* 542, 232–236. doi: 10.1038/nature21066

Cherniak, C. (1995). Neural component placement. *Trends Neurosci.* 18, 522–527. doi: 10.1016/0166-2236(95)98373-7

Davidson, E. H., and Peter, I. (2015). *Genomic Control Process: Development and Evolution*. Cambridge, MA: Academic Press.

De Robertis, E. M. (2008). Evo-devo: variations on ancestral themes. *Cell* 132, 185–195. doi: 10.1016/j.cell.2008.01.003

Deco, G., Tononi, G., Boly, M., and Kringelbach, M. L. (2015). Rethinking segregation and integration: contributions of whole-brain modelling. *Nat. Rev. Neurosci.* 16, 430–439. doi: 10.1038/nrn3963

Duellman, W. E., and Trueb, L. (1986). *Biology of Amphibians*. Baltimore: Johns Hopkins University Press.

Dupre, C., and Yuste, R. (2017). Non-overlapping neural networks in hydra vulgaris. *Curr. Biol.* 27, 1085–1097. doi: 10.1016/j.cub.2017.02.049

Ebbesson, S. O. E. (1980). The parcellation theory and its relation to interspecific variability in brain organization, evolutionary and ontogenetic development, and neuronal plasticity. *Cell Tissue Res.* 213, 179–212. doi: 10.1007/BF00234781

Fodor, J. A. (1983). *The Modularity of the Mind*. Cambridge, MA: The Massachusetts Institute of Technology.

Fortuna, M. A., Bonachela, J. A., and Levin, S. A. (2011). Evolution of a modular software network. *Proc. Natl. Acad. Sci. U.S.A.* 108, 19985–19989. doi: 10.1073/pnas.1115960108

Franks, N. R., Worley, A., Grant, K. A. J., Gorman, A. R., Vizard, V., Plackett, H., et al. (2016). Social behaviour and collective motion in plant-animal worms. *Proc. R. Soc. BBiol. Sci.* 283:20152946. doi: 10.1098/rspb.2015.2946

Gonda, A., Herczeg, G., and Merilä, J. (2013). Evolutionary ecology of intraspecific brain size variation: a review. *Ecol. Evol.* 3, 2751–2764. doi: 10.1002/ece3.627

Hamada, F. N., Rosenzweig, M., Kang, K., Pulver, S. R., Ghezzi, A., Jegla, T. J., et al. (2008). An internal thermal sensor controlling temperature preference in *Drosophila*. *Nature* 454, 217–220. doi: 10.1038/nature07001

Han, S., Taralova, E., Dupre, C., and Yuste, R. (2018). Comprehensive machine learning analysis of Hydra behavior reveals a stable basal behavioral repertoire. *ELife* 7, 1–26. doi: 10.7554/eLife.32605

Han, Z., Boas, S., and Schroeder, N. E. (2016). Unexpected variation in neuroanatomy among diverse nematode species. *Front. Neuroan.* , 9:162. doi: 10.3389/fnana.2015.00162

Harris, J. J., Jolivet, R., and Attwell, D. (2012). Synaptic energy use and supply. *Neuron* 75, 762–777. doi: 10.1016/j.neuron.2012.08.019

Harris, R. M., Pfeiffer, B. D., Rubin, G. M., and Truman, J. W. (2015). Neuron hemilineages provide the functional ground plan for the *Drosophila* ventral nervous system. *ELife*4 1–34. doi: 10.7554/eLife.04493

Havrilak, J. A., Faltine-Gonzalez, D., Wen, Y., Fodera, D., Simpson, A. C., Magie, C. R., et al. (2017). Characterization of NvLWamide-like neurons reveals stereotypy in Nematostella nerve net development. *Dev. Biol.* 431, 336–346. doi: 10.1016/j.ydbio.2017.08.028

Hille, B. (2001). *Ion Channels of Excitable Membranes* (3rd edn). Sunderland, MA: Sinauer Associates.

Holló, G., and Novák, M. (2012). The manoeuvrability hypothesis to explain the maintenance of bilateral symmetry in animal evolution. *Biolo. Dir.* 7, 1–7. doi: 10.1186/1745-6150-7-22

Howard, J., Blakeslee, B., and Laughlin, S. B. (1987). The intracellular pupil mechanism and photoreceptor signal: noise ratios in the fly *Lucilia cuprina*. *Proc. R. Soc. Lond. B. Biol. Sci.* 231, 415–435. doi: 10.1098/rspb.1987.0053

Inglis, I. R. (1983). "Towards a cognitive theory of exploratory behaviour," in *Exploration in Animals and Humans*, eds J. Archer and L. Birke (London: Van Nostrand Reinhold), 72–116.

Jacyna, S. (2009). The most important of all the organs: darwin on the brain. *Brain* 132, 3481–3487. doi: 10.1093/brain/awp283

Jékely, G., Colombelli, J., Hausen, H., Guy, K., Stelzer, E., Nédélec, F., et al. (2008). Mechanism of phototaxis in marine zooplankton. *Nature* 456, 395–399. doi: 10.1038/nature07590

Jékely, G., Paps, J., and Nielsen, C. (2015). The phylogenetic position of ctenophores and the origin(s) of nervous systems. *Evo Devo* 6, 1. doi: 10.1186/2041-9139-6-1

Kaiser, M., and Hilgetag, C. C. (2006). Nonoptimal component placement, but short processing paths, due to long-distance projections in neural systems. *PLoS Computat. Biol.* 2:e95. doi: 10.1371/journal.pcbi.0020095

Koch, C. (2019). *The feeling of Life Itself*. Cambridge, MA: MIT Press.

Kohonen, T. (1995). *Self-Organizing Maps*. Heidelberg: Springer.

Larderet, I., Fritsch, P. M., Gendre, N., Neagu-Maier, G. L., Fetter, R. D., Schneider-Mizell, C. M., et al. (2017). Organization of the *Drosophila* larval visual circuit. *eLife* 6:e28387. doi: 10.7554/eLife.28387

Lee, S. C. S., Cowgill, E. J., Al-Nabulsi, A., Quinn, E. J., Evans, S. M., and Reese, B. E. (2011). Homotypic regulation of neuronal morphology and connectivity in the mouse retina. *J. Neurosci.* 31, 14126–14133. doi: 10.1523/JNEUROSCI.2844-11.2011

Levy, W. B., and Baxter, R. A. (1996). Energy efficient neural codes. *Neural Comput.* 8, 531–543. doi: 10.1162/neco.1996.8.3.531

Lewitus, E. (2018). Inferring evolutionary process from neuroanatomical data. *Front. Neuroanat.* 12:54. doi: 10.3389/fnana.2018.00054

Leys, S. P., Mackie, G. O., and Meech, R. W. (1999). Impulse conduction in a sponge. *J. Exp. Biol.* 202(Pt 9), 1139–1150.

Makarieva, A. M., Gorshkov, V. G., Li, B. A., Chown, S. L., Reich, P. B., and Gavrilov, V. M. (2008). Mean mass-specific metabolic rates are strikingly similar across life's major domains: evidence for life's metabolic optimum. *Proc. Natl.Acad. Sci. U.S.A.* 105, 16994–16999. doi: 10.1073/pnas.0802148105

Marinković, M., Berger, J., and Jékely, G. (2019).) Neuronal coordination of motile cilia in locomotion and feeding. *Philos. Trans. R. Soc. Lond. B Biol. Sci.* 375, 20190165. doi: 10.1098/rstb.2019.0165

Martín-Durán, J. M., and Hejnol, A. (2019). A developmental perspective on the evolution of the nervous system. *Dev. Biol.* S0012-1606:30475–X. doi: 10.1016/j.ydbio.2019.10.003

Martinez, P. (2018). The comparative method in biology and the essentialist trap. *Front. Ecol. Evol.* 6:130. doi: 10.3389/fevo.2018.00130

Martinez, P., Perea-Atienza, E., Gavilán, B., Fernandez, C., and Sprecher, S. (2017). The study of xenacoelomorph nervous systems. *Mol. Morphol.Perspect.* 14, 32–44. doi: 10.1098/rstb.2015.0039

Moroz, L. (2012). Phylogenomics meets neuroscience: how many times might complex brains have evolved? *Acta Biol. Hungarica* 63(Suppl. 2), 3–19. doi: 10.1556/ABiol.63.2012.Suppl.2.1

Moroz, L. L. (2015). The genealogy of genealogy of neurons. *Commun. Integr. Biol.* 7:e993269. doi: 10.4161/19420889.2014.993269

Moroz, L. L., Kocot, K. M., Citarella, M. R., Dosung, S., Norekian, T. P., Povolotskaya, I. S., et al. (2014). The ctenophore genome and the evolutionary origins of neural systems. *Nature* 510, 109–114. doi: 10.1038/nature13400

Moroz, L. L., and Kohn, A. B. (2016). Independent origins of neurons and synapses: insights from ctenophores. *Philos. Trans. R. Soc. Lond. B Biol. Sci.* 371, 20150041. doi: 10.1098/rstb.2015.0041

Nakanishi, N., Renfer, E., Technau, U., and Rentzsch, F. (2012). Nervous systems of the sea anemone *Nematostella vectensis* are generated by ectoderm and endoderm and shaped by distinct mechanisms. *Development* 139, 347–357. doi: 10.1242/dev.071902

Niven, J. E., Anderson, J. C., and Laughlin, S. B. (2007). Fly photoreceptors demonstrate energy-information trade-offs in neural coding. *PLoS Biol.* 5:e116. doi: 10.1371/journal.pbio.0050116

Niven, J. E., and Laughlin, S. B. (2008). Energy limitation as a selective pressure on the evolution of sensory systems. *J. Exp. Biol.* 211(Pt 11), 1792–1804. doi: 10.1242/jeb.017574

Northcutt, R. G. (2012). Evolution of centralized nervous systems: two schools of evolutionary thought. *Proc. Natl.Acad. Scie. U.S.A* 109(Suppl._1), 10626–10633. doi: 10.1073/pnas.1201889109

Ortega-Hernández, J., Lerosey-Aubril, R., and Pates, S. (2019). Proclivity of nervous system preservation in Cambrian Burgess Shale-type deposits. *Proc. . Biol. Sci.* 286:20192370. doi: 10.1098/rspb.2019.2370

Rudolf, J., Dondorp, D., Canon, L., Tieo, S., and Chatzigeorgiou, M. (2019). Automated behavioural analysis reveals the basic behavioural repertoire of the urochordate *Ciona intestinalis*. *Sci. Rep.* 9, 1–17. doi: 10.1038/s41598-019-38791-5

Ryan, J. F., and Chiodin, M. (2015). Where is my mind? How sponges and placozoans may have lost neural cell types. *Philos. Trans. R. Soc. Lond. B Biol. Sci.* 370:20150059. doi: 10.1098/rstb.2015.0059

Sakarya, O., Armstrong, K. A., Adamska, M., Adamski, M., Wang, I. F., Tidor, B., et al. (2007). A Post-synaptic scaffold at the origin of the animal kingdom. *PLoS One* 2:506. doi: 10.1371/journal.pone.0000506

Schlosser, G. (2015). Vertebrate cranial placodes as evolutionary innovations-The ancestor's tale. *Curr. Topics Dev.Bio.* 111, 235–300. doi: 10.1016/bs.ctdb.2014.11.008

Shanahan, M., Bingman, V. P., Shimizu, T., Wild, M., and Güntürkün, O. (2013). Large-scale network organisation in the avian forebrain: a connectivity matrix and theoretical analysis. *Front. Comput. Neurosci.* 7:98. doi: 10.3389/fncom.2013.00089

Sherrington, C. S. (1906). *The Integrative Action of the Nervous System*. New Haven: Yale University Press.

Sherman, S. M., and Guillery, R. W. (2013). *A Deep Look at the Thalamocortical Continuum - Functional Connections of Cortical Areas: A New View from the Thalamus*. Cambridge, MA: The MIT Press.

Shigeno, S. (2017). in *Brain Evolution by Design. Diversity and Commonality in Animals*, eds N. T. Shigeno and S. Murakami (Tokyo: Springer).

Shigeno, S., Andrews, P. L. R., Ponte, G., and Fiorito, G. (2018). Cephalopod brains: an overview of current knowledge to facilitate comparison with vertebrates. *Front. Physiol.* 9:952. doi: 10.3389/fphys.2018.00952

Smith, S. M., Fox, P. T., Miller, K. L., Glahn, D. C., Fox, P. M., Mackay, C. E., et al. (2009). Correspondence of the brain's functional architecture during

activation, and rest. *Proc. Natl.Acad. Sci.U.S.A.* 106, 13040–13045. doi: 10.1073/pnas.0905267106

Sterling, P., and Laughlin, S. (2017). *Principles of Neural Design*. Cambridge, MA: MIT Press.

Strausfeld, N. J., and Hirth, F. (2013a). Deep homology of arthropod central complex and vertebrate basal ganglia. *Science.* 340, 157–161. doi: 10.1126/science.1231828

Strausfeld, N. J., and Hirth, F. (2013b). Homology versus convergence in resolving transphyletic correspondences of brain organization. *Brain Behav. Evol.*82, 215–219. doi: 10.1159/000356102

Strausfeld, N. J., Ma, X., Edgecombe, G. D., Fortey, R. A., Land, M. F., Liu, Y., et al. (2016). Arthropod eyes: the early Cambrian fossil record and divergent evolution of visual systems. *Arthropod Struct. Dev.* 45, 152–172. doi: 10.1016/j.asd.2015.07.005

Sugahara, F., Murakami, Y., Pascual-Anaya, J., and Kuratani, S. (2017). Reconstructing the ancestral vertebrate brain. *Dev.Growth Differ.* 59, 163–174. doi: 10.1111/dgd.12347

Telford, M. J., Moroz, L. L., and Halanych, K. M. (2016). Evolution: a sisterly dispute. *Nature* 529, 286–287. doi: 10.1038/529286a

Tononi, G., Edelman, G. M., and Sporns, O. (1998). Complexity and coherency: integrating information in the brain. *Trends Cogn. Sci.* 2, 474–484. doi: 10.1016/S1364-6613(98)01259-5

Tosches, M. A. (2017). Developmental and genetic mechanisms of neural circuit evolution. *Dev. Biol.* 431, 16–25. doi: 10.1016/j.ydbio.2017.06.016

von Neumann, J. (1958). *The Computer and the Brain*. New Haven: Yale University Press.

Wagner, G. P. (2014). *Homology, Genes, and Evolutionary Innovation*. Princeton: Princeton University Press.

Wolff, G. H., Thoen, H. H., Marshall, J., Sayre, M. E., and Strausfeld, N. J. (2017). An insect-like mushroom body in a crustacean brain. *Elife* 6:e29889. doi: 10.7554/eLife.29889

Zarin, A. A., Mark, B., Cardona, A., Litwin-kumar, A., and Doe, C. Q. (2019). A multilayer circuit architecture for the generation of distinct locomotor behaviors in. *ELife* 8:e51781. doi: 10.7554/eLife.51781

Conflict of Interest: The authors declare that the research was conducted in the absence of any commercial or financial relationships that could be construed as a potential conflict of interest.

frontiers | Frontiers in Cell and Developmental Biology

ORIGINAL RESEARCH
published: 14 June 2022
doi: 10.3389/fcell.2022.894434

Midbody-Localized Aquaporin Mediates Intercellular Lumen Expansion During Early Cleavage of an Invasive Freshwater Bivalve

Elisabeth Zieger[1]*, *Thomas Schwaha*[1], *Katharina Burger*[2], *Ina Bergheim*[2], *Andreas Wanninger*[1]* and *Andrew D. Calcino*[1]*

[1]Integrative Zoology, Department of Evolutionary Biology, University of Vienna, Vienna, Austria, [2]Molecular Nutritional Science, Department of Nutritional Sciences, University of Vienna, Vienna, Austria

OPEN ACCESS

Edited by:
Juan Jesus Tena,
Spanish National Research Council, Spain

Reviewed by:
Makoto Kamei,
South Australian Health and Medical Research Institute, Australia
Andrea J. Yool,
University of Adelaide, Australia

***Correspondence:**
Andreas Wanninger
andreas.wanninger@univie.ac.at
Andrew D. Calcino
andrew.calcino@gmail.com
Elisabeth Zieger
elisabeth.zieger@univie.ac.at

Specialty section:
This article was submitted to Evolutionary Developmental Biology, a section of the journal Frontiers in Cell and Developmental Biology

Received: 11 March 2022
Accepted: 24 May 2022
Published: 14 June 2022

Citation:
Zieger E, Schwaha T, Burger K, Bergheim I, Wanninger A and Calcino AD (2022) Midbody-Localized Aquaporin Mediates Intercellular Lumen Expansion During Early Cleavage of an Invasive Freshwater Bivalve. Front. Cell Dev. Biol. 10:894434. doi: 10.3389/fcell.2022.894434

Intercellular lumen formation is a crucial aspect of animal development and physiology that involves a complex interplay between the molecular and physical properties of the constituent cells. Embryos of the invasive freshwater mussel *Dreissena rostriformis* are ideal models for studying this process due to the large intercellular cavities that readily form during blastomere cleavage. Using this system, we show that recruitment of the transmembrane water channel protein aquaporin exclusively to the midbody of intercellular cytokinetic bridges is critical for lumenogenesis. The positioning of aquaporin-positive midbodies thereby influences the direction of cleavage cavity expansion. Notably, disrupting cytokinetic bridge microtubules impairs not only lumenogenesis but also cellular osmoregulation. Our findings reveal a simple mechanism that provides tight spatial and temporal control over the formation of luminal structures and likely plays an important role in water homeostasis during early cleavage stages of a freshwater invertebrate species.

Keywords: lumenogenesis, midbody, blastomere cleavage, aquaporin, osmoregulation, freshwater invertebrate

INTRODUCTION

Cytokinetic bridges keep cells interconnected throughout cytokinesis. They contain antiparallel bundles of microtubules that overlap at the midbody, an organelle responsible for recruiting the components required for abscission (Hu et al., 2012; D'Avino et al., 2015; Capalbo et al., 2019). This evolutionary ancient mode of daughter cell separation likely dates back to the last common ancestor of animals and even shares numerous features with those of choanoflagellates, plants and archaeans (Otegui et al., 2005; Eme et al., 2009; Laundon et al., 2019; Yagisawa et al., 2020). In addition to controlling the timing and location of final daughter cell separation, the midbody acts as a polarity cue (Dionne et al., 2015). Many proteins recruited via cytokinetic bridges play dual roles in cytokinesis and apical membrane specification (Román-Fernández and Bryant, 2016). Prior to abscission, positioning of the cytokinetic bridge can thus determine the site of apical domain and apical lumen formation (Frémont and Echard, 2018).

In order to organize cells into tissues, metazoan development relies on lumenogenesis, which can be achieved via diverse mechanisms (Datta et al., 2011). Coupling cytokinesis with the *de novo* generation of intercellular lumens requires the delivery of both, apical determinants and lumen-promoting factors to the cytokinetic bridge. This process appears to be chiefly mediated by

endosomes carrying specific Rab GTPases on their surface (Jewett and Prekeris, 2018). Proper trafficking of these Rab endosomes is orchestrated by complex molecular networks that have been extensively investigated in a range of *in vivo* and tissue culture models (Jewett and Prekeris, 2018; Rathbun et al., 2020). However, while numerous targeting regulators have been identified, much less is known about the relevant cargoes transported via different Rab pathways and how they might influence lumen morphogenesis.

Prime candidates for driving luminal expansion, which generally involves redirection of intracellular water to an extracellular space, are aquaporins (AQPs). These channel proteins exist in most living organisms, where they mediate the transport of water and other small solutes across membranes (Campbell et al., 2008; Ishibashi et al., 2017). AQPs thus contribute to diverse physiological processes across cells, tissues and developmental stages (Liu and Wintour, 2005; Day et al., 2014; Martínez and Damiano, 2017) and play a particularly important role in mammalian blastocoel formation (Watson et al., 2004; Offenberg and Thomsen, 2005). Rapid changes to membrane permeability and lumenogenesis generally rely on the agonist-induced and microtubule-mediated redistribution of AQPs from an intracellular vesicular compartment to the general, apical or basolateral plasma membrane (Huebert et al., 2002; Conner et al., 2012; Mazzaferri et al., 2013; Sundaram and Buechner, 2016; Vukićević et al., 2016). It is becoming increasingly clear that not only cytoskeletal activity, but also water flux and hydrodynamics are of fundamental importance for the determination of cell shape, fate, movement and division (Li et al., 2017; Chan et al., 2019; Dumortier et al., 2019). Yet, very little information is available on the sub-cellular localization and functions of AQPs throughout both, early embryogenesis and cytokinetic processes.

Here we explore the dynamic distribution of a maternally inherited AQP during initial cleavage stages of the quagga mussel, *Dreissena rostriformis*, an invasive freshwater bivalve known for its enormous ecological and economic impact (Karatayev et al., 2015; Rudstam and Gandino, 2020). Early dreissenid embryos are especially suited for observing lumenogenesis, since a large intercellular cleavage cavity forms with each blastomere division, to allow for the excretion of excess water in an hypoosmotic environment (Meisenheimer, 1901; Calcino et al., 2019). Furthermore, only a single AQP ortholog, *Dro-lt-AQP1*, is highly expressed in unfertilized eggs and early cleavage stages of *D. rostriformis* (Gene.75921, Figure S18 in Calcino et al., 2019). The lophotrochozoan-specific Dro-lt-AQP1 protein belongs to the classical (i.e., water-selective) AQP subtype (Calcino et al., 2019) and was analyzed with respect to microtubular rearrangements, using immunofluorescence and pharmacological treatments. Our findings reveal a previously undescribed cell biological process that allows precise control over the timing and direction of intercellular lumen formation during cytokinesis by utilizing the ancient molecular machinery that underlies polarized trafficking to the midbody.

MATERIALS AND METHODS

Animals

Adult specimens of the freshwater mussle *Dreissena rostriformis* were collected in the New Danube (Georg-Danzer-Steg, Vienna, Austria, 48°14′44.8″N 16°23′39.3″E) and kept in a large aquarium filled with Danube river water at 18°C. To induce spawning, animals were cleaned with a toothbrush, rinsed with tap water and placed into 2 µm filtered river water. Serotonin (#H9523, Sigma-Aldrich, St. Louis, Missouri, United States) was added at a final concentration of 0.1 mg/ml and the animals were incubated for 20 min at room temperature in the dark. They were then placed into individual glass dishes, where most individuals spawned within 1–2 h of serotonin exposure. Eggs were pooled into a fresh dish, inseminated with a few drops of pooled sperm solution and incubated on a shaker for 30 min. Excess sperm was then washed from fertilized zygotes with several changes of 2 µm filtered river water. Embryos were left to develop at 21°C in the dark and fixed for 1 h in ice-cold 4% PFA (paraformaldehyde, #158127, Sigma-Aldrich) in PBS (0.01 M phosphate buffered saline, #1058.1, Carl Roth, Karlsruhe, Germany) containing 2% acetic anhydride (#CP28.1, Carl Roth GmbH + Co. KG, Karlsruhe, Germany). The samples were then washed three times in PBS and stored at 8°C in PBS containing 0.1% sodium azide (#106688, Merck, Darmstadt, Germany).

Immunofluorescence

A polyclonal antibody against Dro-lt-AQP1_Gene.75921 was generated by Eurogentec (Seraing, Belgium) using their Speedy Mini immunization program. Specifically, one rabbit was immunized with a synthetic peptide (nh2- C + VIDGKGDFQRLPTEE–conh2) corresponding to amino acids 396–410 of the Dro-lt-AQP1_Gene.75921 protein (Calcino et al., 2019). Following the initial immunization and three subsequent boosters, a pre-immune bleed and a final bleed were obtained. The latter was used for affinity purification. Upon receipt, the purified antibody (in PBS, 0.01% thimerosal and 0.1% BSA) was diluted 1:1 in glycerol (#104201, Merck, Darmstadt, Germany) and 4 µl aliquots were stored at -20°C.

Antibody specificity was assessed by Western Blotting, which revealed a strong band at the expected molecular weight for Dro-lt-AQP1_Gene.75921 protein (~50 kDA, **Supplementary Figure S1E**). Pooled eggs of *D. rostriformis* were pelleted, washed twice with 2 µm filtered river water and flash frozen in liquid nitrogen. Samples were stored at -80°C until further processing. Eggs were resuspended in 50 µl RIPA lysis buffer (20 mM 3-(N-morpholino)propanesulfonic acid (MOPS), 150 mM NaCl, 1 mM ethylenediaminetetraacetic acid (EDTA), 1% Nonidet P-40) and 0.1% sodium dodecyl sulfate (SDS)) containing protease and phosphatase inhibitor cocktails (P8340 and P0044, Sigma-Aldrich, Steinheim, Germany). The samples were homogenized with a Tissue Lyser at 45 Hz for 30 s, placed into an ultrasonic bath for 10 s and centrifuged at maximum speed for 15 min. Total protein concentration of the supernatant was quantified using a

Bradford protein assay (#5000001, Bio-Rad Protein Assay Kit II, Bio-Rad Laboratories, Hercules, CA, United States). The protein lysate with DTT (100 mM, #1114740001, VWR, Vienna, Austria) and 4x loading buffer (0.3 M Tris base/10% SDS/50% glycerol/0.05% bromphenol blue) was denatured at 95° for 5 min and separated by electrophoresis on a 10% SDS-polyacrylamide gel in electrophoresis buffer (25 mM Tris base/192 mM Glycin/0.1% SDS) at 110 V for 1.5 h. Separated proteins were transferred to an Immun-Blot®-polyvinylidene difluoride membrane (#1620177, Bio-Rad Laboratories, Hercules, CA, United States) using a Trans Blot® Turbo Transfer System (STANDARD SD Program (25V, 1A, 30 min), #1704150, Bio-Rad Laboratories, Hercules, CA, United States). The membrane was dried overnight and nonspecific binding sites were blocked in 5% nonfat dry milk (MMP, A0830.0500, Applichem, Darmstadt, Germany) diluted in tris buffered saline with Tween 20 (TBST; 10 x TBS, 48,4 g Tris base, 160 g NaCl) for 1 h. For immunological detection of Dro-lt-AQP1, the membrane was incubated with the primary antibody diluted 1:200 (in 5% MMP in TBST) at 4°C overnight. Following 3 times washing, incubation with the secondary antibody (#7074 anti-rabbit IgG, HRP-linked Antibody, Cell Signaling, Danvers, MA, United States) diluted 1:5000 in 5% MMP in TBST was carried out at room temperature for 1 h. Following another washing step, protein bands were detected using a luminol-based enhanced chemiluminescence horseradish peroxidase (HRP) substrate (#34075, Super Signal West Dura kit, Thermo Fisher Scientific, Waltham, MA, United States) and the ChemiDoc XRS System (#1708265, Bio-Rad Laboratories, Hercules, CA, United States).

For immunofluorescence, early cleavage stage embryos of *D. rostriformis* were rinsed three times with PBS and incubated for 1 h in blocking solution, i.e., in PBS containing 1% Tween®20 (#9127.1, Carl Roth, Karlsruhe, Germany) and 3% normal goat serum (#PCN5000, Invitrogen, Molecular Probes). The embryos were then incubated overnight at 8°C in the primary antibodies diluted in blocking solution. For this step, our custom Dro-lt-AQP1 antibody (diluted 1:200), anti-acetylated α-tubulin (1:800, mouse, monoclonal, #T6793, Sigma, St. Louis; MO, United States) and anti-tyrosinated α-tubulin (1:800, mouse, monoclonal, #T9028, Sigma, St. Louis; MO, United States) were used. Following six washes with PBS, the embryos were incubated overnight at 8°C in PBS containing the secondary antibodies goat anti-rabbit Alexa Flour 633 (1:500, #A21070, Invitrogen, Molecular Probes) and goat anti-mouse Alexa Flour 488 (1:500, #A11001, Invitrogen, Molecular Probes) as well as the nucleic acid stain Hoechst (1:5000, Sigma-Aldrich; St. Louis; MO, United States). After a final six washes in PBS, specimens were mounted in Fluoromount-G (Southern Biotech, Birmingham, AL, United States) and stored at 4°C. Negative controls were performed by omitting the primary antibodies and yielded no signal (**Supplementary Figure S1A–D**).

Nocodazole Treatments

Pharmacological experiments were carried out with pooled embryos from three females and three males and in three technical replicates. Nocodazole (#M1404, Merck KGaA, Darmstadt, Germany) was dissolved in DMSO (#A994.2, Carl Roth GmbH + Co. KG, Karlsruhe, Germany) and stored as 33 mM stock solution at -20°C. Embryos were incubated in 2 µm filtered river water containing 10 µM nocodazole and 42 nM DMSO (= 0.033%). Control embryos were treated with 42 nM DMSO. Treatments were carried out in the dark at 21°C and maintained for the entire duration of the experiments. Embryos were either treated from 45 mpf (minutes post fertilization) or from 1 hpf (hours post fertilization) until fixation at 1.5 hpf and 2 hpf, respectivley.

Imaging, Volumetric Measurements and Statistical Analyses

Confocal laser scanning microscopy was performed on a Leica TCS SP5 II microscope (DMI6000 CFS, Leica Microsystems, Wetzlar, Germany). Maximum projections of image stacks were generated and global brightness and contrast were adjusted in ImageJ (Schneider et al., 2012).

Volumetric measurements of blastomeres and cleavage cavities were conducted with the software Amira (v. 2020.2, ThermoFisher). Each respective structure was segmented by manual labelling (**Figure 4B**) and interpolation between sections. Segmented areas were subsequently measured with the Material Statistics tool.

To document nocodazole treatment effects, n > 23 embryos were analyzed for each condition. Raw measurement data is provided in **Supplementary Data S1**. To compare median cell and cavity volumes between different conditions, a two-sided Wilcoxon rank-sum test was performed with several *p*-value thresholds (****p =< 1e-04, ***p =< 0.001, **p =< 0.01, *p =< 0.05, n. s $p > 0.05$, **Figure 4**).

RESULTS AND DISCUSSION

AQP Recruitment to the Cytokinetic Midbody Coincides With Lumen Expansion

During cytokinesis, spindle microtubules become partially reorganized into a cytokinetic bridge, which can be observed particularly well in early cleavage stages of *D. rostriformis* (**Figures 1**, **2**). Maternally inherited Dro-lt-AQP1 is then recruited to this cytokinetic bridge (**Figures 1B–D**, **Figure 2E**, arrows). Dro-lt-AQP1 accumulation at the midbody coincides with the onset of cleavage cavity formation (**Figures 1A–H**, **Figures 2F–I**). While the cleavage cavity expands, Dro-lt-AQP1 immunoreactivity increases within the midbody (**Figures 1G,L**). Importantly, however, Dro-lt-AQP1 is otherwise absent from the plasma membrane. Once abscission is completed (**Figures 1I–L**), the Dro-lt-AQP1-immunoreactive midbody is inherited by one of the two daughter cells and persists within its membrane, at least until the four-cell stage (**Figures 2A–M**). The tubulin fibers of the cytokinetic bridge, in contrast, dissolve rapidly and the cleavage cavity collapses (**Figures 2B–E**), expelling its contents to the exterior. Although numerous studies have addressed AQP recruitment to specific plasma membrane domains (Mazzaferri et al., 2013; Vukićević et al., 2016; Arnspang et al., 2019) as well as their emerging roles

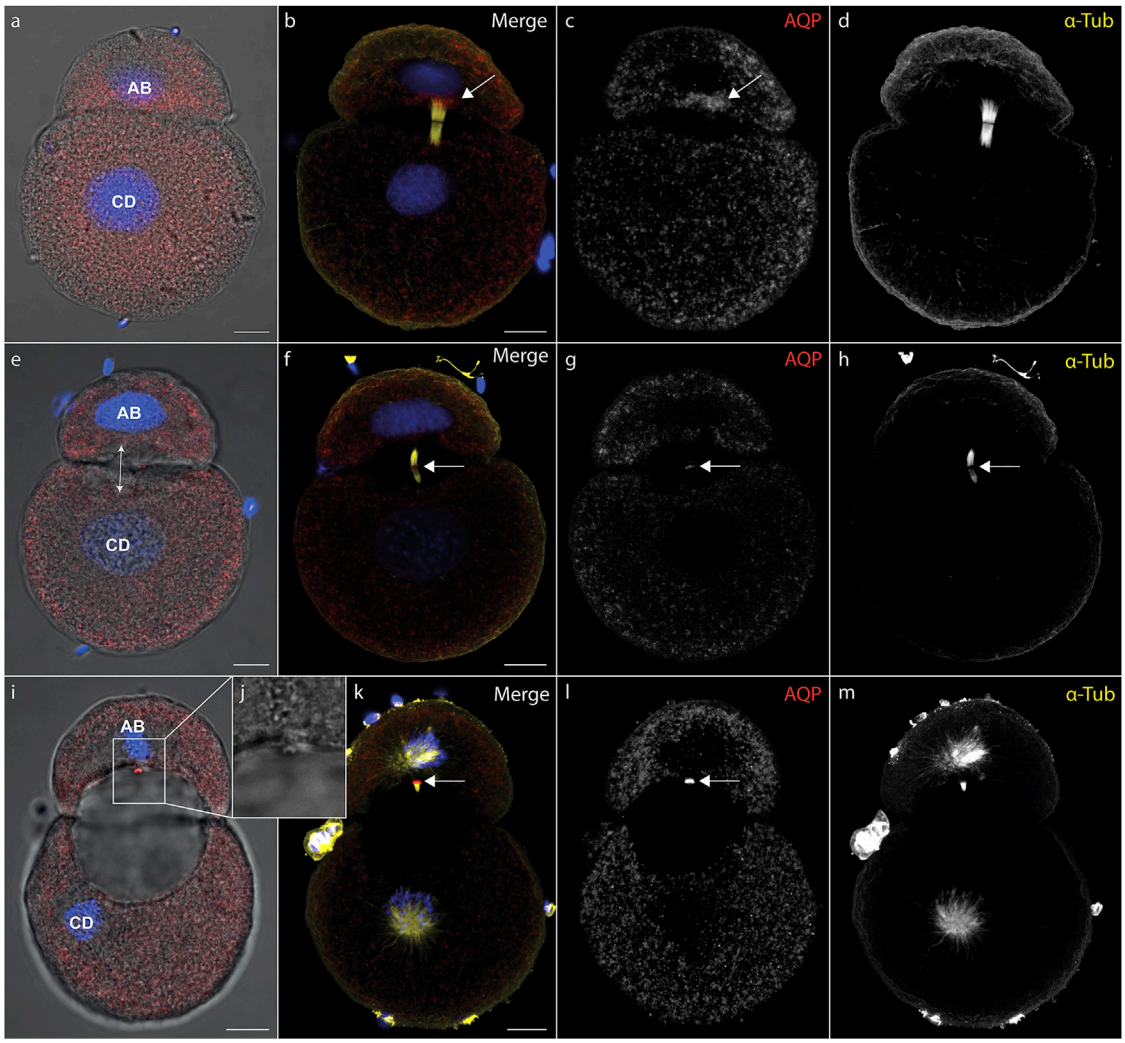

FIGURE 1 | Recruitment of midbody aquaporin and formation of the first cleavage cavity. **(A–I)** Maximum intensity projections of *Dreissena rostriformis* embryos at 1 hpf **(A–D)**, 1.25 hpf **(E–H)** and 1.5 hpf **(I–L)**. Hoechst labeling of nuclei is shown in blue, Dro-lt-AQP1 immunofluorescence is shown in red **(A,B,E,F,I,K)** or grey-scale **(C,G,L)** and acetylated/tyrosinated alpha-tubulin immunofluorescence is shown in yellow **(B,F,K)** or grey-scale **(D,H,M)**. AB and CD blastomere morphology and cleavage cavity expansion are shown in overlays of brightfield images with Dro-lt-AQP1 immunofluorescence **(A,E,I)**. Arrows in **(B,C)** indicate Dro-lt-AQP1 accumulation at the cytokinetic bridge. Arrows in **(F,G,H,K,L)** indicate the location of the Dro-lt-AQP1 immunoreactive midbody. The double-headed arrow in **(E)** indicates the direction of cleavage cavity expansion. **(J)** Brightfield close-up of the Dro-lt-AQP1 immunoreactive midbody remnant shown in **(I)**. Scale bars, 10 μm.

in cell proliferation and cancer biology (Galán-Cobo et al., 2016; Dajani et al., 2018), detailed analyses of the sub-cellular localization of AQP during early embryonic development and during cytokinesis are currently lacking. Accordingly, this is the first report, to our knowledge, of AQP recruitment to the midbody.

The two-cell stage of *D. rostriformis* consists of a smaller AB blastomere and a larger CD blastomere (**Figure 1**) (Meisenheimer, 1901). Interestingly, the larger CD blastomere divides slightly earlier than the smaller AB blastomere, giving rise to a transient three-cell stage (**Figures 2B–H**). The second round of cleavages results in two additional cytokinetic bridges that do not form centrally between the dividing A/B and C/D blastomeres, but instead are displaced towards the interface between the A/D and B/C cousin blastomeres in the center of the embryo (**Figures 2E–M**). Consequently, the two new cleavage cavities form between these cousin blastomeres and not between the A/B and C/D daughter blastomeres (**Figures 2I,M**, double-headed arrows). This is consistent with vertebrate studies linking cytokinetic bridge and midbody positioning to the site of lumen formation (Rodriguez-Fraticelli et al., 2010; Klinkert et al., 2016; Frémont and Echard, 2018; Rathbun et al., 2020).

Since the CD blastomere divides first, Dro-lt-AQP1 accumulation in the C/D cytokinetic midbody precedes that in the A/B cytokinetic midbody (**Figures 2E–I**). However, the remnant of the Dro-lt-AQP1-immunoreactive midbody from the first cleavage (**Figure 2**, red "1") might compensate for this time lag, since the two new cleavage cavities expand

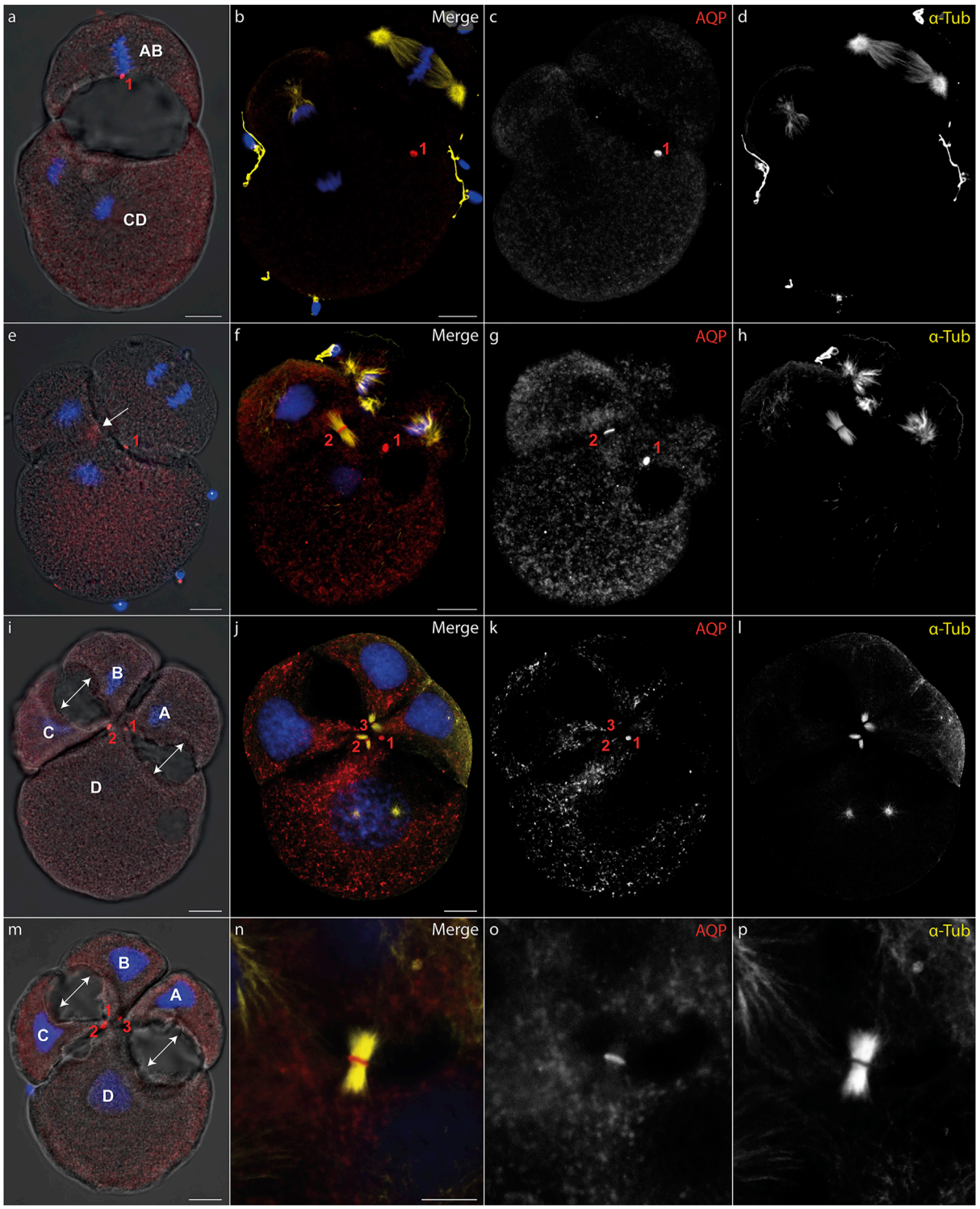

FIGURE 2 | Midbody localization determines the direction of cleavage cavity expansion. **(A–P)** Maximum intensity projections of *Dreissena rostriformis* embryos at 1.5 hpf **(A)**, 1.75 hpf **(B–H)** and 2 hpf **(I-P)**. Hoechst labeling of nuclei is shown in blue, Dro-lt-AQP1 immunofluorescence is shown in red **(A,B,E,F,I,J,M,N)** or grey-scale **(C,G,K,O)** and acetylated/tyrosinated alpha-tubulin immunofluorescence is shown in yellow **(B,F,J,N)** or grey-scale **(D,H,L,P)**. AB and CD blastomere morphology and cleavage cavity expansion are shown in overlays of brightfield images with Dro-lt-AQP1 immunofluorescence **(A,E,I,M)**. Midbodies are numbered in the order of their formation during the first (1) and second cleavages (2 and 3). The arrow in (**e**) indicates Dro-lt-AQP1 accumulation prior to formation of the second midbody between blastomeres C and D. Double-headed arrows in **(I,M)** indicate the direction of cleavage cavity expansion. **(N–O)** Close-up of a cytokinetic bridge and Dro-lt-AQP1 immunoreactive midbody. Scale bars, 10 μm.

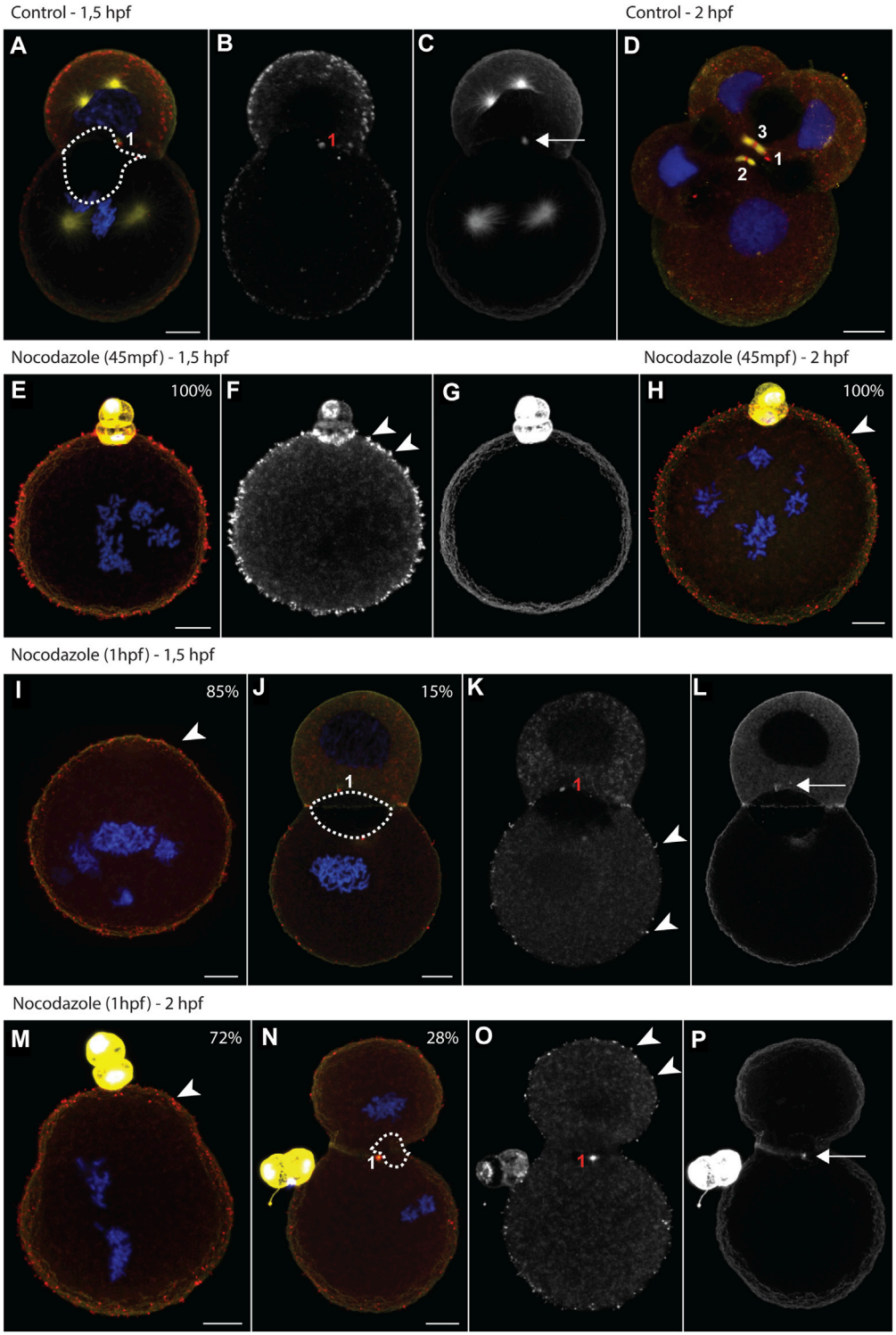

FIGURE 3 | Nocodazole treatments trigger aquaporin translocation and impair lumenogenesis. **(A–P)** Maximum intensity projections of *Dreissena rostriformis* embryos at 1.5 hpf **(A–C, E–G, I–L)** and 2 hpf **(D,H,M–P)**. Embryos were treated with 10 μM nocodazole either from 45 mpf **(E–H)** or from 1 hpf onwards **(I–P)**. Values in the upper right corner of an image indicate the percentage of embryos with the depicted phenotype for the respective treatment condition. Hoechst labeling of nuclei is shown in blue, Dro-lt-AQP1 immunofluorescence is shown in red **(A,D,E,H,I,J,M,N)** or grey-scale **(B,F,K,O)** and acetylated/tyrosinated alpha-tubulin immunofluorescence is shown in yellow **(A,D,E,H,I,J,M,N)** or grey-scale **(C,G,L,P)**. Midbodies are numbered in the order of their formation during the first (1) and second cleavages (2 and 3). The dotted outline in **(A,J,N)** indicates the maximal expansion of the cleavage cavity. Arrows indicate remnants of the cytokinetic bridge **(C,L,P)** and arrowheads point to Dro-lt-AQP1-immunoreactive membrane protrusions **(F,H,I,K,M,O)**. Scale bars, 10 μm.

almost simultaneously (**Figures 2I,M**). Notably, the midbody remnant gradually shifts towards the newly formed Dro-lt-AQP1-immunoreactive midbodies in the center of the developing embryo (**Figures 2I–M**). This likely allows for a precise temporal and spatial control over the water efflux from each blastomere, since we observed no Dro-lt-AQP1 accumulation in other areas of the embryos' cell membranes. Midbody remnants have been shown to influence multiple postmitotic processes, including lumenogenesis, cell proliferation, cell signalling, cell polarity and fate specification as well as the formation of polarized structures such as neurites and cilia (Antanavičiūtė et al., 2018; Peterman and Prekeris, 2019; Labat-de-Hoz et al., 2021). As such, there is a noteworthy overlap with known roles of AQPs not only in lumenogenesis (Huebert et al., 2002; Hashizume and Hieda, 2006; Ferrari et al., 2008; Khan et al., 2013), but also in the regulation of cell stemness and proliferation (Galán-Cobo et al., 2016; Dajani et al., 2018; Jung et al., 2021).

Our findings show that intercellular lumenogenesis in early cleavage stages of *D. rostriformis* is likely mediated by Dro-lt-AQP1 localized in the midbody and midbody remnant. Given their above-mentioned multifunctional properties, this close association between midbodies and AQPs may have important implications for various cellular events, warranting further investigations.

Depolymerisation of Cytokinetic Bridge Microtubules Triggers Ectopic AQP Translocation and Impairs Both Lumenogenesis and Osmoregulation

Our next aim was to prevent Dro-lt-AQP1 targeting to the midbody in order to assess its potential involvement in lumenogenesis and osmoregulation. For early animal cleavage stages, 10 μM nocodazole has been shown to be sufficient to completely depolymerize spindle microtubules (Chenevert et al., 2020). Such treatments can have confounding effects, since they interrupt cellular trafficking. However, nocodazole is widely used in cell biology studies and is not known to impair cellular osmoregulation [i.e., no significant increase in cell volume and no significant effect on a cells ability to recover from hypoosmotic shock, e.g., see (Fernández and Pullarkat, 2010)]. Furthermore, we timed our experiments to specifically target the period of midbody formation and to minimize the duration of drug exposure.

One-cell stage embryos of *D. rostriformis* were exposed to nocodazole either from 45 mpf (minutes post fertilization), i.e., after nuclear division but prior to cytokinetic bridge formation, or from 1 hpf (hours post fertilization), i.e., from early stages of cytokinetic bridge and midbody formation. Drug treatments were maintained for 30, 45, 60 or 75 min. Afterwards, the embryos were fixed either at the two-cell stage (1.5 hpf) or at the four-cell stage (2 hpf) (**Figure 3**). For each condition, the exact number of specimens analyzed ($n > 20$) and all raw data are provided in **Supplementary Data S1**.

Nocodazole treatment at 45 mpf inhibits cytokinesis entirely (**Figures 3E–H**, **Figure 4A**). By 1.5 hpf, 95% of the control embryos are at the two-cell stage (**Figures 3A–C**), whereas 100% of the treated embryos remain at the one-cell stage (**Figures 3E–G**, **Figure 4A**). By 2 hpf, 90% of the control embryos are at the four-cell stage (**Figure 3D**), whereas 100% of the treated embryos still remain at the one-cell stage (**Figure 3H**, **Figure 4A**). One-cell stage embryos lack a cytokinetic bridge and a Dro-lt-AQP1-immunoreactive midbody that could mediate water excretion. However, nocodazole treatment at 45 mpf triggers the ectopic formation of Dro-lt-AQP1-immunoreactive membrane protrusions that are not present in control embryos (**Figures 3E–H**, arrowheads). Such protrusions can be caused by AQP-mediated water effluxes from a cell (Karlsson et al., 2013), which is consistent with our observation that the total cell volume of embryos treated at 45 mpf increases only slightly (but significantly) compared to control embryos (**Figure 4F**). Accordingly, ectopic translocation of AQP to the cell membrane likely allows for a limited compensation of osmotic water influx, preventing cell swelling beyond a certain point and osmotic lysis.

This is consistent with data from vertebrates, where various triggers have been shown to induce the reversible sub-cellular translocation of AQPs in order to maintain water homeostasis (Conner et al., 2013). However, it remains to be determined whether the observed Dro-lt-AQP1 redistribution is a natural response to increased hypoosmotic stress or due to nocodazole-induced disruption of polarized membrane trafficking. It should further be noted that early treated embryos are unable to revert to their original volume at later stages (2 hpf, **Figure 4F**), which shows that their osmoregulation capacity is long-term impaired.

Nocodazole treatment from 1 hpf results in two phenotypes (**Figures 3I–P**, **Figure 4A**). At 1.5 hpf, 15% of the embryos are at the two-cell stage (**Figures 3J–L**), while the rest remain at the one-cell stage (**Figure 3I**). By 2 hpf, the number of embryos at the two-cell stage increases to 28%, while the rest still remain at the one-cell stage (**Figures 3M–P**). The two-cell stage embryos show a Dro-lt-AQP1-immunoreactive midbody remnant and a small cleavage cavity (**Figures 3J–L, N–P**). At 1.5 hpf, the cell volume of both their AB and CD blastomeres is significantly increased (**Figure 4C**). Furthermore, embryos at 1.5 hpf show a significantly higher total cell volume if treated from 1 hpf than if treated from 45 mpf onwards (**Figure 4F**). This is likely because they had 15 min less time to react to nocodazole exposure, e.g., by forming Dro-lt-AQP1-immunoreactive membrane protrusions (**Figures 3F,I–K** arrowheads). The cleavage cavity volume of late treated embryos at both 1.5 and 2 hpf is significantly decreased (**Figure 4E**), indicating reduced water excretion into this intercellular space after cytokinetic bridge disruption. Importantly, however, embryos at 2 hpf show a significantly lower total cell volume, if treated from 1 hpf compared to if treated from 45 mpf (**Figures 3H,N–P**, **Figure 4F**). Reversal of the initial cell volume increase in late treated embryos shows that their osmoregulation capacity is not long-term impaired (as in early treated embryos) but only briefly interrupted, when cytokinetic bridge and midbody formation is not prevented but only partially disrupted (**Figure 4F**).

These data illustrate how cytokinetic bridge disruption impairs lumenogenesis and cellular osmoregulation, although

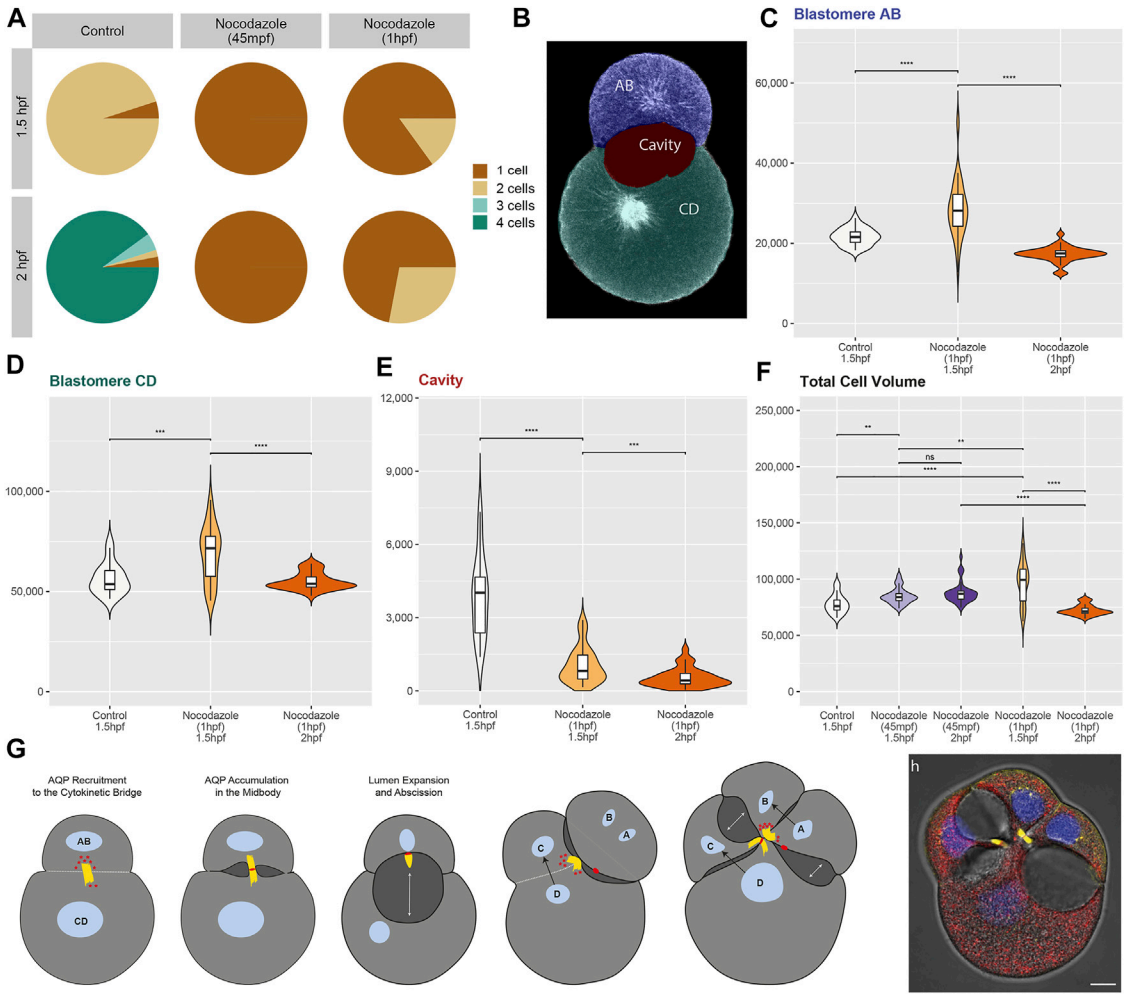

FIGURE 4 | Statistical analyses of nocodazole phenotypes and model of aquaporin function in *Dreissena rostriformis*. **(A)** Pie charts depict the percentage of one-, two-, three- and four-cell stages for embryos at 1.5 and 2 hpf that were exposed to different treatment conditions as indicated. **(B)** Single optical section with areas used for image segmentation and volumetric measurements colorized. **(C–F)** Violin plots illustrate volume distributions in μm³ for the AB blastomere **(C)**, the CD blastomere **(D)**, the cleavage cavity **(E)** and the total cell volume (i.e., AB + CD volumes) **(F)** of embryos exposed to different treatment conditions. For nocodazole treatments from 1hpf, only embryos with a two-cell stage phenotype were analyzed. To compare different conditions, a two-sided Wilcoxon rank-sum test was used with several *p*-value thresholds (****p =< 1e-04, ***p =< 0.001, **p =< 0.01, *p =< 0.05, n. s $p > 0.05$). Comparisons were only made between embryos that are either at the same stage, have the same number of blastomeres or were exposed to the same treatment. **(G)** Schematic representation of the here-proposed model of lumenogenesis. Recruitment of AQP (red) via a cytokinetic bridge (yellow) to the midbody leads to the formation of cleavage cavities (dark grey). Black arrows indicate the direction of blastomere division and double-headed white arrows indicate the direction of cleavage cavity expansion. **(H)** Overlay of a brightfield image and a maximum intensity projection of a control embryo at 2 hpf labeled for Dro-lt-AQP1 immunoreactivity (red), acetylated/tyrosinated alpha-tubulin immunoreactivity (yellow) and Hoechst nuclear staining (blue). Scale bar, 10 μm.

the latter was partially restored through subsequent translocation of Dro-lt-AQP1 to the cell membrane. We further show that presence of at least an incomplete Dro-lt-AQP1-immunoreactive midbody remnant after cytokinetic bridge depolymerization greatly improves the ability of embryos to compensate for hypoosmotic water influx. Accordingly, since Dro-lt-AQP1 is the only water channel expressed in early developmental stages of *Dreissena rostriformis* (Gene.75921, Figure S18 in Calcino et al., 2019) and exclusively detected in the cytosol (storage) and in the midbody of untreated embryos (**Figures 1**, **2**), we argue that midbody-localized Dro-lt-AQP1 plays a central role in cleavage cavity formation.

In sum, we propose a novel mode of lumenogenesis (**Figures 4G,H**) that involves AQP recruitment specifically to the midbody during cytokinesis. Temporal and spatial control over cellular water release is likely achieved through placement, inheritance and maintenance of AQP-containing midbodies and midbody remnants. The large cleavage cavities of the quagga mussel, *Dreissena rostriformis,* are an adaptation to freshwater habitats (Calcino et al., 2019). However, the relatively simple mechanism underlying their controlled formation is likely to be widespread among Metazoa. As summarized in **Supplementary Data S2**, AQPs are present in the zygotes and initial cleavage stages of all investigated species, ranging from cnidarians to vertebrates.

While AQPs may serve various functions in these different embryos, they have been implicated in blastocyst cavity formation in mouse (Barcroft et al., 2003; Offenberg and Thomsen, 2005; Frank et al., 2019). Moreover, previously published AQP immunostainings in mammalian oocytes and embryos from zygote to bastocyst stages actually appear to show labelling of cytokinetic bridge- and midbody-like structures that have not been addressed (Xiong et al., 2013; Park et al., 2014; Park and Cheon, 2015). We therefore suggest that the here-described mechanism of lumenogenesis, via AQP-recruitment to the cytokinetic midbody, may be critical for early animal embryogenesis and should be investigated in more taxa.

DATA AVAILABILITY STATEMENT

The original contributions presented in the study are included in the article/**Supplementary Material**, further inquiries can be directed to the corresponding authors.

AUTHOR CONTRIBUTIONS

AC and EZ conceptualized the study, EZ carried out experiments and drafted the manuscript, TS and EZ analyzed the data, IB and KB contributed to antibody validation, AW contributed to interpretation and discussion of the data and to finalizing the manuscript. All authors commented on and approved the final version of the manuscript.

FUNDING

The research leading to these results has received funding from the Austrian Research Fund (FWF) grant P29455-B29 to AW.

ACKNOWLEDGMENTS

We thank Christian Baranyi and Nadja Hattinger for support with animal logistics and handling as well as Nicolas S.M. Robert for help with statistical analyses.

SUPPLEMENTARY MATERIAL

The Supplementary Material for this article can be found online at: https://www.frontiersin.org/articles/10.3389/fcell.2022.894434/full#supplementary-material

REFERENCES

Antanavičiūtė, I., Gibieža, P., Prekeris, R., and Skeberdis, V. A. (2018). Midbody: From the Regulator of Cytokinesis to Postmitotic Signaling Organelle. *Medicina* 54, 53. doi:10.3390/medicina54040053

Arnspang, E. C., Sengupta, P., Mortensen, K. I., Jensen, H. H., Hahn, U., Jensen, E. B. V., et al. (2019). Regulation of Plasma Membrane Nanodomains of the Water Channel Aquaporin-3 Revealed by Fixed and Live Photoactivated Localization Microscopy. *Nano Lett.* 19, 699–707. doi:10.1021/acs.nanolett.8b03721

Barcroft, L. C., Offenberg, H., Thomsen, P., and Watson, A. J. (2003). Aquaporin Proteins in Murine Trophectoderm Mediate Transepithelial Water Movements during Cavitation. *Dev. Biol.* 256, 342–354. doi:10.1016/S0012-1606(02)00127-6

Calcino, A. D., de Oliveira, A. L., Simakov, O., Schwaha, T., Zieger, E., Wollesen, T., et al. (2019). The Quagga Mussel Genome and the Evolution of Freshwater Tolerance. *DNA Res.* 26, 411–422. doi:10.1093/dnares/dsz019

Campbell, E. M., Ball, A., Hoppler, S., and Bowman, A. S. (2008). Invertebrate Aquaporins: a Review. *J. Comp. Physiol. B* 178, 935–955. doi:10.1007/s00360-008-0288-2

Capalbo, L., Bassi, Z. I., Geymonat, M., Todesca, S., Copoiu, L., Enright, A. J., et al. (2019). The Midbody Interactome Reveals Unexpected Roles for PP1 Phosphatases in Cytokinesis. *Nat. Commun.* 10, 4513. doi:10.1038/s41467-019-12507-9

Chan, C. J., Costanzo, M., Ruiz-Herrero, T., Mönke, G., Petrie, R. J., Bergert, M., et al. (2019). Hydraulic Control of Mammalian Embryo Size and Cell Fate. *Nature* 571, 112–116. doi:10.1038/s41586-019-1309-x

Chenevert, J., Roca, M., Besnardeau, L., Ruggiero, A., Nabi, D., McDougall, A., et al. (2020). The Spindle Assembly Checkpoint Functions during Early Development in Non-chordate Embryos. *Cells* 9, 1087. doi:10.3390/cells9051087

Conner, A. C., Bill, R. M., and Conner, M. T. (2013). An Emerging Consensus on Aquaporin Translocation as a Regulatory Mechanism. *Mol. Membr. Biol.* 30, 101–112. doi:10.3109/09687688.2012.743194

Conner, M. T., Conner, A. C., Bland, C. E., Taylor, L. H. J., Brown, J. E. P., Parri, H. R., et al. (2012). Rapid Aquaporin Translocation Regulates Cellular Water Flow. *J. Biol. Chem.* 287, 11516–11525. doi:10.1074/jbc.M111.329219

Dajani, S., Saripalli, A., and Sharma-Walia, N. (2018). Water Transport Proteins-Aquaporins (AQPs) in Cancer Biology. *Oncotarget* 9, 36392–36405. doi:10.18632/oncotarget.26351

Datta, A., Bryant, D. M., and Mostov, K. E. (2011). Molecular Regulation of Lumen Morphogenesis. *Curr. Biol.* 21, R126–R136. doi:10.1016/j.cub.2010.12.003

D'Avino, P. P., Giansanti, M. G., and Petronczki, M. (2015). Cytokinesis in Animal Cells. *Cold Spring Harb. Perspect. Biol.* 7, a015834. doi:10.1101/cshperspect.a015834

Day, R. E., Kitchen, P., Owen, D. S., Bland, C., Marshall, L., Conner, A. C., et al. (2014). Human Aquaporins: Regulators of Transcellular Water Flow. *Biochimica Biophysica Acta (BBA) - General Subj.* 1840, 1492–1506. doi:10.1016/j.bbagen.2013.09.033

Dionne, L. K., Wang, X.-J., and Prekeris, R. (2015). Midbody: from Cellular Junk to Regulator of Cell Polarity and Cell Fate. *Curr. Opin. Cell Biol.* 35, 51–58. doi:10.1016/j.ceb.2015.04.010

Dumortier, J. G., Le Verge-Serandour, M., Tortorelli, A. F., Mielke, A., de Plater, L., Turlier, H., et al. (2019). Hydraulic Fracturing and Active Coarsening Position the Lumen of the Mouse Blastocyst. *Science* 365, 465–468. doi:10.1126/science.aaw7709

Eme, L., Moreira, D., Talla, E., and Brochier-Armanet, C. (2009). A Complex Cell Division Machinery Was Present in the Last Common Ancestor of Eukaryotes. *PLoS ONE* 4, e5021. doi:10.1371/journal.pone.0005021

Fernández, P., and Pullarkat, P. A. (2010). The Role of the Cytoskeleton in Volume Regulation and Beading Transitions in PC12 Neurites. *Biophysical J.* 99, 3571–3579. doi:10.1016/j.bpj.2010.10.027

Ferrari, A., Veligodskiy, A., Berge, U., Lucas, M. S., and Kroschewski, R. (2008). ROCK-mediated Contractility, Tight Junctions and Channels Contribute to the Conversion of a Preapical Patch into Apical Surface during Isochoric Lumen Initiation. *J. Cell Sci.* 121, 3649–3663. doi:10.1242/jcs.018648

Frank, L. A., Rose, R. D., Anastasi, M. R., Tan, T. C. Y., Barry, M. F., Thompson, J. G., et al. (2019). Artificial Blastocyst Collapse Prior to Vitrification Significantly Improves Na+/K+-ATPase-dependent Post-warming Blastocoel Re-expansion Kinetics without Inducing Endoplasmic Reticulum Stress Gene Expression in the Mouse. *Reprod. Fertil. Dev.* 31, 294. doi:10.1071/RD17500

Frémont, S., and Echard, A. (2018). Membrane Traffic in the Late Steps of Cytokinesis. *Curr. Biol.* 28, R458–R470. doi:10.1016/j.cub.2018.01.019

Galán-Cobo, A., Ramírez-Lorca, R., and Echevarría, M. (2016). Role of Aquaporins in Cell Proliferation: What Else beyond Water Permeability? *Channels* 10, 185–201. doi:10.1080/19336950.2016.1139250

Hashizume, A., and Hieda, Y. (2006). Hedgehog Peptide Promotes Cell Polarization and Lumen Formation in Developing Mouse Submandibular Gland. *Biochem. Biophysical Res. Commun.* 339, 996–1000. doi:10.1016/j.bbrc.2005.11.106

Hu, C.-K., Coughlin, M., and Mitchison, T. J. (2012). Midbody Assembly and its Regulation during Cytokinesis. *MBoC* 23, 1024–1034. doi:10.1091/mbc.e11-08-0721

Huebert, R. C., Splinter, P. L., Garcia, F., Marinelli, R. A., and LaRusso, N. F. (2002). Expression and Localization of Aquaporin Water Channels in Rat Hepatocytes. *J. Biol. Chem.* 277, 22710–22717. doi:10.1074/jbc.M202394200

Ishibashi, K., Morishita, Y., and Tanaka, Y. (2017). "The Evolutionary Aspects of Aquaporin Family," in Aquaporins *Advances in Experimental Medicine and Biology*. Editor B. Yang (Dordrecht: Springer Netherlands), 35–50. doi:10.1007/978-94-024-1057-0_2

Jewett, C. E., and Prekeris, R. (2018). Insane in the Apical Membrane: Trafficking Events Mediating Apicobasal Epithelial Polarity during Tube Morphogenesis. *Traffic* 19, 666–678. doi:10.1111/tra.12579

Jung, H. J., Jang, H.-J., and Kwon, T.-H. (2021). Aquaporins Implicated in the Cell Proliferation and the Signaling Pathways of Cell Stemness. *Biochimie* 188, 52–60. doi:10.1016/j.biochi.2021.04.006

Karatayev, A. Y., Burlakova, L. E., and Padilla, D. K. (2015). Zebra versus Quagga Mussels: a Review of Their Spread, Population Dynamics, and Ecosystem Impacts. *Hydrobiologia* 746, 97–112. doi:10.1007/s10750-014-1901-x

Karlsson, T., Bolshakova, A., Magalhães, M. A. O., Loitto, V. M., and Magnusson, K.-E. (2013). Fluxes of Water through Aquaporin 9 Weaken Membrane-Cytoskeleton Anchorage and Promote Formation of Membrane Protrusions. *PLoS ONE* 8, e59901. doi:10.1371/journal.pone.0059901

Khan, L. A., Zhang, H., Abraham, N., Sun, L., Fleming, J. T., Buechner, M., et al. (2013). Intracellular Lumen Extension Requires ERM-1-dependent Apical Membrane Expansion and AQP-8-Mediated Flux. *Nat. Cell Biol.* 15, 143–156. doi:10.1038/ncb2656

Klinkert, K., Rocancourt, M., Houdusse, A., and Echard, A. (2016). Rab35 GTPase Couples Cell Division with Initiation of Epithelial Apico-Basal Polarity and Lumen Opening. *Nat. Commun.* 7, 11166. doi:10.1038/ncomms11166

Labat-de-Hoz, L., Rubio-Ramos, A., Casares-Arias, J., Bernabé-Rubio, M., Correas, I., and Alonso, M. A. (2021). A Model for Primary Cilium Biogenesis by Polarized Epithelial Cells: Role of the Midbody Remnant and Associated Specialized Membranes. *Front. Cell Dev. Biol.* 8, 622918. doi:10.3389/fcell.2020.622918

Laundon, D., Larson, B. T., McDonald, K., King, N., and Burkhardt, P. (2019). The Architecture of Cell Differentiation in Choanoflagellates and Sponge Choanocytes. *PLoS Biol.* 17, e3000226. doi:10.1371/journal.pbio.3000226

Li, Y., He, L., Gonzalez, N. A. P., Graham, J., Wolgemuth, C., Wirtz, D., et al. (2017). Going with the Flow: Water Flux and Cell Shape during Cytokinesis. *Biophysical J.* 113, 2487–2495. doi:10.1016/j.bpj.2017.09.026

Liu, H., and Wintour, E. M. (2005). Aquaporins in Development - a Review. *Reprod. Biol. Endocrinol.* 3, 18. doi:10.1186/1477-7827-3-18

Martínez, N., and Damiano, A. E. (2017). "Aquaporins in Fetal Development," in Aquaporins *Advances in Experimental Medicine and Biology*. Editor B. Yang (Dordrecht: Springer Netherlands), 199–212. doi:10.1007/978-94-024-1057-0_13

Mazzaferri, J., Costantino, S., and Lefrancois, S. (2013). Analysis of AQP4 Trafficking Vesicle Dynamics Using a High-Content Approach. *Biophysical J.* 105, 328–337. doi:10.1016/j.bpj.2013.06.010

Meisenheimer, J. (1901). Entwicklungsgeschichte von *Dreissensia polymorpha* Pall. *Z. für Wiss. Zool.* 69, 1–13. doi:10.5962/bhl.title.47150

Offenberg, H., and Thomsen, P. D. (2005). Functional Challenge Affects Aquaporin mRNA Abundance in Mouse Blastocysts. *Mol. Reprod. Dev.* 71, 422–430. doi:10.1002/mrd.20306

Otegui, M. S., Verbrugghe, K. J., and Skop, A. R. (2005). Midbodies and Phragmoplasts: Analogous Structures Involved in Cytokinesis. *Trends Cell Biol.* 15, 404–413. doi:10.1016/j.tcb.2005.06.003

Park, J.-W., and Cheon, Y.-P. (2015). Temporal Aquaporin 11 Expression and Localization during Preimplantation Embryo Development. *Dev. Reprod.* 19, 53–60. doi:10.12717/devrep.2015.19.1.053

Park, J.-W., Shin, Y. K., and Choen, Y.-P. (2014). Adaptive Transition of Aquaporin 5 Expression and Localization during Preimplantation Embryo Development by *In Vitro* Culture. *Dev. Reproducit.* 18, 153–160. doi:10.12717/DR.2014.18.3.153

Peterman, E., and Prekeris, R. (2019). The Postmitotic Midbody: Regulating Polarity, Stemness, and Proliferation. *J. Cell Biol.* 218, 3903–3911. doi:10.1083/jcb.201906148

Rathbun, L. I., Colicino, E. G., Manikas, J., O'Connell, J., Krishnan, N., Reilly, N. S., et al. (2020). Cytokinetic Bridge Triggers De Novo Lumen Formation *In Vivo*. *Nat. Commun.* 11, 1269. doi:10.1038/s41467-020-15002-8

Rodriguez-Fraticelli, A. E., Vergarajauregui, S., Eastburn, D. J., Datta, A., Alonso, M. A., Mostov, K., et al. (2010). The Cdc42 GEF Intersectin 2 Controls Mitotic Spindle Orientation to Form the Lumen during Epithelial Morphogenesis. *J. Cell Biol.* 189, 725–738. doi:10.1083/jcb.201002047

Román-Fernández, A., and Bryant, D. M. (2016). Complex Polarity: Building Multicellular Tissues through Apical Membrane Traffic. *Traffic* 17, 1244–1261. doi:10.1111/tra.12417

Rudstam, L. G., and Gandino, C. J. (2020). Zebra or Quagga Mussel Dominance Depends on Trade-Offs between Growth and Defense-Field Support from Onondaga Lake, NY. *PLoS ONE* 15, e0235387. doi:10.1371/journal.pone.0235387

Schneider, C. A., Rasband, W. S., and Eliceiri, K. W. (2012). NIH Image to ImageJ: 25 Years of Image Analysis. *Nat. Methods* 9, 671–675. doi:10.1038/nmeth.2089

Sundaram, M. V., and Buechner, M. (2016). The *Caenorhabditis elegans* Excretory System: A Model for Tubulogenesis, Cell Fate Specification, and Plasticity. *Genetics* 203, 35–63. doi:10.1534/genetics.116.189357

Vukićević, T., Schulz, M., Faust, D., and Klussmann, E. (2016). The Trafficking of the Water Channel Aquaporin-2 in Renal Principal Cells-A Potential Target for Pharmacological Intervention in Cardiovascular Diseases. *Front. Pharmacol.* 7, 23. doi:10.3389/fphar.2016.00023

Watson, A. J., Natale, D. R., and Barcroft, L. C. (2004). Molecular Regulation of Blastocyst Formation. *Animal Reproduction Sci.* 82 (83), 583–592. doi:10.1016/j.anireprosci.2004.04.004

Xiong, Y., Tan, Y.-J., Xiong, Y.-M., Huang, Y.-T., Hu, X.-L., Lu, Y.-C., et al. (2013). Expression of Aquaporins in Human Embryos and Potential Role of AQP3 and AQP7 in Preimplantation Mouse Embryo Development. *Cell Physiol. Biochem.* 31, 649–658. doi:10.1159/000350084

Yagisawa, F., Fujiwara, T., Takemura, T., Kobayashi, Y., Sumiya, N., Miyagishima, S.-y., et al. (2020). ESCRT Machinery Mediates Cytokinetic Abscission in the Unicellular Red Alga Cyanidioschyzon Merolae. *Front. Cell Dev. Biol.* 8, 169. doi:10.3389/fcell.2020.00169

Conflict of Interest: The authors declare that the research was conducted in the absence of any commercial or financial relationships that could be construed as a potential conflict of interest.

Publisher's Note: All claims expressed in this article are solely those of the authors and do not necessarily represent those of their affiliated organizations, or those of the publisher, the editors and the reviewers. Any product that may be evaluated in this article, or claim that may be made by its manufacturer, is not guaranteed or endorsed by the publisher.

frontiers in Ecology and Evolution

PERSPECTIVE
published: 03 December 2021
doi: 10.3389/fevo.2021.745564

On the Nature of Organs and Organ Systems – A Chapter in the History and Philosophy of Biology

*Alessandro Minelli**

Department of Biology, University of Padova, Padua, Italy

Contrasting definitions of organs based either on function or on strictly morphological criteria are the legacy of a tradition starting with Aristotle. This floating characterization of organs in terms of both form and function extends also to organ systems. The first section of this review outlines the notions of organ and body part as defined, explicitly or implicitly, in representative works of nineteenth century's comparative morphology. The lack of a clear distinction between the two notions led to problems in Owen's approach to the comparative method (definition of homolog vs. nature of the vertebrate archetype) and to a paradoxical formulation, by Anton Dohrn, of the principle of functional change. Starting from the second half of the twentieth century, with the extensive use of morphological data in phylogenetic analyses, both terms – organ and body part – have been often set aside, to leave room for a comparison between variously characterized attributes (character states) of the taxa to be compared. Throughout the last two centuries, there have been also efforts to characterize organs or body parts in terms of the underlying developmental dynamics, both in the context of classical descriptive embryology and according to models suggested by developmental genetics. Functionally defined organ are occasionally co-extensive with morphologically defined body parts, nevertheless a clear distinction between the former and the latter is a necessary prerequisite to a study of their evolution: this issue is discussed here on the example of the evolution of hermaphroditism and gonad structure and function.

Keywords: organ, body part, organ system, Dohrn, Owen, hermaphroditism, homology, evolutionary morphology

OPEN ACCESS

Edited by:
Andreas Wanninger, University of Vienna, Austria

Reviewed by:
James Richard Griesemer, University of California, Davis, United States
Pedro Martinez, University of Barcelona, Spain
Ignacio Maeso, Andalusian Center for Development Biology (CABD), Spain

***Correspondence:**
Alessandro Minelli
alessandro.minelli@unipd.it

Specialty section:
This article was submitted to Evolutionary Developmental Biology, a section of the journal Frontiers in Ecology and Evolution

Received: *22 July 2021*
Accepted: *08 November 2021*
Published: *03 December 2021*

Citation:
Minelli A (2021) On the Nature of Organs and Organ Systems – A Chapter in the History and Philosophy of Biology. Front. Ecol. Evol. 9:745564. doi: 10.3389/fevo.2021.745564

INTRODUCTION

Five years ago, in a paper published in a medical journal, Coffey and O'Leary (2016) proposed that the mesentery is an organ of the human body and, as such, should be added to the traditional list of human organs, as item No. 79. In a timely review of that article, Neumann (2017) remarked that "no two anatomists are likely to compile identical lists of the organs of the human body," largely because of the vague current notions of organ, "commonly defined in medical dictionaries as a (somewhat independent) part of the body that performs a (vital or special) function."

Despite an admittedly high level of indeterminacy, this tentative definition of organ as a body part with a well-defined function reveals two important features that have accompanied the usage of the term since classical antiquity: on the one side, individual organs *are parts of the body*; on the other, individual organs *perform distinct functions*. Sensible (or poorly informative, according to personal preferences) as it may appear, this twofold identity of organs opens a series of questions. First, are there body parts that are not organs? Yes, there are, for example body regions such as head,

thorax and abdomen, or complex morphological units such as the trunk segments of centipedes. Second, and more interesting, is function, rather than morphology (form, position), the criterion based on which we can (must?) recognize organs?

Russell's (1916) classic monograph on the history of morphology is still a good guide to learn how (or how little) the notion of organ has being changing over the centuries, endlessly oscillating between a functional and a strictly morphological definition, but a look at the original texts is often necessary. In the next section I will thus provide short excerpts from the old literature: for the texts originally in French or German, translation is mine.

As recognized by Haeckel (1866) in his sensible dissection of mid nineteenth century's comparative morphology, this floating characterization of organs in terms of both form and function also extends to the characterization of organ complexes.

We will subsequently see how the lack of a clear distinction between the two notions led to a paradoxical formulation, by Dohrn (1875), of the principle of functional change.

Starting from the second half of the twentieth century, with the extensive use of morphological data in phylogenetic analyses, both terms – organ and body part – have been often set aside, to leave room for a comparison between variously characterized attributes (character states) of the taxa to be compared.

In a number of instances, a functionally defined organ will be co-extensive with a morphologically defined body part, nevertheless a clear distinction between the former and the latter is a necessary prerequisite to a study of their evolution: in a later section of this article, I will discuss this issue on the example of hermaphroditism.

THE DEFINITION OF AN ORGAN

Organ: Morphological or Functional Concept?

The primacy of function over morphology seems to be largely accepted. To cite from the introduction (p. 1) to Schmidt-Rhaesa's (2007) book on *The Evolution of Organ Systems*: "Despite their diversity, all animals have several basic requirements. They have to gather and digest food, get rid of excretes, receive and process information, and so on. The animal body is made up of parts that deal with these requirements and these parts are generally called organs or organ systems."

Eventually, Schmidt-Rhaesa's (2007) catalog of organs includes both items defined by function (e.g., acoustic, balance, cerebral, chordotonal, copulatory, excretory, hydrostatical, phagocytotic, pumping, reproductive, respiratory, sensory, spermatophore-forming, sperm-receiving, and statoacustic organs, plus eyes, gonads, muscles, and ocelli) and items defined by morphology, especially by position (e.g., apical, caudal, intertentacular, nuchal, and ventral organs). This seems to be uncontroversial, but in fact reveals a conceptual interweaving of concepts and definitions originated from within the different disciplines – medicine, natural history and philosophy – that contributed to emergence of biology as the science of the living (e.g., Zammito, 2018; Minelli, 2020).

From Aristotle to Geoffroy Saint-Hilaire

Russell (1916) defined Aristotle's *De Partibus Animalium* (cf. Lennox, 2001) as "a comparative organography": the term may suggest attention to the shape of the various organs and their spatial relationships, but Aristotle was interested above all in the function of the different organs.

Two thousand years later, this was still true of the first great comparative anatomists of the French school, both of those in the medical profession (therefore especially knowledgeable and interested in human anatomy), like Félix Vicq-d'Azyr, and of those, like Georges Cuvier, who developed in the natural sciences their whole scientific and academic careers.

Vicq-d'Azyr (1792) opened his long essay on comparative anatomy with a list of the "nine characters or general properties of life; namely: 1. digestion; 2. nutrition; 3. circulation; 4. breathing; 5. secretions; 6. ossification; 7. generation; 8. irritability; and 9. sensibility." (p. iv). Organs are the tools through which the different functions are performed. The author examined them in the order indicated and for each function he reviewed the various zoological groups (and also plants, occasionally), in order of decreasing complexity of the organs that serve the specific function. But in the following pages Vicq-d'Azyr reversed the perspective, adopting instead a morphological criterion: in his "Table of animals according to the order of their anatomical composition," he recognized twelve groups, from the simplest, such as hydra and other polyps, that have only one organ, the stomach, up to the most complex, i.e., mammals (incl. cetaceans, although listed in the table as a distinct class). And in building an "Essay of physiological classification of the Insects" Vicq-d'Azyr adopted mixed criteria (both the function and the shape of the organs).

Function was also in the foreground in Bichat's (1801, p. lxxix) approach: "All animals are an assemblage of various organs, each performing a function, that contribute, each in its own way, to the conservation of the whole," but the French anatomist also remarked (ibid.) that organs are "themselves formed by several tissues of very different nature, and which truly form the elements of these organs."

Moving at last into zoology as studied by zoologists, the first author to be cited is Cuvier. His position has been well characterized by Remane (1952): "Not even Cuvier managed to accomplish a theoretical distinction between functional and structural units" (p. 22). Indeed, the terms by which he identified body parts have partly functional, partly structural content; see for example the opening sentence of his "Summary idea of the functions and organs of the body of animals, as well as the various degrees of their complication": "After what we have just said of the organic elements of the body, of its chemical principles and of the forces which act in it, we have only to give a summary idea of the detailed functions of which life is composed, and of the organs that are assigned to them" (Cuvier, 1817, p. 36).

Geoffroy Saint-Hilaire's approach to comparative anatomy was very different, in that he tried to find out correspondences between pure morphological units, i.e., body parts. His message

was clear, despite the frequent differences between his and the current usage of some technical terms. For example, in the *Discours préliminaire* of his *Cours de l'histoire naturelle des Mammifères* he stressed the need to exclude the consideration of functions in any philosophical (theoretically acceptable) comparison of organs (Geoffroy Saint-Hilaire, 1828, p. 25).

ORGAN VS. BODY PART

Owen's Ambiguity: Homolog vs. Archetype

Reading the works of the comparative anatomists of the early 19th century is often difficult, not only due to the widespread uncertainty of the meaning attributed to the word "organ" by different authors, and sometimes by the same author on different pages, but also due to the frequent use of technical terms with a different meaning from what the latter have taken in the biology of our times. In the case of Geoffroy Saint-Hilaire, in particular, we must keep in mind that the entities dealt with in his *Théorie des analogues* (Geoffroy Saint-Hilaire, 1830) are, in fact, those we call homologs, while Geoffroy's *homologues* coincide more or less precisely with the body units that Owen (1849) will later describe as serial homologs. For this relationships, such as the one between the fore and hind limbs of a tetrapod, Lankester (1870) will coin the term homoplasy, which is still in use, but with completely different meaning, as structural similarity due to convergence or parallelism (Osborn, 1902, 1905; cf. Toepfer, 2011) and eventually also reversal.

The use of terms such as analogy and homology remained fluctuating, at least up to the famous definitions of Owen (1843), according to which analog is "a part or organ in one animal which has the same function as another part or organ in a different animal" (p. 374) while homolog is "the same organ in different animals under every variety of form and function" (p. 379).

Owen's definition of homolog is the starting point of all subsequent comparative morphology, largely because it seemed to be amenable to reinterpretation in evolutionary terms. Many authors, however, have pointed to an intrinsic weakness in Owen's notion of homology, i.e., the indeterminate nature of that *sameness* for which it is not easy to imagine an empirical assessment. Actually, in Owen's comparative approach there was another problematic issue, namely the failure to overcome the ambiguity between a morphological and a functional determination of the structures under comparison. In other words, Owen inherited all the uncertainty of previous authors regarding a possible distinction between organ and body part.

The ambiguity is apparent when we pass from the abstract notion of homolog to the archetypal model of the vertebrate endoskeleton that Owen developed in the following years (Owen, 1847, 1848, 1849). This archetype is a series of skeletal segments, osteocommata or vertebrae, each of which is formed in turn, "in its typical completeness," by a specified set of elements and parts. Both in its entirety and in the analytical detail of the parts that compose it, this archetype is not an organ (or an organ system) at all, but a structurally ordered set of body parts.

This archetype lends itself to the most diverse transformations, which involve changes, even radical, of both form and function, as magnificently illustrated in the large plate included in the essay *On the Nature of Limbs (*Owen, 1849). Owen's archetype is therefore an invariant on the basis of which it is possible to identify homologies – but these are clearly correspondences between body parts (essentially, the parts of the skeleton) based on their mutual topological relationships rather than correspondences between the units traditionally described as organs.

Aware of this ambiguity, Haeckel (1866) observed that there are problems with the traditional classification of body parts into tissues, organs, systems, apparatuses, etc., in that one thinks sometimes more of their morphological, sometimes more of their physiological individuality. Moreover, this terminology has been mostly produced by human anatomists who lack adequate knowledge of the diversity of morphological conditions throughout the animal kingdom.

Important traces of this anthropocentrism are still present in today's comparative anatomy. The catalog of functions recognized in our species and the names of the corresponding organs remain, as far as possible, at the basis of the organography of all animals. Of course, as studies extend to zoological groups further away from vertebrates, the discovery of organs for which it is difficult (sometimes impossible) to suggest a correspondence with an organ in the human body becomes increasingly probable. In some cases it has been found convenient to identify the newly discovered organ by the name of its discoverer, such as the "eyes" of fly larvae, known as Bolwig's organs (described in Bolwig, 1946) and the vomeronasal olfactory organ of many tetrapods, known as Jacobson's organ (named after Jacobson who described it in 1813). Human anatomy has had little need to resort to names of this type, but at least two can be cited, the organ of Corti (1851) and the organ of Zuckerkandl (1901).

The Principle of Function Change

Nowhere are the dramatic consequences of the missed distinction between organ and body part more evident than in Dohrn's (1875, p. 60) enunciation of the principle of function change (*Funktionswechsel*):

> The organ is remodeled through the succession of functions, the bearer of which remains one and the same organ. Each function is a resultant of several components, one of which is the main or primary function, while the other is an accessory or secondary function. The decrease in the main function and the increase in a secondary function change the overall function; the secondary function gradually becomes the main function, the overall function becomes different, and the consequence of the whole process is the transformation of the organ.
>
> In these words I believe I have expressed a principle, the general validity of which has not yet been adequately appreciated, however, often it may be recognized in individual cases and secretly assumed to be effective.

The difficulty of enunciating this principle in terms of organ, rather than body part, is evident in Dohrn's words. If organs are anatomical units identified by their functions, how is it possible that an organ whose functions have changed remains the same organ it was before? Dohrn tries go over this riddle by saying that the correspondence between organ and function is not one-to-one, but one-to-many. Thus, the identity of the organ is initially ensured by its main or primary function at the moment; after the *Funktionswechsel* the characterizing function will be another, but this function is not entirely new, because it was part of the complex of functions associated with the same organ before the functional shift. As a formalization of an evolutionary step, this corresponds quite closely to exaptation (Gould and Vrba, 1982) and is therefore reasonable in evolutionary terms. However, in terms of categories applicable to the structure of an organism, Dohrn's effort is perhaps the most paradoxical evidence that missing the distinction between organ and body part can lead to weak or wrong arguments.

Organ Systems

Shortly after Dohrn proposed his principle of functional change, Gegenbaur (1878, p. 14) summarized the current views on the relationship between structure and function, at last from an evolutionary perspective:

> The complication of the organism arises from separation that transfers to individual parts the physiological performance of the originally uniform body. What was previously done by the whole body, individual parts of it do after that process. The function is then either carried out by a larger number of discrete but similar parts, or the individual parts become different from one another. In the first case the division of labor is quantitative, in the latter it is also carried out qualitatively, and the division of the individual parts corresponds to a diversity of the work.

Meanwhile, Haeckel begun to address a further level of complexity that in his *Generelle Morphologie der Organismen* (General Morphology of Organisms; Haeckel, 1866) corresponds to the highest levels of the structural hierarchy he recognized in the living organisms.

If at the level of what are called organs an ambiguity has dragged on over time with respect to the two possible identification criteria, morphological and functional, can the same be said about organ systems?

According to Haeckel, the hierarchical structure of organisms is the product of two "most essential and supreme laws which guide this union of the simple form individuals [. . .] into composite ones, [. . .] the laws of aggregation or community building and of differentiation or division of labor" (p. 289). But the distinction between organ systems and apparatuses is to some extent an arbitrary one, because "In the case of an organ system one has in mind the unity of the form of its essential constituent form-elements, in an apparatus the unity of the performance of these elements" (p. 301); in other terms, "the former is based on a morphological concept, the latter on a physiological concept." "Thus, the term organ system [. . .] must [. . .] be used exclusively in its original morphological sense to denote a continuously connected organ complex in which a single tissue, i.e., a single type of cells or cell blocks occurs predominantly as an essential component, as is, e.g., the case with the nervous system, the muscular system, the system of the outer skin layers and their appendages. The situation is different with the expression organ apparatus, which is originally and usually employed in a more physiological sense, to denote a complex of organs (often [. . .] spatially separated and discontinuous, which only appears to be connected by the common criterion of the same function)" (p. 293). However, "in the concept of the organ apparatus, as it so often occurs in most other such general conceptualizations, physiological and morphological ideas are mixed up in a more or less unclear way and it is therefore difficult to establish satisfactory definitions of these higher organ units" (p. 293). Summing up, Haeckel provided a sensible analysis of the uncertain and to some extent contradictory definitions of structural and functional parts, but failed to provide a valid alternative to an unsatisfactory state of affairs that to some extent is still lasting.

Organs Without Actual Function?

To determine the importance of the functional criterion in the definition of organ (in particular, the persistence of this association in today's biology), it is worth asking: Are there organs without actual function? In other terms, is it useful (and legitimate) to define an organ in terms of its potential (rather than actual) function? The question is suggested, for instance, by the following remark: "We do not know a single instance of an organ which in the phylogenetic history first appeared as a simple Anlage without subsequent functional stage and only later in phylogeny acquired its functional stage" (Remane, 1952, p. 277). Consider for example the wing imaginal disks of holometabolous insects. It is very difficult to assign them a function in the economy of the larva. Therefore, as long as the insect is in a larval state and the imaginal disk has not yet unfolded into a wing, the imaginal disk should be considered a functionsless body part rather than an organ. A wing disk is a wing in potentiality, but not in actuality. (However, this does not rule out exaptation, as in the case of *Drosophila*, where the wing disk in the larva secretes an insulin-like peptide that coordinates tissue growth with developmental timing: Colombani et al., 2012; Garelli et al., 2012).

One may be tempted to follow the traditional adultocentric perspective, by saying that function should be best, or exclusively, determined as manifested in the adult, but this would worsen the problem. There are indeed a number of exclusively larval (and even embryonic) organs (think of the apical organ of many invertebrate larvae; Marlow et al., 2014), irrespective of their possible persistence, in modified form, in the adult of some species (as hypothesized, for example, with the possible origin of the frontal sensory organ in adults of the hoplonemertean *Quasitetrastemma stimpsoni* from the larval apical organ; Magarlamov et al., 2020). In addition, even some of the most basic vital functions, such as feeding, are frequently limited to larval or juvenile stages, as in mayflies and several other insects.

EVOLUTIONARY MORPHOLOGY

Organs and Body Parts as Attributes

In recent decades, the search for homologies and, more generally, comparative biology as a whole (not necessarily limited to morphology) have undergone important developments in the context of phylogenetics. This step was accompanied by the rapid spread of a new language, where terms such as organ or body part appear very rarely. Actually, as rightly observed by Wagner (2014), already in Simpson's (1961) and Mayr's (1969, 1982) historical approach to homology there was no longer trace of organs. Comparisons were proposed instead between *attributes* of the species under comparison. With the consolidation of phylogenetic systematics, even the term "attribute" disappeared soon: data collected in the matrices used for phylogenetic reconstructions are almost universally described as coded states of characters potentially informative from a phylogenetic perspective. In Sereno's (2007) detailed study (2007) on the *Logical basis for morphological characters in phylogenetics*, the term "organ" was mentioned only in the line reporting Owen's definition of homology. And the latter is often reformulated today without even mentioning "organ," for example: "homologous features (or states of features) in two or more organisms are those that can be traced back to the same feature (or states) in the common ancestor of those organisms" (Mayr, 1969, p. 85).

Declining interest in descriptive morphology and the common usage in comparative biology (phylogenetics) of "character" for both morphological and molecular units are probably the main reasons for this terminological mix. However, dissecting an animal's body into organs or body parts is not the same as picking convenient characters to fill a morphological data matrix for phylogenetic analysis. The nature of entries in the latter is the most diverse and these entries only occasionally correspond to the organs or body parts of descriptive morphology, less rarely in phylogenetic analyses of phylum- or class-level interrelationships, such as Eernisse et al. (1992), Backeljau (1993), Zrzavý et al. (1998), Brusca and Brusca (2003), Glenner et al. (2004), Schierwater et al. (2009), and Neumann et al. (2021).

As in the case of "organ" in the oldest literature, so the term "character" is used today in different and, very often, not explicitly defined meanings. It is likely, however, that most of the authors who use it, especially among phylogeneticists, would subscribe to Wiley's (1981, p. 8) definition of character as "a feature (attribute, observable part) of an organism" or, better perhaps, "a part or attribute of an organism that may be described, figured, measured, weighed, counted, scored, or otherwise communicated by one biologist to other biologists."

Developmental Perspectives on Organs

In addition to characterizing organs and/or parts of the body in functional or morphological terms, there have been many attempts to establish their homologies starting from the identity of their primordia, or Anlagen, or the mechanisms by which their morphogenesis unfolds (DiFrisco et al., 2020).

For example, Geoffroy Saint-Hilaire (1807) traced the homologies (*analogies*, in his terminology) between the bones of the skull of vertebrates based on the identity of the ossification centers from which their formation visibly begins, regardless of whether the anatomical part resulting from each center eventually retains its identity as a separate bone, or merges with neighboring units to form a single bone.

Later, especially under the influence of Haeckel's (1866) views on the relationships between ontogeny and phylogeny, zoologists have often accepted that each organ type derives always from the same embryonic germ layer, thus providing a homology criterion on which to rely even for anatomical comparisons between distantly related animals. Germ layers were discovered in the chicken embryo by Pander (1817), who described them as blastodermal layers (*Keimhautblätter*). von Baer (1828) regarded them as primitive organs that develop into definitive organs, typically by folding. Remak (1855, pp. 2–3) gave them the name germ layers (*Keimblätter*) and characterized them in terms of position and function, thus distinguishing an upper, sensory (*sensorielles Blatt*, *Sinnesblatt*; p. 86), an intermediate, motor and germinative (*motorisch-germinatives Blatt*; p. 101) and a lower, trophic germ layer (*trophisches Blatt*, *Darmdrüsenblatt*; p. 112). This has been eventually translated into the textbook rough summary: the ectoderm gives rise to the epidermis and the nervous system, the endoderm to the (mid)gut, the mesoderm to the remaining organs. Conserved derivation of specific organs from the same germ layer would support the homology of these organs, in the light of Owens' concept.

But this embryological criterion of homology has not been universally accepted without reservations (e.g., Wilson, 1896), as discussed by Maienschein (1978) and Hall (1995). "Homologous structures need not, and often do not, arise from the same germ layer" (Hall, 1998, p. 171; see also Oppenheimer and Hamburger, 1976); "if there is essentially similar adult structure and relative position the organs are homologous, whether they come from the same or different 'germ layers' …. After all, the different germ layers of a single individual do have the same genes" (Boyden, 1943, p. 239). But different cells, tissues and organs are more or less strictly characterized by different patterns of expression of their genes.

Some recent approaches have suggested that organs may be defined by the locally expressed gene regulatory networks (GRNs). Specifically, Wagner (2014, p. 97) introduced the notion of Character Identity Network, defined as a set of genes whose "main function is to enable the activation of a position specific and organ specific developmental program." More precisely, "The members of the network are jointly necessary for the development of the morphological character, and some of the network members are also individually sufficient to trigger the morphogenesis and differentiation of the character" (Wagner, 2014, p. 118).

However, in a subsequent revisitation, DiFrisco et al. (2020, p. 16) acknowledge that "insisting on a GRN as the basis of character identity in general would not respect the different levels of organization that these anatomical units represent," thus introduce a new conceptual model of Character Identity Mechanisms (ChIMs). This analysis involves a remarkable level of abstraction, that allows "to hypothesize level-specific 'parts' of the ChIM, appropriate for the focal anatomical unit: transcription

factors for cell types, cell types for tissue types, and signaling centers for organs." (p. 16): ChIMs are intended as "cohesive mechanisms with a recognizable causal profile that allows them to be traced through evolution as homologs despite having a diverse etiological organization. Our model hypothesizes that anatomical units at different levels of organization—cell types, tissues, and organs—have level-specific ChIMs with different conserved parts, activities, and organization." (p. 1).

However, "Some traceable body parts, such as elements of the vertebrate vascular system, may not be endowed with an identifiable ChIM [. . .] many elements of the vascular system develop from a network of blood vessels that are shaped by epigenetic factors, such as shear stress caused by blood flow and pressure differences. In these cases, an anatomical unit that bears a name and can be compared across divergent lineages does not have a specific ChIM."

Hierarchy Challenged

The latter sentence signals an interesting step away from a century-long tradition according to which units such as organs, tissues or cells are objectively given and hierarchically ordered kinds for which there must be specific causes.

Rather than representing tiers in a hierarchical organization, cells, tissues, organs or body parts are units of non-necessarily overlapping decompositions. Many tissues, such as blood, are not clearly confined spatially. In the ctenophoran *Mnemiopsis leidyi*, the patterns recognizable based on transcriptomes disclose a diversity of cell types, most of which cannot be associated with cell types distinguished by morphology or function (Sebé-Pedrós et al., 2018) and well-characterized cell types are recognizable in sponges, despite the lack in those animals of a tissue organization. Other examples are discussed in Minelli (2021).

Organs and body parts are only two of the several kinds of units into which the body has been segmented by morphologists of different times and schools. To put the discussion in full context we should broaden the scope at least to considerations of tissues and cells. However, because of strict limitation to this article's length and of the focus on organs and organ system of the whole Research Topic collection that includes it, this aspect will be simply mentioned here.

Similar to what happens at the level of organ or body part, morphology and function are not always congruent also at the level of cells. Eventually, despite the fact that morphology is usually much more accessible than evidence about function, the first criterion for classification of cell types, at least at the coarsest level (neurons, muscular fibers, secretory cells, etc.) has remained function. We may therefore say that cell types are populations of cells performing different functions (Blainey, 2017; Wagner, 2019). But a satisfactory, exhaustive classification of cell types based on function is often unattainable in practice (Lundberg and Uhlen, 2017; Sanes, 2017).

Position: Tension Between Body Part and Organ

A fascinating but little investigated aspect of the evolution of animal architecture is the tension between organs and body parts due to non-congruent evolutionary constraints. This happens frequently in miniaturized animals (reviewed in Minelli and Fusco, 2019), especially because of the resistance of the central nervous system to follow the trend in size reduction to which structural units such as segments and body regions (tagmata: head, thorax, abdomen) accommodate more easily. For example, in the larva or the adult, or both, of several miniaturized insects, a part at least of the brain is not hosted within the cephalic capsule, that is, in the head. In the larva of *Mikado* sp. (Coleoptera Ptiliidae) the brain is shifted to the thoracic segments and in the first instar larva its posterior limit reaches the second abdominal segment. In the first instar larva of *Mengenilla chobauti* (Strepsiptera) both the brain and the suboesophageal complex are hosted within the thorax and the anterior segments of the abdomen.

A CASE STUDY: THE EVOLUTION OF HERMAPHRODITISM

If nothing in biology makes sense except in the light of evolution (Dobzhansky, 1973), there is also scope for a study of the evolution of a function or a particular functional state.

If organs are defined in terms of function, while body parts are defined in terms of relative position, organs rather than body parts should be the units about which we will reconstruct a history of evolutionary change. But things are not so simple.

Let's focus on the evolutionary transitions from gonochorism to hermaphroditism and vice versa. For the sake of simplicity, let's ignore here that the term hermaphroditism covers a variety of ways in which sexes can be distributed in a population: very often, all individuals in a population produce both eggs and sperms, either sequentially or simultaneously, but in other species hermaphrodites coexist with unisexuals, more often (in animals) male only (cf. Fusco and Minelli, 2019).

One approach to the evolution of hermaphroditism, perhaps the most popular or most attractive one, is to investigate the contexts in which selection would favor either a transition from gonochorism to hermaphroditism, or the fixation of the latter condition in a more or less large lineage (e.g., Ghiselin, 1969, 1974). However, strictly focusing on the adaptive aspects we would not be able to interpret the distribution of hermaphroditism in the different clades of metazoans, because we would neglect the different constraints caused by the different architecture of the reproductive system in different lineages – that is, by their identity as body parts, rather than as organs.

Examples of the importance of distinguishing between the evolution of hermaphroditism as a function from the evolution of the uni- or bisexual gonads where sperms and eggs are produced are offered by nemerteans (ribbon worms). Most nemerteans are gonochoric, but those that produce both eggs and sperm cells have likely evolved several times independently, judging from the widely different anatomy and topography of their reproductive systems (Hyman, 1951). In ribbon worms generally, there is a row of gonads on each side of the intestine (with a single gonad or a group of gonads between two subsequent diverticula of the gut), but there are exceptions. Some hermaphroditic species have

separate male and female gonads; others produce both kinds of sex cells in the same gonad; and in *Dichonemertes*, the anterior gonads are male, the posterior ones are female (Coe, 1938): same functional status (hermaphroditism), but distinct histories of body part evolution.

Hermaphroditism is widespread in crustaceans, but very unequally distributed in the different groups. Cephalocarids and remipeds, all hermaphrodite, have distinct male and female gonads, which occupy distinct segments (Hessler et al., 1995; Kubrakiewicz et al., 2012). Most barnacles, i.e., the members of the Cirripeda Thoracica, are also hermaphrodite (but in several species dwarf functional males also occur, and a few species are gonochoric; Yusa et al., 2013). Here too, male and female gonads are well separate (Gruner, 1993). In the remaining crustacean groups, were hermaphroditism is rare and accidental, or even unknown, eggs and sperms are produced in distinct lobes of the same gonad (e.g., Larsen et al., 2015; Chen et al., 2019; Aneesh and Kappalli, 2020).

Eventually, the evolution of hermaphroditism as a function is not the same as the evolution of the uni- or bisexual gonads involved in the production of sperms and eggs. While functional considerations can explain the presence vs. absence of hermaphroditism in more or less closely related members of a clade, the evolvability of this character (and its actual phylogenetic history) are different in lineages with different body organization, that is, with different gross anatomy – number and distribution of body parts. Hermaphroditism has become the rule in groups where eggs and sperms mature in distinct gonads, but is limited to a small number of species (although, occasionally prevalent in a few lower clades, e.g., the fish families Serranidae and Sparidae) in the groups where male and female germ cells are produced within the same gonad, either simultaneously or in sequence.

CONCLUSION

Caution in respect to the conceptual or theoretical implications of terminology is of fundamental importance to sort out the mix of categories we have carried with us since the origins of biology, often concealed under polysemic terms derived from ordinary language. However, classic terms of animal morphology such as organ and organ system are probably too rooted in use to expect that they can be replaced by more precisely defined terms.

Complex systems can be decomposed in many different ways, and a choice among the alternatives is not necessarily easy (Levins, 1970; Kauffman, 1971), but this is hardly a disturbing issue from the perspective of the practicing biologist. As noted by Wimsatt (2007, p. 180), "scientists must work with this plurality of incompletely articulated and partially contradictory, partially supplementary theories and models," and different "authors make different conceptual choices in developing their technical concepts all aimed at dealing with the long-recognized fact of nature that morphology and physiology, form and function, are deeply entangled by the development, operation, and evolution of life itself" (Wimsatt, 2007, p. 190).

In a number of instances, a functionally defined organ will be co-extensive with a morphologically defined body part, nevertheless a clear distinction between the former and the latter is a necessary prerequisite to a study of their evolution: the brief discussion on hermaphroditism in the previous section has shown how attention to the categories keeps us away from the risk of collecting under the same heading phenomena or conditions that are comparable only from perspectives other than the one we are currently interested in. For comparative morphologists there is still a lot of work ahead.

AUTHOR CONTRIBUTIONS

AM is responsible for planning and writing this article.

ACKNOWLEDGMENTS

I am grateful to Andi Wanninger for inviting me to contribute to this topic collection and to James DiFrisco, Giuseppe Fusco and three reviewers for their precious remarks on previous versions of this article.

REFERENCES

Aneesh, P. T., and Kappalli, S. (2020). Protandrous hermaphroditic reproductive system in the adult phases of *Mothocya renardi* (Bleeker, 1857) (*Cymothoidae*: *Isopoda*: *Crustacea*) – light and electron microscopy study. *Zool. Stud.* 59:e61.

Backeljau, T. (1993). Cladistic analysis of metazoan relationships: a reappraisal. *Cladistics* 9, 167–181. doi: 10.1006/clad.1993.1010

Bichat, X. (1801). *Anatomie générale, appliquée à la physiologie et à la médecine*. 4 vols. Paris: Brosson, Gabon et Cie.

Blainey, P. (2017). Dynamic cellular personalities. *Cell Syst.* 4:258. [Part of: Clevers, H., Rafelski, S., Elowitz, M., Klein, A., Shendure, J., Trapnell, C., Lein, E., Lundberg, E., Uhlen, A., Martinez-Arias, A., Sanes, J. R., Blainey, P., Eberwine, J., Kim, J., and Love, J. C. (2017). What is your conceptual definition of "cell type" in the context of a mature organism? *Cell. Syst.* 4, 255–259. doi: 10.1016/j.cels.2017.03.006],

Bolwig, N. (1946). Senses and sense organs of the anterior end of the house fly larvae. *Vidensk. Med. Dansk Naturh. Foren.* 109, 81–217.

Boyden, A. (1943). Homology and analogy: a century after the definitions of "homologue" and "analogue" of Richard Owen. *Quart. Rev. Biol.* 18, 228–241. doi: 10.1086/394676

Brusca, R. C., and Brusca, G. J. (2003). *Invertebrates*, 2nd Edn. Sunderland: Sinauer Associates.

Chen, D., Liu, F., Zhu, Z., Lin, Q., Zeng, C., and Ye, H. (2019). Ontogenetic development of gonads and external sexual characters of the protandric simultaneous hermaphrodite peppermint shrimp, *Lysmata vittata* (*Caridea: hippolytidae*). *PLoS One* 14:e0215406. doi: 10.1371/journal.pone.0215406

Coe, W. R. (1938). A new genus and species of Hoplonemertea having differential bipolar sexuality. *Zool. Anz.* 124, 220–224.

Coffey, J. C., and O'Leary, D. P. (2016). The mesentery: structure, function, and role in disease. *Lancet Gastroenterol. Hepatol.* 1, 238–247. doi: 10.1016/S2468-1253(16)30026-7

Colombani, J., Andersen, D. S., and Leopold, P. (2012). Secreted peptide DILP8 coordinates *Drosophila* tissue growth with developmental timing. *Science* 336, 582–585. doi: 10.1126/science.1216689

Corti, A. (1851). Recherches sur l'organe de l'ouïe des mammiferes. *Ztschr. Wiss. Zool.* 3, 106–169.

Cuvier, G. (1817). *Le règne animal distribué d'après son organisation pour servir de base à l'histoire naturelle des animaux et d'introduction à l'anatomie comparée, vol. 1*. Paris: Deterville.

DiFrisco, J., Love, A. C., and Wagner, G. P. (2020). Character identity mechanisms: a conceptual model for comparative–mechanistic biology. *Biol. Philos.* 35:44. doi: 10.1007/s10539-020-09762-2

Dobzhansky, T. (1973). Nothing in biology makes sense except in the light of evolution. *Am. Biol. Teach.* 35, 125–129. doi: 10.2307/4444260

Dohrn, A. (1875). *Der Ursprung der Wirbelthiere und das Princip des Funktionswechsels*. Leipzig: Engelmann.

Eernisse, D. J., Albert, J. S., and Anderson, F. E. (1992). Annelida and Arthropoda are not sister taxa: a phylogenetic analysis of spiralian metazoan morphology. *Syst. Biol.* 41, 305–330. doi: 10.1093/sysbio/41.3.305

Fusco, G., and Minelli, A. (2019). *The Biology of Reproduction*. Cambridge: Cambridge University Press. doi: 10.1017/9781108758970

Garelli, A., Gontijo, A. M., Miguela, V., Caparros, E., and Dominguez, M. (2012). Imaginal discs secrete insulin-like peptide 8 to mediate plasticity of growth and maturation. *Science* 336, 579–582. doi: 10.1126/science.1216735

Gegenbaur, C. (1878). *Elements of Comparative Anatomy*. London: Macmillan & Co.

Geoffroy Saint-Hilaire, E. (1807). Considérations sur les pièces de la tête osseuse des animaux vertébrés, et particulièrement sur celles du crâne des oiseaux. *Ann. Mus. Hist. Nat.* 10, 342–365.

Geoffroy Saint-Hilaire, E. (1828). *Cours de l'histoire naturelle des Mammifères*. Paris: Pichon et Didier.

Geoffroy Saint-Hilaire, E. (1830). *Principles de philosophie zoologique discutés en mars 1830, au sein de l'Academie Royale des Sciences*. Paris: Pichon et Didier. doi: 10.5962/bhl.title.2163

Ghiselin, M. T. (1969). The evolution of hermaphroditism among animals. *Q. Rev. Biol.* 44, 189–208.

Ghiselin, M. T. (1974). *The Economy of Nature and the Evolution of Sex*. Berkeley: University of California Press.

Glenner, H., Hansen, A. J., Sørensen, M. V., Ronquist, F., Huelsenbeck, J. P., and Willerslev, E. (2004). Bayesian inference of the metazoan phylogeny; a combined molecular and morphological approach. *Curr. Biol.* 14, 1644–1649. doi: 10.1016/j.cub.2004.09.027

Gould, S. J., and Vrba, E. (1982). Exaptation-a missing term in the science of form. *Paleobiology* 8, 4–15. doi: 10.1017/S0094837300004310

Gruner, H. E. (1993). "Klasse Crustacea," in *Lehrbuch der Speziellen Zoologie, Band I: Wirbellose Tiere, 4. Teil. Arthropoda (begründet von A. Kaestner)*, ed. H. E. Gruner (Jena: Gustav Fischer), 448–1030.

Haeckel, E. (1866). *Generelle Morphologie der Organismen. Allgemeine Grundzüge der organischen Formen-Wissenschaft, mechanisch begründet durch die von Charles Darwin reformirte Descendenz-Theorie*. Berlin: Reimer. doi: 10.1515/9783110848281

Hall, B. K. (1995). Homology and embryonic development. *Evol. Biol.* 28, 1–36. doi: 10.1007/978-1-4615-1847-1_1

Hall, B. K. (1998). Germ layers and the germ-layer theory revisited. Primary and secondary germ layers, neural crest as a fourth germ layer, homology, and the demise of the germ-layer theory. *Evol. Biol.* 30, 121–186. doi: 10.1007/978-1-4899-1751-5_5

Hessler, R. R., Elofsson, R., and Hessler, A. Y. (1995). Reproductive system of *Hutchinsoniella macracantha* (Cephalocarida). *J. Crust. Biol.* 15, 493–522. doi: 10.2307/1548771

Hyman, L. H. (1951). *The Invertebrates: Vol. II. Platyhelminthes and Rhynchocoela, the Acoelomate Bilateria*. New York: McGraw-Hill.

Kauffman, S. A. (1971). Gene regulation networks: a theory of their global structure and behavior. *Curr. Top. Dev. Biol.* 6, 145–182. doi: 10.1016/S0070-2153(08)60640-7

Kubrakiewicz, J., Jaglarz, M. K., Iliffe, T. M., Bilinski, S. M., and Koenemann, S. (2012). Ovary structure and early oogenesis in the remipede, *Godzilliognomus frondosus* (Crustacea, Remipedia): phylogenetic implications. *Zoology* 115, 261–269. doi: 10.1016/j.zool.2012.01.001

Lankester, E. R. (1870). On the use of the term homology in modern zoology, and the distinction between homogenetic and homoplastic agreements. *Ann. Mag. Nat. Hist.* 6, 34–43. doi: 10.1080/00222937008696201

Larsen, K., Guțu, M., and Sieg, J. (2015). "Order Tanaidacea Dana," in *Treatise on Zoology—Anatomy, Taxonomy, Biology. The Crustacea Revised and Updated, as Well as Extended From the Traité de Zoologie*, eds J. C. von Vaupel Klein, M. Charmantier-Daures, and F. R. Schram (Brill: Leiden), 249–329. doi: 10.1163/9789004232518_007

Lennox, J. G. (2001). *Aristotle. On the Parts of Animals I-IV. Translation, Introduction and Commentary*. Oxford: Clarendon Press. doi: 10.1093/oseo/instance.00262098

Levins, R. (1970). "Complex systems," in *Towards a Theoretical Biology*, Vol. 3, ed. C. H. Waddington (Chicago: Aldine), 73–88. doi: 10.4324/9781315125893-8

Lundberg, E., and Uhlen, M. (2017). Mapping as a key first step. *Cell Syst.* 4:257. [Part of: Clevers, H., Rafelski, S., Elowitz, M., Klein, A., Shendure, J., Trapnell, C., Lein, E., Lundberg, E., Uhlen, A., Martinez-Arias, A., Sanes, J. R., Blainey, P., Eberwine, J., Kim, J., and Love, J. C. (2017). What is your conceptual definition of "cell type" in the context of a mature organism? *Cell. Syst.* 4, 255–259. doi: 10.1016/j.cels.2017.03.006],

Magarlamov, T. Y., Dyachuk, V., and Chernyshev, A. V. (2020). Does the frontal sensory organ in adults of the hoplonemertean *Quasitetrastemma stimpsoni* originate from the larval apical organ? *Front. Zool.* 17:2. doi: 10.1186/s12983-019-0347-4

Maienschein, J. (1978). Cell lineage, ancestral reminiscence, and the biogenetic law. *J. Hist. Biol.* 11, 129–158. doi: 10.1007/BF00127773

Marlow, H., Tosches, M. A., Tomer, R., Steinmetz, P. R., Lauri, A., Larsson, T., et al. (2014). Larval body patterning and apical organs are conserved in animal evolution. *BMC Biol.* 12:7. doi: 10.1186/1741-7007-12-7

Mayr, E. (1982). *The Growth of Biological Thought. Diversity, Evolution and Inheritance*. Cambridge: Belknap Press of Harvard University Press.

Mayr, W. (1969). *Principles of Systematic Zoology*. New York: McGraw-Hill.

Minelli, A. (2020). Biology and its disciplinary partitions – intellectual and academic constraints. *Sci. Filosofia* 24, 105–126.

Minelli, A. (2021). "What's a cell type?," in *Origin and Evolution of Metazoan Cell Types*, eds S. Leys and A. Hejnol (Boca Raton: CRC Press), 1–11. doi: 10.1201/b21831-1

Minelli, A., and Fusco, G. (2019). No limits: breaking constraints in arthropod miniaturization. *Arthropod. Struct. Dev.* 48, 4–11. doi: 10.1016/j.asd.2018.11.009

Neumann, J. S., Desalle, R., Narechania, A., Schierwater, B., and Tessler, M. (2021). Morphological characters can strongly influence early animal relationships inferred from phylogenomic data sets. *Syst. Biol.* 70, 360–375. doi: 10.1093/sysbio/syaa038

Neumann, P. E. (2017). Organ or not? Prolegomenon to organology. *Clin. Anat.* 30, 288–289. doi: 10.1002/ca.22848

Oppenheimer, J. M., and Hamburger, V. (1976). The non-specificity of the germ-layers. *Q. Rev. Biol.* 51, 96–124. doi: 10.1086/408987

Osborn, H. F. (1902). Homoplasy as a law of latent or potential homology. *Am. Nat.* 36, 259–271. doi: 10.1086/278118

Osborn, H. F. (1905). The ideas and terms of modern philosophical anatomy. *Science* 21, 959–961. doi: 10.1126/science.21.547.959-b

Owen, R. (1843). *Lectures on the Comparative Anatomy and Physiology of the Invertebrate Animals, Delivered at the Royal College of Surgeons*. London: Longman Brown Green and Longmans.

Owen, R. (1847). Report on the archetype and homologies of the vertebrate skeleton. *Report Br. Assoc. Adv. Sci.* 1846, 169–340. doi: 10.5962/bhl.title.61890

Owen, R. (1848). *On the Archetype and Homologies of the Vertebrate Skeleton*. London: John Van Voorst. doi: 10.5962/bhl.title.118611

Owen, R. (1849). *On the Nature of Limbs*. London: John van Voorst. doi: 10.5962/bhl.title.50117

Pander, C. H. (1817). *Dissertatio inauguralis sistens historiam metamorphoseos, quam ovum incubatum prioribus quinque diebus subit*. Wirceburgi: Nitribitt. doi: 10.5962/bhl.title.48488

Remak, R. (1855). *Untersuchungen über die Entwicklung der Wirbeltiere*. Berlin: Reimer.

Remane, A. (1952). *Die Grundlagen des natürlichen Systems, der vergleichenden Anatomie und der Phylogenetik*. Zweite Auflage. Leipzig: Akademische Verlagsgesellschaft Geest and Portig.

Russell, E. S. (1916). *Form and Function*. London: Murray.

Sanes, J. R. (2017). Moving forward despite quarrels. *Cell Syst.* 4:257. [Part of: Clevers, H., Rafelski, S., Elowitz, M., Klein, A., Shendure, J., Trapnell, C., Lein, E., Lundberg, E., Uhlen, A., Martinez-Arias, A., Sanes, J. R., Blainey, P., Eberwine, J., Kim, J., and Love, J. C. (2017). What is your conceptual definition of "cell type" in the context of a mature organism? *Cell. Syst.* 4, 255–259. doi: 10.1016/j.cels.2017.03.006],

Schierwater, B., Eitel, M., Jakob, W., Osigus, H.-J., Hadrys, H., Dellaporta, S. L., et al. (2009). Concatenated analysis sheds light on early metazoan evolution and fuels a modern "urmetazoon" hypothesis. *PLoS Biol.* 7:e1000020. doi: 10.1371/journal.pbio.1000020

Schmidt-Rhaesa, A. (2007). *The Evolution of Organ Systems*. Oxford: Oxford University Press. doi: 10.1093/acprof:oso/9780198566687.001.0001

Sebé-Pedrós, A., Chomsky, E., Pang, K., Lara-Astiaso, D., Gaiti, F., Mukamel, Z., et al. (2018). Early metazoan cell type diversity and the evolution of multicellular gene regulation. *Nat. Ecol. Evol.* 2, 1176–1188. doi: 10.1038/s41559-018-0575-6

Sereno, P. C. (2007). Logical basis for morphological characters in phylogenetics. *Cladistics* 23, 565–587. doi: 10.1111/j.1096-0031.2007.00161.x

Simpson, G. G. (1961). *Principles of Animal Taxonomy*. New York: Columbia University Press. doi: 10.7312/simp92414

Toepfer, G. (2011). *Historisches Wörterbuch der Biologie*. Stuttgart: Metzler. doi: 10.1007/978-3-476-00439-0

Vicq-d'Azyr, F. (1792). *Encyclopédie méthodique. Système anatomique. Quadrupèdes. Tome second*. Paris: Panckoucke.

von Baer, K. E. (1828). *Über Entwicklungsgeschichte der Thiere: Beobachtung und Reflexion, Erster Theil*. Königsberg: Bornträger.

Wagner, G. P. (2014). *Homology, Genes, and Evolutionary Innovation*. Princeton: Princeton University Press. doi: 10.23943/princeton/9780691156460.001.0001

Wagner, G. P. (2019). "Devo-evo of cell types," in *Evolutionary Developmental Biology*, eds L. Nuno de la Rosa and G. B. Müller (Cham: Springer), 511–528. doi: 10.1007/978-3-319-33038-9_153-1

Wiley, E. O. (1981). *Phylogenetics*. New York: Wiley.

Wilson, E. B. (1896). *The Embryological Criterion of Homology*. Woods Hole, MA: Biological Lectures of the Marine Biological Laboratory, 101–124.

Wimsatt, W. (2007). *Re-Engineering Philosophy for Limited Beings: Piecewise Approximations to Reality*. Cambridge: Harvard University Press.

Yusa, Y., Takemura, M., Sawada, K., and Yamaguchi, S. (2013). Diverse, continuous, and plastic sexual systems in barnacles. *Integr. Comp. Biol.* 53, 701–712. doi: 10.1093/icb/ict016

Zammito, J. H. (2018). *The Gestation of German Biology. Philosophy and Physiology from Stahl to Schelling*. Chicago: Chicago University Press. doi: 10.7208/chicago/9780226520827.001.0001

Zrzavý, J., Mihulka, S., Kepka, P., Bezdek, A., and Tietz, D. (1998). Phylogeny of the Metazoa based on morphological and 18S ribosomal DNA evidence. *Cladistics* 14, 249–285. doi: 10.1111/j.1096-0031.1998.tb00338.x

Zuckerkandl, E. (1901). Ueber Nebenorgane des Sympathicus im Retroperitonaealraum des Menschen. *Verh. Anat. Ges* . 15, 85–107.

Conflict of Interest: The author declares that the research was conducted in the absence of any commercial or financial relationships that could be construed as a potential conflict of interest.

frontiers in Cell and Developmental Biology

ORIGINAL RESEARCH
published: 19 May 2020
doi: 10.3389/fcell.2020.00356

The TMJ Disc Is a Common Ancestral Feature in All Mammals, as Evidenced by the Presence of a Rudimentary Disc During Monotreme Development

Neal Anthwal and Abigail S. Tucker*

Centre for Craniofacial and Regenerative Biology, King's College London, London, United Kingdom

The novel mammalian jaw joint, known in humans as the temporomandibular joint or TMJ, is cushioned by a fibrocartilage disc. This disc is secondarily absent in therian mammals that have lost their dentition, such as giant anteaters and some baleen whales. The disc is also absent in all monotremes. However, it is not known if the absence in monotremes is secondary to the loss of dentition, or if it is an ancestral absence. We use museum held platypus and echidna histological sections to demonstrate that the developing monotreme jaw joint forms a disc primordium that fails to mature and become separated from the mandibular condyle. We then show that monotreme developmental anatomy is similar to that observed in transgenic mouse mutants with reduced cranial musculature. We therefore suggest that the absence of the disc on monotremes is a consequence of the changes in jaw musculature associated with the loss of adult teeth. Taken together, these data indicate that the ancestors of extant monotremes likely had a jaw joint disc, and that the disc evolved in the last common ancestor of all mammals.

Keywords: TMJ disc, monotreme, mammalian evolution, jaw joint, evo devo, muscle, tendon

OPEN ACCESS

Edited by:
Neva P. Meyer,
Clark University, United States

Reviewed by:
Zerina Johanson,
Natural History Museum,
United Kingdom
Patrick Tschopp,
University of Basel, Switzerland

****Correspondence:***
Neal Anthwal
n.anthwal@kcl.ac.uk

Specialty section:
This article was submitted to Evolutionary Developmental Biology, a section of the journal Frontiers in Cell and Developmental Biology

Received: *31 January 2020*
Accepted: *21 April 2020*
Published: *19 May 2020*

Citation:
Anthwal N and Tucker AS (2020) The TMJ Disc Is a Common Ancestral Feature in All Mammals, as Evidenced by the Presence of a Rudimentary Disc During Monotreme Development. Front. Cell Dev. Biol. 8:356. doi: 10.3389/fcell.2020.00356

INTRODUCTION

The temporomandibular joint (TMJ) is the one of the most used joints in the body, articulating the upper and lower jaw in mammals. A fibrous articular disc sits between the skeletal elements of the joint and acts as a cushion.

TMJ development occurs by the coming together of two membranous bones: the condylar process of the dentary bone in the mandible and the squamosal bone in the skull. The interaction of the condylar with the squamosal induces the formation of a glenoid (or mandibular) fossa on the latter (Wang et al., 2011). The articular disc sits between the two within a synovial capsule. The TMJ disc attaches to the superior head of the lateral pterygoid muscle anteriorly, and to ligaments posteriorly including the disco-mallear ligament that runs thought the capsule of the middle ear, joining the malleus to the TMJ disc. The TMJ articulates the jaw in all mammals and is referred to as the squamosal dentary joint (SDJ) in those mammals without a fused temporal bone. In non-mammals the upper and lower jaw articulate via the endochondral quadrate and articular, known as the primary jaw joint (Wilson and Tucker, 2004). TMJ developmental anatomy reflects

its evolutionary history as this novel jaw joint forms after the development of the primary joint, which, in mammals, is integrated into the middle ear (Takechi and Kuratani, 2010; Anthwal et al., 2013; Maier and Ruf, 2016; Tucker, 2017). In recent years, a number of studies have advanced the understanding of middle ear evolution in the context of anatomical development (Luo, 2011; Anthwal et al., 2013, 2017; Urban et al., 2017; Wang et al., 2019), but little work has sought to understand the TMJ in an evolutionary and comparative developmental biology context. This is despite the crucial role that the formation of the TMJ has in mammalian evolution.

An important part of the TMJ is the disc that cushions its action. The origin of the disc is uncertain. The insertion of the lateral pterygoid muscle into the disc on the medial aspect, and the presence of the disco-malleolar ligament, has led to speculation that the disc represents a fibrocartilage sesamoid within a tendon (Herring, 2003). According to this hypothesis, this tendon, originally associated with the musculature of the articular (homologous to the malleus) of the primary jaw joint, would have become trapped as the dentary and squamosal moved together to create the mammalian jaw joint. However, studies in mice indicate that the disc develops from a region of flattered mesenchyme cells adjacent to, or possibly part of, the perichondrium of the developing condylar cartilage (Purcell et al., 2009, 2012; Hinton et al., 2015). Formation of the disc condensation is dependent on Ihh signaling from the cartilage (Shibukawa et al., 2007; Purcell et al., 2009; Yang et al., 2016), and Fgf signaling via Spry 1 and 2 genes from the adjacent muscles (Purcell et al., 2012). Therefore, the disc may have its origins in either a tendon, the novel secondary cartilage of the condylar process, or a combination of the two.

Interestingly the disc is absent in extant monotremes (Sprinz, 1964). Monotremes and therian mammals (marsupials and eutherians) are evolutionary distant, with the common ancestor of the two subclasses being a mammal-like reptile from around 160 million years ago (Kemp, 2005; Luo et al., 2015). Monotremes have a number of "reptile" like anatomical features such as a cloaca, external embryonic development in an egg, a straight cochlea in the inner ear and a sprawling posture (Griffiths, 1978). The absence of a disc in both echidna and platypus suggests that the disc evolved after the split between monotremes and therian mammals, and is therefore a therian novelty. Alternatively, absence of the TMJ disc in extant monotremes might be due to a secondary loss linked to the loss of teeth, and associated changes in the muscles of mastication. Extant adult monotremes are edentulous, possibly due to the expansion of the trigeminal during the evolution of electroreceptivity limiting the available space for tooth roots within the maxilla (Asahara et al., 2016). The juvenile platypus has rudimentary teeth that regress (Green, 1937), while the echidna shows only thickening of the dental epithelium during development. In contrast, fossil monotremes have a mammalian tribosphenic dentition, a structure unique to the mammal lineage that allows occlusion of upper and lower molar teeth for grinding of food in addition to crushing and shearing during mastication (Kemp, 2005). This indicates that extant monotremes evolved from animals with the ability to chew in the mammalian manner, involving lateral and rotational movements. The presence or absence of a disc in such fossils is difficult to ascertain due to lack of preservation of soft tissue. In support of mastication playing a role in disc formation, edentulous therian mammals, or those lacking enamel, often lack a disc. These species include some (but not all) baleen whales (El Adli and Deméré, 2015), giant ant eaters and sloths (Naples, 1999).

In order to discriminate between these two scenarios, we have examined the development of the TMJ in monotremes and made comparison with mouse developmental models where muscle development is perturbed.

MATERIALS AND METHODS

Platypus *(Ornithorhynchus anatinus)* and short-beaked echidna *(Tachyglossus aculeatus)* slides were imaged from the collections at the Cambridge University Museum of Zoology. Details of samples imaged are in **Table 1**. All museum samples have been studied in previously published works (Watson, 1916; Green, 1937; Presley and Steel, 1978). Stages for platypus are after Ashwell (2012). Staging of echidna H.SP EC5 is estimated by cross-referencing previous studies (Griffiths, 1978; Rismiller and McKelvey, 2003). CT scans of adult platypus were a gift of Anjali Goswami, the Natural History Museum, London.

Mesp1Cre;Tbx1flox (Tbx1CKO) mice were derived as previously described (Anthwal et al., 2015).

Tissue processing and histological staining: embryonic samples for histological sectioning were fixed overnight at 4°C in 4% paraformaldehyde (PFA), before being dehydrated through a graded series of ethanol and stored at −20°C. For tissue processing, samples were cleared with Histoclear II, before wax infiltration with paraffin wax at 60°C. Wax embedded samples were microtome sectioned at 8 μm thickness, then mounted in parallel series on charged slides.

For histological examination of bone and cartilage, the slides were then stained with picrosirius red and alcian blue trichrome stain using standard techniques.

This work was carried out under UK Home Office license and regulations in line with the regulations set out under the United Kingdom Animals (Scientific Procedures) Act 1986 and the European Union Directive 2010/63/EU.

TABLE 1 | Museum held specimens used in the current study.

Species	Collection	ID	Estimated stage	CRL
Ornithorhynchus anatinus	Cambridge	Specimen X	6.5 days*	33 mm
Ornithorhynchus anatinus	Cambridge	Specimen Delta	10 days*	80 mm
Ornithorhynchus anatinus	Cambridge	Specimen Beta	80 days*	250 mm
Tachyglossus aculeatus	Cambridge	Echidna H.SP EC5	18 days†	83 mm

*CRL, Crown rump length. *Estimate based on Ashwell (2012). †Estimate based on Griffiths (1978) and Rismiller and McKelvey (2003).*

RESULTS

If the TMJ disc is a therian novelty, then no evidence of a disc would be expected in extant monotremes during development of the TMJ. The development of the jaw joint was therefore examined in museum held histological sections of developing post-hatching platypus and compared with the mouse.

As other authors have previously described (Purcell et al., 2009; Hinton, 2014), in embryonic day (E) 16.5 mice the disc anlage is observed as thickened layer of mesenchyme connected to the superior aspect of the condylar cartilage (**Figure 1A**). At postnatal day (P) 0, the disc has separated from the condylar process and sits within the synovial cavity of the jaw joint (**Figure 1B**). In a platypus sample estimated to be 6.5 days post-hatching, the TMJ had been initiated, but the joint cavity had not yet formed (**Figures 1C,D**). Close examination of the superior surface of the condylar cartilage revealed a double layer of thickened mesenchyme in the future fibrocartilage layer of the condylar (**Figures 1C',D'**). The outer layer is similar to that known to develop into the articular disc in therian mammals (Purcell et al., 2009). This thickened mesenchyme persisted in older samples, estimated to be 10 days post-hatching, where the synovial cavity of the TMJ was beginning to form above (**Figures 1E,E'**). In the most mature platypus sample examined (around P80) the fibrocartilage layer of the condylar process was thick and had a double-layered structure (**Figure 1F**). The outer layer was connected via a tendon to the lateral pterygoid muscle. At this late stage of postnatal development, the platypus puggle would have been expected to start leaving the burrow and to be eating a mixed diet, although full weaning does not occur until around 205 days post-hatching (Rismiller and McKelvey, 2003). In the mature platypus, the condylar process sits within a glenoid fossa (**Figure 1G**), which was not fully formed at earlier stages. A disc-like structure lying over the condylar and connected to the adjacent muscles was therefore evident in the platypus postnatally but did not lift off the condylar at any stage.

Next we examined the development of the TMJ in a museum derived young short-beaked echidna puggle specimen with a crown-rump length of 83mm, which we estimate to be around 18 days post-hatching. The TMJ is not fully developed (**Figure 2**). The condylar process possessed a thick, doubled fibrocartilage outer layer (**Figure 2**), much as was observed in the platypus (**Figure 1D**). The outer fibrocartilage layer was connected by connective tissue to the lateral pterygoid muscle (**Figure 2B'**). Clear disc-like structures were therefore present during development in both extant monotremes.

Taken together, the developmental evidence suggests that extant monotremes initiate a layer of fibrocartilage connected to the lateral pterygoid muscle, similar to the initiation of the TMJ disc in therian mammals. However, unlike in therian mammals, the monotreme fibrocartilage failed to separate from the condylar to form an articular disc in the TMJ. Interactions with musculature, both mechanical (Habib et al., 2007; Purcell et al., 2012; Jahan et al., 2014; Nickel et al., 2018) and molecular (Shibukawa et al., 2007; Gu et al., 2008; Purcell et al., 2009, 2012; Kinumatsu et al., 2011; Michikami et al., 2012; Yasuda et al., 2012; Kubiak et al., 2016), have been suggested to be

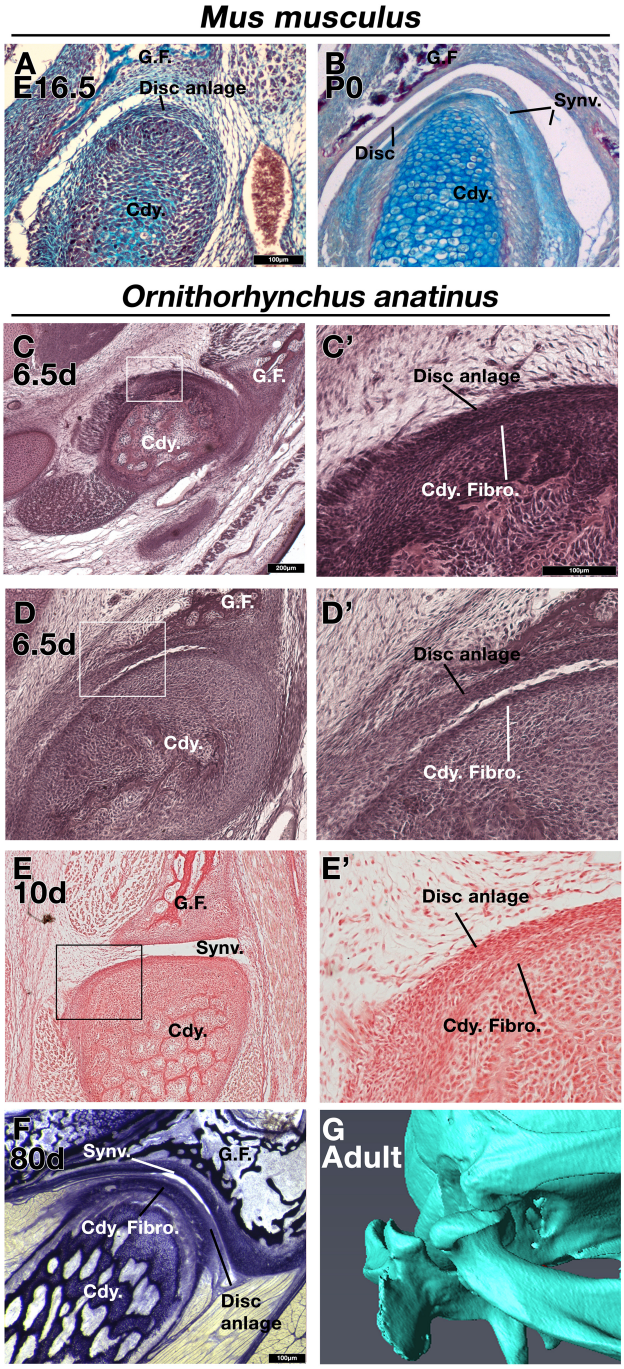

FIGURE 1 | Comparison of mouse (*Mus musculus*) and platypus (*Ornithorhynchus anatinus*) developing jaw joint reveals the presence of a jaw joint disc anlage in early post-hatching platypus despite absence of the disc in adults. **(A,B)** Histological sections of mouse jaw joint disc development at embryonic day 16.5 **(A)** and postnatal day 0 **(B)**. **(C–D')** Histological sections of estimated post-hatching day 6.5 jaw joint at two different levels **(C,D)** Note that the separation between the disc anlage and condylar in D is probably a processing artifact. **(E,E')** Histological sections of estimated post-hatching day 10 jaw joint. **(F)** Histological section of mature jaw joint in a juvenile platypus estimated post-hatching day 80. **(G)** μCT scan of jaw joint region of adult platypus. G.F., glenoid fossa; Cdy., condylar process; Cdy. Fibro., condylar fibrocartilage; Synv., synovial cavity of the jaw joint.

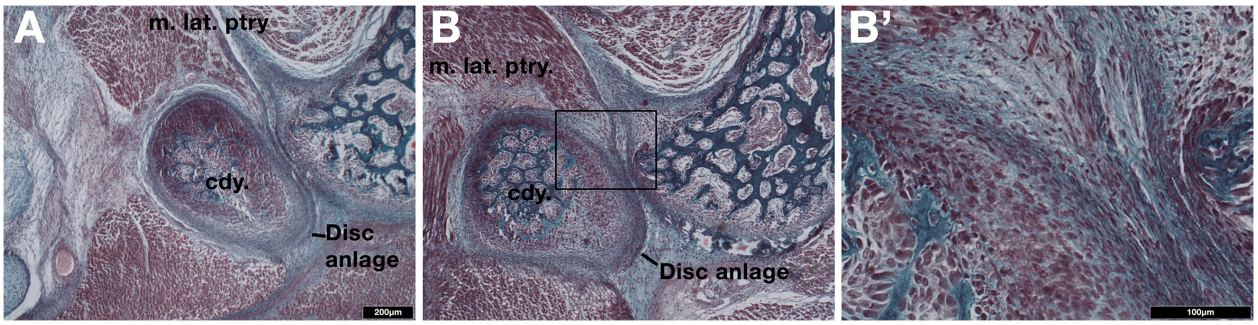

FIGURE 2 | Examination of the developing jaw joint reveals the presence of a jaw joint disc anlage in post-hatching day 18 short-beaked echidna (Tachyglossus aculeatus). **(A,B)** Histological staining at the forming jaw articulation in echidna young estimated to be 18 days post-hatching at two different level. Fibrocartilage disc anlage superior to the condylar and connected by tendon to the lateral pterygoid muscle is observed. **(B')** High-powered view of boxed region in B showing the connection between the muscle and the developing disc anlage. Cdy., condylar process; m. lat. ptry., lateral pterygoid muscle.

responsible for the proper formation of the TMJ disc. Lack of mechanical force or changes in signaling from the muscle in monotremes might therefore result in the disc remaining attached to the condylar. In order to examine how changes in muscle might influence disc development, we next examined disc development in the *Mesp1Cre;Tbx1flox* conditional mutant mouse (*Tbx1CKO*). This mouse has a mesoderm specific deletion of the T-box transcription factor *Tbx1*, resulting in severely perturbed development of the pharyngeal arch mesoderm-derived muscles of the head, resulting in their significant reduction or absence (Grifone et al., 2008; Aggarwal et al., 2010; Anthwal et al., 2015).

We used alcian blue/alizarin red stained histological sections to investigate the development of the TMJ disc in *TbxCKO* mice at embryonic day 15.5. This is the stage when future disc mesenchyme is first observed. In wildtype embryos, the future disc mesenchyme was observed as a condensation attached to the superior surface of the condylar fibrocartilage (**Figure 3A**). A distinct disc-like mesenchyme was also observed superior to the condylar of the *Tbx1CKO* (**Figure 3B**). This mesenchyme and the fibrocartilage layer of the condylar cartilage both appeared thicker in the *Tbx1CKO* compared to its wildtype littermate. At E18.5, the wildtype TMJ disc had separated from the condylar process and sat within a synovial joint cavity (**Figure 3C**). In the *Tbx1CKO* an upper synovial cavity had formed, similar to the WT, but there was little evidence of the earlier disc with no separation from the condylar (**Figure 3D**). Instead, a thickened band of fibrocartilage was observed on the superior surface of the condylar process. The lateral pterygoid muscle was either massively reduced or absent in the *Tbx1CKO*, while other muscles, such as the temporalis, were present but much reduced in volume (see Anthwal et al., 2015).

DISCUSSION

The absence of an articular disc in monotremes has been thought to be either a secondary loss related to the absence of a mature dentition, or the disc being a later acquisition in the therian clade. The data presented here show that a mesenchyme similar to the TMJ disc is initiated in both platypus and echidna jaws during post-hatching development, but fails to mature and separate from the dentary condyle. In the light of the failure of the disc to fully separate in transgenic mouse models with hypomorphic muscle development, it seems likely that the disc has been secondarily lost in edentulous mammals, including monotremes.

The earliest stem mammals, such as *Morganuconodon,* have a mandibular middle ear where the middle ear bones are fully attached to the mandible and have been proposed to act in both hearing and feeding. The secondary jaw joint of these animals were likely to be able to withstand the biomechanical stresses sufficient for feeding on the hard keratinized bodies of insects, while others such as *Kuehneotherium* could not (Gill et al., 2014). More crownward stem-mammals developed

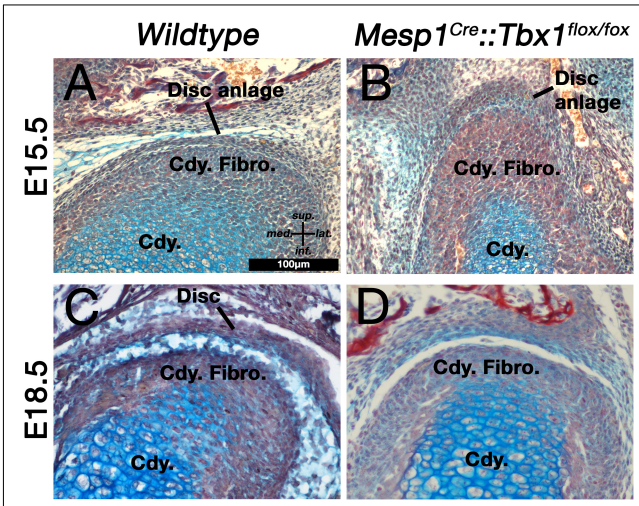

FIGURE 3 | Muscle-disc interactions are required for the maturation and separation of the jaw joint articular disc. **(A,B)** The disc anlage is observed at E15.5 in both wildtype mice **(A)** and *Mesp1Cre;Tbx1fl/fl* mice with a hypomorphic muscle phenotype **(B)**. **(C,D)** By E18.5 the disc has separated from the condylar process in wildtype mice **(C)**, but not in *Mesp1Cre;Tbx1fl/fl* mice. Cdy., condylar process; Cdy. Fibro., condylar fibrocartilage.

a range of mandibular movements during chewing, including rolling, yaw and front to back movements (Kemp, 2005; Luo et al., 2015; Grossnickle, 2017; Lautenschlager et al., 2017, 2018; Bhullar et al., 2019). It is not clear if these species had evolved an articular disc, since fibrocartilage is rarely fossilized. However, the synovial secondary jaw joint was likely present in stem mammals such as *Morganuconodon* (Allin and Hopson, 1992), and the lateral pterygoid has been proposed to have inserted into the condylar of the dentary forming the secondary articulation in basal mammaliforms (Lautenschlager et al., 2017). When this is considered alongside the presence of the first stages of disc formation during monotreme development, it is likely that the common stem Jurassic mammal-like reptilian ancestor of both monotremes and therian mammals had a disc. The data presented here confirms an essential biomechanical component in disc development. Therefore, we are able to consider when during mammalian evolution these forces were able to act to enable disc formation. For example, it is probable that many late Triassic and early Jurassic mammaliaforms such *Hadrocodium* (Luo, 2001) possessed an articular disc, since they possessed a well-formed squamosal dentary joint and occluding teeth capable of grinding food between the cusps of tribosphenic teeth during mastication.

One hypothesis for the origin of the articular disc is that it formed from the tendon of a muscle of jaw closure of the primary jaw joint interrupted by the formation of the novel mammalian jaw joint (Herring, 2003). The tendons and skeleton of the front of the head are derived from the cranial neural crest, whereas the musculature is mesoderm derived (Santagati and Rijli, 2003; Yoshida et al., 2008). Interactions between the mesoderm and neural crest co-ordinate the muscular skeletal development of the head (Grenier et al., 2009). A striking piece of evidence for the tendon origin of the disc is the expression in the developing articular disc of *Scleraxis* (Purcell et al., 2012; Roberts et al., 2019), a specific regulator of tendon and ligament development (Schweitzer et al., 2001; Sugimoto et al., 2013). If the disc is derived from a tendon, then it may be thought of as a fibrocartilage sesamoid. Such sesamoids are found in joints and in tendons that are subject to compression, like the tendons that pass around bony pulleys such as the flexor digitorum profundus tendon in quadrupeds, the patella tendon and ligament (Benjamin and Ralphs, 1998),

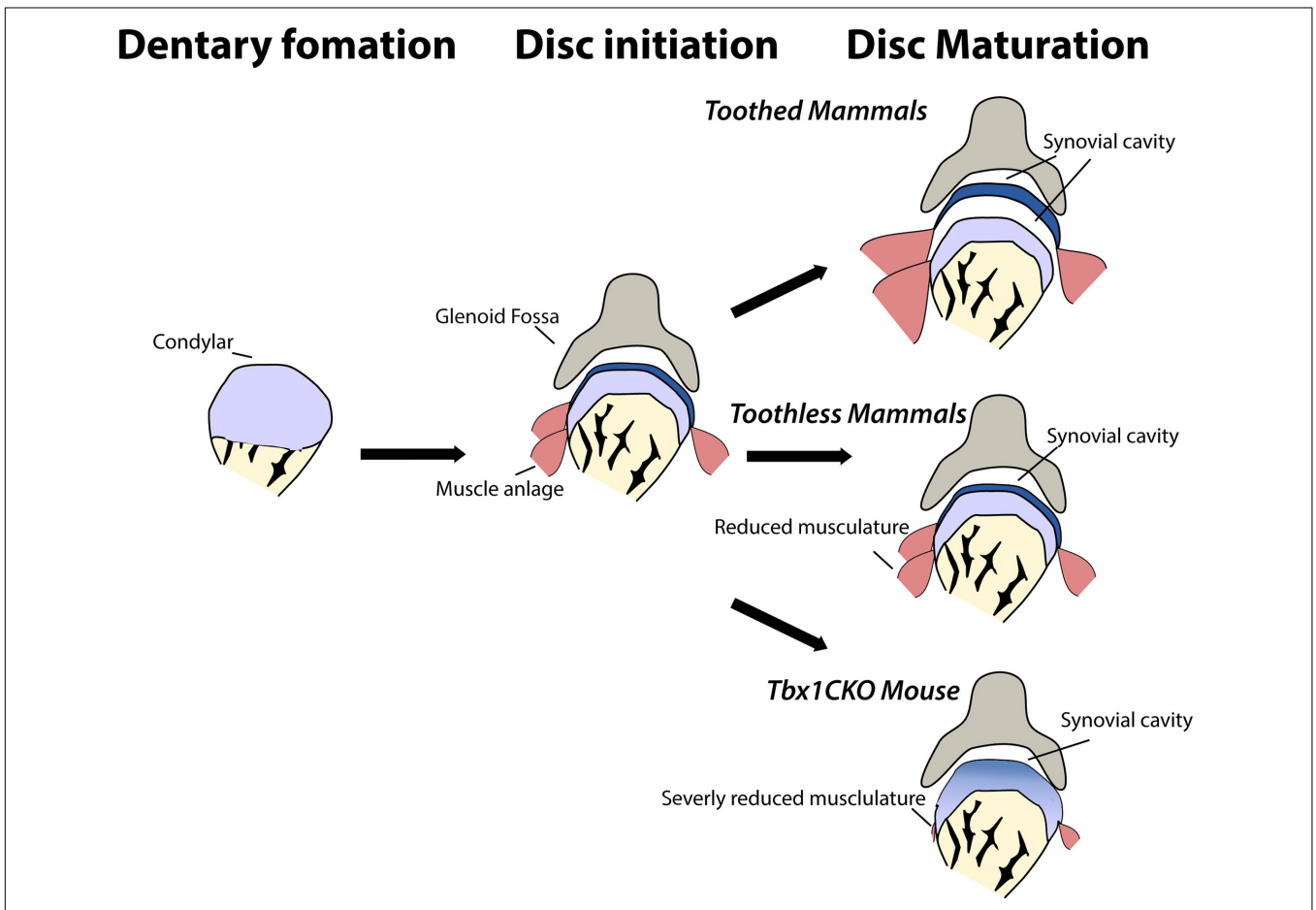

FIGURE 4 | Maturation of the jaw joint articular disc in mammals is dependent on muscle interactions. In toothless mammals and in *Tbx1CKO* mice, reduction or loss of jaw musculature results in changes in muscle-disc interaction and so the disc does not separate from the mandibular condyle to sit within the synovial joint capsule.

and the cartilago transiliens in crocodilians (Tsai and Holliday, 2011). Fibrocartilages also form at the enthesis of long bones. Interestingly, it has been demonstrated that much like the TMJ disc, enthesis fibrocartilage cells are derived from Hh responsive cells and that these cells are responsive to mechanical loading (Schwartz et al., 2015). To support the tendon origin of the TMJ disc, our data show that the formation of the disc is dependent on interactions between the skeletal and muscle components of the TMJ. Such tissue interaction is also a key process in the formation of tendons and ligaments (Eloy-Trinquet et al., 2009; Huang, 2017).

The mechanism by which the disc fails to separate from the condylar in monotremes is not yet clear. Hh signaling is known to be involved in both the initiation of the disc, and the later separation from the condylar (Purcell et al., 2009). It is still possible that the role in Hh in separation of the disc is a therian innovation, and as such the reason that monotremes fail to do so is a lack of the later Hh dependent developmental program for disc separation. However, the absence of the disc in therian edentates, such as some whales and giant anteaters (Naples, 1999; El Adli and Deméré, 2015), strongly suggests that the loss is secondary. The absence of teeth and associated changes in jaw function in monotremes lends itself to the hypothesis that related changes in the lateral pterygoid muscle are responsible for the failure of disc maturation. Secondary loss, through changes in interactions between the developing disc and muscles, is supported by the failure of the disc to elevate off the condylar in *Tbx1CKO* mice that fail to form the lateral pterygoid muscle. These interactions may be either, or a combination of, biomechanical stimulation acting in addition to the compressive force of the TMJ joint, or molecular signaling from the muscles, such as Fgf and Tgf-beta signaling pathways that are known to act in the muscle-tendon-bone/cartilage axis (Purcell et al., 2012; Woronowicz et al., 2018; Roberts et al., 2019; Tan et al., 2020). The source of this signal is likely the lateral pterygoid muscle, which acts to abduct, protrude and laterally move the jaw. These movements are of decreased importance in extant tooth-less monotremes due to feeding modalities that do not rely on chewing with an occluded dentition. As such the formation and maturation of the disc is unlikely to be directly dependent on the presence of teeth, and its absence in edentates is instead a function of the associated changes in musculature. This is supported by the fact that the TMJ disc forms during embryonic development in mice, quite some time before the eruption of the teeth at the end of the second postnatal week. Baleen whales vary in the presence or absence of TMJ discs, and indeed TMJ synovial cavities (El Adli and Deméré, 2015). Significantly, the toothless gray whale has no disc and the lateral and medial pterygoid muscles are fused and function as the medial pterygoid (El Adli and Deméré, 2015), a situation also reported in the adult platypus (Edgeworth, 1931). In addition, although they have a full carnivore dentition, the marsupial Tasmanian Devil has a poorly developed lateral pterygoid muscle and completely lacks the TMJ disc (Hayashi et al., 2013). Evidence that disc maturation is, at least in part, dependent on biomechanical, rather than molecular signaling, cues is found in the disrupted development of the disc in mice after *ex utero* surgical manipulation, where the jaw is sutured closed at E15.5 but the muscle is unaffected (Habib et al., 2007).

Monotremes appear to have two distinct layers in the disc remnant attached to the upper surface of the condylar cartilage (**Figure 1F**), whereas the *Tbx1CKO* mouse has only one continuous fibrocartilage by E18.5 (**Figure 3D**). This may reflect the near total absence of the lateral pterygoid muscle in the mouse mutant, compared to its presence in a reduced form in monotremes. Unfortunately, due to the rarity of fresh material, it is not possible to further examine the mechanistic aspects of TMJ development in edentulous monotreme species at the present time.

CONCLUSION

In conclusion, we demonstrate that during development, monotremes show evidence of initiation of a fibrocartilage articular disc, despite all adult monotremes not having an articular TMJ disc. Maturation and separation of the disc is dependent on interaction with the developing musculature, either through biomechanical stimulation or molecular signals, as demonstrated by the failure of disc maturation and separation in mouse mutants with hypomorphic cranial muscles. Therefore, toothed ancestors of monotremes likely had a TMJ disc. Our research suggests that changes in the cranial musculature that occurred as a consequence of a move toward edentulous dietary niches resulted in absence of the TMJ disc in monotremes, a parallel loss occurring in edentulous therian mammals (**Figure 4**). Finally, the presence of the disc anlage in monotremes indicates that the mammal-like reptile ancestor of all modern mammals likely possessed a disc to cushion the novel jaw articulation.

DATA AVAILABILITY STATEMENT

All datasets generated for this study are included in the article/supplementary material.

ETHICS STATEMENT

Ethical review and approval was not required for the animal study because all tissues used were archival, and in some cases museum specimens. No live studies were carried out.

AUTHOR CONTRIBUTIONS

NA carried out all mouse work, imaged monotreme samples, and wrote the manuscript. AT imaged monotreme samples and critically appraised and edited the manuscript.

FUNDING

This work was supported by the Wellcome Trust (102889/Z/13/Z).

ACKNOWLEDGMENTS

We would like to thank and acknowledge the following people. Anjali Goswami provided μCT images of the adult platypus. Robert Asher provided access to samples held at the Zoological Museum in Cambridge University. Peter Giere provided access to the Hill Collection at the Berlin Museum für Naturkunde. Andrew Gillis provided assistance with imaging. This manuscript has been released as a pre-print at https://doi.org/10.1101/2020.01.17.910471 (Anthwal and Tucker, 2020).

REFERENCES

Aggarwal, V. S., Carpenter, C., Freyer, L., Liao, J., Petti, M., and Morrow, B. E. (2010). Mesodermal Tbx1 is required for patterning the proximal mandible in mice. *Dev. Biol.* 344, 669–681. doi: 10.1016/j.ydbio.2010.05.496

Allin, E. F., and Hopson, J. A. (1992). "Evolution of the auditory system in Synapsida ("mammal-like reptiles" and primitive mammals) as seen in the fossil record," in *The Evolutionary Biology of Hearing*, eds D. B. Webster, R. R. Fay, and A. N. Popper (Berlin: Springer-Verlag), 587–614.

Anthwal, N., Joshi, L., and Tucker, A. S. (2013). Evolution of the mammalian middle ear and jaw: adaptations and novel structures. *J. Anat.* 222, 147–160. doi: 10.1111/j.1469-7580.2012.01526.x

Anthwal, N., Peters, H., and Tucker, A. S. (2015). Species-specific modifications of mandible shape reveal independent mechanisms for growth and initiation of the coronoid. *Evodevo* 6:35. doi: 10.1186/s13227-015-0030-6

Anthwal, N., and Tucker, A. S. (2020). The TMJ disc is a common ancestral feature in all mammals, as evidenced by the presence of a rudimentary disc during monotreme development. *bioRxiv* . doi: 10.1101/2020.01.17.910471

Anthwal, N., Urban, D. J., Luo, Z.-X., Sears, K. E., and Tucker, A. S. (2017). Meckel's cartilage breakdown offers clues to mammalian middle ear evolution. *Nat. Ecol. Evol.* 1:0093. doi: 10.1038/s41559-017-0093

Asahara, M., Koizumi, M., Macrini, T. E., Hand, S. J., and Archer, M. (2016). Comparative cranial morphology in living and extinct platypuses: feeding behavior, electroreception, and loss of teeth. *Sci. Adv.* 2:e1601329. doi: 10.1126/sciadv.1601329

Ashwell, K. W. S. (2012). Development of the hypothalamus and pituitary in platypus (*Ornithorhynchus anatinus*) and short-beaked echidna (*Tachyglossus aculeatus*). *J. Anat.* 221, 9–20. doi: 10.1111/j.1469-7580.2012.01508.x

Benjamin, M., and Ralphs, J. R. (1998). Fibrocartilage in tendons and ligaments–an adaptation to compressive load. *J. Anat.* 193(Pt 4), 481–494. doi: 10.1046/j.1469-7580.1998.19340481.x

Bhullar, B.-A. S., Manafzadeh, A. R., Miyamae, J. A., Hoffman, E. A., Brainerd, E. L., Musinsky, C., et al. (2019). Rolling of the jaw is essential for mammalian chewing and tribosphenic molar function. *Nature* 566, 528–532. doi: 10.1038/s41586-019-0940-x

Edgeworth, F. H. (1931). On the Development of the external ocular, masticatory, and hyoid muscles of monotremata. *Proc. Zool. Soc. London* 101, 809–815. doi: 10.1111/j.1096-3642.1931.tb01045.x

El Adli, J. J., and Deméré, T. A. (2015). On the Anatomy of the temporomandibular joint and the muscles that act upon it: observations on the gray whale. Eschrichtius robustus. *Anat. Rec.* 298, 680–690. doi: 10.1002/ar.23109

Eloy-Trinquet, S., Wang, H., Edom-Vovard, F., and Duprez, D. (2009). Fgf signaling components are associated with muscles and tendons during limb development. *Dev. Dyn.* 238, 1195–1206. doi: 10.1002/dvdy.21946

Gill, P. G., Purnell, M. A., Crumpton, N., Brown, K. R., Gostling, N. J., Stampanoni, M., et al. (2014). Dietary specializations and diversity in feeding ecology of the earliest stem mammals. *Nature* 512, 303–305. doi: 10.1038/nature13622

Green, H. L. H. H. (1937). VIII—The development and morphology of the teeth of ornithorhynchus *. *Philos. Trans. R. Soc. Lond. B. Biol. Sci.* 228, 367–420. doi: 10.1098/rstb.1937.0015

Grenier, J., Teillet, M.-A., Grifone, R., Kelly, R. G., and Duprez, D. (2009). Relationship between neural crest cells and cranial mesoderm during head muscle development. *PLoS One* 4:e4381. doi: 10.1371/journal.pone.0004381

Griffiths, M. (1978). *The Biology of the Monotremes*. London: Academic Press.

Grifone, R., Jarry, T., Dandonneau, M., Grenier, J., Duprez, D., and Kelly, R. G. (2008). Properties of branchiomeric and somite-derived muscle development in Tbx1 mutant embryos. *Dev. Dyn.* 237, 3071–3078. doi: 10.1002/dvdy.21718

Grossnickle, D. M. (2017). The evolutionary origin of jaw yaw in mammals. *Sci. Rep.* 7:45094. doi: 10.1038/srep45094

Gu, S., Wei, N., Yu, L., Fei, J., and Chen, Y. (2008). Shox2-deficiency leads to dysplasia and ankylosis of the temporomandibular joint in mice. *Mech. Dev.* 125, 729–742. doi: 10.1016/j.mod.2008.04.003

Habib, H., Hatta, T., Rahman, O. I. F., Yoshimura, Y., and Otani, H. (2007). Fetal jaw movement affects development of articular disk in the temporomandibular joint. *Congenit. Anom. (Kyoto)* 47, 53–57. doi: 10.1111/j.1741-4520.2007.00143.x

Hayashi, K., Sugisaki, M., Kino, K., Ishikawa, T., Sugisaki, M., and Abe, S. (2013). Absence of the articular disc in the Tasmanian devil temporomandibular joint. *J. Vet. Med. Ser. C Anat. Histol. Embryol.* 42, 415–419. doi: 10.1111/ahe.12031

Herring, S. W. (2003). TMJ anatomy and animals models. *J. Musculos. Neur. Interact.* 3, 997–1003. doi: 10.1016/j.biotechadv.2011.08.021.Secreted

Hinton, R. J. (2014). Genes that regulate morphogenesis and growth of the temporomandibular joint: a review. *Dev. Dyn.* 243, 864–874. doi: 10.1002/dvdy.24130

Hinton, R. J., Jing, J., and Feng, J. Q. (2015). Genetic influences on temporomandibular joint development and growth. *Craniofacial Dev.* 115, 85–109. doi: 10.1016/bs.ctdb.2015.07.008

Huang, A. H. (2017). Coordinated development of the limb musculoskeletal system: tendon and muscle patterning and integration with the skeleton. *Dev. Biol.* 429, 420–428. doi: 10.1016/j.ydbio.2017.03.028

Jahan, E., Matsumoto, A., Rafiq, A. M., Hashimoto, R., Inoue, T., Udagawa, J., et al. (2014). Fetal jaw movement affects Ihh signaling in mandibular condylar cartilage development: the possible role of Ihh as mechanotransduction mediator. *Arch. Oral Biol.* 59, 1108–1118. doi: 10.1016/j.archoralbio.2014.06.009

Kemp, T. S. (2005). *The Origin and Evolution of Mammals*. Oxford: Oxford University Press.

Kinumatsu, T., Shibukawa, Y., Yasuda, T., Nagayama, M., Yamada, S., Serra, R., et al. (2011). TMJ development and growth require primary cilia function. *J. Dent. Res.* 90, 988–994. doi: 10.1177/0022034511409407

Kubiak, M., Ditzel, M., Kubiak, M., and Ditzel, M. (2016). A joint less ordinary: intriguing roles for hedgehog signalling in the development of the temporomandibular synovial joint. *J. Dev. Biol.* 4:25. doi: 10.3390/jdb4030025

Lautenschlager, S., Gill, P., Luo, Z.-X., Fagan, M. J., and Rayfield, E. J. (2017). Morphological evolution of the mammalian jaw adductor complex. *Biol. Rev.* 92, 1910–1940. doi: 10.1111/brv.12314

Lautenschlager, S., Gill, P. G., Luo, Z.-X., Fagan, M. J., and Rayfield, E. J. (2018). The role of miniaturization in the evolution of the mammalian jaw and middle ear. *Nature* 561, 533–537. doi: 10.1038/s41586-018-0521-4

Luo, Z.-X. (2001). A new mammaliaform from the early jurassic and evolution of mammalian characteristics. *Science* 292, 1535–1540. doi: 10.1126/science.1058476

Luo, Z.-X. (2011). Developmental patterns in mesozoic evolution of mammal ears. *Annu. Rev. Ecol. Evol. Syst.* 42, 355–380. doi: 10.1146/annurev-ecolsys-032511-142302

Luo, Z.-X., Gatesy, S. M., Jenkins, F. A., Amaral, W. W., and Shubin, N. H. (2015). Mandibular and dental characteristics of Late Triassic mammaliaform haramiyavia and their ramifications for basal mammal evolution. *Proc. Natl. Acad. Sci. U.S.A.* 112, E7101–E7109. doi: 10.1073/pnas.1519387112

Maier, W., and Ruf, I. (2016). Evolution of the mammalian middle ear: a historical review. *J. Anat.* 228, 270–283. doi: 10.1111/joa.12379

Michikami, I., Fukushi, T., Honma, S., Yoshioka, S., Itoh, S., Muragaki, Y., et al. (2012). Trps1 is necessary for normal temporomandibular joint development. *Cell Tissue Res.* 348, 131–140. doi: 10.1007/s00441-012-1372-1

Naples, V. L. (1999). Morphology, evolution and function of feeding in the giant anteater (*Myrmecophaga tridactyla*). *J. Zool.* 249:S0952836999009036. doi: 10.1017/S0952836999009036

Nickel, J. C., Iwasaki, L. R., Gonzalez, Y. M., Gallo, L. M., and Yao, H. (2018). Mechanobehavior and ontogenesis of the temporomandibular joint. *J. Dent. Res.* 97, 1185–1192. doi: 10.1177/0022034518786469

Presley, R., and Steel, F. L. D. (1978). The pterygoid and ectopterygoid in mammals. *Anat. Embryol. (Berl)* 154, 95–110. doi: 10.1007/BF00317957

Purcell, P., Jheon, A., Vivero, M. P., Rahimi, H., Joo, A., Klein, O. D., et al. (2012). Spry1 and spry2 are essential for development of the temporomandibular joint. *J. Dent. Res.* 91, 387–393. doi: 10.1177/0022034512438401

Purcell, P., Joo, B. W., Hu, J. K., Tran, P. V., Calicchio, M. L., O'Connell, D. J., et al. (2009). Temporomandibular joint formation requires two distinct hedgehog-dependent steps. *Proc. Natl. Acad. Sci. U.S.A.* 106, 18297–18302. doi: 10.1073/pnas.0908836106

Rismiller, P. D., and McKelvey, M. W. (2003). Body mass, age and sexual maturity in short-beaked echidnas, *Tachyglossus aculeatus*. *Comp. Biochem. Physiol. Part A Mol. Integr. Physiol.* 136, 851–865. doi: 10.1016/S1095-6433(03)00225-3

Roberts, R. R., Bobzin, L., Teng, C. S., Pal, D., Tuzon, C. T., Schweitzer, R., et al. (2019). FGF signaling patterns cell fate at the interface between tendon and bone. *Development* 146:dev170241. doi: 10.1242/dev.170241

Santagati, F., and Rijli, F. M. (2003). Cranial neural crest and the building of the vertebrate head. *Nat. Rev. Neurosci.* 4, 806–818. doi: 10.1038/nrn1221

Schwartz, A. G., Long, F., and Thomopoulos, S. (2015). Enthesis fibrocartilage cells originate from a population of Hedgehog-responsive cells modulated by the loading environment. *Development* 142, 196–206. doi: 10.1242/dev.112714

Schweitzer, R., Chyung, J. H., Murtaugh, L. C., Brent, A. E., Rosen, V., Olson, E. N., et al. (2001). Analysis of the tendon cell fate using Scleraxis, a specific marker for tendons and ligaments. *Development* 128, 3855–3866.

Shibukawa, Y., Young, B., Wu, C., Yamada, S., Long, F., Pacifici, M., et al. (2007). Temporomandibular joint formation and condyle growth require Indian hedgehog signaling. *Dev. Dyn.* 236, 426–434. doi: 10.1002/dvdy.21036

Sprinz, R. (1964). A note on the mandibular intra-articular disc in the joints of marsupialia and monotremata. *Proc. Zool. Soc. London* 144, 327–337. doi: 10.1088/1751-8113/44/8/085201

Sugimoto, Y., Takimoto, A., Hiraki, Y., and Shukunami, C. (2013). Generation and characterization of *ScxCre* transgenic mice. *Genesis* 51, 275–283. doi: 10.1002/dvg.22372

Takechi, M., and Kuratani, S. (2010). History of studies on mammalian middle ear evolution: a comparative morphological and developmental biology perspective. *J. Exp. Zool. B. Mol. Dev. Evol.* 314, 417–433. doi: 10.1002/jez.b.21347

Tan, G.-K., Pryce, B. A., Stabio, A., Brigande, J. V., Wang, C., Xia, Z., et al. (2020). TGFβ signaling is critical for maintenance of the tendon cell fate. *eLife* 9:e52695. doi: 10.7554/eLife.52695

Tsai, H. P., and Holliday, C. M. (2011). Ontogeny of the alligator cartilago transiliens and its significance for sauropsid jaw muscle evolution. *PLoS One* 6:e24935. doi: 10.1371/journal.pone.0024935

Tucker, A. S. (2017). Major evolutionary transitions and innovations: the tympanic middle ear. *Philos. Trans. R. Soc. B Biol. Sci.* 372:20150483. doi: 10.1098/rstb.2015.0483

Urban, D. J., Anthwal, N., Luo, Z.-X., Maier, J. A., Sadier, A., Tucker, A. S., et al. (2017). A new developmental mechanism for the separation of the mammalian middle ear ossicles from the jaw. *Proc. R. Soc. B Biol. Sci.* 284:20162416. doi: 10.1098/rspb.2016.2416

Wang, H., Meng, J., and Wang, Y. (2019). Cretaceous fossil reveals a new pattern in mammalian middle ear evolution. *Nature* 576, 102–105. doi: 10.1038/s41586-019-1792-0

Wang, Y., Liu, C., Rohr, J., Liu, H., He, F., Yu, J., et al. (2011). Tissue interaction is required for glenoid fossa development during temporomandibular joint formation. *Dev. Dyn.* 240, 2466–2473. doi: 10.1002/dvdy.22748

Watson, D. M. S. (1916). The monotreme skull: a contribution to mammalian morphogenesis. *Philos. Trans. R. Soc. London. Ser. B, Contain. Pap. Biol. Character* 207, 311–374. doi: 10.2307/92025

Wilson, J., and Tucker, A. S. (2004). Fgf and Bmp signals repress the expression of Bapx1 in the mandibular mesenchyme and control the position of the developing jaw joint. *Dev. Biol.* 266, 138–150. doi: 10.1016/j.ydbio.2003.10.012

Woronowicz, K. C., Gline, S. E., Herfat, S. T., Fields, A. J., and Schneider, R. A. (2018). FGF and TGFβ Signaling Link Form and Function During Jaw Development and Evolution. *Dev. Biol.* 1(Suppl. 1), S219–S236. doi: 10.1016/J.YDBIO.2018.05.002

Yang, L., Gu, S., Ye, W., Song, Y., and Chen, Y. P. (2016). Augmented Indian hedgehog signaling in cranial neural crest cells leads to craniofacial abnormalities and dysplastic temporomandibular joint in mice. *Cell Tissue Res.* 364, 105–115. doi: 10.1007/s00441-015-2306-5

Yasuda, T., Nah, H. D., Laurita, J., Kinumatsu, T., Shibukawa, Y., Shibutani, T., et al. (2012). Muenke syndrome mutation, FgfR3 P244R, causes TMJ defects. *J. Dent. Res.* 91, 683–689. doi: 10.1177/0022034512449170

Yoshida, T., Vivatbutsiri, P., Morriss-Kay, G., Saga, Y., and Iseki, S. (2008). Cell lineage in mammalian craniofacial mesenchyme. *Mech. Dev.* 125, 797–808. doi: 10.1016/j.mod.2008.06.007

Conflict of Interest: The authors declare that the research was conducted in the absence of any commercial or financial relationships that could be construed as a potential conflict of interest.

frontiers in Ecology and Evolution

ORIGINAL RESEARCH
published: 09 December 2021
doi: 10.3389/fevo.2021.741851

Tooth Structure and Replacement of the Triassic *Keichousaurus* (Sauropterygia, Reptilia) From South China

Jun-ling Liao[1,2], *Tian Lan*[1]*, *Guang-hui Xu*[3,4], *Ji Li*[1], *Yan-jiao Qin*[5], *Ming-sheng Zhao*[6], *Yu-lan Li*[1] and *Yue Wang*[1]*

[1] College of Resource and Environmental Engineering, Key Laboratory of Karst Georesources and Environment, Ministry of Education, Guizhou University, Guiyang, China, [2] College of Economics and Management, Xingyi Normal University for Nationalities, Xingyi, China, [3] Key Laboratory of Vertebrate Evolution and Human Origins of Chinese Academy of Sciences, Institute of Vertebrate Paleontology and Paleoanthropology, Chinese Academy of Sciences, Beijing, China, [4] CAS Center for Excellence in Life and Paleoenvironment, Beijing, China, [5] Research Department of Science and Technology, Guizhou Geological Museum, Guiyang, China, [6] College of Paleontology, Shenyang Normal University, Shenyang, China

The small-sized sauropterygian *Keichousaurus hui* was one of the most abundant marine reptiles from the Triassic Yangtze Sea in South China. Although *Keichousaurus* has been studied in many aspects, including the osteology, ontogeny, sexual dimorphism, and reproduction, the dentition of this marine reptile was only briefly described in external morphology. In this study, we provide new information on *Keichousaurus* tooth implantation, histology, and replacement based on a detailed examination of well-preserved specimens collected in the past decades. The tooth histology has been investigated for the first time by analyzing cross-sections of premaxillary teeth and the tooth attachment and implantation have been further revealed by X-ray computed microtomography. We refer the tooth replacement of *Keichousaurus* to the iguanid replacement type on the basis of the observed invasion of small replacement tooth into the pulp cavity of the functional tooth. Given the resemblance to other extinct and modern piscivorous predators in the morphology and structure of teeth, *Keichousaurus* might mainly feed on small or juvenile fishes and some relatively soft-bodied invertebrates (e.g., mysidacean shrimps) from the same ecosystem.

Keywords: pulp cavity, plicidentine, tooth replacement, *Keichousaurus*, Triassic, South China

OPEN ACCESS

Edited by:
Pedro Martinez,
University of Barcelona, Spain

Reviewed by:
Mark Joseph MacDougall,
Museum of Natural History Berlin (MfN), Germany
Domenic D'Amore,
Daemen College, United States

***Correspondence:**
Tian Lan
lantianing@sina.com
Yue Wang
gzyuewang@126.com

Specialty section:
This article was submitted to Evolutionary Developmental Biology, a section of the journal Frontiers in Ecology and Evolution

Received: *15 July 2021*
Accepted: *05 November 2021*
Published: *09 December 2021*

Citation:
Liao JL, Lan T, Xu GH, Li J, Qin YJ, Zhao MS, Li YL and Wang Y (2021) Tooth Structure and Replacement of the Triassic Keichousaurus (Sauropterygia, Reptilia) From South China. Front. Ecol. Evol. 9:741851. doi: 10.3389/fevo.2021.741851

INTRODUCTION

Teeth are complex mineralized tissues that originated in jawed vertebrates more than 400 million years ago (Rücklin et al., 2012). The shape, implantation, and replacement of teeth differ widely across vertebrates and promote the radiation of this clade (Owen, 1841, 1842; Edmund, 1960, 1962; Peyer, 1968; Mehler and Bennett, 2003; Maxwell et al., 2012; Buchtová et al., 2013; LeBlanc et al., 2017; McCurry et al., 2019). Reptiles show a diverse array of tooth shapes from homodont to heterodont (Peyer, 1968; Rieppel, 2002) and from simple unicuspid to complex multicuspid teeth (Ungar, 2010; Handrigan and Richman, 2011), reflecting functional adaptation to various diets. Additionally, reptiles exhibit numerous combinations of tooth implantation and attachment (Peyer, 1968; Mehler and Bennett, 2003; Buchtová et al., 2013; LeBlanc et al., 2017), ranging from teeth possessing roots and lying within a socket (thecodonty), to teeth lying against the lingual wall

of the jawbone (pleurodonty), and to teeth without roots or sockets that are attached to the apex of the marginal jawbones (acrodonty). Continuous tooth replacement (polyphyodonty) is common for the vast majority of reptiles, although some groups (e.g., acrodont lepidosaurs) have lost the ability to replace their dentition (monophyodonty) (Edmund, 1960, 1962; Peyer, 1968; Motani, 1997; Rieppel, 2001; Fastnacht, 2008; Maxwell et al., 2012; Buchtová et al., 2013; Neenan et al., 2014; LeBlanc and Reisz, 2015).

The small-sized sauropterygian *Keichousaurus hui* (rarely exceeding 50 cm in total length) is one of the most abundant reptiles from the Triassic Yangtze Sea in South China (Young, 1958; Rieppel and Lin, 1995; Jiang, 2002; Holmes et al., 2008; Cheng et al., 2009; Fu et al., 2013; Xue et al., 2013). The genus was originally classified by Young (1958) in Pachypleurosauridae or in its own family (Keichousauridae) (Young, 1965) before formal phylogenetic analyses. Recent analyses of the sauropterygian phylogeny place *Keichousaurus* either at a relative basal position of the Eosauropterygia (Shang et al., 2020) or within Pachypleurosauridae (Li and Liu, 2020; Lin et al., 2021). Represented by large quantities of well-preserved specimens, *Keichousaurus* has been studied in many aspects including the ontogeny, taphonomy, reproduction, sexual dimorphism, allometry, and living style (Lin and Rieppel, 1998; Cheng et al., 2004, 2009; Holmes et al., 2008; Fu et al., 2013; Xue et al., 2013; Motani et al., 2015). However, the teeth of *Keichousaurus*—significant organs for taxonomy and ethology (Radinsky, 1961; Handrigan and Richman, 2011; Hwang, 2011)—were only briefly described in their external morphology (Young, 1958, 1965; Lin and Rieppel, 1998; Jiang, 2002; Holmes et al., 2008; Fu et al., 2013). Compared with those in other marine reptiles (Maisch and Matzke, 1997; Motani, 1997; Rieppel, 2001; Ciampaglio et al., 2005; Caldwell, 2007; Maxwell et al., 2012; Neenan et al., 2014; Sassoon et al., 2015), the teeth of *Keichousaurus* remain poorly known in their internal structure, function, and replacement.

In this study, through a detailed examination of well-preserved specimens, we aim to describe the tooth morphology, internal structure, and tooth histology of *Keichousaurus* and to discuss the tooth replacement, dental function, and food preference of this taxon.

MATERIALS AND METHODS

All the studied specimens of *Keichousaurus* are housed in the Resource and Environmental Engineering College of Guizhou University (GZU), China. They were collected from the lower part of the Zhuganpo (lower) member of the Falang Formation in southwestern Guizhou (Dingxiao) and eastern Yunnan (Fuyuan), South China (**Figure 1B**). This member of fossil beds, composed of dark gray thin-to medium-bedded limestones or muddy limestones with dolomitic limestones, indicates a carbonate platform deposit environment (Liu and Xu, 1994; Wang, 1996, 2002; Rieppel, 1999; Rieppel et al., 2000; Jiang, 2002) (**Figure 1A**). Also, from the fossil beds, rich invertebrates, bony fishes, and several other types of marine reptiles are also found; the whole fossil assemblage represents the renowned Xingyi Biota (Su, 1959; Jin, 2001; Liu et al., 2002, 2003; Li, 2006; Geng and Jin, 2009; Xu et al., 2012, 2015, 2018a,b; Tintori et al., 2015; Sun et al., 2016; Ni et al., 2017; Xu and Ma, 2018; Shang et al., 2020; Xu, 2020). The age of this biota was controversial (Benton et al., 2013). Biostratigraphical studies of marine reptiles and ammonites (Young, 1958; Chen, 1985; Li, 2006; Zou et al., 2015) consistently support a late Middle Triassic (late Ladinian), but conodont biostratigraphy (Yang et al., 1995; Wang, 1996, 2002; Wang et al., 1998) suggests a younger Late Triassic (Carnian) age for this biota. Zou et al. (2015) commented that the previous conodont identification is inaccurate; the conodont "*Paragondolella polygnathiformis*" identified by Wang et al. (1998) is actually a transition *Paragondolella polygnathiformis-P. nodosa* recovered from a sample 3 m above the vertebrate-bearing interval. A recent zircon U-Pb age dating (240.8 ± 1.8 Ma) (Li et al., 2016) supports the determination of late Middle Triassic (Ladinian) for the Xingyi Biota.

The specimens were prepared mechanically with sharp steel needles and air scribe under optical microscope and some were washed by dilute oxalic acid to further remove the matrix. Tooth section and photography were performed at the Key Laboratory of Vertebrate Evolution and Human Origins of Chinese Academy of Sciences, Beijing, China. The whole skull of the specimen (GZU V0056) was removed and embedded in resin for preparation of transverse sections. Thin sections of four premaxillary teeth (about 30 μm in thickness) were obtained from the bases of tooth crowns (perpendicular or nearly perpendicular to the long axis of the tooth). These sections were analyzed and photographed under cross-polarized light using the Zeiss Imager A2m microscope. X-ray computed microtomography was performed at the Yunnan Key Laboratory for Palaeobiology of the Institute of Palaeontology, Yunnan University, China, using a micro-CT (Xradia 520 Versa) with a pixel size of 14.71 μm in three axes.

TOOTH MORPHOLOGY AND INTERNAL STRUCTURE

The general morphology of the dentition of *Keichousaurus* has been described by Holmes et al. (2008) in their revision of the skull of this taxon. The heterodont teeth with variation of sizes are implanted in deep sockets of the premaxilla and maxilla in the upper jaw and the anterior portion of the dentary in the lower jaw (**Figures 2A,B**). The teeth in the premaxilla are strongly procumbent (visible in dorsal view) and five in number, larger than the anterior three teeth in the maxilla. The fourth and fifth maxillary teeth are fang-like (caniniform), nearly as large as the largest premaxillary teeth in size (**Figures 2A–C**), and the sixth and remaining (about 10) maxillary teeth are notably smaller, becoming angled more mesial than labial (**Figures 2A,C,D**). A nearly complete series of 19 dentary teeth is discernable in the specimen GZU V0028 including 6 enlarged teeth near the symphysis followed by 13 smaller teeth posteriorly.

As typically in other marine reptiles, the tooth of *Keichousaurus* can be divided into three parts: a crown, a root, and the neck or cervical margin where these two parts

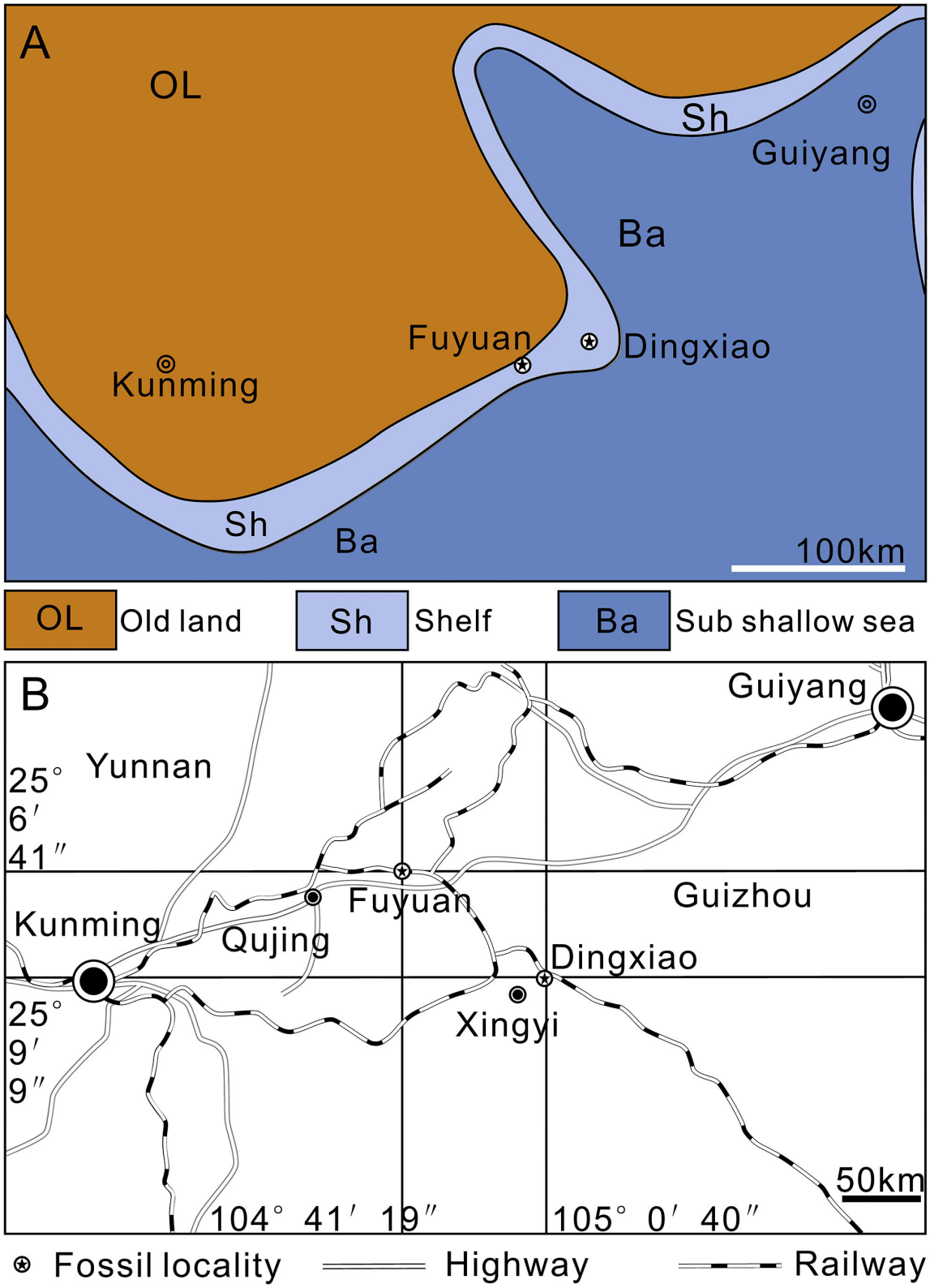

FIGURE 1 | Maps. **(A)** Paleogeography of Southwest China near the Middle/Late Triassic boundary (modified from Liu and Xu, 1994). **(B)** Traffic map of fossil localities.

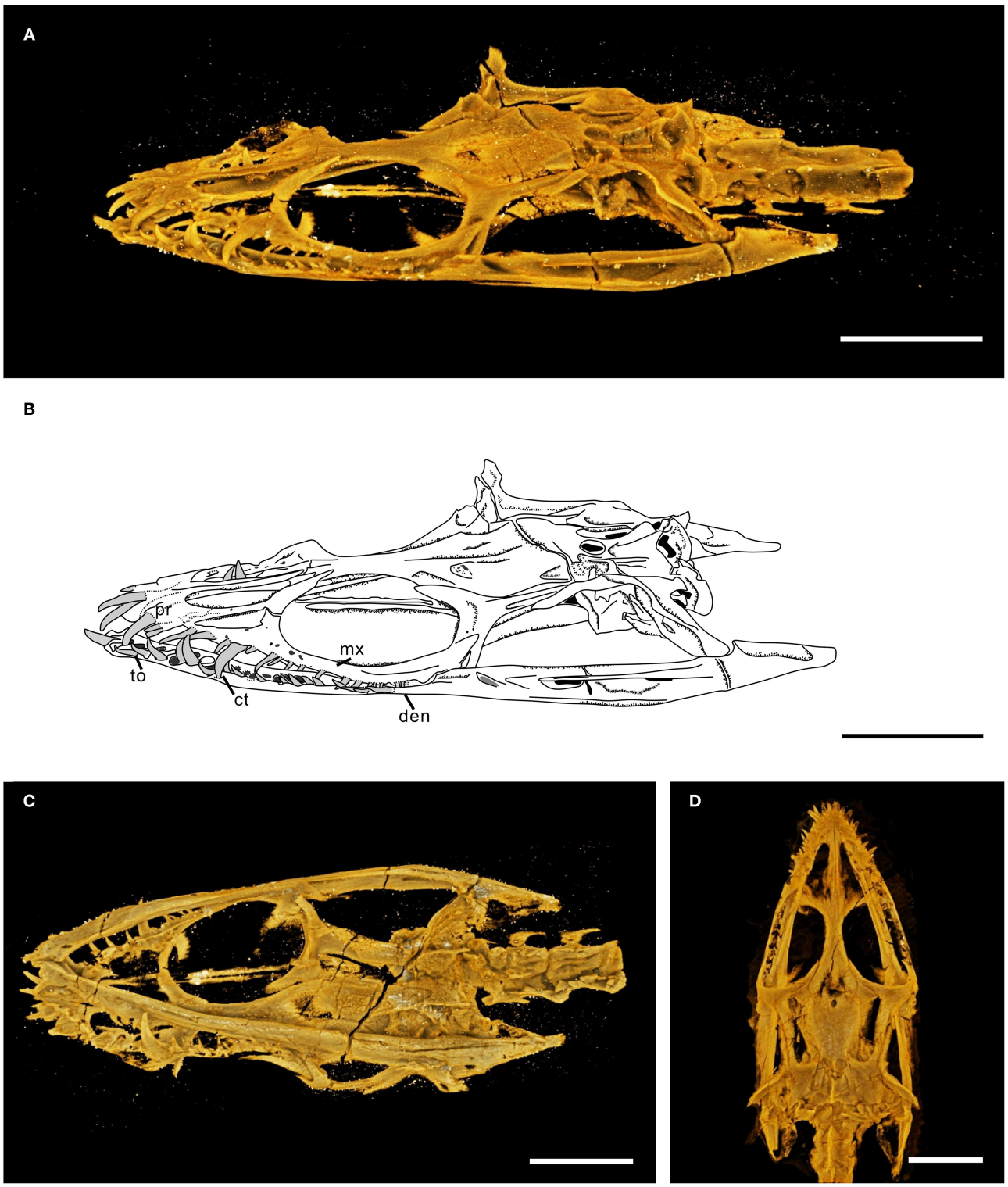

FIGURE 2 | CT scans of skull of *Keichousaurus*. **(A)** Dorsolateral view (GZU V0028), scale bars = 5 mm. **(B)** Line drawing of **(A)**, scale bars = 5 mm. **(C)** Ventrolateral view (GZU V0028), scale bars = 5 mm. **(D)** Ventral view (GZU V0516), scale bars = 5 mm. ct, caniniform tooth; den, dentary; mx, maxilla; pr, premaxilla; to, tooth.

meet. The root is invisible *in situ*, but can be observed when it is detached from the jawbone (**Figures 3A,F**). It has a contracted basal pedicel deeply intercalated within the concave alveolus (**Figures 3D,E**). The nearly cylindrical root gradually shrinks from near the neck toward the opened root apex (**Figure 3F**). The average length of the root is 0.73 mm, accounting for about half

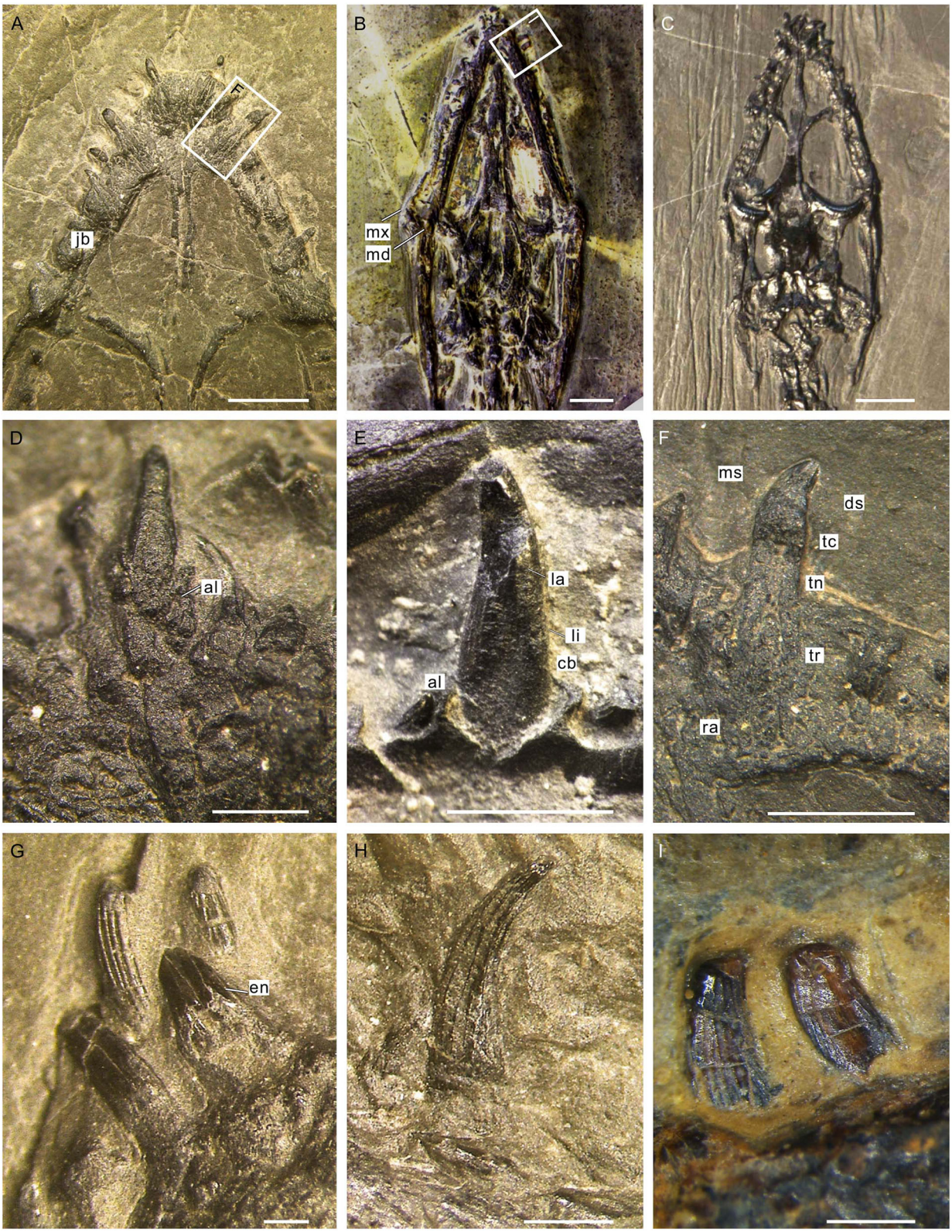

FIGURE 3 | Teeth of *Keichousaurus*. **(A)** Premaxillary teeth (GZU V0036), scale bar = 2 mm. **(B)** Ventral view of the skull (GZU V0095), scale bar = 3 mm. **(C)** Dorsal view of the skull (GZU V0057), scale bar = 4 mm. **(D)** Premaxillary tooth, showing the root inserted into a concaved alveolus (GZU V0043), scale bar = 500 μm. **(E)** A

(Continued)

FIGURE 3 | caniniform tooth (GZU V0028), scale bar =1 mm. **(F)** Magnified view of **(A)**, showing an elongated root, scale bar = 1 mm. **(G)** Left mandibular anterior teeth (GZU V0023), showing the tooth neck, scale bar = 250 μm. **(H)** Right mandibular tooth (GZU V0035), showing the apicobasal ridges, scale bar = 500 μm. **(I)** Right mandibular teeth (GZU V0095), showing the transverse furrows, scale bar = 500 μm. al, alveolus; cb, crown base; ds, distal side; en, enamel; jb, jaw bone; la, labial surface; li, lingual surface; md, mandible; ms, mesial side; mx, maxilla; ra, root apex; tc, tooth crown; tn, tooth neck; tr, tooth root.

to two-thirds of the whole length of the tooth. The waist-shaped neck is presented as an annular depression (**Figures 3F,G**), having a depth of 0.21–0.34 mm. The crown is conical with a sharp, slightly recurved dental cusp (**Figures 3E,F,H**). Lingually, it is concave with an arc-shaped mesial surface (**Figures 3G,H**). The crown has a maximal length of 1.51 mm in the premaxillary teeth and the ratio of height to width ranges from 2.5 to 3.5. The external surface of the crown is ornamented with fine, longitudinal ridges separated by multiple regularly spaced grooves (**Figures 3G–I**). These longitudinal ridges, termed as apicobasal ridges (Young et al., 2012, 2014a,b; Zverkov et al., 2018; McCurry et al., 2019), are straight or slightly curved and unbranched; they extend from the crown base to the apex of cusp, tapering in width along the basal–apical direction. The apicobasal ridges are continuous or interrupted by some shallow, traverse furrows (**Figure 3I**).

The oval cross-section of the tooth crown (viewed from its basal part) has two dark-colored layers (enamel and dentine layer) surrounding a light-colored pulp cavity (**Figures 4A,B,F**, **5A,B**). A relatively bright and transparent (unevenly mineralized) globular zone is discernable between the enamel and dentine layers (**Figures 5A,B**). The enamel layer is densely mineralized and very thin (about 5 μm), indicated by a black ring in the tooth section (**Figures 5A,B**); it gradually becomes sparse toward the neck (**Figure 4C**). The dentine layer, as the main component of the tooth, is relatively low in density and bears some ridges and cracks in its internal wall (**Figures 4A,B**). In tooth sections, the annular dentine is simply folded, in which irregular white calcites and centripetally curved, fibril-like dentinal tubules are also present (**Figures 5A,C**). The circumpulpal dentinal tubules are closely packed near the pulp cavity to make this area darker in color than the surrounding areas of the dentine layer. It appears that some tubules nearly extend into the center of the pulp cavity, indicated by some irregular dark patches in the cavity (**Figures 5A,D**).

The pulp cavity (including pulp chamber and root canal) is largely spindle shaped (**Figures 4A,B,E**), completely filled with euhedral crystal grains of white calcites after the internal connective tissue decayed. The average length from the recurved tip of the pulp chamber to the apical portion of the dental cusp (**Figures 4A,B,D,E**) is 0.36 mm. At the horizontal level of the base of the tooth crown, the pulp cavity reaches its maximum width, which ranges from 0.16 to 0.27 mm and accounts for about fourth-fifths of the width of the tooth crown.

TOOTH REPLACEMENT

The tooth replacements of *Keichousaurus* are traceable in some specimens (GZU V0021, 0044, 0049, 0053), in which small replacement teeth are associated with the pulp cavities of larger predecessor teeth (functional teeth) (**Figures 6A–D**). Among them, the replacement teeth in the specimens GZU V0049 (**Figures 6A,E**) and GZU V0021 (**Figures 6B,F**) are the smallest ones, which are exposed near the mesial-lingual side of the pulp cavities of the predecessor teeth, accounting for slightly less than half of the cavity of predecessor teeth in size. Both have only a loose dentine layer without a distinct enamel layer. In the specimen GZU V0044 (**Figures 6C,G**), the replacement tooth is larger, accounting for slightly more than half of the pulp cavity of the predecessor tooth. Within the predecessor tooth, the replacement tooth extends anterodorsally from the posteroventral edge of the root to the mesial-labial margin of the pulp cavity. The replacement tooth (GZU V0044) (**Figure 6C**) bears a triangular pulp cavity larger than that in the replacement tooth of specimens GZU V0021 (**Figure 6B**). In specimen GZU V0053 (**Figures 6D,H**), the replacement tooth is the largest one, nearly occupying the whole space of this pulp cavity. The replacement tooth has enamel and dentine layers with an even larger pulp cavity.

Two typical tooth replacement types are present in reptiles (Edmund, 1960; Rieppel, 1978; De Ricqlès and Bolt, 1983): iguanid and varanid tooth replacement types. In the former, a replacement tooth germinates at the lingual surface of root of a functional tooth and then invades into the pulp cavity of its related functional tooth during tooth growth; in the latter, the replacement tooth erupts in the interdental location and does not migrate into the pulp cavity during tooth development. Moreover, there is an intermediate replacement type in some reptiles, in which the replacement tooth adopts the replacement path of the iguanid type (existence of an invasion into the pulp cavity of the functional tooth), but the erupting position is similar to that of replacement tooth in the varanid type, with a distal deviation (Rieppel, 1978; Bertin et al., 2018). Based on the presence of replacement teeth inside the pulp cavity of the functional teeth (**Figures 6A–H**), we conclude that the tooth replacement of *Keichousaurus* can largely be referred to the iguanid replacement type. This replacement type was also found in plesiosaurs, Jurassic ichthyosaurs, *Platypterygius*, and extant crocodilians (Edmund, 1960, 1962; Motani, 1997; Fastnacht, 2008; Maxwell et al., 2012).

TOOTH FUNCTION AND FOOD PREFERENCE

The teeth of *Keichousaurus* are thecodont and their roots deeply insert into individual alveoli (**Figures 3D,E**), such as those of some other eosauropterygians (e.g., *Nothosaurus* and *Simosaurus*) and crocodiles (Rieppel, 2001; LeBlanc et al., 2017). The waist-shaped tooth neck has a certain depth (0.21–0.34 mm) and the interdental gap is likely filled by gums, which contribute

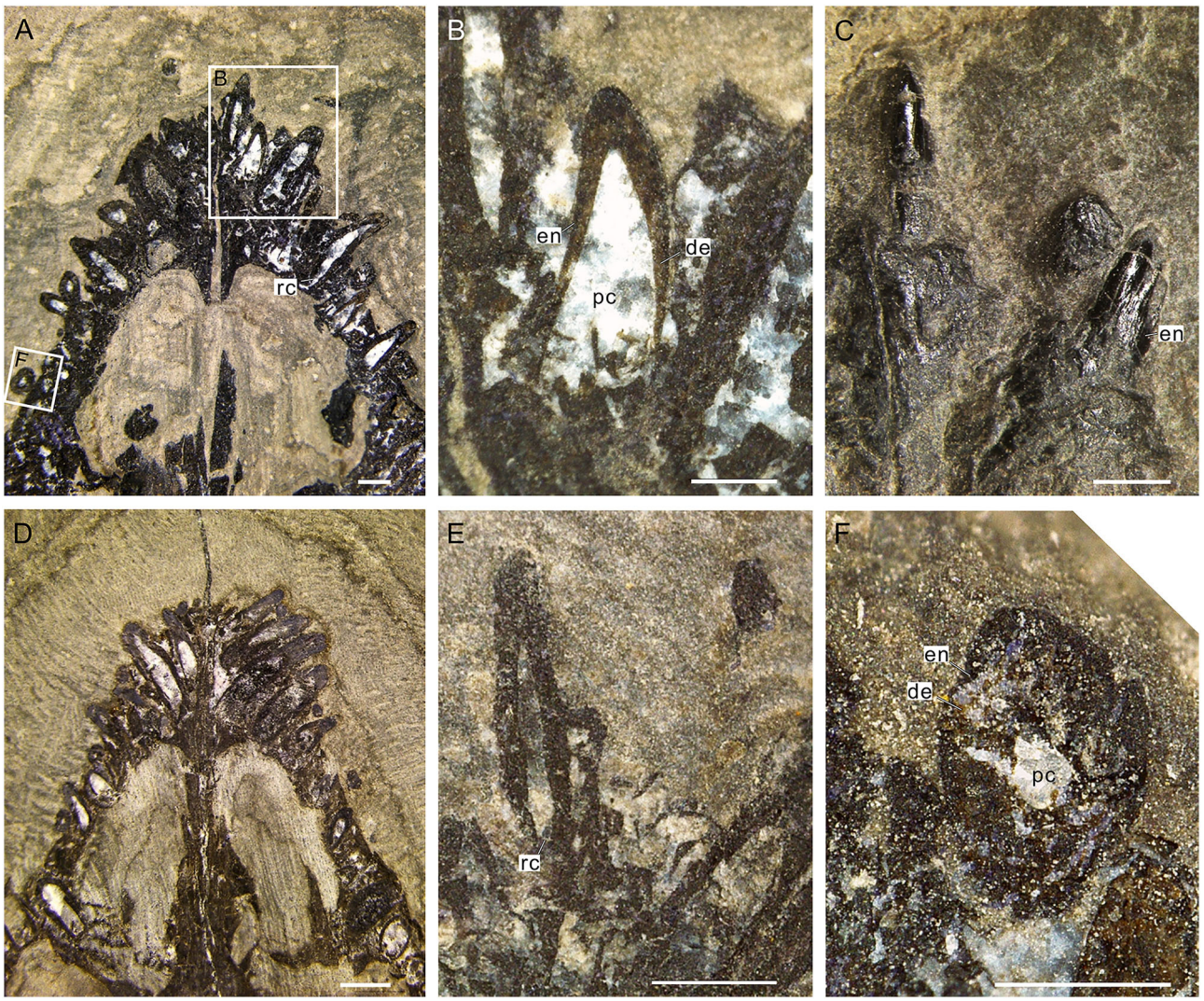

FIGURE 4 | Internal structure of teeth of *Keichousaurus*. **(A)** Dorsal view of teeth (GZU V0049), scale bar = 500 μm. **(B)** Three right premaxillary teeth, showing the large pulp cavities (GZU V0049), scale bar = 250 μm. **(C)** Two teeth of the central premaxilla side, showing the rare faction of enamel on the neck (GZU V0042), scale bar = 500 μm. **(D)** Dorsal view (GZU V0050), scale bar = 1 mm. **(E)** Second teeth on the left premaxilla side (GZU V0046), showing the narrower root canals, scale bar = 500 μm. **(F)** Cross-section (GZU V0049), showing a two-layer structure, scale bar = 250 μm. de, dentine; en, enamel; rc, root canal; pc, pulp cavity.

to the tooth stability (Chung et al., 2006; Carnio et al., 2007; Bourie et al., 2008). The teeth of *Keichousaurus* in anterior portions of jaws are elongated, fang like, and loosely arranged (Young, 1958, 1965; Jiang, 2002; Holmes et al., 2008; Fu et al., 2013). These teeth might exert the main force used to control prey by latching onto it and preventing escape (**Figures 2A,B,D**). The small teeth in posterior portions of jaws (**Figures 2A,C**) could act as a ratchet, transporting the prey posteriorly to the esophagus (Taylor, 1987; Taylor and Cruickshank, 1993).

The crowns of *Keichousaurus* are ornamented with apicobasal ridges (**Figures 3G,H**). These ridges, also present in other sauropterygians (e.g., *Pliosaurus* and *Helveticosaurus*) and some crocodylomorphs (Young et al., 2012, 2014a,b), might help pierce slippery or scaly struggling prey, facilitate blood drain, and prevent the prey from escaping (Frazzetta, 1966; Wright et al., 1979; Vaeth et al., 1985; Kardong and Young, 1996; Massare, 1997; Young et al., 2014b; McCurry et al., 2019). Plicidentine manifested as apicobasal ridges externally (**Figures 3H**, **5A,C**; Tomes, 1878; Maxwell et al., 2012; Macdougall et al., 2014; McCurry et al., 2019) is regarded as a functional property of large predators (Scanlon and Lee, 2002; Modesto and Reisz, 2008). It, commonly seen in labyrinthodonts (Owen, 1841, 1842), mosasaurs (Schultze, 1970), ichthyosaurs (Maxwell et al., 2011), plesiosaurs (Owen, 1841), extant varanoids (Zaher and Rieppel, 1999), and snakes (Scanlon and Lee, 2002), could enhance the stress resistance and strength of the tooth-to-jaw anchoring (Peyer, 1968; Scanlon and Lee, 2002; Maxwell et al., 2011; Macdougall et al., 2014).

Based on the conical crown shape, sharp cusp (**Figures 3E,H**), moderate size (crown height to width between 2.5 and 3.5), and

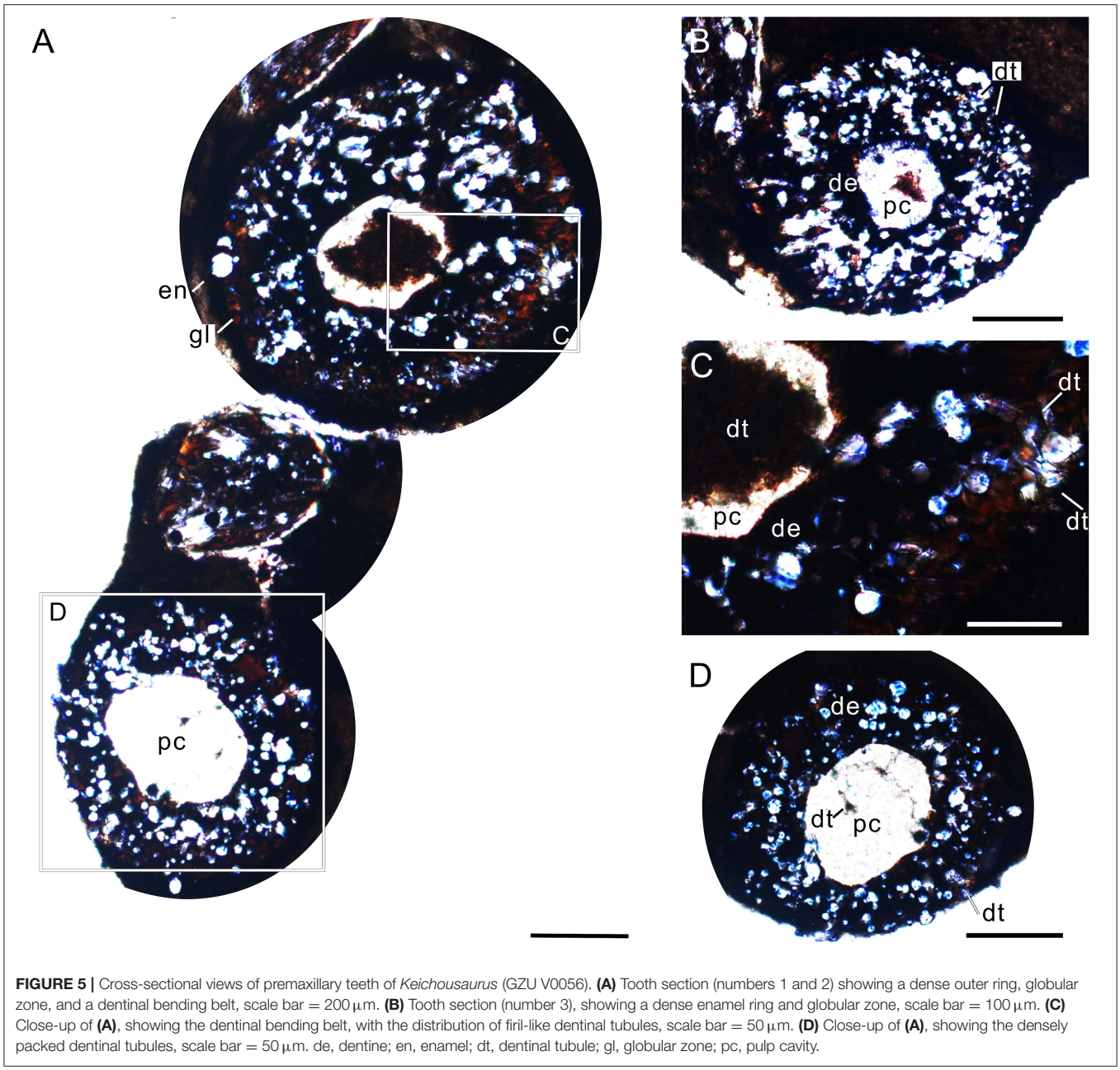

FIGURE 5 | Cross-sectional views of premaxillary teeth of *Keichousaurus* (GZU V0056). **(A)** Tooth section (numbers 1 and 2) showing a dense outer ring, globular zone, and a dentinal bending belt, scale bar = 200 μm. **(B)** Tooth section (number 3), showing a dense enamel ring and globular zone, scale bar = 100 μm. **(C)** Close-up of **(A)**, showing the dentinal bending belt, with the distribution of firil-like dentinal tubules, scale bar = 50 μm. **(D)** Close-up of **(A)**, showing the densely packed dentinal tubules, scale bar = 50 μm. de, dentine; en, enamel; dt, dentinal tubule; gl, globular zone; pc, pulp cavity.

ornamentation of apicobasal ridges (**Figures 3G,H**), the teeth of *Keichousaurus* could be categorized as pierce II (Massare, 1987). This type of piercing teeth (**Figures 3A,D,H**), unlike those in the filter-feeder *Atopodentatus* with needle-like teeth (Cheng et al., 2014) or those in durophagous placodontian predators with bulbous teeth (Neenan et al., 2013), are similar to the "fish-trap" teeth of exclusively piscivorous predators such as many mesozoic marine reptiles (ancient plesiosaurs, pliosauroids, teleosaurs, geosaurs, and nothosaurs) and extant river dolphins and gavial (Massare, 1987, 1997; Taylor and Cruickshank, 1993; Sander, 1999; Rieppel, 2002; Ciampaglio et al., 2005; Shang, 2007).

The teeth of *Keichousaurus* with large pulp cavities (**Figures 4A,B,F**) might have had sound microcirculation systems and keen sensory nerves to perform well in many respects including eliciting endogenous mechanisms of defense, moderating inflammation, providing pain tolerance, and promoting postinjury healing (Gazelius et al., 1987; Silverman and Kruger, 1987; Kimberly and Byers, 1988; Byers et al., 1990; Olgart, 1990; Taylor and Byers, 1990; Byers and Taylor, 1993; Chen et al., 1994; Walton and Nair, 1995; Evans et al., 1999; Hahn and Liewehr, 2007; Caviedes-Bucheli et al., 2008; Couve et al., 2013; Satoko et al., 2013). The large pulp cavities

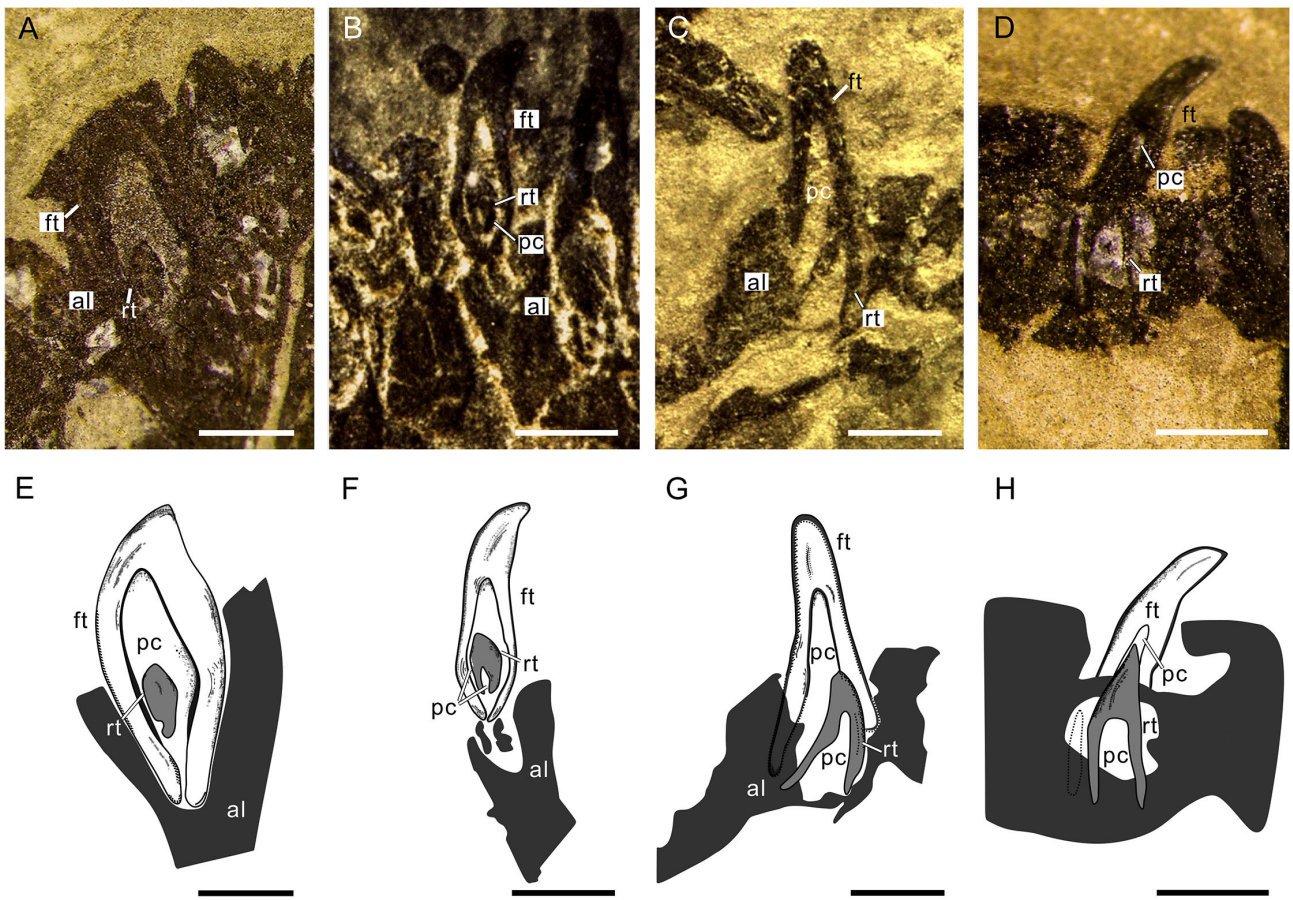

FIGURE 6 | Tooth replacement of *Keichousaurus*. **(A)** Left premaxillary teeth in dorsal view (GZU V0049), scale bar = 500 μm. **(B)** Right premaxillary teeth in ventral view (GZU V0021), scale bar = 500 μm. **(C)** Left maxillary teeth in dorsal view (GZU V0044), scale bar = 500 μm. **(D)** Right maxillary teeth in dorsal view (GZU V0053), showing the, scale bar = 500 μm. **(E)** Line drawing of **(A)**, scale bar = 500 μm. **(F)** Line drawing of **(B)**, scale bar = 500 μm. **(G)** Line drawing of **(C)**, scale bar = 500 μm. **(H)** Line drawing of **(D)**, scale bar = 500 μm. al, alveolus; ft, functional tooth; rt, replacement tooth; pc, pulp cavity.

are prevalent among aquatic carnivores such as dolphins and the crocodilian *Alligator* (Westergaard and Ferguson, 1990; Slooten, 1991). Considering the large pulp cavity is surrounded by a thin wall, the bending resistance and strength of the tooth might be achieved by the radial foldings of the dentine (Plicidentine) (**Figures 5A–C**) (Preuschoft et al., 1991). The teeth of *Keichousaurus*, thus, might respond sensitively to external stimuli and have a relatively strong piercing force.

A rich diversity of small scaly or naked ray-finned fishes has been recovered from the same fossiliferous layer as *Keichousaurus* including thoracopterids, peltopleurids and luganoiids (Xu et al., 2012, 2015, 2018b; Xu, 2020), holosteans (Liu et al., 2002, 2003; Xu et al., 2018a), and stem teleosts (Tintori et al., 2015). These fishes, as primary consumers in the food web of the Xingyi Biota, appear the potential prey of *Keichousaurus* and other piscivorous marine reptiles (e.g., nothosaurs). Other primary consumers in the same ecosystem include mysidaceans, gastropods, brachiopods, bivalves, ammonoids, etc. Among them, the small and relatively soft-bodied mysidaceans are probably the alternative prey of *Keichousaurus*, but other invertebrates with hard shells are unlikely in the diet of *Keichousaurus*.

CONCLUSION

Our detailed examination of well-preserved specimens of *Keichousaurus* provides new information on its tooth implantation, histology, and replacement. The thecodont teeth of *Keichousaurus* resemble the "fish-trap" teeth of other extinct and modern piscivorous predators: the cylindrical root deeply inserts into the alveolus with its depth accounting for about a half to two-thirds of the tooth; the dental neck is presented as an annular depression (0.21–0.34 mm in depth); and the conical, thin-enameled crown bears apicobasal ridges on its surface with a sharp, slightly recurved tooth cusp apically. These ridges might help pierce slippery or struggling scaly prey, facilitate blood drain, and prevent the prey from escaping. In the cross-section of the basal portion of the crown, the tooth has two dark-colored layers (dense enamel and radially folded dentine) surrounding a light-colored large pulp cavity, with some dentinal tubules

invading the cavity. The tooth replacement of *Keichousaurus* can largely be referred to the iguanid replacement type on the basis of the invasion of small replacement tooth into the pulp cavity of the predecessor tooth. Deduced from the functional morphology of the tooth, the potential prey of *Keichousaurus* is mainly composed of small or juvenile fishes and some relatively soft-bodied invertebrates (e.g., mysidacean shrimps) from the same ecosystem.

DATA AVAILABILITY STATEMENT

The original contributions presented in the study are included in the article/**Supplementary Material**, further inquiries can be directed to the corresponding authors.

AUTHOR CONTRIBUTIONS

YW and TL put forward the concept. J-lL wrote this manuscript with comments from G-hX. Y-jQ performed data analysis. JL proposed some suggestions to the article. M-sZ and Y-lL made contributions to data visualization. All authors contributed to the article and approved the submitted version.

FUNDING

This study was supported by the National Natural Science Foundation of China (Grant No. 41762001), the Guizhou Science and Technology Project (No. 2017-5788), the Strategic Priority Research Program (B) of Chinese Academy of Sciences (Grant No. XDB 26000000), the National Natural Science Foundation of China (No. 41902003), and the Natural Science Foundation of Guizhou (No. 20171057).

ACKNOWLEDGMENTS

We are grateful to Dr. Qiang Wang (Institute of Vertebrate Paleontology and Paleoanthropology, Chinese Academy of Sciences) for helping in teeth sections, Mr. ShiLong Ye (Fossil Restoration Center, Dingxiao, Guizhou, China) and Mr. Anjing Zhang (Wusha Village of Xingyi, Guizhou, China) for helping in fossil collection and preparation.

SUPPLEMENTARY MATERIAL

The Supplementary Material for this article can be found online at: https://www.frontiersin.org/articles/10.3389/fevo.2021.741851/full#supplementary-material

REFERENCES

Benton, M.J., Zhang, Q., Hu, S., Chen, Z. Q., Wen, W., Liu, J., et al. (2013). Exceptional vertebrate biotas from the Triassic of China, and the expansion of marine ecosystems after the Permo-Triassic mass extinction. *Earth-Sci. Rev.* 125, 199–243. doi: 10.1016/j.earscirev.2014.08.004

Bertin, T. J., Thivichon-Prince, B., LeBlanc, A. R., Caldwell, M. W., and Viriot, L. (2018). Current perspectives on tooth implantation, attachment, and replacement in amniota. *Front. Physiol.* 9:1630. doi: 10.3389/fphys.2018.01630

Bourie, A., Bissada, N., Al-Zahrani, M. S., Faddoul, F., and Nouneh, I. (2008). Width of keratinized gingiva and the health status of the supporting tissues around dental implants. *Int. J. Oral. Maxillofac. Implants.* 23, 323–326. doi: 10.1016/j.ijom.2007.09.170

Buchtová, M., Zahradníček, O., Balková, S., and Tucker, A. S. (2013). Odontogenesis in the veiled chameleon (*Chamaeleo calyptratus*). *Arch. Oral. Biol.* 58, 118–133. doi: 10.1016/j.archoralbio.2012.10.019

Byers, M. R., and Taylor, P. E. (1993). Effect of sensory denervation on the response of rat molar pulp to exposure injury. *J. Dent. Res.* 72, 613–618. doi: 10.1177/00220345930720031001

Byers, M. R., Taylor, P. E., Khayat, B. G., and Kimberly, C. L. (1990). Effects of injury and inflammation on pulpal and periapical nerves. *J. Endod.* 16, 78–84. doi: 10.1016/S0099-2399(06)81568-2

Caldwell, M. W. (2007). Ontogeny, anatomy and attachment of the dentition in Mosasaurs (Mosasauridae: Squamata). *Zool. J. Linn. Soc.* 149, 687–700. doi: 10.1111/j.1096-3642.2007.00280.x

Carnio, J., Camargo, P. M., and Passanezi, E. (2007). Increasing the apico-coronal dimension of attached gingiva using the modified apically repositioned flap technique: a case series with a 6-month follow-up. *J. Periodontol.* 78, 1825–1830. doi: 10.1902/jop.2007.060414

Caviedes-Bucheli, J., Muñoz, H. R., Azuero-Holguín, M. M., and Ulate, E. (2008). Neuropeptides in dental pulp: the silent protagonists. *J. Endod.* 34, 773–788. doi: 10.1016/j.joen.2008.03.010

Chen, X. M., Zhao, H. P., and He, G. H. (1994). Preliminary study on the biological clock of pulp. *W. Chin. J. Stomatol.* 12, 36–38. (in Chinese with English abstract). doi: 10.CNKI:SUN:HXKQ.0.1994-01-014

Chen, Z. F. (1985). Stratigraphical position of kueichousaurushuiyoung of middletriassic and itssingificance in southwestern guizhou. *Guiz. Geol.* 2, 289–290. (in Chinese with English abstract). Available online at: http://en.cnki.com.cn/Article_en/CJFDTOTAL-GZDZ198503010.htm.

Cheng, L., Chen, X. H., Shang, Q. H., and Wu, X. C. (2014). A new marine reptile from the Triassic of China, with a highly specialized feeding adaptation. *Naturwissenschaften.* 101, 251–259. doi: 10.1007/s00114-014-1148-4

Cheng, Y. N., Holmes, R., Wu, X. C., and Alfonso, N. (2009). Sexual dimorphism and life History of *Keichousaurushui* (Reptilia: Sauropterygia). *J. Vertebr. Paleontol.* 29, 401–408. doi: 10.org/10.1671/039.029.0230

Cheng, Y. N., Wu, X. C., and Ji, Q. (2004). Triassic marine reptiles gave birth to live young. *Nature* 432, 383–386. doi: 10.1038/nature03050

Chung, D. M., Oh, T. J., Shotwell, J. L., Misch, C. E., and Wang, H. L. (2006). Significance of keratinized mucosa in maintenance of dental implants with different surfaces. *J. Periodontol.* 7, 1410–1420. doi: 10.1902/jop.2006.050393

Ciampaglio, C. N., Wray, G. A., and Corliss, R. H. (2005). A toothy tale of evolution: convergence in tooth morphology among marine Mesozoic-Cenozoic sharks, reptiles, and mammals. *Sediment. Res.* 3, 4–7. Available online at: http://www.sites.biology.duke.edu (accessed October, 2020).

Couve, E., Osorio, R., and Schmachtenberg, O. (2013). The amazing odontoblast: activity, autophagy, and aging. *J. Dent. Res.* 92, 765–772. doi: 10.1177/0022034513495874

De Ricqlès, A., and Bolt, J. R. (1983). Jaw growth and tooth replacement in *Captorhinus aguti* (Reptilia: Captorhinomorpha): a morphological and histological analysis. *J. Vertebr. Paleontol.* 3, 7–24. doi: 10.1080/02724634.1983.10011952

Edmund, A. G. (1960). *Tooth Replacement Phenomena in the Lower Vertebrates*. Toronto: Royal Ontario Museum Toronto, Life Sciences Division Press.

Edmund, A. G. (1962). *Sequeuce and Rate of Tooth Replacement in the Crocodilia*. Toronto: Royal Ontario Museum Toronto, Life Sciences Division Press.

Evans, D., Reid, J., Strang, R., and Stirrup, D. (1999). A comparison of laser doppler flowmetry with other methods of assessing the vitality of traumatisedanterior teeth. *Dent. Traumatol.* 15, 284–290. doi: 10.1111/j.1600-9657.1999.tb00789.x

Fastnacht, M. (2008). Tooth replacement pattern of *Coloborhynchus robustus* (Pterosauria) from the Lower Cretaceous of Brazil. *J. Morphol.* 269, 332–348. doi: 10.1002/jmor.10591

Frazzetta, T. H. (1966). Studies on the morphology and function of the skull in the Boidae (Serpentes). Part II. Morphology and function of the jaw apparatus in *Python sebae* and *Python molurus*. *J Morphol.* 118, 217–295.

Fu, W. L., Zhang, X., Ji, C., Jiang, D. Y., Sun, Z. Y., and Hao, W. C. (2013). Morphology of *Keichousaurushui* from the Middle Triassic of Xingyi, Guizhou Province with comments on its reproduction mode. *ActaSci. Natur. Univ. Pekinensis*. 49, 102–109. (in Chinese with English abstract). Available online at: http://ir.nigpas.ac.cn/handle/332004/8444

Gazelius, B., Edwall, B., Olgart, L., Lundberg, J. M., Hökfelt, T., and Fischer, J. A. (1987). Vasodilatory effects and coexistence of calcitonin gene-related peptide (CGRP) and substance P in sensory nerves of cat dental pulp. *Acta. Physiolo. Scand*. 130, 33–40. doi: 10.1111/j.1748-1716.1987.tb08108.x

Geng, B. H, Zhu, M., and Jin, F. (2009). A revision and phylogenetic analysis of *Guizhoucoelacanthus* (Sarcopterygii, Actinistia) from the Triassic of China. *Vertebr. Palasiat*. 47, 165–177. doi: 10.1039/b409327e

Hahn, C., and Liewehr, F. R. (2007). Innate immune responses of the dental pulp to caries. *J. Endod*. 33, 643–651. doi: 10.1016/j.joen.2007.01.001

Handrigan, G. R., and Richman, J. M. (2011). Unicuspid and bicuspid tooth crown formation in squamates. *J. Exp. Zool*. 316, 598–608. doi: 10.1002/jez.b.21438

Holmes, R., Cheng, Y. N., and Wu, X. C. (2008). New information on the skull of *Keichousaurus* hui (Reptilia: Sauropterygia) with comments on sauropterygian interrelationships. *J. Vertebr. Paleontol*. 28, 76–84. doi: 10.1671/0272-4634(2008)2876: NIOTSO2.0.CO;2

Hwang, S. H. (2011). The evolution of dinosaur tooth enamel microstructure. *Biol. Rev*. 86, 183–216. doi: 10.1111/j.1469-185X.2010.00142.x

Jiang, Z. W. (2002). Discovery and significance of *Keichousaurus* Fauna in Fuyuan, Yunnan. *J. Yunn. Geol*. 21, 183–191. (in Chinese with English abstract). doi: 10.3969/j.issn.1004-1885.2002.02.008

Jin, F. (2001). Notes on the discovery of *Birgeria* in China. *Vertebr. Palasiat*. 39, 168–176. (in Chinese with English abstract). doi: 10.3969/j.issn.1000-3118.2001.03.002

Kardong, K. V., and Young, B. A. (1996). Dentitional surface features in snakes (Reptilia: Serpentes). *Amphibia-Reptilia*. 17, 261–276. doi: 10.1163/156853896X00432

Kimberly, C. L., and Byers, M. R. (1988). Inflammation of rat molar pulp and periodontium causes increased calcitonin generelated peptide and axonal sprouting. *Anat. Record* 222, 289–300. doi: 10.1002/ar.10922 20310

LeBlanc, A. R., Brink, K. S., Cullen, T. M., and Reisz, R. R. (2017). Evolutionary implications of tooth attachment versus tooth implantation: a case study using dinosaur, crocodilian, and mammal teeth. *J. Vertebr. Paleontol*. 37:e1354006. doi: 10.1080/02724634.2017.1354006

LeBlanc, A. R., and Reisz, R. R. (2015). Patterns of tooth development and replacement in captorhinid reptiles: a comparative approach for understanding the origin of multiple tooth rows. *J. Vertebr. Paleontol*. 35:e919928. doi: 10.1080/02724634.2014.919928

Li, J. L. (2006). A brief summary of the Triassic marine reptiles of China. *Vertebr. Palasiat*. 44, 99–108. doi: 10.3969/j.issn.1000-3118.2006.01.006

Li, Q., and Liu, J. (2020). An Early Triassic sauropterygian and associated fauna from South China provide insights into Triassic ecosystem health. *Commun. Biol.* 3:63. doi: 10.1038/s42003-020-0778-7

Li, Z. G, Sun, Z. Y., Jiang, D. Y., and Ji, C. (2016). LA-ICP-MS Zircon U-Pb age of the fossil layer of Triassic Xingyi Fauna from Xingyi, Guizhou, and its significance. *Geol. Rev*. 62, 779–790. (in Chinese with English abstract). doi: 10. 16509/j.georeview.2016.03.018

Lin, K., and Rieppel, O. (1998). Functional morphology and ontogeny of *Keichousaurus hui* (Reptilia, Sauropterygia). *Fieldiana. Geol*. 39, 1–35.

Lin, W. B., Jiang, D. Y., Rieppel, O., Motani, R., Tintori, A., Sun, Z. Y., et al. (2021). *Panzhousaurus rotundirostris* Jiang et al., 2019 (Diapsida: Sauropterygia) and the recovery of the monophyly of Pachypleurosauridae. *J. Vertebr. Paleontol*. 41:e1901730. doi: 10.1080/02724634.2021.1901730

Liu, B. J., and Xu, X. S. (1994). *Atlas of the Lithofacies and Palaeogeography of South China (Sinian-Triassic)*. Shanghai: Science Press.

Liu, G. B., Yin, G. Z., and Wang, X. H. (2002). On the most primitive amid fish from Upper Triassic of Xingyi, Guizhou. *Acta. Palaeontolo. Sin*. 41, 461–463. (in Chinese with English abstract). doi: 10.3969/j.issn.0001-6616.2002. 03.015

Liu, G. B., Yin, G. Z., Wang, X. H., Luo, Y. M., and Wang, S. Y. (2003). New discovered fishes from *Keichousaurus* bearing horizon of Late Triassic in Xingyi of Guizhou. *Acta. Palaeontolo. Sin*. 42, 346–366. (in Chinese with English abstract). doi: 10.CNKI:SUN:GSWX.0.2003-03-003

Macdougall, M.J., LeBlanc, A. R., and Reisz, R.R. (2014). Plicidentine in the Early Permian parareptile *Colobomycter pholeter*, and its phylogenetic and functional significance among coeval members of the clade. *PLoS ONE* 9:e96559. doi: 10.1371/journal.pone.0096559

Maisch, M. W., and Matzke, A. T. (1997). Observations on Triassic Ichthyosaurs. Part I. structure of the palate and mode of tooth implantation in Mixosaurus Cornalianus (bassani, 1886). *Neues. Jahrb. Geol. P-M*. 12, 717–732. doi: 10.1127/njgpm/1997/1997/717

Massare, J. A. (1987). Tooth morphology and prey preference of Mesozoic marine reptiles. *J. Vertebr. Paleontol*. 7, 121–137. doi: 10.1080/02724634.1987. 10011647

Massare, J. A. (1997). "Faunas, behavior, and evolution," in *Ancient Marine Reptiles*, ed. J. M. Callaway, and E. L. Nicholls (London, UK, and San Diego, USA: ACAD Press), 403–410.

Maxwell, E. E., Caldwell, M. W., and Lamoureux, D. O. (2012). Tooth histology, attachment, and replacement in the Ichthyopterygia reviewed in an evolutionary context. *Paläeontolo. Z*. 86, 1–14. doi: 10.1007/s12542-011-0115-z

Maxwell, E. E., Caldwell, M. W., Lamoureux, D. O., and Budney, L. A. (2011). Histology of tooth attachment tissues and plicidentine in *Varanus* (Reptilia: Squamata), and a discussion of the evolution of amniote tooth attachment. *J. Morphol*. 272, 1170–1181. doi: 10.1002/jmor.10972

McCurry, M. R., Evans, A. R., Fitzgerald, E. M., McHenry, C. R., Bevitt, J., and Pyenson, N. D. (2019). The repeated evolution of dental apicobasal ridges in aquatic-feeding mammals and reptiles. *Biol. J. Linn. Soc*. 127, 245–259. doi: 10.1093/biolinnean/blz025

Mehler, S. J., and Bennett, R. A. (2003). Oral, dental, and beak disorders of reptiles. *Vet. Clin. Exot. Pract*. 6, 477–503. doi: 10.1016/S1094-9194(03)00032-X

Modesto, S. P., and Reisz, R. R. (2008). New material of *Colobomycter pholeter*, a small parareptile from the lower permian of oklahoma. *J. Vertebr. Paleontol*. 28, 677–684. doi: 10.1671/0272-4634(2008)28677:NMOCPA2.0.CO;2

Motani, R. (1997). "Temporal and spatial distribution of tooth implantations in Ichthyosaurs," in *Ancient Marine Reptiles*, ed. J. M. Calloway, and E. L. Nicholls (London, UK, and San Diego, USA: ACAD Press), 81–103. doi: 10.1016/B978-012155210-7/50007-7

Motani, R., Jiang, D. Y., Rieppel, O., Xue, Y. F., and Tintori, A. (2015). Adult sex ratio, sexual dimorphism and sexual selection in a Mesozoic reptile. *Proc. R. Soc. B-Biol. Sci*. 282:1658. doi: 10.1098/rspb.2015. 1658

Neenan, J. M., Klein, N., and Scheyer, T. M. (2013). European origin of placodont marine reptiles and the evolution of crushing dentition in placodontia. *Nat. Commun*. 4:1621. doi: 10.1038/ncomms2633

Neenan, J. M., Li, C., Rieppel, O., Bernardini, F., Tuniz, C., Muscio, G., et al. (2014). Unique method of tooth replacement in durophagous placodont marine reptiles, with new data on the dentition of Chinese taxa. *J. Anat*. 224, 603–613. doi: 10.1111/joa.12162

Ni, P. G., Tintori, A., Sun, Z. Y., and Jiang, D. Y. (2017). A new specimen of *Birgeria liui* (Osteichthyes, Actinopterygii) from the Longobardian (Ladinian, Middle Triassic) of Xingyi, Guizhou Province, South China. *Research* 3, 55–58. doi: 10.14456/randk.2017.27

Olgart, L. M. (1990). "Functions of peptidergic nerves," in *Dynamic Aspects of Dental Pulp*, ed. R. Inoki, T. Kudo, and L. M. Olgart (Dordrecht, NL: Springer Press), 349–362.

Owen, R. (1841). XXXI.—On the teeth of species of the genus Labyrinthodon (*Mastodonsaurus* of jaeger) common to the German keuper formation and the Lower sandstone of Warwick and Leamington. *Trans. Geol. Soc. Lond*. 5, 503–513.

Owen, R. (1842). XXXII.—Description of parts of the Skeleton and Teeth of five species of the Genus Labyrinthodon (Lab. leptognathus, Lab. pachygnathus, and Lab. ventricosus, from the Coton-end and Cubbington Quarries of the Lower Warwick Sandstone; Lab. Jægeri, from Guy's Cliff, Warwick; and Lab. scutulatus, from Leamington); with remarks on the probable identity of the Cheirotherium with this genus of extinct Batrachians. *Trans. Geol. Soc. Lond*. 2, 515–543. Available online at: http://trn.lyellcollection.org/ at Dalhousie University (accessed June 24, 2015).

Peyer, B. (1968). *Comparative Odontology*. Chicago: Univeristy of Chicago Press.

Preuschoft, H., Reif, W. E., Loitsch, C., and Tepe, E. (1991). "The function of labyrinthodont teeth: big teeth in small jaws," in Constructional morphology and evolution, ed. N. Schmidt-Kittler and K. Vogel (Bln-Heidelb, De: Springer), 151–171. doi: 10.1007/978-3-642-76156-0_12

Radinsky, L. (1961). Tooth histology as a taxonomic criterion for cartilaginous fishes. *J. Morphol* 109, 73–92. doi: 10.1002/jmor.1051090106

Rieppel, O. (1978). Tooth replacement in anguinomorph lizards. *Zoomorphologie* 91, 77–90. doi: 10.1007/BF00994155

Rieppel, O. (1999). Phylogeny and paleobiogeography of Triassic Sauropterygia: problems solved and unresolved. *Palaeogeogr. Palaeocl.* 153, 1–15. doi: 10.1016/S0031-0182(99)00067–X

Rieppel, O. (2001). Tooth implantation and replacement in Sauropterygia. *Palaeontol. Z.* 75, 207–217. doi: 10.1007/BF02988014

Rieppel, O. (2002). Feeding mechanics in Triassic stem-group sauropterygians: the anatomy of a successful invasion of Mesozoic seas. *Zool. J. Linn. Soc.* 135, 33–63. doi: 10.1046/j.1096-3642.2002.00019.x

Rieppel, O., and Lin, K. (1995). Pachypleurosaurs (Reptilia: Sauropterygia) from the lower Muschelkalk, and a review of the Pachypleurosauroidea. *Fieldiana. Geol.* 32, 1–44.

Rieppel, O., Liu, J., and Bucher, H. (2000). The first record of a thalattosaur reptile from the Late Triassic of southern China (Guizhou Province, PR China). *J. Vertebr. Paleontol.* 20, 507–514. doi: 10.1671/0272-4634(2000)0200507:TFROAT2.0.CO;2

Rücklin, M., Donoghue, P., Johanson, Z., Trinajstic, K., Marone, F., and Stampanoni,. M. (2012). Development of teeth and jaws in the earliest jawed vertebrates. *Nature* 491, 748–751. doi: 10.1038/nature11555

Sander, P. M. (1999). The microstructure of reptilian tooth enamel: terminology, function, and phylogeny. *Münch. Geow. Abhandl. A. Geologie. Palae.* 38, 87–97

Sassoon, J., Foffa, D., and Marek, R. (2015). Dental ontogeny and replacement in Pliosauridae. *R. Soc. Open Sci.* 2:150384. doi: 10.1098/rsos.150384

Satoko, K., Shinya, K., Azusa, Y., Zenzo, M., Yuzo, T., and Yuji, M. (2013). Optical measurement of blood oxygen saturation of dental pulp. *Biomed. Eng.* 2013, 1–6. doi: 10.1155/2013/502869

Scanlon, J. D., and Lee, M. S. (2002). Varanoid-like dentition in primitive snakes (Madtsoiidae). *J. Herpetol.* 36, 100–106.

Schultze, H. P. (1970). Folded teeth and the monophyletic origin of tetrapods. *Am. Mus. Nat. Hist.* 2408, 1–10.

Shang, Q. H. (2007). New information on the dentition and tooth replacement of nothosaurus (reptilia: sauropterygia). *Palaeoworld*. 16, 254–263. doi: 10.1016/j.palwor.2007.05.007

Shang, Q. H., Wu, X. C., and Li, C. (2020). A New Ladinian Nothosauroid (Sauropterygia) from Fuyuan, Yunnan Province, China. *J.Vertebr. Paleontol.* 40:e1789651. doi: 10.1080/02724634.2020.1789651

Silverman, J. D., and Kruger, L. (1987). An interpretation of dental innervation based upon the pattern of calcitonin gene-related peptide (cgrp)-immunoreactive thin sensory axons. *Somatosens. Res.* 5, 157–175. doi: 10.3109/07367228709144624

Slooten, E. (1991). Age, growth, and reproduction in Hector's dolphins. *Can. J. Zool.* 69, 1689–1700. doi: 10.1139/z91-234

Su, D. Z. (1959). Triassic fishes from Kueichow, Southwest China. *Vertebr. Palasiat.* 3, 205–210. (in Chinese with English abstract). doi: 10.CNKI:SUN:GJZD.0.1959-04-006

Sun, Z. Y., Jiang, D.Y., Ji, C., and Hao, W. C. (2016). Integrated biochronology for Triassic marine vertebrate faunas of Guizhou Province, South China. *J. Asian. Earth. Sci.* 118, 101–110. doi: 10.1016/j.jseaes.2016.01.004

Taylor, M. A. (1987). How tetrapods feed in water: a functional analysis by paradigm. *Zool. J. Linn. Soc* 91, 171–195. doi: 10.1111/j.1096-3642.1987.tb01727.x

Taylor, M. A., and Cruickshank, A. R. I. (1993). Cranial anatomy and functional morphology of *Pliosaurus brachyspondylus* (Reptilia: Plesiosauria) from the Upper Jurassic of Westbury, Wiltshire. *Philos. T. R. Soc. B.* 341, 399–418. Available online at: http://www.jstor.org/page/info/about/policies/terms.jsp (accessed May, 2021).

Taylor, P. E., and Byers, M. R. (1990). An immunocytochemical study of the morphological reaction of nerves containing calcitonin gene-related peptide to microabscess formation and healing in rat molars. *Arch. Oral. Biol.* 35, 629–638. doi: 10.1016/0003-9969(90)90029-A

Tintori, A., Sun, Z. Y, Ni, P. G., Lombardo, C., Jiang, D.Y., and Ryosuke, M. (2015). Oldest stem Teleostei from the late Ladinian (Middle Triassic) of southern China. *Riv. Ital. Paleontolo. Stratigrafia* 121, 285–296. doi: 10.13130/2039-4942/651

Tomes, C. S. (1878). II. On the structure and development of vascular dentine. *Proc. R. Soc. Lond.* 169, 25–47. doi: 10.1098/rstl.1878.0003

Ungar, P. (2010). *Mammal Teeth: Origin, Evolution and Diversity*. Baltimore: Johns Hopkins University Press.

Vaeth, R. H., Rossman, D. A., and Shoop, W. (1985). Observations of tooth surface morphology in snakes. *J. Herpetol.* 19, 20–26. doi: 10.2307/1564416

Walton, R. E., and Nair, P. N. R. (1995). Neural elements in dental pulp and dentin. *OralRadiol. Endodontol.* 80, 710–719. doi: 10.1016/S1079-2104(05)80256-2

Wang, C. Y., Kang, P. Q., and Wang, Z. H. (1998). Conodont based age of the *Keichousaurus* hui Yang, 1958. *Acta. Micropalaeontol. Sin.* 15, 196–198. (in Chinese with English abstract). doi: 10.1088/0256-307X/15/12/010

Wang, L. T. (2002). Study advances on triassic marine reptiles in guizhou. *Guiz. Geol.* 19, 6–9. (in Chinese with English abstract). doi: 10.3969/j.issn.1000-5943. 2002.01.002

Wang,. L. T. (1996). A discussion on horizon and age of *Keichousaurus* hui occurrence. *Guizh. Geol.* 3, 209–216. (in Chinese with English abstract). doi: 10.GZUVDZ.0.1996-03-002

Westergaard, B., and Ferguson, M. W. (1990). Development of the dentition in *Alligator mississippiensis*: upper jaw dental and craniofacial development in embryos, hatchlings, and young juveniles, with a comparison to lower jaw development. *Am. J. Anat.* 187, 393–421. doi: 10.1002/aja.1001870407

Wright, D. L., Kardong, K. V., and Bentley, D. L. (1979). The functional anatomy of the teeth of the western terrestrial garter snake, *Thamnophis elegans*. *Herpetologica* 35, 223–228. Available online at: http://www.jstor.org/stable/3891690

Xu, G. H. (2020). A new species of *Luganoia* (Luganoiidae, Neopterygii) from the Middle Triassic Xingyi Biota, Guizhou, China. *Vert. Palasiat.* 58, 267–282. doi: 10.19615/j.cnki.1000-3118.200624

Xu, G. H., Ma, X.Y., and Ren, Y. (2018a). *Fuyuanichthys wangi* gen. et sp. nov. from the Middle Triassic (Ladinian) of China highlights the early diversification of ginglymodian fishes. *PeerJ* 6:e6054. doi: 10.7717/peerj.6054

Xu, G. H., Ma, X.Y., and Zhao, L. J. (2018b). A large peltopleurid fish (Actinopterygii: Peltopleuriformes) from the Middle Triassic of Yunnan and Guizhou, China. *Vert. Palasiat* 56, 106–120. doi: 10.19615/j.cnki.1000-3118.171225

Xu, G. H., and Ma, X. Y. (2018). Redescription and phylogenetic reassessment of *Asialepidotus shingyiensis* (Holostei: Halecomorphi) from the Middle Triassic (Ladinian) of China. *Zool. J. Linn. Soc.* 184, 95–114. doi: 10.1093/zoolinnean/zlx105

Xu, G. H., Zhao, L. J., Gao, K. Q., and Wu, F. X. (2012). A new stem-neopterygian fish from the Middle Triassic of China shows the earliest over-water gliding strategy of the vertebrates. *Proc. R. Soc. B-Biol. Sci.* 280:20122261. doi: 10.1098/rspb.2012.2261

Xu, G. H., Zhao, L. J., and Shen, C. C. (2015). A Middle Triassic thoracopterid from China highlights the evolutionary origin of over-water gliding in early ray-finned fishes. *Biol. Lett.* 11:20140960. doi: 10.1098/rsbl.2014.0960

Xue, Y. F., Jiang, D. Y., Motani, R., Rieppel, O., Sun, Y. L., Sun, Z. Y., et al. (2013). New information on sexual dimorphism and allometric growth in Keichousaurus hui, a pachypleurosaur from the middle triassic of Guizhou, South China. *Acta. Palaeontol. Pol.* 60, 681–687. doi: 10.4202/app.00006.2013

Yang, S. R., Liu, J., and Zhang, M. F. (1995). Conodonts of the Falang Formation of southwestern Guizhou and their age. *J. Stratigra.* 19, 161–170. (in Chinese with English abstract). Available online at: http://www.cnki.com.cn/Article/CJFDTotal-DCXZ503.000.htm (accessed August, 2020).

Young, C. C. (1958). On the new Pachypleurosauroidea from Keichow, southwest China. *Ver. PalAsiat.* 2, 69–82.

Young, C. C. (1965). On the new nothosaurs from Hupeh and Kweichou. *China. Ver. PalAsiat.* 9, 315–356. doi: 10.1111/j.1745-7254.2008.00827.x

Young, M. T., Brusatte, S. L., De Andrade, M. B., Desojo, J. B., Beatty, B. L., Steel, L., et al. (2012). The cranial osteology and feeding ecology of the metriorhynchid crocodylomorph genera Dakosaurus and Plesiosuchus from the Late Jurassic of Europe. *PLoS ONE* 7:e44985. doi: 10.1371/journal.pone.0044985

Young, M. T., De Andrade, M. B., Cornée, J. J., Steel, L., and Foffa, D. (2014a). April. Re-description of a putative Early Cretaceous "teleosaurid" from France, with implications for the survival of metriorhynchids and teleosaurids across the Jurassic-Cretaceous Boundary. *Ann. Paléontol.* 100, 165–174. doi: 10.1016/j.annpal.2014.01.002

Young, M. T., Steel, L., Brusatte, S. L., Foffa, D., and Lepage, Y. (2014b). Tooth serration morphologies in the genus *Machimosaurus* (Crocodylomorpha, Thalattosuchia) from the Late Jurassic of Europe. *Roy. Soc. Open. Sci.* 1:140269. doi: 10.1098/rsos.140269

Zaher, H., and Rieppel, O. (1999). *Tooth Implantation and Replacement in Squamates, with Special Reference to Mosasaur Lizards and Snakes*. New York: American museum of nature history Press.

Zou, X., Balini, M., Jiang, D.Y., Tintori, A., Sun, Z. Y., and Sun, Y. L. (2015). Ammonoids from the Zhuganpo Member of the Falang Formation at Nimaigu and their relevance for dating the Xingyi fossil-lagerstätte (late Ladinian, Guizhou, China). *Riv. Ital. Paleontol. S.* 2, 135–161. doi: 10.13130/2039-4942/6511

Zverkov, N. G., Fischer, V., Madzia, D., and Benson, R. B. (2018). Increased pliosaurid dental disparity across the Jurassic–Cretaceous transition. *Palaeontology*. 61, 825–846. doi: 10.1111/pala.12367

Conflict of Interest: The authors declare that the research was conducted in the absence of any commercial or financial relationships that could be construed as a potential conflict of interest.

frontiers in Cell and Developmental Biology

ORIGINAL RESEARCH
published: 09 February 2022
doi: 10.3389/fcell.2022.823283

Expanding of Life Strategies in Placozoa: Insights From Long-Term Culturing of *Trichoplax* and *Hoilungia*

Daria Y. Romanova[1]*, *Mikhail A. Nikitin*[2,3], *Sergey V. Shchenkov*[4] and *Leonid L. Moroz*[5,6]*

[1]Institute of Higher Nervous Activity and Neurophysiology of RAS, Moscow, Russia, [2]Belozersky Institute for Physico-Chemical Biology, Lomonosov Moscow State University, Moscow, Russia, [3]Kharkevich Institute for Information Transmission Problems, Russian Academy of Sciences, Moscow, Russia, [4]Department of Invertebrate Zoology, Faculty of Biology, Saint Petersburg State University, Saint Petersburg, Russia, [5]Departments of Neuroscience and McKnight Brain Institute, University of Florida, Gainesville, FL, United States, [6]Whitney Laboratory for Marine Biosciences, University of Florida, St. Augustine, FL, United States

Placozoans are essential reference species for understanding the origins and evolution of animal organization. However, little is known about their life strategies in natural habitats. Here, by maintaining long-term culturing for four species of *Trichoplax* and *Hoilungia*, we extend our knowledge about feeding and reproductive adaptations relevant to the diversity of life forms and immune mechanisms. Three modes of population dynamics depended upon feeding sources, including induction of social behaviors, morphogenesis, and reproductive strategies. In addition to fission, representatives of all species produced "swarmers" (a separate vegetative reproduction stage), which could also be formed from the lower epithelium with greater cell-type diversity. We monitored the formation of specialized spheroid structures from the upper cell layer in aging culture. These "spheres" could be transformed into juvenile animals under favorable conditions. We hypothesize that spheroid structures represent a component of the innate immune defense response with the involvement of fiber cells. Finally, we showed that regeneration could be a part of the adaptive reproductive strategies in placozoans and a unique experimental model for regenerative biology.

Keywords: Placozoa, fiber cells, immunity, aging, development, nervous system evolution, regeneration, behavior

OPEN ACCESS

Edited by:
Pedro Martinez,
University of Barcelona, Spain

Reviewed by:
Bernd Schierwater,
University of Veterinary Medicine Hannover, Germany
Hiroaki Nakano,
University of Tsukuba, Japan

***Correspondence:**
Daria Y. Romanova
darjaromanova@gmail.com
Leonid L. Moroz
moroz@whitney.ufl.edu

Specialty section:
This article was submitted to Evolutionary Developmental Biology, a section of the journal Frontiers in Cell and Developmental Biology

Received: *27 November 2021*
Accepted: *20 January 2022*
Published: *09 February 2022*

Citation:
Romanova DY, Nikitin MA, Shchenkov SV and Moroz LL (2022) Expanding of Life Strategies in Placozoa: Insights From Long-Term Culturing of Trichoplax *and* Hoilungia. *Front. Cell Dev. Biol. 10:823283. doi: 10.3389/fcell.2022.823283*

INTRODUCTION

Placozoans are essential reference species to understand the origins and evolution of the animal organization. Despite the long history of investigations, Placozoa is still one of the most enigmatic animal phyla. Placozoans have the simplest, among-free living animals, body plan—three cell "layer"s organization (Schulze, 1883; Metschnikoff, 1886; Noll, 1890; Graff, 1891; Metschnikoff, 1892; Stiasny, 1903; Ivanov, 1973; Rassat and Ruthmann, 1979; Dogel, 1981; Malakhov and Nezlin, 1983; Okshtein, 1987; Malakhov, 1990; Smith et al., 2014; Mayorova et al., 2019; Romanova, 2019; Smith et al., 2019; Romanova et al., 2021; Ruthmann et al., 1986; Ivanov et al. 1982), but surprisingly complex behaviors (Kuhl and Kuhl, 1963; Kuhl and Kuhl, 1966; Seravin and Karpenko, 1987; Seravin and Gudkov, 2005a; Eitel and Schierwater, 2010; Eitel et al., 2011; Smith et al., 2015; Senatore et al., 2017; Armon et al., 2018; Zuccolotto-Arellano and Cuervo-González, 2020; Romanova et al., 2020b) with social feeding patterns (Okshtein, 1987; Fortunato and Aktipis, 2019).

The phylum Placozoa contains many cryptic species because differences in morphological phenotypes are minor. The broad sampling across the globe revealed ~30 haplotypes (Aleshin

et al., 2004; Eitel and Schierwater, 2010; Miyazawa et al., 2012; Eitel et al., 2013; Schierwater and DeSalle, 2018; Miyazawa et al., 2021), based upon the mitochondrial 16S. In an initial molecular genetic diversity survey, Voigt et al. (2004) assigned the original Grell strain as the mitochondrial 16S haplotype H1, equal to the classical *Trichoplax adhaerens* (Schulze, 1883).

Among other haplotypes described so far, the H13 haplotype has been recognized as a separate species and genus—*Hoilungia hongkongensis* (Eitel et al., 2018). *Polyplacotoma mediterranea* is the third formally described genus of Placozoa (Osigus et al., 2019). Moreover, emerging data related to genomics, physiology, feeding, and ecology suggest that the H4 haplotype is a separate species of *Hoilungia* (=*Hoilungia* sp.). Similarly, the H2 haplotype can also be viewed as a distinct species of *Trichoplax* (=*Trichoplax* sp. - (Laumer et al., 2018; Schierwater and DeSalle 2018). Therefore, we refer to these four cultured haplotypes in the current manuscript as different species.

Placozoans can predominantly be collected from tropical and subtropical regions (Ueda et al., 1999; Signorovitch et al., 2006; Pearse and Voigt, 2007; Eitel and Schierwater, 2010; Nakano, 2014; Maruyama, 2004; Eitel et al., 2011); they live in a wide range of salinity (20–55 ppm), temperature (11–27°C), depth (0–20 m), and pH (Schierwater, 2005; Schierwater et al., 2010; Eitel et al., 2013). However, their lifestyles are essentially unknown. The morphotypes and reproductive strategies of placozoans vary depending on feeding conditions. Pearse and Voigt, (2007) had suggested that placozoans may be opportunistic grazers, scavenging on organic detritus, algae, and bacteria biofilms.

Long-term culturing helps to explore the life histories of placozoans further. Most of the knowledge about placozoans had been obtained from culturing of just one species, *Trichoplax adhaerens* (Pearse, 1989; Signorovitch et al., 2006; Eitel and Schierwater, 2010; Eitel et al., 2013; Heyland et al., 2014). Both rice and algae had been used as alternative food sources. For example, the feeding substrates could be: *Cryptomonas* (Grell, 1972; Ruthman, 1977), red algae *Pyrenomonas helgolandii* (Signorovitch et al., 2006), green algae (*Ulva sp*; Seravin and Gerasimova, 1998), or a mix of green, *Nannochloropsis salina*, and red algae, *Rhodamonas salina*, *Pyrenomonas helgolandii* (Jackson and Buss, 2009; Smith et al., 2014), as well as yeast extracts (Ueda et al., 1999).

In addition to the disk-like flattened placozoan bodyplan, various culturing conditions resulted in different morphological forms. Thiemann and Ruthmann (1988); Thiemann and Ruthmann (1990); Thiemann and Ruthmann (1991) described several spherical structures and swarmers as asexual/vegetative reproductive stages. These original observations have been made on *T. adhaerens* only. There are no reports about similar structures and functions in other species/haplotypes of placozoans. Here, by maintaining long-term culturing for four species of *Trichoplax* and *Hoilungia*, we provided additional details about feeding and reproductive adaptations relevant to placozoan ecology and immune mechanisms.

MATERIAL AND METHODS

Culturing of Placozoans

We used axenic clonal cultures of four species of Placozoa: *Trichoplax adhaerens* (Grell's strain H1, from the Red Sea), *Trichoplax* sp. (H2 haplotype, collected in the vicinity of Bali island), *Hoilungia* sp. (H4 haplotype, collected in coastal waters of Indonesia), and *Hoilungia hongkongensis* (H13 haplotype, found in coastal waters of Hong Kong). We maintained all species in culture for 3–5 years (2017–2021), allowing long-term observations and adjustments of culture conditions for each haplotype/species.

We cultured H1, H2, and H13 in closed Petri dishes with artificial seawater (ASW, 35 ppm, pH 7.6–8.2), which was changed (70% of the total volume) every 7–10 days. On average, 5–10 Petri dishes were used every week with 200–300 animals on each plate. Monitoring and observation occurred daily.

A suspension of the green alga *Tetraselmis marina* (WoRMS Aphia, ID 376158) was added to the culture dishes. When the biofilm of microalgae became thinner or depleted, freshly prepared, 1–2 ml suspension of *T. marina* could be added to the culture dishes weekly. Mixtures of other algal clonal strains were also occasionally used (for example, the cyanobacteria *Leptolyngbya ectocarpi* (WoRMS Aphia, ID 615645) and *Spirulina versicolor* (WoRMS Aphia, ID 495757), the red algae such *Nannochloropsis salina* (WoRMS Aphia, ID 376044) or *Rhodomonas salina* (WoRMS Aphia, ID 106316). H1, H2, and H13 were maintained at the constant temperature of 24°C and natural light in environmental chambers (see Modes 1–3 in Result section). In parallel, H1, H2, and H13 were also successfully cultured using rice grains as nutrients, with 5–7 rice grains per dish (**Figure 1**).

Placozoans are transparent, but their color could be changed depending on the algae they are feeding on. For example, light-brownish color occurs with *T. marina* as a food source, medium brownish coloration was observed in animals fed on diatoms (*Entomoneis paludosa* (WoRMS Aphia, ID 163646)), or pinkish colors were seen when animals were fed on cyanobacteria. Pinkish coloration might be due to the accumulation of phycobilins from cyanobacteria, red algae, and cryptophytes.

Under long-term culturing, animals were divided every 1–2 days without signs of sexual reproduction (Malakhov, 1990; Zuccolotto-Arellano and Cuervo-González, 2020).

In contrast to other placozoans, the H4 haplotype (or *Hoilungia* sp.) could be successfully cultured at 28°C using a green algae *T. marina* mixture and two cyanobacteria *Spirulina versicolor* and *Leptolyngbya ectocarpi* (see also Okshtein, 1987). However, if the H4 was maintained on *T. marina* only, the population growth was significantly declined.

Cryofixation for Transmission Electron Microscopy

Animals were placed in cryo capsules 100 μm deep and 6 mm diameter in ASW. After specimens adhered, the media was replaced with 20% bovine serum albumin solution in ASW.

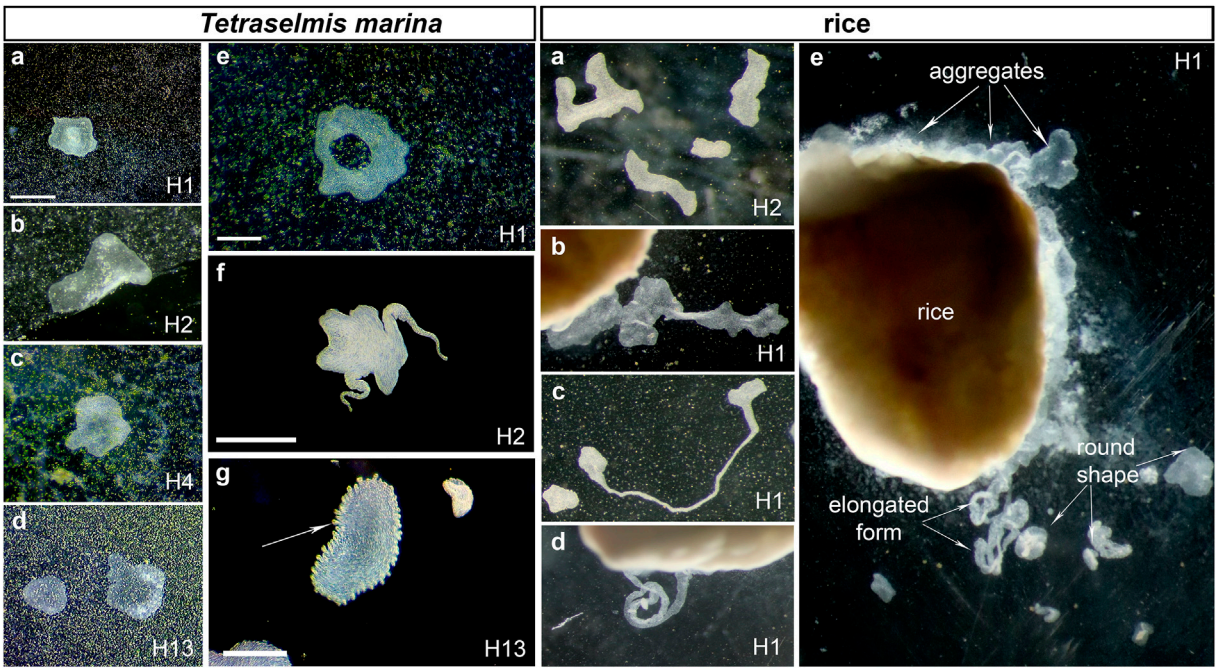

FIGURE 1 | The diversity of placozoan body forms. Illustrated examples from long-term culturing of different haplotypes (indicated in each photo) on two feeding substrates (*Tetraselmis marina* and Rice boxes). *Tetraselmis marina* box shows both canonical placozoans body shapes **(A–D)** and unusual morphologies (animals with a "hole" in the middle of the body (**E** and **Supplementary Video S1**), elongated "pseudopodia"-like structures (**Supplementary Figure S3**), and animals with numerous small ovoid formations in the rim area **(G)**. The 'rice box' illustrate examples of different body morphology in cultured placozoans using different feeding substrate. Rice grains support a stable population growth rate but often facilitate the formation of aggregations of animals around grains (rice box **A–D**: different shapes of placozoans **(A–B)**, including those with highly elongated forms **C,D**). Scale bar: *Tetraselmis marina* box: 500 μm; Rice box: grain: 1 mm.

Animals were frozen with a High-Pressure Freezer for Cryofixation (Leica EM HPM 100). After fixation, animals were embedded in epoxy resin (EMS, Hatfield, UK). Ultrathin (65 nm) serial sections were made using Leica EM UC7 ultramicrotome. Sections were stained in uranyl acetate and lead citrate (Reynolds, 1963) and studied using JEOL JEM-2100 and JEOL JEM-1400 (JEOL Ltd., Tokyo, Japan) transmission electron microscopes with Gatan Ultrascan 4000 (Gatan Inc., Pleasanton, CA) and Olympus-SIS Veleta (Olympus Soft Imaging Solutions, Hamburg, Germany) transmission electron microscopy (TEM) cameras. TEM studies were done at the Research center "Molecular and Cell Technologies" (Saint Petersburg State University).

Laser Scanning Microscopy

Swarmer-like structures and "spheres" were transferred from cultivation dishes to sterile Petri dishes using a glass Pasteur pipette. Individual animals were allowed to settle on the bottom overnight. Fixation was achieved by gently adding 4% paraformaldehyde in 3.5% Red Sea salt (at room temperature) and maintained at 4°C for 1 h. Next, preparations were washed in phosphate buffer solution (0.1 M, pH = 7.4, 1% Tween-20) three times (20 min) and mounted on a slide using Prolong gold antifade reagent with DAPI, and stored in the dark at 4°C. The samples were examined using Zeiss LSM 710 confocal laser scanning microscope with a Plan-Apochromat 63x/1.40 Oil DIC M27 immersion lens (Zeiss, Germany). The images were obtained using the ZEN software package (black and blue edition) (Zeiss, Germany). Image processing was carried out using ZEN (blue edition), Imaris, ImageJ software.

Statistical Analysis

For population growth rate (PGR) experiments, we cultured axenic lines of H1, H2, H4, and H13 at constant temperature (24°C) and natural light in environmental chambers for 13 experimental days. PGR, locomotion, regeneration analysis, number of animals and occurrences of aggregates were monitored daily at the same time and calculated using standard statistical (*t*-test) and heatmap packages in R. We use triplicates for population growth rates; see additional details in Result section (for original datasets and all details for row data, see **Supplementary Tables S1, S2, Supplementary Doc S3, Supplementary Figure S6**). We observed exponential-type growth rates for H1 (Avg = 477), H2 (Avg = 312), and H13 (Avg = 232) haplotypes in triplicate experimental groups.

An average (Avg) daily growth of the culture was calculated as numbers of animals per dish in each independent replicate:

$$v_{absi} = \frac{n_i - n_{i-1}}{t},$$

n—numbers of animals, *i*—day for which the speed is estimated $(i = \overline{2, 11\,(13)})$, *t*—1 day.

The average values for 2–11 and 13 days were calculated from three replicates, and the confidence intervals for the average values. For each independent replication, the relative rate of population growth was presented as:

$$\frac{\frac{v_{absi}}{n_{i-1}} \cdot 100\%}{t}$$

We use the Student's *t*-test for each analyzed parameter ($\alpha < 0.05$ and $\alpha < 0.01$).

Treatment of *T. adhaerens* With Antibiotics

Trichoplax might contain potentially symbiotic bacteria in fiber cells (Driscoll et al., 2013; Kamm et al., 2019a). To control levels of potential bacterial endosymbionts, we used treatment with different antibiotics (ampicillin (5 μg/ml), doxycycline (1.25 μg/ml), ciprofloxacin (7 μg/ml), and rifampicin (1.25 μg/ml).

Total DNA from individual animals was extracted using a silica-based DiaTom DNAprep 100 kit (Isogene, Moscow, Russia) according to the manufacturer's protocol. Amplification was performed using EncycloPlus PCR kit (Evrogen, Moscow, Russia) using the following program: 95°C—3 min, 35 cycles of PCR (95°C—20 s, 50°C—20 s, 72°C—1 min), and 72°C—5 min. We have used universal forward primer 27F (AGA GTT TGA TCM TGG CTC AG) and specific reverse primer 449R (ACC GTC ATT ATC TTC YCC AC). The reverse primer was designed against 16S RNA of *Rickettsia belli* (NR_074484.2) and sequences from *Trichoplax* DNA found through NCBI Trace Archive Blast using NR_074484.2 as the query. After 6 months of ampicillin treatment, the *Rickettsia* were not detected. Other antibiotics were less effective (**Supplementary Figure S5**, see Supplement).

RESULTS

Three States of Long-Term Culturing and Feeding in Placozoa

Analysis of growth and behavioral patterns during the long-term culturing allowed us to distinguish three distinct conditions shared across placozoans.

Optimized Culture Conditions

This first mode describes a population with a stable growth rate on the established algal mat (~6.5×10^6 cells of *T. marina* per 1 μL, added once a week) or rice grains (4–5 grains in one Petri dish, diameter 9 cm), and refreshing liquid medium once in 7–10 days. We observed regular fission of placozoans, at average once 1–2 days, during a few months (**Figure 3**, Mode 1, **Supplementary Figure S6**). Here, we transferred an excess of animals to other dishes maintaining about 500 individuals per dish. This culturing allows keeping stable populations of placozoans for a long time (from a few months to 2–5 years).

Figures 1, **2** show a diversity of canonical placozoans body shapes (**Figures 1A–D**). However, unusual morphologies were also observed in all haplotypes. For example, we noted animals with a "hole" in the middle of the body (**Figure 1E**), elongated "pseudopodia"-like structures (**Supplementary Figure S3**, **Supplementary Figure S3**), or numerous small ovoid formations in the rim area (**Figure 1G**).

Depleted Food Substrate

If no additional food source was added within 2–3 weeks, the biofilm of microalgae became thinner or depleted. When the layer of microalgae became less than 4.2×10^5 cells/μL, we observed a 1.5-2 fold reduction in animals' surface areas in all tested haplotypes (H1, H2, and H13), and the population size decreased from ~500 to ~200 animals per one cultivation dish (**Figure 3**, Mode 2). Under these conditions, the animals were concentrated in the densest areas of the algal substrate. In 4–5 weeks, several percent of placozoans formed unusual spherical structures described in *Spherical Formations and Systemic Immune Response*.

High Density of Food Substrate and "Social" Behavior

The third mode of culturing was observed on dense substrates such as 3–4-layer algal biofilm with 8×10^8 cell/μL of suspension or 7–8 rice grains (per Petri dish, diameter 9 cm for H1, H2, and H13). Placozoans often formed clusters consisting of multiple animals within a few days on abundant food sources (**Figure 2**). These aggregates of 2–15 animals have been described as "social" behavior (Okshtein, 1987; Fortunato and Aktipis, 2019). These conditions also induced social feeding patterns in the 20 L aquaria system for *Hoilungia* sp. (H4 haplotype, **Figure 3**, Mode 3).

This collective behavior differed from typical alterations of search/exploratory and feeding cycles observed in sparked individuals under conditions with limited food sources (Modes 1 and 2, **Figure 3**). When animals were feeding, they usually stayed on the food substrate or rotated for ~15–30 min within a small region, comparable to their body length (**Figure 3**).

LIFE STRATEGIES

Vegetative (Asexual) Reproduction

Long-term culturing provided additional insights into the life-history strategies of Placozoa. In addition to the fission, the formation of smaller daughter animals or "swarmers" had been described in *Trichoplax adhaerens*, and swarmers were reportedly derived from the upper epithelium (Thiemann and Ruthmann, 1990; Thiemann and Ruthmann, 1991). Here, we observed the development of swarmer-like forms in all haplotypes studied (H1, H2, H4, and H13; **Figures 4**, **5**), suggesting that it is an essential part of adaptive strategies for Placozoa [see **Supplementary Video S4** for *Trichoplax* sp. (H2), and **Supplementary Video S5, S6** for *Hoilungia* (H4 haplotype)].

The formation of "swarmers" occurred spontaneously (in about 2 or 5 weeks from a cultivation start) both on algal biofilms and rice. But we noted that swarmer-like forms could be formed at the lower, substrate-facing side (**Figure 4**, **Supplementary Video S3**), with a significantly greater cell-type diversity than in the upper layer (Smith et al., 2014; Mayorova et al., 2019; Romanova et al., 2021). Therefore, the formation of swarmer-type forms from the lower layer might be

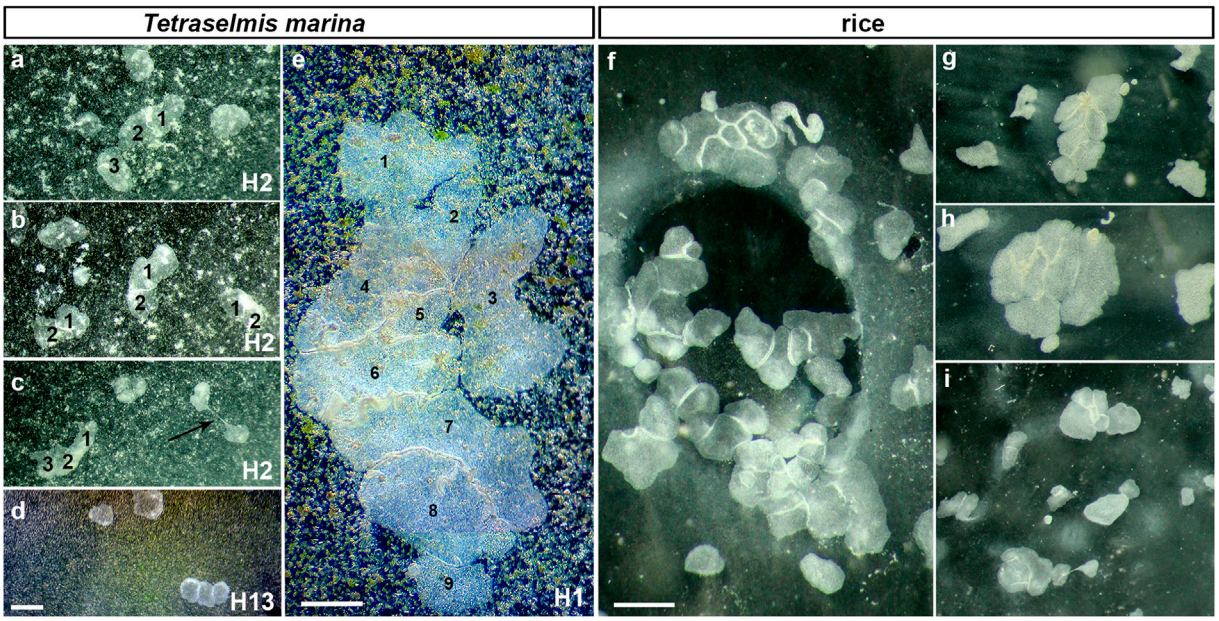

FIGURE 2 | Social feeding behavior during long-term culturing on the dense algal (*Tetraselmis marina* box) and rice (for H1-f) substrates (illustrated examples). The aggregation of animals depended upon the density of the substrates (see mode #3 in the text and **Figure 3**). This behavioral pattern was observed for all haplotypes (H1, H2, H13—in Petri dishes). The arrow in c indicates a fission process. Aggregates often included 2–15 individuals. For example, there were aggregates of 2-3 animals in H2 **(A–C)** on *Tetraselmis marina*, and 9 H1 individuals **(E)** at the same substrate; but H2 often forms aggregates for 10–15 animals around rice grains **(G–I)**. pH = 8.2. Scale bar: **(A–D)**—100 μm, **(E)**—1 mm, **(F–I)**—500 μm.

facilitated by the preexisting heterogeneity of cell types in this region. After physical separation, these progeny could be temporally located under the "mother" animal (**Supplementary Video S3**), moving together on substrates or biofilms.

Regeneration as a Part of Adaptive Life Strategies in Placozoans

An overpopulated/fast-growing culture with a high density of placozoans (over 500–700 animals per 1 Petri dish 9 cm in diameter) often contains many floating individuals or individuals on walls, which are frequently aggregated under the surface film (**Supplementary Figure S2**). The animals could be raptured as a result of contact with air and/or other mechanical damage. Nevertheless, such fragmentation often led to regeneration, which we consider an essential part of life strategy in placozoans.

We investigated the regeneration in model experiments (using H1 and H2 haplotypes, 1–2 mm in size). Individuals were damaged in two ways: mechanical injury by pipetting and by cutting animals with a scalpel (into two parts). The former protocol allows obtaining small cell aggregates (~20–30 cells) placed in Petri dishes with biofilms of *Tetraselmis marina*. The regeneration process lasted approximately 7–10 days. The first stage of recovery was an increase in cell numbers within the aggregates, which were immobile (**Figure 6**). Notably, intact placozoans had a negative phototaxis (animals moved to the darkened areas of experimental Petri dishes, see **Supplementary Figure S1**). However, at the early stages of regeneration, *Trichoplax* aggregates did not respond to changes in light intensity, remaining motionless. After the 4th day, locomotion was restored (**Figure 6**).

On the 7th day, original aggregates became small individual animals with active locomotion and feeding behaviors as well as capable of fission and negative phototaxis. Interestingly, if dissociated cells and aggregates were transferred to Petri dishes without a food source, then aggregates were lysed after 2–3 days.

After dissection individuals into two parts, we observed a slight contraction of animals. Still, within a few minutes, animals curled up, closed the wound, and moved without detectable changes in their locomotion patterns (**Figure 6**, **Supplementary Video S7**).

Spherical Formations and Systemic Immune Response

In 4–5 weeks (Mode 2 of culturing with depleting food source), some animals started developing specific spheroid structures (**Figures 7**, **8**, **Supplementary Video S8–S12**). The formation of these "spheres" occurred randomly in 2–5% of individuals, and data reported below are based on observations of about one hundred animals with such structures. We hypothesize that "spheres" can be viewed as a component of innate immune (e.g., bacterial infection) responses; and separated three stages of this process.

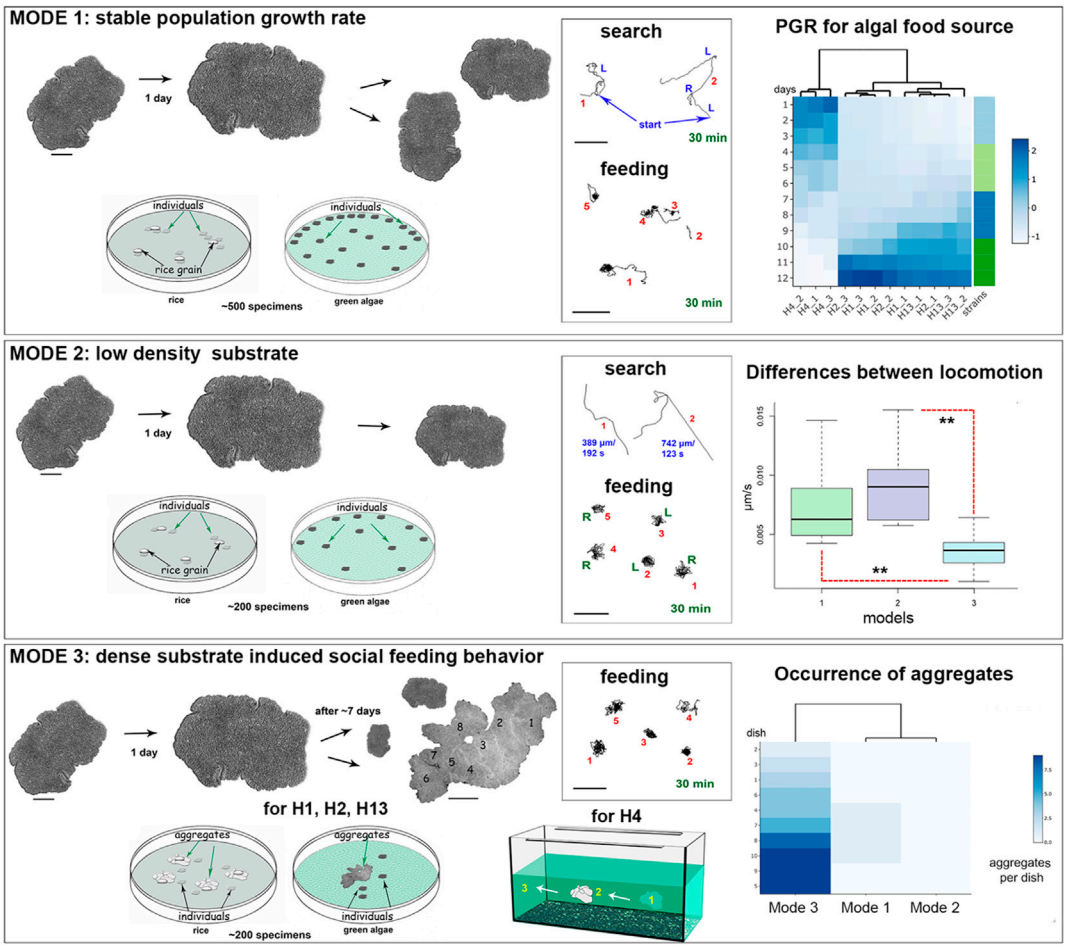

FIGURE 3 | Three separate model schemes of long-term culturing/aging of Placozoa. Mode 1—optimized conditions; Mode 2—low and Mode 3—high densities of the green alga mat (*Tetraselmis marina*) or rice grains; see text for details. Mode 1: Optimized culture conditions with dispersal animals and their moderate concentration on feeding substrates. The middle diagram shows examples of exploratory and feeding locomotion for five animals (numbers) within 30 min. The right diagram shows the representative dynamics of the population growth rate (PGR) for all haplotypes (H1, H2, H4, and H13). 3 separate dishes were used for each haplotype (e.g., H4_1, H4_2, H4_3, etc.), starting with 10 animals per dish. All datasets were normalized to absorb the variation between columns for all four haplotypes of Placozoa. Under these conditions, animals steadily increase their body surface area and have vegetative (non-sexual) reproduction by fission. Mode 2: Low-density substrate. Limit of food source led to decreasing of animal sizes and numbers of animals in culture dishes. Mode 3: High-density substrate. There is both increasing in animal sizes and the aggregation of 2–15 individuals around rice grains or on the dense algal mat. The heat diagram on the right shows the predominant occurrence of aggregates compared to Mode 1 (no aggregates were observed on low-density substrates in Mode 2). H4 expressed the same behavior patterns on the walls of 20L aquarium, where individuals within the aggregate could move together (1-2-3, arrows). However, most animals stay at the substrate (central diagram) with significantly reduced overall locomotion during the feeding, as indicated in the right middle diagram. Each set of video images (Mode 1–3) was analyzed using ImageJ (NIH), calculating for velocity, animal area, and perimeter (n = 3–6), as was reported elsewhere (Romanova et al., 2020a). Difference between locomotion in Modes 1 and 3: p-value is 0.003002; between Modes 2 and 3: p-value is 0.000072 (unpaired Student's test). Scale bars: for individual animals—200 µm; for the aggregate in Mode 3—1 mm; for all locomotory tracks—200 µm.

The first stage was an apparent lengthening of body shape (**Figure 7C**) and inability to fission (**Figures 7C–F**). This phenomenon was observed during the aging of populations, which occurred without systematic refreshing of ASW. When ASW was replaced within 2–3 days, we restored healthy populations of placozoans without any noticeable morphological changes compared to control individuals (as in Mode 1).

The second stage: the upper epithelium begins to exfoliate (**Figures 7D–F**, **Supplementary Figure S7**), and spherical formations become visible. We could observe elongated animals with one "sphere" (**Figure 7E**) or several spheres (**Figure 7F**), as well as rounded animals with one "sphere" (**Figure 7D**).

The third stage was a separation of the spherical structures from a mother animal (**Figures 7G–7G**). "Spheres" consisted of upper epithelium, fiber cells, and, probably, "shiny spheres" cells (with large lipophilic inclusions). Light microscopic analysis revealed cavities inside "spheres" (**Figures 7G–7G**). We damaged the surface tissue of the "sphere" with laser beams (using confocal microscopy), which released numerous bacteria-sized particles (unknown identity, **Figures 7H–K**), suggesting

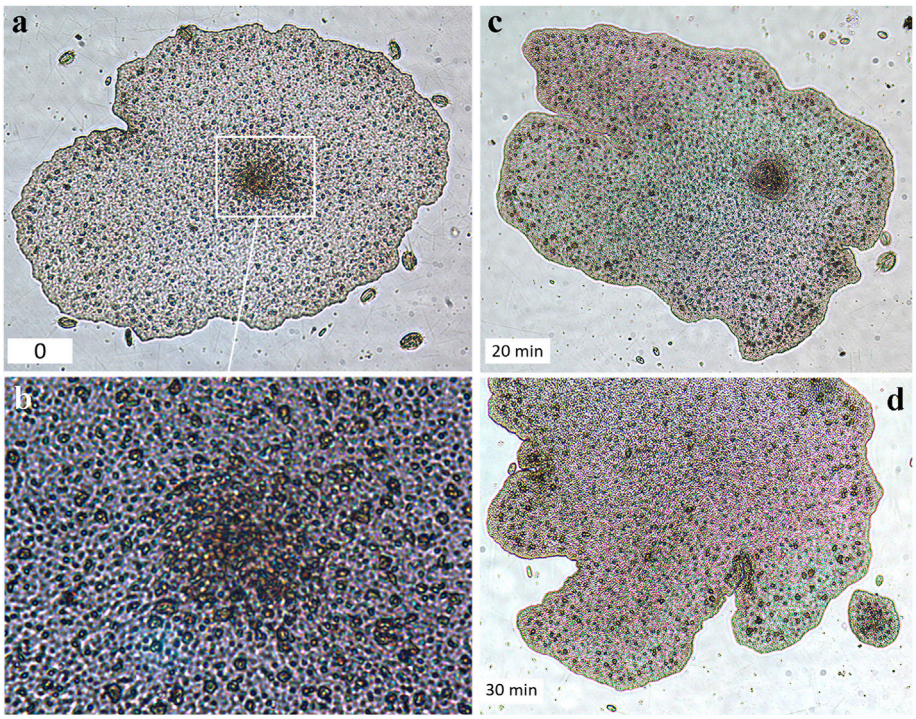

FIGURE 4 | Swarmer-like forms were formed at the lower (substrate-facing) side of the "mother"-animal (H1 haplotype, *T. adhaerens*). **(A,C,D)**—A unique illustrated example of the swarmer formation's time course (bottom left corners indicate time intervals in minutes). **(A)**. The formation of a higher density cell region in the middle part of the mother animal (white square outline, and the higher magnification of the same region in **(B,C)**. The formation of the swarmer and its separation from the mother animal **(D)**.

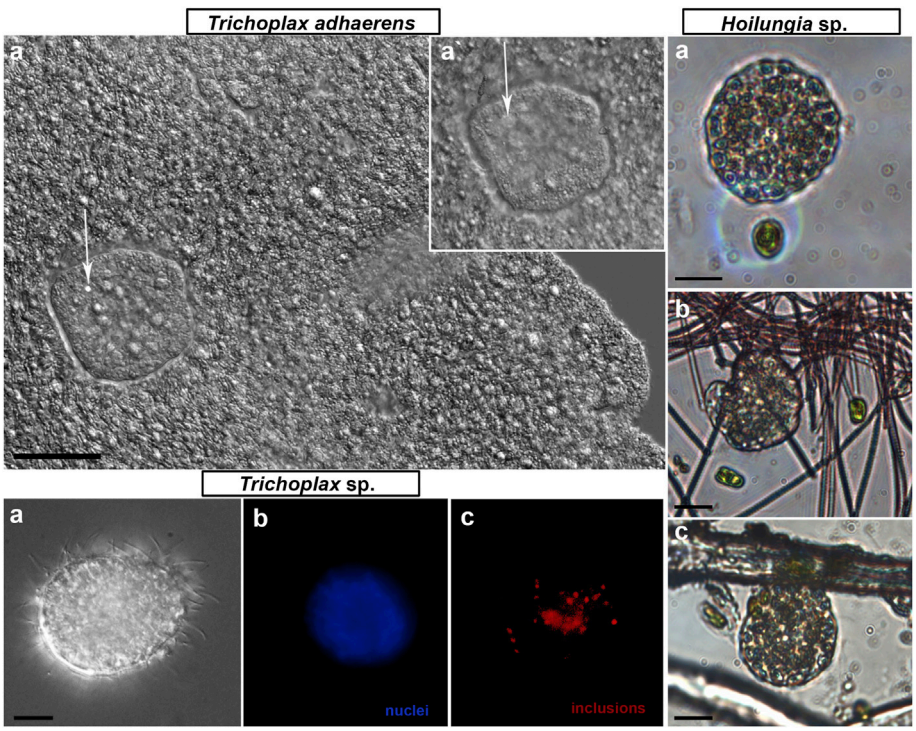

FIGURE 5 | "Swarmers" were formed in the long-term culture in every studied species of Placozoa. "Swarmers" are small (15–30 μm diameter) juvenile animals (white arrows in *T. adhaerens* box, **(A–A')**—different Z-layer). "Swarmers" expressed coordinated exploratory and feeding behaviors (*Hoilungia* sp. box, H4 haplotype, three illustrative images of different juvenile animals). *Trichoplax* sp. box: (a)—DIC view of the solid swarmer-like animal; (b)—high density of nuclei in the center; (c)—autofluorescence. Scale bar: 10 μm.

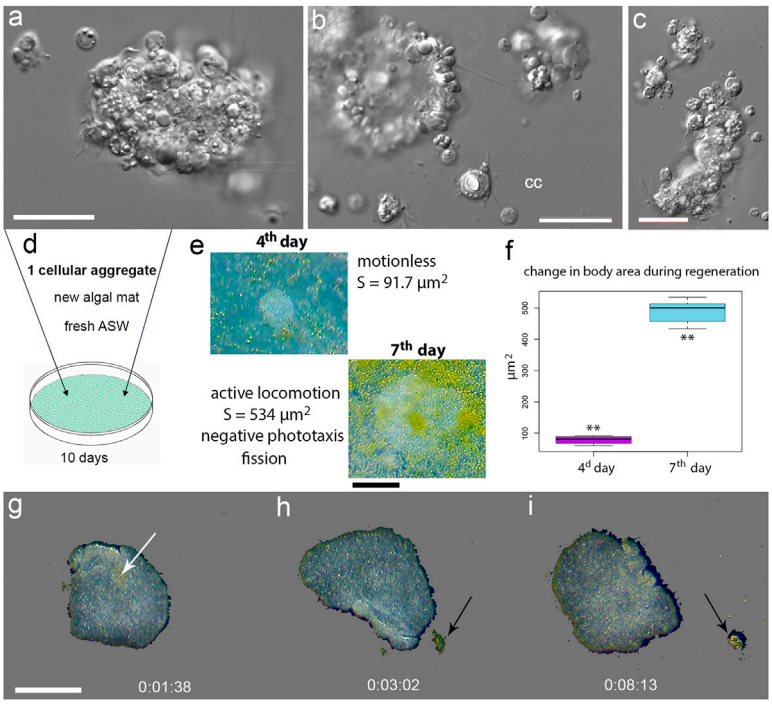

FIGURE 6 | Regeneration in Placozoa. **(A,B,C)**—Illustrative examples of small cellular aggregates from *T. adhaerens*. Aggregates consist of ciliated epithelial cells, lipophil, crystal, and fiber cells, which were identified based on their distinct morphology. cc-isolated crystal cell. **(D)**—Placement of a single aggregate in a new culture cell with fresh ASW and algal mat. **(E)**—4th and 7th day of regeneration with calculated surface area (S) of a newly formed animal. The ciliated locomotion, negative phototaxis and fission started on the 7th day of regeneration. **(F)**—increasing surface areas occurred from 4th to 7th day. The t-value: –23.48979. The *p*-value: < 0.00001. **(G–I)**—time-lapse images after splitting an animal into two parts; locomotion and feeding continued (see text and **Supplementary Video S7**). Arrows indicate a cluster of algae. Scale bar: **(A,B,C)**—20 µm, **(E)**—200 µm, **(G–I)**—500 µm.

that these spherical formations could encapsulate bacteria inside (**Supplementary Video S13**, **Supplementary Figure S8**).

Reversed Nature of "Spheres"

When we transferred 28 already separated "spheres" (**Supplementary Figure S4**) to new Petri dishes with algal mats, then within 3–5 days, we observed the restoration of classical placozoan bodyplan. During the next few days, stable populations of placozoans could be established. In contrast, when we placed 28 control spheres in sterile Petri dishes without algal mats, all "spheres" were degraded within 2–5 days.

Fiber cells are capable of phagocytosis (Thiemann and Ruthmann, 1990; Jacob et al., 2004; Moroz and Romanova, 2021) and contain bacterial cells (Guidi et al., 2011; Gruber-Vodicka et al., 2019; Kamm et al., 2019a; Romanova et al., 2021). We also confirmed that bacteria were localized in fiber cells of H1, H4, and H13 (**Figure 8B**). It was hypothesized that bacteria could be endosymbionts (Kamm et al., 2019a; Gruber-Vodicka et al., 2019). Moreover, the ultrastructural analysis of fiber cells suggested the engulfment of bacteria (**Figure 7B**) by the endoplasmic reticulum, which can also be viewed as a stage of intracellular phagocytosis (**Figure 8B**).

The treatment of *Trichoplax* with ampicillin eliminated potential bacteria from placozoans (**Supplementary Figure S5**) and their fiber cells (**Figures 8F–I**). Furthermore, ampicillin prevented the formation of "spheres" in bacteria-free culture: none were seen during 12 months of cultivating *Rickettsia*-free animals (over 10,000 animals, **Supplementary Figure S5**). Of note, in our culture, animals lived in the presence of ampicillin for more than 4 years without bacteria.

The fiber cell type contains the massive mitochondrial cluster (**Figures 7B**, **8F**,G; Grell et al., 1991; Smith et al., 2014; Mayorova et al., 2018; Romanova et al., 2021, **Figure 5**) as a reporter of high energy production. Ampicillin-treated, *Rickettsia*-free animals had additional morphologic features such as numerous small and clear inclusions inside fiber cells (**Figures 8F,G**). The control group with bacteria has one or two large inclusions (**Figures 8H,I**) with a less visible mitochondrial cluster. The functional significance of these ultrastructural changes is unclear.

DISCUSSION

Grazing on algal and bacterial mats might be an ancestral feeding mode in early Precambrian animals (Rozhnov, 2009). And placozoans may have preserved this evolutionarily conserved adaptation from Ediacaran animals (Sperling and Vinther, 2010). Under this scenario, we view the long-term culturing of placozoans as an essential paradigm to study interactions among relatively small numbers of cell types for integration of

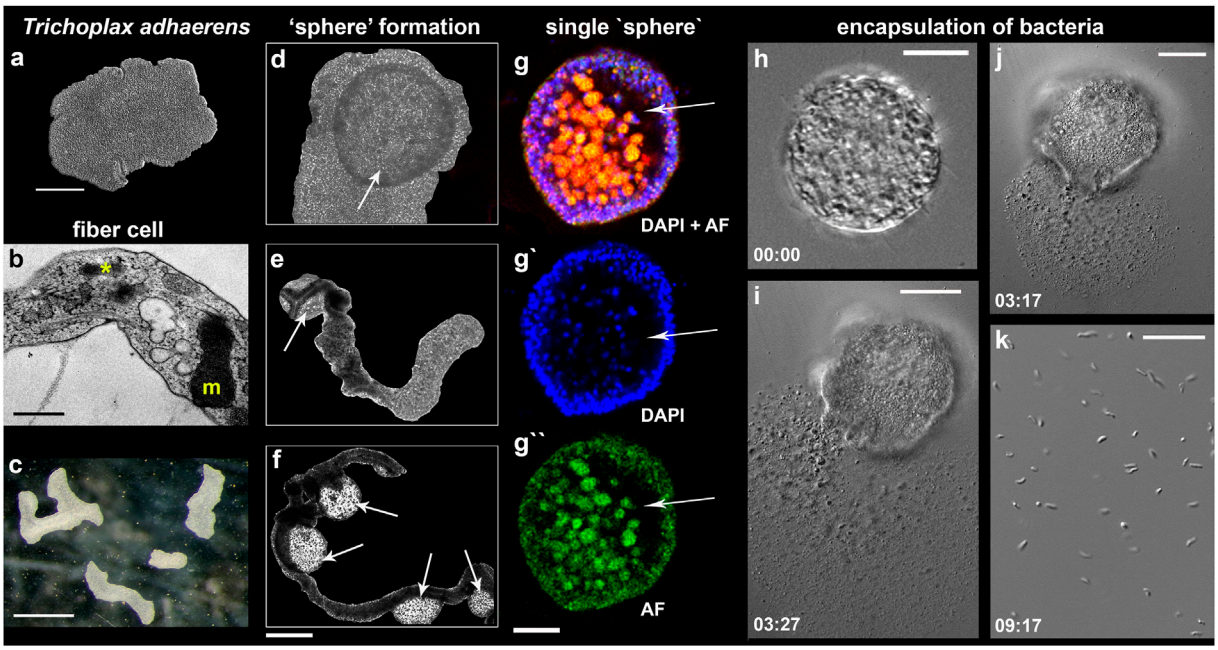

FIGURE 7 | "Sphere"-type formations in *Trichoplax adhaerens*. **(A–C)** control animals under optimal culture conditions (mode #1, see text and **Figure 3**); **(B)**—Transmission electron microscopy (TEM) image of the fiber cell with a bacterium (asterisk) and a large mitochondrial complex (m). **(D–H)**–Formation of spheres (arrows) from the upper/dorsal epithelium. **(D)**—disk-like animal; **(E,F)** -animals with elongated bodies; **(E)**—one "sphere" (arrow); **(D)**—four "spheres" (arrows). (**G–G∋)**—Separated spheres with internal cavities (arrows); Nuclear DAPI staining—blue [excited by the violet (~405 nm) laser with blue/cyan filter (~460–470 nm)]; Autofluorescence (AF)—green (excitation 490 nm and emission 516 nm). **(I–K)**—Spherical formations encapsulate bacteria inside; **(I–J)**—the damage of the sphere's surface by laser released numerous bacteria (magnified in **(K)**; see text for details). Time intervals following the laser-induced injury are indicated in the left corners of each image. Scale: a 200 μm, **(B)**—500 nm, **(C)**—1 mm, (**G–G∋)**—400 μm, **(G–I)**—20 μm, **(K)**—10 μm.

morphogenesis and reproduction, immunity, and behaviors. **Figure 9** summarizes the complementary life-history strategies present in at least four species of Placozoa (=H1, H2, H4, and H13 haplotypes).

The directional (ciliated) locomotion in placozoans depends upon distributions of food sources, which differentially alternate exploratory and feeding patterns. Dense biofilms triggered social-type interactions and elementary cooperation, whereas limited food supplies, stress, and aging triggered systemic immune and morphogenic responses as well as alternative modes of reproduction.

Placozoans are virtually immortal with dominant clonal reproduction strategies (see Schierwater et al., 2021 and below). Furthermore, our data with small cell aggregates (*Regeneration as a Part of Adaptive Life Strategies in Placozoans*) suggest that regenerative responses might also be part of adaptive reproduction mechanisms.

Placozoans have two classical types of non-sexual reproduction: 1) fragmentation into two daughter animals or fission and 2) formation of swarmers (Thiemann and Ruthmann, 1988; Thiemann and Ruthmann, 1990; Thiemann and Ruthmann, 1991; Seravin and Gudkov, 2005a, b)—juvenile animals with small body size (20–30 μm). Thiemann and Ruthmann showed that the "budding" of a daughter animal started from the dorsal side for 24 h, and a released swarmer had all four morphologically defined cell types at that time (Thiemann and Ruthmann, 1988; Thiemann and Ruthmann, 1990; Thiemann and Ruthmann, 1991; Ivanov et al., 1980b). Here, we observed that the formation of swarmer-like juvenile animals could also occur from the lower layer in all placozoans tested here. This type of arrangement might have some rationale: the lower epithelium consists of a greater diversity of cell types (compared to the upper layer) such as epithelial, lipophil, and gland cells with various subtypes (e.g., Smith et al., 2014; Mayorova et al., 2019; Romanova et al., 2021; Prakash et al., 2021).

The Emerging Diversity of Life Forms in Placozoa

In addition to classical flat, disk-like animals, the earlier literature suggests that at least six different spherical morphological forms occur in Placozoa. Thiemann and Ruthmann (1988); Thiemann and Ruthmann (1990); Thiemann and Ruthmann (1991) used electron microscopy to characterize the budding process in *Trichoplax adhaerens*. They provided morphological descriptions of "swarmers" and "spherical forms" as well as the distributions of the different cell types within these structures. The spherical forms were named as follows: 1) Moribund or non-viable spherical forms (degenerative, non-reproductive phase) according to Grell, 1971; 2) Hollow spheres, type A, which cannot be

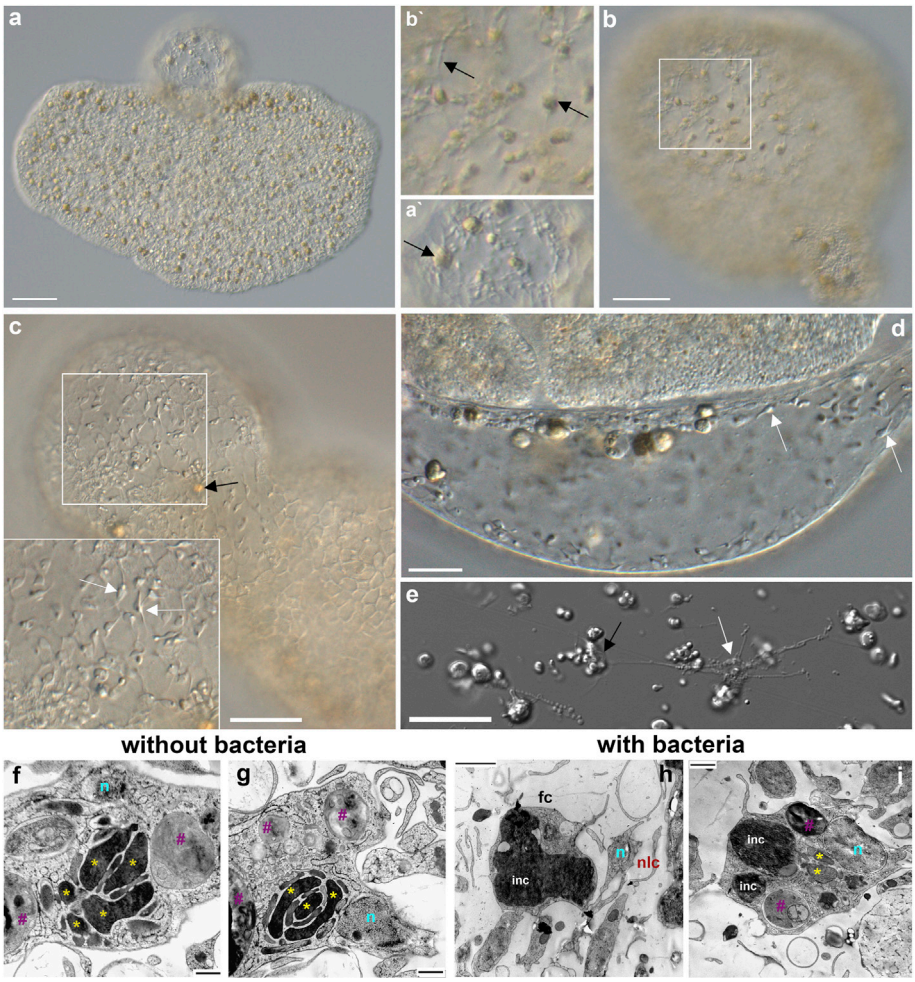

FIGURE 8 | Fiber cells in spherical structures **(A–C)** and their microanatomy **(F–I)**. Both fiber cells (black arrows) and smaller neuroid-like cells (white arrows) are present in "spheres'". **(A)**—*Trichoplax adhaerens* with a sphere on the upper side. **A'**– a part of the sphere with two fiber cells (arrow). **(C,D,E)**—smaller neuroid-like cells (white arrows) with elongated processes **(E)** that can form connections among themselves and fiber (black arrow) cells (Romanova et al., 2021). Both cell types are located in the middle layer of placozoans **(B/B')**. **(F–I)**—Transmission electron microscopy (TEM) of the fiber cells in *Rickettsia*-free *Trichoplax* (ampicillin-treated for 12 months) and control animals with endosymbiotic bacteria (see also **Figure 7B**). Of note, fiber cells in ampicillin-treated populations of placozoans had more elaborate mitochondrial clusters and clear inclusions. In contrast, in animals with bacteria, fiber cells possessed large dark (by TEM) inclusions (light microscopy also shows brownish inclusions—black arrows in **A–C**). Yellow asterisks (*) - mitochondria, n—nuclei, purple #—clear inclusions, inc—dark inclusions, fc—fiber cells, nlc—neuroid-like cells.

transformed to flat animals (Thiemann and Ruthmann, 1990); 3) Hollow spheres, type B, which can be transformed to flat animals or "big" (40–60 μm) swarmers (Grell and Benwitz, 1974; Ivanov et al., 1980a; Thiemann and Ruthmann, 1988); 4) Solid small (12–20 μm) swarmers-like forms, or solid swarmers, vegetative reproduction stage (Grell and Benwitz, 1971; Thiemann and Ruthmann, 1988; Thiemann and Ruthmann, 1991); they can be similar to small swarmer-type forms derived from the ventral surface and discussed here; 5) Solid spheres without cavities (120–200 μm), which are not connected to vegetative reproduction (Thiemann and Ruthmann, 1990); 6) Dorsal stolons, which form small daughter animals by mechanisms different from fission and swarmers (Thiemann and Ruthmann, 1991).

The exact relationships between classical "swarmers" (Grell and Benwitz, 1974; Ivanov et al., 1980b; Thiemann and Ruthmann, 1988) and other spherical structures described in previous papers and this manuscript are less evident due to the lack of established terminology, cross-referenced microscopic methods, and details. No electron microscopic observations of these budding processes were undertaken in the present study, but light microscopy confirmed the presence of similar main cell types as described before.

In a broad sense, the formation and morphology of most separated spherical structures overlap with the far-reaching definition of swarmers as small vegetative progeny (Thiemann and Ruthmann, 1988; Thiemann and Ruthmann, 1990; Thiemann and Ruthmann, 1991). In more precise terms, some physically separated spheroid forms described here match the

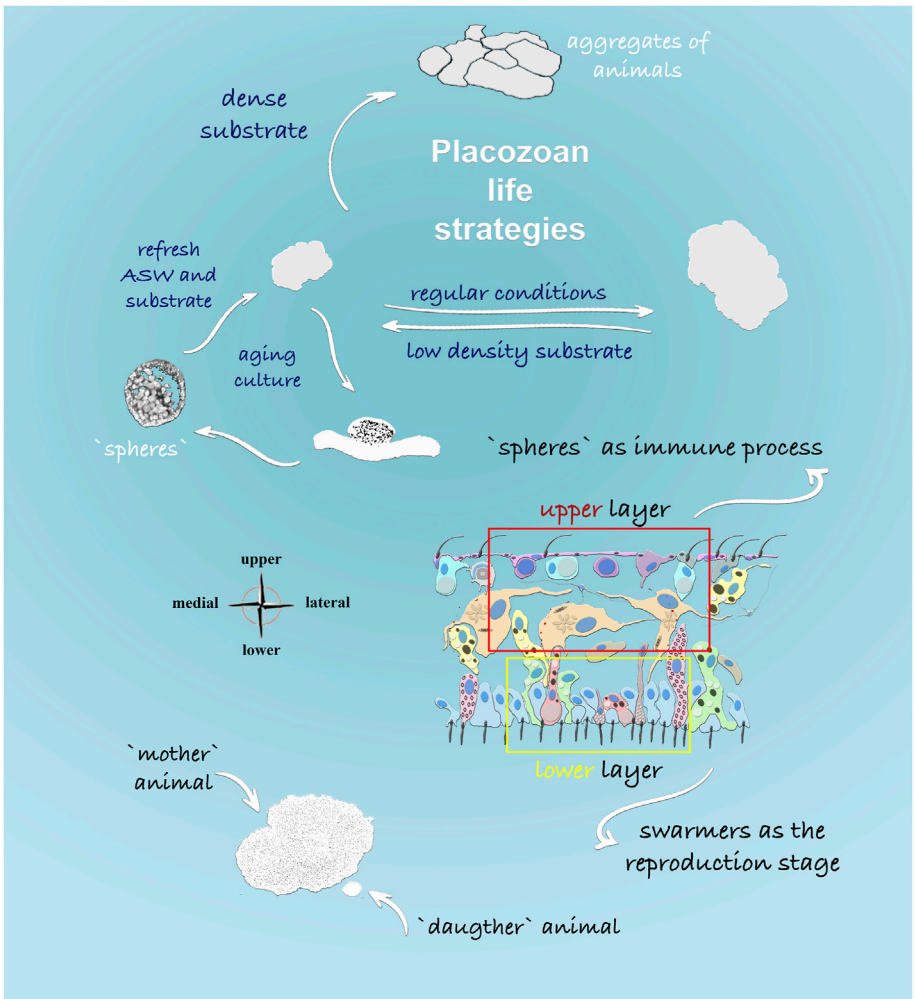

FIGURE 9 | Life Strategies in Placozoa: Schematic representation of feeding and reproductive stages described in this study. The density of food substrate predominantly determines formations of different morphological stages. Dense algal substrate led to the formation of aggregates from multiple animals ("social" feeding behavior). In aging culture, the formation of specialized spherical structures was observed from the upper cell layer of placozoans, and it was shown that spheres could harbor multiple bacteria. In contrast, the formation of small juvenile animals or "swarmers" might have different etiology and development from the lower cell layer, as shown in the cross-section of *Trichoplax*.

definition of "hollow spheres", type B (Thiemann and Ruthmann, 1988; Thiemann and Ruthmann, 1990; Thiemann and Ruthmann, 1991), and their potential transformations to juvenile animals. Specifically, solid small swarmers-like forms (Grell, 1981; Thiemann and Ruthmann, 1988; Thiemann and Ruthmann, 1991) can be similar to small swarmer-like forms discussed here and derived from the ventral surface. They can be naturally transformed into "canonical" juvenile animals under favorable conditions in both cases. To sum, the differences between the current and earlier observations on swarmer-type forms might be clarified if we consider the dynamic nature of sphere formation (e.g., **Supplementary Video S14**), which varies depending on the conditions in which animals are cultivated. We observed the enhanced formation of spherical buds in animals maintained with reduced food sources and aging cultures.

The Roles of Spheres in Innate Immunity Responses

We hypothesize that the spheres could be developmentally linked to the innate immune response, possibly induced by bacteria in aging populations or unhealthy culture conditions. Thus, hollow spheres developed from the upper layer could also be a path to vegetative reproduction under stress conditions. If the

microenvironment became more favorable for placozoans, "spheres" can be transformed into swarmer-like forms as pelagic stages of benthic placozoans and eventually juvenile animals.

The Nature of Bacterial Species and Immunity

Since we did not observe these structures in antibiotic-treated cultures, the budded spheres could be formed as morphological defensive responses to bacterial infection. Bacteria-shaped cells were also released from one of these spherical structures when it was damaged with laser illumination, and we observed their division and labeling with DAPI (**Supplementary Figure S8**). However, we did not characterize the placozoan microbiome with metagenomic tools and inferred putative bacterial sources as the most likely explanation of morphological observations. Also, we did not know whether these bacteria differed from the previously reported endosymbionts (Kamm et al., 2018; Kamm et al., 2019a). On the other hand, our ultrastructural data confirmed the presence of bacteria in fiber cells of all studied species, and fiber cells could be critical players in the integration of immunity, morphogenesis, defense, and behaviors.

One of the forms of nonspecific defense in invertebrates is the encapsulation of foreign objects, and this process is similar to the systemic sphere formation in Placozoa. We see that opsonization has been observed inside the fiber cells (**Figures 7**, **8**). Plus, the fiber cells can perform the functions of macrophages with a well-developed capacity for phagocytosis (Thiemann and Ruthmann, 1990).

Cellular immunity by phagocytosis is the most ancient and widespread mechanism among basal Metazoa. For example, in sponges and cnidarians, the encapsulation is carried out by amoebocytes (=archeocytes) or collencytes (Musser et al., 2021). Phagocytosis in invertebrates, like in vertebrates, includes several stages: chemotaxis, recognition, attachment of a foreign agent to the phagocyte membrane, intracellular lysis, etc. (Bang, 1975; Lackie, 1980; Bayne, 1990). Due to the limited diversity of cell types, humoral and cellular immune responses could likely be relatively simple in Placozoa (Kamm et al., 2019b; Popgeorgiev et al., 2020).

Chemoattractant/repellents can be signaling molecules from microorganisms or other cell types. Symbiont-host signaling can include changes in nitric oxide gradients (Moroz et al., 2020b) or regional differences in amino acid composition, interconversion of D- and L-forms (Moroz et al., 2020a), the formation of oxygen radicals, which are toxic to bacteria, etc.

Fiber cells are perfectly suitable for the placozoan immune system's sensors, integrators, and effectors. Fiber cells are located in the middle layer of placozoans with multiple elongated processes, spread around many other cell types, including the crystal cells. Fiber cells have specialized contacts among themselves (Grell and Ruthmann, 1991). A new class of neural-like/stellar-like cells is localized in the vicinity of fiber cells. Together they form a meshwork of cellular processes from the middle layer to the upper and lower layers (Moroz et al., 2021a; Romanova et al., 2021). This "network" can be a functional integrative system sharing some immune and neural features and pools of signaling molecules in multiple microcavities for volume transmission (Moroz et al., 2021b).

We propose that such a placozoan-type integrative system is conceptually similar to the ancestral integration of innate immune and primordial neuroid-like systems, which controlled adaptive stress responses and behavior and regulated morphogenesis and regeneration.

Early (and present) animals strongly depended on the environmental and symbiotic bacteria, and fiber-type cells (or similar/homologous classes of amoebocytes as recently described in sponges - Musser et al., 2021) might be critical elements in the shared evolution of immune and neural systems to integrate both morphogenesis and behaviors (Fields et al., 2020). Here, the defense against bacterial infections can be an inherent part of such integrative ancestral adaptive responses.

Comments added to proof: When this manuscript was under review, Mayorova et al. (2021) provided additional experimental evidence and highlighted the importance of placozoan fiber cells in regeneration, innate immunity, and phagocytosis emphasizing the significance of macrophage-like cells in the evolution of basal animal lineages.

DATA AVAILABILITY STATEMENT

The original contributions presented in the study are included in the article/**Supplementary Material**, further inquiries can be directed to the corresponding authors.

AUTHOR CONTRIBUTIONS

DR and LM designed the study; DR visualized; MN and DR cultured of all haplotypes; DR involved to LM and LSM microscopy, behavioral observations, and experiments of population growth rate; SS involved to TE microscopy; MN designed tests with antibiotics; DR and LM wrote the draft of the paper; and all authors reviewed, commented on, and edited the manuscript.

FUNDING

This work was supported in part by the Human Frontiers Science Program (RGP0060/2017) and National Science Foundation (1146575, 1557923, 1548121, 1645219) grants to LM. Research reported in this publication was also supported in part by the National Institute of Neurological Disorders and Stroke of the National Institutes of Health under Award Number R01NS114491 (to LM). The content is solely the authors' responsibility and does not necessarily represent the official views of the National Institutes of Health.

ACKNOWLEDGMENTS

The authors thank Drs. M. Eitel and F. Varoqueaux for H2 and H13 haplotypes access, and A. Pronosin for his help in maintaining cultural dishes.

SUPPLEMENTARY MATERIAL

The Supplementary Material for this article can be found online at: https://www.frontiersin.org/articles/10.3389/fcell.2022.823283/full#supplementary-material

Supplementary Figure S1 | Negative phototaxis during long-term culturing of *Trichoplax* and *Hoilungia* genera. a. Culture dishes in the environmental chamber; **(B)**, **(C—A)** Petri dish with *T. adhaerens*; animals were concentrated at the darker side of the dish **(B)** vs. more illuminated side **(C)**; **(D)**, **(E—A)** Petri dish with *Hoilungia hongkongensis*; animals were more concentrated at the darker side of the dish **(D)** vs. brighter side **(E)**.

Supplementary Figure 2 | Floating individuals in an aging culture of placozoans. The photo in **(A)** shows both single floating animals (red arrows) and aggregations under the water surface (white arrows). **(B)**. An illustrated example from **Supplementary Video S2** with a free-floating animal (white arrow); a white circle indicates an animal at the bottom of the cultured dish. Scale bar: A—1 cm, B—1 mm.

Supplementary Figure S3 | Dynamic changes in the body shape of *Trichoplax* sp. (H2 haplotype). Note unusual morphological features such as "pseudopodia"-like elongations in a single individual during ~7 min of time-lapse. Scale bar: 200 μm.

Supplementary Figure S4 | Restoration of a disk-shaped morphology from a sphere to a juvenile placozoan *T. adhaerens*. Separation of "spheres": The photo shows two separate spheres from an animal. Recovery: A particular sphere (~ 30 μm) was placed in a Petri dish with a freshly prepared algal mat (*T. marina*) and ASW (Mode 1). Note an appearance of flattened/elongated body parts from the sphere (2–6 hrs, first three images). In 24 hrs the sphere was transformed into a disk-shaped animal capable of locomotion. In 2 days, small individuals were capable of fission.

Supplementary Figure S5 | Isolation of intracellular bacteria-free *Trichoplax* culture. Table of antibiotics used in experiments. **(A)** Agarose gel electrophoresis of the PCR test of individual *Trichoplax adhaerens* with specific primer for Rickettsiales 16S rRNA (n = 5 per antibiotic, total n = 20 individuals). After 6 weeks of treatment with three different antibiotics, only a minor decrease in bacterial DNA was detected for doxycyclinum, and no effect for two other antibiotics. Treatments with rifampicinum and ciprofloxacin were terminated after 1.5 and 7 months, respectively, because of inefficiency, while doxycyclinum treatment continued for additional time. **(B)** 6 months after the beginning of the experiment, we started treatment with the fourth antibiotic, ampicillin. Agarose gel electrophoresis with tests for 12 months of doxycyclinum and 6 months of ampicillin treatment. Doxycyclinum culture still contains a minor amount of rickettsial DNA, while the ampicillin line is entirely negative. DNA of 10 animals was pooled for each PCR tube, a total of n = 60. The ampicillin-treated line was cultivated with the constant addition of ampicillin for four years by now, and all subsequent tests for rickettsial DNA were negative (not shown). This culture line was used for microscopic imaging shown in Figure 8.

Supplementary Figure S6 | Dynamics of the placozoan population growth and pH variations in culture conditions (artificial seawater 35 ppm, pH = 8.0, 24 ± 2°C, and daylight illumination). Two H1 **(A)** or one H2 **(B)** individuals were added into a 9-cm Petri dish with *Tetraselmis marina* biofilm. Two/thirds of the water were replaced on Day 8. The numbers of individuals and the value of the pH in the media were assessed daily (at the same time of the day) for all days. H13 **(C)** population growth was monitored under similar conditions except that the water was changed daily, yielding a constant pH of 8.0. All experiments were done in triplicates (error bars represent standard error of the mean, confidence intervals $*p < 0.05$, $**p < 0.01$).

Supplementary Figure S7 | Illustrated examples of the "hollow" sphere formation in *Trichoplax adhaerens*.

Supplementary Figure S8 | The overall architecture of a "spherical structure" **(A, B)**. DAPI labeling (blue) and cellular autofluorescence (green). Total image size by Z: 41.24 μm, including **(A–A′)**—12.37 μm depth, **(B–B′)**—16.49 μm depth. White arrows **(A, B)** indicate two putative bacterial cells in the sphere, which are different from *Trichoplax* cells with a larger nucleus and autofluorescence in the cytoplasm. **(C, D)**–bacteria-shaped particles released after the sphere's damage by laser (confocal microscopy and DIC). **(C–C′)** shows the same area with DIC and DAPI fluorescence; blue arrows—*Trichoplax* cell; white circles—putative bacteria cells with a distinct rood-type morphology, which was not observed for *Trichoplax*. Scale bar: **(A–A′)**, **(B–B′)**, **(C–C′)**, **(E)**—20 μm, **(D)**–10 μm.

Supplementary Video S1 | The unusual morphology—*T. adhaerens* with a "hole" in the middle of the body (see also **Figure 1E**).

Supplementary Video S2 | Floating individual in an aging culture of *T. adhaerens*. The photo in **(A)** shows both single swimming animals (red arrows) and aggregations under the water surface (white arrows).

Supplementary Video S3 | After physical separation of a "swarmer," this juvenile animal could be temporally located under the "mother organism," moving together on substrates (*T. adhaerens*).

Supplementary Video S4 | A swarmer of *Trichoplax* sp. (H2 haplotype).

Supplementary Video S5 | A swarmer *Hoilungia* sp. (H4 haplotype).

Supplementary Video S6 | A swarmer *Hoilungia* sp. (H4 haplotype).

Supplementary Video S7 | Locomotion of *Trichoplax adhaerens* on the clean glass before and after splitting the animal by a thin steel needle. 5X magnification, 250X time-lapse. The animal was cut at the site marked by a white circle and letter R. Tracks of the two halves are displayed as red and yellow circles. Tracks of the second animal halves are displayed in blue and cyan. All halves of cut animals continue locomotion after the cut without a noticeable pause. Note, halves of the same animal turn synchronously.

Supplementary Video S8 | An example of the "hollow sphere" formation from the upper layer. The lower layer is responsible for locomotion and feeding.

Supplementary Video S9 | An early stage of the "hollow sphere" separation from *Trichoplax adhaerens*.

Supplementary Video S10 | An elongated form of *Trichoplax adhaerens* with two spherical dorsal structures.

Supplementary Video S11 | An elongated form of *Trichoplax adhaerens* with four dorsal spheres.

Supplementary Video S12 | *Trichoplax adhaerens* with two isolated hollow spheres.

Supplementary Video S13 | Putative bacteria from damaged "sphere".

Supplementary Video S14 | Comparison of a swarmer and a free-floating "sphere". The "solid" swarmer resembles a small juvenile animal with ciliated locomotion, and its interior is filled with cells, without a recognized cavity. A "hollow sphere" has a well-defined micro-cavity, no recognized behaviors, and a low density of ciliated cells on the surface (which might represent dorsal/upper epithelial cells; see also Thiemann and Ruthmann, 1988; 1990, 1991).

REFERENCES

Aleshin, V. V., Konstantinova, A. V., Nikitin, M. A., and Okshteĭn, I. L. (2004). On the Genetic Uniformity of the Genus Trichoplax (Placozoa). *Genetika* 40 (12), 1714–1716. (in Russ). doi:10.1007/s11177-005-0015-y

Armon, S., Bull, M. S., Aranda-Diaz, A., and Prakash, M. (2018). Ultrafast Epithelial Contractions Provide Insights into Contraction Speed Limits and Tissue Integrity. *Proc. Natl. Acad. Sci. USA* 115 (44), E10333–E10341. doi:10.1073/pnas.1802934115

Bang, F. B. (1975). *Invertebrate Immunity*. New York: Academic Press, 137–151. doi:10.1016/b978-0-12-470265-3.50016-5Phagocytosis in Invertebrates

Bayne, C. J. (1990). Phagocytosis and Non-self Recognition in Invertebrates. *Bioscience* 40 (10), 723–731. doi:10.2307/1311504

Dellaporta, S., Holland, P., Schierwater, B., Jakob, W., Sagasser, S., and Kuhn, K. (2004). The Trox-2 Hox/ParaHox Gene of *Trichoplax* (Placozoa) marks an Epithelial Boundary. *Develop. Genes Evol.* 214, 170–175. doi:10.1007/s00427-004-0390-8

Dogel, V. A. (1981). *Zoology of Invertebrates. Izd*. Moscow: High School. (in Russ).

Driscoll, T., Gillespie, J. J., Nordberg, E. K., Azad, A. F., and Sobral, B. W. (2013). Bacterial DNA Sifted from the Trichoplax Adhaerens (Animalia: Placozoa) Genome Project Reveals a Putative Rickettsial Endosymbiont. *Genome Biol. Evol.* 5 (4), 621–645. doi:10.1093/gbe/evt036

Eitel, M., Guidi, L., Hadrys, H., Balsamo, M., and Schierwater, B. (2011). New Insights into Placozoan Sexual Reproduction and Development. *PloS ONE* 6 (5), e19639. doi:10.1371/journal.pone.0019639

Eitel, M., Osigus, H. J., DeSalle, R., and Schierwater, B. (2013). Global Diversity of the Placozoa. *PloS ONE* 8 (4), e57131. doi:10.1371/journal.pone.0057131

Eitel, M., Francis, W. R., Varoqueaux, F., Daraspe, J., Osigus, H. J., Krebs, S., et al. (2018). Comparative Genomics and the Nature of Placozoan Species. *PLOS Biol.* 16 (7), e2005359c. doi:10.1371/journal.pbio.3000032

Eitel, M., and Schierwater, B. (2010). The Phylogeography of the Placozoa Suggests a Taxon-Rich Phylum in Tropical and Subtropical Waters. *Mol. Ecol.* 19 (11), 2315–2327. doi:10.1111/j.1365-294x.2010.04617.x

Fields, C., Bischof, J., and Levin, M. (2020). Morphological Coordination: a Common Ancestral Function Unifying Neural and Non-neural Signaling. *Physiology* 35 (1), 16–30. doi:10.1152/physiol.00027.2019

Fortunato, A., and Aktipis, A. (2019). Social Feeding Behavior of *Trichoplax Adhaerens*. *Front. Ecol. Evol.* 7, 19. doi:10.3389/fevo.2019.00019

Graff, L. (1891). *Die Organization der Turbellaria Acoela*. Leipzig: W. Engelmann, 90.

Grell, K. G., and Benwitz, G. (1971). Die Ultrastruktur von *Trichoplax adhaerens* F.E. Schulze. *Cytobiologie* 4, 216–240.

Grell, K. G., and Benwitz, G. (1974). Elektronenmikroskopische beobachtungen über das wachstum der eizelle und die bildung der "befruchtungsmembran" von *Trichoplax adhaerens* FE Schulze (Placozoa). *Z. für Morphologie der Tiere* 79 (4), 295–310.

Grell, K. G. (1972). Eibildung und furchung von Trichoplax adhaerens F. E. Schulze (Placozoa). *Z. Morph. Tiere* 73 (4), 297–314. doi:10.1007/bf00391925

Grell, K. G., Ruthmann, A., Harrison, F. W., and Westfall, J. A. (1991). *Microscopic Anatomy of Invertebrates: Placozoa, Porifera, Cnidaria, and Ctenophora*. Harrison, FW & Westfall, JA.

Grell, K. G., and Ruthmann, A. (1991). "Placozoa," in *Microscopic Anatomy of Invertebrates*. Editors F. W. Harrison, and J. A. Westfall (New York: Wiley-Liss), 13–27.

Grell, K. G. (1981). Trichoplax adhaerens *and the origin of Metazoa. Origine dei Grandi Phyla dei Metazoi, Accademia Nazionale dei Lincei, Convegno Intern*. Rome, Italy: Accademia Nazionale dei Lincei. 107–121c.

Grell, K. G. (1971). *Trichoplax adhaerens* F.E. Schulze und die Entstehung der Metazoen. *Naturwiss. Rundschau.* 24, 160–161.

Gruber-Vodicka, H. R., Leisch, N., Kleiner, M., Hinzke, T., Liebeke, M., McFall-Ngai, M., et al. (2019). Two Intracellular and Cell Type-specific Bacterial Symbionts in the Placozoan *Trichoplax* H2. *Nat. Microbiol.* 4 (9), 1465–1474. doi:10.1038/s41564-019-0475-9

Guidi, L., Eitel, M., Cesarini, E., Schierwater, B., and Balsamo, M. (2011). Ultrastructural Analyses Support Different Morphological Lineages in the Phylum Placozoa Grell, 1971. *J. Morphol.* 272 (3), 371–378. doi:10.1002/jmor.10922

Heyland, A., Croll, R., Goodall, S., Kranyak, J., and Wyeth, R. (2014). *Trichoplax Adhaerens*, an Enigmatic Basal Metazoan with Potential. *Methods Mol. Biol.* 1128, 45–61. doi:10.1007/978-1-62703-974-1_4

Ivanov, A. V. (1973). *Trichoplax Adhaerens* – Phagocitella-like Animal. *Zool. Zh.* 52, 1117–1130. (in Russ).

Ivanov, D. L., Malakhov, V. V., and Tsetlin, A. B. (1980b). Fine Morphology and Ultrastructure of the Primitive Multicellular Organism *Trichoplax* Sp. 1. Morphology of Adults and Vagrants According to the Data of Scanning Electron Microscopy. *Zool. Zh.* 59 (12), 1765. (in Russian).

Ivanov, D. L., Malakhov, V. V., and Tsetlin, A. B. (1980a). New Find of a Primitive Multicellular Organism *Trichoplax* Sp. *Zool. Zh.* 59, 1735–1739. (in Russian). doi:10.1016/0016-2361(80)90151-9

Ivanov, D. L., MalakhovPrilepsky, G. B. V. V., and Tsetlin, A. B. (1982). Fine Morphology and Ultrastructure of the Primitive Multicellular Organism *Trichoplax* Sp. 2. Ultrastructure of Adults. *Zool. Zh.* 61, 645–652. (in Russian).

Jackson, A. M., and Buss, L. W. (2009). Shiny Spheres of Placozoans (Trichoplax) Function in Anti-predator Defense. *INVERTEBR BIOL.* 128 (3), 205–212. doi:10.1111/j.1744-7410.2009.00177.x

Kamm, K., Osigus, H. J., Stadler, P. F., DeSalle, R., and Schierwater, B. (2019a). Genome Analyses of a Placozoan Rickettsial Endosymbiont Show a Combination of Mutualistic and Parasitic Traits. *Sci. Rep.* 9 (1), 17561. doi:10.1038/s41598-019-54037-w

Kamm, K., Osigus, H. J., Stadler, P. F., DeSalle, R., and Schierwater, B. (2018). *Trichoplax* Genomes Reveal Profound Admixture and Suggest Stable Wild Populations without Bisexual Reproduction. *Sci. Rep.* 8 (1). doi:10.1038/s41598-018-29400-y

Kamm, K., Schierwater, B., and DeSalle, R. (2019b). Innate Immunity in the Simplest Animals - Placozoans. *BMC Genomics* 20 (1), 1–11. doi:10.1186/s12864-018-5377-3

Kuhl, W., and Kuhl, G. (1963). Bewegungsphysiologische Untersuchungen an *Trichoplax Adhaerens* F.E.Schulze. *Zool. Anz. Suppl.* 26, 460–469.

Kuhl, W., and Kuhl, G. (1966). Untersuchungen uber das bewegungsverhalten von Trichoplax adhaerens F. E. Schulze (Zeittransformation: Zeitraffung). *Z. Morph. U. Okol. Tiere* 56, 417–435. doi:10.1007/bf00442291

Lackie, A. M. (1980). Invertebrate Immunity. *Parasitology* 80 (2), 393–412. doi:10.1017/s0031182000000846

Laumer, C. E., Gruber-Vodicka, H., Hadfield, M. G., Pearse, V. B., Riesgo, A., Marioni, J. C., et al. (2018). Support for a Clade of Placozoa and Cnidaria in Genes with Minimal Compositional Bias. *Elife* 7, e36278. doi:10.7554/eLife.36278

Malakhov, V. V. (1990). *Mysterious Groups of marine Invertebrates: Trichoplax, Orthonectids, Dicyemids, Sponges*. Moscow: Publishing house of Moscow State University. (in Russian).

Malakhov, V. V., and Nezlin, L. P. (1983). *Trichoplax* - a Living Model of the Origin of Multicellular Organisms. *Nauka* 3, 32–41. (in Russian).

Maruyama, Y. K. (2004). Occurrence in the Field of a Long-Term, Year-Round, Stable Population of Placozoans. *Biol. Bull.* 206 (1), 55–60. doi:10.2307/1543198

Mayorova, T. D., Hammar, K., Winters, C. A., Reese, T. S., and Smith, C. L. (2019). The Ventral Epithelium of *Trichoplax Adhaerens* Deploys in Distinct Patterns Cells that Secrete Digestive Enzymes, Mucus or Diverse Neuropeptides. *Biol. Open* 8 (8), bio045674. doi:10.1242/bio.045674

Mayorova, T. D., Hammar, K., Jung, J. H., Aronova, M. A., Zhang, G., Winters, C. A., et al. (2021). Placozoan Fiber Cells: Mediators of Innate Immunity and Participants in Wound Healing. *Sci. Rep.* 11, 23343. doi:10.1038/s41598-021-02735-9

Mayorova, T. D., Smith, C. L., Hammar, K., Winters, C. A., Pivovarova, N. B., Aronova, M. A., et al. (2018). Cells Containing Aragonite Crystals Mediate Responses to Gravity in *Trichoplax Adhaerens* (Placozoa), an Animal Lacking Neurons and Synapses. *PloS ONE* 13 (1), e0190905. doi:10.1371/journal.pone.0190905

Metschnikoff, E. (1886). *Embriologische Studien an Medusen. Ein Beitrag zur Genealogie der Primitive-Organe*. Wien: A. Holder.

Metschnikoff, E. (1892). La Phagocytose Musculaire. *Ann. de L'institut Pasteur* 6, 1–12.

Miyazawa, H., Osigus, H. J., Rolfes, S., Kamm, K., Schierwater, B., and Nakano, H. (2021). Mitochondrial Genome Evolution of Placozoans: Gene Rearrangements and Repeat Expansions. *Genome Biol. Evol.* 13 (1), evaa213. doi:10.1093/gbe/evaa213

Miyazawa, H., Yoshida, M.-a., Tsuneki, K., and Furuya, H. (2012). Mitochondrial Genome of a Japanese Placozoan. *Zoolog. Sci.* 29 (4), 223–228. doi:10.2108/zsj.29.223

Moroz, L. L., Nikitin, M. A., Poličar, P. G., Kohn, A. B., and Romanova, D. Y. (2021b). Evolution of Glutamatergic Signaling and Synapses. *Neuropharmacology* 199, 108740. doi:10.1016/j.neuropharm.2021.108740

Moroz, L. L., Romanova, D. Y., and Kohn, A. B. (2021a). Neural versus Alternative Integrative Systems: Molecular Insights into Origins of Neurotransmitters. *Phil. Trans. R. Soc. B.* 376, 20190762. doi:10.1098/rstb.2019.0762

Moroz, L. L., Romanova, D. Y., Nikitin, M. A., Sohn, D., Kohn, A. B., Neveu, E., et al. (2020a). The Diversification and Lineage-specific Expansion of Nitric Oxide Signaling in Placozoa: Insights in the Evolution of Gaseous Transmission. *Sci. Rep.* 10, 13020. doi:10.1038/s41598-020-69851-w

Moroz, L. L., and Romanova, D. Y. (2021). Selective Advantages of Synapses in Evolution. *Front. Cel Dev. Biol.* 9, 726563. doi:10.3389/fcell.2021.726563

Moroz, L. L., Sohn, D., Romanova, D. Y., and Kohn, A. B. (2020b). Microchemical Identification of Enantiomers in Early-Branching Animals: Lineage-specific Diversification in the Usage of D-Glutamate and D-Aspartate. *Biochem. Biophysical Res. Commun.* 527, 947–952. doi:10.1016/j.bbrc.2020.04.135

Musser, J. M., Schippers, K. J., Nickel, M., Mizzon, G., Kohn, A. B., Pape, C., et al. (2021). Profiling Cellular Diversity in Sponges Informs Animal Cell Type and Nervous System Evolution. *Science* 374 (6568), 717–723. doi:10.1126/science.abj2949

Nakano, H. (2014). Survey of the Japanese Coast Reveals Abundant Placozoan Populations in the Northern Pacific Ocean. *Sci. Rep.* 4, 5356. doi:10.1038/srep05356

Nikitin, M. (2015). Bioinformatic Prediction of *Trichoplax Adhaerens* Regulatory Peptides. *Gen. Comp. Endocrinol.* 212, 145–155. doi:10.1016/j.ygcen.2014.03.049

Noll, F. C. (1890). *Zber das Leben niederer Seatiere*. Franfurt: Ber. Senckenberg. Ges, 85–87.

Okshtein, I. L. (1987). On the Biology of *Trichoplax* Sp. (Placozoa). *Zool. Zh.* 66 (3), 339.

Osigus, H.-J., Rolfes, S., Herzog, R., Kamm, K., and Schierwater, B. (2019). *Polyplacotoma Mediterranea* Is a New Ramified Placozoan Species. *Curr. Biol.* 29 (5), R148–R149. doi:10.1016/j.cub.2019.01.068

Pearse, V. B. (1989). Growth and Behavior of *Trichoplax Adhaerens*: First Record of the Phylum Placozoa in Hawaii. *Pac. Sci.* 43 (2), 117–121.

Pearse, V. B., and Voigt, O. (2007). Field Biology of Placozoans (*Trichoplax*): Distribution, Diversity, Biotic Interactions. *Integr. Comp. Biol.* 47 (5), 677–692. doi:10.1093/icb/icm015

Popgeorgiev, N., Sa, J. D., Jabbour, L., Banjara, S., Nguyen, T. T. M., Akhavan-E-Sabet, A., et al. (2020). Ancient and Conserved Functional Interplay between Bcl-2 Family Proteins in the Mitochondrial Pathway of Apoptosis. *Sci. Adv.* 6 (40), eabc4149. doi:10.1126/sciadv.abc4149

Prakash, V. N., Bull, M. S., and Prakash, M. (2021). Motility-induced fracture reveals a ductile-to-brittle crossover in a simple animal's epithelia. *Nat. Phys.* 17(4), 504–511. doi:10.1038/s41567-020-01134-7

Rassat, J., and Ruthmann, A. (1979). *Trichoplax Adhaerens* FE Schulze (Placozoa) in the Scanning Electron Microscope. *Zoomorphologie* 93 (1), 59–72. doi:10.1007/bf02568675

Reynolds, E. S. (1963). The Use of lead Citrate at High pH as an Electron-Opaque Stain in Electron Microscopy. *J. Cel Biol.* 17 (1), 208–212. doi:10.1083/jcb.17.1.208

Romanova, D. Y. (2019). Cell Types Diversity of H4 Haplotype Placozoa Sp. *Mar. Biol. J.* 4, 81–90. (in Russ). doi:10.21072/mbj.2019.04.1.07

Romanova, D. Y., Heyland, A., Sohn, D., Kohn, A. B., Fasshauer, D., Varoqueaux, F., et al. (2020a). Glycine as a Signaling Molecule and Chemoattractant in Trichoplax (Placozoa): Insights into the Early Evolution of Neurotransmitters. *Neuroreport* 31, 490–497. doi:10.1097/WNR.0000000000001436

Romanova, D. Y., Smirnov, I. V., Nikitin, M. A., Kohn, A. B., Borman, A. I., Malyshev, A. Y., et al. (2020b). Sodium Action Potentials in Placozoa: Insights into Behavioral Integration and Evolution of Nerveless Animals. *Biochem. Biophys. Res. Commun.* 532, 120–126. doi:10.1016/j.bbrc.2020.08.020

Romanova, D. Y., Varoqueaux, F., Daraspe, J., Nikitin, M. A., Eitel, M., Fasshauer, D., et al. (2021). Hidden Cell Diversity in Placozoa: Ultrastructural Insights from Hoilungia Hongkongensis. *Cell Tissue Res* 385 (3), 623–637. doi:10.1007/s00441-021-03459-y

Rozhnov, S. V. (2009). Development of the Trophic Structure of Vendian and Early Paleozoic marine Communities. *J. Paleontol.* 43, 1364–1377. doi:10.1134/S0031030109110021

Ruthman, A. (1977). Cell Differentiation, DNA Content and Chromosomes of *Trichoplax Adhaerens* F.E.Schulze. *Cytobiologie* 15, 58–64.

Ruthmann, A. G., Behrendt, G., and Wahl, R. (1986). The Ventral Epithelium of *Trichoplax Adhaerens* (Placozoa): Cytoskeletal Structures, Cell Contacts and Endocytosis. *Zoomorphology* 106 (2), 115–122. doi:10.1007/bf00312113

Schierwater, B., and DeSalle, R. (2018). Placozoa. *Cur. Biol.* 28 (3), R97–R98. doi:10.1016/j.cub.2017.11.042

Schierwater, B., Eitel, M., Osigus, H. J., von der Chevallerie, K., Bergmann, T., Hadrys, H., et al. (2010). "Trichoplax and Placozoa: One of the Crucial Keys to Understanding Metazoan Evolution," in *Key Transitions in Animal Evolution* (Boca Raton: CRC Press), 289–326.

Schierwater, B. (2005). My Favorite Animal, *Trichoplax Adhaerens*. *BioEssays* 27 (12), 1294–1302. doi:10.1002/bies.20320

Schierwater, B., Osigus, H. J., Bergmann, T., Blackstone, N. W., Hadrys, H., Hauslage, J., et al. (2021). The Enigmatic Placozoa Part 1: Exploring Evolutionary Controversies and Poor Ecological Knowledge. *BioEssays* 43, 2100080. doi:10.1002/bies.202100080

Schulze, F. E. (1883). *Trichoplax Adhaerens*, Nov. gen., Nov. Spec. *Zool. Anz.* 6, 92–97.

Senatore, A., Reese, T. S., and Smith, C. L. (2017). Neuropeptidergic Integration of Behavior in *Trichoplax Adhaerens*, an Animal without Synapses. *J. Exp. Biol.* 220, 3381–3390. doi:10.1242/jeb.162396

Seravin, L. N., and Gerasimova, Z. P. (1998). Features of the fine Structure of *Trichoplax Adhaerens* Trichoplax, Feeding on Dense Plant Substrates. *Cytologiya* 30, 1188–1193. (in Russ).

Seravin, L. N., and Gudkov, A. V. (2005a). Ameboid Properties of Cells in the Process of Early Morphogenesis and the Nature of a Possible Protozoal Ancestor of Metazoa. *Zh. Obsh. Biol.* 66 (3), 212–223. (in Russ).

Seravin, L. N., and Gudkov, A. V. (2005b). Trichoplax Adhaerens *(Type Placozoa) - One of the Most Primitive Multicellular Animals*. St. Petersburg, Russia: TESSA. (in Russ).

Seravin, L. N., and Karpenko, A. A. (1987). Features of Orientation of Invertebrates in Three-Dimensional Space. *Zool. Zh.* 66 (9), 1285–1292. (in Russ).

Signorovitch, A. Y., Dellaporta, S. L., and Buss, L. W. (2006). Caribbean Placozoan Phylogeography. *Biol. Bull.* 211 (2), 149–156. doi:10.2307/4134589

Smith, C. L., Pivovarova, N., and Reese, T. S. (2015). Coordinated Feeding Behavior in *Trichoplax*, an Animal without Synapses. *PLoS One* 10, e0136098. doi:10.1371/journal.pone.0136098

Smith, C. L., Reese, T. S., Govezensky, T., and Barrio, R. A. (2019). Coherent Directed Movement toward Food Modeled in *Trichoplax*, a Ciliated Animal Lacking a Nervous System. *Proc. Natl. Acad. Sci. U S A.* 116, 8901–8908. doi:10.1073/pnas.1815655116

Smith, C. L., Varoqueaux, F., Kittelmann, M., Azzam, R. N., Cooper, B., Winters, C. A., et al. (2014). Novel Cell Types, Neurosecretory Cells, and Body Plan of the Early-Diverging Metazoan *Trichoplax Adhaerens*. *Cur. Biol.* 24 (14), 1565–1572. doi:10.1016/j.cub.2014.05.046

Sperling, E. A., and Vinther, J. (2010). A Placozoan Affinity for *Dickinsonia* and the Evolution of Late Proterozoic Metazoan Feeding Modes. *Evol. Dev.* 12, 201–209. doi:10.1111/j.1525-142X.2010.00404.x

Stiasny, G. (1903). Einige histologische Details über *Trichoplax adhaerens*. *Z. für wissenschaftliche Zoologie* 75, 430–436.

Thiemann, M., and Ruthmann, A. (1991). Alternative Modes of Asexual Reproduction in *Trichoplax* (Placozoa). *Zoomorphology* 110 (3), 165–174c. doi:10.1007/bf01632872

Thiemann, M., and Ruthmann, A. (1990). Spherical Forms of *Trichoplax Adhaerens* (Placozoa). *Zoomorphology* 110 (1), 37–45. doi:10.1007/bf01632810

Thiemann, M., and Ruthmann, A. (1988). *Trichoplax Adhaerens* FE Schulze (Placozoa): the Formation of Swarmers. *Z. für Naturforschung C* 43 (11-12), 955–957. doi:10.1515/znc-1988-11-1224

Ueda, T., Koya, S., and Maruyama, Y. K. (1999). Dynamic Patterns in the Locomotion and Feeding Behaviors by the Placozoan. *Trichoplax Adhaerence. Biosyst.* 54 (1-2), 65–70. doi:10.1016/s0303-2647(99)00066-0

Varoqueaux, F., Williams, E. A., Grandemange, S., Truscello, L., Kamm, K., Schierwater, B., et al. (2018). High Cell Diversity and Complex Peptidergic Signaling Underlie Placozoan Behavior. *Curr. Biol.* 28, 3495–3501. e3492. doi:10.1016/j.cub.2018.08.067

Voigt, O., Collins, A. G., Pearse, V. B., Pearse, J. S., Ender, A., Hadrys, H., et al. (2004). Placozoa–no Longer a Phylum of One. *Cur. Biol.* 14 (22), R944–R945. doi:10.1016/j.cub.2004.10.036

Zuccolotto-Arellano, J., and Cuervo-González, R. (2020). Binary Fission in *Trichoplax* Is Orthogonal to the Subsequent Division Plane. *Mech. Dev.* 162, 103608. doi:10.1016/j.mod.2020.103608

Conflict of Interest: The authors declare that the research was conducted in the absence of any commercial or financial relationships that could be construed as a potential conflict of interest.

frontiers | Frontiers in Ecology and Evolution

REVIEW
published: 13 May 2022
doi: 10.3389/fevo.2022.806414

Ontogeny, Phylotypic Periods, Paedomorphosis, and Ontogenetic Systematics

Alexander Martynov[1], Kennet Lundin[2,3] and Tatiana Korshunova[4]*

[1] Zoological Museum, Moscow State University, Moscow, Russia, [2] Gothenburg Natural History Museum, Gothenburg, Sweden, [3] Gothenburg Global Biodiversity Centre, Gothenburg, Sweden, [4] Koltzov Institute of Developmental Biology (RAS), Moscow, Russia

The key terms linking ontogeny and evolution are briefly reviewed. It is shown that their application and usage in the modern biology are often inconsistent and incorrectly understood even within the "evo-devo" field. For instance, the core modern reformulation that ontogeny not merely recapitulates, but *produces* phylogeny implies that ontogeny and phylogeny are closely interconnected. However, the vast modern phylogenetic and taxonomic fields largely omit ontogeny as a central concept. Instead, the common "clade-" and "tree-thinking" prevail, despite on the all achievements of the evo-devo. This is because the main conceptual basis of the modern biology is fundamentally ontogeny-free. In another words, in the Haeckel's pair of "ontogeny and phylogeny," ontogeny is still just a subsidiary for the evolutionary process (and hence, phylogeny), instead as in reality, its main driving force. The phylotypic periods is another important term of the evo-devo and represent a modern reformulation of Haeckel's recapitulations and biogenetic law. However, surprisingly, this one of the most important biological evidence, based on the natural ontogenetic grounds, in the phylogenetic field that can be alleged as a "non-evolutionary concept." All these observations clearly imply that a major revision of the main terms which are associated with the "ontogeny and phylogeny/evolution" field is urgently necessarily. Thus, "ontogenetic" is not just an endless addition to the term "systematics," but instead a crucial term, without it neither systematics, nor biology have sense. To consistently employ the modern ontogenetic and epigenetic achievements, the concept of ontogenetic systematics is hereby refined. Ontogenetic systematics is not merely a "research program" but a key biological discipline which consistently links the enormous biological diversity with underlying fundamental process of ontogeny at both molecular and morphological levels. The paedomorphosis is another widespread ontogenetic-and-evolutionary process that is significantly underestimated or misinterpreted by the current phylogenetics and taxonomy. The term paedomorphosis is refined, as initially proposed to link ontogeny with evolution, whereas "neoteny" and "progenesis" are originally specific, narrow terms without evolutionary context, and should not be used as synonyms of paedomorphosis. Examples of application of the principles of ontogenetic

OPEN ACCESS

Edited by:
Pedro Martinez, University of Barcelona, Spain

Reviewed by:
Alessandro Minelli, University of Padua, Italy
Guillaume Lecointre, Muséum National d'Histoire Naturelle, France

***Correspondence:**
Alexander Martynov
martynov@zmmu.msu.ru

Specialty section:
This article was submitted to Evolutionary Developmental Biology, a section of the journal Frontiers in Ecology and Evolution

Received: *31 October 2021*
Accepted: *14 March 2022*
Published: *13 May 2022*

Citation:
Martynov A, Lundin K and Korshunova T (2022) Ontogeny, Phylotypic Periods, Paedomorphosis, and Ontogenetic Systematics. Front. Ecol. Evol. 10:806414. doi: 10.3389/fevo.2022.806414

systematics represented by such disparate animal groups as nudibranch molluscs and ophiuroid echinoderms clearly demonstrate that perseverance of the phylotypic periods is based not only on the classic examples in vertebrates, but it is a universal phenomenon in all organisms, including disparate animal phyla.

Keywords: ontogeny, evolution, phylogeny, ontogenetic systematics, paedomorphosis

INTRODUCTION

The field of ontogeny is a core biological concept and has enormous applications. Thus, not surprisingly, a significant confusion has arisen during usage and application of the various ontogeny-related terms over centuries. Ontogeny is such a commonly used term, that its meaning has become blurred and is usually referring solely to individual development and also contrasting to phylogeny, with both terms rooted in Haeckel (1866). For Haeckel ontogenesis meant "...die Ontogenie weiter nichts ist als eine kurze Rekapitulation der Phylogenie." (" = ...*ontogeny is nothing more than a brief recapitulation of phylogeny*, Haeckel, 1866, II, p. 7, our italics). However, evolutionary changes (and hence, a phylogeny) are based on alterations in ontogenetic processes, and this modern understanding is among main general achievements of the evolutionary developmental biology (e.g., Gilbert et al., 1996; Hall, 1999, 2011): "The real Phylogeny of Metazoa has never been direct succession of adult forms, but a *succession of ontogenies or life-cycles* [thus include *both adult and larval* periods of ontogeny]" and, the most importantly, "*Ontogeny does not recapitulate phylogeny: it creates it.*" (Garstang, 1922, p. 82, our italics). Therefore, a further generalization is that the direction of character changes is from ontogeny to evolution, and this has a key meaning for the taxonomy and the entire enormous biodiversity field, since ontogenetic modifications is the basis of the diversity of all organisms (Martynov, 2012a). Without ontogeny and its modifications evolution could not proceed.

Despite this, the incorporation of the ontogeny in the modern taxonomy and biology is only superficial. It is widely acknowledged that there is a modern field of the evolutionary developmental biology ("evo-devo") in which an apparently exhaustive consideration of the ontogeny has been performed. But in reality, the situation is completely vice versa. There are exceedingly few publications that in some degree discuss biological systematics (taxonomy) and "evo-devo" (e.g., Hawkins, 2002; Minelli, 2007, 2015a,b), and this does not promote the real importance of the ontogeny for taxonomy as a central biological phenomenon. The clearest indication for this, is that while some apparently new terms have been proposed, for instance "phylo-evo-devo" (Minelli, 2009) or "morpho-evo-devo" (Wanninger, 2015), quite contrary these concepts basically rely on the persisting *centrality of phylogeny*, not on the ontogeny or morphology, *per se* (see for example the notable comment in Neumann et al., 2021). Compared to the modern time, Haeckel recognized the importance of *systematics* in the ontogenetic sense: "...die Systematik' erklärt sich dann einfach aus dem Umstände, dass die individuelle Entwickelungsgeschichte oder die Ontogenie nur eine kurze und gedrungene Wiederholung, gleichsam eine Recapitulation der paläontologischen Entwickelungsgeschichte oder der Phylogenie ist." = "...systematics' explained then simply from the fact that the individual evolutionary history or ontogeny is only a short and concise repetition, as it were a recapitulation of the paleontological evolutionary history or phylogeny." (Haeckel, 1866, II, p. XVIII).

However, in a strong contradiction with the lines above, the fundamental modern neglect of the ontogeny is rooted in the basic works of the major founders of the phylogenetic and ontogenetic thinking in the modern biology: Haeckel (1866), Garstang (1922), and Hennig (1966) as well. Although Haeckel (1866) laid foundation of the evolutionary understanding of ontogeny, his famous aphorism that "ontogeny recapitulates phylogeny" obscured the fact that ontogeny does not mechanistically accumulate evolutionary changes but instead *produces* them (**Figure 1**). In a support of this initial Haeckel's contrasting terms separated ontogeny from phylogeny is the fact that Haeckel equals ontogeny with merely embryology, whereas phylogeny...with paleontology (!): "...dass wir den Begriff der Embryologie (Ontogenie) und der Palaeontologie (Phylogenie) nach Umfang und Inhalt scharf bestimmen." = "...that we define the concept of *embryology (ontogeny)* and *paleontology (phylogeny)* sharply according to scope and content" (Haeckel, 1866, I, p. 53, our italics). Remarkably, this was performed by Haeckel with a very positive intention: to instead make closer exactly ontogeny and phylogeny, "According to the usual biological point of view, however, embryology and paleontology

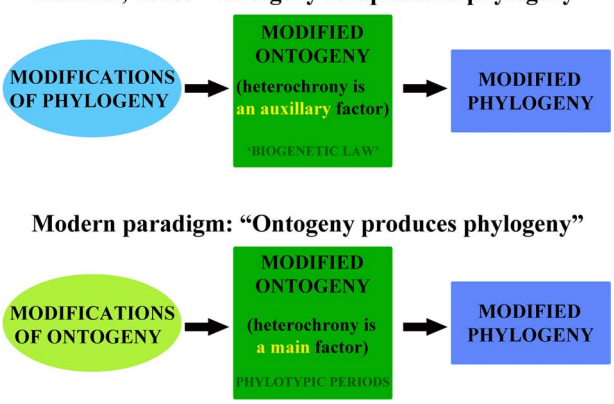

FIGURE 1 | The scheme illustrates changes in the understanding of the "ontogeny and phylogeny" conceptual framework compared with Haeckel's (1866) and modern paradigm since Garstang (1922) seminal work.

are completely diverse and distant branches of biology, which have nothing in common with one another but the object of the organism" (Haeckel, 1866, I, p. 53). However, more than 150 years after Haeckel's fundamental insight, the "usual biological point of view" have persisted perfectly, at the level of the scientific publications, educational programs and as "a common comprehension," represented for example in Wikipedia: "*Ontogeny is the developmental history of an organism within its own lifetime, as distinct from phylogeny, which refers to the evolutionary history of a species*" (Ontogeny, 2022, Wikipedia, our italics), despite all achievements of the evo-devo! This is not the result which Haeckel would have expected from his scientific descendants. The words and scientific terms are crucial not only for thinking and communication, but also for the proper development of the key scientific fields, such as evolutionary one. The persisting and very strict *pre*-Haeckelian sharp contrast between "ontogeny and phylogeny" has strongly postponed real development of the entire evolutionary field. Without new terminological (re)formulation furthers steps forward in that ontogenetic and evolutionary field, so strongly perplexed and confused over centuries, will be impossible.

This statement has implications to a much larger extent than currently recognized. Despite that Garstang (1922) subsequently clearly indicated that fundamental deficiency of the Haeckel's understanding of the ontogeny, in the modern general biological framework, the "ontogeny" and "phylogeny" are usually sufficiently contrasted. This is easy to prove that in majority of the molecular phylogenetic studies, including such crucial as phyla interrelations, ontogeny (or at least a "development") usually either not mentioned, or if mentioned, but only as a highly subsidiary evidence (e.g., Laumer et al., 2019). The major approach of the phylogenetic inference is a suite of statistical methods based exclusively on the DNA sequences (e.g., Yang, 2014), which cannot be equated with the ontogeny as entire life cycle in all its complexity. The best balanced of the recent studies, which consider the development still make a major focus on the disparity along the clade evolution, than on a common shared ontogenetic patterns among different at adult stages phylum subgroups (Deline et al., 2020). Hennig (1966), despite that discussed ontogeny, concentrated on the *phylogenetic* aspects from the "ontogeny and phylogeny" pair, and by this, made a significant contribution to the modern persisting theoretical and practical fundamental omission of the ontogeny as a central process, which produced biodiversity.

However, each individual ontogeny is not only a product of the genetic mutations and selection that apparently allow that very formal scheme in Hennig (1966), but interlinks ancestral and descendant ontogenies through epigenetic and other developmental processes (e.g., Danchin et al., 2019; Anastasiadi et al., 2021; Loison, 2021; Yi and Goodisman, 2021; Lemmen et al., 2022). Therefore, the current unprecedented rise of the epigenetic data provides not only strict evidence for the reality of "every day"- ontogenetic modifications, but also some indulgence for a straightforward refusement by Garstang (1922) of the Haeckel's initial paradigm! Although this is by no means reverse the correct Garstang (1922) conclusion on the major Haeckel's misconception, that the phylogeny is not only a succession of adults, but alterations of the ontogenetic cycles, in which ontogeny plays the role of a central process. The profound linkage between adult and embryonic/larval parts of an ontogenetic cycles can, however, partly reconcile both Haeckel's initial variant and Garstang's reformulation. This is because since the time of Garstang the epigenetic influence of the adult modifications on the gametes has been confirmed (e.g., Anastasiadi et al., 2021). It was also noted that Haeckel adherence with phylogeny and consideration of ontogeny as a dependent process was result of an incorrect formulation, rather than Haeckel's misunderstanding of the real ontogenetic data (Ezhikov, 1940). Furthermore, and even more paradoxically, Garstang (1922, p. 100, our italics) in turn made too much stress on the disproving of the Haeckel's "biogenetic law": "Inevitably there is recapitulation of successive grades of differentiation, *but repetition of adult ancestral stages* is necessarily and *entirely lacking*." While Haeckel's motto "ontogeny recapitulates phylogeny" masked the fundamental fact that phylogeny is not a separate process, but modification of ontogenetic cycles throughout time, however, Garstang's definition in turn strongly disrupted the phylogenetic succession of the modified ontogenies, and by refusing of the importance of the linkage between adult and embryonic/larval stages, actually partly returned the ontogeny field to the antievolutionary "types concept" by von Baer (1828/1837). Therefore, in order to formulate true modern paradigm, both Haeckel's original and Garstang's subsequent formulations, need to be refined and reunited (**Figure 1**).

In a great concordance with the main line of the present work, it has been highlighted recently that ontogeny and phylogeny must be considered as a single process—"ontophylogenesis" (Kupiec, 2009)—and this is in turn remarkably mirrored not only the "phylembryogenesis" concept developed more than a century ago using a different argumentation (although still on the ontogeny-based background, Severtsov, 1912), but immediately recalled the basically unsuccessful, although heroic attempt by Haeckel (1866) to make "ontogeny" and "phylogeny" closer. The Severtsov concept, however, during less a century of its further development by its successors, turned to be not a modern reformulation of the Haeckel's heritage, but became a new dogma, when within the complex and dynamic ontogeny, only three major modes that affects evolutionary modifications have been recognized: "anaboly, deviation and arhallaxis" (e.g., Severtsov, 1939; Ivanova-Kazas, 1995, 2004; see also discussion in Martynov, 2012a), which insufficiency has been already recognized, and limited "phylembryogenesis" was proposed to be substituted exactly with "phylontogenesis" (Vorobyeva, 1991, p. 73). This rigid "three-part" ontogenetic scheme significantly underestimated the real diversity of the ontogenies and phylogenetic results of its modification, and most importantly, did not help to overcome the persisting modern, strong contrasting of "ontogeny and phylogeny." Obviously, on the immediate contrary to Severtsov (1912, 1939) assert that Haeckel biogenetic law is putatively justified only when ontogeny modified through "an extension of development, anaboly" is based on fundamental underestimation that a descendant

ontogeny can be completely free from any ancestral ontogenetic patterns (either adult or larval), which is contradicted by all that is known about real ontogenies (e.g., Martynov and Korshunova, 2015; Korshunova et al., 2020; present work, **Figure 2**).

In parallel with the Kupiec's (2009) remarkable implication that ontogeny and phylogeny represent in reality the same process, it was unequivocally and independently concluded on the paedomorphosis as a process *linking individual and historical development* (Martynov, 2012a, p. 839). In this respect it is most importantly, that every individual ontogeny incorporates phylotypic periods, which have originated and persisted over a large evolutionary range (Arthur, 2002; Irie and Kuratani, 2011; Martynov, 2014; Martynov and Korshunova, 2015), and therefore ontogeny cannot be easily separated from the "phylogeny," that was omitted by both Haeckel (1866) and Hennig (1966). However, Garstang (1922) in turn critically omitted the partial perseverance of the adult ancestral organization in form of the Haeckel's "recapitulations," and which have been later reformulated as phylotypic stage (Slack et al., 1993) or phylotypic periods (Richardson, 1995, 1999; Arthur, 2002, 2015). This is therefore, although at first glance very surprising, but consistent with these founders of the phylogenetic thinking in biology, when even the core achievement of the "evo-devo," phylotypic periods, has been disregarded using precisely *phylogenetic logic* (Hejnol and Dunn, 2016).

Thus, the current situation is truly a most paradoxical one. Everybody understands the importance of ontogeny. This is an open secret at least since Garstang (1922) that the initial Haeckel's definition of the relation between ontogeny and phylogeny contains a fundamental deficiency. However, the evidence for the phylotypic periods as a key concept of the "evo-devo" (Arthur, 2002; Cridge et al., 2019) and can be considered as partial modern reformulation of the "biogenetic law" (Levit et al., 2022) is almost negligible in the vast "phylogenetic" discipline. There also is an impressive number of the references which since 1866 attempted to discuss the "ontogeny and phylogeny" field under various names and using different aspects (Gould, 1977), or in some way criticize or reformulate Haeckel's "biogenetic law" and concepts of the Haeckel's immediate predecessor Müller (1864), and the citations provided here do not pretend to be exhaustive, but to show some punctuated time line (e.g., Gegenbaur, 1888; Hurst, 1893; Bateson, 1894; Sedgwick, 1894; Mehnert, 1897; Keibel, 1898; Morgan, 1908; Smith, 1911; Severtsov, 1912, 1939; Garstang, 1922; de Beer, 1930, 1958; Needham, 1933; Kryzhanovsky, 1939; Schmalhausen, 1942; Ivanov, 1945; Bonner, 1965; Emelyanov, 1968; Mirzoyan, 1974; Gould, 1977; Alberch et al., 1979; Peters, 1980; Raff and Kaufman, 1983; Kluge and Strauss, 1985; McNamara, 1986; McKinney, 1988; Vorobyeva, 1991; Ivanova-Kazas, 1995; Gilbert et al., 1996; Müller, 1997; Bininda-Emonds et al., 2002; Hall, 2003, 2011; Belousov, 2005; Wiens et al., 2005; Minelli, 2007, 2009, 2015a,b; Kupiec, 2009; Martynov, 2009, 2011a,b, 2012a; Wanninger, 2015; Lamsdell, 2020; Martynov et al., 2020; Núñez-León et al., 2021; Levit et al., 2022; Richardson, 2022; Uesaka et al., 2022; and many others). However, despite on all these tremendous efforts, by year 2022, *ontogeny remains to be a subsidiary discipline of the broadly phylogenetic studies*. The original Haeckel's definition, Garstang's reformulation and the apparently modern phylotypic periods concept existed largely separate from each other, despite they are all must be inevitably intersected. Thus, before ontogeny will be a real basis for any biological discipline including taxonomy (and hence a fundamental to immense biodiversity patterns and studies), exactly theoretical basis of the "ontogeny and phylogeny" field must be (one more time) revised. This is a key starting point that can further help to merge the achievements of the evolutionary developmental biology with the true keeper of the worldwide biodiversity—systematics and taxonomy.

Because the ontogenetic field and related evolutionary problems is immense, in the present work we cannot address all arisen questions, but we instead will focus on the clarification of some core concepts which are related to the field of "ontogeny and evolution" and present perspective for the further development of the emerging interdisciplinary field of *ontogenetic systematics* with an emphasis to the paedomorphosis process linked to the ancestral organization *via* phylotypic periods.

TERMINOLOGICAL CLARIFICATION

Ontogeny, Evolution, and Phylogeny

Ontogeny must not be restricted to a developmental stage or a metamorphosis, but it should be explicitly stated that ontogeny is an entire life cycle in all its evolutionary dynamics. The term "evolution" (and therefore, phylogeny) is unfortunately loosely connected with the term "ontogeny," and the fact that ontogeny is meaningless without invoking ontogeny which produces phylogeny (**Figure 1**) and it is notable that the original meaning of the term "evolution" was "ontogeny" (Bowler, 1975). Any ontogenetic patterns and processes, among them such central as phylotypic periods and heterochronies, are therefore not solely specific terms of the "evo-devo" field but have direct importance for the origin of the biological diversity and hence is of paramount importance for the biological taxonomy. For example, in a conditional evolutionary-free framework and without consideration of ontogeny as entire life cycle, the juvenile and adult stages can be putatively considered as separate sets of data (**Figure 2**, red arrows). However, for instance, *juveniles* of dorid nudibranchs represent from one hand the key features of the pleurobranchid ancestral organization (joined rhinophores and ventral anal opening) and form respective phylotypic periods (**Figure 2**, dark green box). From the other hand, *adult* dorid family Corambidae also possess ventral anal opening and gills due to the process of paedomorphosis, which secondarily returns the phylotypic patterns to the adult stages (**Figure 2**, light green arrow). By these and more examples (**Figures 3–5**) it became obvious that modifications of ontogeny is a basis for appearing of the biological diversity and that a "phylogenetic" study cannot be performed without consistent incorporation of ontogeny. This is therefore not a surprise that very significant efforts have been done by antievolutionists in attempts to of course unsuccessfully disprove the real existence of the Haeckel's recapitulations (see e.g., Richards, 2009), which are currently can be partly reformulated as phylotypic periods. This is because

exactly phylotypic periods provide *direct evidence* of the reality of *evolution*. Modern strict phylogenetists must therefore not attempt to disprove (e.g., Hejnol and Dunn, 2016) the reality of the universal conserved periods in ontogeny of the very different at adult stage organisms (**Figures 2–4**), but instead highly praise this essential for the understanding of evolution and *phylogeny* phenomenon.

Phylotypic Periods, Recapitulations, and Biogenetic Law

The concept of phylotypic period implies the presence of similar, homologous and conservative periods of ontogeny shared by various groups with disparate adult morphology (e.g., Arthur, 2002; Martynov and Korshunova, 2015; Cridge et al., 2019; **Figure 2**). Phylotypic periods and their underlying transcriptomic activity have been documented in disparate metazoan phyla (e.g., Domazet-Lošo and Tautz, 2010; Kalinka et al., 2010; Ninova et al., 2014). The term phylotypic period (sometimes as denounced as a phylotypic stage) largely substituted the term recapitulation (Slack et al., 1993; Richardson, 1995), but this was rather terminological than a biologically founded proposal. Ontogeny, in many cases, preserves major features of an ancestral ontogenetic cycle (which thus can be directly partly observable in form of the phylotypic periods), but not an entire sequence of evolutionary alterations. This is very important to note, that phylotypic periods from one hand do not preserve entire ancestral evolutionary sequence and cannot be considered as completely "uniform" across major subtaxa of a given higher taxonomic group, e.g., vertebrates (Richardson et al., 1997), but this should be not used as a substantiation against its fundamental importance for the inferring of phylogenetic patterns (Richards, 2009; Arthur, 2015). From the other hand, the phylotypic period should be not restricted only to a search for a "single" hourglass-like pattern within an ontogeny that is commonly performed in the "evo-devo" field. Any ontogeny obviously preserve *several layers* of the ontogeny of ancestors, and therefore several phylotypic periods can be potentially recognized within a given ontogeny of a given group, and every phylotypic periods can potentially roughly corresponds

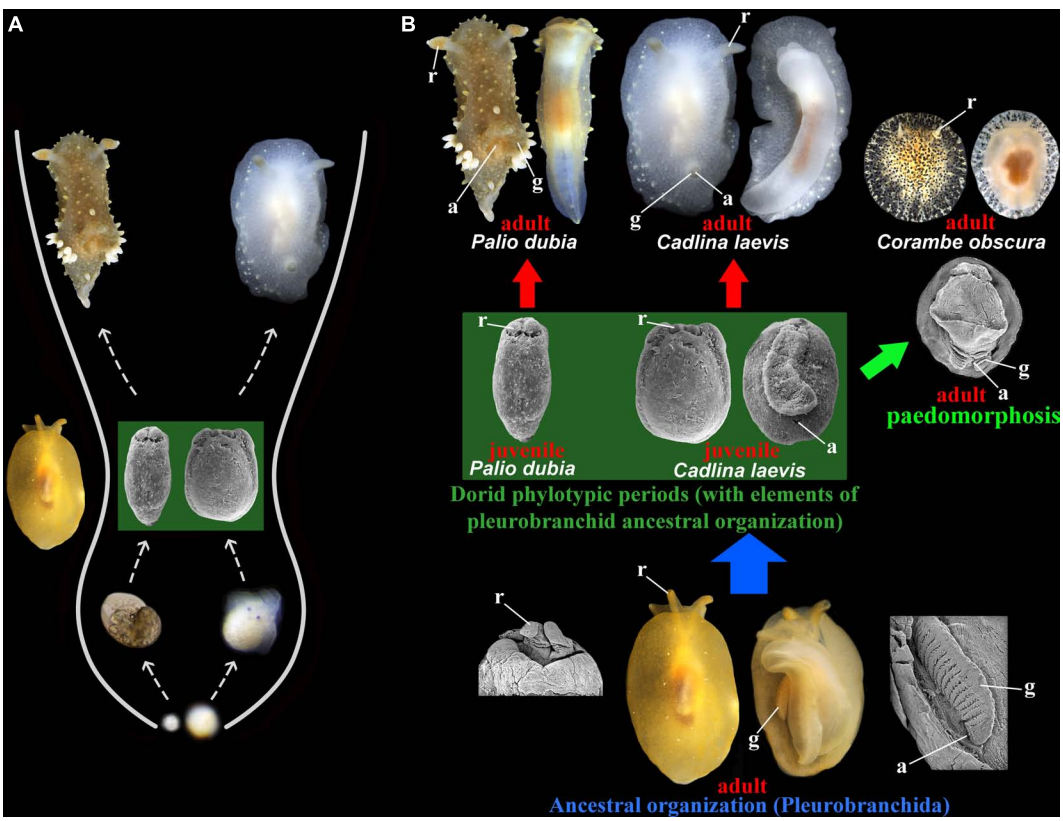

FIGURE 2 | (A) The presentation of phylotypic periods (dark green box) in the disparate at adult phases dorid nudibranch families Polyceridae (represented by *Palio dubia*) and Cadlinidae (represented by *Cadlina laevis*) showing essentially similar to the classic vertebrate phylotypic period an irregular hourglass-like earlier ontogenetic patterns. **(B)** Adult morphological disparity (red arrows) and juvenile conservativeness of the dorid nudibranchs manifesting in the phylotypic periods (dark green box). The dorid phylotypic periods keeps several essential features of the adult pleurobranchid organization (joined rhinophores, ventral anus), which is ancestral for dorids. Thus, evolutionary modifications (blue arrow) of the adult pleurobranchid ontogenetic periods into dorid descendant organization partly remains as some key features in the early ontogenetic dorid phylotypic periods. See Korshunova et al. (2020) for molecular phylogenetic data. Dorid paedomorphic taxa (e.g., *Corambe obscura*, light green arrow) reveal some key features (including ventral anal opening and gills) which link both adult ancestral organization of pleurobranchids and phylotypic periods of majority of non-paedomorphic dorids. a, anal opening, g, gills, r, rhinophores.

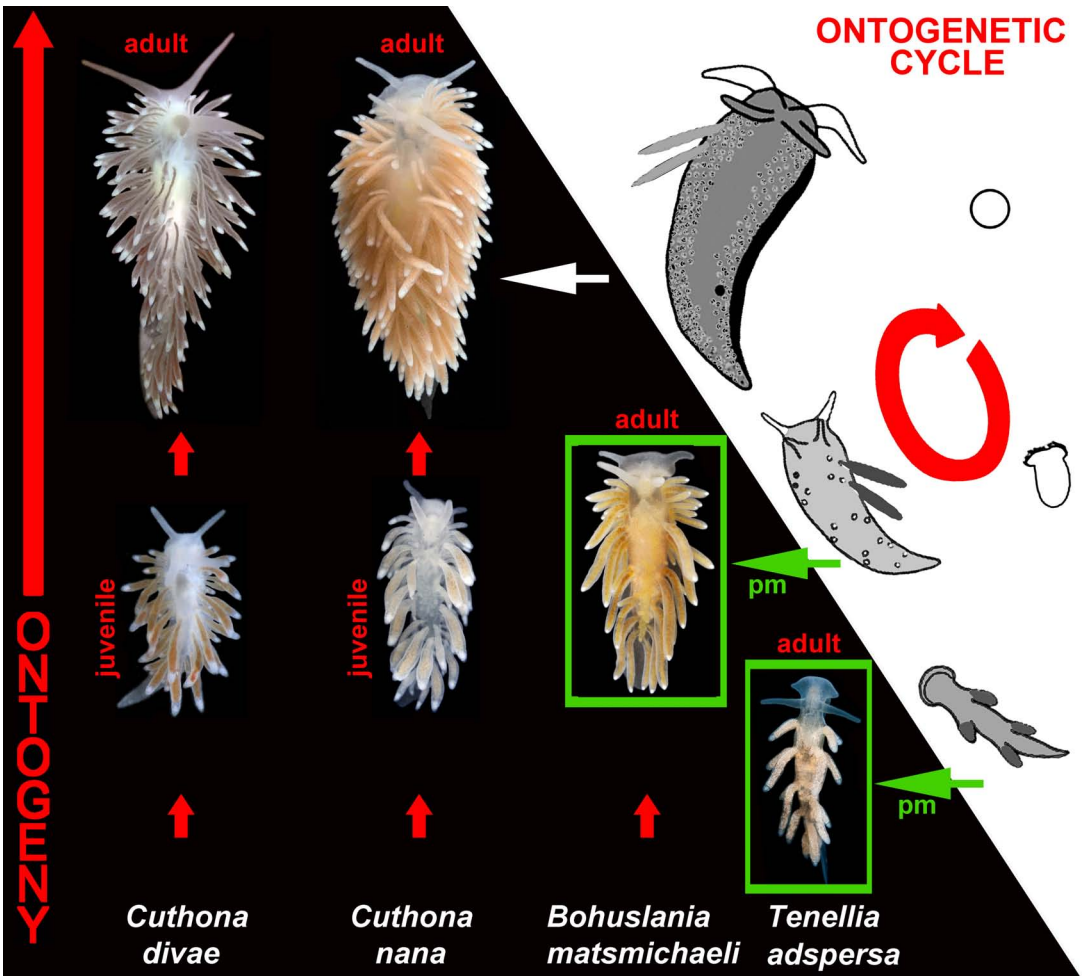

FIGURE 3 | Ontogenetic-and-evolutionary linkage through the modifications of the ontogenetic cycles of aeolidacean nudibranchs. Note significant similarity between aeolidacean ontogenetic periods (hence, phylotypic periods) and adult organization of particular paedomorphic (pm) aeolidacean taxa (e.g., *Bohuslania* and *Tenellia*, green boxes). See Korshunova et al. (2018) and Martynov et al. (2020) for molecular phylogenetic data.

not to single, but several "higher taxa" of traditional taxonomic hierarchy (Martynov and Korshunova, 2015; present work). This novel approach to recognize several phylotypic periods within a given ontogeny is also highlighted here (**Figures 2–4**).

A very relevant example of the phylotypic periods is dorid nudibranchs, when at early juvenile periods phylogenetically distant and morphologically disparate taxa, such as *Cadlina* and *Palio* from different families, see details and molecular phylogeny in Korshunova et al. (2020), show significantly similar morphologies, of course not absolutely identical (**Figure 2**), exactly as phylotypic periods of birds, although essentially similar to that of mammals are different in some details (Cridge et al., 2019). Such a strong adult divergence and juvenile fundamental similarity essentially conforms to the classic examples of the phylotypic periods in vertebrates (Haeckel, 1866; Slack et al., 1993; Arthur, 2002) and imply direct contributions for the origin of the taxonomic diversity. This is also very important example to show tight linkage between ontogeny and evolution: on the **Figure 2** we show that ancestral organization of the order Pleurobranchida (proved also using the molecular phylogenetics, see e.g., Pabst and Kocot, 2018) while modified into disparate dorid descendent organization (**Figure 2**, blue arrow), however, preserved at the juvenile phylotypic periods some elements of the adult pleurobranchid ancestors, including such key patterns as joined rhinophores and ventral anal opening (**Figure 2**, dark green box).

This example is very important because demonstrates ontogenetic patterns principally similar to the classic vertebrate "regular or irregular" hourglass-like phylotypic patterns (Cordero et al., 2020) in a completely different animal phylum, Mollusca (**Figures 2**, **3**), as well as within Echinodermata phylum (**Figure 4**). This also well demonstrates that evolution and resulting phylogeny is not a some theoretical process that needs to be specially proved, but that *elements of adult* organization of remote ancestors is still integral part of ontogenies of the modern, really existed descendants, and this pattern of the partial preservation of the ancestral morphologies in form of the respective phylotypic periods can be revealed among

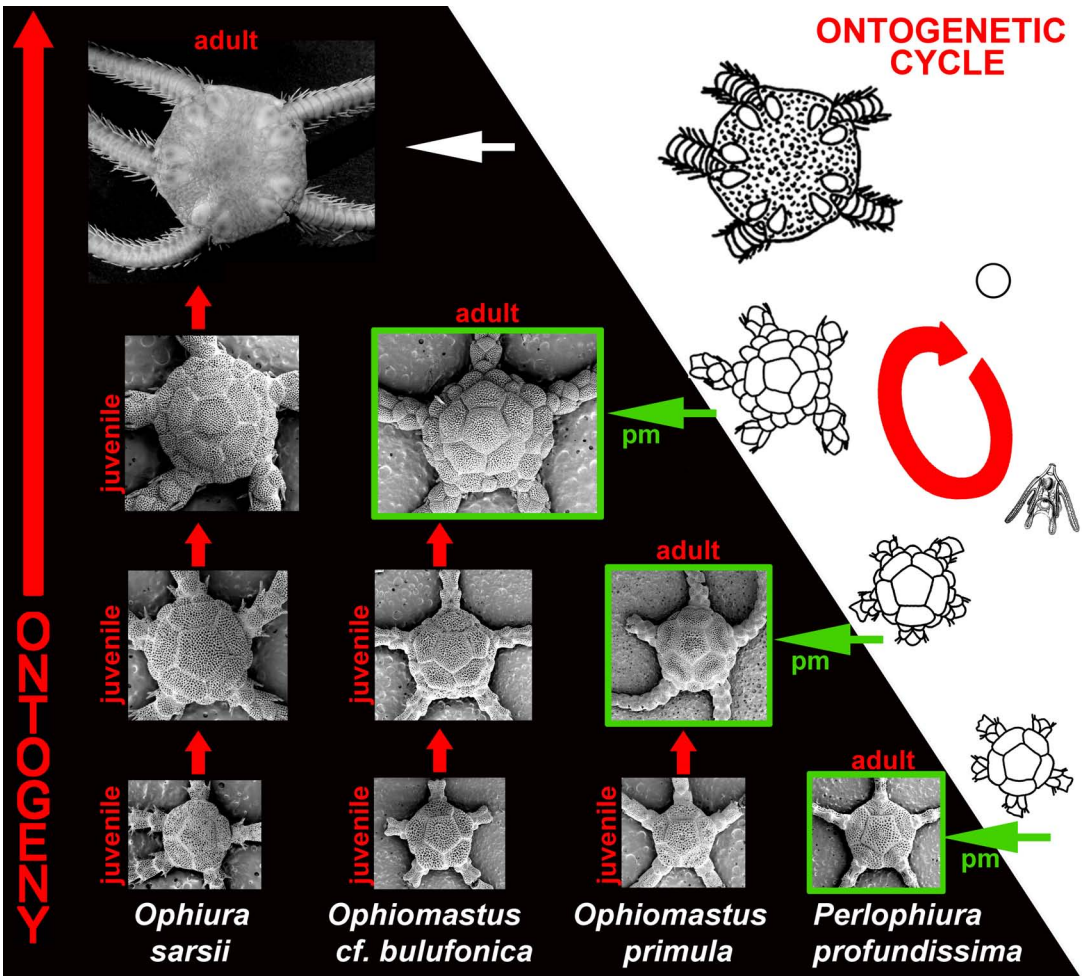

FIGURE 4 | Ontogenetic-and-evolutionary linkage through the modifications of the ontogenetic cycles of ophiuroid echinoderms. Note significant similarity between ophiuroid ontogenetic periods (hence, phylotypic periods) and adult organization of particular paedomorphic (pm) ophiuroid taxa (e.g., *Ophiomastus* and *Perlophiura*, green boxes).

representatives of such disparate phyla as molluscs (**Figure 2**) or chordates (e.g., Arthur, 2015). This naturally existed and proved here to be universal ontogenetic preservation of the elements of adult ancestral morphologies (with respective molecular ground, e.g., specific transcriptomic activity) between very different animal phyla (**Figures 2–5**) was critically omitted by Garstang (1922) in his reformulation of the Haeckel's "biogenetic law." It is also possible to recognize several ancestral layers within dorid ontogenies, which represent several phylotypic periods corresponded to the several modifications of ancestral organizations and have been named separately, e.g., as phylotypic periods dp1 and dp2 (see Martynov and Korshunova, 2015). Also, in a remarkable coincidence with partially- or irregularly resembling the famous "hourglass" ontogenetic pattern (with all possible reservations, see Arthur, 2015), because early larval modifications (e.g., planctonic larva in dorid *Palio* and direct-developed larva in dorid *Cadlina*, **Figure 2**) apparently more different than subsequent "middle" phylotypic stage dp. 1 (**Figure 2**). Therefore, Haeckel's recapitulations are partly compatible with the both "funnel model" and the hourglass model, the latter dominating in today's evo-devo. However, as an important comment to this, it is needed to highlight, that despite on the differences, the larval earliest ontogenetic periods in the adult shell-less *Palio* and *Cadlina* are still can be considered as phylotypic periods common with the predominantly shelled molluscan class Gastropoda since both *Palio* and *Cadlina* bear essentially the same veliger-like structures, although highly reduced in the direct developer *Cadlina* (**Figure 2**). Therefore, the "evo-devo" hourglass concept should not disrupt and mask the key ontogenetic consideration, that even within strong "larval adaptations" obvious remnants of the shelled gastropod ancestral organization can be recognized and traced within shell-less at adult stage nudibranchs. By this, it is also relevant to make a special reservation, that although all evidences, including molecular data should be used to confirm evolutionary models and ancestral patterns, we refer to the "molecular phylogenetic data" as a proof not because we cannot provide evidence using ontogenetic data, but because of the obvious dominance of

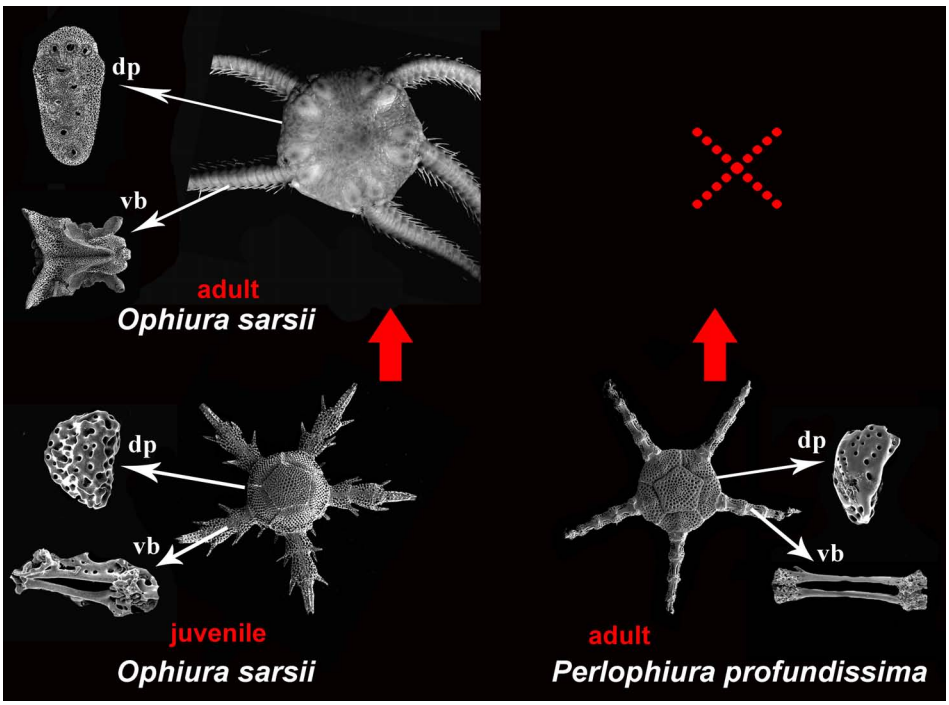

FIGURE 5 | Evidence for essential, unique similarity between respective homologous ophiuroid characters, including external primary disk plates and internal ossicles (dp, dental plate; vb, vertebrae) of the adult strongly paedomorphic ophiuroid *Perlophiura profundissima* and phylotypic periods of early juveniles (postlarvae) of the complex non-paedomorphic ophiuroid *Ophiura sarsii*. The considerable reducing of the paedomorphic life cycle, which lacking complex adult stage is indicated by dashed red cross. By this unique similarity between adult paedomorphic taxa and juveniles of the complex taxa makes almost direct ontogenetic-and-evolutionary linkage as impossible to deny.

the "phylogenetic thinking" over ontogenetic one, the theory and practice of the ontogenetic systematics were largely not developed. It is now time to explicitly start and reintroduce that "new old" discipline, which consistently encompassed and re-untied "ontogeny and phylogeny" immense field.

It is also necessary to highlight, that manifestation in the ontogeny of descendants only partial, but still key characters of the adult ancestors (e.g., **Figure 2**) do not disprove recapitulations. Therefore, the past sometimes very harsh and unsubstantiated critic on the entire Haeckel's fundamental works (e.g., Borzenkov, 1884, p. 130–135) and currently persisted common view that *biogenetic law* (which is based on the partial recapitulation in ontogeny of descendants of an ancestral organization) has been completely abandoned (e.g., Raff and Kaufman, 1983, p. 19) are in reality profoundly incorrect and does not correspond to the real ontogenetic patterns. Recapitulation in the renewed sense should be understood not as "recapitulation of phylogeny" in strict Haeckel's sense, but as *partial recapitulation of* ***ontogeny*** *of ancestors.* This reformulation is important challenge for the contemporary biology since directly influences understanding of the key role of phylotypic periods for the fields of taxonomy and phylogeny. The fact that modern ontogeneses preserve in the phylotypic periods some key features of adult ancestral organization of remote ancestors (for example pharyngeal clefts (arches) in terrestrial mammals) is significantly undervalued by modern evolutionary biologists (e.g., Futuyma and Kirkpatrick, 2017, p. 371), despite clear evidence from the evolutionary developmental biology in presence of various conserved periods (e.g., Irie and Kuratani, 2011; Cridge et al., 2019; Cordero et al., 2020; Hao et al., 2021; Liu et al., 2021; Levit et al., 2022; Uesaka et al., 2022). Therefore, typical modern understanding (e.g., Barnes, 2014) that Haeckel's core contributions as largely wrong due to the putative failure of the concepts of recapitulations and biogenetic law is in fact fundamentally incorrect and must be no more continue to be mentioned as "wrong" in numerous educational as well as targeted for broad audience sources. We must praise Haeckel for the first consistent application of the evolutionary idea to the ontogeny (e.g., Levit and Hossfeld, 2019), even with respective reformulation of the Haeckel's key concepts. Especially dangerous sometimes continuing association of Haeckel with the Nazis regime, even in a softened form (e.g., review in Rieppel, 2016), because Haeckel died more than 10 years before that regime has been established, and although Haeckel has made controversial statements of the role of artificial selection in the human society, the potential subsequent malicious usage of his heritage by Nazis by no means should be considered as his guilt. In this respect, Rieppel (2016, p. 78, 79) specially highlighted that "In his own time, at any rate, Haeckel had defend himself not as protagonist of right-wing politics or fascism, but instead of socialism and academic liberalism," and remarkably, "believe that continuing evolution of the human brain would one time render

armed conflicts a thing of the past" (!). Thus, whatever of the Haeckel's controversies, more than one century later, by the end of February of 2022 we must only conclude that sadly, Haeckel's desperate call has not been yet implemented by the politicians and the human society.

The tight practical linkage between ontogeny and evolution (instead of the contrasting notion of "ontogeny and phylogeny") is further reinforced by the widespread phenomenon of paedomorphosis. Paedomorphosis in turn almost directly links juvenile ancestral organization (which is partially kept in ontogeneses in form of phylotypic periods, **Figure 2**, dark green box) with actual existing adult stages of modern descendants (**Figure 2**, light green arrow), although it was attempted to deny this (e.g., Mayr, 1963), and with the reinforcement of the solely "phylogeny-part" from the undividable pair of the ontogeny and phylogeny, this "phylogenetic denying" of reality of the universal ontogenetic patterns across distantly related taxa is continuing (e.g., Hejnol and Dunn, 2016). Here, we will present several striking examples of the reality of ontogenetic linkage (see also Martynov et al., 2020) between ancestral juvenile (but at a preceding ancestral level, still representing past *adult* organization) and descendant adult characters among taxa of very disparate phyla such as molluscs and echinoderms (**Figures 2–5**).

Phyla Are Real in the Sense of Natural Ontogenetic Properties

Originally, we did not plan to specially emphasize this point, because it is apparently an obvious one. However, a kind comment of one of the reviewers point that situation with the neglecting of the ontogeny in biology (not speaking of taxonomy) is so serious, so we need to specially emphasize this question there. Thus, we find that the phyla can be considered as "not real ones" (with all reservations to the word "real" in a taxonomic context), and at best can be comprehended as a collection of an endless number of phylogenetic clades, those, and not the phyla itself must be a central focus of evolutionary study (e.g., Hejnol and Dunn, 2016). Because in the latter paper even most serious, *naturally* ontogenetic evidence of the real existence of the ontogenetic phylotypic periods across at adult stages dramatically different taxa (Levin et al., 2016), has received a severe critic from the "phylogeny-centered" colleagues, it will be not very convincing to provide just logical or theoretical arguments in support of the existence of the universal ontogenetic patterns. Instead, we will provide here a very simple and a very practical test. Given a marine location, where we have performed some sampling. In the obtaining samples we may find at a first glance, an endless diversity of invertebrate animals. However, such diversity is endless only putatively. Almost 300 years of long and controversial development of the systematic zoology starting from just a structural comparison (still within a non-evolutionary thinking), through acceptance of the evolution and following by the phylogeny-based boom, do not only disprove, but instead strongly strengthened an obvious and natural fact: in any sample obtaining at any depth and at any environment we will be not able to find more than 40 major structural multicellular animal-related organizations, which the systematic zoology assessed as animal phyla, i.e., any endless number of individuals and subgroups will be encompassed by just less than forty major structural plans (with only minor disagreement since some of the phyla can be treated as subphyla/other subgroups). This is a remarkable scientific achievement that judge from the comments from the phylogeny field (e.g., Hejnol and Dunn, 2016) either do not acknowledge at all, or misleadingly interpreted.

The next test, that even if we have a strong intention, this will be highly unlikely that someone will easily describe *a completely new phylum*. A description of a new phylum is a rare, exceptional, and obviously not a routine event. Furthermore, even the most recent phylogenies confirmed validity of absolute majority of the animal phyla (e.g., Laumer et al., 2019), and the main alterations rather concern mostly the status of annelid-related phyla (subgroups). Therefore, someone may wish to find more or deny the existence of the very limited number of the basic animal organizations, when you will come across with a real sample from a real environment, it will be an exceedingly rare and lucky chance that you will be able to detect some completely new organization, beyond that less than 40 main animal structural organizations (even it is still possible to somewhat extend or reduce in number). Notably, there is a recent proposal from the "evo-devo" to consider vertebrates as a separate phylum (Irie et al., 2018). However, again, even with possible somewhat extension of the main structural organizations, they will be still very limited in number, and the "phylum-hypothesis" continues to be confirmed on daily basis by practicing biologists. We specially avoid here the term "body-plan" in order not to be aligned with the pre-evolutionary thinking, but for the majority of phyla, even despite on the subgroup diversity and reduction it is possible to provide a diagnosis that will contain a specific for every phylum set of the adult and juvenile (larval) characters.

Which the most important facts evolutionary developmental biology has added to this well established and obviously natural structural pattern of the highest conservatism discovered by the systematic zoology and largely supported by the molecular phylogenetics? Evolutionary developmental biology has concluded that even in the highly disparate at adult stages representatives of an animal phylum, there are some ontogenetic stage(s) of highly conserved period(s), which even with all reservations and subgroups diversity (e.g., Richardson et al., 1997, Richardson, 2022; Richards, 2009; Arthur, 2015; Levin et al., 2016; Deline et al., 2020) are persisted in their inter-taxon conservatism. For every extant phyla, despite on all the class diversity and reductions it is possible to provide a particular, unique enough set of adult and larval patterns, both according to the classic "structural" approach with some evolutionary ground (e.g., Brusca and Brusca, 1990) or framed in apparently very strict "modern phylogenetic framework" (e.g., Schierwater and DeSalle, 2021).

The latter book is especially relevant for the main topic of the present contribution. It is titled as "Invertebrate Zoology: A Tree of Life Approach," despite that in an abstract it is described as "Synthesizing …. classical morphology, sequencing data, and evo-devo studies"! This is a best proof that even if ontogeny in some way is included into modern studies and reviews, it is an important but still an "add-one" to the phylogeny. Therefore, it is absolutely justified to conclude that there is no "ontogeny" as a primary discipline compared to the resulting process of phylogeny in the contemporary biology. The continuous urgent call for the necessity of the independent, primary discipline of the ontogenetic systematics is therefore fully justified.

Thus, the concept of the phylotypic periods ("stages") instead of being falsely alleged to be an "idealistic discipline," at a new level synthesizes the achievements of the systematic zoology exactly in the evolutionary sense. The newest data in support of the real existence of the phylotypic periods in the ontogeny of such fundamentally different divisions of organisms as animals and plants are continued to be available (e.g., Liu et al., 2021). If we will discard phylotypic periods from the core concept of the evolutionary developmental biology, then the entire field of the "evo-devo" must be discarded, because otherwise "evo-devo" is just a supplementary to a phylogenetic analysis, which will be always primary to the ontogeny. Indeed, a lot of efforts still need to be done in the recognition of the shared phylotypic periods at many different levels of ontogeny across majority of the animal and plant phyla (divisions), but this do not mean that if we do not have a clearly recognized phylotypic periods for all phyla and for many subgroups, we should refuse this key ontogenetic and evolutionary approach. The inclusion of paleontological data is special challenge, but as we already mentioned above, in every phylogeny there are not just "single phylotypic period," but several layers of ancestral ontogenies (e.g., **Figures 2–4**), and therefore shared phylotypic periods can be assessed also for supraphyletic taxa, including extinct phyla and other taxonomic groups. That is why a separate field of *ontogenetic systematics* which is clearly put forward the fundamental precedence of the ontogeny for the evolution, and hence for any phylogenetic analysis is fully justified and highly necessary. The key proposal of the ontogenetic systematic is that the phylotypic periods are no more "isolate Baer's entities" but inevitably reflect *elements* of ancestral organization, and hence indispensable for the reconstruction of the ancestral organizations at *any taxonomic levels*. That can be a better involvement of truly evolutionary principles and that could be a better antidote against any antievolutionary approaches, than the very phylotypic periods approach? It is therefore really important to present why apparently profoundly evolutionary phylogeneticists deny for the ontogeny field the ability to even more clearly present an ancestral organization that it partially manifested at the phylotypic periods of ontogeny. With the only reservation perhaps that the entire ontogeny itself as entire set of several phylotypic periods. To clearly understand this, we need to more strictly outline the basic principles of the ontogenetic systematics, as we presented in this contribution, respectively.

Paedomorphosis

Paedomorphosis is a next to the phylotypic periods very important evidence for the very tight linkage between ontogeny and phylogeny, as well as between ontogeny and evolution (Martynov, 2012a). This is because while a paedomorphic organism is formed, partial structural patterns which in ancestors persist only at larval or juvenile stage, in paedomorphic adult descendants, become part of *adult* organization. Although this is partly evident, but in reality this is a highly underestimated consideration. Because in this case, a paedomorphic organism partly became… a functional, *adult* phylotypic period of ancestral ontogenies! This is not a stretch or a pure theoretical consideration. Adult paedomorphic dorids of the family Corambidae essentially similar externally to the phylotypic periods of the complex non-paedomorphic dorids (**Figure 2**), paedomorphic cuthonid aeolidacean nudibranch genus *Bohuslania* essentially similar to the juvenile phylotypic periods of the genus *Cuthona* (**Figure 3**), and strongly paedomorphic ophiuroid of the genus *Perlophiura* fundamentally similar to postlarvae of the non-paedomorphic ophiuroids both externally and internally in such degree (Martynov, 2009, 2011a,b, 2012a; Stöhr and Martynov, 2016), that can be confused with a real postlarva/earlier juvenile (**Figures 4**, **5**). This is in turn, very nicely corroborated the classic example of paedomorphosis, the axolotl and further examples of various obligate or non-obligate paedomoprhosis cases among amphibians (e.g., Wiens et al., 2005), and also partially evokes the "fish-like" ancestral organization (usually kept only as the ontogenetic phylotypic period), but at the adult stage.

In this respect, in relations to the phylotypic periods and adult and juveniles ancestral and descendant organization, paedomorphosis represent several remarkable layers of primary modifications of an adult ancestral phase into juvenile phylotypic periods of descendants, and then, a secondary partial restoration of the primary adult ancestral organization at the descendant secondary adult paedomorphic organization (**Figure 2**). These consequential and complex interactions between adult, juvenile phases in ontogeny linked by phylotypic periods is fundamentally omitted in the modern taxonomy and biology. To further complicate that picture, some ontogenetic level can be exclusively larval since the most ancestral organization, e.g., sponges-like biphasic adult-larval ontogenetic cycle persisted in the majority of the modern bilaterians, and the larval phases can be only partially involved into formation of the adult organization. Of course, since there is an almost endless number of ancestral ontogenies, the term "primary and secondary" in the given example are applying only to illustrate that general principle. Therefore, that yet unnoticed for Haeckel, and rather exotic modus of phylogeny for Hennig, paedomorphosis is a widespread and in reality the central and one of the most important evidence of the indivisible linkage between ontogeny and phylogeny. And hence paedomorphosis is among also most striking and most "self-evident" strongest evidence of the evolution.

However, currently just at a terminological level, there is incorrect usage around the term "paedomorphosis," that needs to be clarified here. Particularly, "neoteny" and "progenesis" are still sometimes used interchangeable and as plain synonyms of paedomorphosis, without reference to original meaning. This generates considerable confusion despites on previous attempts to clarify the definition (e.g., Reilly et al., 1997). Therefore, below terminological clarification is given. The term *paedomorphosis* was initially suggested (Garstang, 1928) and subsequently revised (McNamara, 1986) to encompass various phenomena of the appearance of larval/juvenile characters of ancestors at the adult stages of descendants and to highlight its role in (macro)evolution. It is needed to be noted here, as it clearly implied by the all ontogeny-centered field, the strict distinction between "micro-" and "macro"-evolution can generate significant exaggeration of putatively "separate macroevolutionary" processes instead of universal ontogeny-based evolutionary process, and this distinction must be therefore avoided. The terms "progenesis" and "neoteny" were instead originally proposed for very restricted cases without phylogenetic context. "Neoteny" was proposed by Kollman (1885, p. 391) specifically to indicate the retardation of development in a few amphibian species including the axolotl. Kollman clearly described "neoteny" as an intraspecific process, without link to evolution. However, the term "neoteny" has been incorrectly applied to describe the evolutionary process, particularly in humans (Gould, 1977), and despite on subsequent clarification (Reilly et al., 1997) still is sometimes being wrongly used in this sense (Skulachev et al., 2017). "Progenesis" was first suggested by Giard (1887, p. 23) in a highly specific sense, in reference to precocious maturation in some decapod crustaceans due to parasitic castration (!).

The term "paedomorphosis" is currently universally accepted as a higher-level term encompassing both "neoteny" and "progenesis" (McNamara, 1986; Smirnov, 1991; Martynov et al., 2020), however, especially "progenesis" is sometimes used separately and as a substitute for the term paedomorphosis (e.g., Yushin and Malakhov, 2014). This is wrong because originally the terms "progenesis" and "neoteny" lacked the key evolutionary component and were highly inconsistent with the initial and modern meanings of the term paedomorphosis. It is especially important to highlight the wrong application of "neoteny" and "progenesis" as synonyms of the entire paedomorphosis central concept, because especially in Russia there is a long tradition of the wrong substitution of the paedomorphosis with "neoteny" (e.g., Karavaev, 1934; Ivanova-Kazas, 1936).

Another crucial consideration is that "progenetic" and "neotenic" patterns are just different sides of the same paedomorphic process. In various organismal groups, often a taxon that demonstrates evident juvenile characters at the adult state is difficult to attribute exactly to "progenetic" or "neotenic" ones due to a strong heterochronic mosaicism of delayed and accelerated growth characters (Godfrey and Sutherland, 1996; Rundell and Leander, 2010; Lecointre et al., 2020). It is therefore is of key importance in assessing of the paedomorphic features not to make the strict differences between patterns and processes, between basic ontogenetic (including paedomorphosis) processes and "morphological results," otherwise the artificial substitution of "neoteny" over paedomorphosis may appear (Gould, 1977; Smirnov, 1991). Because if both retardation of the development of somatic organs or acceleration of maturation may lead to paedomorphosis (Gould, 1977, p. 8), then in the latter case a retardation of somatic development will be also required, otherwise the resulting morphology will be not paedomorphic. In this respect, it is especially relevant to indicate that the original definitions of "progenesis" and "neoteny" did not refer to the evolutionary heterochronic processes, *per se*, and did not necessarily link shifting maturation time with somatic differentiations. Therefore, the general term paedomorphosis should be used instead of controversial terms "progenesis" and "neoteny" (Reilly et al., 1997). As an important reservation it should be clearly stated, that although paedomorphosis is a very important mode of the evolution (e.g., Gould, 1977; Korshunova et al., 2018; Lamsdell, 2020; present review), this does not imply that ancestral developmental patterns are easily disappeared in a course of an evolutionary modification. Practical confirmed examples of paedomorphosis in nudibranch molluscs show that before a distinct paedomorphic organization has been formed, e.g., in the nudibranch families Corambidae or Okadaiidae (Korshunova et al., 2020), or in aeolidacean genus *Bohuslania* (Korshunova et al., 2018) a significant amount of gradual modifications of an ancestral organizations (= ancestral ontogenetic cycles) were occurred.

Paedomorphosis and Progress as Integral Parts of Heterochronies, Whereas "Peramorphosis" Is a Redundant Term

Paedomorphosis is a part of broader ontogenetic processes, heterochronies (different timing of character appearance in ontogeny) (e.g., Lamsdell, 2020; Lecointre et al., 2020). While paedomorphosis can be clearly defined in terms of correspondence of the juvenile characters of ancestors to the adult features of descendants, an "opposite term" peramorphosis has been proposed (review in McNamara, 1986) with the main meaning of "development beyond ancestral organization." Such definition may generate confusion since basically it does not differ from evolution of novelties, i.e., *progressive development* (or just *progress*) in a broader sense (see also discussion in Martynov, 2012a). In this respect the term "peramorphosis" appears as redundant and confusing and we recommend avoiding it, and use instead "progress," "progressive." However, any real organism, even which represent strong paedomorphic characters is a mixture of paedomorphic and progressive traits. A remarkable example of mixture of paedomorphic and progressive features have been assessed for modern humans, which show general paedomorphic delay of many features of body similar to the juveniles of apes, but in contrast demonstrate a highly progressive development of brain (e.g., Godfrey and Sutherland, 1996). Further notable example of such intricate mixture of the paedomorphic and progressive traits is the dorid nudibranch family Corambidae, which secondarily returned the phylotypic condition of ventral anal opening and gills (the paedomorphic

part of corambid evolution, **Figure 2**, *Corambe obscura*), but acquired also a special shedding cuticle unique among molluscs (Martynov, 1994; Martynov and Schrödl, 2011) that can be considered as a progressive side of the evolution of the family Corambidae. We also understand that the usage of the progress instead of "peramorphosis" can be partly misleading too, because progress can be also used in the sense of not a progressive increasing of a complexity, but for example in an ecological sense, like morphological over-simplified nematodes are highly abundant and thus can represent a "progress." However, taking into consideration all that pro and contra we still consider that "peramorphosis" is an obscure and much later rather unnecessary term, compare to the basic term "progress," which in relations to the ontogeny we propose to clarify and partly re-defined and refer to solely of an evident material increasing of complexity of organization, which is based on addition of a particular new periods in ontogeny including specific number of new characters/elements, which were lacked in the ancestral ontogeny, and not just some vague ecological considerations. In some respect, the progress is a formation of an obvious, new, well recognized phylotypic periods, which have been absent in preceding ancestral ontogenies.

For example, dorid nudibranchs (order Doridida) represent a well-defined progressive development since during modification of its ontogeny has been firmly fixed the specific of increasing of complexity by appearing of the closed gill cavity which is formed by the folding and complete closing of the posterior mantle lobes (Martynov, 2011a,b, 2012a; Martynov and Korshunova, 2015; **Figure 2**). Such phylotypic period of ontogeny definitely absent in any other gastropod molluscs including the nudibranchs sensu stricto (order Nudibranchia without dorids, see Martynov and Korshunova, 2011; Korshunova et al., 2020). Additional problem may be posed that any ontogeny is not a straightforward row of mechanistic additions (Haeckel, 1866) or rigid modifications (Severtsov, 1912, 1939), but often "a novelty" is arisen from an alterations of several ancestral features, that not easily to align with either progressive or a regressive, paedomorphic ontogenetic processes. All these complications should be carefully considered while step by step a theory of the organismal form evolution, e.g., true theory of the modifications of the ontogenetic cycles over a time, will be finally completed.

ONTOGENETIC SYSTEMATICS

Because the organismal diversity is generated during alterations of ontogeneses, hence ontogeny must be central to the theory and practice of taxonomy. Therefore, establishing robust hypotheses of phylogenetic lineages critically omits the underlying dynamics of ontogenetic cycles, including broad array of epigenetic and heterochronic processes (**Figures 1–5**). However, due to the domination of the almost exclusively phylogenetic, lineage-based thinking throughout the second part of the twentieth century, the organism, *per se*, and hence its underlying ontogenetic cycles have been largely removed from the central consideration of the evolutionary theory. There are a number of previous and recent attempts to highlight or return importance of the organism (e.g., Godfrey-Smith, 1996; Nicholson, 2014; Baedke, 2019), but still a phylogenetic lineage gains a central position within the evolutionary theory, whereas organism just a subsidiary part of an "endless" evolutionary/phylogenetic flow. To prove the latter statement no particular citation is needed, because all the modern biology and "taxonomy" are just completely "phylogenetic," and some recent doubts in the absolute importance of the "lineage-thinking" (Freudenstein et al., 2017) do not change that still persisted general picture. Therefore, previous attempts to accommodate ontogeny into taxonomy either are exceedingly scarce, and never gained any broad attention (e.g., Orton, 1955) or were fundamentally based on the phylogenetic thinking, in which ontogeny, like the organism is always auxiliary, either explicitly or implicitly compare to the phylogeny, despite on discussions and proposals (e.g., Kluge and Strauss, 1985). Whereas some ontogenetic traits can be indeed indicated just as part of taxonomic descriptions (e.g., Costa et al., 2021) or the application in some "phylogeny-based" studies with inclusion of ontogenetic elements (e.g., Wolfe and Hegna, 2013; Gee, 2020), the "phylogeny-first" still basically implied. As a best confirmation of the absence (despite on putative claims) of any "ontogeny-first" central concept, is that within the apparent inevitable keeper of the "everything ontogenetic" in the biology, the very evolutionary developmental biology, taxonomy has been mentioned rather as an exception (e.g., Minelli, 2007). Furthermore, a publication remarkably entitled "Ontogenetic systematics, molecular developmental genetics, and the angiosperm petal" (Albert et al., 1998), although was an important attempt to link ontogenetic patterns with character evolution, did not offer challenging theoretical (to return ontogeny as a central place within the evolutionary theory) proposal. Another highly symptomatic feature of the modern understanding of the ontogeny, it is the continuous mentioning of Karl Baer among founders of the modern evolutionary biology (e.g., Futuyma and Kirkpatrick, 2017). It must therefore make very clearly, that Baer was a strong *antievolutionist* and his misleading concept widely cited as one of his "laws" directly implies that an embryo of an organism only similar to an embryo of another organism (taxon), *but not to its adult*! (von Baer, 1828/1837). It must be therefore explicitly stated, that Baer's unequivocal prohibition of the linkage between an embryo of one taxon and an adult form of another taxon is not a basis of the modern evolutionary theory, but, on a complete contrary, *the evolutionary blind alley*. Therefore, perhaps the most counterintuitive that despite on apparent more than two hundred centuries of "ontogenetic studies," despites on the Haeckel name and potential large number of references regarding "ontogeny and evolution" topic, but there is a strong *suppression of ontogeny as a central phenomenon in the evolutionary theory and taxonomy*. Thus, this is not researchers from the evo-devo field who on the obviously strictly *evolutionary* grounds provide strong evidences for the reality of the common ontogenetic phylotypic periods between very different taxa (e.g., Levin et al., 2016) have applied a "non-scientific idealistic theory of the body plans," but exactly the entire biological field still lauds the antievolutionist Karl Baer as a founder of the "modern developmental biology."

Therefore, there is nothing stretch that taxonomy has remained essentially ontogeny-free (Martynov, 2012a; Stöhr and Martynov, 2016), and the few twentieth-century publications failed to evoke the deserved paradigm shift in understanding of the key importance of ontogeny for the classification of the world biological diversity. The term *ontogenetic systematics* was independently proposed and unambiguously applied to the field of taxonomy (Martynov, 2009; see also Martynov et al., 2020) not as an attempt just to add some theoretical consideration, but exactly as return of the *centrality of the ontogeny* in the evolutionary studies. Colleagues may clearly feel that obvious shortage of the "ontogeny in phylogeny" (e.g., Minelli, 2015a; Faria et al., 2020), and these attempts are obviously in support of our present approach, and we are very thankful for that. However, still commonly any consideration of ontogeny in a broadly taxonomic/biodiversity field involves a rather basic phylogenetic approach with some addition of "evo-devo" (e.g., Minelli, 2009; Wanninger, 2015), instead of started the real theory of evolutionary processes and modifications (i.e., *the evolution*), with real underlying process, i.e., the *ontogeny*. Notably, Kupiec (2009) just radically avoided the Haeckel's dichotomy of "ontogeny and phylogeny" by introducing of the "ontophylogenesis," and this concept greatly corroborates the long-term previous achievements of the ontogeny/evolution field (Severtsov, 1912; Garstang, 1922). Unfortunately, since that no real shift in the paradigm of the modern profound misunderstanding of the fundamental role of the ontogeny, and the "tree of life" instead of an "ontogeny of life" remains fashionable in the recent publications (Schierwater and DeSalle, 2021). Kupiec (2009) in the introduction also mentioned that yet several decades ago, he was rather a dissident to the contemporary biology, but currently his contribution in the field of the stochastic understanding of the ontogeny is recognized (e.g., Viñuelas et al., 2012). Remarkably, two of the completely independent reviewers of the present paper asked us why we do not referred in the initial version of our manuscript to the Kupiec's book! Such coincidence in asking to cite that once almost neglected approach from one side makes us hope that ontogenetic understanding of the phylogeny will finally overcome that unfortunately persisted dichotomy of the "ontogeny and phylogeny," but from the other hand, the undisrupted integrity of ontogeny and phylogeny was absolutely clear for us yet started our initial works on the ontogenetic systematics (Martynov, 2009, 2011a,b, 2012a,b), when this approach has been developed completely independently from the very supportive for our conception Kupiec's conceptualizations. However, this did not result in a real paradigm shift, the tree-thinking not only prevails, but colleagues from the phylogeny field continue to allege even the most notable contribution from the evo-devo field, the phylotypic-based approach (e.g., Levin et al., 2016) in an adherence with a "pre-evolutionary body plan thinking." As a further very important reservation, in Kupiec (2009), neither taxonomy nor phylogenetics itself does not mention, therefore, even in a most rigorous way, the attempt to merge "phylogeny and ontogeny" does not directly relevant for the present approach. Although the discussion on the stochastic understanding of the ontogeny vs. strict "genetic programming" largely beyond of the limits of the present paper, but ontogenesis, despite on the undisputable at least partly stochastic grounds able to keep very complex and essentially similar ancestral morphological traits over a number of generations.

Facing such obvious not just bias toward the phylogeny-centered modern research, but like an indisputable and unequivocal central modern dogma, that only a phylogeny can resolve relationship within organisms, irrelevantly either colleagues are strict phylogeneticists or a morphology-/"evo-devo"-advocates (e.g., Lee and Palci, 2015; Wanninger, 2015; Hejnol and Dunn, 2016). It would be not a surprise, when such approach also attempted to be omitted nowadays, or it is considered as just something secondarily, insignificant, as some "research program" among many others (Pavlinov, 2020). This is instead of promoting help to return the ontogeny as central component of evolutionary theory, and therefore as central component of any biodiversity studies (since all that enormous biodiversity that we observed currently, have originated as evolutionary *modifications of ontogenetic cycles*) is partly contributing to its further postponing. Thus, one more time, "morpho-evo-devo" and even "evo-devo" at a general scale did no help the ontogenetic-taxonomic and morphology field to stop to be a "secondarily" and scarcely promoted discipline compared to the phylogenetics. First of all this happen because at the main theoretical level there is still no clear understanding that *ontogeny (interacting with other ontogenies and environment) is real primary process in evolution*, whereas phylogeny is instead is a secondary result. To make this absolutely clear and to make the synthesis between ontogeny and phylogeny broadly understood and irreversible one is a task for the near future development of the ontogenetic systematics.

For Haeckel (1866) importance of ontogeny for the systematics was evident ("systematics' *explained* . . . . .ontogeny is only a short and concise repetition. . .of phylogeny"), however through the following "century of acceptance of the evolution" resulting in the Hennig (1966) *phylogenetic* systematics (Rieppel, 2016), ontogeny largely vanished from the taxonomy. And, again, most paradoxically Haeckel takes a significant responsibility for that, because instead of initial proposing something like "evolving ontogenies" or "ontogenetic evolution" he instead strictly contrasted "ontogeny" and "phylogeny" at the terminological level. And his successors instead of carefully reversing "evolution" to its original meaning "ontogeny" (Bowler, 1975), and by this strongly highlight the natural unity of the "ontogeny and phylogeny," instead made strongest accent on "phylogeny" (Hennig, 1966) and by this, the enormous confusion in such a most important biological field is persisted and the problem is growing. This is therefore, one more time to conclude, that it is always possible to find some references in the history of the biological studies that already somehow state the importance of ontogeny in taxonomy (Danser, 1950), which in reality based on that very ancient consideration that living organisms indeed represent a quasicyclical development, and this obvious fact have been indicated both antievolutionists (e.g., Agassiz and Gould, 1857) and apparently strict phylogeneticists (Hennig, 1966). However, this does not help when the "lineage-thinking" obviously engulfed the ontogeny, and the organism, *per se*. It

was remarkably echoed when Lyubischev concluded yet in 1960 (published only in 1982) briefly discussing exactly the Haeckel's heritage, that toward later works of Haeckel compared to his opus magnum of 1866 year "historical morphology *devoured* constructional [structural] one" (Lyubischev, 1982, p. 202, our italics). This should not be interpreted as revival of any idealistic shadow, but this is a great metaphor that exaggeration of the solely *phylogeny* in the reality hardly divisible pair "ontogeny and phylogeny" in course of the last 150 years of the biology development has led to the fundamental negation that *ontogeny* (and their respective structural patterns, including phylotypic periods) is a basis of any evolutionary processes, whereas *phylogeny* it is just result of ontogenetic modifications over a time period. Therefore, truly insignificant if there were some attempts "between Haeckel and Hennig" or not, to remind about existence of ontogeny, when it was almost completely shadowed by the "phylogenetic thinking" and with the rise of the molecular phylogenetics, this ontogenetic neglecting was reinforced enormously. This is now time to clearly formulate that profound neglecting and practical steps how to fundamentally improve the current situation. The key implications therefore that this is not "a phylogeny" itself constitutes material basis for evolutionary modifications, but ontogeny. Thus, by removal of the ontogeny as primary *evolutionary* process and by refusing of the crucial importance of phylotytpic periods for the reconstruction of the ancestral organization we in reality remove phylogenetics (and even more, the entire evolutionary field!) from *scientific* disciplines.

Therefore, facing such fundamental neglecting of the primacy of the ontogeny, the additional citations of five, ten or more sources will not change that obvious fact: *despite on the all achievements of the evo-devo, and despite this year we are celebrating 100th anniversary of the seminal Garstang (1922) publication, ontogeny is still not a central process of understanding of evolution.* This is a very easy to prove. Because even the researchers from the evo-devo field, which obviously must be strict advocates of the centrality of ontogeny (and morphology since this is a central part of any ontogeny), however, on a complete contrary argued that "to understand how phenotypic diversity evolved" we need in a phylogeny! Compare Wanninger (2015, p. 12, our italics) "in other words, once all organisms *have been sequenced and once we have agreed on the "true" phylogenetic tree*, we will still need morphology to understand how phenotypic diversity evolved" and Neumann et al. (2021, p. 1) "The assumption that genomic data will automatically "swamp out" morphological data is not always true for the sister of all metazoan question." In another words, the question that constitutes a major basis of the understanding the ancestral patterns in the animal and organismal evolution is not necessarily can be correctly addressed exactly by the molecular phylogenetics.

This is a best "litmus probe" (if to rephrase a well-recognized Russian idiom) that while evolutionary developmental biology is claimed to be a separate, just relatively recently emerged discipline (Gilbert et al., 1996), in reality it is just a subsidiary discipline of a (molecular) phylogenetic study. Especially indicative that in the same paper Wanninger (2015, p. 12, citing also Scholtz, 2010, our italics) definitely said that: "...morphologists should further and proactively embrace the evolutionary disciplines that are currently *dominated by molecular approaches*, especially phylogenetics and EvoDevo, and integrate these into their own research programs, in order to avoid becoming *a mere add-on to these and degenerate* to a "shrinking or even vanishing field" (!). However, this in reality appears as more an "advertising slogan" than a true program to challenge the "shrinking or even vanishing field" because despite that other colleagues, which since at least 2009 explicitly warned on the true ongoing catastrophe exactly with the evaluation of the importance of the morphology and ontogeny facing of the molecular phylogenetic dominance, have not been cited or acknowledged. Therefore, if ontogeny with all their internal complexity is truly underlying basis of any evolutionary processes (and hence, phylogeny), including the epigenetics which clearly breaks straightforward purely genetic inheritance (the main initial basis for "evo-devo," e.g., Raff and Kaufman, 1983; Ivanova-Kazas, 1995), then ontogenetic field is of its own importance and developmental evidences must be at least of equal weight with the molecular phylogenetic, and not just by definition as a secondary one. This is one of the most important implications of the present work, since there are number of examples, when obvious developmental data were uncritically and uncarefully discarded in favor of molecular phylogenetic data.

Nobody would of course refuse strong necessity of a "time-scale phylogeny" (e.g., Lee and Palci, 2015). However, the main problem that currently the all "final evidences" still expected and referred to a "molecular phylogenetic study," a notoriously known cliché of a necessity of a "robust phylogeny." In this respect, the robustness of the even most expensive and most complicated phylogenomic analyses has been repeatedly contested in that very notable "molecular phylogenetic controversy" of the "porifera-first vs. ctenophora-first." This is very relevant and one of the most notable example when overhyped contemporary molecular phylogenetics, strongly put forward the "ctenophora-first" story, when evident morphological and developmental data (in another words, *ontogenetic* in its real sense) of the fundamental similarity of sponges to the choanoflagellate colonial protists have been disregarded, just because a molecular phylogenetic analysis has been published in a high-impacted journal (Moroz et al., 2014) putatively disproved the well-established ontogenetic (in the *broad*, but real sense) data (e.g., Martynov, 2012b; Nielsen, 2012; Adamska, 2016). And despite that a number of subsequent analysis recovered serious errors in the molecular phylogenetic assessments of the "ctenophora-first" (e.g., Pisani et al., 2015; Simion et al., 2017), the gravity of putative "authority" of the molecular phylogenetic analysis still forced researches to claim and search for a non-existed ambiguity of the "sponges-first" (Li et al., 2021). In spite of the significant amount of the recent data which strongly conclude that the analyses which showed the "ctenophora-first" have been affected by the critical errors (e.g., Juravel et al., 2021; Nejad Kourki, 2021; Redmond and Mclysaght, 2021). However, while still continuing allegation of the evolutionary morphology and ontogeny-based data for an arbitrary approach, we then must placed a similar "disclaimer"

to any molecular phylogenetic study, especially dangerous when they presented a putatively challenging "truth" in journals with a high impact. In order the researches from other fields should not be used a molecular phylogeny as an "unequivocal truth," as it was already regularly happen to make a crucial claim using data of subsequently contested molecular data (e.g., Brown et al., 2008; Dunn et al., 2015).

By this statement we need to specially emphasize that we by no means deny importance of the molecular phylogenetic data, and we themselves are profoundly use it (e.g., Korshunova et al., 2017a,b. Korshunova et al., 2018, 2020, 2021; Martynov et al., 2020). However, it is very important to remove ontogeny from the strong tenets and label of an "outdated" science, and to put at least as equally important to the molecular phylogenetic inference. Symptomatically, although surprisingly, the necessity of the revival of morphological data (which is inevitable part of any ontogeny) has been recently emerged not from the "non-fashionable and arbitrary" evolutionary morphology, but from the very rigorous statistical-based phylogenetics, but with a strong implications, that molecular phylogenetic does not necessary may answer "difficult phylogenetic questions" (Neumann et al., 2021). While this is just a lesser critics to the molecular phylogenetic field, however the fundamental deficiency of the strictly molecular phylogenetic approach is that it unable to reconstruct the ancestral organization, and only considers "sister relationship" that as, practice clearly shown can be very misleading (compare Moroz et al., 2014 vs. Redmond and Mclysaght, 2021, or Cameron et al., 2000 vs. Tassia et al., 2016). Thus, despite on any past and recent claims on importance of ontogeny and "evo-devo" (Haeckel, 1866; Garstang, 1922; Gould, 1977; Minelli, 2009; Wanninger, 2015), the morphology, ontogeny and "evo-devo" field remained to be just a "supplementary" to the molecular phylogenetics.

Therefore, ontogenetic systematics is not just an auxiliary to the "phylogenetic and development" field, but highlights phylotypic periods as a real, and not just "hypothetically inferred" proxy for an ancestral organization. The ontogenetic systematics is therefore a real synthetic discipline that consider all possible evidence, including molecular phylogenetic data, but in a consequential, consistent ontogenetic framework. As another crucial implication that because obviously ontogeny bears a lot of truly evolutionary information about ancestral organization, the reliable framework how to turn ontogenetic field into truly evident discipline, much more theoretical and practical efforts need to be done. The current concept of the ontogenetic systematics is one more step towards to the development of such "ontogeny-evident" theory of the modifications of the organisms (= ontogenetic cycles) in course of the time. Nobody will claim that this will be easy and straightforward. However, without the urgent necessity to form the ontogeny-centered, consistent taxonomic field, any next steps to develop detailed practical applications of the ontogenetic systematics will be impossible.

Thus, the history of the term *ontogenetic systematics* is itself remarkable since, being actually introduced two times independently in different senses from two different fields: *molecular* and *taxonomic*, but both definitions are clearly indicated the obvious necessity of further and real synthesis of the immense modern data on the ontogeny (both at molecular and morphological levels) with astonishing taxonomic diversity of the organisms. Whilst the significance of ontogeny is well understood in the evolutionary developmental biology *per se*, it is still not applied to the major biological fields of taxonomy and phylogenetics. And there is not any stretch in the conclusion, that a search of publications in the Web of Science (Martynov et al., 2015; Stöhr and Martynov, 2016) confirmed the absence of general ontogenetic principles in modern taxonomy. It is possible to list some works where metamorphic stages are used for taxonomic diagnostic, but the fundamental understanding that not a still strictly pre-evolutionary typological taxonomic diagnosis or some "phylogeny" are primary for the taxonomy, but instead universal for any organisms ontogenetic process (with different complexity) is fundamental to the systematics. Therefore, the main field of biodiversity studies is really still devoid of consideration of ontogeny as the central biological process, that fundamentally encompasses all other biological processes. In that sense, ontogenetic systematics is not merely one of many "research programs" in taxonomy, but a fundamental, core discipline that encompasses "static" taxonomic assessments of biodiversity and dynamic evolutionary aspects. By this, ontogenetic systematics cannot be alleged in any way as a "typological discipline" (Pavlinov, 2020). Our earlier analyses (Martynov, 1994, 2009, 2011a,b, 2012a,b) clearly pointed to the problems of taxonomy if ontogenetic basis would be removed, and this is especially justified because of subsequent recent appearance of proposals in a fundamentally similar direction, i.e., to integrate evolutionary developmental biology, phylogenetics and to point to a shortage of the morphological and ontogenetic studies in the molecular era (e.g., Richter and Wirkner, 2014; Wanninger, 2015; Faria et al., 2020).

The failure to incorporate ontogenetic data into systematic biology inevitably limits the precision of taxonomic representations of natural patterns. The premise that the same genes determine an organism's identity at the egg and adult stage of an individual, thereby obviating the need to include ontogenetic data in phylogenetic studies (Mayr, 1963), strongly ignores epigenetic and other processes beyond strict inherent genetic control (e.g. Müller, 2017). Therefore, molecular analysis cannot substitute the ontogenetic approach. Yet few decades ago, when "phylogenetic thinking" reached its peak, such a statement would be controversial. However, the currently accumulated developmental evidence instead strongly favor a shift to a further change of the paradigm (Martynov, 2009) and place ontogeny not as "just a possible research program" but as a core of taxonomy: "We argue that evolutionary biologists should return from a purely gene-centric view of evolution and place more focus on analyzing and defining conserved developmental processes and periods" (Ferretti et al., 2020: 1). This is because *there is no "biological reality" beyond ontogeneses* and all living organisms, even prokaryotes have a complex underlying system of patterns and processes. Ontogenetic systematics instead of drifting toward some "formal-logical" biology-free theories is therefore a most natural integrator of traditional evolutionary-free taxonomy, ontogeny-free phylogenetics and

evolutionary developmental biology. Ontogenetic systematics is based not only on formalized molecular genealogies of taxa, but on analysis and description of the major structural modifications and transformations of organisms, particularly in analysis of degree of shared ontogenetic conservativeness (as expressed in phylotypic periods, see e.g., Richardson, 1995; Arthur, 2002; Martynov and Korshunova, 2015; present work) among taxa which are disparate at adult stages, with a careful integration of the molecular data (Korshunova and Martynov, 2020; Korshunova et al., 2020; Martynov et al., 2020), instead of giving an absolute priority to the molecular phylogenetic data. By this ontogenetic systematics is perfectly verifiable science. The major structural modifications of every taxonomic groups are manifested in the phylotypic periods at different taxonomic levels (very importantly: not only at the phylum level, see e.g., Martynov and Korshunova, 2015), and this, compared to misleading comments from the strict phylogeny-based field, not a return to "pre-evolutionary" thinking or "circular arguing," but instead most natural recognition of the really existed, common between taxonomically disparate organisms ontogenetic periods, as a major basis for the reconstruction of ancestral organization(s). This is an essence of the ontogenetic systematics. That could be least "idealistic" and instead directly evolutionary discipline!

The ontogenetic challenge for taxonomy is a practical call to make systematics of the world biodiversity as science to be really based on the underlying patterns and processes of majority of organisms (i.e., ontogeny). Below are given several examples from different phyla of the ontogenetic systematics approach implying ontogenetic-and-evolutionary linkage of the adult and juvenile features among both closely related and disparate taxa in frames of the modifications of the ontogenetic cycles, carefully aligned (whenever this possible) with molecular phylogenies, but this is an outstanding goal of the ontogenetic systematics for the vast majority of the living organisms. Although previously we outlined several principles in ontogenetic systematics (e.g., Martynov, 2009, 2011a,b, 2012a; Stöhr and Martynov, 2016; Korshunova et al., 2017a,b, 2018, 2021; Martynov et al., 2020), and while more detailed practical principles will be outlined elsewhere, the refined basic principles of the *ontogenetic systematics* still need to be more rigorously presented here:

1. *Ontogeny* is the central underlying process of the evolution.
2. *Phylogeny* is a secondary result of the (evolutionary) modification of ontogeny.
3. *Ontogeny and phylogeny* must not be strictly separated as they are closely interlinked through epigenetic inheritance and other developmental processes.
4. Biological organisms are not just subsidiary part of an endless evolutionary/phylogenetic flow, but separate entities, which represent most complex ever appeared natural objects, encompassed trillions of interlinked elements, which underlie the basic energy- and external-resources depended organism functioning, such as growth, defense, feeding and reproduction.
5. Organisms do not exist only as a separate either embryonal, or juvenile, or adult stages, but exist only as ontogenetic cycles of various degree of complexity, from very simple in viruses, bacteria and archaea, and most complex in the bilaterian animals.
6. The term *ontogeny* therefore implies not a developmental stage, but equal to an ontogenetic cycle of any organism. This must be understand very clearly and do not restrict ontogeny only to the "embryonal-juvenile" period which is still commonly used in the current literature.
7. *Taxonomy* is the multi-level understanding of the biological diversity of the organisms, those emergence result of the evolutionary modifications of ontogeny.
8. Without *centrality of the ontogenetic principles* it is impossible to correctly classify the organisms (and hence taxonomy is impossible without ontogeny).
9. Taxonomy therefore is not a pure typological or a "service-based" discipline that just technically assign some names to organismal groups to define the enormous diversity and allow study (provides the service—names) to other "proper" scientific fields such as any molecular investigations, but *is a central biological discipline that encompass all organismal-related process at all levels*.
10. Since any organisms are existed in frames of only a specific ontogenetic process (ontogenetic cycle), therefore ontogeny (by definition) is a real natural object that must be basic and central for any evolutionary and phylogenetic studies.
11. Molecular phylogenetics must not be considered as solely central evidence for the relationships of the organisms (ontogenetic cycles), as it currently widely claimed because modifications of ontogeny are not restricted only to the genetic inheritance, but as shown by numerous studies, also significantly influenced by epigenetic processes.
12. Phylotypic periods are not "flawed heritage" of the pre-evolutionary "idealistic body plan" concepts, but a key object of ontogenetic systematics, *the naturally existed inter-taxon nodes that linked at the earlier ontogenetic periods taxa with very different adult morphologies*. Beyond classical examples of the vertebrates taxonomy, here we present evidence of the universal occurrence of the phylotypic periods across such both morphologically and phylogenetically very disparate animal phyla as molluscs (nudibranchs) and echinoderms (ophiuroids) (**Figures 2–4**).
13. Therefore, we cannot just restrict the main target of the all biology—inference of unequivocal order of emergence and modifications (evolution) of consequential ancestral organizations (ancestral ontogenetic cycles) either to the plain "taxonomy/systematics," which have an exceeding number of negative connotations and still basically non-evolutionary, real typological discipline, or morphological and molecular phylogenetics. The latter has been claimed to be a strictly evolutionary field, but in reality critically removed ontogeny as the central biological process. Instead, a separate term is in a strong need. Such term is proposed as *ontogenetic systematics* since it is a most general way encompassed both the apparently "static" taxonomic assessments and the developmental

(evolutionary aspect), and hence both putatively strictly "individual" and "historical "development" will be conjoined under universal ontogeny-based term.

Practical Examples of Applications of Ontogenetic Systematics

These examples are not just target "to illustrate" using few selected cases, but first of all aim to provide robust evidence that such only putatively well-known central ontogenetic phenomena as phylotypic periods and paedomorphosis by no way restricted merely to the well-recognized vertebrate taxonomic groups, but they also universally occurs in such very different animal phyla as molluscs and echinoderms, and inevitably, similar ontogenetic patterns present in absolute majority of the organisms. The reality and most important predictive power of the universally existed phylotypic periods can be proved by the practices. If for example we will find a new species of a vertebrate mammal, bird, and reptilians, or dorid nudibranch molluscs, or ophiuroid echinoderms, for which earlier ontogenetic patterns are yet completely unknown, we can with a high confidence predict that the basic organization of their respective phylotypic periods will be essentially similar (despite on some inevitable differences). The predictive power is a central attribute of any scientific study, and therefore the ontogenetic systematics reinforced by the concept of the phylotypic periods represents true scientific discipline with its own set of theories, concepts and practical applications. Some of them are briefly explained below.

Nudibranch Molluscs

Dorid Nudibranchs

Cryptobranch and phanerobranch dorids that are morphologically and taxonomically disparate in the adult stage are essentially similar in the early juvenile stages (Martynov and Korshunova, 2015; Zaitseva et al., 2015; Korshunova et al., 2020; **Figure 2**). The following developmental processes are the same in both cryptobranchs and phanerobranchs: (1) the strictly separated rhinophores form later in development; (2) the ventral anus forms before its dorsal translocation and (3) the gills start to develop significantly later, after juveniles reach more than 1 mm in length. This conserved development conforms to the evolutionary phenomenon of phylotypic periods, i.e., similarity of early developmental patterns across large taxonomic groups with considerably different adult morphology (e.g., presence of the ancestral pharyngeal arches in early ontogeny of all vertebrates, even if they no longer have gills in the adult state). This intersection of development and evolution is well established at the morphological level (Richards, 2009) and has been confirmed using transcriptomic analysis (Irie and Kuratani, 2011). There are several partly or considerably paedomorphic lineages arisen independently among dorids, notably Corambidae (Martynov, 1994; Martynov et al., 2011), but also Okadaiidae and other groups (Korshunova et al., 2020). This is also important to highlight, that not merely ontogenies, but ontogeny-based integration of the molecular phylogenetic data (Korshunova et al., 2020; this study) directly contributes to the evolutionary models and based on it classification of the gastropod nudibranch molluscs. The predictive power of the present dorid ontogenetic model, that recognized phylotypic stages essentially similar with the adult disparate *Cadlina* and *Palio* (Martynov and Korshunova, 2015; present study, **Figure 2**) has been detected by an independent study (Moles et al., 2017) in a very different dorid taxonomic group. As important practical example, from the ontogenetic field must be removed the previously widely promoted, and still sometimes applied in Russia, these Severtsov (1912, 1939) inflexible schemes that all ontogenetic modifications fall to the Procrustean bed of the only three major changes: "anaboly, deviation and archalaksis". Despite previously we partially praised Severtsov as a conceptual predecessor of Garstang (1922) work (Martynov, 2011a). The real ontogenetic patterns strongly contradict to that theoretical scheme. For example, even highly modified direct developers such as dorid nudibranch *Cadlina* still preserve major features of the dorid ontogeny representing by the phylotypic periods (Martynov and Korshunova, 2015; Korshunova et al., 2020; **Figure 2**). Another major misunderstanding, when in an extreme case of strongly modified direct development is difficult to recognize major features of ancestral dorid organization at early ontogenetic stages in the dorid families Bathydoridiidae (Moles et al., 2017), or Okadaiidae (Martynov and Korshunova, 2011) *it is result of long series of reductions* proved also by the molecular data (Korshunova et al., 2020), and not only a putative solely drastic "earlier development changes." In addition, earlier stages of ontogeny was not yet studied and still may contain although reduced but still remnants of the dorid phylotypic periods. By this we also would like to one more time warn, that despite that paedomorphosis (as a very substantial reversal, although only partial to an ancestral organization, *via* partial "adultization" of phylotypic periods) is a highly important evolutionary concept, it must be applied very carefully, without typical consideration, when a complex ancestral organization is disappeared "to nowhere," as it is sometimes has been proposed recently (e.g., Nielsen, 2008).

Aeolid Nudibranchs

During the ontogeny of all aeolidacean nudibranchs, a few juvenile ceratal rows (1–2 anterior rows in earlier postlarval stages, about 3–4 anterior rows in more advanced juveniles) precede the adult state with numerous ceratal rows (commonly more than ten in total, more than four in anterior rows) (**Figure 3**). Therefore, the presence of a smaller number of ceratal rows in the adult stage is a sign of at least partial paedomorphosis, and not just an overall reduction/loss, especially if small-sized taxa with a smaller number of anterior ceratal rows are sister to large-sized taxa with numerous cerata. The recent confirmation of the evidently paedomorphic adult characters of the family Pseudovermidae using both morphological and molecular data (see details in Flammensbeck et al., 2019; Martynov et al., 2020) is exactly in line with the core approach of the ontogenetic systematics outlined above. As a direct practical application of the principles of ontogenetic systematics in

the aeolidacean group, morphological and molecular data indicate that brackish water speciation was triggered by paedomorphic evolution among aeolidacean nudibranchs at least two times independently, i.e., in the Cuthonidae for the genus *Bohuslania* and in the Trinchesiidae for the genus *Tenellia* (see Korshunova et al., 2018). If to apply instead a strictly molecular phylogenetic approach, without ontogenetic data, the flawed concepts of overlumped "*Tenellia*" and "*Flabellina*" will appear (see review in Korshunova et al., 2017a,b).

Ophiuroid Echinoderms

To date, various data have been accumulated on postlarval development for the majority of ophiuroid families (see details in Martynov et al., 2015; **Figures 4**, **5**). The ophiuroid postlarvae have a conserved morphology as follows: 1. The major part of the dorsal disk is occupied by the primary plate rosette comprised of a single central primary plate and usually five radial primary plates; 2. The radial shields and genital plates have yet to appear or are underdeveloped; 3. Each half-jaw is narrow, elongate and bears ventrally a few rudimentary oral papillae, commonly bar-shaped; 4. The dental plate is small, convex and bears a few tooth sockets of unspecific shape; 5. Each adoral shield bears a papilla (spine) of various length and shape; 6. Arm segments are limited in number and considerably elongated proximally; 7. Vertebrae are comprised of two separate, loosely connected elongated parts; 8. The vertebral articulation is generally underdeveloped without a distally well-defined condyle.

Highly relevant for the above outlined evidence of the almost direct linkage between only putatively disrupted ontogenetic phylotypic periods and phylogenetic (evolutionary) patterns, both juvenile of non-paedomorphic ophiuroid taxa and adult specimens of ophiuroid paedomorphic taxa (see Martynov, 2012a; Martynov et al., 2015) have very short concave dental plate with a single tooth, and considerably elongated, only partially fused vertebrae (**Figure 5**). Therefore, instead to deny of the juvenile—adult ontogenetic (evolutionary) linkage (e.g., Mayr, 1963; Hennig, 1966) there is the remarkable correspondence between the adult shape and placement of primary plates, dental plates and vertebrae of the adult paedomorphic ophiuroids and the homologous structures in early juveniles of related non-paedomorphic taxa (**Figures 4–5**). This is a very important evidence, not merely for "phylogenetic" or "evolutionary" approaches, but for the approach of *ontogenetic systematics*.

Furthermore, the manifestation of the paedomorphic processes varies among various ophiuroid taxa from an almost exact correspondence to the early postlarval stages in adult *Perlophiura*, to the correspondences of the later postlarval stages in paedomorphic *Ophiomastus* to the complex ancestral ophiuroids (**Figure 4**). Indeed, any ontogeny is not a plain scheme, and the direct linkage between earlier juvenile ancestral and adult paedomorphic morphologies are certainly not exact because of the influence from various ontogenetic processes, but generally the similarity between ancestral early juvenile and adult paedomorphic characters are striking (**Figures 4–5**) and the evolutionary linkage through particular periods (stages) of the ontogeny cannot be denied. The independent appearance of paedomorphic taxa within remote ophiuroid families, such as Ophiuridae and Ophiolepididae has been also indicated (Martynov, 2009, 2012a). In some cases, resulting external and internal morphology of adult paedomorphic ophiuroids from remote families is almost indistinguishable. A comprehensive morphological scanning electron study of about 200 species of more than 100 genera of majority of modern ophiuroid families confirmed this. Studying of spine articulations of the lateral arm plates (the shape of which is very conservative at the family level) remains the reliable method to distinguish some taxa of paedomorphic brittle stars (Martynov, 2009, 2010a,b). Recent molecular phylogenomic data on ophiuroids (O'Hara et al., 2017) are generally concordant with the earlier proposed ontogenetic model of ophiuroids (Martynov, 2012a; **Figure 4**) with several independent paedomorphic lineages.

These practical examples confirm that ontogenetic systematics is a natural integrator of morphological and molecular data. The quest for that is an obvious and significant problem of biodiversity studies, since a few decades ago formal molecular phylogenies started to substitute the real biological organisms, which are essentially represented by the ontogenies. In all these cases from two very different metazoan phyla, representing major traditional bilaterian supraphyletic groupings as protostomiens (Mollusca) and deuterostomiens (Echinodermata), the presence of the conservative ontogenetic periods which are linked at different layers of the both adult and juvenile ancestral organizations *via* phylotypic periods and paedomoprhosis are confirmed. By this, the main theme of the present contribution, the tight, indivisible linkage between ontogeny as a primary process, and phylogeny as a secondarily result of the evolutionary modifications of the ontogeny is thoroughly confirmed both at the theoretical and practical levels.

CONCLUSION

1. *Ontogeny* is apparently old and well-established biological term, however there are still significant contradictions and deficiency in its evolutionary and taxonomic applications.
2. *Ontogeny and phylogeny* are two sides of fundamental biological properties of organisms.
3. *Paedomorphosis* (and not "neoteny" or "progenesis") should solely be used as term to describe cases of retention of juvenile features of ancestors at the adult stages of descendants.
4. *Phylotypic periods* represent real manifestation of some features of the ancestral ontogenetic cycles in the ontogenies of modern descendants and therefore partial recapitulations of the ancestral organization.
5. *Recapitulations* and *biogenetic law* are not abandoned concepts but represents actual existing patterns of ontogenies, denoting persistence of phylotypic periods in the ontogenies of the modern taxa.

6. If to remove phylotypic periods which a natural basis for existence of the phyla concepts, as a core concept of'evo-devo," then evolutionary developmental biology will be turned to an auxiliary discipline of the molecular phylogenetics.
7. The evolutionary linkage between juvenile ancestral characters and adult features of descendants (paedomorphosis) is a widespread phenomenon, as evidently showed here using examples from molluscs and echinoderms (**Figures 1–5**).
8. *Ontogenetic systematics* is not merely a "research program" in taxonomy, and not an auxiliary subdivision of "evo-devo." Ontogenetic systematics is an interdisciplinary field which encompasses and further promotes achievements of "evo-devo" and epigenetics to link it to the still separated fields of phylogenetics and taxonomy. Among the main goals of the ontogenetic systematics is to achieve more precise knowledge on the patterns and processes (both universal/conservative and unique ones) in the worldwide biodiversity, that currently is endangered due to ongoing climatic and other challenges.
9. The central paradigm of the *ontogenetic systematics* and "ontogeny and evolution field," applying Haeckel's initial formulation, Garstang's reformulation, and synthesizing it with the material fact of the universal existence of the phylotypic periods across disparate organisms' groups, can be now formulated at a new conceptual level as following: *ontogeny partially keeps (past) ancestral ontogenies (importantly, at adult and larval phases) and produces (future) ontogenies, and both these patterns in total form the phylogenetic (evolutionary) process—which is nothing but modifications of the interacting ontogenies in course of time.*

AUTHOR CONTRIBUTIONS

All authors listed have made a substantial, direct, and intellectual contribution to the work, and approved it for publication.

FUNDING

This study was supported by research project of MSU Zoological Museum (18-1-21 No. 121032300105-0, AM). The work of TK was conducted under the IDB RAS basic research program in 2021 No. 0088-2021-0008.

ACKNOWLEDGMENTS

Electron Microscopy Laboratory MSU thanked for providing electron microscopy facilities. We are thankful to reviewers for the advices that helped to improve the manuscript.

DEDICATION

This article is dedicated to the 100th anniversary of the seminal article by Walter Garstang (1922), which for the first time explicitly concluded, that ontogeny produces phylogeny (and hence, evolution), instead to be solely a "storage room" for the evolutionary process; but with a remained elusive for Garstang key addition: Phylotypic periods are partial, dynamic keepers of the adult ancestral organizations within the constantly evolved ontogenetic cycles!

REFERENCES

Adamska, M. (2016). Sponges as models to study emergence of complex animals. *Curr. Opin. Genet. Dev.* 39, 21–28. doi: 10.1016/j.gde.2016.05.026

Agassiz, A. A., and Gould, A. A. (1857). *Principles of Zoölogy*. Boston, MA: Gould and Lincoln.

Alberch, P. S., Gould, J., Oster, G. F., and Wake, D. B. (1979). Size and shape in ontogeny and phylogeny. *Paleobiology* 5, 296–317. doi: 10.1162/artl.2009.15.2.15200

Albert, V. A., Gustafsson, M. H. G., and Di Laurenzio, L. (1998). "Ontogenetic systematics, molecular developmental genetics, and the angiosperm petal," in *Molecular systematics of plants II*, eds P. S. Soltis, D. E. Soltis, and J. J. Doyle (Boston, MA: Kluwer Acad. Publ.), 349–374. doi: 10.1007/978-1-4615-5419-6_12

Anastasiadi, D., Venney, C. J., Bernatchez, L., and Wellenreuther, M. (2021). Epigenetic inheritance and reproductive mode in plants and animals. *Trends Ecol. Evol.* 36, 1124–1140. doi: 10.1016/j.tree.2021.08.006

Arthur, W. (2002). The emerging conceptual framework of evolutionary developmental biology. *Nature* 415, 757–764. doi: 10.1038/415757a

Arthur, W. (2015). "Internal factors in evolution: the morphogenetic tree, developmental bias, and some thoughts on the conceptual structure of evo-devo," in *Conceptual Change in Biology. Scientific and Philosophical Perspectives on Evolution and Development*, ed. A. C. Love (Dordrecht: Springer Science & Business Media), 343–363. doi: 10.1007/978-94-017-9412-1_16

Baedke, J. (2019). "What is a biological individual?," in *Old Questions and Young Approaches to Animal Evolution, Fascinating Life Sciences*, eds J. M. Martín-Durán and B. C. Vellutini (Cham: Springer Nature Switzerland AG), 269–284. doi: 10.1007/978-3-030-18202-1_13

Barnes, M. E. (2014). *Ernst Haeckel's Biogenetic Law (1866)*. Tempe, AZ: Embryo Project Encyclopedia.

Bateson, W. (1894). *Materials for the Study of Variation*. London: Macmillan.

Belousov, L. V. (2005). *Foundations of General Embryology*. Moscow: MSU Publishing House.

Bininda-Emonds, O. R. P., Jeffery, J. E., Coates, M. I., and Richardson, M. K. (2002). From Haeckel to event-pairing: the evolution of developmental sequences. *Theory Biosci.* 121, 297–320. doi: 10.1007/s12064-002-0016-5

Bonner, J. T. (1965). *Size and Cycle: An Essay on the Structure of Biology*. Princeton, NJ: Princeton University Press.

Borzenkov, Y. A. (1884). Readings on comparative anatomy. *Uch. Zap. Imp. Mosc. Univ. Otd. Estest. Istor.* 4, 1–242. doi: 10.1017/9781108869348.006

Bowler, P. J. (1975). The changing meaning of "evolution". *J. Hist. Ideas* 36, 95–114. doi: 10.2307/2709013

Brown, F. D., Prendergast, A., and Swalla, B. J. (2008). Man is but a worm: chordate origins. *Genes* 46, 605–613. doi: 10.1002/dvg.20471

Brusca, R. C., and Brusca, G. J. (1990). *Invertebrates*. Sunderland, MA: Sinauer Associates.

Cameron, C. B., Garey, J. R., and Swalla, B. J. (2000). Evolution of the chordate bodyplan: new insights from phylogenetic analyses of deuterostome phyla. *Proc. Natl Acad. Sci. U.S.A.* 97, 4469–4474. doi: 10.1073/pnas.97.9.4469

Cordero, G. A., Sánchez-Villagra, M. R., and Werneburg, I. (2020). An irregular hourglass pattern describes the tempo of phenotypic development in placental mammal evolution. *Biol. Lett.* 16:20200087. doi: 10.1098/rsbl.2020.0087

Costa, S. G. D. S., Welbourn, C., Klimov, P., and Pepato, A. G. (2021). Integrating phylogeny, ontogeny and systematics of the mite family Smarididae (Prostigmata, Parasitengona): classification, identification key, and description of new taxa. *Syst. Appl. Acarol.* 26, 85–123. doi: 10.11158/saa.26.1.6

Cridge, A. G., Dearden, P. K., and Brownfield, L. R. (2019). "The developmental hourglass in the evolution of embryogenesis," in *Evolutionary Developmental Biology*, eds L. Nuño de la Rosa and G. B. Müller (Cham: Springer Nature Switzerland AG).

Danchin, E., Pocheville, A., Rey, O., Pujol, B., and Blanchet, S. (2019). Epigenetically facilitated mutational assimilation: epigenetics as a hub within the inclusive evolutionary synthesis. *Biol. Rev.* 94, 259–282. doi: 10.1111/brv.12453

Danser, B. H. (1950). A theory of systemtics. *Bibl. Biother.* 4, 115–180.

de Beer, G. R. (1930). *Embryology and Evolution*. Oxford: Oxford University Press.

de Beer, G. R. (1958). *Embryos and Ancestors*, 3rd Edn. Oxford: Oxford University Press.

Deline, B., Thompson, J. R., Smith, N. S., Zamora, S., Rahman, I. A., Sheffield, S. L., et al. (2020). Evolution and development at the origin of a phylum. *Curr. Biol.* 30, 1672–1679. doi: 10.1016/j.cub.2020.02.054

Domazet-Lošo, T., and Tautz, D. (2010). A phylogenetically based transcriptome age index mirrors ontogenetic divergence patterns. *Nature* 468, 815–818. doi: 10.1038/nature09632

Dunn, C. V., Leys, S. P., and Haddock, S. H. D. (2015). The hidden biology of sponges and ctenophores. *Trends Ecol. Evol.* 30, 282–291. doi: 10.1016/j.tree.2015.03.003

Emelyanov, S.V. (ed.) (1968). *Tempo of Individual Development of Animals and Its Evolutionary Modifications*. Moscow: Nauka.

Ezhikov, I. I. (1940). "The concept of recapitulation and its critics," in *Basic Biogenetic Law*, eds F. Müller and E. Haeckel (Moscow-Leningrad: Academy of Science USSR).

Faria, L. R. R., Pie, M. R., Salles, F. F., and Soares, E. D. G. (2020). The Haeckelian shortfall or the tale of the missing semaphoronts. *J. Zool. Syst. Evol. Res.* 59, 359–369. doi: 10.1111/jzs.12435

Ferretti, L., Krämer-Eis, A., and Schifferet, P. H. (2020). Conserved patterns in developmental processes and phases, rather than genes, unite the highly divergent Bilateria. *Life (Basel)* 10:182. doi: 10.3390/life10090182

Flammensbeck, C. K., Haszprunar, G., Korshunova, T. A., Martynov, A. V., Neusser, T. P., and Jörger, K. M. (2019). Pseudovermis paradoxus 2.0—3D microanatomy and ultrastructure of a vermiform, meiofaunal nudibranch (Gastropoda, Heterobranchia). *Org. Divers. Evol.* 19, 41–62. doi: 10.1007/s13127-018-0386-2

Freudenstein, J. V., Broe, M. B., Folk, R. A., and Sinn, B. T. (2017). Biodiversity and the species concept — lineages are not enough. *Syst. Biol.* 66, 644–656. doi: 10.1093/sysbio/syw098

Futuyma, D. J., and Kirkpatrick, M. (2017). *Evolution*, 4th Edn. Sunderland, MA: Sinauer, Associates, Inc., Publishers.

Garstang, W. (1922). The theory of recapitulation: a critical restatement of the biogenetic law. *Proc. Linn. Soc. Zool.* 35, 81–101. doi: 10.1111/j.1096-3642.1922.tb00464.x

Garstang, W. (1928). The morphology of the Tunicata, and its bearing on the phylogeny of the Chordata. *Q. J. Microsc. Sci.* 72, 52–187. doi: 10.1186/s12862-014-0214-z

Gee, B. M. (2020). Size matters: the effects of ontogenetic disparity on the phylogeny of Trematopidae (Amphibia: Temnospondyli). *Zool. J. Linn. Soc.* 190, 79–113. doi: 10.1093/zoolinnean/zlz170

Gegenbaur, C. (1888). Über Cänogenese. *An. Anz.* 3, 493–499.

Giard, D. (1887). La castration parasitaire et son influence sur les caracteres exterieurs du sexe male ches les crustaces decapodes. *Bull. Sci. Dep. du Nord* 18, 1–28.

Gilbert, S. F., Opitz, J. M., and Raff, R. A. (1996). Resynthesizing evolutionary and developmental biology. *Dev. Biol.* 173, 357–372. doi: 10.1006/dbio.1996.0032

Godfrey, L. R., and Sutherland, M. R. (1996). Paradox of peramorphic paedomorphosis: heterochrony and human evolution. *Am. J. Phys. Anthropol.* 99, 17–42. doi: 10.1002/ajpa.1330990102

Godfrey-Smith, P. (1996). *Complexity and the Function of Mind in Nature*. Cambridge: Cambridge University Press.

Gould, S. J. (1977). *Ontogeny and Phylogeny*. Cambridge: Harvard University Press.

Haeckel, E. (1866). *Generelle Morphologie der Organismen. Bd. 1–2*. Berlin: G. Reimer.

Hall, B. K. (1999). *Evolutionary Developmental Biology*, 2nd Edn. Dordrecht: Kluwer Academic Publishers.

Hall, B. K. (2003). Evo–Devo: evolutionary developmental mechanisms. *Int. J. Dev. Biol.* 47, 491–495.

Hall, B. L. (2011). Ontogeny does not recapitulate phylogeny, it creates phylogeny: a review of The Tragic Sense of Life: Ernst Haeckel and the Struggle Over Evolutionary Thought, by Robert J. Richards. *Evol. Dev.* 13, 401–404. doi: 10.1111/j.1525-142x.2011.00495.x

Hao, Z., Zhang, Z., Xiang, D., Venglat, P., Chen, J., Gao, P., et al. (2021). Conserved, divergent and heterochronic gene expression during *Brachypodium* and *Arabidopsis* embryo development. *Plant Reprod.* 34, 207–224. doi: 10.1007/s00497-021-00413-4

Hawkins, J. (2002). "Evolutionary developmental biology: Impact on systematic theory and practice, and the contribution of systematics," in *Developmental Genetics and Plant Evolution*, eds Q. C. B. Cronk, R. M. Bateman, and J. A. Hawkins (London: Taylor and Francis), 32–51. doi: 10.1201/9781420024982.ch3

Hejnol, A., and Dunn, C. W. (2016). Animal evolution: are phyla real? *Curr. Biol.* 26, 424–426. doi: 10.1016/j.cub.2016.03.058

Hennig, W. (1966). *Phylogenetic Systematics*. Urbana: University of Illinois Press.

Hurst, C. H. (1893). The recapitulation theory. *Nat. Sci.* 2, 195–200, 364–369.

Irie, N., and Kuratani, S. (2011). Comparative transcriptome analysis reveals vertebrate phylotypic period during organogenesis. *Nat. Commun.* 2:248. doi: 10.1038/ncomms1248

Irie, N., Satoh, N., and Kuratani, S. (2018). The phylum Vertebrata: a case for zoological recognition. *Zool. Lett.* 4:32. doi: 10.1186/s40851-018-0114-y

Ivanov, A. N. (1945). On the questions of so called "prophetic phase" in evolution of Kosmoceratidae. *Bull. Mos. Soc. Nat. Geogr.* 20, 1–32.

Ivanova-Kazas, O. M. (1936). Neoteny. *Priroda* 8, 57–67.

Ivanova-Kazas, O. M. (1995). *Evolutionary Embryology of Animals*. St. Petersburg: Nauka.

Ivanova-Kazas, O. M. (2004). Mythlandia, the reproduction of mythozoes. *Priroda* 4, 49–54.

Juravel, K., Porras, L., Höhna, S., Pisani, D., and Wörheide, G. (2021). Improved resolution of recalcitrant nodes in the animal phylogeny through the analysis of genome gene content and morphology. *bioRxiv* [Preprint] doi: 10.1101/2021.11.19.469253

Kalinka, A. T., Varga, K. M., Gerrard, D. T., Preibisch, S., Corcoran, D. L., Jarrells, J., et al. (2010). Gene expression divergence recapitulates the developmental hourglass model. *Nature* 468, 811–814. doi: 10.1038/nature09634

Karavaev, V. (1934). First, recently discovered case of the neoteny in animals. *Priroda* 9, 81–83.

Keibel, F. (1898). Das biogenetische Grundgesetz und die Coengenese. *Erg. Anat. Entw.* 7, 722–792.

Kluge, A. G., and Strauss, R. E. (1985). Ontogeny and systematics. *Ann. Rev. Ecol. Syst.* 16, 247–268. doi: 10.1146/annurev.es.16.110185.001335

Kollman, J. (1885). Das ueberwintern von europeischen frosch- und tritonlarven und die umwandlung des mexikanischen Axolotl. *Verh. Naturfor. Gesell. Basel* 7, 387–398.

Korshunova, T., and Martynov, A. (2020). Consolidated data on the phylogeny and evolution of the family Tritoniidae (Gastropoda: Nudibranchia) contribute to genera reassessment and clarify the taxonomic status of the neuroscience models *Tritonia* and *Tochuina*. *PLoS One* 15:e0242103. doi: 10.1371/journal.pone.0242103

Korshunova, T. A., Driessen, F. M. F., Picton, B. E., and Martynov, A. V. (2021). The multilevel organismal diversity approach deciphers difficult to distinguish nudibranch species complex. *Sci. Rep.* 11:18323. doi: 10.1038/s41598-021-94863-5

Korshunova, T. A., Fletcher, K., Picton, B., Lundin, K., Kashio, S., Sanamyan, N., et al. (2020). The Emperor's Cadlina, hidden diversity and gill cavity evolution: new insights for taxonomy and phylogeny of dorid nudibranchs (Mollusca: Gastropoda). *Zool. J. Linn. Soc.* 189, 762–827.

Korshunova, T. A., Lundin, K., Malmberg, K., Picton, B., and Martynov, A. V. (2018). First true brackish water nudibranch mollusc provides new insights for phylogeny and biogeography and reveals paedomorphosis-driven evolution. *PLoS One* 13:e0192177. doi: 10.1371/journal.pone.0192177

Korshunova, T. A., Martynov, A. V., and Picton, B. E. (2017a). Ontogeny as an important part of integrative taxonomy in tergipedid aeolidaceans (Gastropoda: Nudibranchia) with a description of a new genus and species from the Barents Sea. *Zootaxa* 4324, 1–22. doi: 10.11646/zootaxa.4324.1.1

Korshunova, T. A., Martynov, A., Bakken, T., Evertsen, J., Fletcher, K., Mudianta, I. W., et al. (2017b). Polyphyly of the traditional family Flabellinidae affects a major group of Nudibranchia: aeolidacean taxonomic reassessment with descriptions of several new families, genera, and species (Mollusca, Gastropoda). *Zookeys* 717, 1–139. doi: 10.3897/zookeys.717.21885

Kryzhanovsky, S. G. (1939). Das Rekapitulationsprinzip und die Bedingungen der historischen Auffassung der Ontogenese. *Acta Zool.* 20, 1–87. doi: 10.1111/j.1463-6395.1939.tb00493.x

Kupiec, J. J. (2009). *The Origin of Individuals*. Singapore: World Scientific.

Lamsdell, J. C. (2020). A new method for quantifying heterochrony in evolutionary lineages. *Paleobiology* 47, 1–22. doi: 10.1007/978-3-319-33038-9_71-1

Laumer, C. E., Fernández, R., Lemer, S., Combosch, D., Kocot, K., Riesgo, A., et al. (2019). Revisiting metazoan phylogeny with genomic sampling of all phyla. *Proc. R. Soc. B* 286:20190831. doi: 10.1098/rspb.2019.0831

Lecointre, G., Schnell, N. K., and Teletchea, F. (2020). Hierarchical analysis of ontogenetic time to describe heterochrony and taxonomy of developmental stages. *Sci. Rep.* 10:19732. doi: 10.1038/s41598-020-76270-4

Lee, M. S. Y., and Palci, A. (2015). Morphological phylogenetics in the genomic age. *Curr. Biol.* 25, 922–929. doi: 10.1016/j.cub.2015.07.009

Lemmen, K. D., Verhoeven, K. J. F., and Declerck, S. A. J. (2022). Experimental evidence of rapid heritable adaptation in the absence of initial standing genetic variation. *Funct. Ecol.* 36, 226–238. doi: 10.1111/1365-2435.13943

Levin, M., Anavy, L., Cole, A. G., Winter, E., Mostov, N., Khair, S., et al. (2016). The mid-developmental transition and the evolution of animal body plans. *Nature* 531, 637–641. doi: 10.1038/nature16994

Levit, G. S., and Hossfeld, U. (2019). Ernst Haeckel in the history of biology. *Curr. Biol.* 29, 1276–1284. doi: 10.1016/j.cub.2019.10.064

Levit, G. S., Hoßfeld, U., Naumann, B., Lukas, P., and Olsson, L. (2022). The biogenetic law and the gastraea theory: from Ernst Haeckel's discoveries to contemporary views. *J. Exp. Zool. B Mol. Dev. Evol.* 338, 13–27. doi: 10.1002/jez.b.23039

Li, Y., Shen, X.-X., Evans, B., Dunn, C. W., and Rokas, A. (2021). Rooting the animal tree of life. *Mol. Biol. Evol.* 38, 4322–4333. doi: 10.1093/molbev/msab170

Liu, J., Viales, R. R., Khoueiry, P., Reddington, J. P., Girardot, C., Furlong, E., et al. (2021). The hourglass model of evolutionary conservation during embryogenesis extends to developmental enhancers with signatures of positive selection. *Genome Res.* 31, 1573–1581. doi: 10.1101/gr.275212.121

Loison, L. (2021). Epigenetic inheritance and evolution: a historian's perspective. *Philos. Trans. R. Soc. B* 376:20200120. doi: 10.1098/rstb.2020.0120

Lyubischev, A. A. (1982). *Problems of the Form of the Systematics and Evolution of Organisms*. Moscow: Nauka.

Martynov, A. V. (1994). Materials for revision of nudibranch molluscs of the family Corambidae (Gastropoda, Opisthobranchia). Part II. Origin. *Zool. Zh.* 73, 36–43.

Martynov, A. V. (2009). From ontogeny to evolution: an expectation for changing current systematic paradigm. *Tr. Zool. Muz. Mosk. Gos. Univ.* 50, 145–229. ISBN 978-5-87317-617-5.

Martynov, A. V. (2010a). "Structure of the arm spine articulation ridges as a basis for taxonomy of Ophiuroidea (a preliminary report)," in *Proceedings of the Twelfth International Echinoderm Conference, Durham, NH*, ed. L. Harris (Rotterdam: Balkema), 233–239. doi: 10.1201/9780203869543-c37

Martynov, A. V. (2010b). Reassessment of the classification of the Ophiuroidea (Echinodermata), based on morphological characters: I. General character evaluation and delineation of the families Ophiomyxidae and Ophiacanthidae. *Zootaxa* 2697, 1–154. doi: 10.11646/zootaxa.2697.1.1

Martynov, A. V. (2011a). *Ontogenetic Systematics and a New Model of Evolution of Bilateria*. Moscow: KMK.

Martynov, A. V. (2011b). From 'tree-thinking' to 'cycle-thinking': ontogenetic systematics of nudibranch molluscs. *Thalassas* 27, 193–224.

Martynov, A. V. (2012a). Ontogenetic systematics: the synthesis of taxonomy, phylogenetics, and evolutionary developmental biology. *Paleont. J.* 46, 833–864. doi: 10.1134/S003103011208007

Martynov, A. V. (2012b). Ontogeny, systematics, and phylogenetics: perspectives of future synthesis and a new model of the evolution of Bilateria. *Biol. Bull.* 39, 393–401. doi: 10.1134/s106235901205010x

Martynov, A. V. (2014). "Ontogeny as a central paradigm of biology: declarative importance and practical underestimation," in *Proceedings of the 3rd International Congress on Invertebrate Morphology*, Berlin, 128.

Martynov, A. V., Brenzinger, B., Hooker, Y., and Schrödl, M. (2011). 3D Anatomy of a new tropical peruvian nudibranch gastropod species, *Corambe mancorensis*, and novel hypothesis on dorid gill ontogeny and evolution. *J. Molluscan Stud.* 77, 129–141. doi: 10.1093/mollus/eyq047

Martynov, A. V., Ishida, Y., Irimura, S., Tajiri, R., O'Hara, T., and Fujita, T. (2015). When ontogeny matters: a new Japanese species of brittle star illustrates importance of considering both adult and juvenile characters in taxonomic practice. *PLoS One* 10:e0139463. doi: 10.1371/journal.pone.0139463

Martynov, A. V., and Korshunova, T. A. (2011). *Opisthobranch Molluscs of the Seas of Russia. A Colour Guide to their Taxonomy and Biology*. Moscow: Fiton Press.

Martynov, A. V., and Korshunova, T. A. (2015). A new deep-sea genus of the family Polyceridae (Nudibranchia) possesses a gill cavity, with implications for cryptobranch condition and a 'Periodic Table' approach to taxonomy. *J. Molluscan Stud.* 81, 365–379. doi: 10.1093/mollus/eyv003

Martynov, A. V., Lundin, K., Picton, B., Fletcher, K., Malmberg, K., and Korshunova, T. (2020). Multiple paedomorphic lineages of soft-substrate burrowing invertebrates: parallels in the origin of *Xenocratena* and *Xenoturbella*. *PLoS One* 15:e0227173. doi: 10.1371/journal.pone.0227173

Martynov, A. V., and Schrödl, M. (2011). Phylogeny and evolution of corambid nudibranchs (Mollusca: Gastropoda). *Zool. J. Linn. Soc.* 163, 585–604. doi: 10.1111/j.1096-3642.2011.00720.x

Mayr, E. (1963). *Animal Species and Evolution*. Cambridge: Harvard University Press.

McKinney, M.L. (ed.) (1988). *Heterochrony in Evolution: A Multidisciplinary Approach*. New York, NY: Plenum.

McNamara, K. J. (1986). A guide to the nomenclature of heterochrony. *J. Paleontol.* 60, 4–13. doi: 10.1017/s0022336000021454

Mehnert, E. (1897). Kainogenese. Eine gesetzmässige Abänderung der embryonalen Entfaltung in Folge von erblicher Uebertragung in der Phylogenese erworbener Eigenthümlichkeiten. *Morph. Arb* 7, 1–156. doi: 10.1159/000393310

Minelli, A. (2007). Invertebrate taxonomy and evolutionary developmental biology. *Zootaxa* 1668, 55–60. doi: 10.11646/zootaxa.1668.1.7

Minelli, A. (2009). Phylo–evo–devo: combining phylogenetics with evolutionary developmental biology. *BMC Biol.* 7:36. doi: 10.1186/1741-7007-7-36

Minelli, A. (2015a). Biological systematics in the evo-devo era. *Eur. J. Taxon.* 125, 1–23. doi: 10.1017/9781108873130.003

Minelli, A. (2015b). "EvoDevo and its significance for animal evolution and phylogeny," in *Evolutionary Developmental Biology of Invertebrates 1*, ed. A. Wanninger (Vienna: Springer), 1–23. doi: 10.1007/978-3-7091-1862-7_1

Mirzoyan, E. N. (1974). *The Development of the Recapitulation Concept*. Moscow: Nauka.

Moles, J., Wägele, H., Cutignano, A., Fontana, A., Ballesteros, M., and Avila, C. (2017). Giant embryos and hatchlings of Antarctic nudibranchs (Mollusca: Gastropoda: Heterobranchia). *Mar. Biol.* 164, 114. doi: 10.54173/f512114

Morgan, T. H. (1908). *Evolution and Adaptation*. London: Macmillann.

Moroz, L., Kocot, K. M., Citarella, M. R., Dosung, S., Norekian, T. P., Povolotskaya, I. S., et al. (2014). The ctenophore genome and the evolutionary origins of neural systems. *Nature* 510, 109–114. doi: 10.1038/nature13400

Müller, W. A. (1997). "Comparative review: the phylotypic stage of vertebrates, common versus distinct features, and aspects of evolution," in *Developmental Biology* (New York, NY: Springer). doi: 10.1007/978-1-4612-2248-4_4

Müller, G. B. (2017). Why an extended evolutionary synthesis is necessary. *Interface Focus* 7:20170015. doi: 10.1098/rsfs.2017.0015

Müller, F. (1864). *Für Darwin*. Leipzig: Verlag von Wilhelm Engelmann.

Needham, J. (1933). On the dissociability of the fundamental process in ontogenesis. *Biol. Rev.* 8, 180–223. doi: 10.1111/j.1469-185x.1933.tb01153.x

Nejad Kourki, A. (2021). *Evolution of the Eumetazoan Body Plan*. Ph.D. thesis. Bristol: University of Bristol.

Neumann, J. S., Desalle, R., Narechania, A., Schierwater, B., and Tessler, M. (2021). Morphological characters can strongly influence early animal relationships inferred from phylogenomic data sets. *Syst. Biol.* 10, 360–375. doi: 10.1093/sysbio/syaa038

Nicholson, D. J. (2014). The return of the organism as a fundamental explanatory concept in biology. *Philos. Compass.* 9, 347–359. doi: 10.1111/phc3.12128

Nielsen, C. (2008). Six major steps in animal evolution: are we derived sponge larvae? *Evol. Dev.* 10, 241–257. doi: 10.1111/j.1525-142X.2008.00231.x

Nielsen, C. (2012). *Animal Evolution: Interrelationships of the Living Phyla*, 3rd Edn. Oxford: Oxford University Press.

Ninova, M., Ronshaugen, M., and Griffiths-Jones, S. (2014). Conserved temporal patterns of microRNA expression in *Drosophila* support a developmental hourglass model. *Gen. Biol. Evol.* 6, 2459–2467. doi: 10.1093/gbe/evu183

Núñez-León, D., Cordero, G. A., Schlindwein, X., Jensen, P., Stoeckli, E., Sánchez Villagra, M. R., et al. (2021). Shifts in growth, but not differentiation, foreshadow the formation of exaggerated forms under chicken domestication. *Proc. R. Soc. B* 288:20210392. doi: 10.1098/rspb.2021.0392

O'Hara, T. D., Hugall, A. F., Thuy, B., Stöhr, S., and Martynov, A. V. (2017). Restructuring higher taxonomy using broadscale phylogenomics: the living Ophiuroidea. *Mol. Phyl. Evol.* 107, 415–430. doi: 10.1016/j.ympev.2016.12.006

Ontogeny (2022). *Wikipedia*. Available online at: https://en.wikipedia.org/wiki/Ontogeny (accessed February 27, 2022).

Orton, G. R. (1955). The role of ontogeny in systematics and evolution. *Evolution* 9, 75–83. doi: 10.2307/2405359

Pabst, E. A., and Kocot, K. M. (2018). Phylogenomics confirms monophyly of Nudipleura (Gastropoda: Heterobranchia). *J. Molluscan Stud.* 84, 259–265. doi: 10.1093/mollus/eyy013

Pavlinov, I. Y. (2020). Multiplicity of research programs in the biological systematics: a case for scientific pluralism. *Philosophies* 5:7. doi: 10.3390/philosophies5020007

Peters, S. (1980). Das biogenetische grundgesetz – vorgeschichte und folgerungen. *Medizinhist. J.* 15, 57–69.

Pisani, D., Pett, W., Dohrmann, M., Feuda, R., Rota-Stabelli, O., Philippe, H., et al. (2015). Genomic data do not support comb jellies as the sister group to all other animals. *Proc. Nat. Acad. Sci. U.S.A.* 112, 15402–15407. doi: 10.1073/pnas.1518127112

Raff, R. A., and Kaufman, T. C. (1983). *Embryos, Genes, and Evolution*. Bloomington, IN: Indiana University Press.

Redmond, A. K., and Mclysaght, A. (2021). Evidence for sponges as sister to all other animals from partitioned phylogenomics with mixture models and recoding. *Nat. Comm.* 12:1783. doi: 10.1038/s41467-021-22074-7

Reilly, S. M., Wiley, E. O., and Meinhardt, D. J. (1997). An integrative approach to heterochrony: the distinction between interspecific and intraspecific phenomena. *Biol. J. Linn. Soc.* 60, 119–143. doi: 10.1006/bijl.1996.0092

Richards, R. J. (2009). Haeckel's embryos: fraud not proven. *Biol. Phil.* 24, 147–154. doi: 10.1007/s10539-008-9140-z

Richardson, M. K. (1995). Heterochrony and the phylotypic period. *Dev. Biol.* 172, 412–421. doi: 10.1006/dbio.1995.8041

Richardson, M. K. (1999). Vertebrate evolution: the developmental origins of adult variation. *Bioessays* 21, 604–613. doi: 10.1002/(SICI)1521-1878(199907)21:7<604::AID-BIES9>3.0.CO;2-U

Richardson, M. K. (2022). Theories, laws, and models in evo-devo. *J. Exp. Zool.* 338, 36–61. doi: 10.1002/jez.b.23096

Richardson, M. K., Hanken, J., Gooneratne, M. L., Pieau, C., Raynaud, A., Selwood, L., et al. (1997). There is no highly conserved embryonic stage in the vertebrates: implications for current theories of evolution and development. *Anat. Embr.* 196, 91–106. doi: 10.1007/s004290050082

Richter, S., and Wirkner, C. S. (2014). A research program for evolutionary morphology. *J. Zool. Syst. Evol. Res.* 52, 338–350. doi: 10.1111/jzs.12061

Rieppel, O. (2016). *Phylogenetic Systematics: Haeckel to Hennig*. Boca Raton, FL: Taylor & Francis.

Rundell, R. J., and Leander, B. S. (2010). Masters of miniaturization: convergent evolution among interstitial eukaryotes. *Bioessays* 32, 430–437. doi: 10.1002/bies.200900116

Schierwater, B., and DeSalle, R. (eds). (2021). *Invertebrate Zoology: A Tree of Life Approach*. Boca Raton, FL: CRC press.

Schmalhausen, I. I. (1942). *Organism as a Whole in Individual and Historical Development*. Moscow–Leningrad: Akad. Nauk USSR.

Scholtz, G. (2010). Deconstructing morphology. *Acta Zool.* 91, 44–63. doi: 10.1111/j.1463-6395.2009.00424.x

Sedgwick, A. (1894). On the law of development commonly known as Von Baer's law. *Q. J. Microsc. Sci.* 36, 35–52. doi: 10.1242/jcs.s2-36.141.35

Severtsov, A. N. (1912). *Essays on the Theory of Evolution: Individual Development and Evolution*. Kiev: Imp. Univ. Sv. Vladimira.

Severtsov, A. N. (1939). *Morphological Patterns of Evolution*. Moscow–Leningrad: Akad. Nauk USSR Publishing house.

Simion, P., Philippe, H., Baurain, D., Jager, M., Richter, D. J., Di Franco, A., et al. (2017). A large and consistent phylogenomic dataset supports sponges as the sister group to all other animals. *Curr. Biol.* 27, 1–10. doi: 10.1016/j.cub.2017.02.031

Skulachev, V. P., Holtze, S., Vyssokikh, M. Y., Bakeeva, L. E., Skulachev, M. V., Markov, A. V., et al. (2017). Neoteny, prolongation of youth: from naked mole rats to "naked apes" (Humans). *Physiol. Rev.* 97, 699–720. doi: 10.1152/physrev.00040.2015

Slack, J. M. W., Holland, P. W. H., and Graham, C. F. (1993). The zootype and the phylotypic stage. *Nature* 361, 490–492. doi: 10.1038/361490a0

Smirnov, A. V. (1991). "Paedomorphosis as mechanism of evolutionary transformations of organisms," in *Modern Evolutionary Morphology*, eds E. I. Vorobyeva and A. A. Vronsky (Kiev: Naukova Dumka), 88–103.

Smith, G. (1911). *Primitive Animals*. Cambridge: Cambridge University Press.

Stöhr, S., and Martynov, A. V. (2016). Paedomorphosis as an evolutionary driving force: insights from deep-sea brittle stars. *PLoS One* 11:e0164562. doi: 10.1371/journal.pone.0164562

Tassia, M. G., Cannon, J. T., Konikoff, C. E., Shenkar, N., Halanych, K. M., and Swalla, B. J. (2016). The global diversity of Hemichordata. *PLoS One* 11:e0162564. doi: 10.1371/journal.pone.0162564

Uesaka, M., Kuratani, S., and Irie, N. (2022). The developmental hourglass model and recapitulation: an attempt to integrate the two models. *J. Exp. Zool.* 338, 76–86. . doi: 10.1002/jez.b.23027

Viñuelas, J., Kaneko, G., Coulon, A., Beslon, G., and Gandrillon, O. (2012). Towards experimental manipulation of stochasticity in gene expression. *Prog. Biophys. Mol. Biol.* 110, 44–53. doi: 10.1016/j.pbiomolbio.2012.04.010

von Baer, K. E. (1828/1837). *Entwickelungsgeschichte der Thiere: Beobachtung und Reflexion. 2 Bd*. Königsberg: Bornträger, 264.

Vorobyeva, E. I. (1991). "Modern problems of the evolution of ontogeny," in *Modern Evolutionary Morphology*, eds E. I. Vorobyeva and A. A. Vronsky (Kiev: Naukova Dumka), 72–87.

Wanninger, A. (2015). Morphology is dead – long live morphology! Integrating MorphoEvoDevo into molecular EvoDevo and phylogenomics. *Front. Ecol. Evol.* 3:54.

Wiens, J. J., Bonnet, R. M., and Chippindale, P. T. (2005). Ontogeny discombobulates phylogeny: paedomorphosis and higher level salamander relationships. *Syst. Biol.* 54, 91–110. doi: 10.1080/10635150590906037

Wolfe, J. M., and Hegna, T. A. (2013). Testing the phylogenetic position of Cambrian pancrustacean larval fossils by coding ontogenetic stages. *Cladistics* 30, 366–390. doi: 10.1111/cla.12051

Yang, Z. (2014). *Molecular Evolution: A Statistical Approach*. Oxford: Oxford University Press.

Yi, S. V., and Goodisman, M. A. D. (2021). The impact of epigenetic information on genome evolution. *Philos. Trans. R. Soc. B* 376:20200114. doi: 10.1098/rstb.2020.0114

Yushin, V. V., and Malakhov, V. V. (2014). The origin of nematode sperm: progenesis at the cellular level. *Russ. J. Mar. Biol.* 40, 71–81. doi: 10.1134/S1063074014020114

Zaitseva, O. V., Shumeev, A. N., Korshunova, T. A., and Martynov, A. V. (2015). Heterochronies in the formation of the nervous and digestive systems in

early postlarval development of opisthobranch mollusks: organization of major organ systems of the Arctic dorid *Cadlina laevis*. *Biol. Bull.* 42, 186–195. doi: 10.1134/s1062359015030152

Conflict of Interest: The authors declare that the research was conducted in the absence of any commercial or financial relationships that could be construed as a potential conflict of interest.

Publisher's Note: All claims expressed in this article are solely those of the authors and do not necessarily represent those of their affiliated organizations, or those of the publisher, the editors and the reviewers. Any product that may be evaluated in this article, or claim that may be made by its manufacturer, is not guaranteed or endorsed by the publisher.

Frontiers in
Cell and Developmental Biology

Explores the fundamental biological processes of life, covering intracellular and extracellular dynamics.

The world's most cited developmental biology journal, advancing our understanding of the fundamental processes of life. It explores a wide spectrum of cell and developmental biology, covering intracellular and extracellular dynamics.

Discover the latest Research Topics

See more →

Frontiers

Avenue du Tribunal-Fédéral 34
1005 Lausanne, Switzerland
frontiersin.org

Contact us

+41 (0)21 510 17 00
frontiersin.org/about/contact